



**Depositional processes and controlling factors from
river mouths to slope systems in active tectonic margins:**
insights from middle-upper Eocene to Lower Miocene
records in the Colombian Caribbean

Sergio A. Celis

PhD Thesis

**Doctoral Programme in Earth Sciences
University of Granada
2024**



ugr

Universidad
de Granada



Programa Doctorado
Ciencias de la Tierra



Programa Doctorado
Ciencias de la Tierra



ugr | Universidad
de Granada



El conocimiento
es de todos

Minciencias

**Depositional processes and controlling factors from
river mouths to slope systems in active tectonic margins:
insights from middle-upper Eocene to Lower Miocene records in the Colombian Caribbean**

PhD Dissertation by

Sergio Andres Celis Hurtado

PhD Thesis

Doctoral Programme in Earth Sciences

Department of Stratigraphy and Palaeontology

University of Granada

2024

**Depositional processes and controlling factors from
river mouths to slope systems in active tectonic margins:
insights from middle-upper Eocene to Lower Miocene records in the Colombian Caribbean**

PhD Dissertation by

Sergio Andres Celis Hurtado

Supervised by

Francisco J. Rodríguez-Tovar

Andrés Pardo Trujillo

PhD Thesis

Doctoral Programme in Earth Sciences

Department of Stratigraphy and Palaeontology

University of Granada

2024

Editor: Universidad de Granada. Tesis Doctorales
Autor: Sergio Andrés Celis Hurtado
ISBN: 978-84-1195-752-6
URI: <https://hdl.handle.net/10481/103210>

Doctoral Thesis

**Depositional processes and controlling factors from
river mouths to slope systems in active tectonic margins:
insights from middle-upper Eocene to Lower Miocene records in the Colombian Caribbean**

*Procesos deposicionales y factores de control desde
sistemas de desembocadura de ríos al talud en un margen tectónico activo:
perspectivas a partir de registros del Eoceno medio-superior al Mioceno Inferior en el Caribe colombiano*

Thesis submitted by Sergio Andres Celis Hurtado for the degree of Doctor in Earth Sciences by the
University of Granada.

Sergio A. Celis

This Doctoral Thesis has been supervised by PhD Francisco J. Rodríguez Tovar, Professor of the Department of Stratigraphy and Palaeontology of the University of Granada (Spain), and PhD Andrés Pardo Trujillo, Professor of the Department of Geology of the University of Caldas (Colombia).

Francisco J. Rodríguez-Tovar

Andrés Pardo Trujillo

Doctoral Programme in Earth Sciences
Department of Stratigraphy and Palaeontology
University of Granada

2024

The front cover photograph was taken on the road between the cities of Montería and Planeta Rica and is interpreted as representing fluvial-dominated deltaic deposits from the Oligocene to Early Miocene.

The well-core photograph shows an interval from the ANH-SSJ-La Estrella-1X well-core, illustrating the irregular contact between clast-supported conglomerates and horizontally laminated sandstones, with organic debris highlighting the lamination in upper Eocene deposits.

The photograph on the back cover is from the ANH-SSJ-Nueva Esperanza-1X well-core, featuring *Ophiomorpha* exhibiting infill with rhythmic lamination (tubular tidalites) in Lower Miocene deposits.

Para la realización de la tesis doctoral, Sergio A. Celis obtuvo un Crédito-Beca del Ministerio de Ciencia Tecnología e Innovación (Minciencias Colombia) de Doctorados en el exterior (convocatoria 885-2020).

La Agencia Nacional de Hidrocarburos ANH, el Ministerio de Ciencia, Tecnología e Innovación y el Instituto de Investigaciones en Estratigrafía IIES a partir del Convenio 730/327–2016 permitieron estudiar algunos testigos de sondeo (*well-cores*) perforados en el Caribe colombiano.

Durante esta Tesis Doctoral se realizaron dos estancias en centros extranjeros. La primera en el Instituto Patagónico de Geología y Paleontología (IPGP CONICET-CENPAT; Puerto Madryn, Argentina) bajo la supervisión del Dr. Sebastian Richianno y Dr. José Cuitiño. La segunda en el Centro de Investigaciones Geológicas (CIG- CONICET- Universidad Nacional de La Plata, La Plata, Argentina) bajo la supervisión del Dr. Damián Moyano-Paz y Dr. Gonzalo Veiga. Estas estancias fueron subvencionadas por la AUIP (Becas de movilidad entre universidades andaluzas e iberoamericanas, Convocatoria 2022), Banco Santander y Vicerrectorado de Internacionalización de la UGR (Becas Santander Movilidad internacional doctorado 23/24) y CONICET.

International Association of Sedimentologist (IAS), Society for Sedimentary Geology (SEPM), International Ichnological Association (IIA), el proyecto de I+D+i PID2019-104625RB-100, financiado por MICIU/AEI/10.13039/501100011033, el Instituto de Investigaciones en Estratigrafía IIES y Smithsonian Institution brindaron apoyo económico.

Esta Tesis Doctoral se desarrolló en el marco del Grupo de Investigación RNM-178 de la Junta de Andalucía (España), y del Grupo de Investigación en Estratigrafía y Vulcanología (GIEV) Cumanday de Minciencias (Colombia). Asimismo, se integra dentro del grupo de investigación “Ichnology and Palaeoenvironmental Research Group”, en el Departamento de Estratigrafía y Paleontología de la Universidad de Granada.

For the completion of his doctoral thesis, Sergio A. Celis received a Credit-Scholarship from the Ministry of Science, Technology, and Innovation (Minciencias Colombia) for Doctoral Studies Abroad (Call 885-2020).

The National Hydrocarbons Agency (ANH), the Ministry of Science, Technology, and Innovation, and the Institute of Stratigraphy Research (IIES), through Agreement 730/327–2016, facilitated the study of certain well-cores drilled in the Colombian Caribbean.

During this doctoral research, two research stays were conducted at international institutions. The first was at the Patagonian Institute of Geology and Paleontology (IPGP CONICET-CENPAT; Puerto Madryn, Argentina) under the supervision of PhD. Sebastian Richiano and PhD. José Cuitiño. The second was at the Geological Research Center (CIG-CONICET, National University of La Plata, La Plata, Argentina) under the supervision of PhD Damián Moyano-Paz and PhD Gonzalo Veiga. These research stays were funded by the AUIP (Mobility Grants between Andalusian and Ibero-American Universities, Call 2022), Banco Santander, and the Office of Internationalization at the University of Granada (Santander International Doctoral Mobility Grants 23/24) as well as CONICET.

The International Association of Sedimentologists (IAS), Society for Sedimentary Geology (SEPM), International Ichnological Association (IIA), the R&D&I project PID2019-104625RB-100 funded by MICIU/AEI/10.13039/501100011033, the Institute of Stratigraphy Research (IIES), and the Smithsonian Institution provided financial support.

This doctoral thesis was developed within the framework of the RNM-178 Research Group of the Junta de Andalucía (Spain) and the Research Group on Stratigraphy and Volcanology (GIEV) Cumanday of Minciencias (Colombia). Additionally, it is part of the "Ichnology and Palaeoenvironmental Research Group" within the Department of Stratigraphy and Paleontology at the University of Granada.

A mamá y papá

A tí, mi Susy

During this thesis, adversary knocked at our door twice, trying to force its way in.

Shutting it proved arduous, yet we prevailed, securing it with a padlock.

This thesis is a tribute to every PhD student whose families weathered the storm of uncertainty alongside them, for whom the journey is wrought with challenges. May you find strength and courage in abundance. Do not yield, but do not rush forward either. Pause. In these moments, let your heart guide your actions, not mere reason. Decisions made for those you love should always be led by love.

All will be well.

*“Research is to see what everybody else has seen,
and to think what nobody else has thought”*

Albert Szent-Gyorgyi

*“It’s so much easier to throw rocks
than it is to govern”*

Karen Bass

*...but it is much more difficult to be governed by someone
who seems to have only thrown rocks.*

Si fuera fácil, CUALQUIERA LO HARÍA.

PREFACE

This is only the beginning.
As an apprentice in sedimentology and ichnology,
I remain eager to continue exploring the
field and the rocks... the rocks in the field.
Although, with more lateral continuity.
In the tropics there is a lot of jungle and few rocks,
and journal editors don't like that.

The journey should be marked by an absolute respect for the work of others, for their ideas, and for their positions. We interpret based on what we know, so how can we judge others who may know more and less than we do? This has been my principle, but I have always viewed this position with a lot of criticism and strictness. This has caused me problems. Many confuse this situation and call criticism disrespectful. There is a fine line, of course. The issue is balance.

However, the journey of pursuing a PhD is a delicate balance between critical rigour and a certain degree of permissiveness—between the excuses we allow ourselves and the obligations we must meet. Over the past five years, I've faced numerous moments that have reminded me that not everything can be controlled, nor can everything always go as planned. The world, science, and those who believe in the transformative power of education are indeed on the right path. Yet, this does not imply that everything within that world is perfectly aligned. The challenge lies in learning to manage these imperfections without losing motivation. In every situation, there is always a right place and the right people—the task is to find them. And to put aside what is not suitable. Even if many of them turn out to be indecipherable.

The introduction reflects what I have always aspired to be and study. It represents my dreams: to discuss and contemplate basin depositional processes over countless cups of coffee, to be immersed in this world. I've always dreamed of interacting, traveling, exploring, and discovering new realms within these topics.

The geological framework represents my country—the place I've always wanted to study, out of a desire to contribute to its progress. We, the people of my country, have grown up in a world that often feels inverted. Our ingrained mindset carries many positive aspects, such as warmth and hospitality, but also significant challenges, like the tendency to put oneself above others. It's contradictory, but it's real. However, 'putting oneself above others' should never be misunderstood. Often, when one is strict and demands discipline and rigor, many hide behind protective adjectives that, in reality, only serve to mask mediocrity. I try not to fall into them on a daily basis. My dream is to return and contribute to changing the system, to create more opportunities, and to challenge the limitations that are often mental. Change is unlikely to come from within—it's often easier to see the need for change from the outside. *Colombia is not just a country; it is a sentiment.*

The materials and methods serve as a reminder that without a life project, life becomes more complex. Without a script, without direction, everything becomes random—and that randomness can be dangerous. Methods, in both life and research, are essential to prevent everything from drifting aimlessly.

The results allow me to envision the Eocene flows as sudden and unpredictable as life itself. One day you're here, the next day you're somewhere entirely different, without a fixed course. In contrast, the Oligocene feels more predictable, with future plans and an established project—though who knows if it will remain so over time? Deltas, like life, are inherently unpredictable; even when they seem stable, the domain of rivers, waves, or tides can alter them unexpectedly.

The discussion chapter mirrors my life during my PhD. My path changed radically several times, often leading me to question, "What am I doing here? Why am I not somewhere else?" Finding an explanation is no easy matter. But you must always find the reason for the changes and move on.

But it is always necessary to finish—to conclude is to learn to bring every project, every chapter of life, to a close, so that a new one can begin. That's why I'm grateful to those who believe in future generations, for they are the ones willing to step aside when their time has come.

Finally, the future perspectives are uncertain. But you should always give your best and leave the best impression wherever you go. Because you never know the twists and turns life may take and where you might end up. "The best way to uphold the image of your country is to help the country you are in grow through your actions."

Table of contents

| | |
|---|-----------|
| Index of abbreviations | 21 |
| Abstract..... | 23 |
| Resumen..... | 24 |
| Extended abstract | 25 |
| Resumen extendido | 28 |
| THESIS SCOPE AND FRAMEWORK | 33 |
| I. Motivation | 33 |
| II. Research questions and hypothesis | 34 |
| III. Objectives | 35 |
| IV. Layout..... | 36 |
| PART I INTRODUCTION AND BACKGROUND | 41 |
| Chapter I..... | 43 |
| INTRODUCTION..... | 43 |
| I.1. Coastal sedimentary environments | 44 |
| I.2. Ichnological analysis | 46 |
| I.3. Sediment transfer to the shelf and deep-sea zones | 48 |
| I.4. Allogenic and autogenic factors | 51 |
| I.5. Forearc basins: the Colombian Caribbean..... | 53 |
| I.6. Study area | 54 |
| PART II GEOLOGICAL FRAMEWORK AND MATERIALS AND METHODS | 57 |
| Chapter II | 59 |
| GEOLOGICAL FRAMEWORK | 59 |
| II.1. Present regional tectonic configuration..... | 60 |
| II.2. Geological and stratigraphical context..... | 62 |
| II.3. Middle-upper Eocene to Lower Miocene deposits..... | 63 |
| Chapter III..... | 67 |
| METHODOLOGY | 67 |
| III.1. Basis of the research | 68 |
| III.2. Material selection..... | 69 |
| III.3. Outcrops..... | 69 |
| III.4. Well-cores | 69 |
| PART III RESULTS..... | 73 |
| Chapter IV | 75 |
| EOCENE SHALLOW MARINE SYSTEMS..... | 75 |

| | |
|--|------------|
| Hyperconcentrated to hyperpycnal flow transition along a river-delta system in a tropical humid setting (middle to late Eocene, Caribbean Colombia) | 76 |
| Abstract | 77 |
| IV.1. Introduction..... | 77 |
| IV.2. Geological setting | 79 |
| IV.3. Methods | 81 |
| IV.4. Stratigraphy..... | 83 |
| IV.5. Facies associations analysis | 84 |
| IV.6. Depositional model and control factors | 96 |
| IV.7. Conclusions..... | 101 |
| Chapter V..... | 103 |
| EOCENE DEEP MARINE SYSTEMS..... | 103 |
| Coarse-grained submarine channels: from confined to unconfined flows in the Colombian Caribbean (late Eocene) | 104 |
| Abstract | 105 |
| V.1. Introduction..... | 105 |
| V.2. Geological setting..... | 106 |
| V.3. Methods and data set | 109 |
| V.4. Results | 109 |
| V.5. Depositional model | 126 |
| V.6. Discussion – from confined to unconfined flows in coarse-grained channels: assessing integrative sedimentary facies..... | 128 |
| V.7. Conclusions | 133 |
| Chapter VI..... | 135 |
| OLIGOCENE TO LOWER MIOCENE FLUVIO-DELTAIC SYSTEMS | 135 |
| Evolution of a fluvial-dominated delta during the Oligocene of the Colombian Caribbean: Sedimentological and ichnological signatures in well-cores..... | 136 |
| Abstract | 136 |
| VI.1. Introduction..... | 137 |
| VI.2. Geological setting | 139 |
| VI.3. Material and methods..... | 140 |
| VI.4. Sedimentology and ichnology | 143 |
| VI.5. Interpretation and discussion | 157 |
| VI.6. Conclusions..... | 165 |
| PART IV DISCUSSION..... | 167 |
| Chapter VII | 169 |
| TECTONIC, EUSTASY AND SEDIMENTATION..... | 169 |

| | |
|---|------------|
| Sedimentary evolution of forearc basins in the Colombian Caribbean: insights from middle-upper Eocene to Lower Miocene deposits | 170 |
| Abstract | 171 |
| VII.1. Introduction | 171 |
| VII.2. Geological background..... | 173 |
| VII.3. Dataset and methodology | 177 |
| VII.4. Biostratigraphy | 178 |
| VII.5. Sedimentary facies and facies association..... | 179 |
| VII.6. Evolution of depositional systems..... | 200 |
| VII.7. Discussion..... | 207 |
| VII.8. Conclusions | 216 |
| Chapter VIII..... | 219 |
| RECORDS OF THE ESTABLISHMENT OF DELTAIC SYSTEMS IN THE OLIGOCENE-EARLY MIOCENE | 219 |
| Deciphering influencing processes in a tropical delta system (middle-late Eocene? to Early Miocene, Colombian Caribbean): Signals from a well-core integrative sedimentological, ichnological, and micropaleontological analysis | 220 |
| Abstract | 221 |
| VIII.1. Introduction..... | 221 |
| VIII.2. Geological setting..... | 223 |
| VIII.3. Materials and methods | 224 |
| VIII.4. Results | 226 |
| VIII.5. Depositional systems and evolution..... | 245 |
| VIII.6. Paleogeographic implications | 250 |
| VIII.7. Conclusions..... | 252 |
| Supplementary paper of Chapter VIII | 255 |
| Sediment provenance signal of the Northern Andes during the Oligocene-Pliocene: Insights from the detrital record of the forearc and intra-arc basins, northwestern Colombian margin | 255 |
| PART V FINAL REMARKS, CONCLUSIONS AND FORTHCOMING RESEARCH | 257 |
| Chapter IX..... | 259 |
| CONCLUSIONS | 259 |
| CONCLUSIONES..... | 263 |
| Chapter X..... | 267 |
| FUTURE PERSPECTIVES AND OTHER COASTAL SYSTEMS..... | 267 |
| Ichnological indicators of physico-chemical stresses in wave- to tide-dominated Miocene shallow marine environments (Argentine Patagonia) | 269 |
| Abstract | 270 |

| | |
|---|------------|
| X.1. Introduction..... | 271 |
| X.2. Geological background | 273 |
| X.3. Methodology | 274 |
| X.4. Sedimentological and ichnological features..... | 274 |
| X.5. Vertical facies distribution | 293 |
| X.6. Ichnological signature and physico-chemical stresses | 299 |
| X.7. Conclusions | 303 |
| Agradecimientos / Acknowledgements..... | 307 |
| References | 311 |
| Appendix I. | 363 |

Index of abbreviations

BFS: Bucaramanga Fault System

BI: Bioturbation Index

BoF: Boconó Fault

LMVB: Lower Magdalena Valley Basin

PFS: Palestina Fault System

RFS: Romeral Fault System

SFB: Sinu Fold Belt

SJFB: San Jacinto Fold Belt

SMF: Santa Marta Fault

SMM: Santa Marta Massif

SNSM: Sierra Nevada de Santa Marta

SSJB: Sinu San Jacinto Basin

Abstract

The middle-upper Eocene to Lower Miocene sedimentary successions in the Colombian Caribbean represent complex depositional environments shaped by tectonics and sediment input. The conducted sedimentological, ichnological, well-logs, and micropaleontological analyses reveal both allogenic and autogenic processes influencing sedimentation.

In the southwestern Colombian Caribbean, south of the San Jacinto Fold Belt, middle-upper Eocene coarse-grained deposits are characterized by hyperconcentrated and hyperpycnal flows originating from continental areas. These flows undergo transformations upon reaching coastal and marine settings, exhibiting diverse flow behaviors ranging from high-energy sand-rich flows to fluidal gravel beds. Marine influence, reflected in sedimentological and ichnological features, indicate gravitational flow and tidal modulation. In the central region of the San Jacinto Fold Belt, evidence points to the development of submarine channel systems, with coarse-grained channel-lobe transitions in slope-basin plain systems, marking supercritical to subcritical conditions with sediment transport from land to the marine basin.

During the latest Eocene to earliest Oligocene, transgressive fine-grained deposits overlie coarse-grained successions in the southwestern Colombian Caribbean. Oligocene to Early Miocene successions show meandering fluvial deposits, mudrocks, and rhizoliths, indicating water-logged interdistributary bays and gallery flood forests, marking the beginning of a lower delta plain system. Moreover, typical fluvio-dominated deltaic successions, influenced by tropical torrential rains, show fluctuations in river discharges, with episodic tidal modulation and wave reworking affecting the deltaic system. This period marks a significant shift in sedimentation patterns, driven by tectonic activity, relative sea level changes, and tropical climatic influences. The progradational trend and evolving depositional styles highlight the complex interplay between tectonic convergence, subsidence, and climate, contributing to the understanding of sedimentary processes in tropical regions.

Resumen

Las sucesiones sedimentarias del Eoceno medio-tardío al Mioceno Temprano en el Caribe colombiano representan sistemas deposicionales complejos, modulados por la tectónica y el aporte de sedimentos. Los análisis sedimentológicos, icnológicos y micropaleontológicos llevados a cabo revelan procesos alogénicos y autogénicos que influyen en la sedimentación.

En el suroeste del Caribe colombiano, al sur del Cinturón Plegado de San Jacinto, los depósitos de grano grueso del Eoceno medio-tardío se generaron por flujos hiperconcentrados e hiperpícnicos originados en áreas continentales. Estos flujos se transforman al alcanzar los entornos costeros y marinos, exhibiendo comportamientos de flujo diversos que van desde flujos ricos en arena de alta energía hasta lechos de fluidos de grava. La influencia marina, reflejada en características sedimentológicas e icnológicas, se relaciona con la presencia de flujos gravitacionales y modulación por mareas. En la región central del Cinturón Plegado de San Jacinto hay evidencia del desarrollo de sistemas de canales submarinos, con transiciones de lóbulos y canales de grano grueso que marcan condiciones supercríticas a subcríticas con transporte de sedimentos desde la tierra hacia la cuenca.

Durante el Eoceno tardío al Oligoceno temprano, depósitos transgresivos de grano fino cubren las sucesiones de grano grueso en el suroeste del Caribe colombiano. Las sucesiones del Oligoceno al Mioceno temprano muestran depósitos fluviales meandriformes, lutitas y rizolitos, que indican bahías interdistributarias y bosques anegados, marcando el inicio de un sistema de llanura deltaica inferior. Además, las típicas sucesiones deltaicas dominadas por sistemas fluviales, influenciadas por lluvias torrenciales tropicales, registran fluctuaciones en las descargas de los ríos, con modulación por mareas y retrabajamiento por olas afectando el sistema deltaico de manera episódica. Este período refleja un cambio en los patrones de sedimentación, ocasionado por la actividad tectónica, los cambios relativos del nivel del mar y las influencias climáticas tropicales. La tendencia progradacional y la evolución de los patrones deposicionales resaltan la compleja interacción entre la convergencia tectónica, la subsidencia y el clima, contribuyendo a la comprensión de los procesos sedimentarios en regiones tropicales.

Extended abstract

The middle-upper Eocene to Lower Miocene successions in the Colombian Caribbean are potential reservoirs and seals, representing coarse- and fine-grained depositional systems, associated with an accretion-dominated subduction complex. An integrative sedimentological, ichnological, well-logs and micropaleontological analysis of outcrops and well-cores was conducted to understand the allogenic and autogenic processes that control sedimentation and how they influence the spatial distribution of sedimentary deposits. Complex interactions between processes in shallow marine environments determine stressful paleoenvironmental conditions affecting tracemaker community and organism-substrate relationships. By characterizing facies and facies associations, defining stacking patterns, and establishing stratigraphic correlations (lateral continuity from river mouths to the slope), we gain insights into the interactions between sedimentary dynamics and macrobenthic ecosystems allowing paleoenvironmental reconstructions.

During the middle to late Eocene in the southwestern of the Colombian Caribbean (southern region of the San Jacinto Fold Belt), coarse-grained systems are characterized by hyperconcentrated to hyperpycnal flows from continental areas reaching the coastline where the flow undergoes transformations.

Sharp-based, massive coarse-grained sandstone with outsized pebble-clasts is interpreted as the result of a high competence, sand-concentrated flow, where high-velocity sand settling from suspension led to rapid deposition and a high rate of sediment aggradation. Following this, sharp-based, normally graded gravel beds suggest a more fluidal and turbulent flow, capable of bedload transport of the largest clasts, with grain-size conditioned settling from suspension. Moreover, unstratified deposits contain the largest clasts, likely representing the peak of the flood discharges. However, evidence also suggests that flows may undergo transformations upstream or when they come into contact with the marine system. Transitions to structureless coarse-grained sandstones, horizontal-laminated conglomeratic sandstones, with organic debris highlighting the lamination, and beds with abundant pollen and spores are recognized. These features correlate with records of high-velocity currents, likely associated with bedload under hyperpycnal flow conditions. Sedimentological and ichnological features—presence of *Conichnus*, *Ophiomorpha*, *Thalassinoides*, fluid muds, and mud drapes—indicate that the arrival of flows at the coastline triggers an interaction between gravitational flow processes and marine processes, highlighting the interplay between the feeder system and the receiving basin. Occasional marine influence associated with tidal modulation or wave reworking during upstream avulsion or a decrease in sediment input is also interpreted. The limited accommodation space favoured the accumulation of amalgamated successions in this compressional accretionary forearc basin, with no evidence of deltaic plains.

In the central region of the San Jacinto Fold Belt, evidence suggests that some of these flows reached the shelf, slope and basin plain, where coarse-grained deposits point to the development of a channel-lobe system. It displays a well-preserved channel inception stage in the shelf break represented by sigmoidal to lens-shaped gravels, and planar cross-stratified pebbly sandstones (foreset and backset) interpreted as cyclic steps in an expansion zone. In a later stage, a classical channel-levee complex was developed, represented by channel fill deposits showing thick sharp- and erosional-based, fining-upward successions, having basal massive matrix-supported pebble conglomerates vertically evolving to liquefied massive to planar-laminated coarse-grained

sandstones with phytodetrital carbonaceous laminae. They are interpreted as concentrated flow deposits (high-density turbidites) coming from continental areas or from coastal systems (i.e., delta reworking). Undifferentiated channel-belt thin-bedded turbidites, associated with levee and terrace deposits, are linked to these confined systems, characterized by trace fossils such as *Ophiomorpha* and *Thalassinoides*. This ichnoassemblage belong to the *Ophiomorpha rudis* ichnosubfacies within the *Nereites* ichnofacies, associated with deposition from turbidity currents in the channel. Additionally, *Nereites* and *Phycosiphon* trace fossils, related to the *Nereites* ichnosubfacies from *Nereites* ichnofacies, are common in internal levee and terrace settings, where interbedded bioturbated mudstones settle out of suspension under lower-energy conditions, either from overflowing turbidity currents or hemipelagic processes during the shutdown of the higher energy system.

The channel-lobe transition zone is marked by debrites from cohesionless debris flows in a channel-mouth bar setting, representing bypass processes that developed distally into low-angle, planar cross- and sigmoidally-stratified (upstream antidune) pebble-size to coarse-grained sandstones that fill low-angle scours (cut-and-fill structures) in an antidune field setting with supercritical conditions. As flows lose channel confinement, Froude supercritical flows transition to subcritical flow conditions in the inner lobe to lobe off-axis environment. Here, laminated fine-grained silty and muddy deposits accumulate toward the top when the flow is very slow and close to stopping, eventually being bioturbated by *Ophiomorpha*, *Scolicia*, *Taenidium* and *Thalassinoides*. These trace fossil assemblages, belonging to the *Ophiomorpha rudis* ichnosubfacies, are typically found in channels and proximal lobes of turbidite systems.

In the latest Eocene to earliest Oligocene, in the southwestern part of the Colombian Caribbean (south of the San Jacinto Fold Belt and the western-southwestern Lower Magdalena Valley, San Jorge sub-basin) transgressive fine-grained deposits overlie the coarse-grained successions. Transgression generates an abrupt change in the system. Oligocene to Early Miocene successions exhibit meandering fluvial deposits, abundant fungal remains, morichal palm pollen, mudrocks, coals and rhizoliths, indicating water-logged interdistributary bays and gallery flood forests, and suggesting the onset of a lower delta plain supply system. Vertical changes in depositional style occurred under a dramatic global change (Eocene to Oligocene Transition Zone), but the tectonically active basin makes it very difficult to correlate variations in the effectiveness of fluvial and tidal influence with eustatic sea level fluctuations. Therefore, the ratio of accommodation space to sediment supply is mainly controlled by local active tectonics.

Sedimentation patterns in transitional zones and shallow marine systems reveal terminal distributary channels reaching waterlogged interdistributary areas and marine zones. This process generated fluvio-dominated mouth bars, along with distal delta front and prodelta systems, reactivated by transgressive lag deposits. The system is dominated by fine- to coarse-grained sandstones with tractive structures, often highlighted by organic debris, indicating the coalescence of hyperpycnites. The ichnological assemblage is low in abundance but moderately diverse, comprising *Ophiomorpha*, *Skolithos*, and *Thalassinoides* in fluvio-dominated mouth bars; *Ophiomorpha*, *Skolithos*, *Taenidium*, and *Thalassinoides* in the distal delta front; and *Phycosiphon*, *Planolites*, *Teichichnus*, and *Thalassinoides* in prodelta successions.

The evolution of this complex sedimentary system throughout the Oligocene is reflected in repetitive coarsening-upward successions, which also show variations in sedimentological features (e.g., fluid muds, mud drapes) and ichnological content (e.g., tubular tidalites, burrow size). Mouth bars also exhibit mud drapes and flaser bedding, with an increased bioturbation index and diversity, including *Asterosoma*, *Conichnus*, *Cylindrichnus*, *Dactyloidites*, *Gyrolithes*, *Macaronichnus*, *Ophiomorpha*, *Skolithos*, and *Thalassinoides*, reflecting tidal influences in the deltaic system. Distal delta front successions show wavy bedding with scarce mud drapes and trace fossil assemblage of *Diplocraterion*, *Ophiomorpha*, *Planolites*, *Rhizocorallium*, *Teichichnus*, and *Thalassinoides*. The prodelta is controlled by lenticular and episodic mud drapes and mudrock domains, with *Chondrites*, *Planolites*, *Siphonichnus*, *Teichichnus*, and *Thalassinoides*, indicating tidal influences in the deltaic system. Variations in the system arise from either river discharge or mud flocculation within buoyant plumes that transport brackish water to the sediment-water interface. These processes significantly disrupt the marine signature, impacting macrobenthic tracemaker communities, particularly suspension feeders, and leading to depauperate, monospecific, or stress-dominated trace fossil assemblages. However, the frequency of tropical torrential rains continuously alters system dynamics, with variations suggesting mouth bar migrations upstream, laterally, or downstream, depending on basin morphology and tectonic influences. This episodically increases the impact of tidal modulation or wave reworking on the deltaic system, which may have intensified during the Early Miocene. The Oligocene to Early Miocene fluvio-deltaic system was an important tributary catchment, extending over 250 km since the Oligocene. Its long lifespan and dynamic evolution are likely linked to the development of one of the most significant deltaic systems in the northern Andes during that period.

These patterns reflect a progradational trend with increased fluvial-marine interaction and rising accommodation space as compared to the Eocene, attributed to tectonic realignment and increased subsidence. The changes in depositional style coincide with lower plate convergence velocities and plate obliquities, suggesting margin stabilization in a flat slab subduction accretion scenario. This tectonic setting favors reduced sedimentation rates in forearc basins due to the absence of the magmatic arc, allowing significant sediment accumulation.

Tropical systems in northern South America may be more closely correlated with high- and mid-latitude fluvio-dominated rivers due to their relationship with mountain ranges than with tropical Southeast Asian environments, which are more influenced by monsoons or tides in other tectonic scenarios. The present research improves our understanding of the influence of tectonics versus climatic factors on sedimentation in tropical regions.

Resumen extendido

Las sucesiones del Eoceno medio-superior al Mioceno Inferior en el Caribe colombiano representan reservorios y rocas sello, que abarcan sistemas depositacionales de grano grueso y fino dentro de complejos de subducción dominados por acreción. Se realizó un análisis integrado sedimentológico, icnológico, rayos gamma y micropaleontológico de afloramientos y núcleos de perforación para comprender los procesos alogénicos y autogénicos que controlan la sedimentación y cómo influyen en la distribución de las sucesiones. Las complejas interacciones entre los procesos en ambientes marinos someros determinan condiciones paleoambientales estresantes que afectan a las comunidades de macrobentónicas y las relaciones organismo-sustrato. Al caracterizar facies y asociaciones de facies, definir patrones de apilamiento de facies y establecer las variaciones laterales desde las desembocaduras fluviales hasta el talud, obtenemos información sobre las interacciones entre la dinámica sedimentaria y los ecosistemas macrobentónicos, lo que permite reconstrucciones paleoambientales.

Durante el Eoceno medio a tardío, en el suroeste del Caribe colombiano (al sur del Cinturón Plegado de San Jacinto), los sistemas de grano grueso se caracterizan por flujos hiperpícnicos y altamente concentrados procedentes de áreas continentales que alcanzan la línea de costa, donde los flujos sufren transformaciones. Areniscas gruesas masivas de base neta con clastos de guijarros grandes se interpretan como el resultado de un flujo de alta competencia y concentración de arena, donde la depositación rápida y la alta tasa de aggradación de sedimentos se debieron al asentamiento de arena a alta velocidad. Posteriormente, capas de conglomerados normalmente gradados y de base neta sugieren un flujo más fluido y turbulento, capaz de transportar en carga de fondo los clastos más grandes, con un asentamiento controlado por el tamaño de grano desde la suspensión. Además, depósitos no estratificados que contienen los clastos más grandes probablemente representan el pico de inundación de mayor descarga. Sin embargo, la evidencia también sugiere que los flujos pueden transformarse aguas arriba o cuando entran en contacto con el sistema marino. Se reconocen transiciones a areniscas gruesas con estructuras masivas, areniscas conglomeráticas con laminación horizontal soportadas por matriz, y con esporas y polen abundantes, correlacionándose con registros de corrientes de alta velocidad, probablemente asociadas a flujos hiperpícnicos en condiciones de carga de fondo. Las características sedimentológicas e icnológicas, como la presencia de *Conichnus*, *Ophiomorpha*, *Thalassinoides*, tapones de fango fluido y cortinas de lodo, indican que la llegada de flujos a la costa desencadena una interacción entre los procesos de flujo gravitacional y los procesos marinos, destacando la interacción entre el sistema alimentador y la cuenca receptora. Se interpreta una influencia marina ocasional asociada a la modulación de mareas o al retrabajo de olas durante las avulsiones fluviales o una disminución en el aporte de sedimentos. El espacio de acomodación limitado favoreció la acumulación de sucesiones amalgamadas en esta cuenca de antearco, sin evidencia de planicies deltaicas.

En la región central del Cinturón Plegado de San Jacinto, la evidencia sugiere que algunos de estos flujos alcanzaron la plataforma y el talud, donde los depósitos de grano grueso señalan el desarrollo de un sistema canal-lóbulo de grano grueso. Este muestra una etapa de inicio de canal bien preservada en el borde de la

plataforma, representada por conglomerados sigmoides y lenticulares, y areniscas conglomeráticas con estratificación cruzada planar, interpretadas como escalones cíclicos en una zona de expansión. En una etapa posterior, se desarrolló un complejo canal-*levee* clásico, representado por depósitos de relleno de canal que muestran sucesiones gruesas de base erosiva, grano decrecientes, con facies que pasan de conglomerados de guijarros con matriz masiva en la base a areniscas masivas licuefactas o con laminación planar, con láminas carbonosas fitodetríticas, interpretadas como depósitos de flujos concentrados (turbiditas de alta densidad) provenientes de áreas continentales o sistemas costeros. Turbiditas delgadas asociadas a depósitos de terraza y *levee* están vinculadas a estos sistemas confinados, caracterizados por trazas fósiles como *Ophiomorpha* y *Thalassinoides*. Esta icnoasociación pertenece a la icnosubfacies *Ophiomorpha rudis* dentro de la icnofacies *Nereites*, asociada a corrientes de turbidez en canales. Además, las trazas fósiles *Nereites* y *Phycosiphon* son comunes en depósitos de *levee* internos y terrazas, donde las limolitas bioturbadas intercaladas se depositan por suspensión bajo condiciones de menor energía, ya sea por el desbordamiento de corrientes de turbidez o por procesos hemipelágicos durante el cese del sistema de mayor energía.

La zona de transición canal-lóbulo está marcada por debritas de flujos de escombros no cohesivos en un entorno de canal-lóbulo, que representan procesos de transferencia que evolucionan distalmente en areniscas gruesas con laminación cruzada planar y sigmoidal (antidunas) que rellenan surcos poco profundos en un campo de antidunas bajo condiciones supercríticas. A medida que los flujos pierden confinamiento, las condiciones de flujo Froude supercrítico transicionan a subcrítico en ambientes de lóbulo interno y lóbulo fuera del eje principal. Aquí, se acumulan sedimentos finos laminados en la parte superior de la sucesión cuando el flujo pierde velocidad, siendo posteriormente bioturbados por *Ophiomorpha*, *Scolicia*, *Taenidium* y *Thalassinoides*. Estas icnoasociaciones, pertenecientes a la icnosubfacies *Ophiomorpha rudis*, son típicamente encontrados en canales y lóbulos proximales de sistemas turbidíticos.

Durante el Eoceno tardío y el Oligoceno temprano, en la parte suroeste del Caribe colombiano (sur del Cinturón Plegado de San Jacinto y oeste-suroeste de la Cuenca del Valle Inferior del Magdalena, subcuenca San Jorge), depósitos transgresivos de grano fino cubren las sucesiones de grano grueso, a pesar de una caída eustática global del nivel del mar, probablemente superpuesta por la actividad tectónica y un alto aporte de sedimentos. La transgresión genera un cambio abrupto en el sistema. Las sucesiones del Oligoceno al Mioceno temprano exhiben depósitos fluviales meandriformes con abundantes restos de hongos, polen de palma, limolitas y rizolitos, lo que indica la presencia de bahías interdistributarias estancadas y bosques de galería, sugiriendo el inicio de un sistema de aporte desde la planicie deltaica inferior. Cambios verticales en el estilo depositacional ocurrieron bajo un cambio global dramático (zona de transición Eoceno-Oligoceno), pero la actividad tectónica en la cuenca dificulta correlacionar las variaciones en la influencia fluvial y mareal con las fluctuaciones eustáticas del nivel del mar. Por lo tanto, la relación entre el espacio de acomodación y el aporte de sedimentos está principalmente controlado por la tectónica activa.

Los patrones de sedimentación en zonas de transición y sistemas marinos someros revelan canales distributarios terminales que alcanzan áreas interdistributarias inundadas y zonas marinas, generando barras de desembocadura fluvio-dominadas, junto con sistemas de frente deltaico distal y prodelta, reiniciados por depósitos transgresivos. El sistema está dominado por areniscas de grano fino a grueso con estructuras

tractivas, a menudo resaltadas por restos orgánicos, que indican la coalescencia de hiperpícnitas. El contenido icnológico es bajo en abundancia, pero moderadamente diverso, compuesto por *Ophiomorpha*, *Skolithos* y *Thalassinoides* en las barras de desembocadura fluvio-dominadas; *Ophiomorpha*, *Skolithos*, *Taenidium* y *Thalassinoides* en el frente deltaico distal; y *Phycosiphon*, *Planolites*, *Teichichnus* y *Thalassinoides* en las sucesiones de prodelta.

La evolución de este complejo sistema sedimentario a lo largo del Oligoceno se refleja en estas sucesiones repetitivas con tendencia granocreciente, que también muestran variaciones en las características sedimentológicas (e.g., fango fluido, cortinas de lodo) y contenido icnológico (e.g., *tubular tidalites*, tamaño de las madrigueras). Las barras de desembocadura también exhiben cortinas de lodo y laminación flaser, con un aumento del índice de bioturbación y diversidad, que incluyen *Asterosoma*, *Conichnus*, *Cylindrichnus*, *Dactyloidites*, *Gyrolithes*, *Macaronichnus*, *Ophiomorpha*, *Skolithos* y *Thalassinoides*, lo que refleja influencias tanto mareales como fluviales. Las sucesiones del frente deltaico distal muestran laminación ondulante con escasas cortinas de lodo y una icnoasociación compuesta por *Diplocraterion*, *Ophiomorpha*, *Planolites*, *Rhizocorallium*, *Teichichnus* y *Thalassinoides*. El prodelta está controlado por depósitos de lutitas, algunas cortinas de lodo y episódica laminación lenticular, con traza fósiles como *Chondrites*, *Planolites*, *Siphonichnus*, *Teichichnus* y *Thalassinoides*, indicando influencias tanto mareales como fluviales.

Las variaciones en el sistema surgen ya sea del caudal fluvial o de la floculación de lodo en plumas de agua salobre que transportan sedimentos hacia la interfase agua-sedimento. Estos procesos alteran significativamente la señal marina, impactando a las comunidades macrobentónicas, particularmente a los organismos suspensívoros, lo que conduce a asociaciones de trazas fósiles empobrecidas, monoespecíficas o dominadas por organismos oportunistas que se adaptan a las condiciones de estrés ecológico. Sin embargo, la frecuencia de lluvias torrenciales tropicales altera continuamente la dinámica del sistema, con variaciones que sugieren migraciones de las barras de desembocadura aguas arriba, lateralmente o aguas abajo, dependiendo de la morfología de la cuenca y la influencia tectónica. Esto aumenta de manera episódica el impacto de la modulación de mareas o el retrabajo de olas en el sistema deltaico, lo que puede haber sido intensificado durante el Mioceno temprano. El sistema fluvio-deltaico del Oligoceno al Mioceno temprano fue una cuenca tributaria importante, que se extendió más de 250 km desde el Oligoceno. Su longitud y evolución dinámica probablemente están vinculadas al desarrollo de uno de los sistemas deltaicos más importantes de los Andes del norte durante ese período.

Estos patrones reflejan una tendencia progradacional con una mayor interacción fluvial-marina y un aumento del espacio de acomodación en comparación con el Eoceno, atribuida al realineamiento tectónico y al aumento de subsidencia. Los cambios en el estilo depositacional coinciden con velocidades de convergencia de placas más bajas y oblicuidades de placas, lo que sugiere una estabilización del margen en un escenario de subducción plana. Este entorno tectónico favorece tasas de sedimentación reducidas en las cuencas de antearco debido a la ausencia del arco magmático, permitiendo una acumulación sedimentaria significativa.

Los sistemas tropicales en el norte de Sudamérica pueden estar más correlacionados con los ríos fluvio-dominados de latitudes altas y medias debido a su relación con las cordilleras montañosas, en lugar de con los ambientes tropicales del sudeste asiático, que están más influenciados por los monzones o las mareas en otros escenarios tectónicos. La presente investigación mejora nuestra comprensión de la influencia de la tectónica frente a los factores climáticos en la sedimentación en regiones tropicales.

THESIS SCOPE AND FRAMEWORK

I. Motivation

The sedimentological and ichnological study of coastal depositional systems has become increasingly important over the past three decades, driven by the need to understand the sedimentary dynamics of these environments (e.g., MacEachern et al., 2005; Bhattacharya, 2006; Dalrymple and Choi, 2007; MacEachern and Bann, 2008, 2022; Steel and Milliken, 2013; Shchepetkina et al., 2019; Steel et al., 2024). These systems are characterized by a complex interplay of physical, biological, and chemical factors, including waves, tidal currents, storms, fluvial sediment input, salinity, and oxygenation (MacEachern and Bann, 2022). Coastal plains, tidal flats, deltaic systems, and estuarine environments exhibit progradational and retrogradational trends that vary with sediment supply, basin and coastline morphology, and relative sea level (Dalrymple and Choi, 2007; Ainsworth et al., 2011). Recognizing these environments, however, can be challenging due to the similarities that emerge under specific sedimentary conditions (MacEachern et al., 2005; Bhattacharya, 2006). Studies of coastal to marine deposits have focused primarily on sedimentary characteristics, such as structures and textures, alongside paleontological and geochemical data (MacEachern et al., 2005). The advent and growth of ichnology as a key discipline in sedimentology have added a new dimension to these studies. The response of organisms to environmental conditions is reflected in their behavior and the traces they leave behind, making ichnology a valuable tool for characterizing depositional environments (MacEachern and Bann, 2022). In past coastal systems, the fluctuations in physicochemical conditions create significant ecological stress that is captured in the ichnological record through trace fossil features such as morphology, bioturbation intensity, ichnodiversity, and ichnodisparity (MacEachern and Bann, 2008).

On this basis, the integration of sedimentological and ichnological information is essential for the construction of high-resolution paleoenvironmental models. Such models allow for the assessment of key physicochemical parameters including salinity, hydrodynamic energy, sedimentation rates, substrate consistency, turbidity, oxygenation, and temperature, and provide a deeper understanding of the relative importance of fluvial, tidal, and wave-related processes (MacEachern et al., 2005; Bhattacharya, 2006).

In addition to their scientific interest, coastal depositional systems hold significant economic importance, particularly in the context of hydrocarbon exploration. Coastal to marine clastic deposits are associated with major hydrocarbon reservoirs in regions such as the North Sea, Nigeria, Brunei, and Venice (Howell et al., 2008). The internal architecture and heterogeneity of these facies are critical factors influencing reservoir quality (Howell et al., 2008). In deltaic systems, for example, the potential for source rock development is linked to coal formation and organic matter accumulation in different sub-environments. Thus, understanding the factors that control system heterogeneity is critical for reservoir characterization, especially as the energy sector transitions to more sustainable sources.

The Sinú-San Jacinto Basin and the Lower Magdalena Valley Basin (including the Plato and San Jorge sub-basins) in the Colombian Caribbean are emerging as key areas of interest for hydrocarbon exploration. Numerous oil and gas seeps and well cores with evidence of hydrocarbons highlight the potential of the region (e.g., Sánchez and Permanyer, 2006; Osorno and Rangel, 2015; Cortes et al., 2018; Mora et al., 2018). However, the complex structural and stratigraphic nature of these basins, coupled with a controversial geologic

history, pose significant challenges in defining the petroleum system configuration (Mora et al., 2018; Montes et al., 2019). The lack of detailed sedimentological-ichnological and stratigraphical studies further emphasizes the need for continued research.

One lithostratigraphic unit of particular interest is the uppermost Eocene to Lower Miocene Ciénaga de Oro Formation, which is reservoir, particularly in its Miocene coastal deposits (e.g., Osorno and Rangel, 2015). Yet detailed facies characterization remains scarce, with most existing studies relying on inaccessible reports from private companies. The present research aims to fill these gaps through an integrative sedimentological, ichnological, well-logs and micropaleontological study focused on the dynamics of coastal-marine systems in the southwestern Colombian Caribbean basins (with a particular emphasis on the Sinú-San Jacinto Fold Belt), and the factors controlling sediment accumulation in forearc basins.

Recent studies have placed the Colombian Caribbean basins within a forearc setting, giving this research a unique relevance due to the rarity of delta-influenced successions with reservoir potential in such tectonic contexts worldwide (e.g., Hessler and Sharman, 2018; Mora et al., 2018; Montes et al., 2019). By integrating the stratigraphic information obtained and supported by some seismic lines to reduce uncertainty in our interpretations, this study will analyze the evolution of coastal-to-marine successions within this tectonic framework, although the seismic research will depend on the availability of industry-held data and is likely not to be included in the thesis.

This thesis will conduct the integration of distinctive tools for sedimentary basin research, focusing on variations in paleoenvironmental (ecological and depositional conditions) across the basins, with particular emphasis on interpreting depositional processes and trace fossil assemblages across salinity gradients to assess the major controlling factors in the basin's depositional evolution during a period marked by significant global and local changes.

II. Research questions and hypothesis

Several main questions of significant interest have emerged from the proposed research, to be answered according to the traditional, null, and alternative hypotheses:

Research question 1. How did the sedimentary environments of the Colombian Caribbean, with a particular emphasis on the Sinú-San Jacinto Fold Belt, evolve from the middle-late Eocene to the Early Miocene, and what were the processes and patterns of sediment dispersal from river mouths to the shelf and slope break?

Research hypothesis. The deltaic systems previously inferred for the Oligocene-Miocene are the only sedimentary evidence in the basin from the Eocene Oligocene transition, and therefore, the earlier deposits were subject to erosion. During the Oligocene a deltaic system is established with significant changes due to the active tectonic margin.

Null hypothesis. The coastal to shelf marine sedimentary dynamics of the Colombian Caribbean were initially dominated by fully marine environments (offshore to shelf deposits) in the middle-late Eocene. These systems transitioned to predominantly deltaic systems in the Oligocene-Early Miocene, reflecting a significant sea level drop associated with platform denudation due to eustatic sea level fall during the Eocene-Oligocene transition.

Alternative hypothesis. During this geologic period, sedimentary environments did not experience significant variations from previous ones. Consequently, the deltaic systems previously inferred in the Oligocene persisted from the middle late Eocene to the Early Miocene without significant changes.

Research question 2. How do the Colombian Caribbean basins, with a particular emphasis on the Sinú-San Jacinto Fold Belt, record tectonic and eustatic events from the middle-late Eocene to the Early Miocene, and what insights do these records provide into sedimentary dynamics during this period?

Research hypothesis. The fall in sea level during the Eocene-Oligocene transition, leads to the formation of amalgamated deposits, unconformities, and consequently, deposits that are more susceptible to erosion. Later, during the Oligocene, the system became more stable, with normal variations associated with the active tectonic margin.

Null hypothesis. Sedimentation processes within these basins are expected to show a significant sea level fall during the Eocene-Oligocene transition, akin to the widespread denudation observed on various platforms globally. This sea level decline may obscure tectonic activity and manifest as depositional hiatuses, providing evidence for eustatic changes.

Alternative hypothesis. Tectonic processes, particularly those related to variations in subsidence, obscure the typical eustatic signals. As a result, no discernible evidence of changes in depositional dynamics is observed in the sedimentary deposits.

III. Objectives

The main objective of this thesis is to conduct a paleoenvironmental analysis of two onshore basins in the southwestern Colombian Caribbean, with a particular emphasis on the Sinú-San Jacinto Fold Belt, from the middle-upper Eocene to the Early Miocene. This analysis will be situated within the context of a dynamic ecological and depositional setting—characterized by complex coastal-marine systems with deltaic influence, transitioning to shelf and slope—framed by the tectonic evolution of the basin. The study will integrate sedimentological, ichnological, well-log, and micropaleontological data from outcrops and well cores. Specifically, the research aims to identify the main allogenic and autogenic controls on sedimentation, focusing on the most significant changes in sedimentation patterns.

To achieve this overall objective, the thesis will address the following specific objectives:

- (i) Interpret the processes involved in deposition, their interactions and relative importance, and the lateral and temporal variations within the Colombian Caribbean basins (particular emphasis on the Sinú-San Jacinto Fold Belt) from the middle-late Eocene to the Early Miocene.
- (ii) Characterize the animal-substrate relationship and assess the response of the macrobenthic tracemaker communities to variations in paleoenvironmental (ecological and depositional) conditions.
- (iii) Evaluate the potential of ichnology as a fundamental tool for the characterization of coastal-marine systems, based on the comparison with past and modern analogues.
- (iv) Propose a paleogeographic model for the middle-late Eocene to Early Miocene period in the southwestern Colombian Caribbean basins.

Initially, this project had a primarily petroleum-oriented focus, aimed at characterizing sedimentary systems with potential for hydrocarbon exploration. However, as the world moves rapidly toward an energy transition, the project could be redirected towards the exploration of gas source rocks and their CO₂/gas storage capacity, which are likely to be key components for the future. Integrative research allowing a detailed and rigorous characterization and understanding of these systems would prove useful in any application.

IV. Layout

The results of this research have been published or are currently under review in scientific journals indexed in the Journal Citation Report. This dissertation is organized into five parts consisting of: Introduction, Geological framework and materials and methods, Results, Discussion, and Final remarks, conclusions and forthcoming research. Six scientific papers form the core of several chapters, including three in Results, two in Discussion, and one in Final Remarks, conclusions and forthcoming research.

PART I INTRODUCTION AND BACKGROUND

Chapter I INTRODUCTION

This chapter provides a comprehensive review of the state of the art in coastal sedimentary systems, highlighting their growing significance in recent years due to advances in classification methods aimed at characterizing them as important reservoirs. In this context, ichnology has emerged as an indispensable tool for their characterization, given the response of tracemakers to physico-chemical stressors. The chapter emphasizes the importance of coastal processes in determining the potential remobilization of coastal deposits to shelf and slope areas, also considering the major allogenic and autogenic factors that influence depositional processes. Special attention is given to forearc basins, such as those in the Colombian Caribbean, where the sedimentological and ichnological complexities are explored. Presenting an analysis of such components, this chapter seeks to frame research in basin analysis by highlighting the intricate interactions and processes within coastal environments and sediment bypass zones.

PART II GEOLOGICAL FRAMEWORK AND MATERIALS AND METHODS

Chapter II GEOLOGICAL FRAMEWORK

This chapter sets the geologic context for the evolution of the Colombian Caribbean basins, focusing on how sedimentary deposits have been influenced by different tectonic stages. First, the tectonic history of the region is outlined, emphasizing the relationship between basin evolution and tectonic activity. It then presents the subsurface configuration, derived from previous seismic studies that have shaped our current understanding of the area. In addition, a review of previous research on the study formations is provided, highlighting the predominance of regional-scale tectonic studies over detailed investigations. This review also identifies gaps in the existing knowledge that our research aims to fill. Overall, the chapter establishes a foundation for understanding the complex geologic framework of the Colombian Caribbean and provides essential background for the subsequent analysis.

Chapter III METHODOLOGY

This chapter provides the methodology used to conduct the integrative sedimentological, ichnological, and micropaleontological analysis of exposed rock formations within the San Jacinto Fold Belt of the Colombian Caribbean, using field descriptions, plus photo-panel constructions for the mapping of 3D architectural elements and bounding surfaces. Moreover, we present a detailed description of the methods used to study drill cores.

PART III RESULTS

Results already published or currently under review are presented in the next three chapters, focusing on middle-late Eocene (shallow and deep marine) and Oligocene (fluvio-dominated delta) systems.

Chapter IV EOCENE SHALLOW MARINE SYSTEMS

Hyperconcentrated to hyperpycnal flow transition along a river-delta system in a tropical humid setting (Late Eocene, Caribbean Colombia). This chapter examines the transition from hyperconcentrated to hyperpycnal flows within a river-delta system in the late Eocene of the Caribbean Colombian, emphasizing its rare occurrence in a non-volcanic, humid tropical setting. Typically associated with lahars or dry alluvial systems, hyperconcentrated flows are rarely documented in such environments. The study highlights how these flows, driven by tectonically active reliefs, high water and sediment discharge, and steep sedimentary systems, played a dominant role in sedimentation. Hyperconcentrated flow transitions are better developed and preserved in the sedimentary record when the flows are controlled by long-term processes (i.e. seasonal rainfall in humid tropical environments) than by catastrophic events (i.e. volcanic eruptions). This section also discusses the implications of these sedimentary processes for hydrocarbon exploration, where coarse-grained mouth-bar deposits, acting as potential reservoirs, are capped by fine-grained distributary channel sediments, potentially creating flow barriers.

Chapter V EOCENE DEEP MARINE SYSTEMS

Coarse-grained submarine channels: from confined to unconfined flows in the Colombian Caribbean (late Eocene). This chapter addresses the preservation and evolution of submarine channel mouths deposits, focusing on their under-represented role in the stratigraphic record. By examining upper Eocene deposits from the San Jacinto Fold Belt in the Colombian Caribbean, it sheds light on a coarse-grained delta-fed, coarse-grained channel-lobe system. Key findings include the identification of an initial stage characterized by sigmoidal gravels and cyclic steps, and the development of a channel-levee complex with distinctive fining-upward settings. The study highlights the channel-lobe transition zone, marked by debris flows and supercritical flow conditions, which evolve into low-angle, planar cross-stratified deposits associated with subcritical flows. Seasonal precipitation variations play a critical role in sedimentation, influencing the formation of high-erosive coarse-grained deltas and submarine channels. This research advances our understanding of turbiditic systems by refining depositional models and improving criteria for interpreting preserved channel mouth systems in ancient records.

Chapter VI OLIGOCENE FLUVIO DELTAIC SYSTEMS

Evolution of a fluvial-dominated delta during the Oligocene of the Colombian Caribbean: Sedimentological and ichnological signatures in well-cores. This chapter is focused on the sedimentological and ichnological characteristics of an Oligocene siliciclastic succession from the south of the Sinú-San Jacinto Basin in the Colombian Caribbean, emphasizing its significance as a reservoir rock. The ~330-m thick well-core section, representing a deltaic system, reveals a complex sedimentary evolution characterized by a coarsening-upward trend. The successions show a transition from bioclastic sediments to bioturbated sandy mudrocks and carbonaceous mudrocks, and to sandstones and conglomerates with variable ichnological assemblages. Despite the predominance of fluvial processes, local tidal and wave influences are also recorded. Detailed analysis of the sedimentological and ichnological data allows the identification of deltaic sub-environments such as prodeltaic bay, distal delta front, proximal delta front, distributary channels, mouth bars, and lower delta plain, providing crucial insights for understanding sedimentary processes and potential areas of economic interest.

PART IV DISCUSSION

Chapter VII TECTONICS, EUSTASY AND SEDIMENTATION

Sedimentary evolution of forearc basins in the Colombian Caribbean: insights from middle-upper Eocene to Lower Miocene deposits. This chapter reviews the middle to upper Eocene to Lower Miocene successions in the Colombian Caribbean, revealing complex sedimentary dynamics within an accretion-dominated subduction complex. The integration of sedimentological and ichnological data identifies 12 distinct facies associations, highlighting a trend from coarse-grained mouth-bars (hyperconcentrated to hyperpycnal flows) during the middle-late Eocene, to thick coal-bearing mixed-energy fine-grained deltaic deposits in the Oligocene to Early Miocene punctuated by a transgression. The Eocene succession shows tidal and wave influence in a compressional forearc basin with limited accommodation. In contrast, the Oligocene to Lower Miocene successions show coarsening-upward patterns reflecting increased fluvial-marine interaction and greater accommodation space due to tectonic subsidence and realignment. The study suggests that tropical sedimentation in northern South America has more in common with high- and mid-latitude fluvial systems than with Southeast Asian tropical environments, emphasizing the significant role of tectonics over climatic factors in shaping sedimentary processes. This research advances the understanding of sedimentary dynamics in tectonically active regions, as well as sedimentary processes and their relationship to eustatic sea level.

Chapter VIII OLIGOCENE TO LOWER MIOCENE FLUVIO-DELTAIC SYSTEMS

Deciphering influencing processes in a tropical delta system (middle-late Eocene? to Early Miocene, Colombian Caribbean): Signals from a well-core integrative sedimentological, ichnological, and micropaleontological analysis. This chapter focuses on the fine-grained deltaic system established during the Oligocene to Early Miocene, which reflects a complex interplay of coastal processes within an active tectonic setting under tropical conditions. This system is characterized by a coal-bearing, mixed-energy deltaic succession. The analysis of this interval used multidisciplinary tools, such as sedimentology, ichnology, and micropaleontology, to unravel the sedimentary dynamics and the establishment of what is probably the most significant fluvio-deltaic system in northwestern South America during the Oligocene. Additionally, general

provenance data from this study, along with those from complementary research, provided insights into the sediment supply and the tectonic evolution of the Sinú-San Jacinto Basin, elucidating the sedimentary processes of the region. This integrated approach highlights the role of tectonics and subsidence, as well as relative sea level changes and internal delta dynamics, in shaping the stratigraphy and sedimentation style of the Caribbean basins during the Oligocene to Early Miocene.

PART V FINAL REMARKS, CONCLUSIONS AND FORTHCOMING RESEARCH

Chapter VIII CONCLUSIONS

This final part, including final remarks and conclusions, provides a comprehensive synthesis of the main findings of the thesis, offering a structured overview of the key outcomes and conclusions. This section distils the essence of the research and underlines the most important insights.

Chapter IX FUTURE PERSPECTIVES: OTHER COASTAL SYSTEMS

Ichnological indicators of physico-chemical stresses in wave- to tide-dominated Miocene shallow marine environments (Argentine Patagonia). This section on future research perspectives highlights a recent study that integrates sedimentology and ichnology in wave- to tide-dominated coastal systems in Argentine Patagonia, illustrating the high complexity of these environments. The example underscores that no single model can serve as a global solution, emphasizing the need for case-by-case analysis. This section also outlines emerging research areas and methodologies to suggest potential avenues for interdisciplinary collaboration so as to deepen our understanding of coastal to shelf environmental responses, and to identify departures from the archetypal expression of Seilacherian ichnofacies in order to improve existing ichnological models.

PART I INTRODUCTION AND BACKGROUND

Chapter I

INTRODUCTION

I.1. Coastal sedimentary environments

Coastal sedimentary environments are highly dynamic natural systems, experiencing morphological changes across different scales while maintaining an unstable equilibrium (Ainsworth et al., 2011; Collins et al., 2020; Morales, 2022). It should be noted that these changes are primarily caused by short-term sedimentary dynamics, which can mobilize sediments, cause erosion or deposition, and reshape the pre-existing topography (Bhattacharya, 2006). However, the tectonic setting also influences the dynamics of all processes involved (Matenco and Haq, 2020). Deciphering processes in shallow marine systems from the geological record constitutes a cutting-edge field of research, focusing on the study of the structure and origin of all components of the coastal margin, from the emerged waterfront to the sublittoral areas, and even their transport to shelf, slope, or even abyssal plain systems (e.g., Galloway, 1975; Dalrymple et al., 1992; Carvajal and Steel, 2009; Tonkin, 2012; Steel et al., 2024; Zavala et al., 2024). Particular emphasis is placed on understanding the processes such as weathering, erosion, transport and deposition, from source to sink (e.g., Howell et al., 2008; Ainsworth et al., 2011; Nyberg et al., 2018; Gugliotta and Saito, 2019; Steel et al., 2024). The deposits along a given coastline are the result of combined physical, chemical, and biological processes that act upon that coastline over time (MacEachern et al., 2005; Bhattacharya, 2006; Ainsworth et al., 2011; Collins et al., 2020; Isla et al., 2020, 2023; Steel et al., 2024). Understanding erosion, sediment transport, and deposition phenomena in coastal environments requires analysis of the movement of sediments through wave action, tidal currents, and other marine factors. The study should emphasize identifying hydrodynamic processes and sedimentary facies, along with the long-term impacts of sediment supply patterns and changes in relative sea level (Porebski and Steel, 2006; Morales, 2022).

Coastal systems have been classified over the years using a variety of criteria. Early approaches focused on their relationship to the sea, distinguishing between emergent and submerged coasts (Johnson, 1919). Later classifications considered dominant processes, categorizing coasts based on marine versus non-marine influences (Davies, 1964; Shepard, 1973) or the direction of shoreline migration, identifying transgressive and regressive coasts (Curry, 1964). Structural controls have also served as a basis for classification (Inman and Nordstrom, 1971; Bloom, 1978). More recently, a ternary classification system that emphasizes the role of waves, tides, and river discharge has gained prominence (Galloway, 1975; Wright, 1977; Boyd et al., 1992; Orton and Reading, 1993; Ainsworth et al., 2011). This ternary approach is particularly valuable because it provides a detailed characterization of coastal systems that can be applied at multiple scales and further refined with additional classification criteria.

The characterization of fluvial-, wave-, and tidal-dominated sedimentary successions in tropical regions has received widespread attention in scientific and exploratory studies due to their high sediment loads and potential as reservoirs (e.g., Dalrymple et al., 2003; Howell et al., 2008; Shchepetkina et al., 2019; Collins et al., 2020). The interplay of fluvial, wave, and tidal processes over short spatial and temporal scales produces high variability in marine mixed shoreline systems, as observed in both modern environments and the geologic record (e.g., Yang et al., 2005; Rossi and Steel, 2016; Collins et al., 2020; Fig. I.1). To capture the great variability and complexity of ancient mixed-process shoreline systems, classifications using qualitative

descriptors—such as dominated-, influenced-, or affected-—by fluvial, wave, and tidal processes have often been employed to characterize sedimentary deposits (Ainsworth et al., 2011) (Fig. I.1). Alternative means of characterizing the internal facies complexity include techniques that quantify the likelihood that a deposit was formed by wave, tidal, or fluvial processes, based on dominant sedimentary structures, textures, and bioturbation. This approach is particularly useful for core data, where 3D features of sedimentary bodies (e.g., bed geometry) are difficult to observe (MacEachern et al., 2005; Bhattacharya, 2006; Wei et al., 2016; Rossi et al., 2017b). However, although specific sedimentary environments within coastal successions have characteristic facies associations, their recognition should not be based on physical structures alone; under certain depositional conditions, they may appear similar depending on the interactions of various parameters (MacEachern et al., 2005; Bhattacharya, 2006; Dalrymple and Choi, 2007; Ainsworth et al., 2011). Ichnology has therefore proven to be an indispensable tool in the study of these types of systems (MacEachern et al., 2005, 2007a; Gingras et al., 2011; Buatois et al., 2012; Schwarz and Buatois, 2012; MacEachern and Bann, 2020, 2022; Moyano-Paz et al., 2022; Ponce et al., 2023).

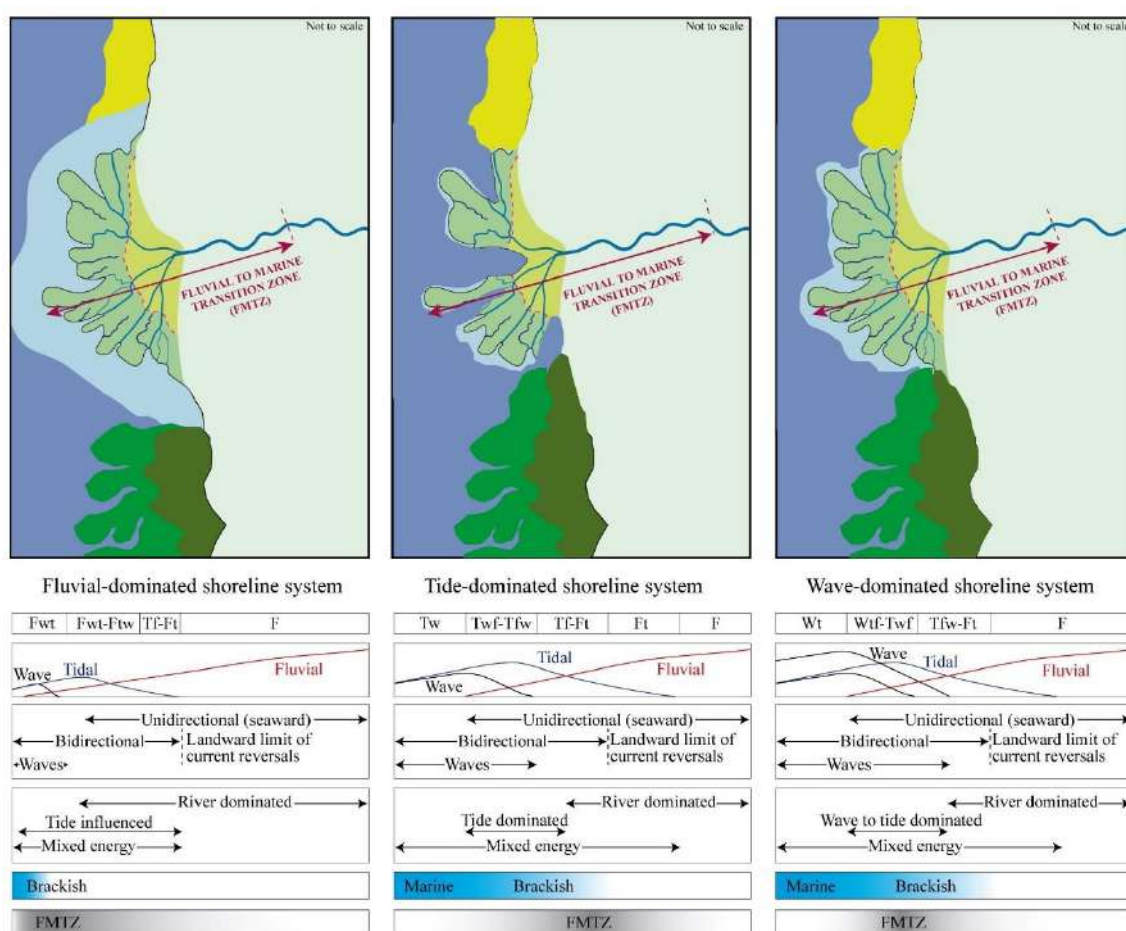


Fig. I.1. Schematic plan-view subdivision of major deltaic environments adjacent to and encompassing the fluvial to marine transition zone (FMTZ), from fluvial-dominated shorelines to tide-dominated shorelines and wave-dominated shorelines. Moreover, generalized process-based models for the FMTZ in distributary channels in relatively fluvial- tide- and wave-dominated systems, as well as sediment transport directions, salinity and suspended-sediment concentrations are included. The spatial and temporal variability in the balance of processes can vary significantly among systems. Modified from Collins et al. (2020), after Dalrymple and Choi (2007) and Gugliotta et al. (2016).

Note: F-: fluvial domain; -f: fluvial subordinate; T-: tidal domain; -t: tidal subordinate; W-: wave domain; -w: wave subordinate. FMTZ: Fluvial to marine transition zone.

I.2. Ichnological analysis

Sedimentology integrated with detailed ichnological and micropaleontological analyses have become fundamental tools for interpreting coastal depositional environments (e.g., Nagy, 1992; MacEachern et al., 2005; Gani et al., 2007; MacEachern and Bann, 2008, 2020; Slater et al., 2017; Chalabe et al., 2022; Zuchuat et al., 2023). In particular, most descriptions indicate the presence of biogenic sedimentary structures, and given the increasing application of trace fossil analysis in sedimentary basin research (i.e., McIlroy, 2008; MacEachern et al., 2010; Buatois and Mángano, 2011; Knaust and Bromley, 2012), ichnological studies are becoming an increasingly essential tool for understanding these environments (e.g., Pemberton and Wightman, 1992; MacEachern et al., 2005; Gani et al., 2007; Dashtgard et al., 2012; Buatois et al., 2012; Tonkin, 2012; Shchepetkina et al., 2019; Bayet–Goll and Neto de Carvalho, 2020; Moyano Paz et al., 2020). Ichnology is particularly useful for paleoenvironmental interpretation because of the response of tracemakers—their behavior and the structures they generate—to specific environmental conditions (Ekdale et al., 1984, Bromley, 1996; MacEachern et al., 2005; MacEachern and Bann, 2008). While the variability of depositional systems has been widely studied, a comprehensive understanding of biological responses to the interplay of processes and environmental (i.e., ecological and depositional) conditions operating in coastal depositional settings with fluvial input is still evolving (e.g., MacEachern and Bann, 2020, 2022).

Wave- tide- and fluvial-influenced coastal systems are characterized by receiving fluvial discharges that, depending on the ability of marine processes (waves, storms or tides) to redistribute sediment and freshwater inputs, can produce significant fluctuations in physicochemical conditions, resulting in a highly stressful ecological environment (e.g., MacEachern et al., 2005; Collins et al., 2020). The macrobenthic trace-maker community, by responding to these environmental changes, provides ichnological evidence of them, in terms of morphology and size of the structures, degree of bioturbation, distribution, ichnodiversity, ichnodisparity, and tiering (e.g., Buatois et al., 2005, 2012; MacEachern et al., 2005; Hansen and MacEachern, 2007; Bann et al., 2008; Collins et al., 2020) (Fig. I.2). Based on this understanding, the integration of sedimentology and ichnology is essential for the development of detailed and accurate paleoenvironmental models that incorporate physicochemical parameters such as salinity, hydrodynamics, sedimentation rates, oxygenation, substrate consistency, turbidity, light, and temperature, among others. This approach allows researchers to determine the relative importance of fluvial, tidal, and wave processes during the stages of coastal development (MacEachern et al., 2005, 2007; Gani et al., 2007).

Ichnology has traditionally relied on the Seilacherian/archetypal ichnofacies concept, which, along with the ichnofabric analysis, is one of the paradigms of modern ichnology (e.g., McIlroy, 2008). This concept categorizes groups of ichnotaxa that evolved under specific environmental conditions, and provides insights into those environments (Seilacher, 1964; MacEachern et al., 2007, 2012). However, the application of this model to coastal and deltaic systems is challenging due to the high variability in physicochemical conditions, which complicates the use of standardized models. To address this, some researchers have proposed unique ichnofacies specifically tailored to deltaic environments, based on common features observed in different systems worldwide (e.g., MacEachern and Bann, 2020, 2022). Nevertheless, the constant, and in most of cases rapid, changes in physicochemical conditions make it difficult to apply certain ichnofacies consistently across

Fig. I.2. Succession of facies models from fluvial- tide- and wave-dominated deltas, and comparison with mixed-influenced deltas, highlighting variations in trace fossil features such as diversity and abundance. *Arenicolites* (*Ar*), *Asterosoma* (*As*), *Chondrites* (*Ch*), *Conichnus* (*Co*), *Cylindrichnus* (*Cy*), *Dactyloidites* (*Da*), *Diplocraterion* (*Di*), *Gyrolithes* (*Gy*), *Helicodriomites* (*He*), *Macaronichnus* (*Ma*), *Ophiomorpha* (*Op*), *Phycosiphon* (*Ph*), *Rhizocorallium* (*Rh*), *Rosselia* (*Ro*), *Schaubcylindrichnus* (*Sch*), *Scolicia* (*Sc*), *Siphonichnus* (*Si*), *Skolithos* (*Sk*), *Taenidium* (*Ta*), *Teichichnus* (*Te*), *Thalassinoides* (*Th*), *Zoophycos* (*Zo*), Root structures (R). In wave-dominated and storm influenced delta – shoreface, u: upper, m: middle, l: lower; offshore, ot: offshore transtition, u: upper, l: lower. In mixed influenced delta – delta front, w: wave; t: tidal.

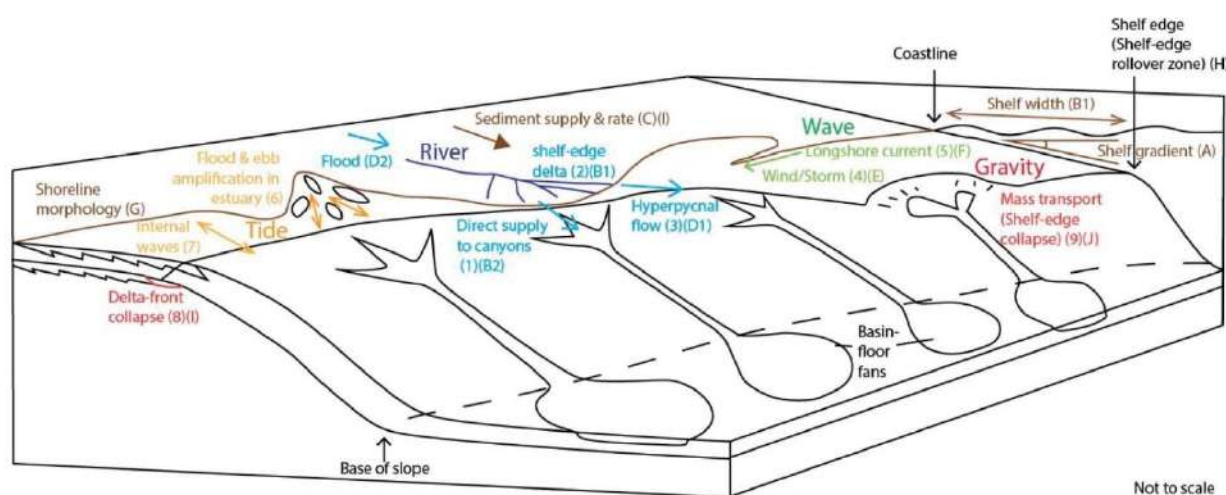
I.3. Sediment transfer to the shelf and deep-sea zones

The dominant processes in coastal zones —whether fluvial, waves including storms, or tidal-influence depositional processes— mark the resulting successions in shelf zones and slope transitions, and finally in the basin plain environments (Fig. I.3) (Mulder et al., 2003; Carvajal and Steel, 2009; Slatt and Zavala, 2011; Zavala and Arcuri, 2016; Gan et al., 2022). These zones exhibit significant sedimentary variability, which is also strongly influenced by tectonic regimes, accommodation, and sediment supply (Syvitski et al., 2003, 2022).

The sediment load and the ability of waves and tides to rework the injected plumes are key factors, leading to different results (e.g., sedimentary structures) depending on the specific processes occurring along the coast (Barrell, 1912; Zavala, 2020; Zuchuat et al., 2023). The continental shelf should not be considered simply as an extension of the coast but rather “*the expansion of the shallow seabed that runs along the coast to the deep*” (Morang, 2004; Morales, 2022). In the case of the world's major river systems, such as the Amazon, Orinoco, Mississippi, and Niger, the flow is so great that freshwater reaches the mouth, and the mixing of waters takes place directly on the shelf or sometimes even in deeper marine environments (Mulder and Syvitski, 1995; Morales, 2022). In smaller rivers, this mixing can occur during large floods. Yet even in small rivers, the finest material from the turbidity maximum generated within the channels may travel long distances, forming a turbidity plume that extends into more distal environments (Gan et al., 2022; Morales, 2022).

Knowledge about sediment transfer from coastal areas to shelf and slope environments has grown significantly, particularly in the context of deltaic sedimentation (e.g., Carvajal and Steel, 2009; Zavala et al., 2021, 2024). Traditionally, deltaic models are defined and classified using both geomorphologic and stratigraphic approaches based on the dominant processes —tidal, wave, or fluvial (Coleman and Wright, 1971; Galloway, 1975; Gani and Bhattacharya, 2005; Bhattacharya, 2006, 2010; Syvitski et al., 2022). However, other classifications that take into account the density of the incoming river discharge, and the density of the water reservoir, have become increasingly popular in recent years (Bates, 1953; Zavala et al., 2021, 2024). Recent studies emphasize the role of sediment-laden river discharges and the interaction between the salinity of the receiving water body and the bulk density of the incoming river (e.g., Zavala, 2020). This has led to the initial classification of deltas into three major types —hypopycnal, homopycnal, and hyperpycnal; Bates, 1953— which can be further subdivided into more specific categories (Zavala et al., 2024). These deltaic processes highlight the complexity of sediment transfer from coastal zones to more distal environments, where river dynamics, sediment concentration, and water body salinity all interact to shape the final deposits (Gan et al., 2022). Bypassing the debate on whether the definition of a delta should be extended to more distal areas beyond

the coastal zones, this work aims to characterize the resulting deposits, the processes involved, and shed light on their characteristics and variations, as well as the potential accumulation scenarios in the transfer zones from shallow to distal environments. Seismic data, especially from shelf margins and deep marine settings, have greatly enhanced our comprehension of marine processes and basin-scale sedimentary features (Steel and Milliken, 2013). Additionally, integrating knowledge about rates and time scales of tectonics, climate dynamics, and sea-level changes has been crucial in identifying the signals of these drivers in sedimentary successions. However, while many of these transition zones have been studied using seismic sections, outcrop studies remain fundamental and require detailed data and paleoenvironmental reconstructions to understand variations not only along the coastline but also in more distal areas, including the shelf and slope.



| Controls on sediment delivery from the shallow marine systems to the shelf-edge zone and deeper marine environments | Recognized processes important to sediment bypass through the shelf-edge zone with importance of controls | | | |
|---|---|-------|-------|---------|
| | Fluvial/River | Waves | Tidal | Gravity |
| A. Gradient | | | | |
| B1. Proximity — shelf width (shoreline to shelf edge) | | | | |
| B2. Proximity sediment source (delta, littoral cell) to conduit (canyon, slope channel...) | | | | |
| C. Sediment supply | | | | |
| D1. River plumes types (hyper, homo, hypo) | | | | |
| D2. River flood frequency | | | | |
| E. Storm intensity | | | | |
| F. Wind direction | | | | |
| G. Shoreline morphology | | | | |
| H. Shelf morphology | | | | |
| I. Sedimentation rate | | | | |
| J. Underlying stratigraphy / sediment type | | | | |

Fig. I.3. Schematic diagram of processes on the shelf that deliver sediment from the coast to the shelf edge and deeper marine zones (in numbers) and their controlling factors (in letters) (from Gan et al., 2022).

Therefore, in coastal environments, the interplay between topography, climate, tectonics, and sediment availability influences the generation of a variety of flow types, each characterized by different durations and bulk densities. Additionally, the dynamics at river mouths—including the reworking by storm waves, longshore currents, and strong tidal currents—play a fundamental role in the transition of gravitational flows from coastal to deep marine systems, from small to very large basins (Gan et al., 2022). Depending on these factors, shallow areas can produce flows ranging from cohesive debris flows to clear water discharges. Notably, when the density of these flows exceeds that of the receiving basin water, a hyperpycnal regime becomes apparent.

In this sense, sediment gravity flows are critical in initiating hyperpycnal flows. Despite their frequent occurrence in the geologic record, there is no consensus on the classification of these flows, largely because early schemes, such as those proposed by Middleton and Hampton (1973), were based on flow behavior and are difficult to apply to the geological records. A more applicable classification may be one that considers the primary characteristics of the final deposits (Fig. I.4), including categories such as cohesive debris flows, hyperconcentrated flows, concentrated flows, and turbidity currents or sediment-laden turbulent flows (Mutti, 1992; Mutti et al., 1996; Mulder and Alexander, 2001; Nemeč, 2009; Zavala, 2020) (Fig. I.4). It is important to consider the ongoing debates surrounding these classifications and to address pertinent discussions with a focus on the dynamics of processes, such as the transitions from hyperconcentrated to hyperpycnal flows versus subaqueous debris flows (e.g., Nemeč and Steel, 1984; Mutti, 1992; Mulder and Alexander, 2001; Benvenuti and Martini, 2002; Zavala, 2020) (Fig. I.4).

There is a clear relationship between the relief of the source and the resulting flow types: steep slopes are essential for triggering and sustaining cohesive debris flows and supercritical flows, as the slopes help to overcome internal cohesion or maintain the velocity necessary to counteract energy loss from grain-to-grain collisions. Consequently, hyperpycnal flows initiated by these mechanisms are typically associated with high-relief coastal areas, although other factors such as torrential rains with high sediment loads can also trigger them (Mutti, 1992; Mulder and Alexander, 2001; Zavala, 2020). From a rheological perspective, hyperpycnal flows may originate from non-Newtonian (cohesive debris flows), Newtonian supercritical (e.g., lahars, hyperconcentrated flows, concentrated flows), or Newtonian subcritical flows (e.g., pebbly, sandy, or muddy turbidity currents) (Zavala, 2020) (Fig. I.4).

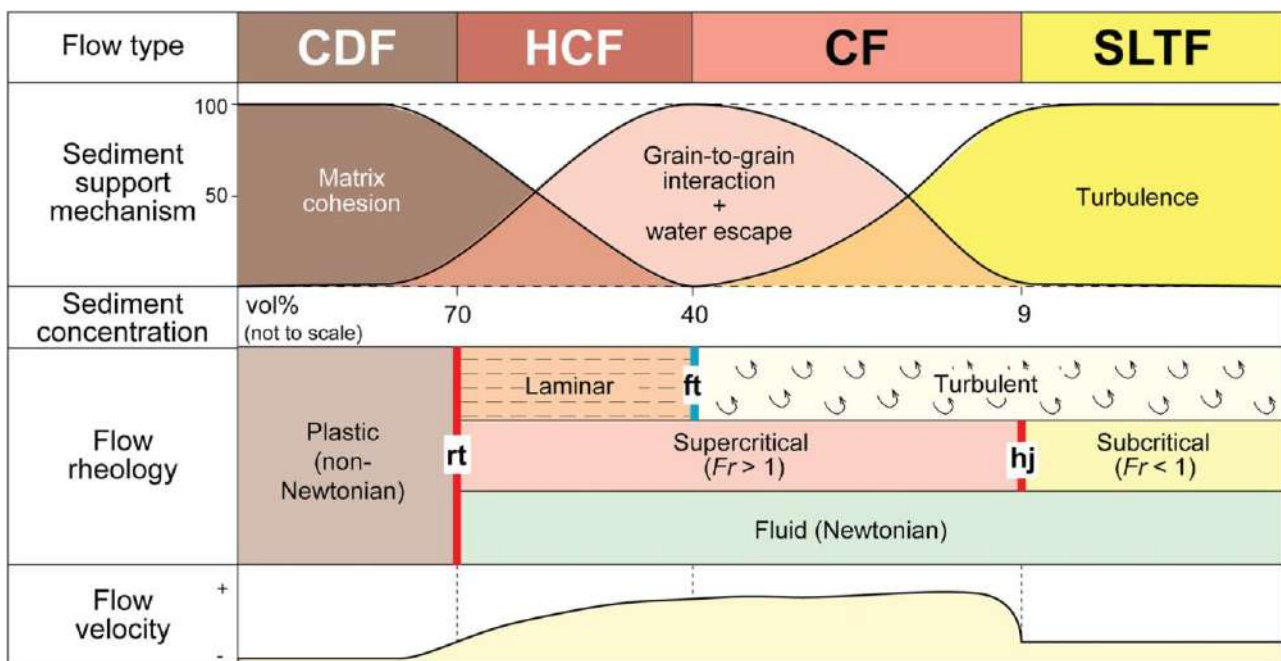


Fig. I.4. Classification of sediment gravity flows (Zavala, 2020; after Mutti, 1992; Mutti et al., 1996; Mulder and Alexander, 2001). CDF: Cohesive debris flow; HCF: Hyperconcentrated flow; CF: Concentrated flow; SLTF: Sediment-laden turbulent flow; rt: Rheological transformation; ft: Flow transformation; hj: Hydraulic jump; Fr: Froude number. Note that sediment concentration (% volume) is not to scale.

I.4. Allogenic and autogenic factors

Significant progress has been made in understanding how changes in allogenic factors, such as sea level, subsidence, or climate, can influence the evolution of coastal systems throughout time, particularly with respect to the balance between sediment supply and accommodation space (e.g., Heller et al., 1993; Cowell et al., 2003; Patruno et al., 2015; Hampson, 2016). This balance determines the distribution of facies, in turn directly reflected in the stratigraphic stacking of sedimentary deposits at different scales, primarily parasequences and sequences (Collier et al., 1990; Muto and Steel, 1997; Catuneanu, 2006; Allen and Allen, 2013).

However, in active margins and forearc basins (see below), research requires an initial focus on the dynamics of sediment transport and its preservation in the sedimentary record. The nature of a coastal system and its evolution over such time scales calls for an understanding of other influential phenomena and autogenic factors, such as sediment transport gradients and internal transfer processes (Aagaard, 2011). The processes controlling both longitudinal and transverse transport dynamics fluctuate over time, influenced by hydrodynamic properties. Meanwhile, fluctuating climatic conditions play a crucial role in this dynamic system, either through their interaction with tectonics or, in tropical regions, through the frequency and intensity of torrential rains, which can suddenly alter the fair-weather dynamics of a coastline. To record how these high-frequency processes are reflected in a sedimentary succession, it is essential to evaluate the record in as much detail as possible and to analyse the major facies features to interpret the depositional and post-depositional processes that govern environmental evolution.

In this context, coastal systems are subject to progradation or retrogradation due to changes in the factors that control the balance between sediment supply and accommodation space (such as relative sea level changes and tectonics) (Matenco and Haq, 2020). In recent years, sedimentological studies of shallow marine environments have enabled the development of more reliable high-resolution stratigraphic models for ancient successions. This has advanced our understanding of the variable recurrence interval controls that may affect these environments (Hampson et al., 2008), such as sediment supply and basin accommodation space (Ainsworth et al., 2008). Numerous analyses of the multiple controls that determine depositional architecture continue to employ predictive numerical models (Charvin et al., 2010; Slott et al., 2010; Burgess et al., 2016) or experimental approaches (Kim et al., 2006; Muto et al., 2007). Yet these results cannot adhere to a fixed format, as a number of assumptions can prevent direct comparison with outcrop or subsurface data (Hampson, 2016). This drawback the need to examine each shallow model independently, especially under active tectonic regimes.

The middle to upper Eocene to Lower Miocene deposits of the Colombian Caribbean were formed during a period of significant global change. The first major continental glaciation in Antarctica occurred during the Eocene-Oligocene transition, characterized by an abrupt, stepwise shift that indicates combined cooling and glacial expansion (Zachos et al., 2001; Mudelsee et al., 2014; Miller et al., 2020), with alternating warm and wet periods and cooler, drier intervals (Katz et al., 2008; Coxall and Wilson, 2011) (Fig. I.5). The initial cooling phase, marked by a 2°C drop in deep-water temperatures, occurred at 33.8 My (EOT-1), and was accompanied by minor continental ice growth and a 25-meter sea level drop (López-Quirós, 2020; Miller et al., 2020; López-

Quirós et al., 2021) (Fig. I.5). A subsequent event at 33.6 My (EOT-2) involved further deep-water cooling and another slight sea level fall (López-Quirós, 2020) (Fig. I.5). The third phase at 33.5 My (Oi-1) resulted in a temperature decrease of 2°C, a sea level drop of 60 ± 25 m, and significant ice sheet development (Coxall et al., 2005; Miller et al., 2009, 2020; López-Quirós et al., 2021) (Fig. I.5). Sedimentological evidence from coastal and continental shelf settings has been reported from certain Antarctic regions, although most models are derived from low-latitude regions, e.g. Weddell Sea (~37.6 to 33.2 My; López-Quirós et al., 2021); Prydz Bay (35 My; O'Brien et al., 2001; Cooper et al., 2009), the Ross Sea (34 My; Barrett, 2007; Galeotti et al., 2016), and the Wilkes-Adelie Land (33.6 My; Escutia et al., 2011, 2014). During the Oligocene, $\delta^{18}\text{O}$ isotope records suggest that ice volumes fluctuated considerably, driven by orbital cycles (Liebrand et al., 2011; Beddow et al., 2016). The Oligocene-Miocene transition saw another significant cooling event at 23.03 My (Zachos et al., 2001; Liebrand et al., 2011). It is important to note that the eustatic curve is constructed from isotopic data, including an empirical correction for carbonate ion changes over the Eocene-Oligocene transition to account for an apparent warming effect of $\sim 1.5^\circ\text{C}$. This correction, when applied to the sea level curve, reduces the amplitude by 28 meters between 34.17 and 34.30 Ma (e.g., Miller et al., 2020). Moreover, global eustasy estimates for the Oligocene (Oi) events, based on Pleistocene calibration and associated sea level variations, range from 50 to 65 meters (Wade and Palike, 2004). Reconstructing eustatic sea level changes from $\delta^{18}\text{O}$ fluctuations during the early Paleogene is more challenging due to the lack of direct evidence for continental ice. The major transgressive-regressive cycles identified in the Paleogene are based on a combination of T-R facies cycles and major sequence boundaries as proposed by Hardenbol et al. (1998), with the major cooling event in the earliest Oligocene also considered (Gradstein et al., 2020). Therefore, models indicating the timing of net ice sheet consolidation and inferences of eustatic sea level change should be treated with caution.

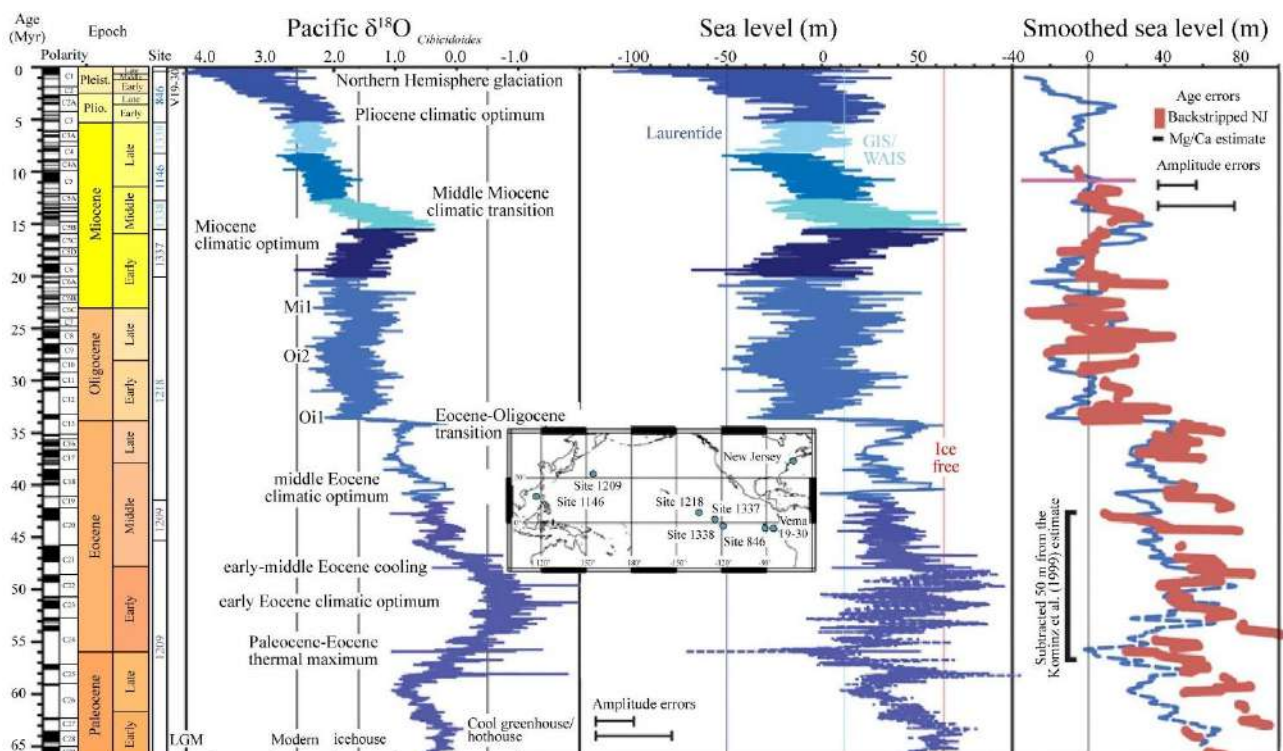


Fig. I.5. Summary of Cenozoic benthic foraminiferal $\delta^{18}\text{O}$, sea level, and smoothed sea level records. Modified from Miller et al. (2020).

I.5. Forearc basins: the Colombian Caribbean

Marine basins that form along active margins are closely linked to orogenic zones, where tectonic loading from thrust and nappe emplacement generates accommodation space (Fuller et al., 2006; Noda, 2016). The loading induces flexure in the subducting oceanic and continental lithosphere, resulting in the creation of significant depositional spaces. These spaces give rise to the formation of accretionary wedges and forearc or back-arc foreland or foredeep basins, which are influenced by various forcing factors (e.g., Beaumont, 1981; Allen et al., 1986; DeCelles and Giles, 1996; Noda, 2016). Ongoing convergence at the leading edge subsequently scrapes off the previously deposited sediments in the flexural accommodation. These sediments become part of the orogenic system as highly deformed accretionary prisms, external fold-and-thrust belts, or deformed foredeeps, where the depositional record can be significantly eroded (Matenco and Haq, 2020). Because this is a major problem in the study of accretionary systems, their records are considered exceptional (e.g., Cloos and Shreve, 1988; Condie, 2007; Cawood et al., 2009; Scholl and von Huene, 2010). Analysis of these sedimentary deposits can reveal whether relative sea level variations are primarily influenced by allogenic or autogenic factors (Catuneanu and Zecchin, 2013; Noda, 2016; Manteco and Haq, 2020), or else help determine the importance of modulation by climatic factors in the case of tropical environments. However, their direct correlation with global eustatic changes is quite complex, and the local tectonic patterns acting on the system must be taken into account, as they are likely to control the sedimentation and depositional mechanisms and thus the resulting successions.

The forearc basins of the southwestern Colombian Caribbean are characterized by two temporally non-parallel systems: the Sinu-San Jacinto Basin and the Lower Magdalena Valley Basin (Fig. I.6). The basement of both basins was formed in a Late Cretaceous "normal" subduction margin due to oblique convergence of the Caribbean Plate relative to South America (Pindell et al., 1998, 2005; Moreno-Sanchez and Pardo-Trujillo, 2003; Pindell and Kennan, 2009; Spikings et al., 2015; Cardona et al., 2018; Hincapié-Gómez et al., 2018; Montes et al., 2019; Mora-Paez et al., 2019).

This convergence was characterized by active dextral strike-slip displacement and possible subduction erosion (Fig. I.6). The onset of more orthogonal, low-angle subduction of the oceanic Caribbean Plateau after the Eocene led to significant changes in the convergent margin, including the cessation of magmatism and the formation of a tectonically segmented accretionary forearc basin in the Lower Magdalena Valley, and forearc highs in the Sinu-San Jacinto Basin. It is also possible, however, that the recorded lower to middle Eocene unconformity is related to the collision of the Caribbean Arc, resulting in a subduction polarity reversal, as proposed by Kroehler et al. (2011). The Sinu-San Jacinto Basin is currently represented by the San Jacinto Fold Belt, a forearc high that has been uplifted since approximately the latest Eocene, exposing Cretaceous to Plio-Pleistocene rocks (Mora-Bohórquez et al., 2020).

Coastal deposits in tectonically active margins play a crucial role in such correlations. In particular, the torrential rainfall that occurs under tropical conditions combined with active tectonics would determine depositional parameters such as accommodation space and sediment supply. Additionally, changes in plate

convergence should control factors that directly affect accommodation spaces, sediment dispersal trajectories, and margin configuration, thereby revealing different types of flow. Although two different scales of study are addressed, there may be a direct or indirect correlation between basin-scale and local-scale deposits. The deposits under study are poorly understood, so that no relationship between allogenic and autogenic processes and sedimentation patterns has been established. Still, this is only one of many questions that need to be addressed when describing the deposits of these basins in northwestern South America.

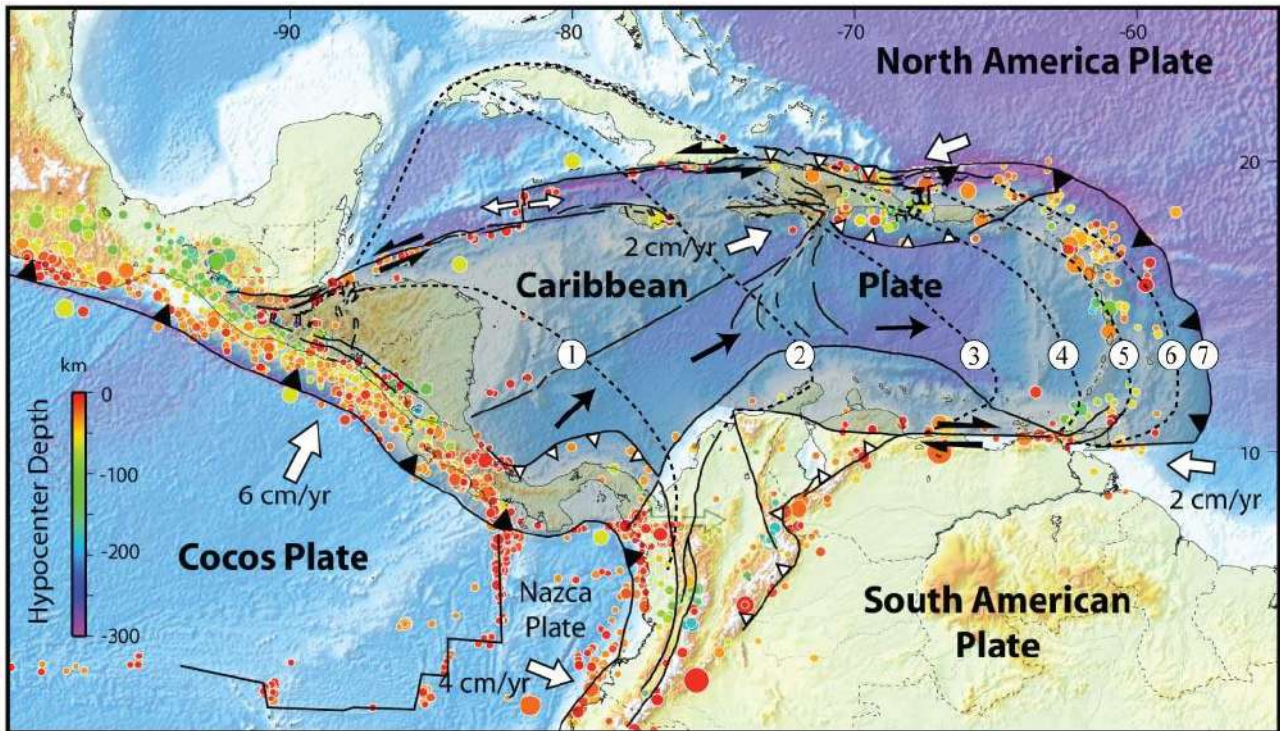


Fig. I.6. Present tectonic configuration of the Caribbean (modified from Harbitz et al. [2012]; after E. Calais [<http://web.ics.purdue.edu/~ecalais/haiti/>] Courtesy: National Science Foundation). Diachronous eastward displacement of the Caribbean Plate relative to the North and South American plates with numbered, dotted black lines representing the inferred positions of the leading edge of the Caribbean Plate at these times: 1 = Late Cretaceous (~80 Ma); 2 = middle Paleocene (~60 Ma); 3 = middle Eocene (~44 Ma); 4 = middle Oligocene (~30 Ma); 5 = middle Miocene (~14 Ma); 6 = Pliocene (~5 Ma); and 7 = Recent (from Escalona and Mann, 2011; modified from Lugo and Mann, 1995).

I.6. Study area

The middle-upper Eocene to lowermost Miocene deposits in the Colombian Caribbean are characterized by progradational systems of significant thickness (~1000 m), where multiple tectonic scenarios occurred during their accumulation (e.g., Mora-Bohórquez et al., 2020). The most widely accepted models suggest a shift in subduction from oblique to orthogonal during the early to middle Eocene, with multiple scenarios of compressional accretionary-type forearc basins (Mantilla-Pimiento et al., 2009; Bernal-Olaya et al., 2015; Mora et al., 2018) (Fig. I.6), which most likely had an impact on sedimentary systems. Although two different research scales would prevent making a direct correlation, this study focuses on discerning the allochthonous and autochthonous factors that control sedimentation in the basins to understand their cause-and-effect relationship within the tectonic context. Since the distribution pattern of sedimentary deposits is a direct response to tectonics and/or eustasy, it sheds light on the movements of thrust loading during subduction, or eustatic variations in a period of strong global change (i.e., Eocene-Oligocene transition).

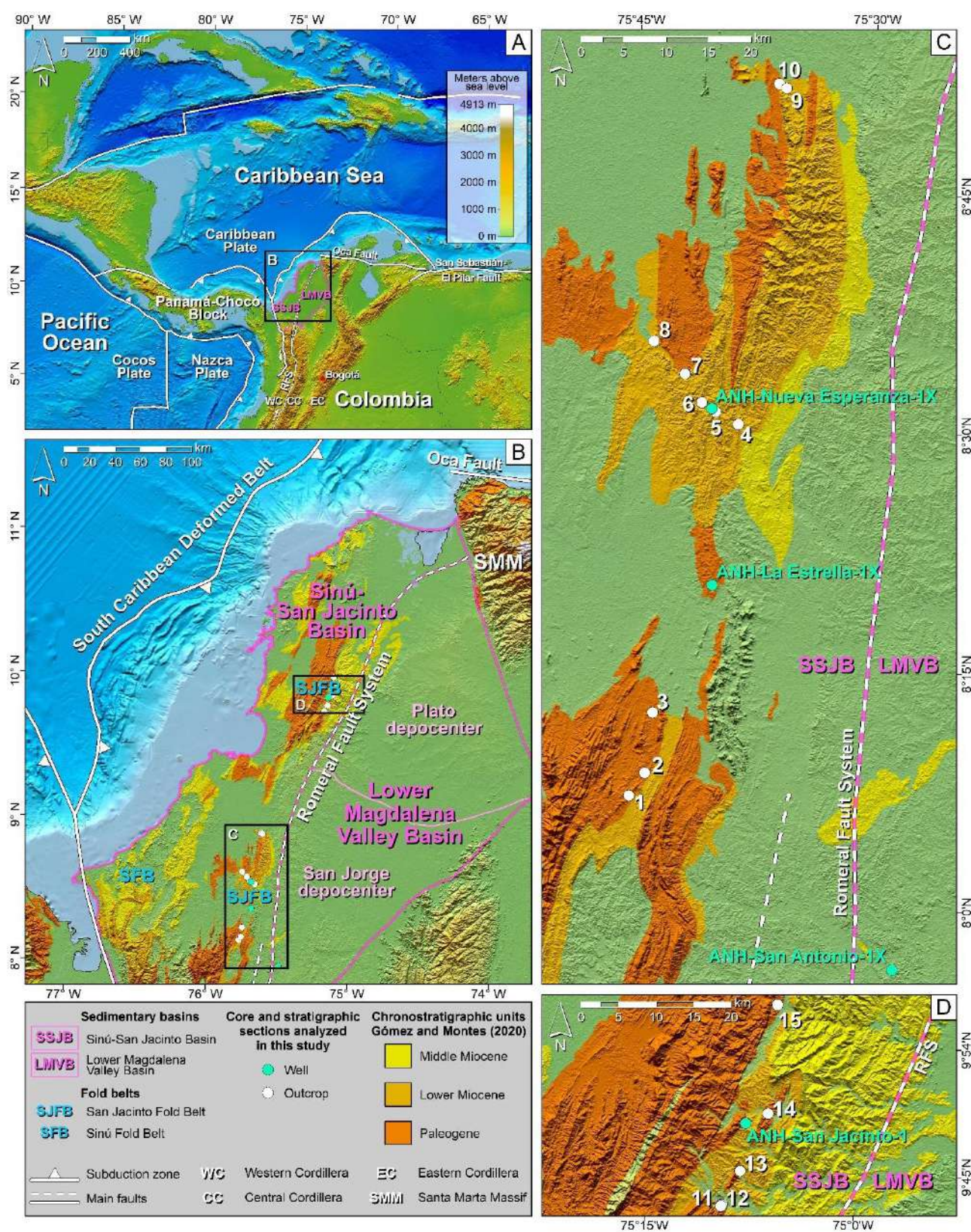


Fig. I.7. A. Location of the Colombian Caribbean basins. B. Study areas in the San Jacinto Fold Belt and the western part of Lower Magdalena Valley Basin. C-D. Outcrop and well-core locations in south (C) and central (D) regions respectively. Paleogene, Lower and Middle Miocene deposits are indicated in the Sinú-San Jacinto Basin (Source: WGS-1984 coordinate system; CIOH, SRTM, NOAA elevation, and ocean models; geology from Gómez and Montes, 2020).

In settings deposited under active tectonic this purpose is commonly hindered by the often-concurrent effects of eustasy and subsidence, which influence spatial and temporal variations in sediment supply and

accumulation (Matenco and Haq, 2020). Despite the intricate accumulation scenario, a careful assessment of unconformity-bounded sediment wedges and lateral features of bounding surfaces can be a key in elucidating stratigraphic relationships. This approach helps distinguish whether fluctuations in relative sea level are driven by eustatic changes or tectonic controls (e.g., Howell and Flint, 1996; Carr et al., 2003; Zecchin et al., 2006; Celma and Cantalamessa, 2007) and constitutes a step forward in comprehending the sedimentation in forearc basins. At the same time, although materials of sedimentary successions are largely influenced by such collisional tectonic scenarios, sedimentation in tropical basins—and the high erosion rates produced by the fast climatic changes of tropical latitudes—can drastically modify the type of resulting successions (e.g., Nummedal et al., 2003). Thus, in addition to changes in subduction processes, the high input of continental sediments into fluvio-deltaic systems during this period must be deciphered in view of the dominant processes on the bases of 15 the outcrop sections and 4 well-cores studied (Fig. I.7).

**PART II GEOLOGICAL FRAMEWORK AND
MATERIALS AND METHODS**

Chapter II

GEOLOGICAL FRAMEWORK

II.1. Present regional tectonic configuration

The geological configuration of Colombia is characterized by a series of allochthonous terranes accreted at different times to the northwestern margin of South America, associated with interaction between the Farallones, Nazca, Cocos and Caribbean plates (Cediel et al., 2003; Restrepo and Toussaint, 2020; Toussaint and Restrepo, 2020). The terranes are bounded by south-north trending regional faults parallel to the Andean Mountain ranges and the current subduction zone between the Nazca and South American plates (Restrepo and Toussaint, 2020).

This combination of tectonic factors has led to the division of the Colombian Andes into three mountain ranges, separated by current extensive intramountain basins through which Colombia's main rivers flow, notably the Magdalena, Cauca, and Atrato. The geological units considered autochthonous to the South American margin are located between the foothills of the Garzón Massif, the Eastern Cordillera, and the Eastern Llanos region (borders with Venezuela, Brazil, and Peru) (Toussaint, 1993; Ibáñez-Mejía and Cordani, 2020; Restrepo and Toussaint, 2020). These units are of Paleoproterozoic age and were affected by syn- and post-tectonic plutonism, some of which is anorogenic, with intermediate to acidic compositions from the Mesoproterozoic to the Mesozoic. They are overlain by Palaeozoic, Mesozoic, and Cenozoic sedimentary rocks (Gómez et al., 2007; Restrepo and Toussaint, 2020).

Regarding the mountain ranges, the Eastern Cordillera has a Precambrian and Paleozoic igneous-metamorphic basement overlain by a Devonian to the Recent sedimentary cover of marine and continental origin (Cooper et al., 1995; Sarmiento-Rojas, 2001, 2019; Gómez et al., 2003; Sarmiento-Rojas et al., 2006).

The Central Cordillera has a Paleozoic basement affected by Permian-Jurassic metamorphism and plutonism, associated with the fragmentation of Pangea, and intruded by Jurassic, Cretaceous and Cenozoic plutons (Cardona et al., 2010; Villagómez et al., 2011; Cochrane et al., 2014; Leal-Mejía et al., 2019). It also concentrates much of the Neogene volcanism and currently has an active volcanic arc along its axis (Marín-Cerón et al., 2019; Vargas, 2020).

The basement of the Western Cordillera consists of blocks of mafic and ultramafic volcanic rocks, gabbros, tonalites, sedimentary and metasedimentary rocks of marine origin, associated with oceanic plateaus, island arcs, and related basins. They form the Colombian Caribbean Igneous Province, or the Western Cretaceous Oceanic Lithospheric Province (Kerr et al., 1996; Nivia, 2001; Cediel et al., 2003; Villagómez et al., 2011), which accreted to the Pacific margin during the Late Cretaceous (Moreno-Sánchez and Pardo-Trujillo, 2002, 2003; Pindell et al., 2005; Villagómez et al., 2011, 2013; Spikings et al., 2015; Pardo-Trujillo et al., 2020).

To the west of the Western Cordillera lies the Chocó Block, described by Duque-Caro (1990b) and redefined by Cediel et al. (2003) as the Panama-Chocó Block. Structural and biostratigraphic evidence, including regional sutures (such as the Garrapatas-Dabeiba Fault or the Uramita Fault System) and the presence of planktonic foraminifers like *Morozobella velascoensis*, common in Guatemala and Mexico, suggest that the Panama-Chocó Block is an allochthonous segment of Central America (Montes et al., 2012; Cardona et al., 2018; Barbosa-Espitia et al., 2019; Botero-García et al., 2023; Vallejo-Hincapié et al., 2024). It accreted on

the northwestern flank of the Western Cordillera (Duque-Caro, 1990a). This accretion occurred during the Oligocene, and the contact is defined by the Uramita Fault System (Duque-Caro, 1990b; Vallejo et al., 2024).

The development and evolution of the sedimentary basins in the Caribbean and the western Colombian margin have been shaped by the oblique and orthogonal collision of allochthonous terranes with the continental margin since the Late Cretaceous (Montes et al., 2019; Mora-Paez et al., 2019; Pardo-Trujillo et al., 2020) (Figs. I.6, II.1 and II.2). This evolution is closely related to the southwest-to-northeast direction, followed by a west-to-east migration of the Caribbean Plate and its interaction with the northwestern margin of the South American Plate (Pindell et al., 1998, 2005; Moreno-Sanchez and Pardo-Trujillo, 2003; Pindell and Kennan, 2009; Spikings et al., 2015; Cardona et al., 2018; Hincapié-Gómez et al., 2018; Montes et al., 2019; Mora-Paez et al., 2019) (Fig. I.6).

Currently, the Caribbean margin has the morphological and tectonic characteristics of a typical accretion-dominated subduction complex (Mantilla-Pimiento et al., 2009). However, based on seismic reflection data, two distinct subduction systems must be considered due to a slab break in the Caribbean Plate (Mora-Bohórquez et al., 2020) (Fig. II.1). Transtension occurs along the Oca-San Sebastián-El Pilar Fault (Echeverri, 2019), causing the Caribbean Plate to subduct beneath the South American/Atlantic Plate, forming the present-day Antilles Arc east of the study area (Escalona and Mann, 2011). South of this transtensional zone, where our study area is located, orthogonal flat-slab subduction of the Caribbean Plate beneath the South American Plate occurs (Escalona and Mann, 2011; Mora-Bohórquez et al., 2020) (Fig. II.1).

The primary tectonic features of this Caribbean margin, from west to east, include the trench, the active accretionary prism, and the outer high and forearc basins (Mantilla-Pimiento et al., 2009). The trench axis aligns with the base of the active accretionary prism, which forms the outer portion of the Sinú-Colombia accretionary wedge (Figs. II.1 and II.2). The outer high domain includes a significant structural complex comprising the easternmost part of the Sinú-Colombia accretionary wedge and the San Jacinto Fold Belt (Mantilla-Pimiento et al., 2009; Figs. I.7 and II.2). This SW-NE trending structure is part of the subduction complex, and crops out Cretaceous to Miocene rocks (Mantilla-Pimiento et al., 2009; Vallejo et al., 2023). The fossil portion of the accretionary prism now serves as a dynamic backstop to the active accretionary prism (Mantilla-Pimiento et al., 2009). The outer high consists of several small sedimentary basins containing post-kinematic Plio-Pleistocene deposits that fossilize the complex structure of the outer high (San Jorge and Plato forearc sub-basins; Mantilla-Pimiento et al., 2009). The landward boundary of the outer high is delineated by the well-developed positive flower structure of the Romeral North or San Jacinto Fault System, representing a structural separation between the minor basins deformed by mud diapirism to the west (Sinú Fold Belt) and the main, deeper forearc Lower Magdalena Valley Basin to the east (Mantilla-Pimiento et al., 2009). This Lower Magdalena Valley Basin, bounded by the Romeral Fault System to the west, and the Central Cordillera, San Lucas, and the Cáchira Structural High to the east (Mora et al., 2018), is the most prominent feature at the transition between the highly deformed forearc domain to the west (San Jacinto Fold Belt) and the less deformed one to the east (Mantilla-Pimiento et al., 2009; Fig. II.2).

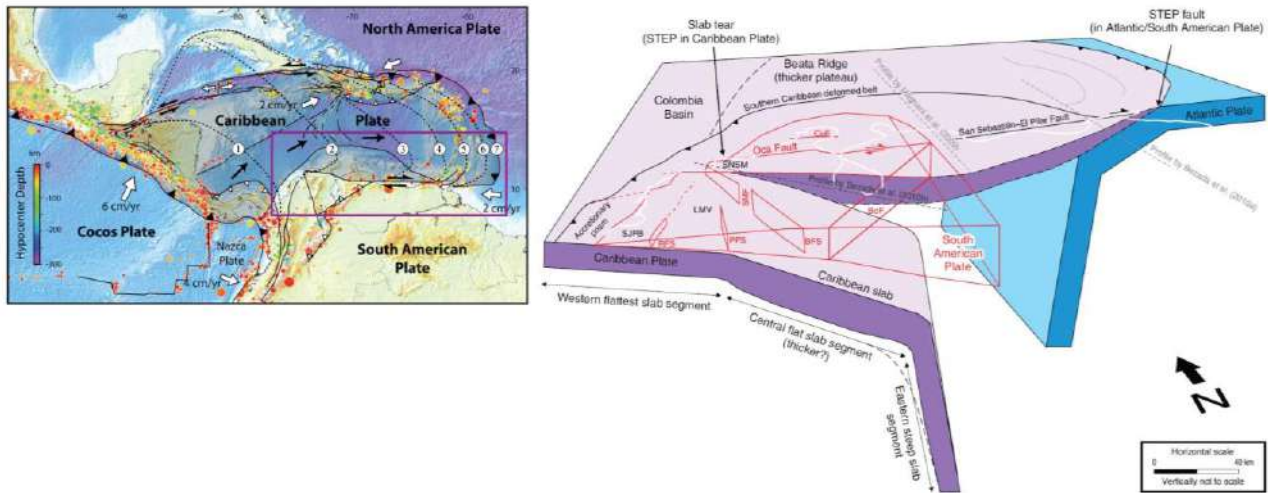


Fig. II.1. Proposed three-dimensional lithospheric configuration of NW South America with a slab tear or STEP (subduction transform edge-propagator) fault (Govers and Wortel, 2005) in the Caribbean Plate, probably represented in the upper crust by the western tip of the Oca–El Pilar–San Sebastián dextral fault system. (SNSM) Sierra Nevada de Santa Marta; (SJFB) San Jacinto Fold Belt; (RFS) Romeral Fault System; (LMV) Lower Magdalena Valley; (PFS) Palestina Fault System; (SMF) Santa Marta Fault; (BFS) Bucaramanga Fault System; (BoF) Boconó Fault. Left: Modified from Courtesy: National Science Foundation; the inferred positions of the leading edge of the Caribbean Plate from Escalona and Mann (2011). Right: from Mora-Bohórquez et al. (2020).

II.2. Geological and stratigraphical context

Seismic data suggest that from the Late Cretaceous to the early-middle Eocene, the convergence between northwest South America and the Caribbean Plate was oblique (SW to NE), while nearly orthogonal convergence (W to E) has taken place from the middle-late Eocene to the present (Pindell et al., 2005; Villagómez et al., 2011; Bayona et al., 2012; Bernal-Olaya et al., 2015; Montes et al., 2019; Mora-Bohórquez et al., 2020).

The San Jacinto Fold Belt presents an oceanic igneous basement of Cretaceous age (Silva-Arias et al., 2016; Mora et al., 2017), and the sedimentary record spans from the Late Cretaceous to recent (Dueñas and Gómez, 2013; Mora et al., 2017, 2018; Montes et al., 2019; Pardo-Trujillo et al., 2020; Angulo-Pardo et al., 2023; Rincón-Martínez et al., 2023; Vallejo-Hincapié et al., 2023; Plata-Torres et al., 2024) (Fig. II.2).

The sedimentary fill includes limestones, mudrocks, cherts and sandstones, from the Cansona Formation of Campanian-Maastrichtian age, that overlie the basement (Duque-Caro, 1968, 1972; Giraldo-Villegas et al., 2023). Subsequently, the collision of the Caribbean Plate against the northern South American margin produced a tectonic event, recognized by a lower Paleocene unconformity-LPU (Guzmán et al., 2004; Mora et al., 2017). Upper Paleocene-lower Eocene conglomerates, sandstones and mudrocks from the San Cayetano Formation overlie the Upper Cretaceous rocks (Duque-Caro, 1972; Guzmán, 2007; Bermúdez et al., 2009; Bermúdez, 2016; Mora et al., 2017). In the early to middle Eocene, the increase in morphotectonic activity generated the lower middle Eocene unconformity-LMEU (Guzmán et al., 2004; Mora et al., 2017). The Chalan/Chengue/Toluviejo Formations, composed of conglomerates, sandstones, limestones and mudrocks of middle-late Eocene age overlie the San Cayetano Formation, and are in turn overlain by the Carmen/San

Jacinto formations of late Eocene-early Oligocene age (Duque-Caro, 1972; Duarte, 1997; Guzmán, 2007; Bermúdez et al., 2009; Bermúdez, 2016; Mora et al., 2017, 2018; Celis et al., 2024). Later, sandstones and siltstones with coal beds associated with the Ciénaga de Oro Formation (Oligocene-Early Miocene age) were deposited (Duque-Caro, 1972; Guzmán, 2007; Bermúdez et al., 2009; Bermúdez, 2016; Mora et al., 2017, 2018; Manco-Garcés et al., 2020). A regional early Miocene tectonic event generated the lower Miocene unconformity-LMU (Mora et al., 2018). During the middle to late Miocene, siltstones and in minor proportion sandstones from the Porquero Formation were deposited (Duque-Caro, 1972; Guzmán, 2007; Bermúdez et al., 2009; Bermúdez, 2016; Duque-Castaño et al., 2023). Upper Miocene-Pliocene sandstones, siltstones and carbonaceous levels associated with the El Descanso, El Cerrito and Tubará formations are registered above (Duque-Caro, 1972; Guzmán, 2007; Molinares et al., 2012). Finally, Pliocene and Quaternary sandstones, siltstones, conglomerates and limestones from the Sincelejo, Morroa and La Popa formations were deposited (Duque-Caro, 1972; Guzmán, 2007; Molinares et al., 2012).

II.3. Middle-upper Eocene to Lower Miocene deposits

The tectonic evolution of the margin and its interaction with the sedimentary environments remains a topic of ongoing debate, in part because of the paucity of detailed scientific work.

In northwestern Colombia, a regional magmatic hiatus occurred during the late Eocene-Oligocene, which has been associated with margin segmentation due to block rotation, basin opening, and deformation in other parts of the continental margin (Montes et al., 2010, 2019; Bayona et al., 2012; Cardona et al., 2012). This tectonic activity generated uplift and exhumation events of the northern regions of the Central and Western cordilleras (Restrepo-Moreno et al., 2009; Villagómez and Spikings, 2013; Cochrane et al., 2014; León et al., 2018) as well as in the basement of the adjacent basins (Mora et al., 2017; Silva et al., 2017), producing coarse-grained sedimentation in several of these basins and explaining the high production of detrital materials transported by rivers to the Caribbean basins at this time (Osorio-Granada et al., 2020).

Deposits prior to coarse-grained sedimentation are associated with the Chengue Formation (Fig. II.2), which is characterized by basinward sedimentation from the ramp, dominated by hemipelagic claystones and siltstones, and small channel-lobe systems in the outer ramp and slope (Salazar-Ortiz et al., 2020b). Later, coarse-grained siliciclastic successions of late Eocene to early Oligocene age, deposited during the tectonic changes of the subduction complex, are associated with the San Jacinto Formation in the San Jacinto Fold Belt (Duque-Caro et al., 1996; Clavijo and Barrera, 2001; Guzman, 2007; Mora et al., 2017; Salazar-Ortiz et al., 2020a; Celis et al., 2023; Vallejo-Hincapié et al., 2023) (Fig. II.2). These coarse-grained siliciclastic materials are interpreted as ancient submarine deposits in slope failures associated with fan-delta environments (Duque-Caro et al., 1996; Duarte, 1997; Barrera et al., 2001; Guzmán, 2007). Overlying the San Jacinto Formation, it is widely agreed that the Ciénaga de Oro Formation was deposited in shallow marine and deltaic systems from the Eocene (?) to Early-Middle Miocene in both the San Jacinto Fold Belt and the Lower Magdalena Valley Basin (Dueñas and Duque-Caro, 1981; Dueñas, 1986; Guzmán et al., 2004; Bermúdez et al., 2009; Bermúdez, 2016; Mendoza-Rodríguez et al., 2018; Manco-Garcés et al., 2020; Celis et al., 2021, 2023; Pardo-Trujillo et al., 2023; Vallejo-Hincapié et al., 2023).

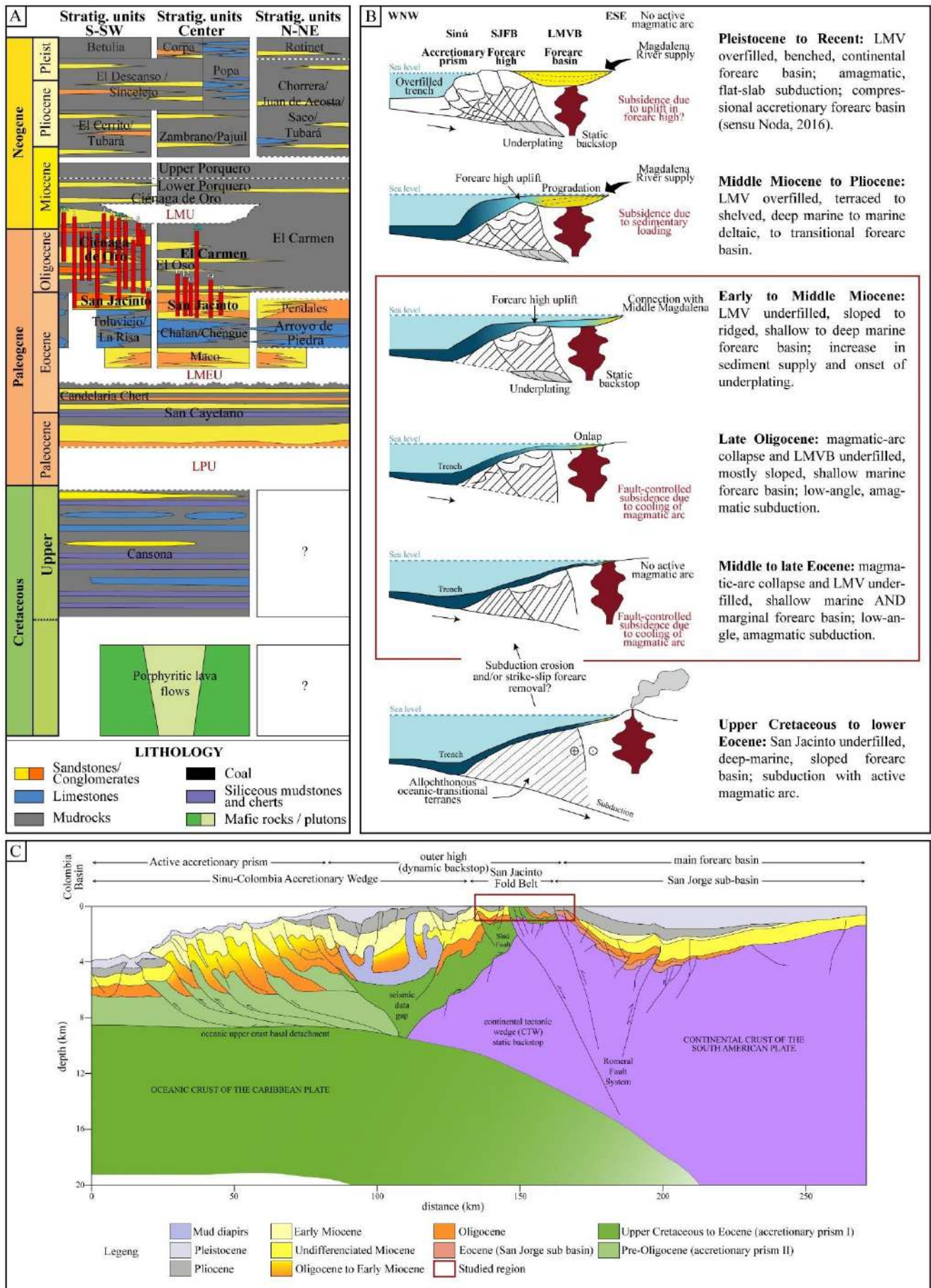


Fig. II.2. A. Schematic chronostratigraphic chart of the San Jacinto Fold Belt (SJFB; modified from Mora et al., 2017, 2018; Osorio-Granada et al., 2020). LPU: lower Paleocene unconformity; LMEU: lower-middle Eocene unconformity; LMU: lower Miocene unconformity. Red bars: studied sections (outcrops and well-cores in map Fig. I.7, and Table III.1). Modified from Celis et al. (2023). **B.** Interpreted evolution of the morphology of the San Jacinto Fold Belt (SJFB) and Lower Magdalena Valley Basin (LMVB) forearc system from Upper Cretaceous to Recent (from Mora-Bohórquez et al., 2020). **C.** Main tectonic features of the Colombian Caribbean margin. The accretionary system between the forearc region and the deformation front is divided into two zones (active accretionary prism and outer high) with different morphological and structural characteristics. The outer high initially evolved by accretion against the static backstop (continental crust of the arc framework). Later, the outer high acts as a dynamic backstop for the younger accretionary prism, which remains active to the present day (from Mantilla-Pimiento, 2009).

Deposits of the same age described mainly to the northwest and northeast of the Sinú San Jacinto Basin — such as the El Floral and El Carmen formations, respectively— are characterized by a predominance of hemipelagic mudstones (Duque-Caro et al., 1996; Raigosa, 2018; Arias-Villegas et al., 2023; Domínguez-Giraldo et al., 2023) and would be associated with the distal facies of the Ciénaga de Oro Formation, linked mainly to the shelf and slope environments (Duque-Caro et al., 1996). Oil company studies (unpublished) also report successions of this age in slope and basin plain environments in the offshore basins, possibly corresponding to the El Carmen Formation. Some authors have divided the Ciénaga de Oro Formation into two settings separated by a Lower Miocene unconformity: Lower Ciénaga de Oro from Oligocene to Lower Miocene and Upper Ciénaga de Oro from Lower Miocene to Lower-Middle Miocene. The data are not yet conclusive, however.

Overlying the Ciénaga de Oro Formation is the Porquera Formation, featuring a predominance of fine-grained deposits accumulated from shelf and deep marine systems during the Middle to Late Miocene (Duque-Caro et al., 1996; Mora et al., 2018; Duque-Castaño et al., 2023).

Chapter III

METHODOLOGY

III.1. Basis of the research

Before initiating the project described here, a preliminary desk-based phase was conducted, for a search and critical review of bibliographic material related to studies carried out in the Colombian Caribbean basins. This review contributed to defining the research problem and establishing the scope of the work. Additionally, the examination of literature on sedimentology and ichnology in coastal systems helped to refine the objectives of our research. The development of the Master's Project, which involved the study of an initial well-core sample provided by the National Hydrocarbons Agency (ANH), further refined the research methodology, identified potential challenges in section correlation, and assessed the value of the data within the context of the future doctoral dissertation.

The theoretical framework of this study—including the tectonic, paleogeographic context and the relevant literature review— was developed using the Tree of Science database (Zuluaga et al., 2022). This tool categorizes all articles on a given topic into four sets: a) the root, which includes the classic and foundational scientific articles on the subject; b) the trunk, consisting of structural articles that currently dominate and consolidate the information on the topic; c) the branches, specific subareas within a knowledge domain, encapsulating articles centered around distinct themes derived from cluster analysis. Moreover, the Branches also signify the trending topics within that area; and d) the leaves, which gather the most recent articles and reviews that should condense very well your topics. Each group is represented by circles of varying sizes; each circle represents an article, and its size depends on the number of citations (Fig. III.1). To ensure a reliable tree, the search engine must yield between 100 and 500 results. It is important to note that this database conducts its searches within the Web of Science (Thomson Reuters) databases, specifically the Science Citation Index.

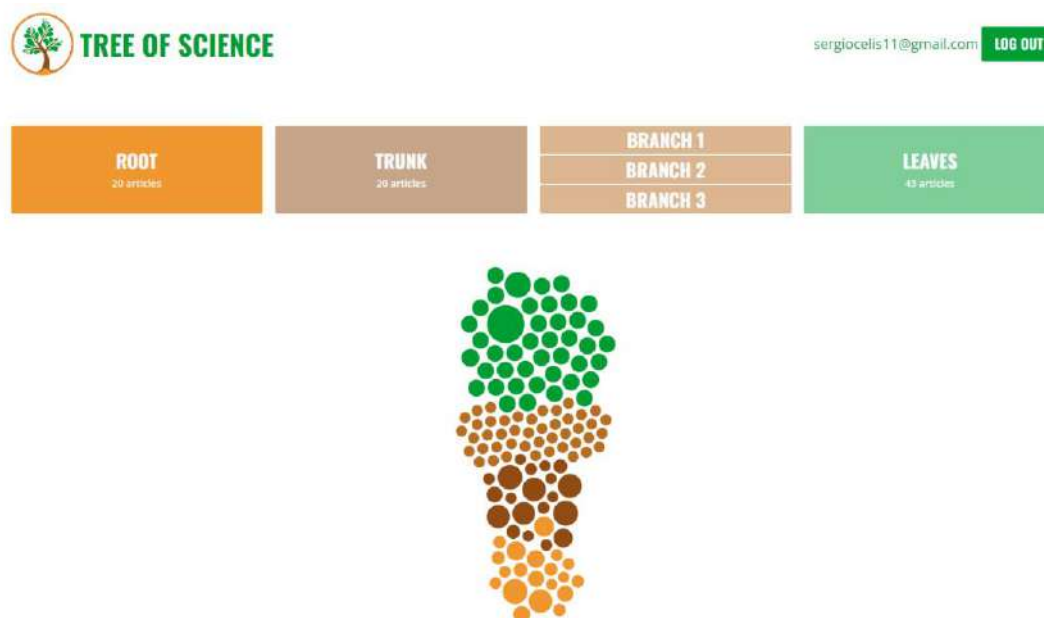


Fig. III.1. Tree diagram obtained from the search for 'fluvio-deltaic systems' where the root (yellow) represents the classical and/or earliest scientific articles on the subject; the trunk (brown) represents the foundational articles, which currently dominate and compile all the information on the topic; the branches represent trending topics, and the leaves (green) represent the most recent articles on the subject. The size corresponds to the number of citations. Tree of Science (Zuluaga et al., 2022).

III.2. Material selection

The structural complexity of the study area, associated with the deformation of the Sinú-San Jacinto Fold Belt, underscores the importance of careful preliminary analysis before undertaking sedimentological and ichnological studies. As a first step, seismic lines and existing geological field information were reviewed to ensure that the sections preliminarily selected for study represented the same deformation framework. In cases where this was particularly challenging, available biostratigraphic information was utilized to guide decision-making. Following this, locations were visited to examine outcrops and evaluate the previous selection, and based on these findings, the well-cores that could best support the research were chosen (Table III.1).

III.3. Outcrops

From the final selection, outcrop study was based on the sedimentological and photo-panel analysis of exposed rock formations in creeks and roads located in the present-day onshore Colombian Caribbean region, specifically the middle-upper Eocene to Lower Miocene rocks within the San Jacinto Fold Belt. Fifteen selected outcrops were analyzed bed-by-bed focusing on sedimentological and ichnological features using a Jacob's staff, encompassing observations of bed geometry and thickness, lithology, texture, sedimentary structures, fossils, and ichnological assemblages. Facies were differentiated and linked to specific depositional processes. Ichnological attributes including ichnotaxobases, ichnodiversity, distribution, and abundance (Bioturbation Index BI *sensu* Taylor and Goldring, 1993) were defined. Then, facies and ichnological attributes were grouped into facies associations based on recurring patterns, revealing similarities in processes and depositional conditions.

Paleoflow directions were defined based on stratigraphic features from planar- and trough-cross stratification, ripple-cross lamination, and clast imbrications. Bed thickness was classified as very thin (<1 cm), thin (1–10 cm), medium (11–30 cm), thick (31–100 cm), or very thick (>100 cm) according to the proposal by Nichols (2009). The gravel-clast fabric terminology used follows Walker's (1975) classification. Integration of field work and photo-panel analysis allowed mapping of the 3-dimensional arrangement of architectural elements and bounding surfaces to configure a larger-scale stacking pattern of facies associations. Sampling for micropaleontological analysis was carried out in mudrock lithologies. Micropaleontological analyses (palynomorphs, foraminifera, calcareous nannoplankton) were conducted for biostratigraphic and paleoenvironmental purposes in collaboration with specialists from the University of Caldas (Colombia) and the University of Salamanca (Spain). Occasionally, sampling stations coincide with those from previous micropaleontological studies on foraminifera and calcareous nannofossils (e.g., Duque-Caro et al., 1996; Duarte, 1997; Guzmán, 2007; Mejía-Molina et al., 2010; Manco–Garcés et al., 2020) for age control.

III.4. Well-cores

In recent years, the National Hydrocarbons Agency (ANH) has drilled several stratigraphic wells in the Colombian Caribbean region to study the basin evolution and assess its hydrocarbon potential. In 2018, through an inter-administrative agreement between the ANH and the University of Caldas, titled "Certification of Physical and Age Stratigraphy of the Drilling Cores Recovered by the National Hydrocarbons Agency –ANH–

in the Sinú-San Jacinto basins and Cordillera" (Project Contract RC 494, 2017), several wells with high potential for sedimentological and ichnological study were identified.

After an initial phase of material selection, we chose four well-cores, considered as the most suitable for this research in view of the project's key objectives. These well-cores offered a comprehensive record of the study interval, excellent preservation of physical and biogenic structures, and good biostratigraphic calibration. Well-core methodology includes step-by-step facies association identification, trace fossil analysis, and microfossil assemblage examination to interpret palaeoenvironmental conditions and depositional patterns. A detailed stratigraphic log (scale 1:1) was created, documenting lithology (texture, composition), sedimentary structures, contact types, and paleontological content (fossils and biogenic sedimentary structures). Bed thickness was described following the terminology of Nichols (2009). Special attention was given to ichnological characterization, focusing on trace fossil size, type of fill, orientation, relationships with facies and stratigraphic surfaces, and tiering. Ichnodiversity, distribution, and abundance were also recorded, using the Bioturbation Index (BI) as defined by Taylor and Goldring (1993). Ichnotaxonomic classification was based on ichnotaxobases observed in cores (Knaust, 2017). Although the well-core was not slabbled, only ichnotaxa that could be confidently identified by ichnotaxonomic features were considered in the analysis. Those that posed any doubts were marked with a question mark and used with caution in the interpretations. Spatial variability challenges are addressed in Chapter VII through integrated analytical techniques. This framework was applied to other well-cores in the study area, offering valuable insights into the dynamic interactions within tropical deltaic systems. Micropaleontological analyses, including studies of palynomorphs, foraminifera, and calcareous nannofossils, were also performed for biostratigraphic and paleoenvironmental objectives in collaboration with researchers from the University of Caldas (Colombia) and the University of Salamanca (Spain).

Table III.1. Location of outcrop and well-core sections studied in this research.

| Number on map (Fig. I.7.) | Section | Coordinates | | Thickness (m) | Age | Chapter associated in thesis |
|---------------------------|--|-------------|------------|---------------|--|------------------------------|
| | | Lat | Long | | | |
| well-core | ANH-SSJ-SAN-ANTONIO-1X | 7.94 | -75.49 | ~293 | Oligocene to Early Miocene | Chapter VII |
| 1 | San Francisco del Rayo | 8.123193 | -75.763709 | ~40 | middle-late Eocene to Oligocene | Chapters IV, VII |
| 2 | San Francisco del Rayo | 8.146999 | -75.746704 | ~10 | Oligocene | Chapter VII |
| 3 | El Arenoso (punto de control) | 8.210035 | -75.738421 | ~7 | Oligocene | Chapter VII |
| well-core | ANH-SSJ-LA-ESTRELLA-1X | 8.34 | -75.68 | ~298 | middle-late Eocene to Oligocene | Chapters IV, VII |
| 4 | Perfil extenso Planeta Rica - Montería | 8.511962 | -75.647603 | ~92 | Oligocene to Early Miocene | Chapter VII |
| 5 | Ladrillera, via Planeta Rica - Montería | 8.524892 | -75.671515 | ~31 | Oligocene to Early Miocene | Chapter VII |
| well-core | ANH-SSJ-NUEVA ESPERANZA-1X | 8.34 | -75.68 | ~690 | middle-late Eocene to Early Miocene | Chapters IV, VI, VII, VIII |
| 6 | Perfil extenso Planeta Rica - Montería | 8.535073 | -75.686713 | ~126 | Oligocene to Early Miocene | Chapter VII |
| 7 | Discordancia via Planeta Rica a Montería | 8.564717 | -75.703663 | ~20 | Paleocene / Oligocene to Early Miocene | Chapter VII |
| 8 | Canal via Planeta Rica a Montería | 8.599307 | -75.736927 | ~15 | Oligocene to Early Miocene | Chapter VII |
| 9 | Via Cienga de Oro - La Y | 8.86354 | -75.596193 | ~35 | Oligocene | Chapter VII |

| Number on map (Fig. I.7.) | Section | Coordinates | | Thickness (m) | Age | Chapter associated in thesis |
|---------------------------|-------------------------------|--------------|--------------|---------------|---------------------------------|------------------------------|
| | | Lat | Long | | | |
| 10 | Via Cienga de Oro - La Y | 8.868001 | -75.603867 | ~62 | middle-late Eocene | Chapters IV, VII |
| 11 | Alfárez Creek (jet section) | 9°43'5.17'' | 75°9'26.08'' | ~245 | middle-late Eocene to Oligocene | Chapters V, VII |
| 12 | Alfárez Creek (curve section) | 9°42'59.47'' | 75°9'29.86'' | ~158 | middle-late Eocene to Oligocene | Chapters V, VII |
| 13 | Piedra Azul Creek | 9°45'27.60'' | 75°8'7.27'' | ~101 | middle-late Eocene | Chapters V, VII |
| well-core | ANH-San Jacinto-1 | 9°48'5.47'' | 75°7'33.95'' | ~524 | middle-late Eocene to Oligocene | Chapter VII |
| 14 | San Jacinto Creek | 9°49'31.75'' | 75°6'6.74'' | ~84 | middle-late Eocene to Oligocene | Chapters V, VII |
| 15 | Salvador Creek | 9°57'13.46" | 75° 5'25.87" | ~50 | middle-late Eocene | Chapter VII |

PART III RESULTS

Chapter IV

EOCENE SHALLOW MARINE SYSTEMS

Hyperconcentrated to hyperpycnal flow transition along a river-delta system in a tropical humid setting (middle to late Eocene, Caribbean Colombia)

Sergio A. Celis^{a,b,c*}, Fernando García-García^a, Francisco J. Rodríguez-Tovar^a, Carlos A. Giraldo-Villegas^{a,b,c}, Andrés Pardo-Trujillo^{b,c}

^a Departamento de Estratigrafía y Paleontología, Universidad de Granada, 18002 Granada, Spain.

^b Grupo de Investigación en Estratigrafía y Vulcanología (GIEV) Cumanday, Universidad de Caldas, Manizales, Colombia.

^c Instituto de Investigaciones en Estratigrafía-IIES, Universidad de Caldas, 170004, Manizales, Colombia.

*Corresponding author sergiocelis11@gmail.com; sergiocelis@correo.ugr.es (Sergio A. Celis).

In progress. It will be submitted to The Depositional Record

The Depositional Record

The journal of the International Association of Sedimentologists

Open Access



Highlights

- Hyperconcentrated flows are rarely reported from non-volcanic, humid tropical settings. They are commonly documented from lahars or alluvial systems in arid settings.
- Hyperconcentrated and hyperpycnal flow deposits are reported as the dominant sedimentation in a river-delta system.
- Hyperconcentrated flow transitions are better developed and preserved in the sediment record when the flows are controlled by long-time processes (i.e. seasonally rainfall in tropical humid settings) than catastrophic events (i.e. volcanic eruption-generated).
- Conditions favouring hyperconcentrated flow (i.e. available sand sediment in the source area, steep sedimentary system, high water and sediment discharge) presumably were encouraged by tectonically active reliefs and tropical humid settings in the Caribbean Colombia during late Eocene.

Abstract

Sediment transport and deposition in fluvial and mouth bar systems are primarily driven by gravity flows, including sediment gravity flows and fluid-gravity flows. While these processes are well-studied, hyperconcentrated flows represent a transitional stage that remains less understood, particularly in the context of mass transport and their arrival at the coastline, forming mouth bars. Hyperconcentrated flows exhibit non-Newtonian, plastic behavior, transitioning between debris flows and fluid flows. This study examines the dynamics of such flows on middle to upper Eocene deposits in the Colombian Caribbean, focusing on their role in shaping deltaic and coastal systems in tectonically active environments.

The deposits studied consist of clast-supported conglomerates, coarse-grained sandstones, interbedding with some mudstones with root structures intervals, which indicate rapid sedimentation during torrential rain events and fluvial flooding. These coarse-grained sediments, characterized by abrupt vertical grain-size transitions and poor sorting, also reveal a complex interplay between fluvial and marine processes. The deposits show evidence of transitions to hyperpycnal flows, followed by a return to hyperconcentrated flows upon reaching the coastline. These flows transitioned from high-energy fluvial systems to marine-influenced environments. Mouth bars in this setting were initially shaped by gravitational flows and later modified by wave and tidal processes during upstream avulsion events, as suggested by the presence of ichnotaxa such as *Conichnus*, *Macaronichnus*, *Ophiomorpha* and *Thalassinoides*.

This study provides valuable insights into the sedimentological processes governing hyperconcentrated flows and their impact on the stratigraphic record, particularly in deltaic systems along tectonically active margins. The findings also emphasize the challenges of interpreting marine influences in hyperconcentrated flow deposits due to the interaction of sediment gravity flows with coastal processes. The results have broader implications for understanding sediment transport, deltaic evolution, and flood hazards, particularly in regions prone to extreme weather events.

IV.1. Introduction

Sediment transport and deposition processes are primarily governed by sediment gravity flows and fluid-gravity flows, influenced by factors such as matrix strength, dispersive pressure, and turbulence (Middleton and Hampton, 1973; Lowe, 1982; Nemeč and Steel, 1984; Lavigne and Suwa, 2004). However, the intermediate stage known as hyperconcentrated flows remains a controversial research topic (Nemeč, 2009). These flows are crucial for understanding the dynamics of mass transport and sudden flow events, especially given the increasing need to assess debris flows and flood hazards in populated areas (Benvenuti and Martini, 2002).

Hyperconcentrated flows represent an intermediate state along the sediment-water ratio spectrum, situated between the two flow end-members such as debris flows (cohesive and non-cohesive) and stream flows (fluid flows) (Benvenuti and Martini, 2002). The rheological behaviour of hyperconcentrated flows typically involves plastic, non-Newtonian properties, where the flow still behaves like a fluid, with solids and water remaining as separate phases (Beverage and Culbertson, 1964; Pierson and Scott, 1985; Smith, 1986; Coussot and Meunier, 1996). These flows are defined as dense, turbulent subaerial flows that exhibit non-tractional

sediment deposition. They begin as non-Newtonian fluids and often transition into pseudoplastic (laminar) flows (Fredrickson, 1964; Barnes et al., 1989; Nemeč, 2009).

Hyperconcentrated flows are commonly reported from catastrophic flood events associated with volcanic eruptions, generating lahars and jökulhlaups (e.g., Smith, 1986; Cronin et al., 2000; Lavigne and Suwa, 2004). They also occur in regions where large volumes of loose, sorted fine- to medium-grained sediments are available, such as glacial or paraglacial settings and loess-dominated regions (e.g., Wasson, 1977; Svendsen et al., 2003; Hornung et al., 2007; Rodríguez-López et al., 2010). Additionally, these flows are documented in steep-gradient alluvial systems typical of arid regions (Ilgar et al., 2024; Larsen et al., 2024a, 2024b, 2024c; Nemeč and Ozaksoy, 2024; Wathne et al., 2024).

Although their definition has sometimes included normal-graded, non-stratified deposits from subaqueous sediment-gravity flows (Mulder and Alexander 2001; Sohn et al. 2002), often classified as high-density turbidity currents (*sensu* Lowe, 1982), the more widely accepted definition of hyperconcentrated flows describes a turbulent subaerial flow that is excessively dense, leading to sediment deposition that is mainly or entirely non-tractional (Nemeč, 2009). These flows may or may not be channelized, and their deposits are typically normal-graded and non-stratified, except possibly at the top (Benvenuti and Martini, 2002; Nemeč, 2009).

Although hyperconcentrated flows have been extensively documented across various environments, reports of their occurrence in coastal mouth bars are relatively scarce (e.g., Dunne and Hempton 1984; Wood and Ethridge 1988), and they are seldom reported in humid tropical settings. This is noteworthy because mouth bars play a critical role where confined flows within distributary channels expand and decelerate as they enter a standing body of water (Bates, 1953; Wright, 1977; Elliott, 1986). The presence of connected voids between grains in these flows allows them to ingest water, expand, and potentially transform into less concentrated density flows. This transformation can differ significantly between subaqueous and subaerial settings (Mulder and Alexander, 2001). With few cohesive particles, turbulence is easily generated (Kneller and Buckee, 2000), and flow transitions can be triggered by changes in topography, leading to concentrated density flows or even turbidity currents (Fisher, 1983). However, in tectonically active regions, hyperconcentrated flows are often generated in small basins with shallow water depths (Mutti et al., 1996). Here, steep ramps enable the transport of large sediment blocks near the flow bottom, but these ramps are typically too short for the flow to fully transform into a turbidity current. As a result, these flows can either lead to the progradation of small alluvial fans (e.g., Mutti et al., 1996; Falk and Dorsey, 1998; Sohn et al., 1999; Alasad et al., 2023) or undergo transformations into hyperpycnal systems (e.g., Nemeč, 1990; Melstrom and Birgenheier, 2021; Larsen et al., 2024b). These transitions are marked by shifts in particle-support mechanisms, with increasing fluid turbulence providing support. Similar transformations are observed in lahars moving down river valleys, where water ingress dilutes the flow, reducing its capacity to carry larger gravels (Thouret et al., 2020). In subaqueous flows, dilution may also occur along the upper surface of the flow (Simpson, 1997) or when a river generates such an underflow this tends to bypass the upper shoreface with little or no record (probably erased by storms) (Larsen et al., 2024).

When an alluvial distributary system delivers sufficient sediment to a tectonically controlled, relatively steep basin margin immediately adjacent to the river mouth, the resulting deposits exhibit Gilbert-type delta architecture (Nemec, 1990; Postma, 1990). In contrast, when water depths seaward of the mouth are shallow or shoaling, a turbulent jet of fluid from the river mixes with the basin water, spreads out, decelerates, and deposits the sediment load (Wright, 1977). Bed load deposited near the river mouth results in the formation of shoal-water delta architecture or fan delta deposits (Nemec and Steel, 1988; Postma, 1990; Nemec, 1993). In this second scenario, the influence of marine processes becomes evident as enhanced bed friction can accelerate spatial expansion and cause deceleration of the river jet (Wright, 1977). However, the influence of wave- and tidal-processes on coarse-grained deltas is poorly documented in geological settings (e.g., Ekdale and Lewis, 1991; Ichaso et al., 2022; Baucon et al., 2023; Giraldo-Villegas et al., 2024), with only a few modern examples, such as the Bella Coola delta in British Columbia (Kostaschuk and McCanna, 1983; Kostaschuk, 1985). The geometry and scale of mouth bars in these settings are shaped by the interaction between riverine flows and coastal processes, as well as by any flow transformations occurring from the source to the receptor basin. However, deciphering marine processes in these scenarios is challenging because the physical processes in shallow marine environments are often altered by the rheology of the incoming flows (matrix strength, dispersive pressure, and turbulence). Therefore, the physical characteristics of shallow marine deposits in such settings may not directly reveal marine input. In this context, ichnology emerges as an essential tool for determining whether macrobenthic ecological niches have been established, thus helping to assess the extent of marine influence on depositional processes (e.g., Giraldo-Villegas et al., 2024).

While significant strides have been made in understanding coarse-grained mouth bars, this complex subject still requires further exploration, particularly regarding their representation in the geological record, subsurface deposits, and implications for risk and disaster management. This study addresses some of these gaps by examining middle to upper Eocene coarse-grained deposits from the Colombian Caribbean. These deposits provide valuable insights into the behaviour of gravitational flow rheology, flow transformations, and discharges along coastline in tropical humid environments, where torrential rains may exert a significant influence. The river mouth morpho-dynamics and facies assemblages of these systems reflect the short-term interplay of fluvial and marine processes, likely driven by stream floods and relative sea-level changes along a tectonically active margin.

IV.2. Geological setting

The tectonic evolution of the SJFB in the Colombian Caribbean is primarily governed by the complex interactions between the Caribbean and South American plates (Fig. IV.1). The collision between these two plates during the Late Cretaceous, followed by its subsequent movement from the southwest to the northeast, significantly influenced the sedimentary dynamics of the Colombian Caribbean basins until the middle Eocene (~45 Ma; Mora et al., 2017). This tectonic activity, characterised by a zipper-like collision against the continental margin, led to the formation of various tectonic features that continue to impact the region's geology (Pindell and Kennan, 2009; Montes et al., 2019; Pardo-Trujillo et al., 2020).

Following the middle Eocene, a shift in the migration direction of the Caribbean Plate from west-east induced a transtensional regime along the pre-Oca lineament, continuing the influence of Caribbean-South American plate interactions on the studied basins up to the present day, with variations in subduction dynamics over time (Echeverri, 2019; Mora-Bohorquez et al., 2020).

The key tectonic features of the margin, arranged from west to east, include the trench, the active accretionary prism, the outer high, and the forearc basins (Mantilla-Pimiento et al., 2009). The trench axis aligns with the base of the active accretionary prism, forming the outermost segment of the Sinú-Colombia accretionary wedge (Fig. IV.1). The outer high encompasses a significant structural complex, which includes the easternmost part of the Sinú-Colombia accretionary wedge and the SJFB. This current SW-NE trending structure of the SJFB is a component of the subduction complex and has exposed Cretaceous to Miocene rocks at the surface since the Pleistocene (Duque-Caro et al., 1996; Guzman, 2007; Mora et al., 2017, 2018; Salazar-Ortiz et al., 2020a, 2020b; Celis et al., 2023, 2024; Giraldo-Villegas et al., 2023; Vallejo-Hincapie et al., 2023) (Fig. IV.1). The fossilized portion of the accretionary prism now acts as a dynamic backstop to the active accretionary prism (Mantilla-Pimiento et al., 2009).

The basement of the Colombian Caribbean basins is part of the Caribbean Plate, with mafic and ultramafic rocks derived from submarine volcanism, and this is overlain by initiating sedimentary dynamics from the Campanian-Maastrichtian, characterized by deposits of the abyssal plain and continental slope, along with turbiditic systems reaching these environments (Cerón et al., 2007; Villagómez et al., 2011; Pardo-Trujillo et al., 2020; Giraldo-Villegas et al., 2023). Although the associated shallow marine environments have not been reported so far, their preservation is not ruled out. Subsequently, coarse-grained deltaic and submarine fans deposits dominated the Paleocene-early Eocene, corresponding with the activity of an active volcanic arc (Duque-Caro et al., 1996; Guzmán, 2007; Cardona et al., 2012). A significant regional unconformity, though poorly dated, have been associated with the transition in the Caribbean Plate's evolution from SW-NE to W-E migration during the early to middle Eocene (Mora et al., 2017). Following this unconformity, carbonate patches and their reworking into the slope and abyssal plain dominated the middle Eocene sedimentation (Salazar-Ortiz et al., 2020a; Silva-Tamayo et al., 2020). However, this scenario underwent an abrupt change, leading to the deposition of coarse-grained deposits, focus of this study, overlaying these carbonate systems.

The contact between these carbonate- and siliciclastic-dominated sedimentary units is poorly preserved, and research on these middle-to-upper Eocene deposits is limited (e.g., Salazar-Ortiz et al., 2020a; Domínguez-Giraldo et al., 2023). The coarse-grained sedimentation has been informally referred to as the San Jacinto Formation in private petroleum industry reports, though the unit lacks a formal definition. These deposits range from shallow to deep marine environments (e.g., Duque-Caro et al., 1996; Duarte, 1997; Guzmán, 2007; Salazar-Ortiz et al., 2020b; Celis et al., 2024). However, dominant literature associates the San Jacinto Formation primarily with slope and slope-break deposits, hence the proximal facies studied here will be referred to as middle-to-late Eocene shallow marine deposits, adhering to the guidelines of international stratigraphic nomenclature, reserving the informal term "San Jacinto Formation" exclusively for deep marine deposits (e.g., Celis et al., 2024).

In the central-northern region of the SJFB (Fig. IV.1), both shallow and deep sedimentary environments have been reported during the middle-to-upper Eocene (e.g., Duque-Caro et al., 1996; Duarte, 1997; Guzmán, 2007; Salazar-Ortiz et al., 2020b; Celis et al., 2024). However, in the southern region, studies reporting coarse facies from this age are scarce, and these facies have been exclusively associated with proximal deposits (e.g., Celis et al., 2023). In the southern SJFB, these facies are overlain by deltaic deposits of the Ciénaga de Oro Formation, dated to the Oligocene-Early to Middle Miocene, with an apparently conformable contact between both units (Dueñas, 1986). In contrast, in the central-northern region, only the deposits interpreted as deep marine are overlain by shelf and continental slope facies, representing the distal facies of the Ciénaga de Oro Formation, which have been referred to as the El Carmen Formation (e.g., Duque-Caro et al., 1996; Osorio-Tabares et al., 2023; Celis et al., 2024).

IV.3. Methods

Fieldwork was conducted at two outcrop locations following an exhaustive search for these deposits, as they do not consistently outcrop in the southern area of the SJFB (Fig. IV.1). This may be the first documented report of these deposits in the region. Detailed facies characterization was a priority, and stratigraphic sections were measured using a Jacob's staff. Key attributes recorded include lithology, grain size, sorting, roundness, color, bed thickness, bedding contacts, physical sedimentary structures, fossil content, and biogenic structures. For the biogenic structures, special attention was given to their distribution, abundance, size, morphology, depth of penetration into the substrate, and cross-cutting relationships. Paleoflow directions were determined using indicators such as planar and trough cross-stratification, ripple cross-lamination, and clast imbrication.

Stratigraphic descriptions of the well cores were performed at a 1:10 scale, with continuous photographic documentation along the studied core sections. The well cores examined include the ANH-SSJ-Nueva Esperanza-1X and ANH-SSJ-La Estrella-1X, which span approximately 250 meters in thickness and were drilled in the southwestern zone of the SJFB (Fig. IV.1). The ANH-SSJ-La Estrella-1X well drilled rocks older than the study interval, thus only the section from 130 to 298 meters in depth was analysed. Due to tectonic deformation, the thickness of the rocks in this well was recalculated (see SM1). These descriptions were carried out at the National Lithology Repository in Piedecuesta, Santander (Colombia).

In both well cores and outcrops, facies were described in detail (Table IV.1), and ichnotaxonomic and ethological identifications of trace fossils were performed. Ichnological analysis was based on qualitative features (e.g., shape, lining, filling, spreite) and quantitative measures (e.g., dimensions, abundance, and orientation). The vertical distribution of trace fossils and their cross-cutting relationships were analyzed to interpret ecological stratification (tiering). This information was complemented by the distribution and abundance of biogenic structures, using the Bioturbation Index as defined by Taylor and Goldring (1993).

Lithofacies analysis was based on texture, grain size, sedimentary structures, and bioturbation, allowing characterization and differentiation of facies, and subsequently integrated in facies associations based in the depositional processes and the lateral and vertical relationships between the facies. Finally, sedimentary sub-environments were interpreted.

Biostratigraphic data from previous micropaleontological studies in the same stratigraphic sections (i.e., palynology, foraminifera, and calcareous nannofossils), were integrated.

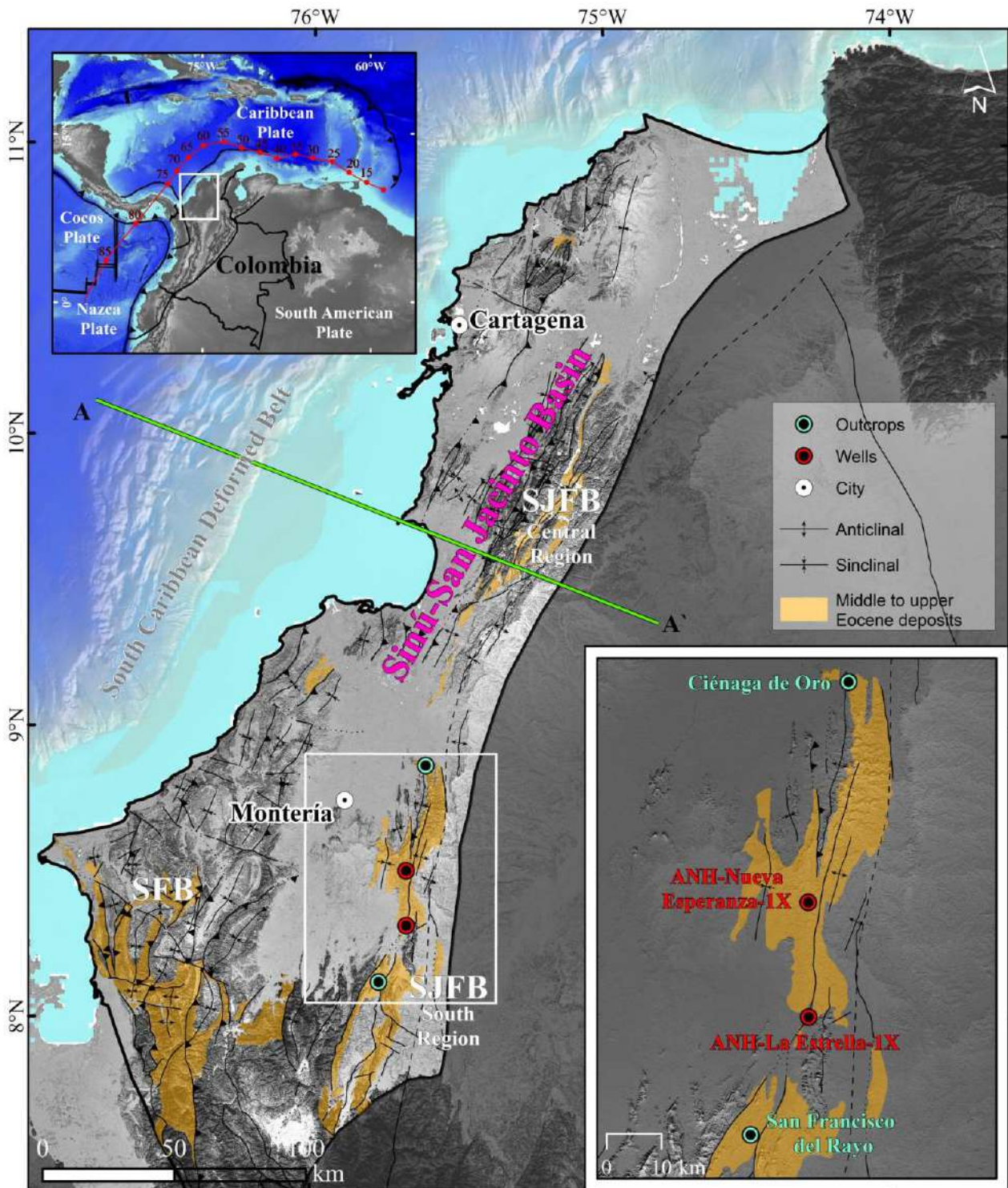


Fig. IV.1. Location of the southwestern Colombian Caribbean basins; red line and dots with Myr indicate the movement of the Caribbean Plate. Study area in the Sinú-San Jacinto Basin. Outcrop and well-core locations in San Jacinto Fold Belt (SJFB) in south region. Middle to upper Eocene deposits are indicated in the Sinú-San Jacinto Basin (Source: WGS-1984 coordinate system; CIOH, SRTM, NOAA elevation, and ocean models; geology from Gómez and Montes, 2020). A-A': Subduction profile with San Jacinto Fold Belt. Note: SFB: Sinú Fold Belt; SJFB: San Jacinto Fold Belt; LMV: Lower Magdalena Valley Basin.

IV.4. Stratigraphy

The four analysed stratigraphic logs, comprising two outcrops and two well cores, 12 distinct lithofacies (F1 to F12) have been differentiated (Table IV.1). These lithofacies were grouped into six facies associations (FA1 to FA6) (Fig. IV.2).

IV.4.1. San Francisco del Rayo town (SFR)

These deposits, comprises an 8-meter-thick record of middle to upper Eocene deposits, are in a quarry 0.5 km north of the town of San Francisco del Rayo (Fig. IV.2). The lower contact is not visible, and the upper contact is faulted against fluvio-deltaic deposits from the Oligocene to Early Miocene. The deposits are characterized by packages of clast-supported and locally matrix-supported conglomerates up to 2-3 meters thick. The clasts range in size from pebbles to cobbles, reaching up to 8 cm in diameter, while the matrix is typically medium to coarse-grained sand. Overall, the deposits are massive, with some sedimentary structures, such as planar cross-bedding highlighted by larger clasts.

IV.4.2. ANH-SSJ-La Estrella-1X well-core (LE)

The initial thickness of the rocks in this well was recalculated due to tectonic deformation (see SM1). The ANH-SSJ-La Estrella-1X well-core drilled rocks down to the Upper Cretaceous deposits, with the overlying succession likely corresponds to the late Palaeocene to early Eocene age. The intermediate interval (298.3 to 130 meters), consisting of middle to upper Eocene deposits, is the focus of this study (Fig. IV.2). The transition between the lower and middle Eocene deposits is marked by an unconformity, although the biostratigraphy is complex due to coarse lithologies, scarcity of palynomorphs and absence of in situ marine microfossils.

Below the deposits studied, sharp contacts with conglomeratic deposits are observed, possibly representing an unconformity. The underlying conglomerates are characterized by a high proportion of lithic fragments and a low quartz content (less than 20-35%). In contrast, the studied deposits have a quartz content of 60-80%. Therefore, the boundary between these units is estimated to be approximately 298 meters from the top (~420 meters from the top based on the initial apparent thickness).

The middle to upper Eocene deposits are characterized by 4-5 m-thick clast-supported and matrix-supported single-story conglomeratic beds, sharp-based and topped, with an overall aggradational trend (Fig. IV.2). Some transitional contacts to mudstone packages with root structures are observed, as well as normal gradations to coarse-grained sandstones with abundant organic matter fragments, highlighting parallel horizontal lamination. Towards the top, some coal layers are interbedded within the mudstones. The occurrence of certain ichnogenera (*Conichnus*, *Ophiomorpha*, *Thalassinoides*) towards the top of the section is observed.

The overlying unit is in concordant contact with the Eocene-Oligocene transition zone and corresponds to deltaic deposits of the Ciénaga de Oro Formation. A relative increase in accommodation space is evident (e.g., Celis et al., 2023).

IV.4.3. ANH-SSJ-Nueva Esperanza-1X well-core (NE)

The ANH-SSJ-Nueva Esperanza-1X well-core drilled middle to upper Eocene deposits, characterized by matrix- and to a lesser extent clast-supported conglomerates composed of pebbles, cobbles, and occasional granules. The matrix consists of medium to fine-grained sandstones with high content in quartz. These deposits have distinct contact types with coarse to medium-grained sandstones that display traction structures, such as planar cross lamination, as well as horizontal parallel lamination, highlighted by abundant layers of organic matter. The general trend of the deposits is aggradational. In some instances, medium-grained massive sandstones exhibit bioturbation (i.e., *Ophiomorpha*), towards the top of the studied succession. Moreover, symmetrical ripples and convolute lamination are recorded. At the top, there is a sharp contact with deltaic deposits of the Ciénaga de Oro Formation at the Eocene-Oligocene transition.

IV.4.4. Ciénaga de Oro road (COR)

These deposits are located 1.5 km southeast of the town of Ciénaga de Oro, along the road to La Y. They exhibit tectonic deformation, with the strata nearly vertical. Neither the contact with the underlying unit nor the overlying unit is preserved. The deposits are characterized by lenticular-shaped conglomeratic bodies, primarily clast-supported with a smaller proportion of matrix-supported; the mean of the clast grain size are cobbles (Fig. IV.2). The matrix consists of medium to coarse-grained sandstones. Transitional contacts to mudstones with root structures are present, as well as sharp contacts with massive coarse- to medium-grained sandstones that display some minor traction structures. Towards the top, the conglomeratic bodies diminish, transitioning to medium to coarse-grained sandy bodies interbedded with thinner mudstones.

IV.5. Facies associations analysis

Facies associations are described from the most proximal (FA1) to the most distal (FA6) and their stratigraphic variation is presented in Fig IV.2. The FA1 represent a 40%, the FA2 25%, FA3 15%, FA4 12%, FA5 3% and FA6 5%, showing a clear predominance of FA1 and FA2 related to proximal settings such as alluvial and fluvial settings.

Table IV.1. Lithofacies.

| Lithofacies code | Lithology, texture and fabric | Sedimentary structures | Bed thickness | Hydrodynamic process |
|------------------|---|---|---------------|-------------------------------------|
| F1: Gms | Matrix-supported, poorly-sorted subangular pebbles to granule | Ungraded or massive, trace fossils (<i>Ophiomorpha</i>) | 30 to 100 cm | Subaqueous cohesionless debris flow |
| F2: Gcs | Clast-supported, poorly-sorted angular pebbles to granule | Ungraded or normal grading, sharp- and erosional bases | 100 to 300 cm | Hyperconcentrated gravel flow |

| Lithofacies code | Lithology, texture and fabric | Sedimentary structures | Bed thickness | Hydrodynamic process |
|------------------|---|--|----------------------------|--|
| F3: SGm | Poorly-sorted, granule to very coarse sandstone (pebbly sandstone-like) | Massive, floating scattered outsized-granule/pebble clasts | | Rapid grain-by-grain aggradation from both suspension and bedload traction - Hyperconcentrated sandy flow |
| F4: Sm | Well-sorted, medium to fine-grained sandstones with carbonaceous detrital (discontinuous) lenses (S1L facies from Zavala <i>et al.</i> , 2011) | Massive, carbonaceous-prone clay chips in diffuse flaser-like lamination, sharp- and irregular-bases with rare mud (coal) clasts (<i>Conichmus</i> , <i>Ophiomorpha</i> and <i>Thalassinoides</i>) | 2 to 10 cm | Rapid deposition, most probably through the deceleration of a heavily sediment-laden current. Destruction of depositional lamination can come about through intense reworking of sediment. Progressive aggradation from quasi-steady turbulent flows (Zavala <i>et al.</i> , 2011) |
| | | | | |
| F5: Sp | Coarse to medium-grained sandstones | Planar cross-lamination/stratification (<i>Ophiomorpha</i> and <i>Thalassinoides</i>) | 10 to 20 cm | Unidirectional migration of 2D straight-crested ripples and thalweg bars in high-energy fluvial channels, under lower flow regime. |
| F6: Sh | Medium to very coarse sandstones (and granule) | Horizontal lamination/bedding | 3 to 5 cm | High velocity currents, probably associated with upper flow regime in fine- to medium-grained sandstones and that it is not very micaceous. |
| F7: St | Fine- to medium-grained sandstones | Trough cross-lamination | 1 to 15 cm | Produced during unidirectional migration of sinuous to linguoid-crested ripples or dunes (depending of the scale) in high to moderate energy |
| F8: Sw | Fine- to medium-grained sandstones | Symmetrical ripples | 1 to 10 cm | Bidirectional, oscillatory wave motion creates straight-crested symmetrical wave ripples. Represents deposition under wave action or in shallow water with stable flow conditions |
| F9: H | Heterolithic deposits (S2L facies from Zavala <i>et al.</i> , 2011) | Fine alternation of fine sand and carbonaceous detrital dark layers | Centimetric to millimetric | Sandy hyperpycnal flow and lofting |
| | | | | |
| F10: M | Homogeneous mudstones | Massive | 5 to 15 cm | Fluid muds |
| F11: Mr | Mottled green -grey mudstones | Massive, root traces, Fe-oxidized nodules | 50 to 150 cm | Soil |
| F12: C | Coal | Massive | 50 to 150 cm | Terrestrial organic matter preservation in suboxic conditions |

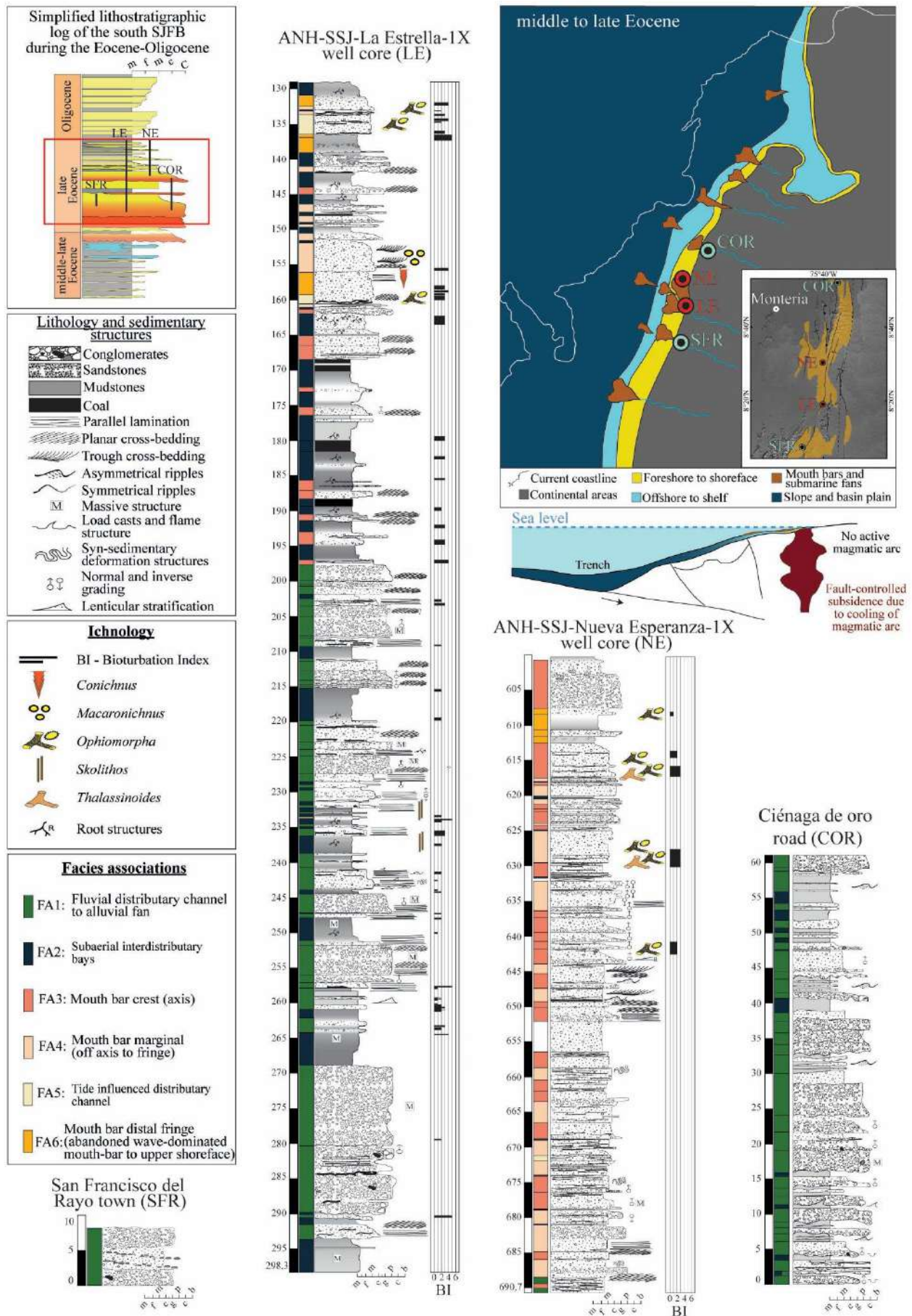


Fig. IV.2. Stratigraphic sections of middle to late Eocene, with data lithology, sedimentary structures, and ichnology. Facies associations have been differentiated.

IV.5.1. FA 1 Fluvial distributary channel to alluvial fan

Description. FA1 consists of clast-supported, pebbles- to granule-size conglomerates, poorly-sorted, angular clasts, displaying ungraded or normal graded structures (Fig. IV.3). The beds have sharp, erosional bases and range in thickness from 1 to 3 m (Fig. IV.3). Lags of outsized subangular clasts (up to pebble-size) are commonly found floating within structureless sandstones overlying the basal surface. FA1 also exhibits transitions to horizontally stratified, centimetre-thick, normal-graded gravel and sandstone beds. Transitions are common, with apparent normal grading from pebbles- to granule- to very coarse-grained sandstones (pebbly sandstone), as well as some inverse grading. These deposits are poorly sorted and massive, with scattered outsized granules or pebble-sized clasts embedded in the sandstone matrix.

Normal grading continues into medium- to fine-grained sandstones, which often contain carbonaceous detrital lenses and are well-sorted and massive. These sandstones feature carbonaceous-prone clay chips in diffuse flaser-like lamination that form mud-drape-like structures. They have sharp, irregular-bases, occasionally containing rare mud (coal) clasts, and range in thickness from 2 to 10 cm. In outcrop, FA1 appears to have a lenticular morphology and is often multi-storey, nested, and offset-stacked. However, due to limited extent of the outcrop, it is difficult to determine definitively whether the structures are channelized. Notable occurrences of FA1 have been documented at San Francisco del Rayo, ANH-SSJ-La Estrella-1X, and along the Ciénaga de Oro Road outcrop.

Interpretation. The random orientation of the outsized clasts within the massive sandstones suggests that these clasts were transported by rolling and subsequently trapped by high rates of sand aggradation (Benvenuti and Martini, 2002). This indicates poorly diluted (liquefaction or fluidization features are lacking), highly aggradational bedload deposits controlled by frictional forces, where high grain concentration prevents fall-out suspension (Mulder and Alexander, 2001). Rapid deceleration immediately seaward of the outlet leads to frictional freezing due to grain-to-grain interaction (Lowe, 1988). Therefore, these facies are interpreted as deposits from hyperconcentrated flows (Wasson, 1977; Nemeč and Muszyński, 1982; Smith, 1986; Mulder and Alexander, 2001; Benvenuti and Martini, 2002).

In contrast, the overlying stratified deposits are interpreted as the result of traction transport and deposition from bedload (gravel) and suspension (coarser sand grains close to the bed). Traction transport is favoured when the flow exhibits more fluidal behaviour, typically as sediment concentration decreases (Mulder and Alexander, 2001). Inverse grading occurs due to an upward velocity gradient within the flow and the laminar flow regime (Mulder and Alexander, 2001), which suggests that subaqueous hyperconcentrated flows may evolve into lower-concentrated flows. These processes are characteristic of alluvial fan environments or fluvial channels (e.g., Rust and Koster, 1984; Nemeč and Steel, 1988; Orton, 1988; Mulder and Alexander, 2001), although the degree of flow confinement cannot be determined with certainty.

IV.5.2. FA2 Subaerial interdistributary bays

Description. FA2 is characterised by mottled green-grey mudstones beds up to 5 m thick, massive, and containing root structures, Fe-oxidised nodules, and coal layers reaching up to 1 m in thickness (Fig. IV.4). Some intervals include very fine- to fine-grained sandstone beds with sharp bases, ranging from 0.1 to 0.3 m

in thickness, and displaying root structures (Fig. IV.4). These sandstone intervals exhibit lateral continuity over distances of 7-8 m. FA2 shows sharp contacts and transitions to FA1. Notable occurrences of FA2 have been documented at San Francisco del Rayo, ANH-SSJ-La Estrella-1X, and along the Ciénaga de Oro Road outcrop.



Fig. IV.3. Facies association 1 (FA1). **A.** Irregular surface (white dashed line) of pebble- to cobble-size conglomerates with normal-grading overlaid by mudrocks with root structures (top to the left). **B.** Irregular sharp-based (white dashed line) and basal inverse grading (black triangle) gravel deposits (lithofacies Gcs) overlying dark mudstones (lithofacies M). **C.** Normal-grading (black triangle) gravel deposits (lithofacies Gcs-SGm) overlaid by ungraded gravels (lithofacies Gcs). **D.** Normal-grading (black triangle) gravel deposits (lithofacies Gcs). **E.** Sharp-topped (white arrow) gravel deposits (lithofacies Gcs) overlaid by well-sorted, massive fine-grained sandstone (lithofacies Sm). Look at largest clasts at the top climbing stepped upper levels toward the right (yellow arrow). **F.** Ungraded gravel (lithofacies Gcs and SGm) with scattered, randomly distributed and oriented outsized pebble clasts (white arrows). **G.** Sharp change of grain size (black arrow) at the boundary between massive sandstone (lithofacies Sm) and clast-supported gravels (lithofacies Gcs). **H.** Heterolithic deposits (lithofacies H) represented by the interbedding of fine-grained “clean” (light colour) and “dirty” (dark colour) sandstones related to variations of terrestrial organic remains. They appear at the top of massive sandstones (lithofacies Sm) occurring at the upper part of the coarse-grained packages. **I.** Centimeter-thick, normal-graded (black triangle), horizontally stratified gravelly-sandstones (lithofacies Gh) at the top of gravel package (lithofacies Gcs). **J.** Massive, very coarse- to coarse-grained sandstone (lithofacies Sm) with scattered, random oriented, subangular pebble clasts (white arrows). **K.** Sharp-based (white arrow) between well-sorted, massive fine-grained sandstone (lithofacies Sm) overlying homogeneous mudstones (lithofacies M). Look at a mud drape (yellow arrow) and lenses of organic laminae into sandstones (orange arrow). **L.** Massive, very coarse- to coarse-grained sandstone (lithofacies Sm) with scattered, random oriented, subangular pebble clasts (white arrows). Look at the vertical orientation of the clast closest to the right, lower part of the core. **M.** Planar-lamination sandstones (lithofacies Sh) constituted of centimeter-thick, normally graded coarse sandy layers.

Interpretation. The variegated mudrocks with rhizoliths in FA2 indicate deposition in low-energy environments. The transitions from FA1 suggest a rapid shift from active flow or fluvial discharge to the establishment of permanent vegetation (Makaske, 2001; Retallack, 2001). These deposits are associated with the preservation of terrestrial organic matter in suboxic conditions, likely representing mire and ponds on the floodplain of the main channel or subaerial interdistributary bays (Makaske, 2001; Retallack, 2001; Bridge, 2003, 2006; Yeste et al., 2020).

IV.5.3. FA3 Mouth bar crest (axis)

Description. FA3 consists of matrix-supported, pebbles- to granule- size conglomerates, subangular and poorly sorted, ungraded or massive in structure, occasionally presenting *Ophiomorpha* (BI = 1), and ranging in thickness from 0.3 to 1 m (Fig. IV.5). Some clasts present a red thin coating around them. Some intervals show coarsening and thickening-upwards trends, transitioning from sandstones to conglomeratic deposits with thicknesses of 2-3 m. The sandy intervals feature coarse- to medium-grained sandstones, planar cross-lamination, and evidence of soft sediment deformation. Millimeter-thick dark mudstone or terrestrial organic debris-prone laminae appear within the dipping laminae forming alternation with sandstones (Fig. IV.5). FA3 overlies the gravel deposits of FA1, which are associated with hyperconcentrated flows. Significant examples of FA3 have been identified at the ANH-SSJ-La Estrella-1X and ANH-SSJ-Nueva Esperanza-1X well-cores.

Interpretation. Sandy intervals with planar cross-lamination represent the migration of 2D dunes under unidirectional flow conditions in the lower flow regime, as well as the migration of 2D-megaripple caused by fluvial traction currents, which induce drag-controlled liquefaction and deformation (Shanmugam, 2009; Miall, 2014; Zavala, 2020). The upward-increasing amalgamation from sandstones to matrix-supported gravelly deposits, occasionally bioturbated by *Ophiomorpha*, is associated with high-energy deposition near

the river mouth (Wright, 1977; MacEachern et al., 2005; Enge et al., 2010; Ainsworth et al., 2016; Fidolini and Ghinassi, 2016). Mouth bar deposits typically display coarsening-upward successions, with the coarser intervals found at the top (e.g., van Yperen et al., 2020). Contorted or deformed cross-beds are commonly observed at the mouth-bar crest and the coarse-grained front of the mouth-bar, where factors such as high sedimentation rate, slope oversteepening, and steep foresets (seaward slopes) promote slope instability and deformation (Kostaschuk and McCann, 1983). Deposition from debris flows that transition to high- and low-density turbidity currents is suggested by the presence of stratified turbulent flows. These are evidenced by clast-supported conglomerates in certain intervals, alternating with structureless, planar laminated, or cross-stratified sandstones. Carbonaceous detrital dark laminae highlight lamination, which is often associated with hyperpycnal flows (Lowe, 1982; Zavala et al., 2011; Talling et al., 2012; Zavala, 2020).



Fig. IV.4. Facies association 2 (FA2), and transitions to and from FA1. **A.** Apparently lenticular body (lithofacies Gcs), 0.7 m thick, with net contact to mudstone (lithofacies M). **B-C-D.** Dark mudstones (lithofacies M; FA2) overlain by irregular-based (white dashed line) gravelly deposits (lithofacies Gcs and SGM). **E.** Mudstones (lithofacies M) with Fe-oxidised nodules (white arrow). **F.** Mudstones (lithofacies M) with root structures (white arrow). **G.** Massive coal (lithofacies C). **H.** Fine-grained sandstones (lithofacies Sm) with root structures (white arrows).

IV.5.4. FA4 Mouth bar marginal (off axis to fringe)

Description. FA4 is composed by medium- to fine-grained, well-sorted sandstones with carbonaceous detrital lenses, which are discontinuous (Fig. IV.6). These sandstones are typically massive, with occasional planar cross-lamination, featuring carbonaceous-prone clay chips in diffuse, flaser-like lamination (Fig. IV.6). The beds have sharp and irregular bases and occasionally contain aligned mud (coal) clasts, ranging in thickness from 2 to 10 cm. Bioturbation by *Ophiomorpha* (BI = 1-2) is present in some cases (Fig. IV.6). Additionally, FA4 includes fine alternations of millimeter-thick mud and fine-grained sandy sheets, with plant remains and carbonaceous-rich dark layers, forming heterolithic deposits with asymmetrical ripples. This facies association often caps coarse-grained sandstones to gravelly deposits (FA1) through an erosional contact. Soft-sediment deformations, such as contorted cross-beds, recumbent folds, or convolute lamination, are also commonly observed. Significant examples of FA4 have been identified at the ANH-SSJ-Nueva Esperanza-1X well-core.

Interpretation. Fine- to medium-grained sandstones with diffuse flaser lamination and levels of parallel-aligned clasts, along with high concentration in plant remains that highlight the lamination, are formed by poorly confined flows with pulsating energy (Mulder and Alexander, 2001). These flows result in alternating fallout and bedload deposition (Zavala, 2020; Melstrom and Birgenheier, 2021). Suspended load facies, include massive, laminated, and rippled fine-grained sandstones, originate from the progressive loss of flow capacity in sustained hyperpycnal flows, leading to the collapse of suspended materials at varying rates of sediment fallout and flow velocity (Zavala and Pan, 2018). The sandy deposits, often containing angular clasts and coal fragments, with *Ophiomorpha*, indicate marine influence, potentially in mouth bar positions away from the central axis of the crest (off axis to fringe), where energy peaks from hyperpycnal flows, potentially linked to flood events, are less intense than FA3 (Mulder and Alexander, 2001; Mulder et al., 2003; Zavala, 2020). Some intervals with rhythmites, alternating between mudstone and sandstone laminae, likely reflect tidal influences in the off-axis mouth bar setting (van Yperen et al., 2020). Liquefaction and fluidization processes, deforming foreset laminae of migrating dunes in tidal environments, are associated with autogenic overloading triggers. Wave-induced liquefaction is also considered a possible mechanism for explaining deformed cross-lamination in crest and stoss ebb megaripples in intertidal settings (Davis and Dalrymple, 2012).

IV.5.5. FA5 Tide influenced distributary channel

Description. FA5 consists of sandy-dominated heterolithic deposits, primarily characterised by very fine- to fine-grained sandstones (Fig. IV.7). These sandy beds are typically structureless with sharp bases, or display trough cross-lamination and reactivation surfaces, ranging in thickness from 0.1 to 0.4 m. They alternate with thin mudrock beds, which are 1 to 10 cm thick.



Fig. IV.5. Facies association 3 (FA3). **A.** Massive, chaotic matrix-supported gravelly deposits (lithofacies Gms). Note the subangular to subrounded texture of some of the bigger clasts and a red thin coating around them (white arrows). **B.** Poorly sorted, granule to very coarse sandstone (lithofacies SGm) overlay by fine alternation of fine-grained and carbonaceous-rich detrital sandy beds (lithofacies H/Sh), and irregular contact at the top with clast-supported, poorly sorted angular pebbles- to granule-size conglomerates (lithofacies Gcs). **C.** Fine-grained sandstone with carbonaceous detrital dark layers (white arrow) (lithofacies Sh) with scattered, random oriented, subangular pebble clasts (yellow arrow) and some intervals with increase grain-size to matrix-supported, poorly sorted subangular pebbles to granule-size conglomerates (lithofacies Gms) (orange arrow). **D.** Poorly sorted featuring planar cross-lamination, granule- to very coarse-grained sandstone (pebbly sandstone-like; lithofacies SGm, Sh) with some carbonaceous detrital sheets (white arrow). **E.** Sharp irregular contact between heterolithic (lithofacies H) – mudstone (lithofacies M) deposits at the base and poorly sorted, granule (white arrow) to very coarse sandstone (lithofacies SGm) with high content of carbonaceous detrital. **F-G.** Fine- to medium-grained sandstone (lithofacies Sm) with some scattered, random oriented, subangular pebble clasts (white arrows) bioturbated by *Ophiomorpha* (Op). **H-I.** Detail of matrix-supported, poorly sorted subangular pebble- to granule-size (white arrow) conglomerates (lithofacies Gms).

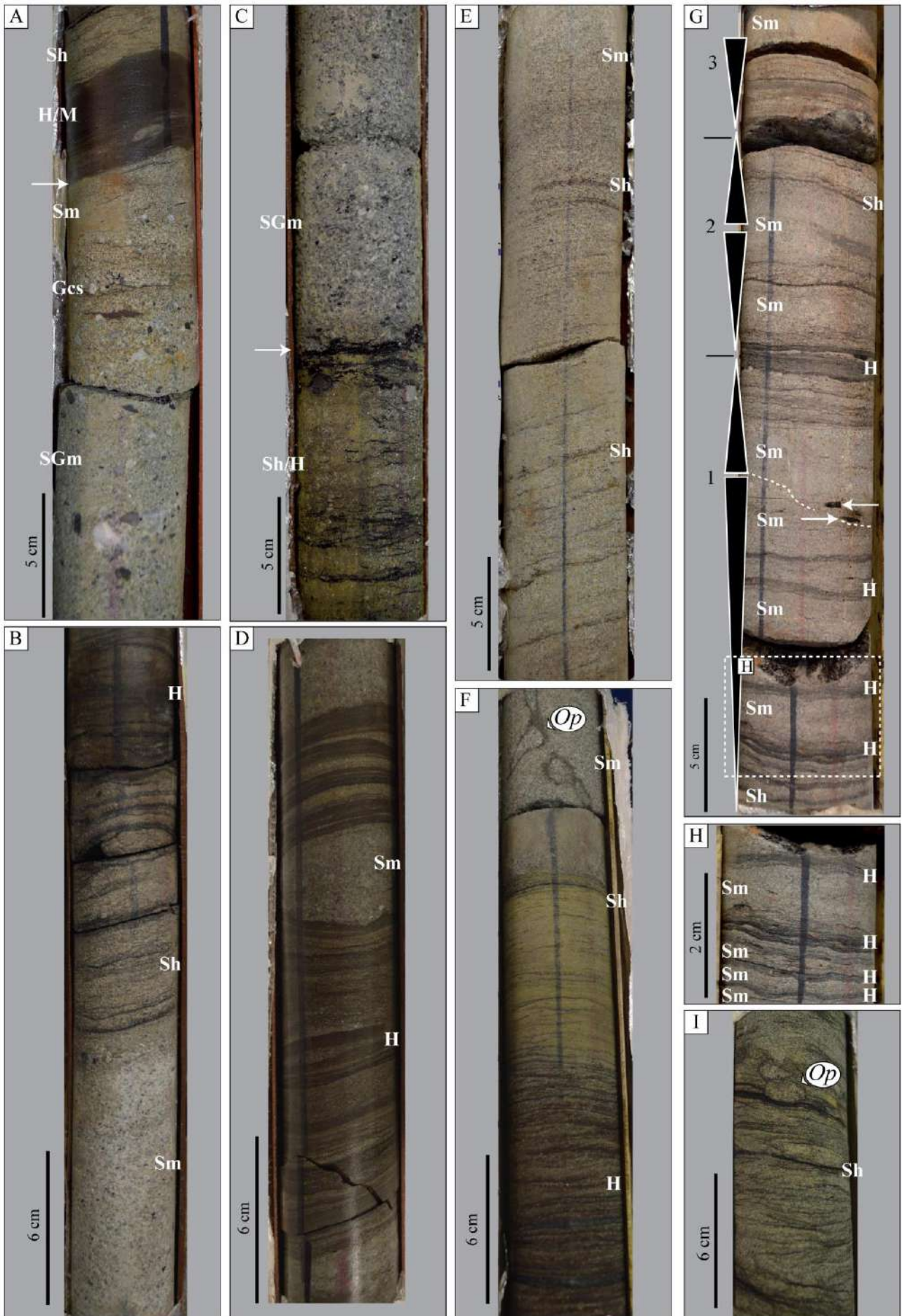


Fig. IV.6. Facies association 4 (FA4). **A.** Sharp contact (white arrow) between underlying gravel/sandstones (lithofacies SGm, Gcs, Sm) and overlying finer lithofacies (lithofacies H/M/Sh). **B.** Transition from medium-grained sandstone (lithofacies Sm) to carbonaceous-rich dark sandy layers highlighting lamination (lithofacies Sh, H). **C.** Sharp and erosional-based (white arrow) between massive coarse-grained sandstone deposits (lithofacies SGm) overlying heterolithic deposits of fine-grained sandstones containing carbonaceous-prone clay chips (lithofacies Sh/H). **D.** Interbedding of fine-grained sandstone with carbonaceous-prone clay chips in flaser-like lamination (lithofacies H) and massive fine-grained sandstone beds (lithofacies Sm). **E.** Planar cross-laminated sandstones (lithofacies Sh) with abundant, upward-decreasing carbonaceous clay chips in the lower part, transitioning into heterolithic facies and massive sandstone (lithofacies Sm) toward the top. **F.** Fine-grained sandstone beds with carbonaceous-rich debris, highlighting horizontal lamination (lithofacies H, Sh). Carbonaceous detritus decreases toward the top, with a sharp contact to massive fine-grained sandstone (lithofacies Sm) containing *Ophiomorpha* (*Op*). **G.** Three (1-3) decimetric-thick, coarsening-and-thickening to finning-and-thinning (black triangles) sandstone (lithofacies Sm) and heterolithic (lithofacies H) alternating successions. Note the mud clasts (white arrows) indicating normal grading on an erosional surface (dotted line). **H.** Detail of the lowermost part from the previous image G, showing alternating sharp-based, massive sandstone (lithofacies Sm) laminae and dark, carbonaceous-prone clay laminae (lithofacies H). **I.** Fine-grained sandstone with irregular horizontal lamination (lithofacies Sh), highlighted by concentrations of carbonaceous detrital laminae, with *Ophiomorpha* (*Op*) present between the laminae.

The muddy layers occasionally feature draped or double-draped mud and show asymmetrical ripples in places (Fig. IV.7). Common elements in FA5 include wood debris and mud rip-up clasts. Bioturbation occurs in both fine-grained sandstones and mudrocks but is sporadic and of low in abundance (BI = 0-2), with trace fossils such as *Macaronichnus*, *Ophiomorpha*, and *Thalassinoides*. FA5 deposits are observed to erosively incise into underlying mouth-bar deposits (FA3). In certain intervals, pebble-sized conglomerates, associated with FA1 and FA3 are sharply in contact with the mudrocks. Significant examples of FA5 have been identified at the ANH-SSJ-Nueva Esperanza-1X well-core.

Interpretation. The heterolithic nature of FA5 likely results from variations in fluvial discharge (Gugliotta et al., 2016). The presence of 10 cm-thick mud drapes or mudrocks intervals suggests periods of mud fluids associated with tidal influence (Baas et al., 2016). Mudstone laminae are formed by mud suspension settling during slackwater periods, when tidal currents are minimal, while sandstone laminae are deposited during more energetic ebb and flood tidal currents. This reflects the cyclical nature of diurnal or semidiurnal tidal regimes (Dalrymple and Choi, 2007). Features such as double mud-draped ripple laminae, trough cross-lamination, and reactivation surfaces, observed in relation to channel fills (FA1) and the mouth bar axis (FA3), are consistent with tidal processes (Nio and Yang, 1991), though not exclusively diagnostic of them. Rather than indicating tidal dominance, FA5 is interpreted as representing the infill of tide-influenced distributary channels, where tidal effects intermittently impact flow energy. The observed bioturbation, though reflective of high-energy conditions, is less pronounced compared to deposits near the mouth bar axis (Gani et al., 2007). Overall, this facies association illustrates the dynamic interplay between fluvial and tidal processes in shaping the sedimentary architecture at the distal fringe of mouth bars (Dalrymple et al., 1992).

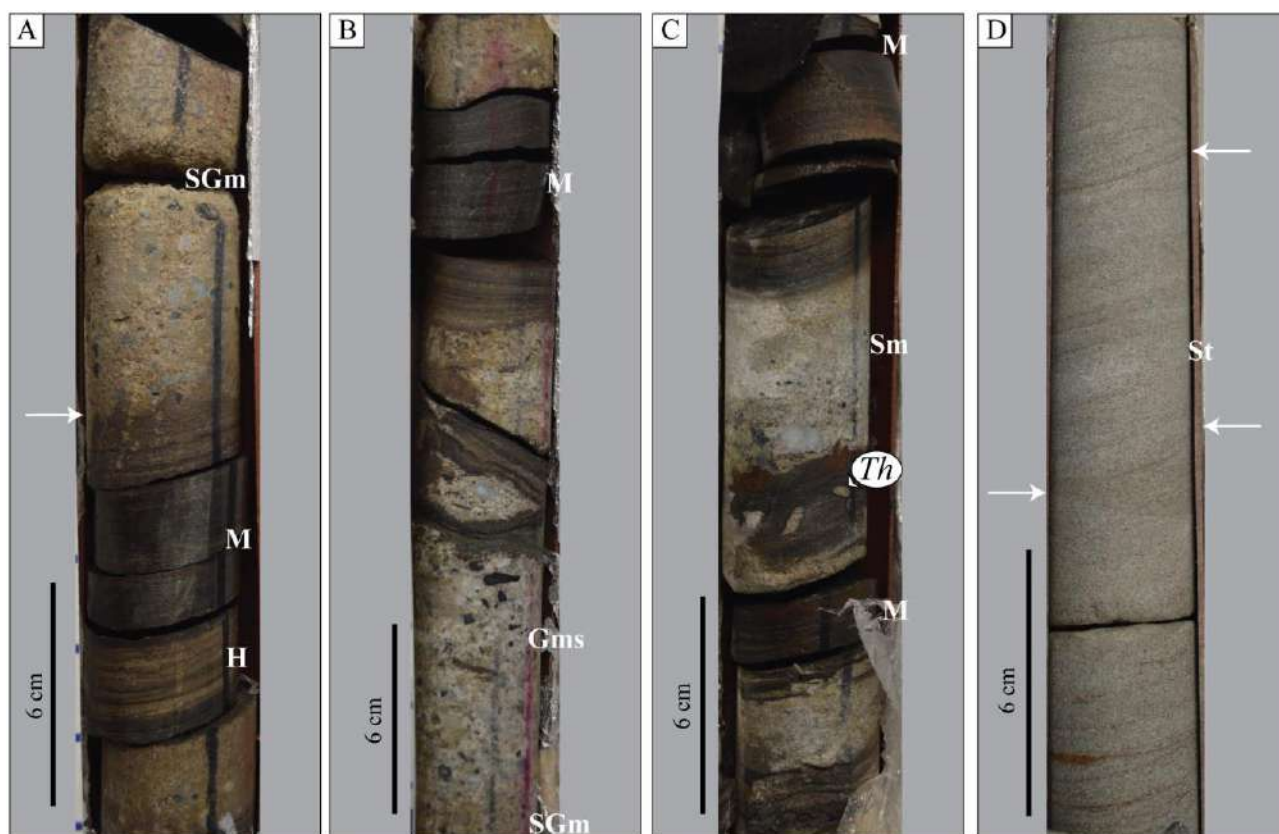


Fig. IV.7. Facies association 5 (FA5). **A.** Sharp irregular contact (white arrow) between mudstone interval (lithofacies M) overlain by poorly sorted, granule- to very coarse sandstone (lithofacies SGm). **B.** Matrix-supported, poorly sorted subangular pebble- to granule-sized conglomerate (lithofacies SGm, Gms) in irregular, deformed contact with a mudstone interval (lithofacies M). **C.** Interbedding of poorly sorted, granule- to very coarse-grained sandstone (lithofacies Sm) with mudstone intervals (lithofacies M), bioturbated by *Thalassinoides* (*Th*). **D.** Fine-grained sandstone displaying trough cross-lamination (lithofacies St) and reactivation surfaces (white arrows).

IV.5.6. FA6 Mouth bar distal fringe (abandoned wave-dominated mouth-bar to upper shoreface)

Description. FA6 are constituted by well-sorted fine-grained sandstones with symmetrical ripples, along with scattered dark mud laminae (Fig. IV.8). Medium-grained sandstones with trough cross-lamination are also present. Some intervals feature poorly sorted fine-grained sandstones with occasional embedded pebble-sized clasts. The beds representing this FA are typically no more than 10 cm thick. Trace fossils such as *Conichnus*, *Ophiomorpha*, and *Thalassinoides* (BI = 1-4; Fig. IV.8) are occasionally observed. Other intervals are characterized by well-sorted, medium- to fine-grained sandstones with discontinuous carbonaceous detrital lenses, massive structures, carbonaceous-prone clay chips in diffuse flaser-like lamination, sharp and irregular bases, rare mud (coal) clasts, and bed thicknesses ranging from 2 to 10 cm. Significant examples of FA6 have been identified at the ANH-SSJ-Nueva Esperanza-1X well-core.

Interpretation. Symmetrical ripples in sandstones suggest a relatively high-energy environment, controlled by oscillatory wave processes in the upper to middle shoreface (Tinterri, 2011). Trough cross-lamination represents the migration of 3D ripples and megaripples under unidirectional flow (i.e. alongshore currents) in the lower flow regime. Prolonged wave action generates high energy, removing mud from the seafloor, but the

energy is not overwhelming, allowing for the presence of suspension-feeding organisms like those producing *Ophiomorpha* (Gani et al., 2007). The local occurrence of mudrocks forming heterolithic lamination suggests a decrease in energy compared to sandstone-dominated areas, with weak tidal influence (e.g., Ainsworth et al., 2016; Cole et al., 2021).

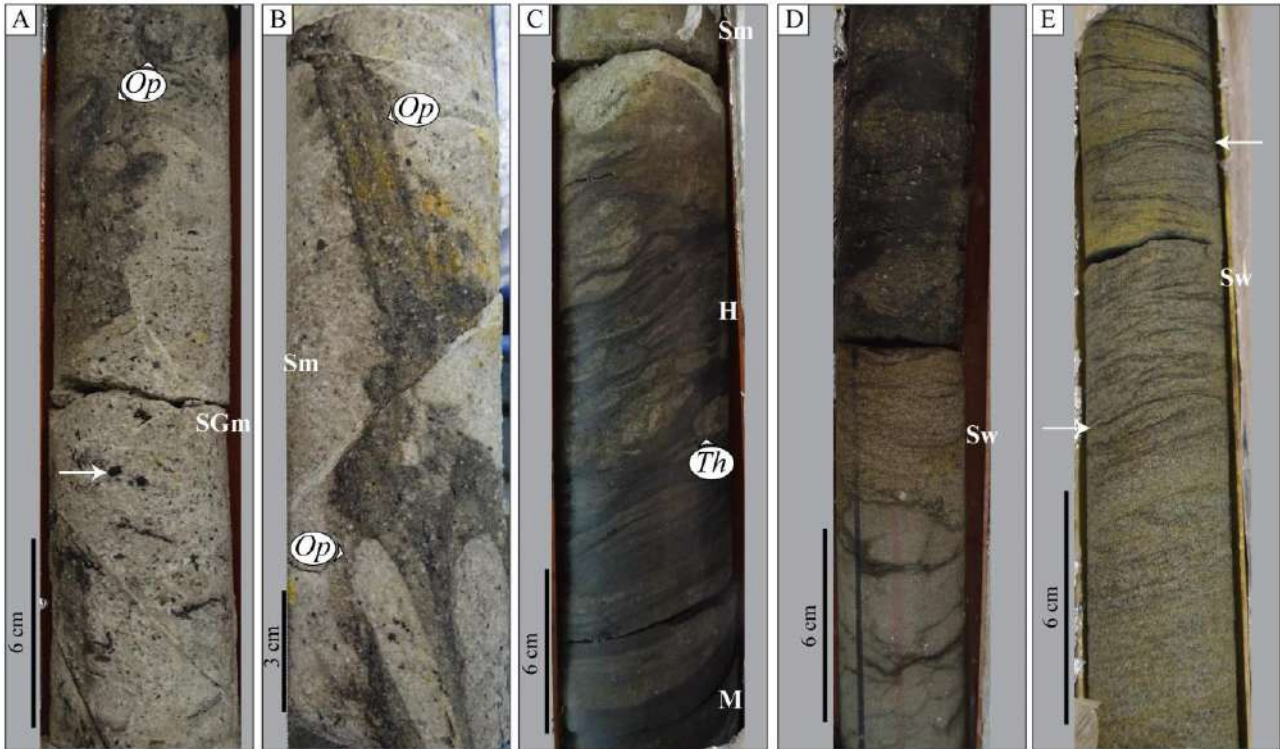


Fig. IV.8. Facies associations 6 (FA6) **A.** Poorly sorted, granule- to very coarse-grained sandstone containing coal pebbles (white arrow), with highly bioturbation by *Ophiomorpha* (*Op*). **B.** Medium-grained sandstones (lithofacies Sm) with a high bioturbation index, dominated by *Ophiomorpha* (*Op*). **C.** Muddy (lithofacies M) interval transitioning into heterolithic (lithofacies H) bioturbated deposits by *Thalassinoides* (*Th*), and massive sandstone (lithofacies Sm). **D-E.** Symmetrical cross-laminated fine-grained sandstones (lithofacies Sw) with scattered dark mud laminae (white arrows).

IV.6. Depositional model and control factors

IV.6.1. Hyperconcentrated to hyperpycnal flows in continental areas

The study of fluvial sedimentation processes and their deposits has been extensively addressed in the geological record across various tectonic settings (e.g., Allen, 1983; Bridge and Tye, 2000; Gouw and Berendsen, 2007; Aslan, 2013). Typical fluvial channel successions are often characterised by sand and gravel fills, appearing as lenticular bodies or thick tabular sheets with complex bedding geometries and erosive bases. These successions may include overbank deposits, such as natural levees, crevasse splays, and flood basins, depending on the fluvial style (e.g., Allen, 1983; Jenson and Pedersen, 2010; Yeste et al., 2020). However, the successions observed in this study deviate from these typical clear-water fluvial deposits commonly found in continental settings. Instead, they are dominated by deposits associated with hyperconcentrated flows (FA1), as indicated by the stratigraphic architecture and rapid facies transitions observed in sections such as San Francisco del Rayo, the base of ANH-La Estrella-1X, and Ciénaga de Oro Road (Figs. IV.2 and IV.3). These repetitive successions provide a unique opportunity to analyse the sedimentary dynamics and depositional

processes of hyperconcentrated and hyperpycnal flows in a fluvial context (e.g., Benvenuti and Martini, 2002; Brenna et al., 2021; Melstrom and Birgenheier, 2021) and the arrive to the coastline (Figs. IV.9, IV.10 and IV.11).

These deposits are primarily clast-supported, with no evidence of matrix support. Grain distribution is predominantly normal- or inverse-graded, characterised by abrupt vertical changes in grain size, transitioning from sand to pebbles or pebbles to sand. The main sedimentary structures observed include massive structures or horizontal stratification/lamination. The deposits are poorly sorted, containing a high volume of subangular granules to coarse sand.

Sharp-based, massive coarse-grained sandstone with outsized pebble clasts is interpreted as the result of high competence, sand-concentrated flows, where high-velocity sand settling from suspension led to rapid deposition and a high rate of sediment aggradation (Fig. IV.9). Following these deposits, sharp-based, normally graded gravel beds suggest a more fluid and turbulent flow, capable of bedload transport of the largest clasts, with grain size-conditioned settling from suspension (Fig. IV.9). The middle part of the gravel package consists of unstratified deposits containing the largest clasts, likely representing the flood peak. The uppermost deposits are horizontally stratified transitioning to coarse- to medium-grained sandstones associated with waning flood flow (Fig. IV.9).

The absence of mud laminae and the lack of abrupt vertical grain size changes within the gravel suggest a single-story depositional process. Each gravel package likely records the rising and falling discharge of a flooding river. Variations in gravel package features —such as thickness, vertical grain size, and the concentration of the largest clasts in the middle— indicate that these gravel deposits represent a prolonged, unsteady flow, likely caused by a seasonal river flood (Fig. IV.9). On the other hand, the intercalation of conglomerate and sandstone beds with mudstone beds containing root structures, associated with FA2, highlights episodes of low hydrodynamic energy and reduced sedimentation rates, as well as probable subaerial exposure (Fig. IV.9). This suggests a possible cessation of the torrential flow.

IV.6.2. Mouth bars (Flow transformations and wave- tidal- signals)

The arrival of flows at the coastline triggers an interaction between gravitational flow processes and marine processes, highlighting the interplay between the feeder system and the receiving basin (Figs. IV.10 and IV.11). In many cases, the absence of marine elements and tractive structures in the gravelly beds may indicate the rapid arrival of gravitational flows to the basin (FA3), linked to distributary channels prograding seaward (Kleinspehn et al., 1984; Nemeč and Steel, 1984; García-García et al., 2006). However, evidence also suggests that flows may undergo transformations upstream or upon contact with the marine system (FA4-FA5-FA6). The driving force behind hyperconcentrated density flows is primarily gravity (Mulder and Alexander, 2001). This suggests a steep delta feeder system (i.e. alluvial fan or braided fluvial systems) and a short fluvial-marine transition upstream from mouth bars (Fig. IV.11). The poor-maturity of coarse-grained deposits reflects short transport from the source (with minimal fluvial or coastal buffering) via sediment-gravity flows with laminar rheology.

Metric-scale successions of unstratified gravel deposits, containing large, poorly sorted, and immature clasts, interbedded with rhizolite-bearing clays from continental areas with pollen and spores, laterally transition to coarse-grained sandstones with massive structures, conglomeratic sandstones with horizontal lamination, and organic debris highlighting the lamination (FA3-FA4). These characteristics align with records of high-velocity currents, likely associated with bedload transport under hyperpycnal flow conditions during torrential rain events (e.g., Zavala, 2020).

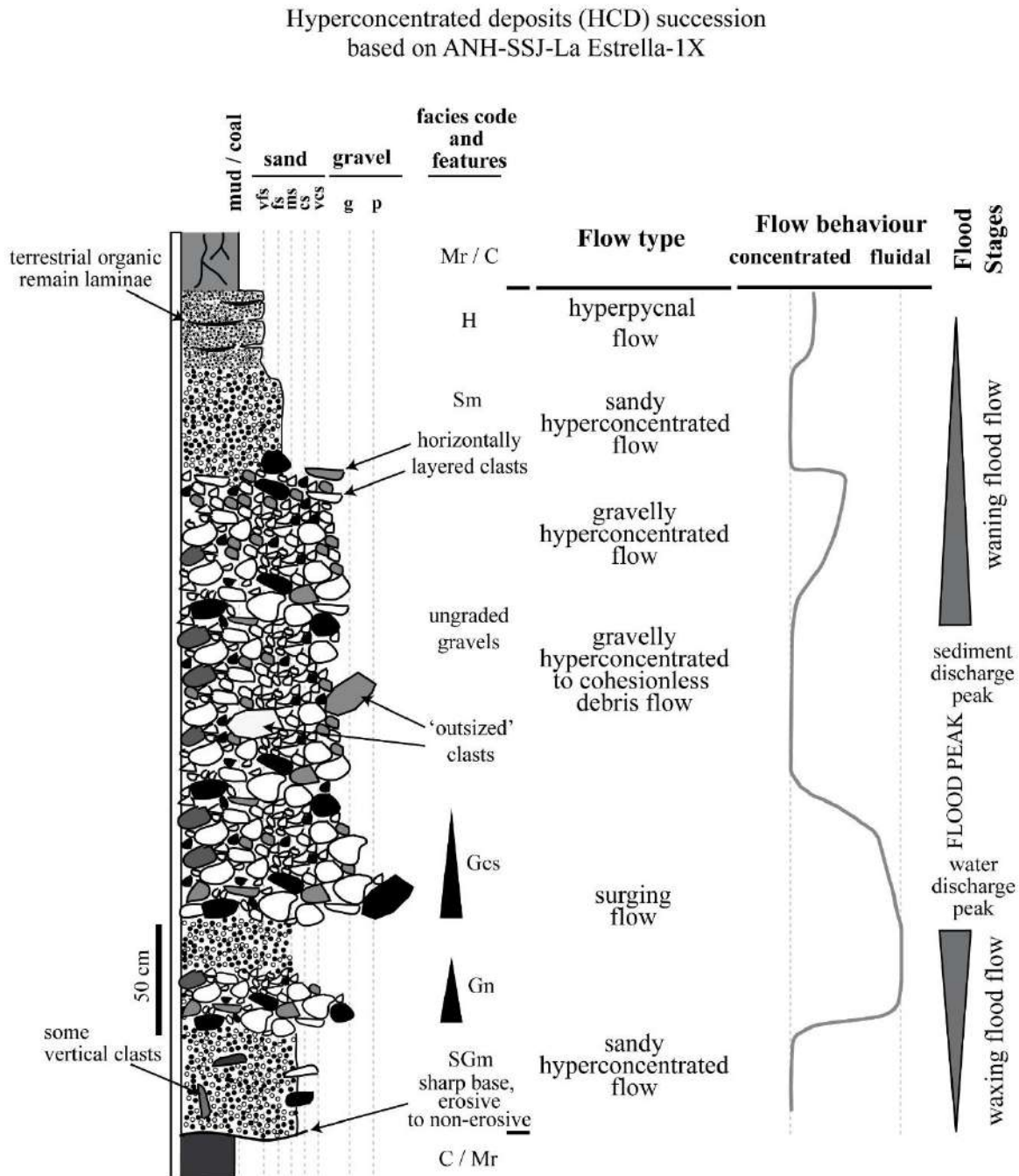


Fig. IV.9. Succession of flow transitions (based on ANH-SSJ-La Estrella-1X), starting with sandy hyperconcentrated flow and waxing flood flow (grey triangle), progressing to flood peak with gravelly hyperconcentrated flow, cohesionless debris flow, and finally waning flood flow (grey triangle). This followed by a return to sandy hyperconcentrated flow and hyperpycnal flows. These transformations occur on floodplains with sharp boundaries or rapid transitions. Additionally, internal changes are observed, including surging flows (black triangles) and shifts from concentrated to fluidal flow behavior.

Asymmetrical ripples, trough cross-lamination, and planar cross-bedding/lamination suggest traction and suspended load deposition during flow slowdowns in a low-flow regime (FA4) (Mulder et al., 2003; Zavala et al., 2011; Slater et al., 2017). Toward the upper parts of the hyperpycnal deposits, thick beds of medium- to coarse-grained sandstones and pebble- to cobble-sized conglomerates (both matrix- and clast-supported) with normal grading exhibit a bigradational trend. The poorly sorted, angular clasts, sometimes overlain by convolute lamination (FA4), are likely associated with gravity flows originating from continental areas (Shanmugam, 2009; Talling et al., 2012; Zavala, 2020) via sediment-gravity flows with laminar rheology, which then change upon reaching the coastline due to interaction with seawater.

Hyperpycnal-dominated succession
based on ANH-SSJ-Nueva Esperanza-1X

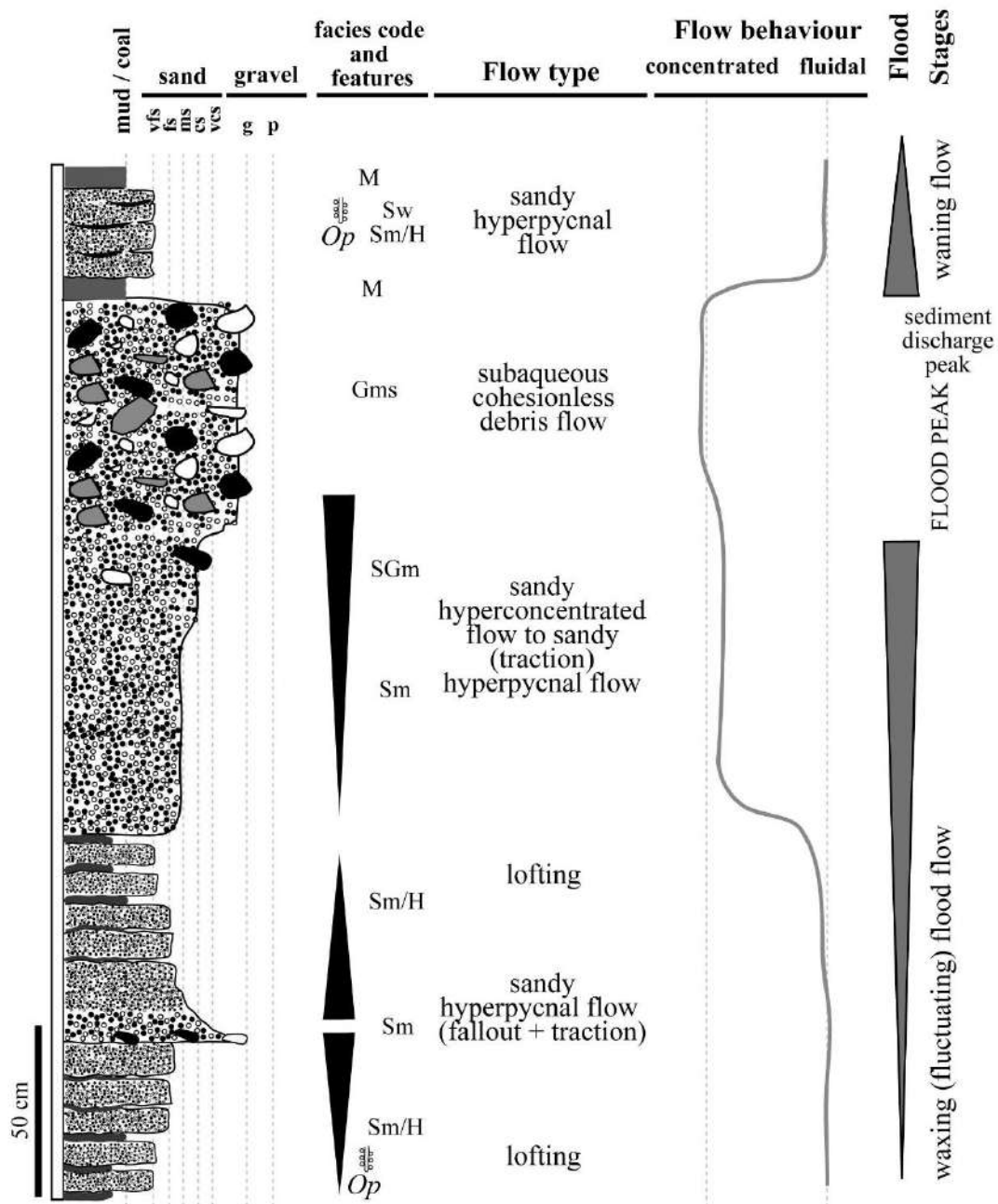


Fig. IV.10. Succession of flow transitions (based on ANH-SSJ-Nueva Esperanza-1X), beginning with sandy hyperpycnal flow and waxing flood flow, progressing to sandy hyperconcentrated flow, where the flood peak results in subaqueous cohesionless debris flow. This is followed by waning flow, returning to sandy hyperpycnal flow. Internal changes are also observed, including fluctuations during the waxing phase (black triangles), where flow behavior shifts from fluidal to concentrated (grey triangles). These changes may be driven by upstream avulsion or a decrease in sediment input, enhancing the marine influence as the flow reaches the coastline. Consequently, wave- or tidal-related signals are detected through ichnological evidence (e.g., *Ophiomorpha Op*) and sedimentary structures associated with reworking by waves or tides.

Some authors propose that the transition between hyperconcentrated and concentrated flows occurs when particles are free to sort through settling as the flow evolves (e.g., Benvenuti and Martini, 2002; Nemeč, 2009). In hyperconcentrated flow deposits, normal grading is minimal or absent, except near the top, where deposition results from a more dilute suspension cloud (Mulder and Alexander, 2001). These flows transport significantly larger loads of sand compared to normal stream flows, even with low clay concentrations (Pierson and Scott, 1985). Hyperpycnal deposits are also interbedded with medium- to fine-grained sandstones, forming well-sorted successions. The presence of structures possibly associated with tidal and wave processes, along with sporadic occurrences of *Ophiomorpha*, indicates interaction between sediment flows and marine environments (FA4-FA6).

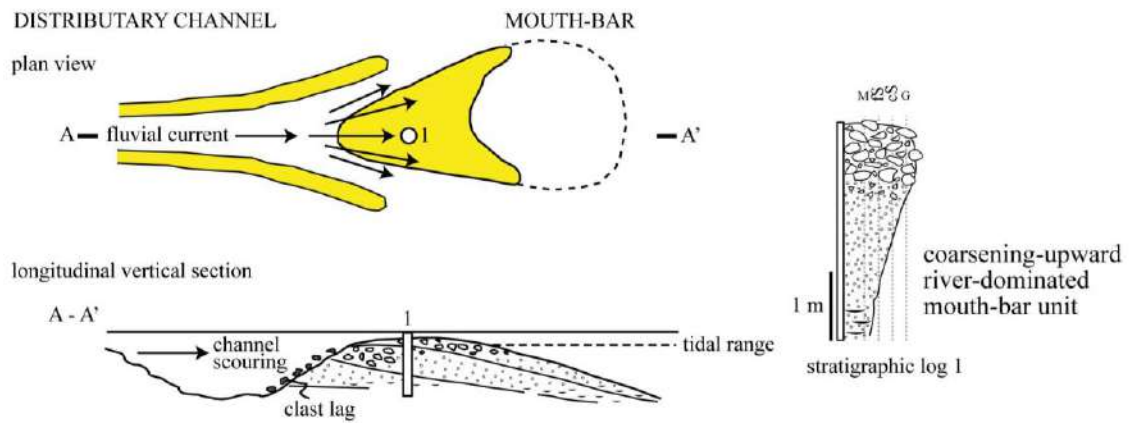
The high sediment yield and bedload dominance of the river suggest frequent channel avulsions and shifts across the lower delta plain. River-dominated distributary mouth bars formed when tidal and wave processes were unable to overpower river dynamics, allowing coarse sediment to accumulate as the distributary channel remained active and its mouth bar prograde seaward (FA3; Fig. IV.11).

However, upstream avulsion of the distributary channel reduced flow energy, enabling tidal and wave influences to dominate (FA5-FA6). These deposits suggest intervals of mouth-bar-type deltas development. The formation of these deltas is typically associated with relatively stable fluvial distributaries in low-energy, shallow-water basins beyond the outlet zone (see mouth-type delta in Postma, 1990). Yet, recurrent periods of torrential rainfall altered the conditions and characteristics of the mouth bar.

Due to the steep gradient of the delta and the presence of coarse-grained deposits in the mouth-bar area, tidal influence remained confined to distributary channels. Sediment from the active distributary channel continued to deposit, while other channels were largely abandoned, as observed in modern examples like the Fly delta in Papua New Guinea (Dalrymple et al., 2003). The coarse deposits at the mouth-bar crest limited tidal reworking, preventing the formation of elongated tidal bars commonly seen in fine-grained nearshore systems. Tidal current velocities in distributary channel were stronger than those on the delta front, as illustrates by the Bella Coola delta in Canada (Kostaschuk and McCann, 1983).

Towards the upper parts of the ANH-SSJ-La Estrella-1X and ANH-SSJ-Nueva Esperanza-1X well-cores, marine influence becomes increasingly prominent. The hyperconcentrated and hyperpycnal flows diminish, and the thickness of mudstone intervals, associated with interdistributary bays, increases. FA5 and FA6 dominate the uppermost sections, intermittently interrupted by FA3 and FA4. Significant increases in bioturbation indexes reflect the growing marine influence within the system. Bars developed on the mouth-bar crest (overlying the coarsest deposits) migrated seaward during the waning stages of flooding.

A FLUVIAL-DOMINATED ACTIVE DISTRIBUTARY CHANNEL AND MOUTH-BAR PROGRADING



B TIDAL-DOMINATED (ABANDONED) DISTRIBUTARY CHANNEL AND WAVE-INFLUENCED MOUTH-BAR

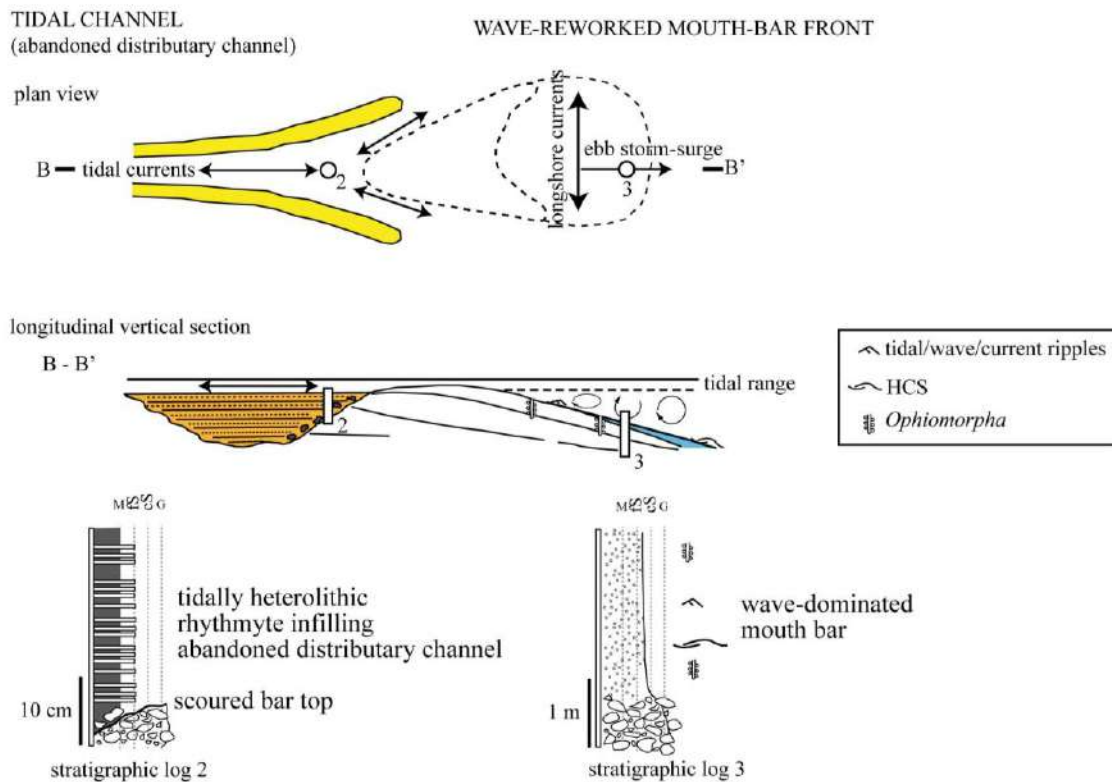


Fig. IV.11. Depositional model. **A.** Fluvial-dominated active distributary channel-mouth-bar. **B.** Tidal-dominated abandoned distributary channel and wave-influenced mouth bar front.

IV.7. Conclusions

This study provides significant insights into gravitational flow sedimentation processes, particularly those associated with hyperconcentrated and hyperpycnal flows in an apparent fluvial to mouth bar context. Unlike typical clear-water fluvial deposits, which are often dominated by sand and gravel fills in lenticular or tabular sheets, the successions observed here are marked by rapid facies transitions and stratigraphic architectures with clast-supported pebble-sized conglomerates linked to hyperconcentrated flows (FA1).

The sedimentary structures, including massive and horizontally stratified coarse-grained deposits, suggest a high-energy system dominated by sand-concentrated flows with rapid sediment aggradation. The presence of sharp-based, graded gravel beds further supports the occurrence of fluid, turbulent flows capable of transporting larger clasts, while interbedded mudstone intervals with root structures (FA2) indicate periodic low-energy phases and possible subaerial exposure.

At the coastline, these gravitational deposits interact with marine processes, leading to complex depositional environments where hyperconcentrated flows give way to hyperpycnal flows with high detrital content highlighting laminations or to more marine-influenced sedimentation (FA4-FA6). The presence of coarse-grained, poorly sorted clasts and high-velocity currents in these deltaic environments underscores the role of gravity-driven sediment-gravity flows, which undergo significant transformations upon reaching the marine realm.

The evolution of the delta, particularly in response to upstream channel avulsions and the periodic dominance of tidal and wave processes, reveals a dynamic system where river-dominated mouth bars give way to tidally influenced environments. The upper parts of the studied successions reflect increasing marine influence, marked by higher bioturbation index and the development of bars overlying the coarsest beds, signaling the waning stages of flood events.

Overall, this study highlights the importance of understanding the interplay between fluvial and marine processes, particularly in systems influenced by hyperconcentrated flows, and contributes to broader knowledge of coarse-grained mouth bars sedimentary environments in tectonically active settings.

Acknowledgements. The National Program for Doctoral Formation provided financial support to Celis and Giraldo-Villegas (Minciencias grants 885-2020, 906-2021, respectively). We want to thank the National Hydrocarbons Agency-ANH, and *Ministerio de Ciencia, Tecnología e Innovación - Minciencias* for allowing the study of well-core (Convenio 730/327-2016). The Vicerrectoría de Investigaciones y Posgrados and the Instituto de Investigaciones en Estratigrafía-IIES of Universidad de Caldas gave economic and logistic support. The research was conducted within the “Technology and Palaeoenvironment RG” (UGR). Financial support for Rodríguez-Tovar was provided by scientific Projects PID 2019- 104625RB-100 (funded by MCIN/AEI/10.13039/501100011033), P18- RT- 4074 (funded by FEDER/Junta de Andalucía-Consejería de Economía y Conocimiento), B-RNM-072-UGR18 and A-RNM-368-UGR20 (funded by FEDER Andalucía).

Chapter V

EOCENE DEEP MARINE SYSTEMS

**Coarse-grained submarine channels: from confined to unconfined flows in the Colombian Caribbean
(late Eocene)**

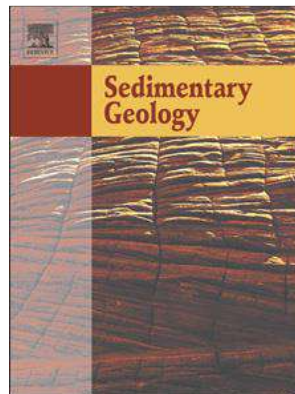
Sergio A. Celis^{a,b,*}, Fernando García-García^a, Francisco J. Rodríguez-Tovar^{a,}, Carlos A. Giraldo-Villegas^{a,b}, Andrés Pardo-Trujillo^{b,c}**

a Departamento de Estratigrafía y Paleontología, Universidad de Granada, 18002, Granada, Spain

*b Grupo de Investigación en Estratigrafía y Vulcanología (GIEV) Cumanday, Universidad de Caldas,
Manizales, Colombia*

c Instituto de Investigaciones en Estratigrafía-IIES, Universidad de Caldas, 170004 Manizales, Colombia

Sedimentary Geology, 459 (2024), 106550



<https://doi.org/10.1016/j.sedgeo.2023.106550>

Highlights

- Sedimentary facies from confined to unconfined flows.
- Evolution of a coarse-grained system from supercritical to subcritical flows.
- Depositional cyclic steps with supercritical conditions.
- Debrites to antidune field settings with supercritical to subcritical conditions.
- Inner lobe to lobe off-axis in subcritical conditions.

Abstract

Submarine channel mouth settings are hardly preserved in the stratigraphic record. Although they are still poorly known with respect to other segments of turbidite systems, conceptual models are being refined in the light of new discoveries in modern and ancient examples. Still, some questions such as the transition between expansion zones and the traditional Channel-Lobe Transition Zone (CLTZ) remains open in ancient systems. Upper Eocene deposits of the Colombian Caribbean (San Jacinto Fold Belt) are interpreted here as a fan-delta-fed, submarine, coarse-grained channel-lobe system. It displays a well-preserved channel inception stage in the shelf break represented by sigmoidal to lens-shaped gravels, and planar cross-stratified pebbly sandstones (foreset and backset) interpreted as cyclic steps in an expansion zone. In a later stage, a classical channel-levee complex was developed, represented by channel fill elements showing sharp- and erosional-based, fining-upward sequences that are meters thick, having basal massive matrix-supported pebble conglomerates (hard—extrabasinal—clasts, rip-up clasts, coastal bioclasts), vertically evolving to liquefied massive to planar-laminated coarse-grained sandstones with phytodetrital carbonaceous laminae. They are interpreted as concentrated flow deposits (high-density turbidites) coming from continental areas or from coastal systems (i.e., delta reworking). Undifferentiated channel belt thin-bedded turbidites associated with levees and terraces deposits are related to these confined systems. The channel-lobe transition zone is characterized by debrites from cohesionless debris flow in a channel-mouth bar setting, representing bypass processes that developed distally into low-angle, planar cross- and sigmoidally-stratified (upstream antidune) pebble-size to coarse-grained sandstones that fill low-angle scours (cut-and-fill structures) in an antidune field setting with supercritical conditions. When the currents lose channel confinement, the setting is characterized by changes from Froude supercritical to subcritical flow conditions in an inner lobe to lobe off-axis environment. Large seasonal fluctuations in precipitation favor high sediment concentrations, promoting the formation of volumetrically significant fan deltas and coarse-grained submarine channels with high erosive capacity; therefore, their record helps refine interpretations of depositional processes, providing criteria for recognizing areas of the turbiditic systems that are hardly preserved. The particular aggradational conditions for the preservation and stratigraphic characterization of the rare exhumed submarine channel mouth systems make it possible to decipher sediment dispersal patterns and thus connect the models proposed here, from supercritical systems to the traditional models of turbiditic systems.

Keywords. High-density turbidites, Submarine channel-mouth bar, Supercritical flow, Cyclic steps, Antidunes, Subcritical flow.

V.1. Introduction

Submarine turbidite channel-lobe complexes have been extensively studied, revealing them to be among the most prevalent hydrocarbon reservoirs discovered in deep ocean environments (e.g., Mayall et al., 2006). Depositional elements (i.e., channel-lobe and levees) have been the main focus of many recent and ancient sedimentary systems reported in the literature, unlike the Channel-Lobe Transition Zone (CLTZ), which is still being explored (e.g., Hand, 1974; Mutti and Normark, 1987; Parker et al., 1987; Kenyon et al., 1995; Palanques et al., 1995; Wynn et al., 2002; Van der Merwe et al., 2014; Dennielou et al., 2017; Brooks et al., 2018; Maier

et al., 2018). Because flows are commonly inferred to be supercritical conditions in channel to lobe transitional settings (Postma et al., 2021), a better knowledge of the sedimentology of supercritical flows is essential to understand the processes and their final results along the settings connecting channels and lobes. A recent revival of sedimentological studies on the supercritical flow in turbidity currents from flumes (Postma et al., 2009; Sequeiros et al., 2010; Cartigny et al., 2014; Postma and Cartigny, 2014; Lang et al., 2021; Ono et al., 2021; Wilkin et al., 2023, among others), modern systems (e.g., Fildani et al., 2006; Armitage et al., 2012; Covault et al., 2014; Hughes Clarke, 2016; Symons et al., 2016; Hage et al., 2018, among others) and outcrops (Ito et al., 2014; Postma et al., 2016, 2021; Lang et al., 2017; Ono and Plink-Björklund, 2018; Postma and Kleverlaan, 2018; West et al., 2019; Navarro and Arnott, 2020, among others) has led to a characterization of deposits from supercritical flows in terms of morphodynamics, erosional structures and bedforms (i.e., antidunes, chute-and-pools, cyclic steps).

In their wake, further studies have focused on CLTZs both in recent and ancient systems (e.g., Hofstra et al., 2015, 2018; Postma et al., 2016, 2021; Lang et al., 2017). However, the identification of channel mouth settings in the stratigraphic record is complicated by their high geomorphological dynamism and low preservation potential in modern examples (Maier et al., 2011; Hofstra et al., 2018; Hodgson et al., 2022). This has meant that facies characterization in the geologic record of these environments is still evolving (e.g., Summer et al., 2012; Postma and Cartigny, 2014; Slootman and Cartigny, 2020; Tinterri et al., 2020). A very recent classification of submarine channel mouth settings highlights the distinction between the traditional submarine CLTZ, plunge and pools, and Channel Mouth Expansion Zones (CMEZs) (Hodgson et al., 2022). CLTZs tend to be associated with abrupt breaks in slope, while CMEZs are characterized by long and broad areas of flaring of the channel and are identified where gradient changes are subtle to absent, as on a slope (Wynn et al., 2002; Navarro and Arnott, 2020; Fildani et al., 2021; Hodgson et al., 2022).

In this study, a coarse-grained unit of late Eocene age, embedded in marine muddy deposits from a forearc subduction complex (San Jacinto Formation, Colombian Caribbean; Fig. V.1A-B-C) is interpreted as a channel mouth system, and proposed as an expansion zone from a confined to unconfined system, thus improving our knowledge of rare exhumed submarine channel mouth systems. The record of these deposits is therefore relevant, and together with a worldwide review of examples of various ages (China, Chile, USA, Nicaragua, Argentina, Spain), it helps to decipher depositional processes in supercritical to subcritical flows in the geological record, and moreover refines sedimentary signatures and facies, which to date have been largely based on data acquired in modern examples and tank experimentation.

V.2. Geological setting

The sedimentation of Colombia's Caribbean basins has been influenced by the ongoing interaction of the Caribbean Plate with the north-west margin of South America since the Cretaceous period (Pindell and Kennan, 2009; Spikings et al., 2015; Montes et al., 2019; Mora-Páez et al., 2019; Romito and Mann, 2020; Mann, 2021). Seismic data indicate that from Late Cretaceous to late Eocene times the convergence of NW South America and the Caribbean was oblique, whereas nearly orthogonal convergence has occurred from the Oligocene until the present day (Pindell et al., 2005; Villagómez et al., 2011; Bayona et al., 2012; Bernal-Olaya et al., 2015; Montes et al., 2019; Mora-Bohórquez et al., 2020). A fore-arc configuration, linked to the

interaction between the Farallones and South American plates during the Late Cretaceous, is the most accepted model for the origin of this basin (Mora et al., 2017, 2018).

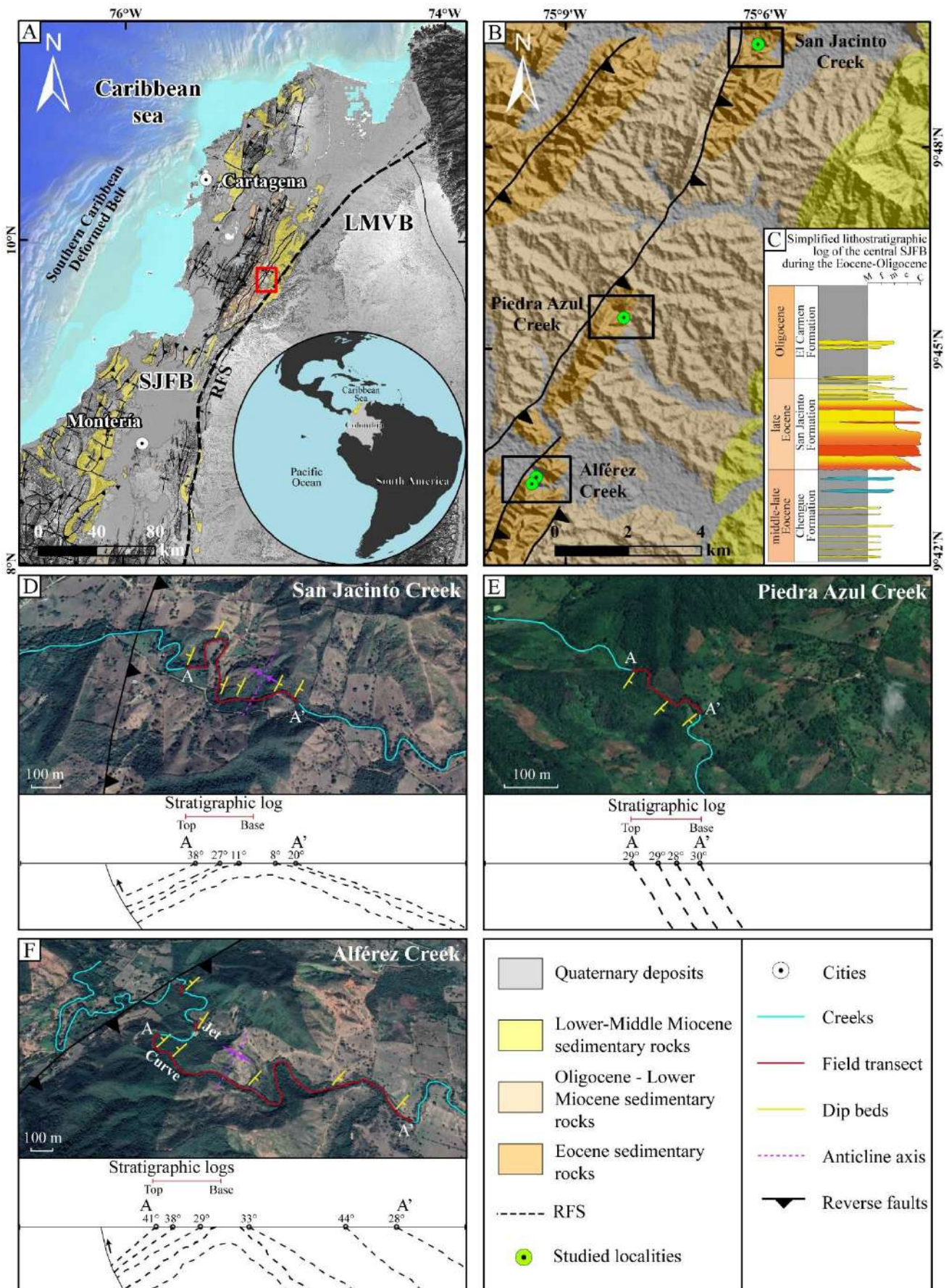


Fig. V.1. A. Location map. Geological map and distribution of the Eocene to Miocene sedimentary units in Colombian Caribbean onshore basins (SJFB - San Jacinto Fold Belt; LMVB – Lower Magdalena Valley Basin; RFS - Romeral Fault System) (Source: WGS-1984 coordinate system; CIOH, SRTM, NOAA elevation, and ocean models; geology from Gómez et al., 2015). **B.** Location of the studied outcrops. **C.** Simplified lithostratigraphic log of the central SJFB with underlying (Chengue Formation) and overlying (El Carmen Formation) lithostratigraphic units. M: mudstones (gray); f: fine sandstones (yellow); m: medium sandstones (yellow); c: coarse sandstones (yellow); C: conglomerates (orange). **D–F.** Inset maps show details of the stratigraphic record in San Jacinto Creek, Piedra Azul Creek, and Alférez Creek (jet and curve sections).

The San Jacinto Fold Belt (SJFB) is a SW-NE trending complex structure that forms part of the subduction complex of northwestern Colombia (Mantilla-Pimiento et al., 2009) and is located between an Oligocene to Recent fore-arc basin to the east [Lower Magdalena Valley Basin (LMVB)] and the Miocene to Recent accretionary prism to the west (Southern Caribbean Deformed Belt) (Duque-Caro, 1984; Mantilla-Pimiento et al., 2009; Bernal-Olaya et al., 2015) (Fig. V.1). The SJFB represents the fossilized part of the accretionary prism of the northwest Colombia subduction complex, which today acts as dynamic backstop (Mantilla-Pimiento et al., 2009). The Romeral Fault System (RFS), which is considered to continue from the south to form the eastern boundary of the SJFB, appears to be separating the oceanic (SJFB) to transitional basement under the belt from the felsic continental basement of the South American crust, which floors the LMVB in the east (Duque-Caro, 1979, 1984; Flinch, 2003; Mora et al., 2017).

The sedimentary infill of the SJFB consists of rocks deposited from deep to shallow marine and continental settings during the Late Cretaceous to Recent, separated by regional unconformities related to tectonic events during the basin evolution (Vallejo-Hincapié et al., 2023). Deep marine environments were dominant during the accumulation of Upper Cretaceous-Paleocene rocks (Angulo-Pardo et al., 2023; Giraldo-Villegas et al., 2023; Rincón-Martínez et al., 2023). Paleocene-lower Eocene deposits have been associated with deposition from turbiditic processes, followed by a development of mixed-carbonate deposits, and finally the accumulation of coarse-grained deposits related to fan delta settings (Guzmán, 2007; Salazar-Ortiz et al., 2020b; Domínguez-Giraldo et al., 2023; Plata-Torres et al., 2023). Shelf and deltaic environments were established during the Oligocene-Early Miocene, allowing the deposition of thick muddy and sandy-carbonaceous sequences (Guzmán, 2007; Celis et al., 2021, 2023). A deepening of the basin is indicated by the regional accumulation of muddy deposits in shelf settings during the Early-Middle Miocene (Duque-Castaño et al., 2023). Shallow marine to fluvial deposits accumulated during the Late Miocene-Early Pliocene (Vargas-González et al., 2022; Ospina-Muñoz et al., 2023). Pleistocene to Recent sequences are poorly known.

V.2.1. San Jacinto Formation (late Eocene to early Oligocene age)

In northwestern Colombia, a regional magmatic hiatus that took place during the late Eocene-Oligocene has been associated with margin segmentation resulting from block rotation, basin opening, and deformation in other parts of the continental margin (Montes et al., 2010, 2019; Bayona et al., 2012; Cardona et al., 2012). This tectonic activity generated uplift and exhumation events of the northern regions of the Central and Western cordilleras (Restrepo-Moreno et al., 2009; Villagómez and Spikings, 2013; Cochrane et al., 2014; León et al., 2018) as well as in the basement of the adjacent basins (Mora et al., 2017; Silva et al., 2017),

producing coarse-grained sedimentation in several of them and explaining the high production of detrital materials transported to the Caribbean basins by rivers at this time (Osorio-Granada et al., 2020).

Deposits prior to coarse-grained sedimentation are associated with the Chengue Formation (Fig. V.1C), characterized by basinward sedimentation from the ramp, dominated by hemipelagic claystones and siltstones, and small channel-lobe systems in the outer ramp and slope (Salazar-Ortiz et al., 2020b). Later, coarse-grained siliciclastic sequence of late Eocene to early Oligocene age, deposited during the tectonic changes of the basin, is associated with the San Jacinto Formation in the SJFB (Duque-Caro et al., 1996; Clavijo and Barrera, 2001; Guzmán, 2007; Mora et al., 2017; Salazar-Ortiz et al., 2020a; Celis et al., 2023; Vallejo-Hincapié et al., 2023) (Fig. V.1C). These deposits are interpreted as ancient submarine deposits in slope failures associated with fan delta environments (Duque-Caro et al., 1996; Duarte, 1997; Barrera et al., 2001). Overlying the San Jacinto Formation, El Carmen Formation (Fig. V.1C) is characterized by a predominance of hemipelagic mudstones deposited in slope settings (Duque-Caro et al., 1996).

V.3. Methods and data set

This study is based on the sedimentological and photo-panel analysis of exposed rock formations in creeks located in the present-day onshore Colombian Caribbean region, specifically the San Jacinto Formation within the San Jacinto Fold Belt (SJFB) (Fig. V.1D-E; Supplementary material V.3). The outcrops were surveyed bed by bed using a Jacob's staff, encompassing observations of bed geometry and thickness, lithology, texture, sedimentary structures, fossils, and ichnological assemblages.

Ichnological attributes such as ichnodiversity, distribution, and abundance were defined with Bioturbation Index BI sensu Taylor and Goldring (1993). Paleoflow directions were defined from planar- and trough-cross stratification, ripple-cross lamination, and clast imbrications. Bed thickness was classified as very thin (<1 cm), thin (1–10 cm), medium (11–30 cm), thick (31–100 cm), or very thick (>100 cm) according to the scheme of Nichols (2009). The gravel-clast fabric terminology used follows Walker's (1975) classification. Through the field work and photo panel analysis, the 3-dimensional arrangement of architectural elements and bounding surfaces was mapped to document the larger-scale stacking pattern of facies associations (employing the terminology of Pickering et al., 1995). Paleoflow conditions and their spatial changes and temporal evolution were taken into consideration when interpreting facies associations and stacking patterns. Biostratigraphic data were adopted from previous micropaleontological research on foraminifera and calcareous nannofossils carried out in the same stratigraphic sections in order to have an age control (e.g., Duque-Caro et al., 1996; Duarte, 1997; Guzmán, 2007; Mejía-Molina et al., 2010).

V.4. Results

V.4.1. Lithofacies and stratigraphy

Twelve lithofacies (L1 to L12) were identified and interpreted in terms of sedimentary processes in the San Jacinto Formation (Supplementary material V.1). The vertical distribution of lithofacies was established through four stratigraphic logs (Fig. V.2). Then, the lithofacies were grouped in seven facies associations (FA1 to FA7) and interpreted in terms of sedimentary subenvironments (Table V.1).

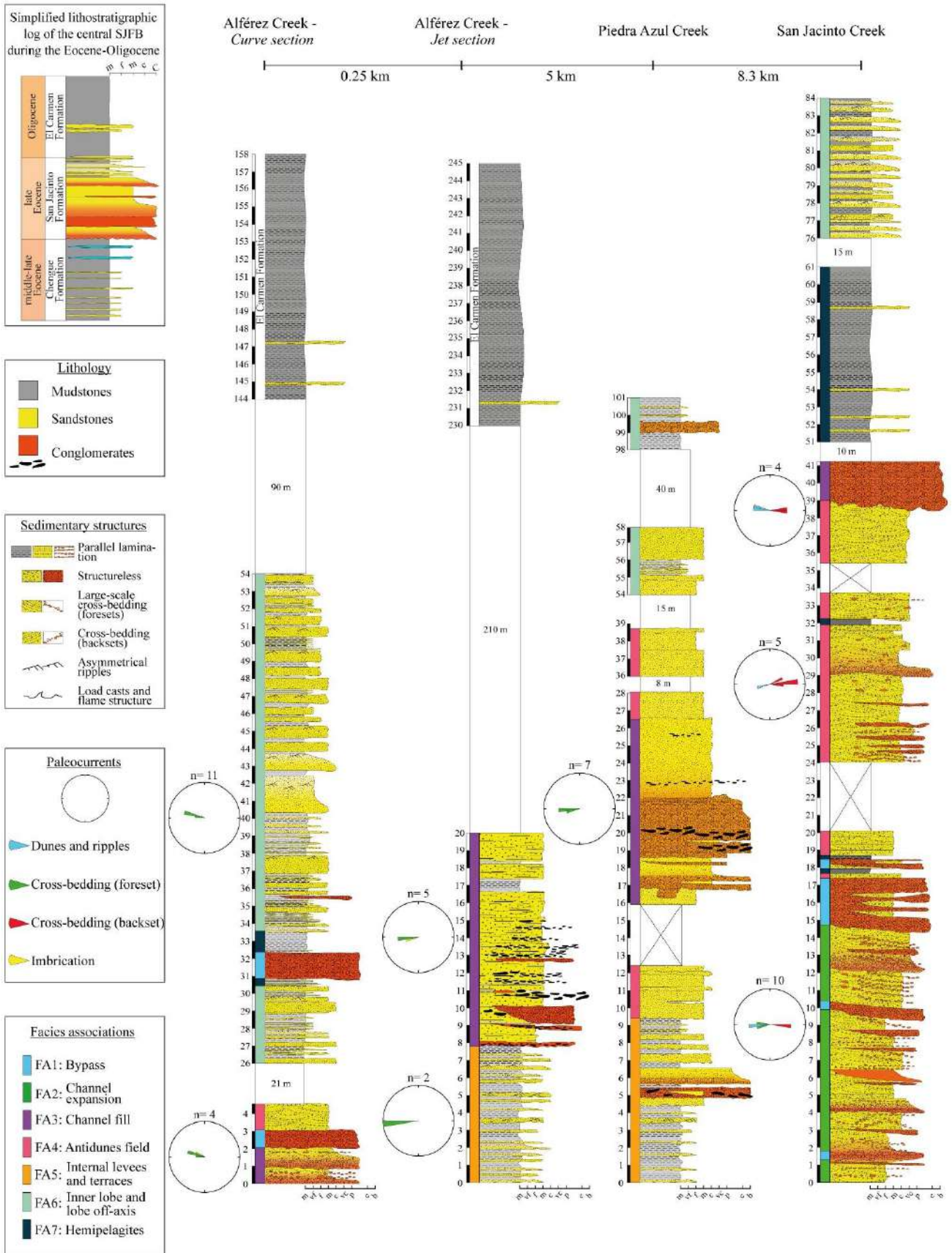


Fig. V.2. Stratigraphic sections of the San Jacinto Formation.

V.4.1.1. San Jacinto Creek

The San Jacinto Creek section is ~84 m thick (Fig. V.2). Its contacts with the underlying Chengue Formation and overlying El Carmen Formation are not recorded. The base of this section is characterized by medium to thick beds of coarse-pebble- to boulder-sized conglomerates and medium to coarse-grained sandstones. Irregular (erosive) surfaces are common, with coarse-pebble-sized conglomerates infilling scours. Additionally, thick to very thick beds having tabular and wavy geometry (boulder- to medium-pebble-sized matrix- to clast-supported conglomerates) mark irregular surfaces at the base. Embedded rip-up clasts are occasionally present. Toward the middle part of the section, flat or irregularly bounded medium to very thick beds of medium- to coarse- grained sandstones and conglomeratic sandstones are recorded, with medium- to coarse-pebble-sized clasts occurring in scour-and-fill structures. Very fine granules and coarse pebbles (up to 2 cm) are common along scour surfaces. Near the top of the section, there is a sharp contact with medium to thick beds of mudstones and fine-grained sandstones. The mean paleocurrent direction measured in planar cross-bedding sandstones and conglomerates is to the W, with some degree of variation to the W-SW and W-NW (Fig. V.2).

V.4.1.2. Piedra Azul Creek

The Piedra Azul Creek section is ~38 m thick of exposure (Fig. V.2), in which the contact with the underlying Chengue Formation is not recorded, nor that with the overlying El Carmen Formation. However, the top of San Jacinto Formation could be inferred. The San Jacinto Formation at the base of this section features a centimeter-thick intercalation of mudstones and fine- to medium-grained sandstones; a bed of cobble-sized conglomerates with normal grading to medium-grained sandstone is also observed. Above this sandstone-mudstone succession lies an irregular erosional base of medium- to coarse-grained sandstones with sigmoidal geometry. Different erosional surfaces are filled by matrix- supported cobble- and boulder-sized conglomerates (rounded to angular, poorly sorted, disorganized rip-up clasts). The matrix consists of very fine-pebble- to medium-grained sandstones. The clasts are moderately sorted, having subrounded to well-rounded cobble and coarse to very coarse pebble-sized sedimentary hard-clasts, rip-up, and bivalve gastropod fragments. Atop these successions are fine to medium sandstones, and pebble-sized conglomerates interbedding with mudstones. Rip-up clasts are imbricated to the WSW.

V.4.1.3. Alférez Creek

At the Alférez Creek, two sections (jet and curve) were studied (Fig. V.2). The jet section is 35 m thick of exposure, in which the contact with the underlying Chengue Formation is not recorded, but the overlying El Carmen Formation is observed above a ~210 m-thick covered interval. The San Jacinto Formation at the base of this section features a decimeter-thick intercalation of bioturbated mudstones and medium- to coarse-grained sandstones having tabular geometry. The sandstones have irregular bases with load casts and asymmetric flame structures. This sandstone-mudstone succession is capped by an irregular erosional base of matrix-supported cobble- and boulder-sized conglomerates (rounded to angular, poorly sorted, disorganized rip-up clasts) commonly occurring above scour surfaces. The matrix consists of very fine-pebble- to medium-grained sandstones. Additionally, meter-scale mudstone beds are embedded within the conglomerate packages.

Successive beds of conglomerates with erosive bases are recognized; they are clast-supported and moderately sorted, having subrounded to well-rounded cobble and coarse- to very coarse-pebble-sized sedimentary hard-clasts of ochre coloration. The matrix is granule to medium- grained sandstone. Atop these successions lie medium- to coarse-grained sandstones with abundant organic matter marking the laminations. Asymmetric flame structures show WSW trends; and some rip-up clasts are imbricated to the WSW.

The Alférez Creek curve section is 68 m thick of exposure and 90 m unexposed (Fig. V.2). The overlying El Carmen Formation is seen above a ~90 m covered interval, but the underlying formation is not observed. This section has a base dominated by matrix-supported conglomerates, featuring coarse to very coarse to pebble-sized clasts consisting of ochre-colored sedimentary lithoclasts, and pockets of highly fragmented bivalves and gastropods. The conglomerates show fining-upward trends: from 1 to 2 m thick coarse and medium to pebble-size to very fine-pebbly sandstones and very coarse-grained sandstones, with irregular erosional bases. Toward the top, where conglomerates decrease in abundance, there are fining- and thinning-upward successions of very coarse to medium-grained sandstone with rip-up clasts, to fine-grained sandstones and mudstones with sharp and erosional bases. Bed thickness ranges from thin to thick. In some cases, thinly interbedded mudstones and very fine-grained sandstones occur at the top of the beds. Bioturbation is seen mainly at the top of the successions. The mean paleocurrent direction is to the WNW.

V.4.2. Facies association analysis

Seven facies associations (FA1 to FA7) were defined in the study sections (Table V.1) based on the grouping of characteristic sedimentary structures, common depositional processes, stacking patterns, architectural features and temporal and spatial evolution.

Table V.1. Facies associations and distinguishing characteristics of stratal elements.

| Facies Association | Order of occurrence in stratal complex | Exposed dimensions (thickness and width) | Basal surface | Sedimentary facies | Vertical and lateral trends and architectural stacking patterns | Interpretation |
|---------------------------|---|---|----------------------|-----------------------------|---|-----------------------|
| FA1 | FA2/FA3/FA7 →FA1→ FA2/FA4/FA7 | Individual: 30 cm to 8 m. | Sharp and irregular. | L1, L2. | None. | Bypass. |
| FA2 | FA1→FA2→FA1 | Sets up to 3 - 8 m. | Sharp and irregular. | L1, L2, L3, L5, L6, L7, L8. | Amalgamated vertical surfaces, and grading to FA4. At the kilometer-scale, gradual lateral changes to FA3/FA5. | Channel expansion. |
| FA3 | FA4/FA5 →FA3→ FA1 | Sets up to 10 m. | Irregular. | L1, L2, L3, L4, L6, L9. | Amalgamated vertical surfaces. Upward changes in facies. Nested offset stacking. Rapid (over a few meters) lateral bed fining, and overlain to FA5. | Channel fill. |
| FA4 | FA1/FA7 →FA4→ FA3/FA7 | Sets up to 12 m. | Sharp. | L6, L7. | Vertical stacking, with subtle vertical and lateral fining and thinning. | Antidunes field. |
| FA5 | FA5→FA3 | Sets up to 8 m. | Irregular. | L7, L8, L9, L10, L11, L12. | Amalgamated vertical surfaces, and erosive top to FA3. At the kilometer-scale, gradual lateral changes to FA2. | Levee/terraces. |

| <u>Facies Association</u> | <u>Order of occurrence in stratal complex</u> | <u>Exposed dimensions (thickness and width)</u> | <u>Basal surface</u> | <u>Sedimentary facies</u> | <u>Vertical and lateral trends and architectural stacking patterns</u> | <u>Interpretation</u> |
|---------------------------|---|---|----------------------|---------------------------|--|------------------------------|
| FA6 | FA7→FA6→FA7 | Sets up to 15 m. | Irregular and sharp. | L3, L9, L10. | Vertical stacking. | Inner lobes / Lobe off-axis. |
| FA7 | FA1/FA4/FA6 →FA7→ FA1/FA4/FA6 | Individual: 30 cm. | Sharp. | L12. | None. | Hemipelagites. |

V.4.2.1. FA1: matrix- to clast-supported, ungraded conglomerates

Description. This facies association consists of ungraded medium to very thick sharply-based conglomerates supported by a coarse-grained sandy matrix (L1), and locally clast-supported (L2). Clasts are subrounded to subangular, granule- to pebble- and occasionally cobble-sized (Fig. V.3A). Bioclasts of oysters and gastropods were recognized. Rare rip-up clasts appear with pebble-sizes (Fig. V.3B). Two sub-facies associations are distinguished mainly based on the bed geometry:

V.4.2.1.1. FA1a: sheet-like, matrix-supported conglomerate beds. This association show tabular geometry (Fig. V.3C) up to 5mthick. The basal surface is irregular (Fig. V.3D), and matrix/clast ratio is low. Rare structureless rip up clasts can be identified at the lower part (Fig. V.3B), whereas the middle to upper part is well-bedded by distinct gravel and coarse- to medium-grained sandstones (Fig. V.3E).

V.4.2.1.2. FA1b: wavy geometry, matrix-supported conglomerate beds. It shows wavy geometry (Fig. V.3F-G) with thicknesses from 30 cm to 1.5m. The basal surface is also sharply irregular. Sharp grain-size breaks occur between FA1b and the overlying FA4 (see description below) (Fig. V.3F-G). It is found at the upper part of the sequences embedded into finer grain-size deposits (FA5-FA7; Fig. V.3F-G). These facies show a high matrix/clast ratio.

Interpretation. Basal scour and rip-up clasts in the lower part of the beds would evidence a turbulent flow regime at the initial stage of bed deposition (Talling et al., 2012). The presence of sandstones between conglomerate beds (FA1a) in the middle to upper part of the succession marks a density-stratified flow that moved gravel as a bedload. When the traction currents declined in competence, the gravel-waves ceased to migrate, and sand that had previously been in suspension was deposited and moved as bedload while the flow was waning (Lowe, 1982; Hughes Clarke et al., 1990). FA1a and FA1b are interpreted as a debrite resulting from cohesionless debris flow, vertically evolving to surging flow (Nemec and Steel, 1984; Ge et al., 2022). The presence of sharp grain-size breaks, as seen between FA1b and FA4, allows FA1b to be interpreted as an indicator of sediment bypass (Stevenson et al., 2015; McArthur et al., 2020).

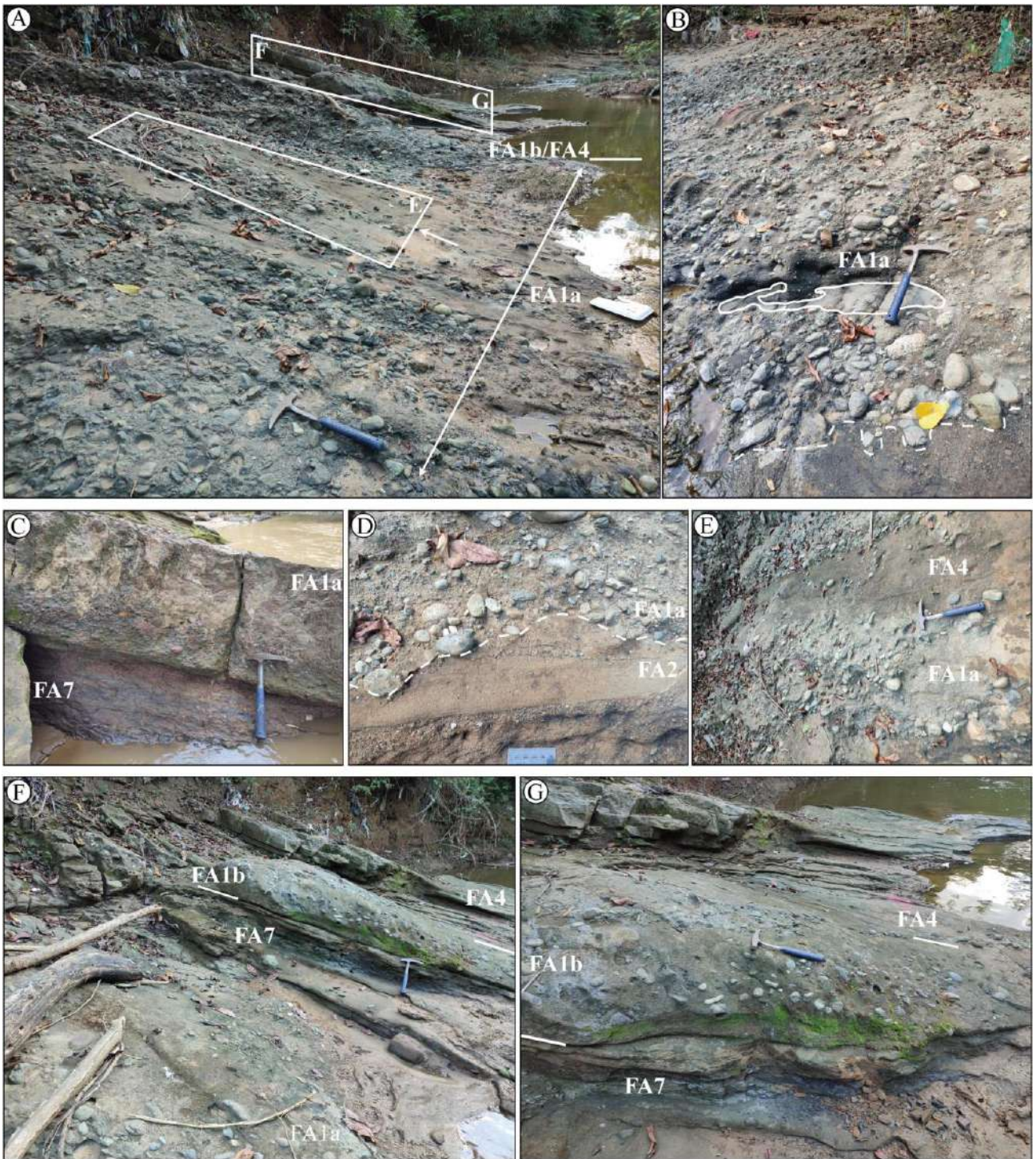


Fig. V.3. Facies association 1 (FA1). **A.** Section showing the vertical transition from matrix-supported rounded pebble clasts (FA1a) to sigmoidally cross-stratified coarse-grained sandstones (FA4) capped by sigmoidal-shaped, matrix-supported conglomerate beds (FA1b) (at the top of the picture) (hammer is 32 cm long). **B.** Large rip-up clasts in the lower part of the matrix supported rounded pebble clasts (FA1a) overlying FA2 through irregular contact. **C.** Mudstones (FA7) in sharp irregular contact with tabular bed of matrix-supported conglomerate (FA1a). **D.** Detail of the irregular base (dashed line) of the matrix-supported rounded pebble clasts (FA1a) (chart to scale: 10 cm). **E.** Sandstone-dominated layers in the middle-upper part of the matrix-supported rounded pebble clast beds (FA1) (see location in panel A). **F–G.** Sigmoid-shaped, matrix-supported conglomeratic beds (FA1b) interbedded with sigmoidally cross-stratified granule to coarse-grained sandstones (FA4) and horizontally laminated dark mudstones (FA7) (see location in panel A).

V.4.2.2. FA2: normally graded conglomerate lenses that transitionally evolve upward to planar cross-stratified coarse to pebbly sandstones

Description. This facies association is represented by amalgamated thick to very thick beds of pebbly sandstones with planar cross-stratified, normal grading (L3) to fine- to medium-grained sandstones, convex-up low angle surfaces (L5, L7), and mound-shaped geometries. The arrangement can be divided into three parts according to textural variations (Fig. V.4 general view and sketch general view). The lower (1–2 m thick) consists of lens-shaped conglomerates with extra-pebble clasts (rip-up clasts are absent), having massive structure (L1), diffuse low-angle and planar cross-stratified, and sigmoidal geometry infilling convex-up erosional surfaces where rare load casts are present (Fig. V.4A-B, and sketch B). Typically, clast- or matrix-supported conglomerates (L1, L2) with subrounded to well-rounded pebbles to cobbles—mostly derived from sedimentary rocks—make up the basal scour infills. Upward, the middle part contains thicker beds (2–4 m thick) of sigmoidal cross-stratified pebbly sandstone deposits (L7; Fig. V.4D) that laterally may pass into lens- and mound-shaped beds of pebbly sandstones with low-angle, trough and planar cross-bedding (L6, L7; backsets and foresets; Fig. V.4C–E, and sketch C). Just upstream, lens-shaped, massive to crudely planar cross-stratified pebbly sandstone occurs (Fig. V.4D). The enclosing facies of the mound-shaped beds consist of coarse- to medium-grained sandstones and pebbly sandstones that appear trough cross-stratified (asymptotic downstream) (Fig. V.4E). Structureless and weakly-bedded sandstone (L8) deposits occur in the upper bed (top), up to 1 m thick (Fig. V.4C and sketch C).

Interpretation. Altogether, the prevalence of convex-up surfaces, scour-and-fill structures, planar cross-stratified pebbly sandstone, lens-shaped geometry with backsets and foresets, and subsequent draping of these surfaces by onlapping of asymptotic downstream cross-bedding pebbly sandstones (Fig. V.4F) would be associated with a supercritical high-density turbidity current that generated small cyclic steps (Cartigny et al., 2014; Hage et al., 2018; Slooman and Cartigny, 2020). Massive or crudely laminated zones just upstream of the lens shaped beds could be associated with the hydraulic jump (Postma and Kleverlaan, 2018). Scour fills display crude and widely spaced low angle stratification, indicating a decrease in sediment concentration and an increase in bedload transport and bed shear stress; it could occur rapidly downflow of the hydraulic jump, where a velocity maximum causes higher boundary shear stress and thus more erosive power (Sequeiros, 2012; Postma and Cartigny, 2014). This transition may take place swiftly downstream of the hydraulic jump (Postma and Cartigny, 2014; Postma et al., 2014; Lang et al., 2017). In the mound-shaped beds, the migration of the crest occurs at an angle of climb that exceeds the dip of the lee side (Fig. V.4D, and sketch D), resulting in an overall aggradational state on both sides of the step. This allows the preservation of continuous beds across cyclic steps, appearing as wave trains in the depositional record (Vellinga et al., 2018; Slooman and Cartigny, 2020).

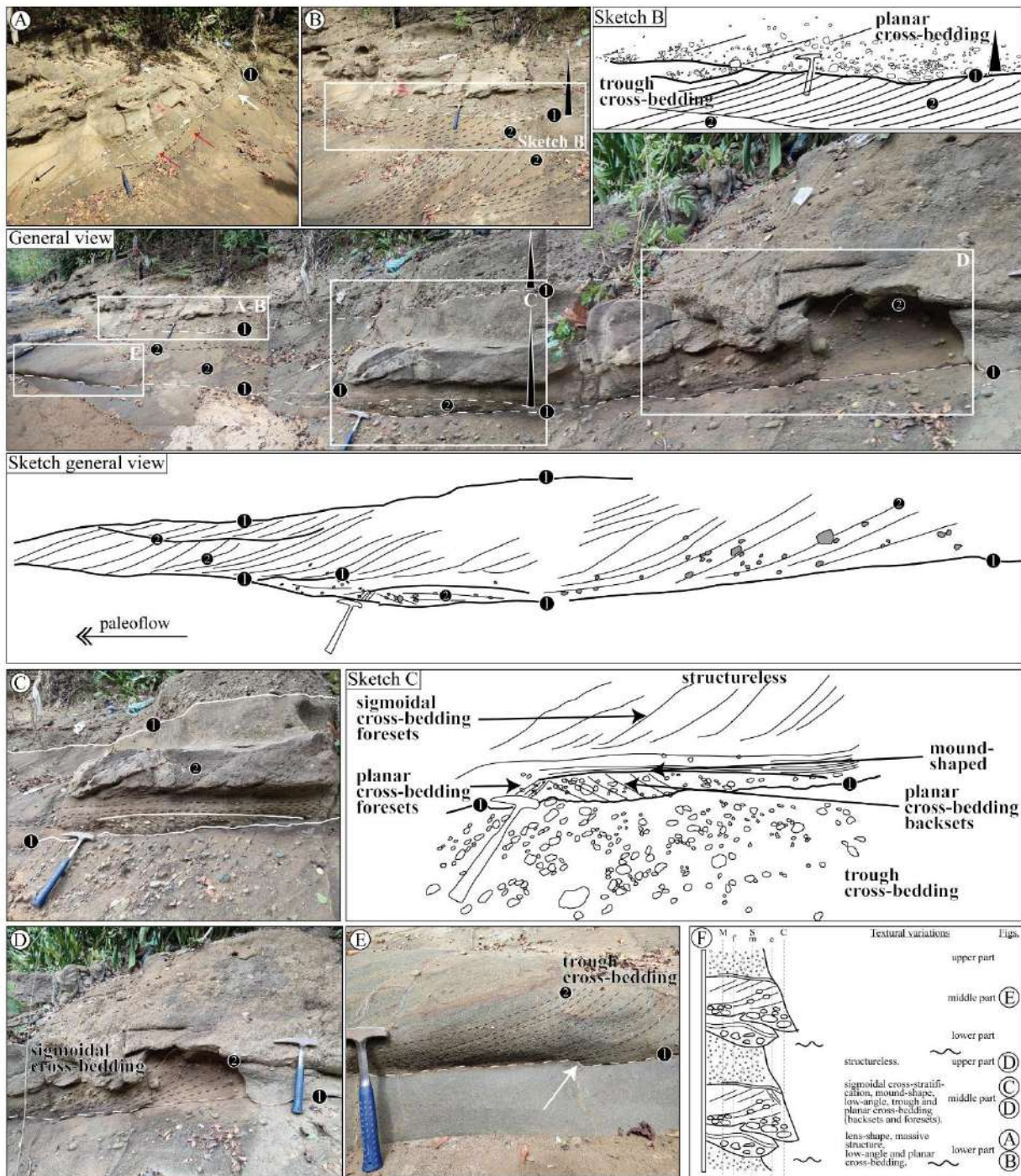


Fig. V.4. Facies association 2 (FA2). General view and sketched general view of the lower part of the San Jacinto Creek section. Two-meter-thick pebbly sandstone beds appear amalgamated. The amalgamation surface stratigraphy hierarchy is marked by numbers: 1. Cross-bedding coset stratigraphic surfaces, 2. cross-bedding set stratigraphic surfaces (hammer is 32 cm long); (see figure locations in General view). **A.** Lens-shaped and mound-shaped structures of normal-graded gravels and sandstone deposits (red arrows), flame structure (black arrow) intruding into structureless sandy upper interval, and sigmoidal gravel deposits infilling a shallower and longer scour (white arrow). **B and sketch B.** Detail and line drawing of the lower part deposits. Note the erosional, scoured basal surface truncating underlying planar cross-bedded sandstones. Gravels show diffuse planar cross-bedding (dipping toward the left) with scattered pebbles dispersed in sand-dominated laminae. **C and sketch C.** Detail and line drawing of the middle part deposits. Mound-shaped with backset-bedded pebbly sandstone deposits cap the amalgamation surface, and a sigmoidal cross-bedded sandstone unit encloses the mound-shaped ones. **D.** Lens of pebbly sandstone deposits at the lower part of the sigmoidal cross-bedded unit. It appears overlying the amalgamation surface (dashed line). **E.** Trough cross-bedded sandstones with scattered very fine and coarse pebbles. **F.** Schematic textural variations for FA2.

They are classified as ‘fully depositional cyclic steps’ following Slooman and Cartigny (2020), in this case formed under high values of sediment concentration, where amalgamation shows that fine sediment deposition is prevented in the upper part of the bed. Deposition in fully depositional cyclic steps occurs from the leeward side in foreset-bedding and aft side in backset bedding (Slooman and Cartigny, 2020). However, the angle of migration of the climb that exceeds the dip on the lee side is not perfectly preserved; therefore, the lee side could have been eroded—the rate of sediment removal being less than the rate of deposition on the stoss side—and the cyclic steps could have been partially depositional (Slooman and Cartigny, 2020).

The bases of slope breaks, when there are gradient changes at the basin bottom (continental slopes and related canyons), appear to favor either already subcritical flows or swift transitions from supercritical to subcritical flow conditions (e.g., Fildani et al., 2021; Hodgson et al., 2022). Although the bedforms developed in the expansion zones are generated by turbidity currents in upper flow regimes, the aggradational and preservation tendencies must occur beneath supercritical to subcritical flows (Fr close to 1) to prevent erosion (Postma et al., 2016; Hodgson et al., 2022).

V.4.2.3. FA3: graded and amalgamated matrix-supported conglomerates to sandstones

Description. This association is represented by vertical and nested offset stacking, irregular and sharply-based conglomerates supported by a medium- and coarse-grained sandy matrix, massive and occasionally graded (L3) to sandstone deposits. Two sub-facies associations are distinguished in view of the stacking pattern and sedimentary structure:

V.4.2.3.1. FA3a: vertical stacking, normally-graded, rip-up- and/or hard-clast conglomerates to sandstones. This is represented by lenticular-shaped geometry and medium to thick beds, normally graded, consisting of three intervals (Fig. V.5): i) A lower interval exhibiting hard-clast- and matrix-supported conglomerates with some angular rip-up clasts (L1, L2, L3; Fig. V.5A-B), ii) a sharp-based, planar-bedded granule- to very coarse-grained sandstone (L9) interval in the middle part (Fig. V.5A-B), and iii) an upper interval characterized by planar cross-bedded upstream (backsets) very fine-pebble-size to sandstone deposits (L6; Fig. V.5C-D).

Interpretation. These deposits forming upward-fining sequences represent the channel fill at the channel axis (Kane et al., 2009). Angular rip-up clasts indicate that these deposits are relatively immature, and they could evolve downslope into fully turbulent flow where sediment would break up (e.g., Mulder and Alexander, 2001; Kane et al., 2009).

V.4.2.3.2. FA3b: nested offset stacking, amalgamated scour-and-fill, rip-up and/or hard-clast conglomerates to sandstones. Coarse-grained lags that include mudstone breccia with frequent deformed shale clasts are overlain by amalgamated thick-bedded conglomerates and sandstones (L1, L2, L4, nested offset stacking; Fig. V.6). Scours are 0.5 m deep and 2–15 m long (Fig. V.6A, and sketch A), and are mostly irregular and asymmetrical. Scour fills consist of matrix-supported conglomerates (L1) with pebbly sandstone or coarse- to medium-grained sandstone as matrix, as well as bivalve and gastropod fragments (Fig. V.6). In some cases, the bases of the larger scours are characterized by deposits associated with FA5, having scoop-shaped and smaller-scale scours (see below in FA5).



Fig. V.5. Facies association 3a (FA3a). **A.** Sharp-based, normally-graded conglomerate to sandstone deposits (FA3a) (hammer is 32 cm long). **B.** Detail of the lower conglomeratic interval in panel A exhibiting clast-supported fabric and normal grading with scattered large clasts at the top (arrow). Note the sharp transition between conglomeratic and overlying granule and sandstone intervals (lines) (scale = 10 cm). **C–D.** Vertical transition from planar-bedded to backset planar cross-bedded (dashed lines) fine-pebble size conglomerates to sandstone intervals (see location in panel A). Sharp transition (lines separating a lower brown interval from an upper gray one) between intervals could indicate an amalgamation surface between two different depositional events or surges of an unstable flow. Lasting would support the vertical decrease in grain size (hammer is 32 cm long in both pictures).

The composition of the clasts filling the scours can be divided into rip-up (Fig. V.6B) and hard (Fig. V.6C), while in rare cases rip-up and hard clasts are mixed. Rip-up clasts consist of mudstone and siltstone ranging from coarse-pebbles to cobbles and rare boulder size (up to 0.40 m in diameter; Fig. V.6D), subangular to subrounded. The hard clasts range from very fine pebbles to coarse pebbles, subangular to angular, ochre-colored, derived sedimentary rocks. The clast fabric is commonly random. In general, the coarsest grain sizes occur within the largest scours with rip-up clasts, and even partially complete layers can be part of the backfill (Fig. V.6D-E). Internally, the rip-up and hard-clast scour fills are massive; rip up clast scours fills are amalgamated. Yet appearing upward in the succession are normally-graded rip-up clasts that are pebble- to cobble-size with imbrication to the SW (L3; Fig. V.6F), along with horizontally laminated coarse- to medium-grained sandstones with plant debris (L9; Fig. V.6G).

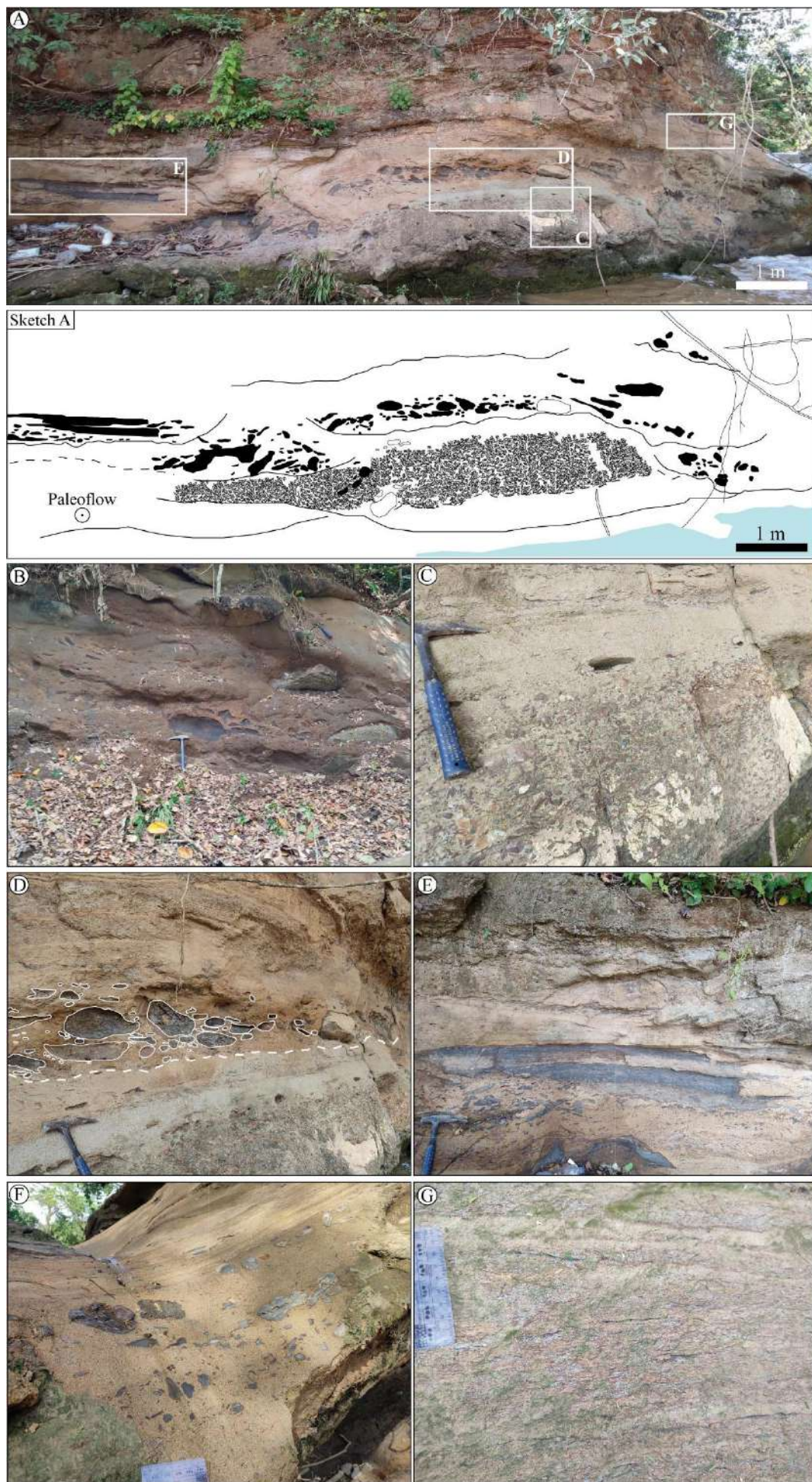


Fig. V.6. Facies association 3b (FA3b). **A and sketch A.** Cross-section of the top of the Alférez Creek (jet section) showing amalgamation of rip-up- and hard-clast channels with high organic content. **B.** Abundant concentration of rip-up clasts with boulder-sized particles. **C.** Coarse-grained turbidite channel composed of hard sedimentary lithics, with massive structure and normal grading at the top. **D.** Abundant concentration of rip-up clasts at the base of the channel, with boulder-sized particles overlying another channel consisting of hard clasts. **E.** Concentration of rip-up clasts and whole bed fragments ripped off the previous basin floor, forming a basal lag deposit. **F.** Rip-up clasts ranging in size from pebbles to cobbles floating in a medium-grained sandy matrix. Some clasts show SW imbrication. Chart to scale: 10 cm. **G.** Abundant layers of organic matter highlighting parallel lamination toward the top of the accumulation of rip-up clasts, emphasizing normal grading in the succession. Chart to scale: 10 cm.

Interpretation. Amalgamated coarse-grained scour fills indicate erosion by a high-velocity water flow, and subsequent filling by subangular to subrounded intraclasts from highly concentrated flows that represent significant sediment bypass or a waning phase of the flow that cuts the scour (Postma et al., 1988, 2014; Peakall et al., 2020). In submarine channels, the occurrence of vigorous substrate scouring and ripping-up of partially complete beds, coupled with the subsequent deposition of unstructured beds, suggests an explosive hydraulic jump phenomenon (Postma et al., 2009). The occurrence toward the top of normal grading beds rich in laminated plant debris may be associated with hyperpycnal flows delivered directly from subaerial settings (Lowe, 1976; Zavala and Pan, 2018; Zavala, 2020; Grundvåg et al., 2023).

V.4.2.4. FA4: sigmoidally stratified pebbly sandstones

Description. This facies association is represented by 15–30 cm thick, coarse-tail, normally-graded to low-angle, sigmoidal cross-stratified pebbly to granule sandstone beds (Fig. V.7A-B). Scours are filled by asymmetrical lenticular beds of foresets and concave-up, low-angle backset planar cross stratified pebbly to granule sandstones (Fig. V.7C-D). The dimensions of the lenticular to sigmoidal elements are characterized of low amplitude (5 cm) and relatively long wavelength (30–50 cm) (Fig. V.7E-F). Laterally the thickness pinches and swells slightly due to converging-diverging stratification (Fig. V.7E-F). Asymmetrical sigmoidal stratified sandstones (e.g., humpback cross-bedding-type) also appear (Fig. V.7E-F).

Interpretation. Low-angle backsets and foresets in gravel sandstones are interpreted as representing deposits of low relief antidunes and chutes or pools due to internal waves, surges or unstable hydraulic jumps (Lang and Winsemann, 2013; Ono and Plink-Björklund, 2018). Humpback dunes are interpreted as dune to upper plane bed transitions in open channel flows (i.e., river channels, Fielding, 2006). However, supercritical flow experiments in density flow showed that humpback dunes may also represent downslope migrating antidunes with high rates of deposition (Lowe, 1982; Fielding, 2006; Lang and Winsemann, 2013; Fedele et al., 2016; Winsemann et al., 2021). The lack of upper plane beds in these deposits (which would be common in supercritical flows occurring in open channel flows; Fielding, 2006) could signal that the density flow did not reach the high Froude numbers required for upper plane beds (higher than the open channel flow analogs, as reported by Fedele et al., 2016 experiments). Thus, this facies association is interpreted as the result of an aggrading antidune-type bedform in granule to coarse-grained sand beds. It would have formed under supercritical flows, as observed in laboratory flumes (e.g., Alexander et al., 2001; Fedele et al., 2016; Ono and Plink-Björklund, 2018; Winsemann et al., 2021). Steep scours filled by foreset and backset planar cross-

bedding are interpreted as the result of breaking waves (Ono and Plink-Bjorklund, 2018). The absence of plane bed zones laterally separating antidunes discounts their stability where flow becomes transcritical (from supercritical flow at relatively low Froude numbers; Cartigny et al., 2014). Here they are capped by cut-and-fill (antidune) structures, thus implying rising flow power conditions during supercritical flow, or deposition by waxing flows that attain supercritical flow conditions (Lowe, 1982; Saunderson and Lockett, 1983; Chakraborty and Bose, 1992; Fielding, 2006).

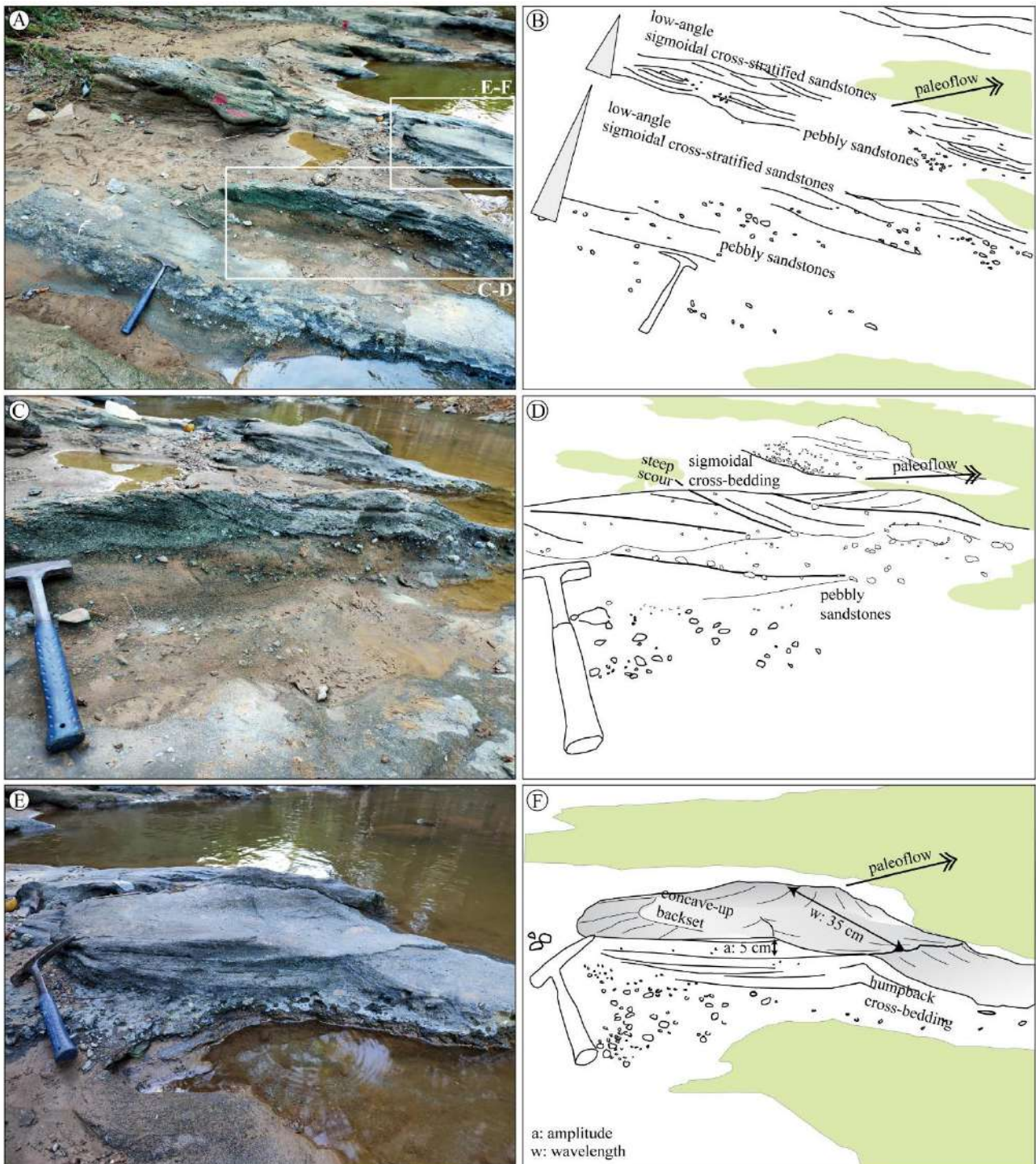


Fig. V.7. Facies association 4 (FA4). **A–B.** Field picture and line drawing showing normally graded, vertical stacking of centimetric-thick, low-angle cross-laminated pebbly sandstone to sandstone beds. See panel A for location of detailed photos C and E. **C–D.** Field photo and line drawing showing a lens of gently sigmoidal cross-bedded pebbly sandstone and asymmetrical cross laminated granule to sandstone bed with scouring and filling structure interpreted as unstable antidune (see text for details), **E–F.** Field picture and line drawing showing gently backflow cross-bedded and humpback cross-bedding sandstone at the top of a pebbly sandstone bed interpreted as antidunes (see text for details) (32-cm long hammer to scale in all the pictures).

V.4.2.5. FA5: burrowed (Ta-e) sandstone and mudstone layers

Description. This facies association comprises interbedded thick to very thick sheet-like beds of massive mudstone, and fine- to medium-grained sandstone beds (L10, L11, L12; Fig. V.8A-B-C) with massive (L8), horizontally laminated (L9), planar cross-bedding (L7), and ripple lamination structures, as well as normal grading (L10), having erosional bases that often contain load casts and flame structures (Fig. V.8C-D-E). Sandstones present moderate ichnodiversity, low to moderate abundance (BI = 1–3), and show *Ophiomorpha* and *Thalassinoides* (Fig. V.8E), while the mudstones show patches of *Nereites* and *Phycosiphon* and locally *Taenidium* (Fig. V.8F-G), with moderate ichnodiversity and a moderate to high intensity of bioturbation (BI = 3–4). The top of these successions is overlain by erosional surfaces associated with FA3, which contains abundant rip-up clasts (Fig. V.8D).

Interpretation. Thick to very thick beds of fine-grained sandstones are attributed to sediment deposition along the channel margin areas (such as internal levees and terraces) where the low-concentrated turbidity flows slow, or because the flow thickness is greater than the channel depth, or because of inertia at channel bends or in encounters with irregularities, leading to escape from the main channel, and sometimes even the formation of minor channels (Kane and Hodgson, 2011; Pickering and Hiscott, 2015; Bayet-Goll et al., 2023). The distinction between inner levees and terraces requires a well-defined channel belt architecture; so, in our study we consider these systems as undifferentiated channel belt thin-bedded turbidites (according to Hansen et al., 2015). The presence of trace fossils such as *Ophiomorpha* and *Thalassinoides* could be related to the *Ophiomorpha rudis* ichnosubfacies within the *Nereites ichnofacies*, associated with deposition from turbidity currents by the channel (Uchman, 2009; Uchman and Wetzel, 2012). In an internal levee and terrace setting, interbedded bioturbated mudstones tend to settle out of suspension under lower-energy conditions from clouds of overflowing turbidity currents, or due to hemipelagic processes when the system shutdown (Heard and Pickering, 2008; Kane and Hodgson, 2011; Hansen et al., 2015). *Nereites* and *Phycosiphon* must be related to *Nereites ichnosubfacies* in the *Nereites ichnofacies*, common in lower energy environments or associated with muddy flysch sediments (Uchman and Wetzel, 2012; Callow et al., 2014; Rodríguez-Tovar, 2022). It should be noted that the distribution and abundance of these ichnological associations vary in the presence of cohesive debris flow, which forces organisms to migrate from areas of higher energy to areas where low-density turbidites predominate (Hubbard et al., 2008, 2012; Callow et al., 2014; Bayet-Goll et al., 2023). The observed sedimentary pattern could be the first stage of an abandonment drape, caused by a number of factors, such as upstream channel avulsion, relative sea-level rise, or changes in the sediment supply brought on by tectonic activity or climate shift in the source area (Clark and Pickering, 1996; Richards et al., 1998).



Fig. V.8. Facies association 5 (FA5). **A.** General view of the internal levee/terrace succession (FA5), overlain at the top by an erosive surface associated with the turbiditic channel (FA3b). **B–C.** Interbedding between massive bioturbated mudstones and fine- to medium-grained sandstones with ripple lamination, parallel lamination, and erosive basal surfaces highlighting load-cast structures. Jacob's Staff for scale: 1.5 m. **D.** Irregular (erosive) surface of a submarine channel overlying internal levee/terrace deposits (FA5), with reworking of rip-up clasts. **E.** Irregular erosional basal surface of fine-grained sandstone with abundant ripple lamination and intense bioturbation by *Ophiomorpha* (*Op*), *Thalassinoides* (*Th*) toward the top. The contact with massive bioturbated mudstones displays a gradational transition. **F–G.** Massive bioturbated mudstones with patches of abundant *Phycosiphon* (*Ph*) and *Nereites* (*Ne*), showing cross-cutting relationships with *Taenidium* (*Ta*).

V.4.2.6. FA6: prograding successions decreasing from coarse, conglomeratic sandstones to bioturbated mudstones

Description. This facies association is characterized by tabular fining- and thinning upward successions from conglomeratic sandstones to mudstones that are up to 2 m thick and show sharp and irregular erosional bases (L3, L10; Fig. V.9A-B-C, and sketch B). Occasionally, scours are infilled by gravel and coarse sandstone, or the basal beds are granule- to pebble-sized matrix-supported conglomerates, with primarily lithic sedimentary angular clasts and a medium-grained sandy matrix. Rare grooves and flute marks are observed. Metric packages of poorly sorted medium-grained sandstones with pebble-sized rip-up clasts also occur, predominantly distributed at the bases of the successions. In some cases, this succession is repeated, showing erosive bases. In other layers, however, normal grading (L10) to medium to fine-grained sandstones with horizontally lamination (L9) are observed, followed by sandstones with ripple lamination and planar cross-lamination toward the top (Fig. V.9D, and sketch D). Synsedimentary deformation structures are sometimes found (Fig. V.9D). The tops of the successions are bioturbated mudstones with *Ophiomorpha*, *Scolicia*, *Taenidium*, and *Thalassinoides* (Fig. V.9E).

Interpretation. The repetition of tabular bedding, erosional basal bed surfaces, and rip-up clasts suggest the presence of high-energy turbiditic currents generating scours prior to deposition, where angular sedimentary clasts indicate a nearby source (Brooks et al., 2022). Normal grading is often associated with the waning stage of turbidity currents — the decrease in flow velocity would allow sediment particles to settle out of suspension, transitioning from depositional to bypass conditions (Komar, 1985; Kneller and Branney, 1995; Kneller and Buckee, 2000; Kneller and McCaffrey, 2003; Stevenson et al., 2014). Fine-grained sandstones with parallel lamination toward the base, followed by a development of planar cross-stratification, could indicate transport by a not very strong current of traction. Convolute laminations may be produced by shear, buoyancy instabilities, and/or water escape (e.g., Allen, 1977, 1985; Gladstone et al., 2018), indicating high suspension fall-out rates. Laminated fine-grained silt and mud accumulate toward the top when the flow is very slow and close to stopping. *Ophiomorpha*, *Scolicia*, *Taenidium* and *Thalassinoides* at the top indicate a post-depositional trace fossil assemblage assigned to the *Ophiomorpha rudis* *ichnosubfacies*, commonly found in channels and/or proximal lobes of turbidite systems (Uchman, 2009; Uchman and Wetzel, 2012; Callow et al., 2014; Rodríguez-Tovar, 2022).

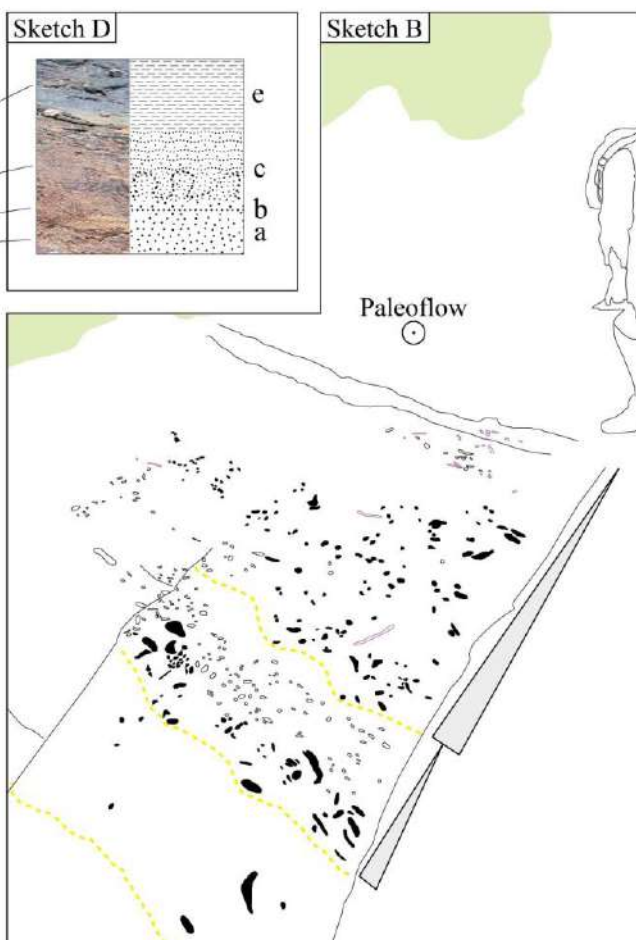
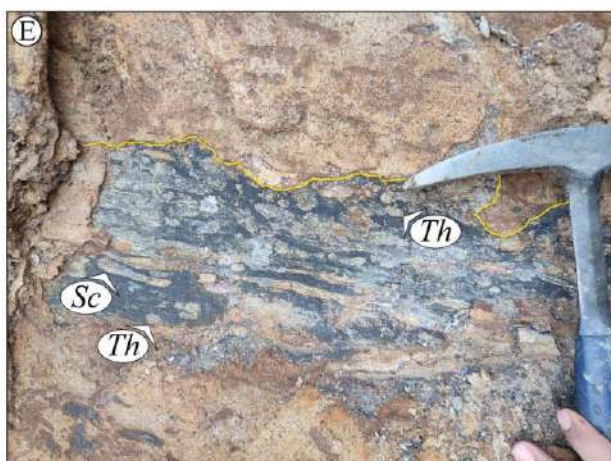
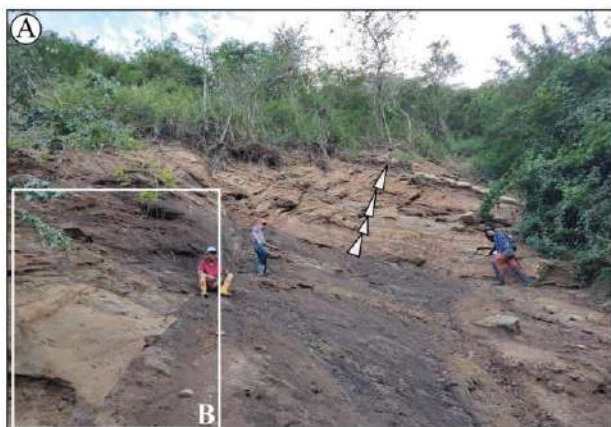


Fig. V.9. Facies association 6 (FA6). **A.** Overview of the outcrop. **B.** Erosional surface and deposit of medium- to coarse-grained structureless sandstone with accumulations of rip-up clasts and subsequent fining-upward successions (see sketch B). **C.** Fining- and thinning-upward successions ranging from poorly sorted granule-sized conglomerates that are matrix- to clast supported, passing transitionally to medium- to coarse-grained sandstone and upward fine-grained sandstone and mudstone. Topping beds are generally bioturbated. **D.** Ripple lamination is detailed at the base. Irregular surface and detail of the fining-upward succession from massive medium-grained sandstone (a), transition to a zone of syn-sedimentary deformation (b), upward ripple lamination (c), and bioturbated mudstones (e) (see sketch D). Chart to scale: 10 cm. Detail of the top of the fining-upward succession consisting of bioturbated mudstone with *Scolicia* (*Sc*) and *Thalassinoides* (*Th*), in addition to unidentified trace fossils.

Therefore, beds with gradations to finer sediments, as well as the presence of Bouma divisions, amalgamated sandstones, bioturbation to the top, laterally adjacent channel fills, and fining- and thinning-upward sequences would be indicative of the waning phase of low-density turbidity currents, suggesting deposition between an inner lobe and lobe off-axis context (Hubbard et al., 2009). The amalgamated massive sandstones and conglomeratic sandstones suggest rapid sediment deposition in marginal sheets of channels by turbidity currents of lower density in internal levees; when there is insufficient space in the channel for the flow to decelerate and deposit most of its sediment before reaching the channel boundary topography, confined sheet deposits or terraces are created (e.g., Babonneau et al., 2004; Kane and Hodgson, 2011; Paull et al., 2013; Hansen et al., 2015).

V.4.2.7. FA7: dark-gray mudstones

Description. This facies consists of sheet-like beds of massive to horizontally laminated gray mudstones and siltstones (L12), 20–30 cm thick, with a few thinner interbedded horizontally-laminated siltstones, 3–5 cm (Fig. V.3C-F-G). They contain mainly agglutinated benthic foraminifera.

Interpretation. Massive mudstone was deposited by suspension, settling in a low-energy environment attributed to hemipelagic sedimentation on the basin floor, where parallel-stratified mudstone beds are associated with low-energy traction-plus-fallout processes of low concentration turbidity currents (Stow and Piper, 1984; Stow, 1985; Stow and Tabrez, 1998; Potter et al., 2005; Navarro and Arnott, 2020; Stow and Smillie, 2020).

V.5. Depositional model

The studied sections of the San Jacinto Formation in Caribbean Colombia consist of predominantly coarse-grained deposits interpreted as the result of highly concentrated flows that occurred during the late Eocene. They would range from cohesionless debris flows to high-density turbiditic currents that persist in both supercritical to subcritical conditions (and transitions in between). The cyclic steps (FA2), antidune field (FA4), fining-upward successions (FA5 and FA6), reworking of fossil fragments from coastal systems (FA3b), benthic foraminiferal assemblages (FA7) associated with outer shelf to upper bathyal environments (Duque-Caro et al., 1996; Guzmán, 2007; Garzón Oyola, 2023), and the high content of organic matter (FA3b) all lead us to interpret that the flows with supercritical conditions were confined in submarine slope channel complexes

that evolved into less confined areas along well-preserved channel mouth depositional settings, with a final transformation to subcritical flows in an inner lobe to lobe off-axis context (Figs. V.10 and V.11).

V.5.1. Stage 1

The lower section in San Jacinto Creek is dominated by deposits of high-density currents in supercritical conditions represented by cyclic steps (FA2). The initiation is marked by depositional cyclic steps in an expansion zone along a shelf break to continental slope from confined flows (CMEZ using the classification of Hodgson et al., 2022) (Figs. V.10 and V.11).

Sedimentary features of the deposits (amalgamation, lack of fine deposits, poorly sorted deposits, and subangular rip-up and extra clast dominated deposits; FA1 and FA2) indicate that highly concentrated flows were confined within this submarine transfer routing system; therefore, it recorded the inception of a submarine channel (i.e., slope channel) fed directly from continental settings (i.e., alluvial fans or steep rivers) (Fig. V.11).

They are preserved as bypass deposits at the channel thalwegs, representing amalgamated infill units at the axis of these channels (Fig. V.11). The presence of gravel lenses and planar cross-stratified coarse-grained sandstone and conglomerate lag facies—as described here—are interpreted to represent bypass in slope channel fills (Mutti, 1992; Stevenson et al., 2015). Confined high-energy flows over a steep slope would impede the deposition of muds draping amalgamation surfaces, as reported in gentler base-of-slope settings (e.g., Mutti and Normark, 1987).

Cyclic steps (lower section in San Jacinto Creek) below and adjacent to stacking channel elements (Piedra Azul Creek, and upper part of Alférez Creek – jet section) would record the overall progradation of a lower slope succession, as interpreted in other ancient records (e.g., Pemberton et al., 2016) (Figs. V.10 and V.11). Channel fill elements are interpreted as cohesionless debris flows (bypass) and concentrated flow deposits (high density turbidites), likewise derived directly from continental areas or from a reworking of coastal systems (i.e., delta). The fine-grained sediment fraction of the flows was deposited outside of the channel belt as undifferentiated thin-bedded turbidites associated with levees or terraces (FA5) (Figs. V.10 and V.11).

V.5.2. Stage 2

Confined deposits in expansion zones (supercritical flows) vertically evolve to sigmoidal lens-shaped gravels, foreset and backset planar cross-stratified pebbly sandstones, and low-angle upstream, undulated-stratified (antidunes) granule to coarse-grained sandstones filling gentle scours (cut-and-fill structures) (FA4), which would represent the transition from CMEZ to CLTZ (San Jacinto Creek) (Figs. V.10 and V.11). Coarse-grained mouth-bar migration and antidunes (FA4) linked to supercritical flows characterize the CLTZ, where the currents lose channel (or canyon) confinement in the mouth to antidune field setting. However, the occurrence of sporadic debrites and channel fill toward the middle part of the San Jacinto Creek section (FA1), as well as interbedding with hemipelagites in a mixed-foraminiferal assemblage (FA7) with species typical of the outer shelf to upper and middle bathyal zones (Duque-Caro et al., 1996; Guzmán, 2007) would indicate other periods of slope instability (Fig. V.10).

The increased tabular bedding and fining-upwards successions, from coarse conglomeratic sandstones to bioturbated mudstones (FA6; Piedra Azul Creek and Alférez Creek – curve section) probably overlapping or

adjacent to an antidune field (San Jacinto Creek) may support a progressive decrease in depositional energy, which is associated with waning phase of low-density turbidity currents, suggesting deposition between an inner lobe and lobe off-axis context (Figs. V.10 and V.11).

Thus, the complete stratigraphic succession of San Jacinto Formation exposes the initiation, progradation and then retrogradation of a coarse grained turbidite channel-lobe system (Figs. V.10 and V.11). The studied sections of this lithostratigraphic unit are interpreted as the expression of decreasing confinement along a coarse-grained, submarine sediment routing system (Fig. V.11). It transferred highly concentrated flows from coarse-grained coastal systems (i.e., fan delta) to deep-water settings. Similar and scarce slope evolution has been documented in view of recent and ancient examples (e.g., Pemberton et al., 2016; Brandes and Winsemann, 2018).

V.6. Discussion – from confined to unconfined flows in coarse-grained channels: assessing integrative sedimentary facies

The CLTZ is perhaps the geomorphic subregion having the least available data among modern and ancient turbidite systems given its high erosive capacity, resulting in poor preservation (Hand, 1974; Mutti and Normark, 1987; Parker et al., 1987; Kenyon et al., 1995; Palanques et al., 1995; Wynn et al., 2002; Van der Merwe et al., 2014; Dennielou et al., 2017; Brooks et al., 2018; Maier et al., 2018; Maestrelli et al., 2020). As a result, knowledge of these zones is still developing worldwide, and their identification in outcrops is challenging. Studies of both modern examples and outcrops have led to new classifications (e.g., Hodgson et al., 2022). While descriptions to date of CLTZs include plunge pools, and distinctive long and flared tracts between channels and lobes, the novel term Channel Mouth Expansion Zone (CMEZ) has been proposed by Hodgson et al. (2022). Fitting these deposits into facies models is nonetheless complex, due to the multiple scenarios that can be generated (e.g., Postma et al., 2014). Multiple allogenic and autogenic factors modify the CLTZs: basin architecture (in active or passive margins); tectonic activity such as subsidence and uplift; sediment supply; weathering processes; amount of rainfall and runoff; temperature and sea-level changes; or sediment transport pathways from the source area. Therefore, the morphology and architecture of CLTZs depend on internal and external factors of the basin and the function of the Froude (Fr) number, with supercritical CLTZs differing from subcritical examples (Postma et al., 2016; McArthur et al., 2020).

Considering the sections visited and previous reports, we consider that this expansion zone would have a width of about 10 km (from San Jacinto Creek and transition to Piedra Azul Creek), with a channel lobe transition area of about 5 km (from Piedra Azul Creek to Alférez Creek); channel fills related to the backfilling phase have lenticular geometries with widths of <100 m (Piedra Azul Creek and Alférez Creek). However, we lack sufficient outcrops to establish the full continuity of the transition zones or interactions with other systems. Although this expansion system seems small in comparison with other examples (see Navarro and Arnott, 2020), it must be taken into account that it corresponds to a single system and that other systems probably developed along the margin.

This study is one of the few that reflects the expansion and then decrease of confinement along a coarse-grained sediment routing system. The compilation of different facies associations and other outcrop examples from deep-sea environments elsewhere (Supplementary material V.2; China, Chile, USA, Nicaragua,

Argentina, Spain) allows us to characterize at the facies level certain expansion zones and transitions to CLTZ under the domain of high-density turbidity currents fed by supercritical flows that transition to subcritical flows at active margins (Supplementary material V.2).

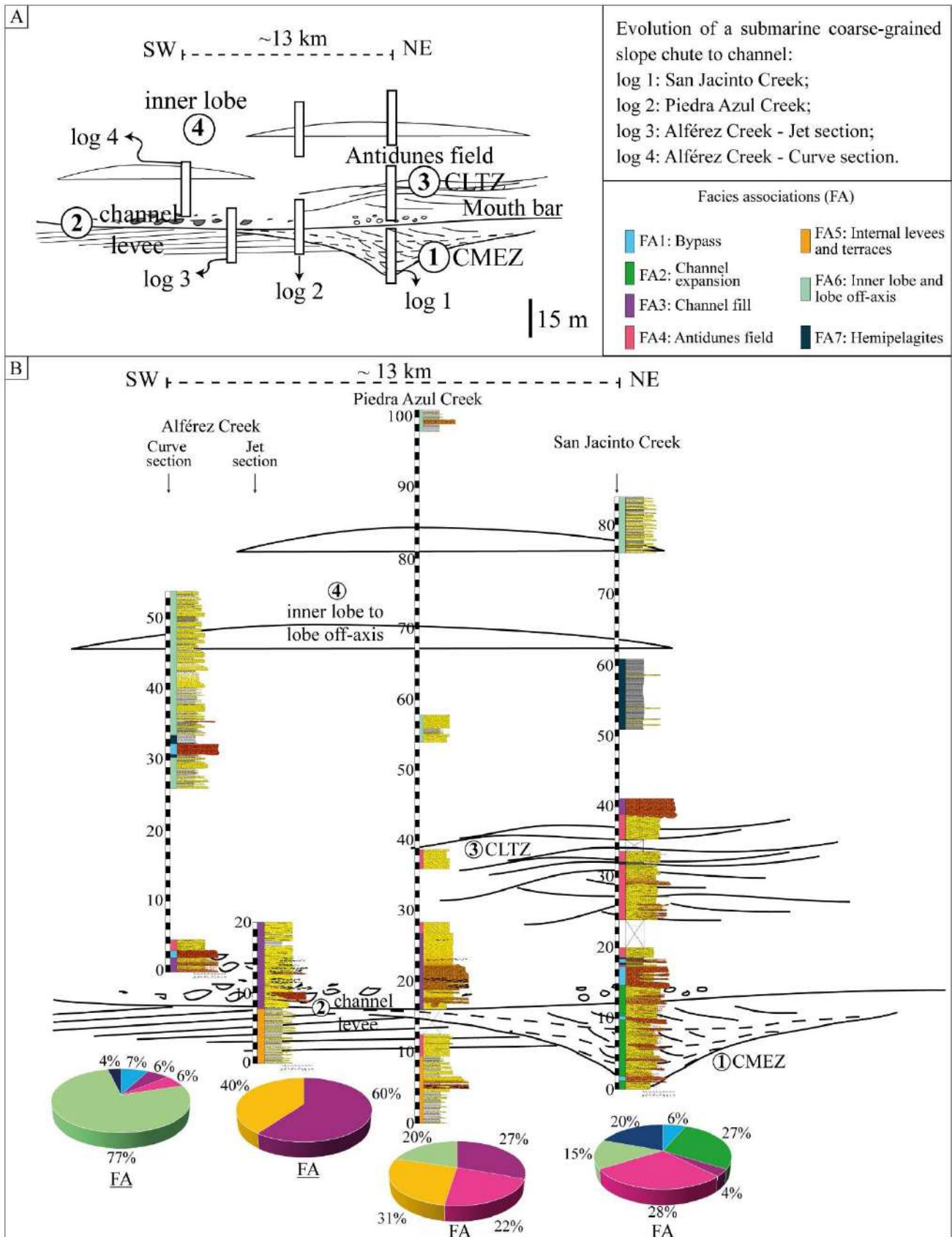


Fig. V.10. A–B. Sketch cross-section showing dominant facies associations and bedforms of the stage of expansion zone (CMEZ according to Hodgson et al., 2022) from proximal to distal settings, marking a stratigraphic correlation between San Jacinto Creek (to the north), Piedra Azul Creek, and Alférez Creek (the curve section and the jet section, to the south) based on sedimentary features recognized in outcrops. Note that the lower part of the sequence (1. CMEZ) is reported only in the San Jacinto Creek; 2. representative channel-levee elements in Piedra Azul Creek and Alférez Creek (the jet section); 3. antidune field and debrite bypass associated with CLTZ as reported in San Jacinto Creek and Piedra Azul Creek; and toward the top, 4. Inner lobes to lobe off-axis recognized in San Jacinto Creek, Piedra Azul Creek and Alférez Creek (curve section).

V.6.1. Mouth expansion zone

By studying the evolution of the San Jacinto Formation, several arguments can be derived about sedimentary systems and factors increasing the likelihood of preservation of ancient expansion zones [CMEZs according to Hodgson et al., 2022] in the sedimentary record. It is recorded at the base (stage 1 of the channel evolution) of a submarine channel lobe system dominated by highly-concentrated flows (cohesionless debris flows and high-density turbidity currents) coming directly from the continent with coastal reworking (fossil fragments, abundant sheets of organic matter). Thus, low-angle, upstream and downstream planar cross-bedding pebbly sandstones (back- and foresets) as well as lens and mound-shaped beds characterized supercritical flows; but near the boundary subcritical flows occurred at the beginning of the slope chute to channel dynamics (Fig. V.11). Coarse grained submarine slope systems (from submarine canyons to slope channel and fan complexes) composed of deposits of high-density turbidity currents are commonly related to short and steep margins with abrupt relief close to the shoreline, or high-gradient alluvial-fluvial systems (i.e., fan deltas, Gilbert type delta, shelf-edge deltas) attached to them. In this case, they may have been fed by products from the erosion of mountain range systems that show contemporaneous faster cooling rates along the entire paleomargin, related to exhumation and/or uplift during the final magmatic shutdown in the late Eocene (e.g., Restrepo-Moreno et al., 2009; Villagómez and Spikings, 2013). This would constitute one of the first evidence of coarse-grained deposits associated with the western margin of the orogen and could become further evidence that the cooling of the margin is indeed related to exhumation-erosion.

Coarse-grained submarine slopes derive from tectonically-active settings such as forearc basins (e.g., La Jolla Group; Maier et al., 2020, or Otadai Formation; Brooks et al., 2022) and from passive-margin contexts (e.g., Azpiroz-Zavala et al., 2017; see review in Navarro and Arnott, 2020). Tectonically active margins, generally with steep gradients and high sediment supply, provide a landscape where strong Froude supercritical flow turbidity currents can occur (e.g., Supplementary material V.2; Ono and Plink-Bjorklund, 2018). This study strongly supports that tectonically active basin fills—such as the Colombian Caribbean forearc basin—represent a favorable host of expansion zones given their steeper slopes than those of relatively tectonically-quiet ones. In addition, aggradational cyclic steps resulting in bed amalgamation in expansion zones (see FA2) require variability in river discharge, favored by the tropical humid conditions that involved large seasonal fluctuations in rainfall during which the deposits were formed (e.g., Martínez et al., 2021).

Hence, early-stage successions having a high proportion of supercritical bedforms and erosion surfaces could be candidates for sedimentary facies of expansion zones (Supplementary material V.2; Postma et al., 2014; Gong et al., 2017; Lang et al., 2017; Cornard and Pickering, 2019; Postma et al., 2021). Notwithstanding, some

examples of early expansion zone stage candidates could be from aggradational systems, where the onset of flow at lobe initiation stages may entail antidune facies associations and subsequently initiate a prograding cycle associated with cyclic steps (e.g., Supplementary material V.2; Postma and Kleverlaan, 2018; Postma et al., 2021).

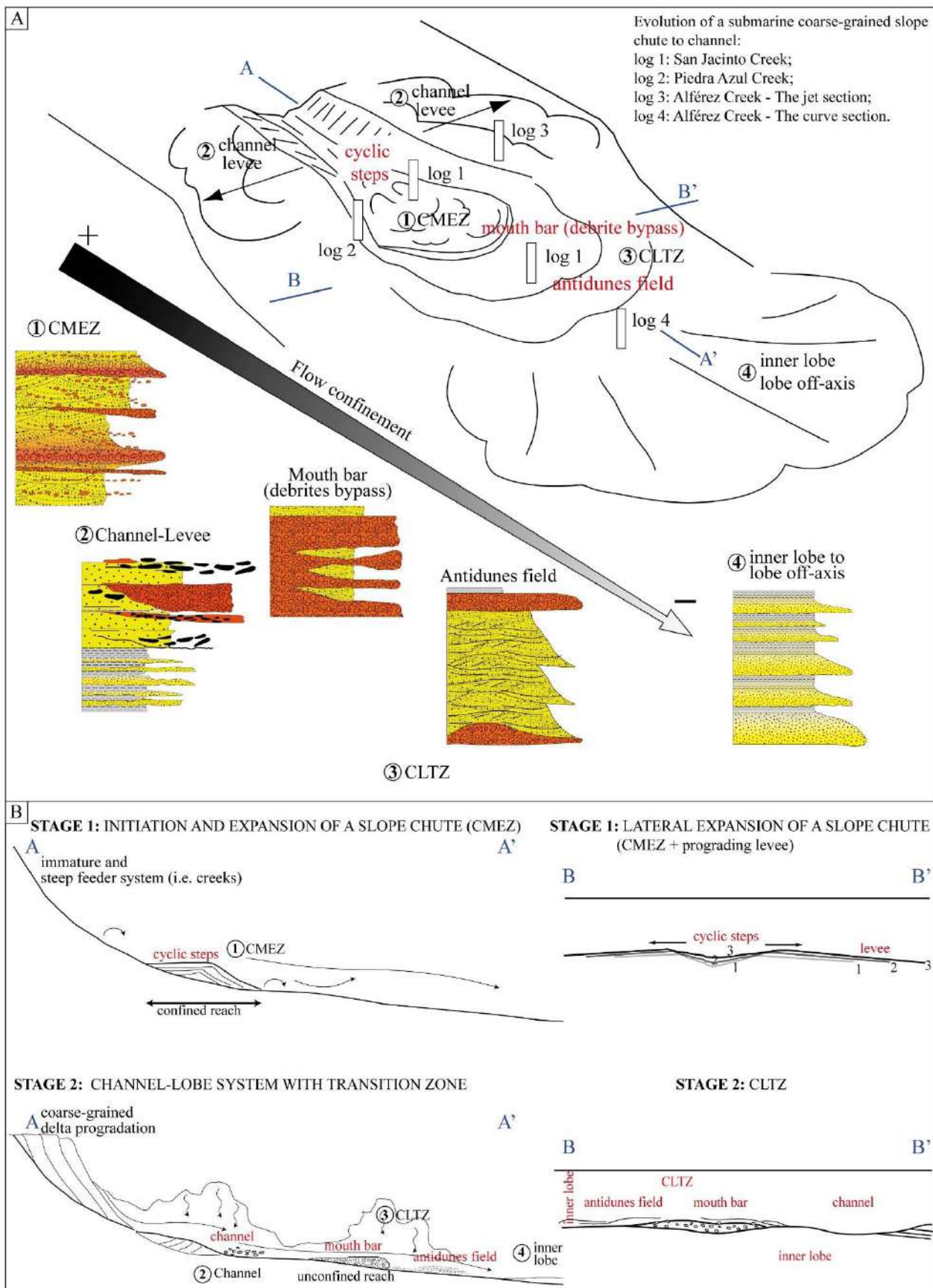


Fig. V.11. A. Supercritical to subcritical flows from CMEZ to classical CLTZ. Sedimentary facies. **B.** Cross-sections (A-A' and B-B') along and perpendicular to the channel axis showing different dominant sedimentary structures from channel-confined proximal settings (cyclic-step-dominated) to unconfined distal settings (inner lobes to lobe off-axis).

V.6.2. Channel-levee complex

Amalgamated scour-and-fill, rip-up- and/or hard-clast conglomerates to sandstones with nested offset stacking and burrowed (Ta-e) sandstone and mudstone layers below and adjacent to the expansion zone represent channeled high-density turbidites, as well as its levees and terraces, marking the onset of gravity flow deconfinement/transit.

Other examples of high gradient slopes and confined settings are known to form the feeder systems that subsequently generate large and small-scale cyclic steps (e.g., Supplementary material V.2; Ponce and Carmona, 2011; Postma et al., 2014, 2021; Cornard and Pickering, 2019). Apart from tectonics, climate is an important factor contributing to the development of the channel-levee complex and expansion zones, as highly concentrated flows coming directly from the continent are generated by river floods (e.g., Gábris and Nagy, 2005; Vellinga et al., 2018). Variable discharge rivers have been shown to support high sediment concentrations, promoting the formation of volumetrically significant fan deltas and coarse grained submarine channels (Gábris and Nagy, 2005; Wagreich and Strauss, 2005; Lang et al., 2017; Yang et al., 2017; Brandes and Winsemann, 2018; Grundvåg et al., 2023). On many occasions, this variability generates re-accelerated flow in the first stages of amalgamation of cyclic steps, hence a repetition of hydraulic jumps from supercritical to subcritical, and back to supercritical flows (e.g., Supplementary material V.2; Lang et al., 2017). Although no repetitions or variations in the cyclic steps could be identified here, the tropical context would favor such scenarios of systems fed by hyperpycnal flows (Supplementary material V.2; Yang et al., 2017; Martínez et al., 2021). Coarse- to medium-grained sandstones with inverse and then normal grading, horizontally laminated with plant debris (FA3b), are considered diagnostic facies of hyperpycnal flow origin (Mulder et al., 2003; Zavala et al., 2011, 2012; Yang et al., 2017; Grundvåg et al., 2023).

V.6.3. CLTZ: mouth bar (debrite bypass and antidune field)

CLTZs are the passage zones between channel-levee systems and well-defined lobes (Hansen et al., 2021; Hodgson et al., 2022). Therefore, they encompass facies associations with depositional and erosional bedforms ranging from cyclic steps to antidunes. Yet using the new classification by Hodgson et al. (2022) and based on the literature review, our study proposes integrative sedimentary facies from confined to unconfined systems. Accordingly, CLTZ would be linked to the second stages of supercritical bedforms, and characterized by sigmoid-shaped centimeter-thick, normally-graded pebbly sandstone to medium grained sandstone deposits having sigmoidal symmetrical or asymmetrical cross-bedding; low-angle bedding at the top with humpback cross bedding capped by sheet-like and lenticular-like matrix-supported conglomerate beds represent the progressive deconfinement of the flow in a transition zone between supercritical to subcritical flows ($Fr \sim 1$). The vertical stratal stacking pattern of the succession is another key to explain the low preservation of the expansion zones (CMEZ, according to Hodgson et al., 2022) in the ancient record.

Candidate San Jacinto expansion zone and other outcrops (i.e., Supplementary material V.2; Ponce and Carmona, 2011; Postma et al., 2014; Gong et al., 2017; Lang et al., 2017; Yang et al., 2017; Ono and Plink-Bjorklund, 2018; Postma and Kleverlaan, 2018; Cornard and Pickering, 2019) are preserved at the base of a succession exhibiting a retrogradational pattern represented from bottom to top by a candidate expansion zone-channel/levee, and initial stages of unconfinement in CLTZ (Fig. V.11; Supplementary material V.2; Postma et al., 2014; Pemberton et al., 2016; Lang et al., 2017; Cornard and Pickering, 2019). Perhaps the most documented prograding slope settings are not very favorable for expansion zone preservation because of a highly erosional depositional history, meaning the transit of flow decelerations to the antidune field is often not well preserved (Supplementary material V.2; Ponce and Carmona, 2011; Pemberton et al., 2016; Postma et al., 2016; Gong et al., 2017). Furthermore, in some zones the first stages of the flow may be completely aggradational (antidune), but progradation begins later (e.g., Postma and Kleverlaan, 2018; Postma et al., 2021).

V.6.4. Overbank to inner lobes

A prograding stacking pattern of successions—decreasing from coarse, conglomeratic sandstones to bioturbated mudstones—is associated with the zones best preserved in the stratigraphic record, and on this basis the facies models of channel-lobe transition zones in deep marine environments are put forth (Postma et al., 2014; Brooks et al., 2022). Typical successions with gradual energy decay—often bioturbated at the top under subcritical conditions in a deconfined state—have allowed us to observe numerous study sequences (e.g., Summer et al., 2012; Postma and Cartigny, 2014; Tinterri et al., 2022). Even facies models and stacking patterns of fine-grain sizes under supercritical conditions have been proposed (Normark et al., 2009; Mukti and Ito, 2010; Postma and Cartigny, 2014; Postma et al., 2014). In this case, however, such successions represent the end of the retrograding pattern, and link the previous facies with models established outside the confined channel suggesting deposition between an inner lobe and lobe off-axis.

V.7. Conclusions

Coarse-grained deposits of the San Jacinto Formation (late Eocene, Colombian Caribbean forearc subduction complex) are interpreted to record an exceptionally complete history of inception and evolution of a submarine channel system dominated by cohesionless debris flow to high-density turbidity currents with highly variable (Froude number) flow conditions. Gravelly amalgamated depositional cyclic step sets developed by highly concentrated flows in supercritical conditions are related to the onset of the confined segment becoming a submarine channel. Laterally, beyond the expansion zone (CMEZ), an aggrading undifferentiated channel belt thin-bedded turbidites associated with levees and terraces complex is built. Distally evolving to the expansion zone, bypass debrite capped by antidunes alternating with mudstone layers can be interpreted as the slope channel-mouth bar and the antidune field of a Channel-Lobe Transition Zone (CLTZ) dominated by cohesionless debris flows to high-density turbidites under supercritical conditions. Finally, the transition to the subcritical domain is determined by the record of bioturbated inner lobe to lobe off-axis deposits. The stratigraphy of the San Jacinto Formation in this area reflects an expanding and then decreasing confinement along a coarse-grained sediment routing system, from the channel mouth expansion zone to channel-lobe

transition zone in the shelf-break context. Clast textural features, abundant organic matter, and reworked coastal bioclasts found within the coarse-grained deposits reveal that the head of the slope channel/canyon cuts across a shallow marine system fed by a fairly high-gradient fluvial system and immature source. This occurred along a tectonically-active, short and abrupt basin margin, with seasonal rainfall variations during the Eocene-Oligocene transition in the forearc subduction complex. The development of expansion zone deposits in the form of cyclic steps takes place in the framework of concurrent active sediment transport, bypass, and deposition of coarse-grained material from a channel-levee system; the antidune field (transition from expansion zones) and loss of confinement in inner lobes to lobe off axis context are compared with further examples of deep marine environments having expansion zones. Thus, the facies evolution proposed here can be linked with traditional facies models in turbiditic systems, to propose advances in our knowledge of the transition from supercritical to subcritical flows.

Acknowledgments. Financial support of Celis and Giraldo-Villegas was provided by the National Program for Doctoral Formation (Minciencias Colombia grants 885-2020, 906-2021 respectively). Financial support for Rodríguez-Tovar was provided by scientific Projects PID2019-104625RB-100 (funded by MCIN/AEI/10.13039/501100011033), P18-RT-4074 (funded by FEDER/Junta de Andalucía-Consejería de Economía y Conocimiento), B-RNM-072-UGR18 and A-RNM-368-UGR20 (funded by FEDER Andalucía). We would like to express our gratitude to Catherine Chagué (Editor-in-Chief) and two anonymous reviewers for their constructive comments and suggestions. Funding for open access charge: Universidad de Granada / CBUA.

Supplementary data

The following are the supplementary data related to this article.

Supplementary material 1. Description and interpretation of lithofacies.

<https://ars.els-cdn.com/content/image/1-s2.0-S0037073823002221-mmc1.docx>

Supplementary material 2. Outcrop examples of facies and processes in supercritical and transition to subcritical bedforms.

<https://ars.els-cdn.com/content/image/1-s2.0-S0037073823002221-mmc2.docx>

Supplementary material 3. Details of the location of the figures.

<https://ars.els-cdn.com/content/image/1-s2.0-S0037073823002221-mmc3.xlsx>

Chapter VI

OLIGOCENE TO LOWER MIOCENE FLUVIO-DELTAIC SYSTEMS

**Evolution of a fluvial-dominated delta during the Oligocene of the Colombian Caribbean:
Sedimentological and ichnological signatures in well-cores**

Sergio A. Celis^{a,b,*}, Francisco J. Rodríguez-Tovar^{b,}, Carlos A. Giraldo-Villegas^{a,b}, Andrés Pardo-Trujillo^{a,c}**

a Instituto de Investigaciones en Estratigrafía-IIES, Universidad de Caldas, 170004 Manizales, Colombia

b Departamento de Estratigrafía y Paleontología, Universidad de Granada, 18002, Granada, Spain

c Departamento de Ciencias Geológicas, Universidad de Caldas, Calle 65 N° 26 - 10, Manizales, 275, Colombia

Journal of South American Earth Sciences, 111 (2021), 103440



<https://doi.org/10.1016/j.jsames.2021.103440>

Highlights

- Integrated sedimentological/ichnological analysis is conducted on deltaic sediments.
- Trace fossil features allow interpret limiting paleoenvironmental conditions.
- Fluvial processes are dominant in the deltaic system, but tidal and wave influence is recognized.
- Deltaic succession type repeats, with minor changes, through the Oligocene.
- Trace fossil abundance and diversity allows characterize different sub-environments.

Abstract

Basin analysis from Colombian Caribbean is particularly important given the interest in finding hydrocarbon reservoirs, but their complex geological evolution, and the frequent lateral and vertical variation of facies difficult a conclusive characterization, highlights the need for detailed sedimentological and ichnological studies. The study succession corresponds to an interval of a well core drilled in the south of the Sinú-San Jacinto Basin (Colombian Caribbean), with 1069 ft (~326 m) thick of an Oligocene siliciclastic succession, interpreted in general terms, as deposited in a deltaic system. The integrated sedimentological/ichnological analysis allows the differentiation of dominant facies, with predominant lithologies such as conglomerates,

sandstones, mudrocks, bioclastic sediments, as well as coal beds. The ichnological assemblage is low in abundance and moderately diverse, composed by *Conichnus*, *Cylindrichnus*, *Dactyloidites*, *Macaronichnus*, *Ophiomorpha*, *Phycosiphon*, *Skolithos*, *Taenidium*, *Teichichnus*, and *Thalassinoides*, as well as rhizoliths.

The complexity of the sedimentary system is reflected in its evolution throughout the Oligocene. A type succession with coarsening-upward trend was identified and it is repeated through the succession studied. It presents a general trend from bioclastic sediments (bioclastic conglomerates, sandstones and mudrocks) that pass into horizontal lamination and massive mudrocks occasionally bioturbated by *Phycosiphon*, and interbedded by mudrocks and sandstones with lenticular bedding, and the occurrence of *Teichichnus*. Above, bioturbated muddy sandstones with *Ophiomorpha*, *Taenidium*, *Thalassinoides*, and rarely *Teichichnus*, muddy sandstones with planar cross-lamination, and horizontal lamination sandstones with *Dactyloidites*, *Ophiomorpha*, *Skolithos*, and *Thalassinoides* are registered. Transition to carbonaceous mudrocks with *Teichichnus*, coal medium beds, and fine-to coarse-grained sandstones sometimes with *Macaronichnus* and/or *Ophiomorpha* is observed. Towards the top, are observed mudrocks with rhizoliths. This succession is interrupted by massive and horizontal lamination sandstones with low bioturbation index generated by the ichnological assemblage and/or by the exclusive occurrence of *Ophiomorpha* and/or *Taenidium*. Massive sandstones with erosive bases, asymmetrical ripples, and high content of organic debris are occasionally recorded. This succession reflects a progradational trend similar to those of fluvial-dominated deltaic sequences.

Detailed analysis revealed that even the fluvial processes were dominant in the deltaic system; however, local tidal and wave influence is recorded. Moreover, integration of sedimentological and ichnological information allows characterizing the evolution of the different sub-environments of the deltaic system, as prodelta bay, distal delta front, proximal delta front, distributary channels, mouth bars, and lower delta plain, and this is essential for areas of economic interest.

Keywords. Trace fossils, Palaeoecological and depositional conditions, Deltaic system, Well-core, Hydrocarbon exploration, Oligocene, Colombia.

VI.1. Introduction

Deltaic environments are complex settings determined by the interactions of fluvial and marine hydrodynamic processes, as well as by the geometry of the receiving basin, and type and amount of sediments delivered from the river (Tonkin, 2012). In this sense, deltas generate variable coastal morphologies depending on their genesis and fluvial, tidal and/or wave interactions (Dalrymple et al., 1992).

Deltas present diagnostic facies trends as the fluvial system incorporated into the sedimentary basin supplies a greater sediment load than can be redistributed outside the mouth bar by the dominant wave and/ or tidal processes, and significantly influence associated coastal environments such as coastal plains and tidal flats (Galloway, 1975; Boyd et al., 1992; Orton and Reading, 1993; Bhattacharya and Giosan, 2003; Bhattacharya, 2006). These trends are observed in outcrops and cores, being generally recognized as coarsening upward successions (Tonkin, 2012). These are progradational, and sometimes retrogradational, siliciclastic sequences associated with the dynamic of the relative sea level (regressive and transgressive phases), according to the

supply of sediment, redistribution capacity, the morphology of the basin, and the coastline (Bhattacharya and Walker, 1992; Dalrymple et al., 1992; Dalrymple and Choi, 2007; Ainsworth et al., 2008, 2011, 2011; Tonkin, 2012).

The study of deltaic deposits has been based, fundamentally, on the analysis of sedimentary features (e.g., sedimentary structures, textures), together with paleontological and geochemical information (MacEachern et al., 2005). In most researches, the presence of biogenic sedimentary structures is indicated, which, according to the growth of ichnology in recent years, determined the integration of ichnological studies as an essential tool for the analysis of deltaic systems (Pemberton and Wightman, 1992; MacEachern et al., 2005; Gani et al., 2007; MacEachern and Bann, 2008, 2020; Dashtgard et al., 2011; Buatois et al., 2012; Tonkin, 2012; Shchepetkina et al., 2019; Bayet-Goll and Neto de Carvalho, 2020; Canale et al., 2020; Moyano Paz et al., 2020). Coastal systems with deltaic influence are characterized by receiving fluvial discharges that, depending on the capacity of marine processes (waves or tides) to redistribute sediment and the fresh water provided by rivers, generate significant fluctuations in the physical-chemical conditions, determining a stressful environment (Collins et al., 2020). Thus, the trace makers, as responding to these environmental changes (ecological and depositional), provides ichnological evidences (i.e., morphology and size of the structures, degree of bioturbation, distribution, ichnodiversity, ichnodisparity, tiering) which contribute to the detail characterization of delta settings (Ekdale et al., 1984; Bromley, 1990; Buatois et al., 2005, 2012, 2012; MacEachern et al., 2005; Hansen and MacEachern, 2007; Bann et al., 2008; Collins et al., 2020). On this basis, the integration of sedimentology and ichnology reveals essential for the interpretation of deltaic environments, and the associated physicochemical parameters such as salinity, hydrodynamics, sedimentation rate, oxygenation, substrate consistency, turbidity, light, or temperature, allowing evaluation of the importance of fluvial, tidal and/or wave processes during delta development (Bhattacharya and Giosan, 2003; MacEachern et al., 2005, 2007a, 2007a; Gani et al., 2007; Buatois and Mángano, 2011).

The Sinú-San Jacinto (SSJB) and Lower Magdalena Valley (LMV) basins of the Colombian Caribbean have currently a particular economic importance, based on the existence of numerous oil and gas seeps, as well as boreholes with evidence of hydrocarbon (Bernal–Olaya et al., 2015; Osorno and Rangel, 2015). Particularly, the SSJB shows evidence of the existence of an active petroleum system, being one of the basins with more petroleum seeps in Colombia, and within which have been tested Upper Cretaceous sequences as hydrocarbon source rocks (Osorno and Rangel, 2015). These characteristics make this basin an ideal area for hydrocarbon exploration.

For this purpose, the National Hydrocarbons Agency (ANH) has drilled several cores of exploratory wells in order to know and understand in detail the petroleum systems of the Colombian Caribbean, because its stratigraphic and structural complexity difficult to understand the geologic evolution of the basin (e.g., Taboada et al., 2000; Cediél et al., 2003; Pindell et al., 2005; Escalona and Mann, 2011; Cardona et al., 2012; Rosello and Cossey, 2012; Alfaro and Holz, 2014; Mora et al., 2017, 2018; Silva–Tamayo et al., 2017; Montes et al., 2019). The stratigraphic studies involving the geological evolution of the SSJB show the difficulty for the establishment of the elements of the petroleum system given the continuous variation of facies both lateral and

vertically (Duque–Caro, 1991; Guzmán et al., 2004; Guzmán, 2007; Bermúdez et al., 2009; Bermúdez, 2016; Mora et al., 2017, 2018; Osorio-Granada et al., 2020; Manco–Garcés et al., 2020).

In 2015, the National Hydrocarbons Agency (ANH) drilled the ANH-SSJ-Nueva Esperanza-1X stratigraphic well, which is located close to the Montería-Planeta Rica road (coordinates 8°31' 42,68' N/ 75°40'31,93' W) reaching a total depth of ~2266 ft (~691 m) (Fig. VI.1). A well core interval drilled a sedimentary succession of Oligocene age associated with Ciénaga de Oro Formation (Fig. VI.1) that, according to its lithological characteristics, have been considered as a potential reservoir within the system (Flinch, 2003; Marín et al., 2010). However, its complex lateral variation of facies within the basin prevents the proposal of a definitive model. On this base, the aim of the present research is the detailed integrative ichnological and sedimentological analysis of a sedimentary succession drilled in the SSJB in order to improve the understanding vertical variations, and characterization of the dynamics of deltaic environments developed in the Colombian Caribbean during the Oligocene.

VI.2. Geological setting

The NW corner of South America is influenced by the interaction between Nazca, Caribbean and South America plates (Montes et al., 2019; Mora-Paez et al., 2019). This complex interaction has controlled the filling of the sedimentary basins from the Upper Cretaceous to the Recent (Mora et al., 2017, 2018, 2018; Montes et al., 2019; Pardo–Trujillo et al., 2020).

Into the onshore sedimentary basins at the north of Colombia, the SSJB and LMV are considered forearc basins, geologically separated by the Romeral Fault System (Bernal–Olaya et al., 2015; Mora et al., 2018; Montes et al., 2019). The SSJB is located on an igneous oceanic basement of Cretaceous age (Geotec, 2003; Guzmán, 2007; Bermúdez et al., 2009; Silva–Arias et al., 2016; Mora et al., 2017). Its sedimentary fill includes rocks from Upper Cretaceous to Recent (Fig. VI.2), linked to the northeastern migration of the Caribbean Plate (Mora et al., 2017, 2018; Montes et al., 2019; Pardo–Trujillo et al., 2020). Limestones, mudrocks, cherts and sandstones, from the Cansona Formation of Campanian – Maastrichtian age overlay the basement (Duque-Caro, 1968, 1972; Guzmán, 2007; Bermúdez et al., 2009; Dueñas and Gomez, 2011; Bermúdez, 2016). Subsequently, the collision of the Caribbean Plate against the northern South American margin produced a tectonic event, recognized by a lower Paleocene unconformity-LPU (Guzmán et al., 2004; Mora et al., 2017). Upper Paleocene – lower Eocene conglomerates, sandstones and mudrocks from the San Cayetano Formation overlay the Upper Cretaceous rocks (Duque-Caro, 1972; Guzmán, 2007; Bermúdez et al., 2009; Bermúdez, 2016; Mora et al., 2017). In the early to middle Eocene, the increase in morphotectonic activity generated another unconformity: lower middle Eocene unconformity-LMEU (Guzmán et al., 2004; Mora et al., 2017). The Chalan/Chengue/Toluviejo formations, composed of conglomerates, sandstones, limestones and mudrocks of middle – late Eocene age overlay the San Cayetano Formation, and are overlaid by the Carmen/San Jacinto formations of late Eocene – early Oligocene age (Duque-Caro, 1972; Guzmán, 2007; Bermúdez et al., 2009; Bermúdez, 2016; Mora et al., 2017, 2018). Later, sandstones and siltstones with coal beds associated with the Ciénaga de Oro Formation (Oligocene – early Miocene age) were deposited (Duque-Caro, 1972; Guzmán, 2007; Bermúdez et al., 2009; Bermúdez, 2016; Mora et al., 2017, 2018; Manco–Garcés et al., 2020). A regional early Miocene tectonic event generated the lower Miocene unconformity-LMU (Mora

et al., 2018). In the middle to late Miocene, were deposited siltstones and in minor proportion sandstones correspond to the Porquero Formation (Duque-Caro, 1972; Guzmán, 2007; Bermúdez et al., 2009; Bermúdez, 2016). Upper Miocene – Pliocene sandstones, siltstones and carbonaceous levels associated with the El Descanso, El Cerrito and Tubará Formation were registered above (Duque-Caro, 1972; Guzmán, 2007; Molinares et al., 2012). Finally, Pliocene and Quaternary sandstones, siltstones, conglomerates and limestones from the Sincelejo, Morroa and La Popa Formation were deposited (Duque-Caro, 1972; Guzmán, 2007; Molinares et al., 2012).

VI.2.1. Ciénaga de Oro Formation

During the Oligocene – early Miocene, thick shallow marine and deltaic deposits accumulated in the southern part of the SSJB corresponding to the Ciénaga de Oro Formation (Dueñas and Duque-Caro, 1981; Dueñas, 1986; Guzmán et al., 2004; Bermúdez et al., 2009; Bermúdez, 2016; Manco– Garcés et al., 2020). Duque-Caro (1972) in the stratigraphic sections of Arroyo Alférez and Carmen-Zambrano defined the Carmen Group that includes from base to top, Ciénaga de Oro, Porquero and Cerrito formations. Subsequently, Duque-Caro (1973) used the term Ciénaga de Oro to designate the succession of sandstones and mudrocks outcropping on the Montería-Planeta Rica road. The term Ciénaga de Oro Formation is derived from unpublished Intercol oil company reports that use it in the Montería-Planeta Rica and Ciénaga de Oro-La Ye regions (Dueñas and Duque-Caro, 1981). Based on palynological, stratigraphic and seismic studies carried out in the Ciénaga de Oro Formation, an Eocene (?) – Oligocene to lower Miocene age is assigned (Dueñas, 1980, 1983, 1986, 1983; Dueñas and Duque-Caro, 1981; Guzmán et al., 2004; Bermúdez et al., 2009; Mora et al., 2018). The thickness of this unit was measured on the Montería-Planeta Rica road and corresponds to at least 2500 m of a domain of sandy facies with intercalations of calcareous gray mudrocks, carbonaceous mudrocks and coal (Dueñas and Duque-Caro, 1981).

Dueñas and Duque-Caro (1981) and Mora et al. (2018) divide the Ciénaga de Oro Formation into two segments: lower and upper. The analysis of planktonic foraminifera in well-cores and outcrops reported by Mora et al. (2018) assign an Oligocene to lower Miocene age for the lower segment. This unit is limited towards the top by a regional unconformity that puts it in contact with the upper segment (Mora et al., 2018), which has a lower to middle Miocene age (Dueñas and Duque Caro, 1981; Mora et al., 2018).

VI.3. Material and methods

In the last years, the National Hydrocarbons Agency (ANH) has drilled several stratigraphic wells in the Colombian Caribbean area in order to characterize the evolution and hydrocarbon potential of the basins. The study succession corresponds to an interval of the ANH-SSJ-Nueva Esperanza-1X stratigraphic well, drilled in the south of the SSJB. The study interval is between 2013 ft–946 ft (~614 m–~288 m) from the top. The well-core was described in detail in the Colombian core repository (Litoteca Nacional-Piedecuesta, Colombia). The Oligocene age data were taken from the biostratigraphic study developed by the Universidad de Caldas for the ANH and Minciencias based mainly on palynomorphs, foraminifera, and calcareous nanofossils (Project Contrato RC 494, 2017) and other previous works in the Ciénaga de Oro Formation (e.g., Dueñas, 1980).

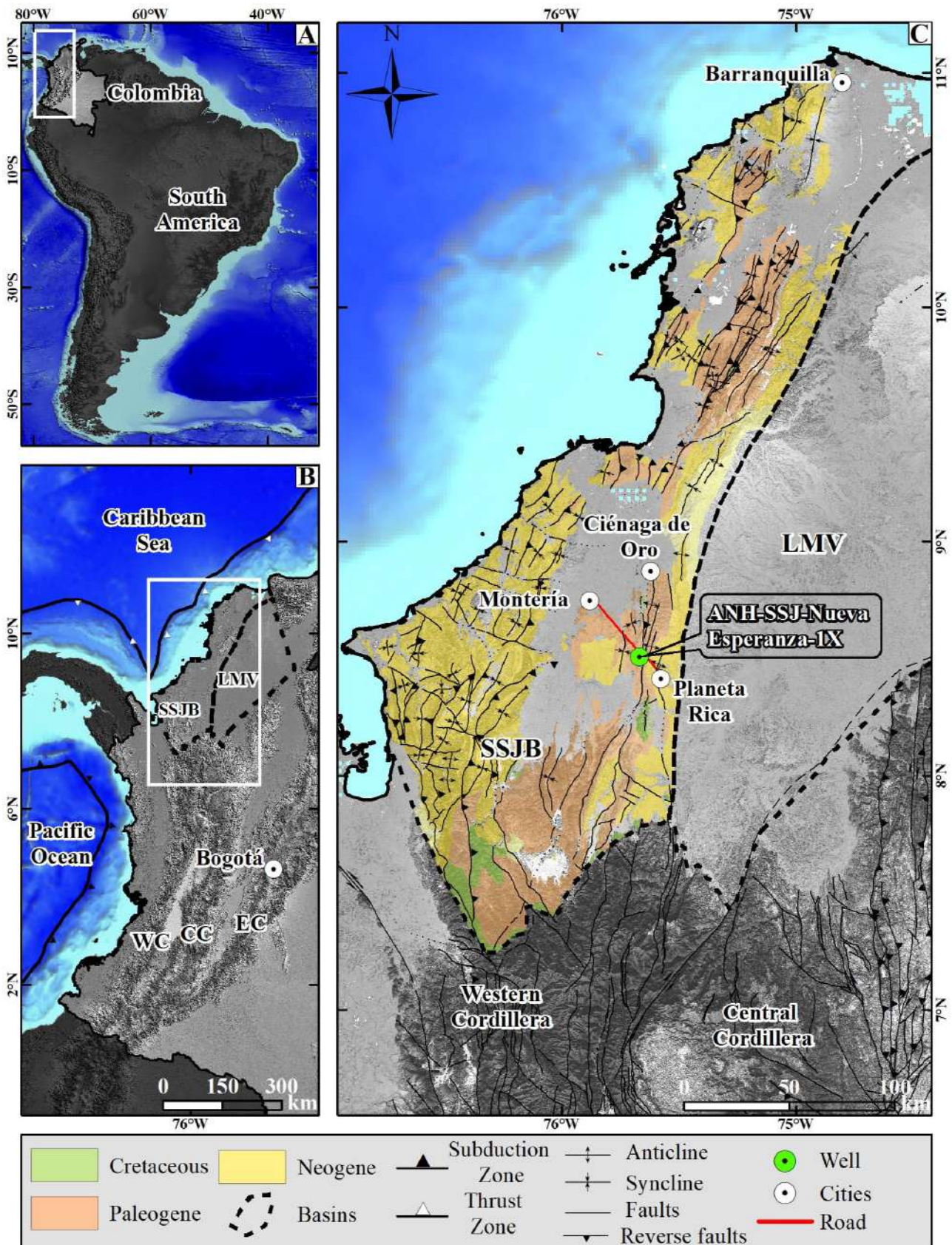


Fig. VI.1. Location map. **A.** Location of Colombia in South America. **B.** Location of the Sinú-San Jacinto Basin (SSJB) and Lower Magdalena Valley Basin (LMV) in the Colombian Caribbean (WC Western Cordillera; CC Central Cordillera; EC Eastern Cordillera). **C.** Sinú-San Jacinto Basin (SSJB). Montería-Planeta Rica road. Geology is only indicated in the SSJB (Source: WGS-1984 coordinate system; CIOH, SRTM, NOAA elevation and ocean models; geology of Gómez et al., 2015).

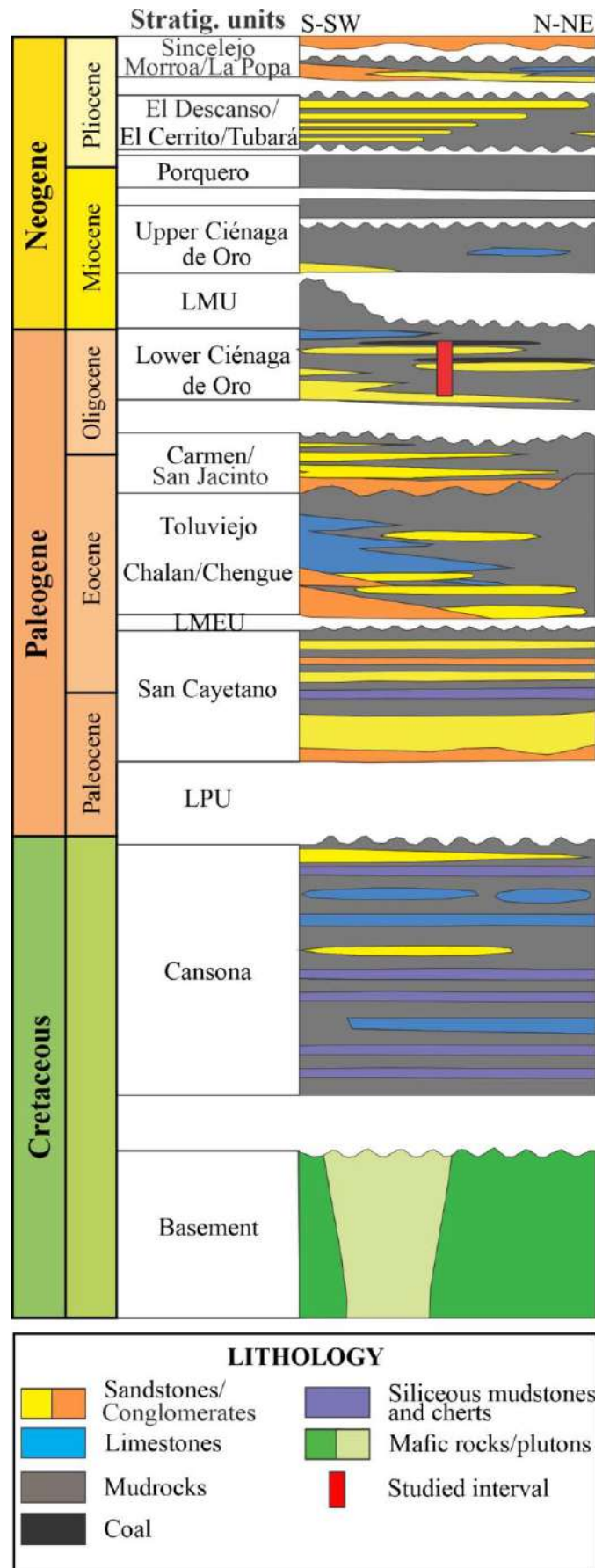


Fig. VI.2. Schematic chronostratigraphic chart of the Sinú-San Jacinto Basin (modified from Mora et al., 2017, 2018; Osorio-Granada et al., 2020). Note: LPU: lower Paleocene unconformity; LMEU: lower-middle Eocene unconformity; LMU: lower Miocene unconformity.

A detailed stratigraphic log (scale 1:1) was carried out taking into account the lithology (texture, composition), sedimentary structures, contact types, and paleontological contents (fossils, and biogenic sedimentary structures). The thicknesses of the beds are described following the nomenclature of Nichols (2009): very thin beds (<1 cm), thin beds (1–10 cm), medium beds (10–30 cm), thick beds (30–100 cm), very thick beds (>100 cm). Special attention was paid to the detailed ichnological characterization, including ichnological features such as size of trace fossils, type of fill, orientation, relationship with the facies and stratigraphic surfaces, and tiering, as well as ichnodiversity, distribution and abundance (Bioturbation Index, BI, sensu Taylor and Goldring, 1993) of the structures. Ichnotaxonomical assignation is based on the recognition of ichnotaxobases as observed in cores (Knaust, 2017). The facies codes were assigned from the terminology used by Collinson and Mountney (2019).

VI.4. Sedimentology and ichnology

VI.4.1. Facies

The well-core segment studied corresponds to a siliciclastic succession approximately 1069 ft (~326 m) thick. Five lithological groups were differentiated in the study succession (sandstones - Fig. VI.3, mudrocks - Fig. VI.4, conglomerates - Figs. VI.3 and VI.4, bioclastic sediments - Figs. VI.3 and VI.4, and coal levels - Fig. VI.4), as well as the definition of sedimentary facies (Table VI.1; Figs. VI.3 and VI.4).

The study interval is formed mainly by thin, medium and thick sandstone beds from very fine-medium to coarse-slightly conglomeratic sizes, gray and yellowish gray. Also, the grain-selection is variable from poor to well sorted. Internally and throughout the well-core, massive structure (Sm; Fig. VI.3A), horizontal lamination (Sh; Fig. VI.3B), low-angle cross-bedding (Sa; Fig. VI.3C), planar cross-bedding (Sp; Fig. VI.3D), and trough cross-bedding are present (St; Table VI.1; Figs. VI.3I and VI.5). Sandstones and mudrocks intercalations are observed, showing flaser (Htf; Fig. VI.4A), wavy (Htw; Fig. VI.4B) and lenticular bedding (Htl; Fig. VI.4C), where the occurrence of mud-drapes is also common (Table VI.1; Fig. VI.5). In addition, in some intervals hummocky cross-stratification (HCS; Fig. VI.3E) is observed, as well as convolute lamination (Sc) (Fig. VI. 3F), flame structure, load casts (Sf, Slc; Fig. VI.3H-M), and asymmetrical (Sr; Fig. VI.3G) and symmetrical ripples (Sw; Fig. VI.3H; Table VI.1; Fig. VI.5). Some massive sandstones (Sm) have rhizoliths. In some intervals, there are medium-to coarse-grained sandstones with fragments of organic matter, erosive bases and tops with normal gradation (Sng; Fig. VI.3J) to fine and very fine-grained sandstones. Occasionally, inverse gradation (Sig; Fig. VI.3K) to conglomeratic sandstones and granule-sized matrix-supported conglomerates, and then normal gradation to coarse and medium-grained sandstones is registered (Table VI.1; Fig. VI.5). Bioturbation index in sandstones range from 0 to 5. Massive sandstones (Sm) generally exhibit the highest values of BI = 4–5 (Table VI.1; Fig. VI.5).

Thin, medium and thick light gray to dark/black mudrock beds are common in the study succession (Table VI.1; Fig. VI.5). They occur mainly with lenticular bedding (Htl; Fig. VI.4C) and, occasionally, massive structure (Mm; Fig. VI. 4D), and horizontal lamination (Mh; Fig. VI.4E), with a variable but low bioturbation index (BI = 0 and 2; Table VI.1; Fig. VI.5). Some syneresis cracks (Ms; Fig. VI.4F), iron and siderite nodules and, occasionally, accompanied by rhizoliths are also observed (Table VI.1; Fig. VI.5). The micropaleontological analysis reveals the presence of mudrocks levels with few calcareous nanofossils,

foraminifera (benthic and planktonic), and marine palynomorphs (dinoflagellates), and in a higher proportion pollen and spores (Project Contrato RC 494, 2017).

Throughout the study interval, thin, medium and thick beds of gray and yellowish gray polymictic granule-sized matrix- and clast-supported conglomerates (Gmm, Gcm; Fig. VI.4H-I) associated with sandstones. To a lesser extent, pebbles-sized conglomerates are observed (Table VI.1; Fig. VI.5). Their clasts are subangular to subrounded, moderately to well sorted. Change to sandstones beds can be gradational (Gng, Gig; Fig. VI.4J-K), erosive or net (Table VI.1; Fig. VI.5). Rarely, pebble-sized oligomictic clast-supported conglomerates (Goc; Fig. VI.4L) are observed consisting of mudrocks clasts (Table VI.1; Fig. VI.5). Woody fragments are also common. Biogenic sedimentary structures in the conglomerates are scarce, although in the variations from medium to coarse sandstones to conglomeratic sandstones and to granule-sized matrix-supported conglomerates, traces of *Ophiomorpha* and bioturbation index between 0 and 2 are observed (Table VI.1; Fig. VI.5).

Frequently, medium to thick bioclastic sandstones beds (Sb; Fig. VI.3L) with indeterminate shell fragments, bivalves and gastropods fragments occur (Table VI.1; Fig. VI.5). They show slight variations to granule-sized bioclastic matrix-supported conglomerates (Gb; Table VI.1; Fig. VI.4M; Fig. VI.5). Thin and medium bioclastic mudrock beds (Mb) with slight variations to bioclastic sandstones (Sb; Fig. VI.4G) are also locally recognized, with, bivalves, and gastropods and indeterminate shell fragments (Table VI.1; Fig. VI.5). On some occasions, granule-sized bioclastic matrix-supported conglomerates (Gb; Fig. VI.4M) are observed in net contact on the sandstones or medium coal beds (Co; Table VI.1; Fig. VI.5). The bioclastic content of the conglomerates consists of indeterminate shell fragments, as well as bivalves and gastropods. Bioturbation index in bioclastic sediments range from 0 to 2.

Very thin, thin, and medium coal beds (Co; Fig. VI.4N) are also observed in the study interval (Fig. VI.4), with a variable relationship with the other lithologies (Table VI.1; Fig. VI.5). The base usually presents net contacts with other lithologies and occasionally transitional contacts from carbonaceous mudrocks. The top of these coal beds shows transitional change to mudrocks, and/or erosive contacts with bioclastic sediments (bioclastic sandstones (Sb) and/or bioclastic conglomerates (Gb)), and to a lesser extent to massive sandstones (Sm; Table VI.1; Fig. VI.5). Bioturbation index 3–4 characterize the top of some of these coal beds (Table VI.1; Fig. VI.5).

VI.4.2. Trace fossils

Trace fossil assemblage in the studied succession is low abundant and moderately diverse. Ten ichnogenera have been recognized, including *Conichnus*, *Cylindrichnus*, *Dactyloidites*, *Macaronichnus*, *Ophiomorpha*, *Phycosiphon*, *Skolithos*, *Taenidium*, *Teichichnus*, *Thalassinoides*, as well as undifferentiated rhizoliths. The bioturbation index ranges from 0 (no traces) to 4–5 (intense bioturbation to almost completely disturbed bedding). In numerous intervals *Ophiomorpha* is the only trace fossil present. In other cases, *Conichnus*, *Cylindrichnus*, *Dactyloidites*, *Macaronichnus*, *Phycosiphon*, *Skolithos*, *Taenidium*, *Teichichnus*, and *Thalassinoides* are also registered as exclusive traces. Furthermore, the associations *Ophiomorpha-Conichnus*, *Ophiomorpha-Thalassinoides*, *Conichnus-Dactyloidites-Ophiomorpha* are recognized.



Fig. VI.3. Main sedimentary structures identified in the sandstones of the study succession. Scale bar: 2 cm. In parentheses, location of the photograph in the well (feet - meters from the top). **A.** Massive sandstone (Sm; 1506 ft - ~459 m). **B.** Horizontal lamination sandstone (Sh; 1053 ft - ~321 m). **C.** Low angle cross-bedding sandstone (Sa; 1884 ft - ~574 m). **D.** Planar cross-bedding sandstone (Sp; 1089 ft - ~332 m). **E.** Hummocky cross-stratification (HCS; 1895 ft - ~578 m); **F.** Convolute lamination sandstone (Sc; 1935 ft - ~590 m). **G.** Asymmetrical ripples in sandstone (Sr; 1681 ft - ~512 m). **H.** Symmetrical ripples in sandstone (Sw), and load casts (Slc; 1948 ft - ~594 m). **I.** Trough cross-bedding sandstone (St; 1783 ft - ~543 m). **J.** Normal gradation of coarse-grained sandstone to medium fine-grained sandstone (Sng; 1776 ft - ~541 m). **K.** Inverse gradation of medium-grained sandstone to coarse-grained sandstone (Sig; 1619 ft - ~493 m). **L.** Massive bioclastic sandstone (Sb; 1153 ft - ~351 m). **M.** Load casts (Slc; 1092 ft - ~333 m).

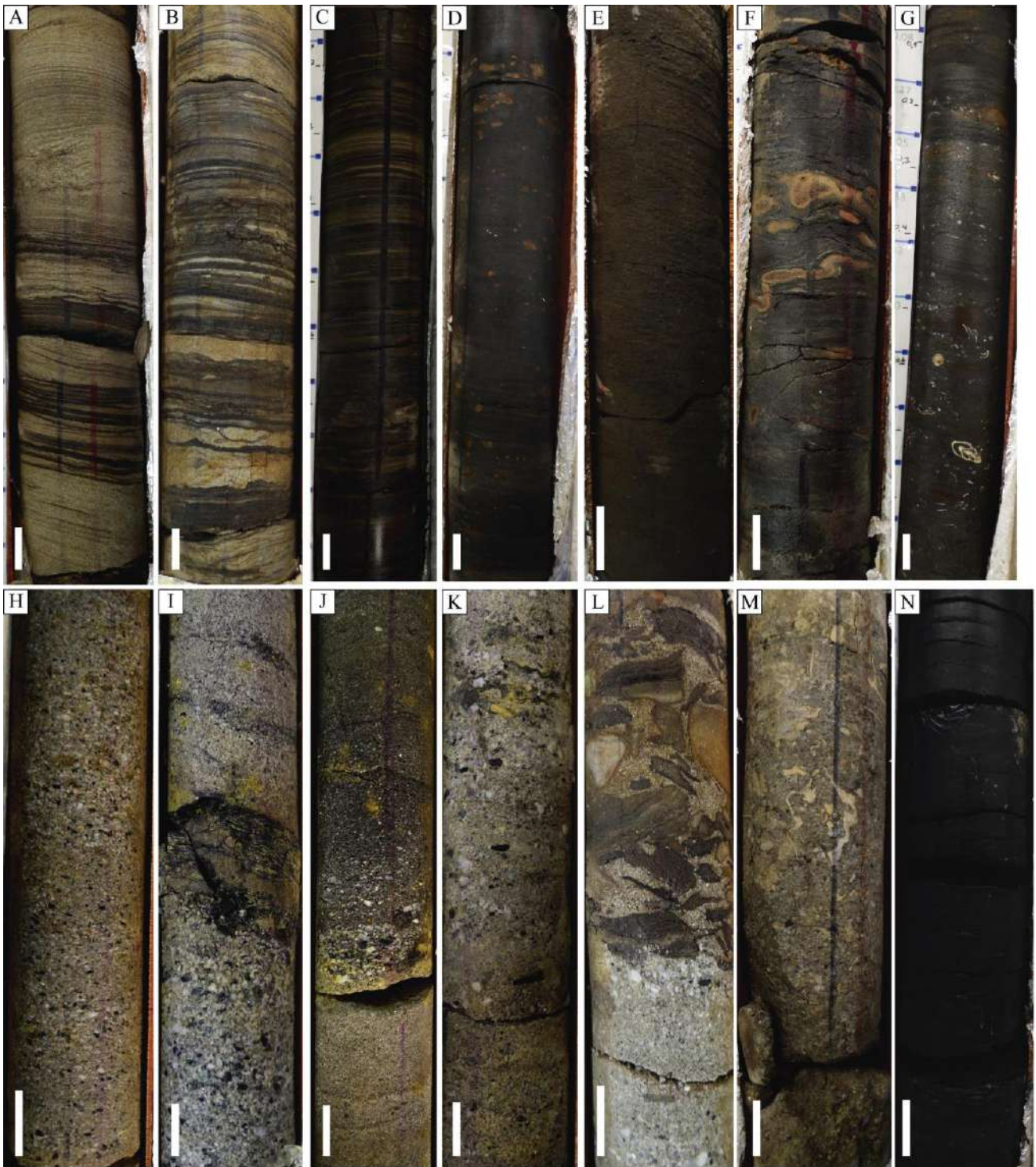


Fig. VI.4. Main sedimentary structures identified in the sandstones and mudrock interbedded, mudrocks, conglomerates, and coal beds of the study succession. Scale bar: 2 cm. In parentheses, location of the photograph in the well (feet - meters from the top). **A.** Flaser bedding (Htf; 1894 ft - ~577 m). **B.** Wavy bedding (Htw; 1299 ft - ~396 m). **C.** Lenticular bedding (Htl; 1934 ft - ~589 m). **D.** Massive mudrock (Mm; 1916 ft - ~584 m). **E.** Horizontal lamination mudrock (Mh; 999 ft - ~304 m); **F.** Syneresis cracks (Ms; 1397 ft - ~426 m). **G.** Massive bioclastic mudrock (Mb; 1923 ft - ~586 m). **H.** Massive polymictic matrix-supported conglomerates (Gmm; 1586 ft - ~483 m). **I.** Massive polymictic clast-supported conglomerates (Gcm; 971 ft - ~296 m). **J.** Normal gradation of granule-sized conglomerate to medium-grained sandstones (Gng; 1583 ft - ~482 m). **K.** Inverse gradation of medium coarse-grained sandstone to granule-sized conglomerate (Gig; 1191 ft - ~363 m). **L.** Massive oligomictic clast-supported conglomerates (Goc; 965 ft - ~294 m). **M.** Massive bioclastic conglomerate (Gb; 1980 ft - ~603 m). **N.** Massive coal (Co; 1842 ft - ~561 m).

Table VI.1. Sedimentary facies and hydrodynamic interpretation.

| Lithological group | Sedimentary structure | Facies Code | Hydrodynamic processes | References |
|-------------------------------------|--|-------------|---|--|
| Sandstones | Massive structure | Sm | Rapid deposition, most probably through the deceleration of a heavily sediment-laden current. Destruction of depositional lamination can come about through intense reworking of sediment. | Collinson et al. (2006), Collinson and Mountney (2019) |
| | Horizontal lamination | Sh | - High velocity currents, probably associated with upper flow regime in fine- to medium-grained sandstones and that it is not very micaceous. | Collinson and Mountney (2019), Heldreich et al. (2017) |
| | Low-angle cross-bedding | Sa | - Washed-out dunes that occur between subcritical flow regimes. - Deposited by traction from relatively weak currents that approach upper flow regime conditions for the size of sediment being deposited. | Picard and High (1973), Heldreich et al. (2017) |
| | Planar cross-bedding | Sp | Unidirectional migration of 2D straight-crested ripples and thalweg bars in high-energy fluvial channels, under lower flow regime. | Heldreich et al. (2017), Collinson and Mountney (2019) |
| | Hummocky cross-stratification | HCS | Deposition during high-energy oscillatory or combined flows. Strong and complex wave activity, mainly in areas below fair-weather wave base. | Collinson and Mountney (2019) |
| | Convolute lamination | Sc | Plastic deformation of partially liquefied sediment, usually occurring soon after deposition. | Collinson and Mountney (2019) |
| | Asymmetrical ripples | Sr | Result from currents flowing in one direction only (unidirectional). | Collinson and Mountney (2019) |
| | Symmetrical ripples | Sw | Bidirectional, oscillatory wave motion creates straight-crested symmetrical wave ripples. Represents deposition under wave action or in shallow water with stable flow conditions. | Heldreich et al. (2017), Collinson and Mountney (2019) |
| | Trough cross-bedding | St | Produced during unidirectional migration of sinuous to linguoid-crested ripples or dunes (depending of the scale) in high to moderate energy. | Collinson and Mountney (2019) |
| | Normal gradation - Medium- to coarse-grained sandstones to fine and very fine-grained sandstones | Sng | This suggests a decelerating current from suspension of sediments, with coarsest particles falling to the bed first. | Collinson and Mountney (2019) |
| Sandstones and conglomerates | Inverse gradation - Medium- to coarse-grained sandstones to conglomeratic sandstones and granule-sized matrix-supported conglomerate | Sig | Dispersive pressure caused by mutual impacts of grains behaving inertially within a rapidly shearing layer. | Reading (1996), Hand (1997), Collinson et al. (2006) |
| Bioclastic sandstones | Massive bioclastic sandstones | Sb | Rapid deposition, most probably through the deceleration of a heavily sediment-laden current. Destruction of depositional lamination can come about through intense reworking of sediment. | Collinson et al. (2006) |

| Lithological group | Sedimentary structure | Facies Code | Hydrodynamic processes | References |
|---------------------------------|--|-------------|---|--|
| Sandstones and mudrocks | Load casts and flame structures | Slc, Sf | Differences in density between the beds. | Collinson and Mountney (2019) |
| | Flaser bedding | Htf | Water movement over a sand bed, as unidirectional currents, oscillatory waves or combination of both. The variation in mud and sand content is the result of increasing/decreasing in current speed. | Collinson et al. (2006). |
| | Wavy bedding | Htw | | |
| | Lenticular bedding | Htl | | |
| Mudrocks | Massive | Mm | Vertical settling by weak suspension currents, intense bioturbation, high viscosity sediment - water flows under low energy conditions or in standing bodies of water (mudflows). | Shanmugam (1997), Potter et al. (2005) |
| | Horizontal lamination | Mh | Vertical settling by weak suspension currents in very low energy conditions. | Potter et al. (2005) |
| | Syneresis cracks | Ms | They are produced by the expulsion of liquid that generates the spontaneous contraction experienced by a recently deposited clay, in contact with a saline solution. This subaqueous shrinkage in argillaceous sediments can also be caused by earthquake-induced dewatering. | Astin and Rogers (1991), Pratt (1998), Tanner (2003) |
| Bioclastic mudrocks | Massive bioclastic mudrocks | Mb | Vertical settling by weak suspension currents, intense bioturbation, dense mudflows along the bottom. | Shanmugam (1997), Potter et al. (2005) |
| Conglomerates | Massive polymictic matrix-supported | Gmm | Transport and deposition of such hyper-concentrated sediments occur in high-energy flow conditions. | Collinson and Mountney (2019) |
| | Massive polymictic clast-supported | Gcm | Transport and deposition of such hyper-concentrated sediments occur in high-energy flow conditions. | Collinson and Mountney (2019) |
| | Normal gradation - Granule-sized and a lesser extent, pebbles matrix-supported conglomerates to medium- to coarse-grained sandstones | Gng | Deceleration of the flow with coarsest particles falling to the bed first. | Lowe (1976), Collinson and Mountney (2019) |
| | Inverse gradation - Medium- to coarse-grained sandstones to conglomeratic sandstones and granule-sized matrix-supported conglomerate | Gig | Dispersive pressures operated, the density-modified grain flow. Inverse grading may also result from growth of low-relief bars though a clast-supported fabric is then more likely. | Todd (1989), Nemeč and Postma (1993) |
| | Massive oligomictic clast-supported | Goc | Transport and deposition of such sediments occur in high-energy, but some of the clasts originated from within the basin of deposition and were eroded from penecontemporaneous sediments. | Collinson and Mountney (2019) |
| Bioclastic conglomerates | Massive bioclastic conglomerates | Gb | Rapid deposition, most probably through the deceleration of a heavily sediment-laden current. Destruction of depositional lamination can come about through intense reworking of sediment. | Collinson et al. (2006) |
| Coal | Massive coal | Co | Calm hydrodynamic conditions that allow the preservation of organic matter suggests low oxygen conditions. | Collinson and Mountney (2019) |

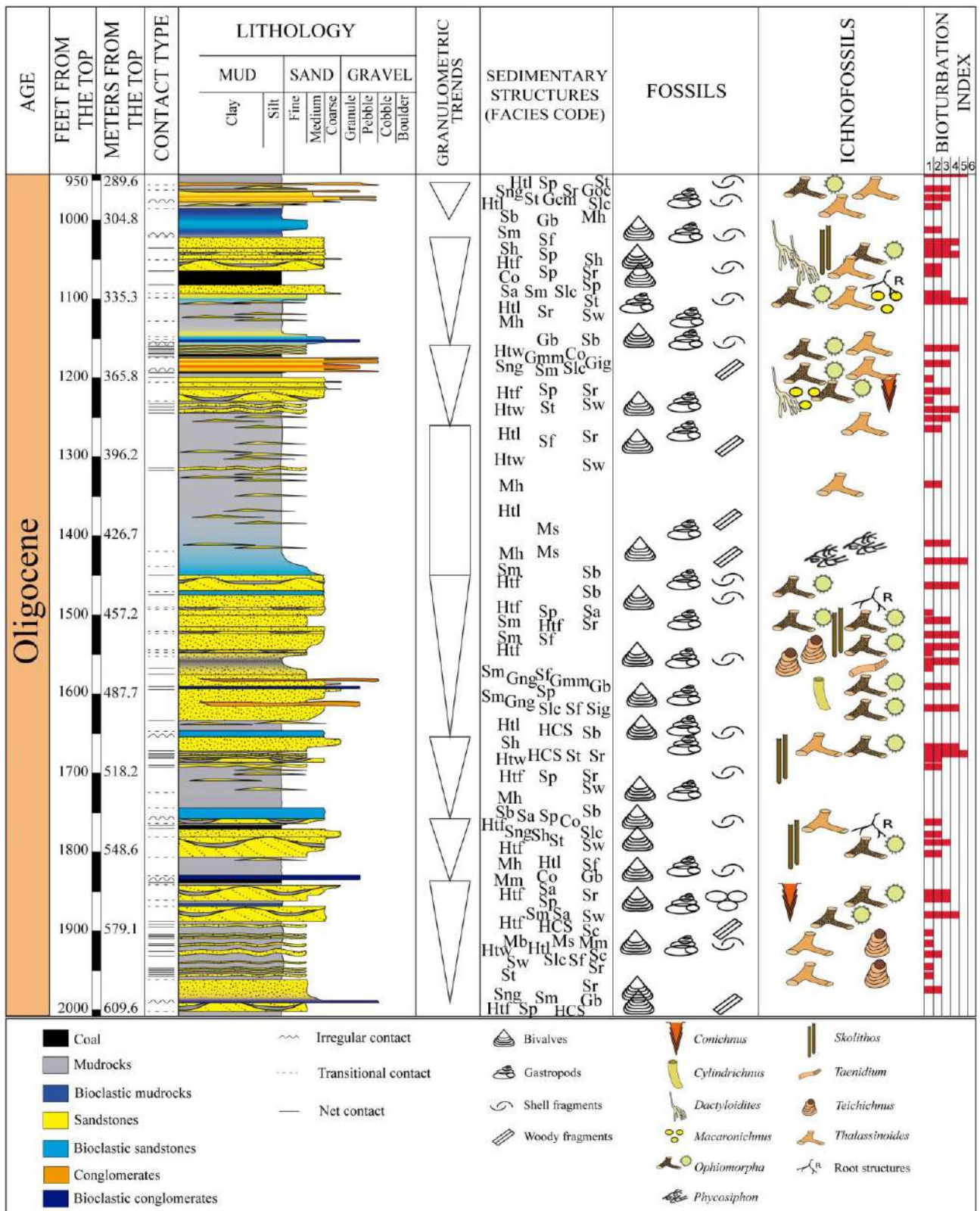


Fig. VI.5. Stratigraphic log of the studied interval (scale 1:2000), including sedimentological (lithology, contact type, grain size, sedimentary structures-facies) and paleontological (fossils, ichnofossils and Bioturbation Index) features. For facies codes see Table VI.1.

Conichnus (Fig. VI.6A), is a relatively large conical burrow with subcircular cross section and subvertical orientation. The passive filling may include a thin lining along the wall of the burrow (Frey and Howard,

1981). Internally, *Conichnus* often show downward deviated blades determining a chevron appearance, primarily in response to the vertical adjustment of the producer (Knaust, 2017).

The recognized specimens have approximately a cross section ~8 cm long and ~2 cm wide. The thin lining along the wall of the burrow is observed, as well as the deviation of the sediment sheets downwards (Fig. VI.6A). Specimens are found in medium-grained sandstones with incipient horizontal lamination (Sh), and massive sandstones (Sm), sometimes together with *Ophiomorpha* (Fig. VI.6A). *Conichnus* is a common element of shallow marine and, nearshore environments where occur high-energy sedimentary processes, high sediment supply, and frequently mobilized substrate (e. g., Abad et al., 2006). It also occurs in shallow intertidal to subtidal environments, and can be associated with wave structures, dunes and megaripples (e.g., Savrda, 2002).

Cylindrichnus (Fig. VI.6B), includes arc-shaped or U-shaped burrows with a passive fill and a concentric laminated lining (Ekdale and Harding, 2015). They are usually unbranched, although branching has been documented (Knaust, 2017). Observed *Cylindrichnus* burrows have subvertical shapes with a slight arc shape with sizes between ~4 and 6 cm long, and ~1 cm wide. Displaying the diagnostic thick lining highlighted by sheets of organic matter enclosing a thin central to eccentric tube (Fig. VI.6B). This trace fossil is found mainly in massive medium-to fine-grained sandstones with a high content of organic matter (Sm). *Cylindrichnus* is characteristic of high-energy deposits, including storm deposits, sand dunes, and sandbanks, where vertical forms predominate (e.g., Howard, 1966; Pemberton and Frey, 1984; Frey, 1990; Knaust, 2017). It is a common component of marine and estuarine environments with brackish conditions (e.g., Netto and Rossetti, 2003; MacEachern and Gingras, 2007; Buatois and Mángano, 2011; Gingras and MacEachern, 2012) and occurs in association with delta front and prodelta deposits (e.g., Tonkin, 2012). In addition, this trace fossil has been frequently reported in moderate to low energy deposits from the shelf to the lower shoreface where horizontal morphologies predominate (e.g., Fürsich, 1974; Belaústegui and de Gibert, 2013).

Dactyloidites (Fig. VI.6C) is a fan-shaped rosette trace formed by radial elements and a vertical central tube. The radial elements, sub-horizontal or inclined with respect to the bedding plane, arise from the vertical tube, and present protrusive connections (spreite) generated by the downward movement of the tube (Fürsich and Bromley, 1985). Radial elements can be sub-horizontal or inclined with respect to the bedding plane (Fürsich and Bromley, 1985). In the study succession, *Dactyloidites* is locally recognized as circular to subcircular sections, occasionally elongated, associated with the terminations of the rosette with a better selected filling and with a lighter coloration than the host rock (Fig. VI.6C). They have average diameters of ~0.5 cm and appear isolated and/or grouped, but no overlap is observed. Sometimes it appears as an exclusive trace or associated with *Ophiomorpha* and always into massive medium-to fine-grained sandstones (Sm), or low angle cross-bedding medium-to fine-grained sandstones (Sa) or horizontal lamination medium-to fine-grained sandstones (Sh) (Fig. VI.6C). Observed specimens show similarities with those described in cores by de Gibert et al. (1995). However, given that the vertical central tube is not observed in the study specimens, its assignment to the ichnogenus is tentative *?Dactyloidites*. This ichnogenus is common in high energy shallow marine environments, and usually present in conditions of warm climates (de Gibert et al., 1995). Furthermore,

it has been described in fluvial-dominated deltas (Gilbert type and mouth bar type; Agirrezabala and de Gibert, 2004), in environments with a high contribution of organic debris (e.g., Boyd and McIlroy, 2016), and in lower shorefaces influenced by storms (e.g., Lazo et al., 2008). Particularly are associated with sediments in the last stages of sedimentary courtship at high sea level (highstand system tract; Uchman and Pervesler, 2007).

Macaronichnus (Fig. VI.6D) includes predominantly horizontal, cylindrical burrows, with a straight, sinuous, meandering or spiral-shaped morphology, although oblique and vertical forms can also occur (Clifton and Thompson, 1978; Knaust, 2017). Burrows are characterized by an active fill of sand lighter than that of the embedded sediment and a rim composed of dark mineral grains (mica or heavy minerals) that commonly occur in high density (Clifton and Thompson, 1978; Knaust, 2017). Here *Macaronichnus* is scarce (2 intervals), consisting of cylindrical burrows with elongated, elliptical and circular sections (Fig. VI.6D). The diameter ranges from 0.1 cm to 0.4 cm and its length can be at least 2 cm. The burrow fill contrasts with the surrounding sediment by its pale colour, and the halo of dark minerals is recognizable. It is registered either as some scattered specimens (Fig. VI.6D) or with a high density in a completely bioturbated interval (~1 m), in massive medium-to fine-grained sandstones (Sm), flaser bedding (Htf), or fine sandstones with planar cross-bedding (Sp), and horizontal lamination (Sh). *Macaronichnus* is typically associated with sandy unconsolidated substrates (Knaust, 2017). *M. segregatis* is a shallow marine trace, very common in beach, shoreface, and delta front deposits, as well as in shallow intertidal and subtidal deposits (e.g., Nara and Seike, 2004; Seike, 2007; Bromley et al., 2009; Quiroz et al., 2010, 2019; Uchman et al., 2016). *M. segregatis degiberti* is also occasionally recorded in deeper environments (e.g., Rodríguez-Tovar and Aguirre, 2014; Knaust, 2017; Giannetti et al., 2018; Miguez-Salas et al., 2020; Dorador et al., 2021).

Ophiomorpha (Fig. VI.6A-E-K), consists of burrows showing a horizontal frame with vertical axes, and circular to elliptical in cross section. The branch is Y- and T-shaped, typically with enlargement of the junctions. Passive filling is common, although some segments of the burrow may have a meniscal filling (Knaust, 2017). Burrow lining is diagnostic of *Ophiomorpha*, consisting of sand and/or mud granules along the wall or pellets (Frey et al., 1978). *Ophiomorpha* is abundant in the studied succession, both as an exclusive trace or associated with other ones (Fig. VI.6A–K). It is recorded in massive sandstones (Sm), massive conglomeratic sandstones (Sm; Fig. VI.6E), and massive polymictic matrix-supported granule-sized conglomerates (Gmm; Fig. VI.6E). The diameter of the burrows varies between ~0.5 cm and ~3 cm, and the longitudinal sections between ~3 cm and ~12 cm (Fig. VI.6E). The presence of pellets in the wall is characteristic in all the observed specimens. *Ophiomorpha* is found in a wide variety of paleoenvironments, being, although not exclusively, a typical component of high-energy environments. Originally considered as a significant element of shallow marine facies (Frey et al., 1978; Pollard et al., 1993), various ichnospecies of *Ophiomorpha* are also characteristic of deep-sea deposits (Uchman, 2009), and their relationship in different facies is discussed (Monaco et al., 2009). Occasionally, *Ophiomorpha* is documented in continental environments, mainly in Permian sediments associated with the first records of crustaceans (e.g., Baucon et al., 2014), although these burrows can also be produced by other organisms and assigned to different ichnotaxa (Goldring and Pollard, 1995).

Phycosiphon (Fig. VI.6F-G) is a small burrow consisting of repeated narrow U-shaped, or hooked lobes, each of which encloses a spreite of millimeter to centimeter scale and branches regularly or irregularly from an axial spreite of similar width (Wetzel and Bromley, 1994). The study specimens have been recognized in a 60 cm-thick interval of massive muddy sediments (Mm) with slight variations to massive very fine sandstones (Sm), distributed in patches, showing various lobe orientations, resulting in a chaotic arrangement. Burrow length varies between ~0.1 cm and ~0.5 cm and rarely reach 1 cm (Fig. VI.6F-G). *Phycosiphon* is a characteristic component of offshore-platform to lower shoreface deposits, commonly occurring as exclusive trace or in higher ichnodiversity siliciclastic successions (Goldring et al., 1991), as well as in deltaic environments (e.g., Rodríguez – Tovar et al., 2014). It also occurs in slope deposits (e.g., Naruse and Nifuku, 2008), and is common in deep marine environments (e.g., Celis et al., 2018). *Phycosiphon* producers are among the first bioturbators of event deposits such as storms, turbidity currents, and bottom current (e.g., Goldring et al., 1991; Wetzel, 2008; Rodríguez–Tovar et al., 2014).

Skolithos (Fig. VI.6H) consist of a subvertical cylindrical tube with or without a liner, and passive filling (Alpert, 1974). A funnel-shaped opening can be developed or preserved at the top (Knaust, 2017). Throughout the study succession, *Skolithos* specimens correspond to vertical/subvertical straight lined burrows, arranged perpendicular to the horizontal lamination of fine- to medium-grained sandstones (Sh). Longitudinal section generally has a millimeter thickness (~0.2 cm on average) and a length between ~4 cm and ~10 cm (Fig. VI.6H). They are also observed in massive medium- to fine-grained sandstones (Sm), and flaser bedding (Htf). *Skolithos* is a common indicator of relatively high energy, shallow water, and nearshore to marginal marine environments (Knaust, 2017). However, some authors record it as a common component of fluvial and other continental deposits (e.g., Hasiotis, 2010).

Taenidium (Fig. VI.6I) is a meniscate cylindrical burrow, predominantly sub-horizontal but can also be subvertical. Burrows have no lining or it is very thin and they are not branched (D'Alessandro and Bromley, 1987). The meniscate filling is usually widely spaced with little contrast in lithology (D'Alessandro and Bromley, 1987). Observed specimens occur in sandy-silty and sandy sediment (Sm), as sub-horizontal (Sa) or inclined (~45°) structures (Sp), respectively, diameter of ~1 cm and variable presence of meniscus (Fig. VI.6I). *Taenidium* has been recorded from a wide variety of environments. It is commonly found in marginal alluvial, fluvial and lake environments (Savrda et al., 2000; Hasiotis, 2010; Melchor et al., 2012). *Taenidium* is also of special interest, particularly in the transition zone between terrestrial and terrestrial aquatic environments (e.g., Rodríguez – Tovar et al., 2016). It is also common in transitional environments (e.g., fluvial-tidal transition; Díez – Canseco et al., 2015), but it also belongs to the *Cruziana* ichnofacies in the offshore zone. *Taenidium* is also in shallow and deep marine deposits (e.g., D'Alessandro and Bromley, 1987; Miguez– Salas and Rodríguez–Tovar, 2019). Recently *Taenidium*, has been registered linked to hyperpycnal systems (García-García et al., 2021).

Teichichnus (Fig. VI.6J) is a spreite burrow with a subvertical wall and a straight or curved plan arrangement containing stacked lamellae and a causative burrow with passive fill (Knaust, 2018). In vertical sections *Teichichnus* usually appear as groups of vertical to highly inclined spreiten, which can pile up one on top of

the other due to different sedimentation events (Knaust, 2017). In the studied section *Teichichnus* is observed showing a subvertical disposition, where the spreite is easily recognized due to the contrast with the hosting sediment that varies between massive siltstone (Mm) and very fine sandstone (Sm). They are ~1 cm wide, and ~3 cm long (Fig. VI.6J). *Teichichnus* is typically in siliciclastic systems, occurring frequently into deltaic deposits (e.g., Tonkin, 2012). Its producers can be considered as euryhaline organisms capable of adapting to a wide range of salinity; it has often been recognized in reduced salinity settings (Knaust, 2018). Such conditions are common in marginal marine environments (e.g., inlets-bays, estuaries, lagoons), where *Teichichnus* is widespread (Knaust, 2017). Furthermore, it is frequently present in tidal deposits including dunes and bars in brackish environments (Desjardins et al., 2012) and hyperpycnal flow deposits (e.g., Buatois et al., 2011). In contrast to such marginal marine occurrences with low ichnodiversity, *Teichichnus* is characteristic of lower shoreface to offshore-platform deposits, in high diverse assemblages (Knaust, 2018). *Teichichnus* has been used in sequence stratigraphy analysis as an indicator of flood events, being characteristic of transgressive system tracts (Pemberton et al., 1992; Taylor et al., 2003). *Thalassinoides* (Fig. VI.6K) consists of burrows horizontal, variable, frames with vertical axes, similar to *Ophiomorpha* (Knaust, 2017). Burrows are circular to elliptical in cross section, unlined, and branching is Y- and T-shaped, typically with bulbous enlargement of the junctions (Knaust, 2017). Passive filling is common, although burrow elements can be actively filled (Knaust, 2017).

Thalassinoides is abundant throughout the studied section, as circular and elliptical cross-sections, with an average diameter ~1 cm (Fig. VI.6K) and, occasionally, with vertical axes. The passive fill, mainly sandy, in most cases contrasts with the embedded sediment. They are recorded in coal levels (Co), and in massive sandstones (Sm). *Thalassinoides* are more common in shallow marine environments such as shoreface, and deltas (Knaust, 2017), but it is found in a wide range of marine environments, from marginal to deep (e.g., Rodríguez-Tovar et al., 2008; Rodríguez-Tovar et al., 2017; Monaco et al., 2009). Given the producer can tolerate fluctuations in salinity, *Thalassinoides* can be found in brackish environments (e.g., estuaries and delta fans) (Knaust, 2017). *Thalassinoides* is often associated with firm substrates, associated with the *Glossifungites* ichnofacies (MacEachern et al., 2007b).

Rhizoliths (Fig. VI.6L). Root structures found in the study succession range in diameter from ~1 mm to ~10 cm. They have irregularly distributed, and unbranched. Their fill is carbonaceous, sandy, or sand-filled with a thin carbonaceous lining (Fig. VI.6L). They occur mainly in massive sandstones (Sm; Fig. VI.6L), and massive clayey siltstones (Mm). Plants commonly colonize terrestrial and aquatic environments in continental settings, such as alluvial, fluvial, lacustrine, and aeolian deposits (e.g., Hasiotis, 2010; Knaust, 2015, 2017; see recent review in Esperante et al., 2021). Mangroves deposits and other rooted deposits are also found in marginal marine environments, including swamps, lagoons, and tidal flats (e.g., Whybrow and McClure, 1980; Knaust, 2009). Transitional zones (marine to continental sequences) that present rhizoliths indicate subaerial exposure (Husinec and Read, 2011; Knaust, 2017).

VI.4.3. Distribution of facies and trace fossils**VI.4.3.1. Study interval**

Throughout the study interval, we recognized seven repetitive successions of different thickness, showing slight variations, but being common the upward increase in grain size (coarsening upward trend), as well as the upward decrease in trace fossils diversity, shell fragments (Fig. VI.5) and marine calcareous microfossils. The successions have thicknesses from ~50 ft (~15 m) to ~160 ft (~49 m), and a succession in the intermediate part of the study interval, which presents a thickness of ~285 ft (~87 m) (Fig. VI.5).

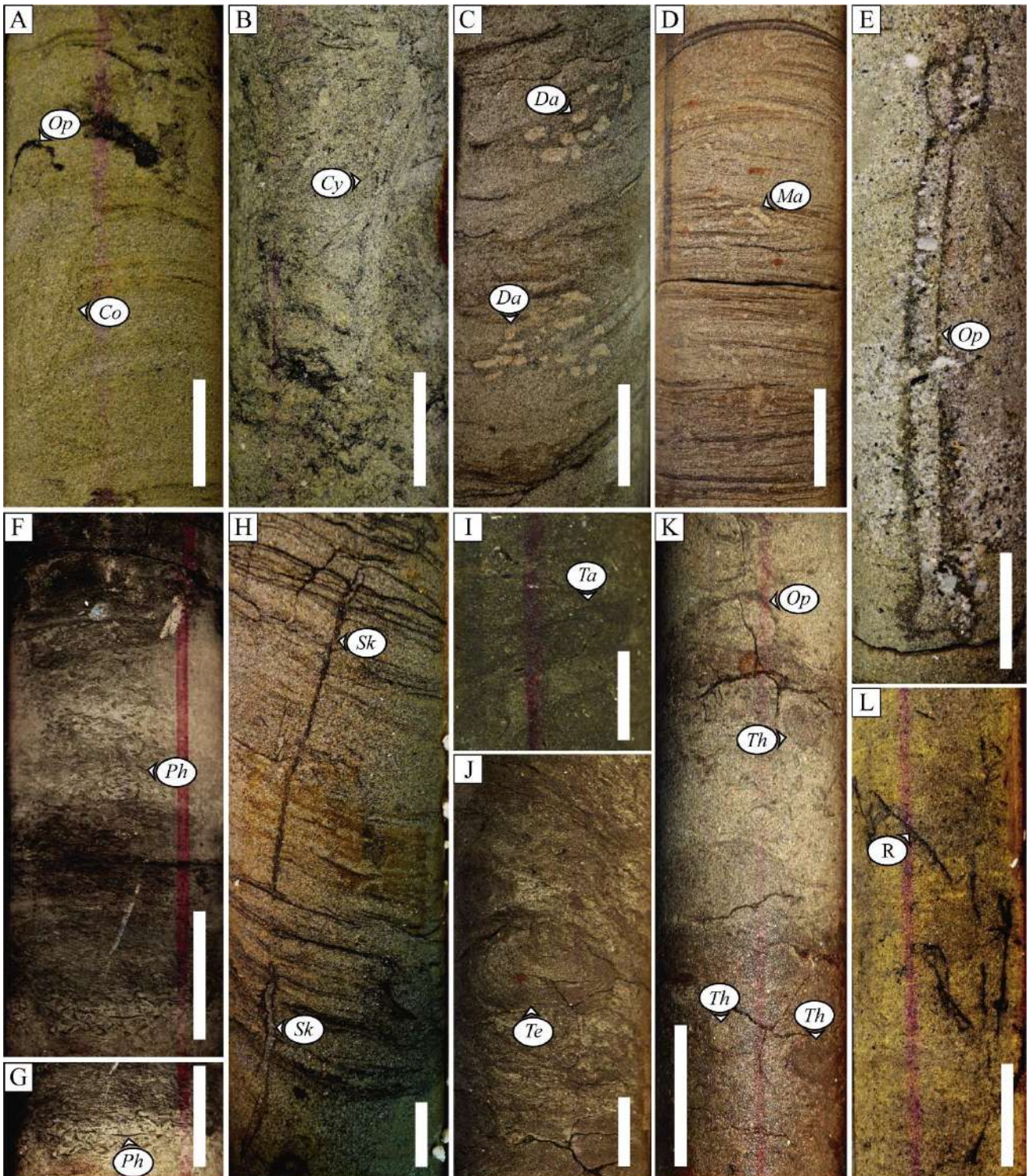


Fig. VI.6. Ichnogenus and rhizoliths recognized in the study succession. **A.** *Conichnus* (*Co*) and *Ophiomorpha* (*Op*) (1875 ft - ~572 m). **B.** *Cylindrichnus* (*Cy*) (1608 ft - ~490 m). **C.** *Dactyloidites* (*Da*) (1045 ft - ~319 m). **D.** *Macaronichnus* (*Ma*) (1231 ft - ~375 m). **E.** *Ophiomorpha* (*Op*) (1186 ft - ~361 m). **F - G.** *Phycosiphon* (*Ph*) (1438 ft - ~438 m). **H.** *Skolithos* (*Sk*) (1043.5 ft - ~318 m). **I.** *Taenidium* (*Ta*) (1578 ft - ~481 m). **J.** *Teichichnus* (*Te*) (1551 ft - ~472,7 m). **K.** *Ophiomorpha* (*Op*) and *Thalassinoides* (*Th*) (1541 ft - ~470 m). **L.** Rhizoliths (*R*) (1775 ft - ~541 m). Scale bar: 3 cm. In parentheses, location of photograph in well (feet - meters).

VI.4.3.2. Succession type

The sedimentological analysis, and the ichnological assemblage of these repetitive successions allowed us to identify the common patterns between them. These can be divided into three parts (Fig. VI.7). The lower part begins with massive bioclastic mudrocks (*Mb*), bioclastic sandstones (*Sb*) or bioclastic conglomerates (*Gb*) and thicknesses between ~3 ft (~0,9 m) and ~10 ft (~3 m). These vary transitionally to massive (*Mm*) or horizontal lamination mudrocks (*Mh*) occasionally bioturbated by *Phycosiphon* (*BI* = 0–5) but with punctual record (Fig. VI.7). These mudrocks exhibit lenticular bedding (*Htl*) and the occurrence of *Teichichnus* (*BI* = 1–2). Moreover, syneresis cracks (*Ms*) and iron and siderite nodules are observed (Fig. VI.7). Thicknesses vary between ~20 ft (~6 m) and ~90 ft (~27 m). However, there is a typical succession where the thickness of this lithology is greater than the others ~200 ft (~61 m). At the middle part, the succession changes progressively to massive (*Sm*) and horizontal lamination silty sandstones (*Sh*) with thin and medium beds of bioturbated mudrocks by *Ophiomorpha*, *Taenidium*, *Thalassinoides*, and rarely *Teichichnus* (*BI* = 2–4). These facies exhibit massive structure (*Sm*), horizontal lamination (*Sh*), wavy bedding (*Htw*), as well as planar cross-bedding (*Sp*), and asymmetrical ripples (*Sr*) (Fig. VI.7). The thicknesses of this part of the succession vary between ~10 ft (~3 m) and ~25 ft (~8 m). Sometimes and less frequently, there is also some hummocky cross-stratification (*HCS*), convolute lamination (*Sc*), and symmetrical ripples (*Sw*; Fig. VI.7). Then, the succession passes upward to massive medium/fine sandstones (*Sm*), and sometimes coarse-grained, with organic matter fragments, and the ichnological assemblage of *Dactyloidites*, *Ophiomorpha*, *Skolithos*, and *Thalassinoides* (*BI* = 2–4) or with punctual record of *Macaronichnus* and/or *Ophiomorpha* (Fig. VI.7). Occasionally and with punctual record the ichnoassemblage consisting of *Conichnus*, *Cylindrichnus*, *Dactyloidites*, *Ophiomorpha*, *Skolithos* and *Thalassinoides* (*BI* = 2–5) is also observed. They present horizontal lamination (*Sh*), planar cross-bedding (*Sp*), trough cross-bedding (*St*), flaser (*Htf*) and wavy bedding (*Htw*), asymmetrical ripples (*Sr*) and, to a lesser extent, symmetrical ripples (*Sw*) (Fig. VI.7), and thicknesses between ~10 ft (~3 m) and ~25 ft (~8 m). At the upper part, the succession passes upward to medium/fine-grained bioturbated sandstones with massive structure (*Sm*), horizontal lamination (*Sh*), and low angle cross-bedding sandstones (*Sa*) (Fig. VI.7). Likewise, this upper part can be characterized by mudrocks with massive structure (*Mm*), horizontal lamination (*Mh*), and lenticular bedding (*Htl*) bioturbated by *Teichichnus* (*BI* = 1–2), as well as coal thin beds (*Co*), and massive (*Sm*) and horizontal lamination (*Sh*) fine-to coarse-grained sandstones sometimes with a punctual record of *Macaronichnus* and/or *Ophiomorpha* (*BI* = 2–4). These sandstones present variations to mudrocks and carbonaceous mudrocks with the presence of rhizoliths (Fig. VI.7). The upper part of the succession presents thicknesses between ~10 ft (~3 m) and ~20 ft (~6 m). This repetitive coarsening upward succession type is interrupted by massive medium-to coarse-grained sandstones (*Sm*), massive conglomeratic sandstones (*Sm*) and/or massive polymictic granule-sized matrix-supported conglomerates (*Gmm*) with a high

content of organic matter fragments, and erosive bases, as well as load casts (Slc), flame structures (Sf), and bioturbated by *Ophiomorpha* and *Taenidium* (BI = 1–2) (Fig. VI.7). Sometimes, normal gradation from granule-sized matrix-supported conglomerates (Gng), and conglomeratic sandstones to medium-, fine-grained sandstones occur (Fig. VI.7). At other times there is a bigradational trend: inverse gradation from fine/medium-grained sandstones (Sig) to conglomeratic sandstones and granule-sized matrix-supported conglomerates, and again normal gradation (Sng) to medium/coarse-grained sandstones. Occasionally, rhizoliths towards the top are observed. The most common thicknesses of these are between ~1 ft (~0,3 m) and ~10 ft (~3 m).

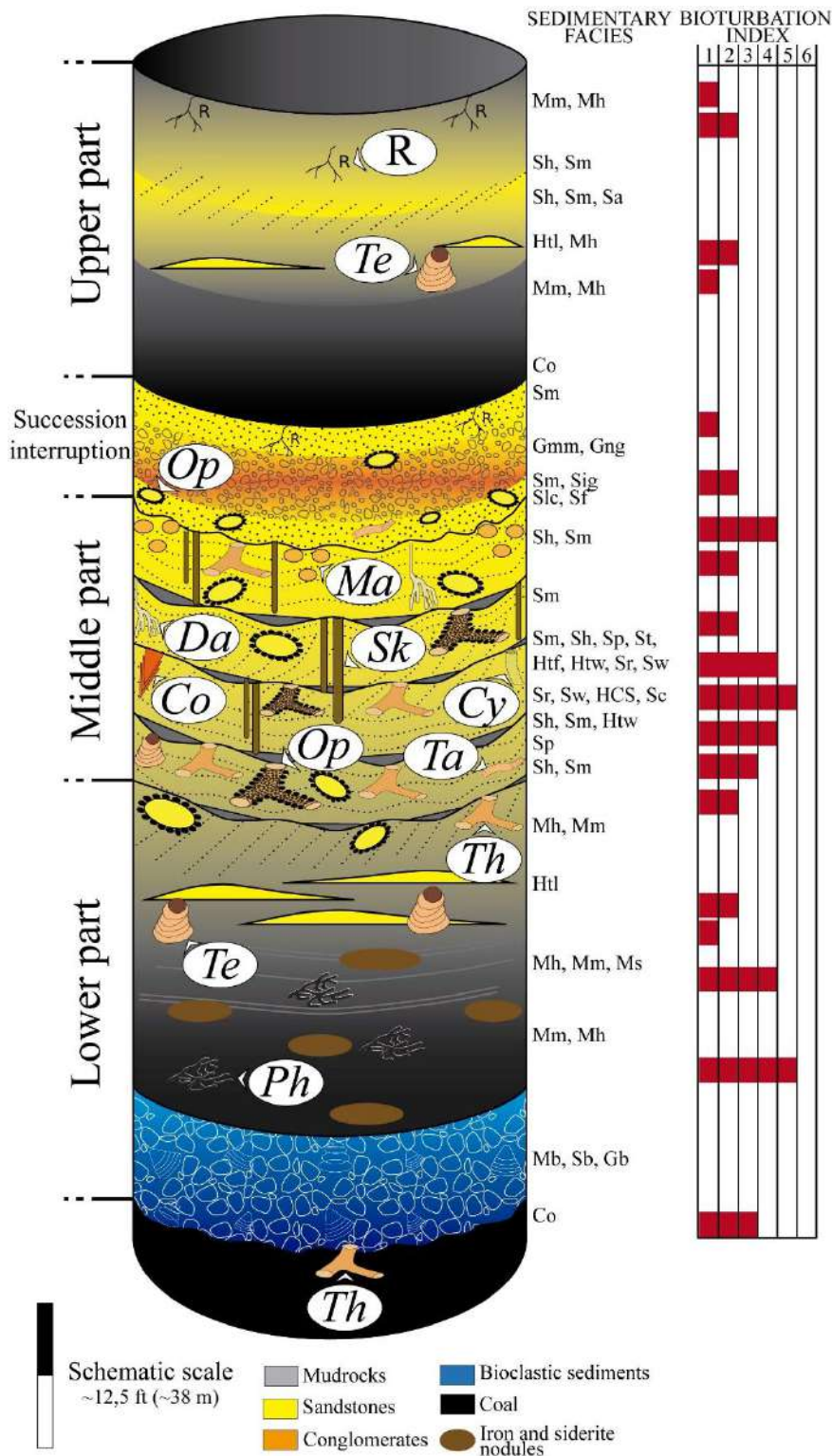


Fig. VI.7. Succession type found in the study succession with characteristic facies evolution and differentiated trace fossils. Note: *Conichnus* (Co), *Cylindrichnus* (Cy), *Dactyloidites* (Da), *Macaronichnus* (Ma), *Ophiomorpha* (Op), *Phycosiphon* (Ph), Rhizoliths (R), *Skolithos* (Sk), *Taenidium* (Ta), *Teichichnus* (Te), and *Thalassinoides* (Th). For facies codes see Table VI.1.

VI.5. Interpretation and discussion

VI.5.1. Depositional environment: fluvial-dominated deltaic system

The registered sedimentological features, as the frequent progradational trend (coarsening upward), the presence of sandstones and conglomerates (Sm, Gmm, Gcm) with erosive bases, the predominance of unidirectional structures such as asymmetric ripples (Sr), medium beds of sandstones with normal gradation (Sng, Gng) are associated with the development of channels (MacEachern et al., 2005; Coates and MacEachern, 2007). The previous facies association, together with the occurrence of coal beds (Co), the high content of organic debris, as well as the occurrence of massive sandstones (Sm) and massive mudrocks (Mm) with rhizoliths, together with the ichnological information, including composition, diversity and abundance of ichnoassemblages, allow the interpretation of a transitional system, more specifically a deltaic system (MacEachern et al., 2005; Bhattacharya, 2006). Furthermore, the dominance in time of these characteristics throughout the succession allows us to interpret a fluvial-dominated deltaic setting, characterized by variations in the coastline with continuous shallowing up sequences (Johnson and Dashtgard, 2014; Dalrymple et al., 2015; Dashtgard and La Croix, 2015; Ainsworth et al., 2017; Shchepetkina et al., 2019; Maselli et al., 2020) (Fig. VI.8).

The occurrence of some beds with flaser (Htf) and wavy bedding (Htw) and mud drapes associated, as well as hummocky cross-stratification (HCS) associated with interbedded sandy and muddy deposits, allows us to interpret local tidal influence on the system with sporadic storms (Dalrymple et al., 1990, 1992; Dashtgard et al., 2009; Desjardins et al., 2012; Shchepetkina et al., 2019). The punctual record of symmetrical ripples (Sw) could be associated with wave processes (Dalrymple et al., 1990, 1992; Bann et al., 2008).

The presence of convolute lamination (Sc) at some intervals and occasional associated hummocky cross-stratification (HCS) and symmetrical ripples (Sw), also reflect sudden episodes of storms (Arnott and Southard, 1990; Frey, 1990; Bann et al., 2008).

In this context, bioclastic deposits (Gb, Sb, Mb) could be related to rapid and short-time transgressive pulses (Savrda et al., 1993; Cattaneo and Steel, 2003; Buatois et al., 2012; Díez – Canseco et al., 2015; Schultz et al., 2020). After the short-time transgressive phase, the sedimentary environment usually returns to the previous conditions quickly. Conditions of a deeper/distal marine environment are not maintained over time but locally registered (e.g., 1833 ft–1811 ft; ~558.7 m–~552 m) (Fig. VI.5). However, at some intervals, the bioclastic deposits change progressively to laminated mudrocks (Mh) with few calcareous microfossils and low bioturbation, which could be related to a flooding phase in a confined interdistributary bay-type context and/or stagnant waters (Buatois et al., 2012; Díez – Canseco et al., 2015) (e.g., 1442 ft–1246 ft; ~439.5 m–~379.8 m; Fig. VI.5). In some intervals, medium beds of fine- to medium-grained sandstones with horizontal lamination (Sh) and low-angle cross-bedding (Sa), and bioturbation associated with *Macaronichnus*, and/or *Ophiomorpha*

(BI = 3–4), typically occur twice at the top of the progradational cycle, could be related to high-energy conditions on the beach-like environments (Pemberton et al., 2001; Buatois et al., 2012).

The interpreted generalized fluvial-dominated deltaic system, with the secondary, minor, tidal and wave influence, is supported by the ichnological record. The low abundant and moderate diverse trace fossil assemblage could be related to a stressful environment for macrobenthic trace maker communities (Buatois et al., 1997; MacEachern and Gingras, 2007), favouring the preservation of physical sedimentary structures (MacEachern et al., 2005; Buatois and Mángano, 2011). Some levels that register a higher abundance and diversity of traces (where *Conichnus*, *Cylindrichnus*, *Dactyloidites*, *Ophiomorpha*, *Skolithos*, *Teichichnus*, *Thalassinoides* can be recognized) (e.g., 1226 ft–1223 ft; ~373.7 m–~372.8 m) (Fig. VI.5) could be associated with mixed delta conditions where the fluvial domain decreases, and the tidal-wave influence increases (Bhattacharya and Giosan, 2003; Buatois et al., 2005; Bayet-Goll and Neto de Carvalho, 2020; Moyano Paz et al., 2020). However, these conditions do not last over time and are interrupted by the establishment of conditions with fluvial domain.

The presence of a high organic debris content, low bioturbation index (*Ophiomorpha* and/or *Taenidium*), together with deposits showing erosive bases and mainly normal gradations (Sng, Gng) with a thickness between ~0,5 ft and 3 ft, and bigradational trends, could be associated with the influence of multiple distributary channels providing hypopychnic feathers during normal fluvial discharges, and hyperpychnic during extraordinary river discharges (Mulder et al., 2003; MacEachern et al., 2005; Bhattacharya and MacEachern, 2009; Buatois et al., 2011, 2019; Zavala et al., 2011; Díez – Canseco et al., 2015; Zavala and Pan, 2018). In this context, an increase in the input of fresh water into the environment is envisaged, determining a considerable decrease in salinity, and then significant variations in a brackish setting (Buatois et al., 2005). This fact, together with the increase in both turbidity and sedimentation rate, would have negatively affected the development of benthic communities (Gingras et al., 1998; MacEachern et al., 2005), evidencing the dominant incidence of fluvial processes in the ecological and depositional environment, and the secondary, minor, tidal and wave influence (Bhattacharya and Giosan, 2003; Buatois et al., 2005; Bayet-Goll and Neto de Carvalho, 2020; Moyano Paz et al., 2020). The punctual record of massive oligomictic clast-supported conglomerates (Goc) show transport and deposition of sediments in these high-energy environments, but some of the clasts originated from within the basin of deposition and were eroded from penecontemporaneous sediments (Collinson and Mountney, 2019).

VI.5.2. Sub-environments into the fluvial-dominated deltaic system

In this generalized deltaic system with fluvial domain interpreted for the study interval, facies association and ichnological analysis allow recognition of different sub-environments, as prodelta-bay, distal delta front, proximal delta front (subaqueous distributary channels, distributary mouth bars), lower delta plain-interdistributary bays, lower delta plain-floodplain, swamps, beach-like, lower delta plain-crevasse splays, channel, bars (Fig. VI.8). These different sub-environments are replaced several times through the studied interval (Fig. VI.8).

VI.5.2.1. Facies association 1 - prodelta - bay (FA1)

Description. Characterized by massive mudrocks (Mm), and horizontal lamination mudrocks (Mh), with the exclusive presence of *Phycosiphon* in the first centimeters after the occurrence of bioclastic sediments (Mb, Sb, Gb), together with a moderate to low occurrence of marine calcareous microfossils (Project Contrato RC 494, 2017). The bioturbation indexes are 0 and when the specific occurrence of *Phycosiphon* occurs it is between 4 and 5. At the top of these facies, there is the occurrence of a) lenticular bedding (Htl) occasionally with *Teichichnus* (BI = 1–2), asymmetrical and symmetrical ripples (Sr, Sw), syneresis cracks (Ms), and siderite nodules and/or b) massive sandstones (Sm) with erosional base truncating the succession.

Interpretation. Bioclastic sediments could represent single episodes of transgressive lags (Gingras et al., 1999, 2012a; MacEachern et al., 1999; Cattaneo and Steel, 2003). The subsequent conditions with the unique occurrence of calcareous marine microfossils throughout the succession, dominance of mudrocks, and the presence of *Phycosiphon*, could be associated with the punctual record of sediments deposited under the most marine conditions of the system related to prodelta environments (Fig. VI.8). Low bioturbation index and low diversity in this scenario, represent the influence of the fluvial system (MacEachern et al., 2005; Buatois et al., 2012). The occurrence of *Phycosiphon* also could be linked to the opportunistic character of the producer organism in an environment with food availability (Wetzel, 2010; Rodríguez – Tovar et al., 2014; Celis et al., 2018), which would be related to high inputs of organic matter from the fluvial system. Towards the top, the facies association described in a) could represent quiet hydrodynamic situations in bay conditions because the conditions of the prodelta are not maintained over time due to the fact that the flood is not representative (Bhattacharya, 2006). There is an overall shallowing-upward facies succession, associated with a trend from more marine to more nonmarine facies, but commonly without the deposition of thick sands (Bhattacharya, 2006) represented by the local occurrence of lenticular bedding (Htl), and symmetrical ripples (Sw) in this case, that would show the tidal and wave influence. However, the dominance of the fluvial system is represented by the continuous occurrence of asymmetrical ripples (Sw) associated with unidirectional currents, and the low bioturbation indexes associated with stressful conditions. Moreover, syneresis cracks (Ms), and siderite nodules reveal salinity fluctuations in the system (MacEachern et al., 2005; Buatois et al., 2012; Gingras et al., 2012a; Dí ez – Canseco et al., 2015). The sequence is sometimes interrupted by the succession described in b) related to distributary channels (Bhattacharya, 2006). The overall shallowing-upward facies succession from massive or laminated mudrocks (Mm, Mh) with *Phycosiphon* to lenticular bedding (Htl) with *Teichichnus* represents the transition from prodelta to bay environments (Bhattacharya and Walker, 1991; Bhattacharya, 2006).

VI.5.2.2. Facies association 2 - distal delta front (FA2)

Description. Characterized by mudrocks, muddy sandstones, and fine-grained sandstones with planar cross-bedding (Sp), massive structure (Mm, Sm), wavy bedding (Htw), horizontal lamination (Sh), asymmetrical ripples (Sr), moderate bioturbation indexes (2–4), and the record of *Ophiomorpha*, *Taenidium*, and *Thalassinoides*. Occasionally there are the occurrence of an association of facies characterized by symmetrical ripples (Sw), convolute lamination (Sc), and hummocky cross-stratification (HCS).

Interpretation. The fine-grain size sediment domain, muddy sandstones with planar cross-bedding (Sp), and the absence of dwelling structures of suspension feeding organisms, suggests distal environments within the deltaic system (MacEachern et al., 2005; Gingras et al., 2011; Buatois et al., 2012; Moyano Paz et al., 2020). However, the variable concentration of organic matter, together with the low ichnodiversity, shows the fluvial domain on the succession (Buatois et al., 2005; MacEachern et al., 2005; Bhattacharya, 2006) (Fig. VI.8). This succession is overlying the characteristic facies of the prodelta-bay or transgressive lag deposits, and towards the top, it transitionally changes to coarser sandstones from the proximal deltaic front (Fig. VI.8). The facies association described could correspond with the record of the influence of waves and storms (Arnott and Southard, 1990; Frey, 1990; MacEachern et al., 2005; Coates and MacEachern, 2007; Bann et al., 2008; Buatois et al., 2012; Solórzano et al., 2017; Moyano Paz et al., 2020).

VI.5.2.3. Facies association 3 - proximal delta front (FA3)

Description. It is characterized by well-sorted fine-to medium grained sandstones, with asymmetrical ripples (Sr), trough cross-bedding (St), horizontal lamination (Sh), wavy (Htw) and flaser bedding (Htf), diffuse planar cross-bedding (Sp), and organic debris, as well as bioturbation indexes between 2 and 3, and the occurrence of the assemblage or exclusive ichnogenus such as *Ophiomorpha*, *Skolithos* and/ or *Thalassinoides*. The occurrence of wavy (Htw), flaser bedding (Htf), and from paired mud drapes within cross-beds, sometimes with *Ophiomorpha*, occurs as punctual record, as well as the occurrence of symmetrical ripples (Sw), and hummocky cross-stratification (HCS).

Interpretation. According to the sedimentological and ichnological characteristics raised in the distal delta front and those evidenced in this facies association, a prograding trend can be interpreted. The most proximal conditions are reflected in the low indexes of bioturbation together with the dominance of sandy sediments with sedimentary structures of unidirectional currents that reveal an environment with high-energy conditions, and well oxygenated waters associated with river discharge (Gingras et al., 1998; Moslow and Pemberton, 1988; MacEachern et al., 2005; Coates and MacEachern, 2007; Buatois and Mángano, 2011; Solórzano et al., 2017; Moyano Paz et al., 2020) (Fig. VI.8). The interbedded of bioturbated sandstones and mudrocks (Htw, Htf), and mud drapes supports the interpretation of tidal influence (Dalrymple and Choi, 2007; Buatois et al., 2012; Díez – Canseco et al., 2015). The occurrence of symmetrical ripples (Sw), and hummocky cross-stratification (HCS) reveals the local influence of waves and/or storms (Arnott and Southard, 1990; Frey, 1990; Coates and MacEachern, 2007; Bann et al., 2008). This association of facies is sometimes interrupted by distributary mouth bar and, subaqueous distributary channels deposits.

VI.5.2.3.1. Facies association 3.1 - distributary mouth bars.

Description. It consists of medium-to fine-grained sandstones with massive structure (Sm), horizontal lamination (Sh), and planar cross-bedding (Sp). Coarsening-upward trends from the sandstones to granule-sized matrix-supported conglomerate (Gmm) is recorded. The bioturbation index varies between 2 and 4, and it is characterized by the ichnological association or by the exclusive occurrence of *Dactyloidites*, *Macaronichnus*, *Ophiomorpha*, *Skolithos* and/or *Thalassinoides*.

Interpretation. The sedimentary structures identified are typical of high energy environments with sheet flows, and migration of two-dimensional dunes where the underlying succession presents the sedimentological and ichnological characteristics of the subaqueous distributary channels (Buatois et al., 2005, 2012, 2012; MacEachern et al., 2005; Coates and MacEachern, 2007) (Fig. VI.8). The coarsening-upward trend indicates continuous progradational succession.

VI.5.2.3.2. Facies association 3.2 - subaqueous distributary channels.

Description. It is represented by massive medium-to coarse-grained sandstones (Sm) with variations to conglomeratic sandstones (Sig), and granule-sized matrix-supported conglomerates with normal and inverse gradation (Gng, Gig) -bigradational trend, asymmetrical ripples (Sr), as well as erosive bases, organic matter debris and bioturbation indexes between 0 and 2 with the exclusive presence of *Ophiomorpha* or *Taenidium*. *Ophiomorpha* present smaller sizes (~0.5–1 cm in diameter, and 3–4 cm long). Furthermore, some associated flame structures (Sf), and load casts (Slc) are recognized. The punctual flaser bedding (Htf), and interbedded mud-drapes record are also given.

Interpretation. These lithological and ichnological characteristics suggest deposition in a brackish to marine environment, with episodic sedimentation of currents with high-water-turbidity in a fluvial-dominated delta front environment, probably associated with collapses of the channel bar deposits, or high-density hyperpychnic flows (Mulder and Syvitski, 1995; Bhattacharya, 2006; Buatois et al., 2011; Zavala and Pan, 2018; Moyano Paz et al., 2020) (Fig. VI.8). The absence of dwelling structures of suspension-feeders, together with the low diversity, is characteristic. Stressful environmental conditions limit the development of a stable, diverse and abundant macrobenthic community, determining low indexes of bioturbation (BI = 0–2) generated mainly by deposit-feeders organisms (Gingras et al., 1998; Moslow and Pemberton, 1988; MacEachern et al., 2005; Coates and MacEachern, 2007; Buatois and Mángano, 2011). The small sizes exhibited by *Ophiomorpha* may indicate fluctuations in salinity conditions (MacEachern et al., 2005; Coates and MacEachern, 2007; Gingras et al., 2011). The sporadic record of flaser bedding (Htf), as well as the occasional occurrence of interbedded mud-drapes, reveals the local tidal influence on the system (Dalrymple and Choi, 2007).

VI.5.2.4. Facies association 4 - lower delta plain

VI.5.2.4.1. Facies association 4.1 - lower delta plain: interdistributary bays with tidal and wave influence (FA4.1).

Description. It is characterized by massive mudrocks (Mm), horizontal lamination mudrocks (Mh), and lenticular bedding (Htl), with occasional bivalves and gastropods fragments, and undifferentiated shells, and to a lesser extent wavy bedding (Htw), as well as asymmetrical ripples (Sr), symmetrical ripples (Sw), syneresis cracks (Ms), and siderite nodules. Bioturbation indexes are very low (BI = 0–2) and only the ichnogenus *Teichichnus* can be recognized. Calcareous microfossils are near absent, except for a few benthic foraminifera (Project Contrato RC 494, 2017).

Interpretation. Syneresis cracks (Ms), and siderite nodules reveal salinity fluctuations in the system (MacEachern et al., 2005; Buatois et al., 2012; Gingras et al., 2012a; Díez – Canseco et al., 2015). These

ichnological and lithological features can be associated with deposits of muddy and mixed plains, accumulated in interdistributary bays that take place after transgression episodes (transgressive lags) and under quiet conditions and low turbidity, but with a high content of organic matter (Gingras et al., 1999, 2012a; MacEachern et al., 1999; Cattaneo and Steel, 2003; Buatois et al., 2012) (Fig. VI.8). The influence of unidirectional currents is evidenced in Sr. The tidal influence in these systems is associated with lenticular bedding (Htl) and mudrocks dominance (Buatois et al., 2012; Gingras et al., 2012; Dí ez – Canseco et al., 2015), and the wave influence may be associated with the symmetrical ripples (Buatois et al., 2012).

VI.5.2.4.2. Facies association 4.2 - lower delta plain: floodplain, swamp, beach-like (FA4.2).

Description. The previous facies association, linked to interdistributary bays, together with the occurrence of very fine- and fine-grained horizontal lamination sandstones (Sh), massive sandstones (Sm) with rhizoliths, massive mudstones (Mm), massive carbonaceous mudrocks (Mm), horizontal lamination mudrocks (Mh), and coal beds (Co), represent this sub-environment. In some rare cases, thin and medium beds of fine-medium-grained sandstones with low angle cross-bedding (Sa) and horizontal lamination (Sh) with intense bioturbation (BI = 4–5) associated with *Macaronichnus* and/or *Ophiomorpha* typically occur at the top of the progradational cycle.

Interpretation. Variations from fine-grained sediments (Mm, Mh) to coal beds (Co) particularly indicate the development of peat bogs in swampy areas constantly waterlogged, enabling the accumulation and preservation of organic matter (Retallack, 2001; Buatois et al., 2012) (Fig. VI.8). However, in this same environment and far from these swampy areas, the occurrence of fine-grained deposits with root traces fossils indicates low energy traction currents developed in the subaerial delta plain (MacEachern et al., 2005, 2007b, 2007b; Bhattacharya, 2006; Buatois et al., 2012). Fine-grained sandstones and mudrocks are interpreted to represent thin sheet sands and distal portions of splays deposited during river flood conditions (Heldreich et al., 2017). The record of Sh and Sa with the trace fossils *Macaronichnus* and/or *Ophiomorpha*, even if it is very scarce, could reveal beach-like environments (Pemberton et al., 2001; Buatois et al., 2012).

VI.5.2.4.3. Facies association 4.3 - lower delta plain: crevasse splays, channel, bars (FA4.3).

Description. It is associated with the described facies of the lower delta plain; there are also fine-to coarse-grained massive sandstones (Sm), planar cross-bedding (Sp), low-angle cross-bedding (Sa), asymmetrical ripples (Sr), and to a lesser extent, some thin horizontal lamination mudrocks beds (Mh). Settings with root trace fossils are also present.

Interpretation. High and low-angle cross-bedding is common in sandy crevasse-splay deposits, but there is also evidence for the cessation of current discharge, in the form of mudrock and sandstones beds with rhizoliths (Bridge, 2006). Overbank crevasse splay deposits closest to the main channel can be confused with upper channel-bar deposits displaying a progressive decrease in grain size with increasing distance from the channel margin (Bridge, 2006; Heldreich et al., 2017). The current structures generated in the sandstones (Sr) could show the influence of channels in this area (Dalrymple and Choi, 2007; Johnson and Dashtgard, 2014; Dalrymple et al., 2015; Dashtgard and La Croix, 2015). The Sa facies could register the down current migration of point and longitudinal bars deposited by traction from relatively weak currents that approach upper-flow

regime conditions for the size of sediment being deposited (Picard and High, 1973). This makes it difficult to interpret this sub-environment, so we consider that it represents a crevasse splay adjacent to fluvial and distributary channel bodies.

VI.5.3. Wave and tidal influenced: the ichnological record

Bioclastic-rich sediments (Gb, Sb, Mb) with approximate thicknesses between ~3 ft (~0,9 m) and ~10 ft (~3 m), associated with transgressive pulses, on some occasions change progressively to muddy and fine sandy sediments with horizontal lamination (Sh), symmetrical ripples (Sw), and locally hummocky cross-stratification (HCS). Its particular characteristic is a higher ichnodiversity (*Ophiomorpha*, *Teichichnus*, *Thalassinoides*) and abundance of trace fossils (BI = 3–5) than are observed in other intervals. Then a coarsening-upward to medium-fine sandstones, flaser bedding (Htf) with mud drapes is registered, showing an ichnoassemblage consisting of *Conichnus*, *Cylindrichnus*, *Dactyloidites*, *Ophiomorpha*, *Skolithos* and *Thalassinoides*. In particular, the intervals that present these characteristics are few and these conditions do not last over time, being rapidly interrupted by a) medium-to fine-grained sandstones with horizontal lamination (Sh), and planar cross-bedding (Sp), and BI = 2–4 with the ichnological association or the exclusive occurrence of *Macaronichnus*, *Ophiomorpha*, and/or *Skolithos*, characteristics of the mouth bar; and/or b) medium to fine sandstones with normal and inverse gradation (Sng, Sig), as well as erosive bases, organic matter debris and bioturbation indexes between 0 and 2 with the exclusive presence of *Ophiomorpha* or *Taenidium* characteristics of the distributary channels. Thus, the dominant ichnological and lithological features contrast with those previously described. These punctual records can probably be associated with episodes where fluvial control decreases, allowing the development of a delta front under mixed conditions (Bhattacharya and Giosan, 2003; MacEachern et al., 2005; Bhattacharya, 2006; Coates and MacEachern, 2007; Bann et al., 2008; Buatois et al., 2012; Bayet-Goll and Neto de Carvalho, 2020; Canale et al., 2020; Moyano Paz et al., 2020) (Fig. VI.8). The association of facies interpreted as beach-like conditions is not related to this mixed environment, since the previous facies to these deposits are associated with the distributary channel and the later facies with the lower delta plain. Therefore, beach-like environments are not directly considered a deposit associated with wave processes. The associated environmental conditions favour the establishment of a more diverse and abundant macrobenthic trace maker community as reflected in the ichnological record. However, the next progradation of the deltaic system through the mouth bar/distributary channels, prevents maintenance of these conditions. The contact surfaces separating these two scenarios (deltaic systems fluvial-dominated vs mixed) could represent regressive surfaces (MacEachern et al., 2007b; Moyano Paz et al., 2020), but a more detailed analysis is needed before any conclusive interpretation. Similar examples have been recognized in tropical deltas (Buatois et al., 2012). Sequences that vary along the coastline but also vertically have been identified and characterized as fluvial deltas dominated with tidal and wave influence. Even, storm dominated successions interrupting the river sequence has been identified (Buatois et al., 2012). In this alternation of conditions, each one of them persists over time and these variations are observed along the coastline, which gives rise to the establishment of ecological niches and stable palaeoenvironmental conditions at each stage. In our case study, low abundance and moderate diversity of trace fossils, as well as unidirectional

structures, and erosive bases predominate throughout the entire succession and therefore, in general terms the fluvial domain has been interpreted.

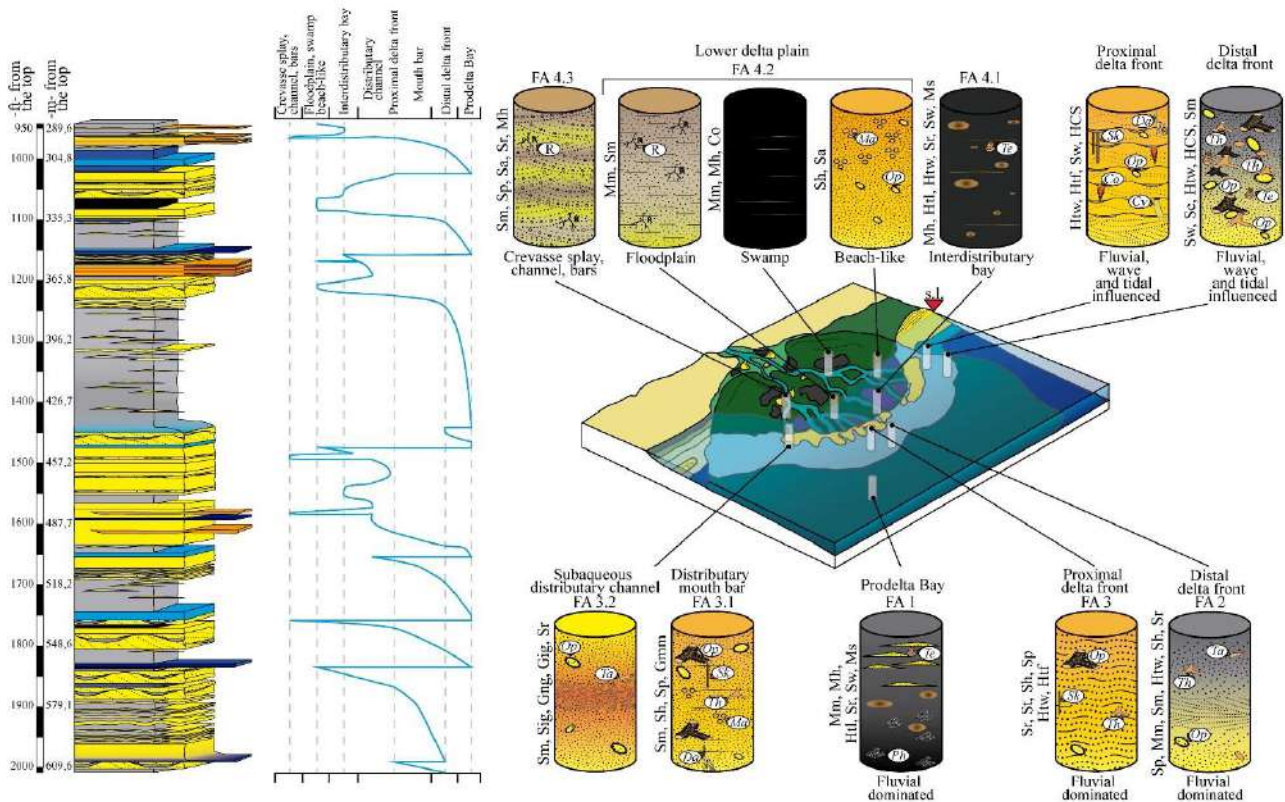


Fig. VI.8. Summarizing sketch showing the differentiated sub-environments of a fluvial-dominated deltaic system interpreted for the studied succession. Note: *Conichnus* (Co), *Cylindrichnus* (Cy), *Dactyloidites* (Da), *Macaronichnus* (Ma), *Ophiomorpha* (Op), *Phycosiphon* (Ph), *Rhizoliths* (R), *Skolithos* (Sk), *Taenidium* (Ta), *Teichichnus* (Te), and *Thalassinoides* (Th). FA facies association. S.l sea level. For facies codes see Table VI.1.

VI.5.4. Prospective considerations

The deposits associated with the fluvial-marine transition zone are of particular interest as hydrocarbon reservoirs (Whateley and Pickering, 1989; Shields and Strobl, 2010). However, depending on the position within this zone, fluvial, tidal and/or wave conditions may dominate, which determines variations in the facies association (Dalrymple and Choi, 2007; Howell et al., 2008). In this sense, the internal architecture and the heterogeneity of the facies, not only lateral but also vertical, are primary factors of great importance in the quality of the reservoir (Miall, 1988; Slatt, 2006). Our detailed analysis suggests that the studied succession drilled by the ANH-SSJ-Nueva Esperanza-1X stratigraphic well, was deposited in a fluvio-dominated delta setting during part of the Oligocene. Obtained data are in agreement with the general deltaic environment previously interpreted for the Ciénaga de Oro Formation (Duque-Caro, 1972; Dueñas, 1983; Guzmán, 2007; Bermúdez et al., 2009; Mora et al., 2017, 2018; Osorio-Granada et al., 2020; Manco–Garcés et al., 2020). However, due to the study succession obeys a highly dynamic depositional context where lateral and vertical variations of facies are evident and frequent, it is necessary to conduct high-resolution sedimentological and ichnological studies to evaluate the continuity, and therefore, the prospectivity of the successions with the

same chronostratigraphic range because not all the interpreted sub-environments represent ideal conditions as reservoirs.

VI.6. Conclusions

Sedimentological and ichnological analysis of a core drilled in the Oligocene deposits of the Sinú-San Jacinto Basin (SSJB) (Colombian Caribbean) allows interpret the development of a fluvial-dominated delta. The studied interval corresponds to a siliciclastic succession with approximately 1069 ft (~326 m) thick. The sedimentological analysis allows the differentiation of dominant facies, with predominant lithologies such as conglomerates, sandstones, mudrocks, bioclastic sediments, as well as coal beds. Ichnological analysis reveals a low abundant, and moderately diverse trace fossil assemblage, consisting of ten ichnogenera *Conichnus*, *Cylindrichnus*, *Dactyloidites*, *Macaronichnus*, *Ophiomorpha*, *Phycosiphon*, *Skolithos*, *Taenidium*, *Teichichnus*, and *Thalassinoides*, together with rhizoliths. The interval studied presents multiple coarsening upward metric successions with a regular order of facies and ichnological assemblage that allows establishing a succession type. Integration of sedimentological and ichnological information allows us to interpret the complexity of the fluvial-dominated deltaic system as reflected in its evolution over time, and in the different sub-environments characterized: prodelta bay, distal delta front, proximal delta front, mouth bars, distributary channels, and lower delta plain. Thus, even the fluvial processes were dominant in the deltaic system; this was affected by the tidal and wave influence. Throughout the succession, the fluvial-dominated deltaic system was punctuated by the episodic development of a mixed deltaic system.

The detailed ichnological analysis conducted shows the usefulness of ichnology for the characterization of complex environments, such as deltaic ones, given the response of tracemakers to stressful and highly variable conditions in these environments. This reveals special interest due to the economic importance of the studied area.

Acknowledgements. We would like to thank Dr. Pazos (JSAES Guest Editor) and two anonymous reviewers by constructive comments and suggestions. Thanks to the National Hydrocarbons Agency-ANH, and *Ministerio de Ciencia, Tecnología e Innovación - Minciencias* to allow the study of well-core (project Contrato RC 494–2017). The Vicerrectoría de Investigaciones y Posgrados and the Instituto de Investigaciones en Estratigrafía-IIES of Universidad de Caldas gave economic and logistic support. The research was conducted within the “Ichnology and Palaeoenvironment RG” (UGR). Financial support of Rodríguez-Tovar was provided by scientific Projects CGL 2015-66835-P and CTM 2016-75129-C3-2-R (Secretaría de Estado de I + D + I, Spain), and B-RNM-072-UGR18 (FEDER Andalucía), and Research Group RNM-178 (Junta de Andalucía). Funding for open access charge: Universidad de Granada / CBUA. Thanks to Fabian Gallego for his contribution in some sedimentological discussions.

PART IV DISCUSSION

Chapter VII

TECTONIC, EUSTASY AND SEDIMENTATION

Sedimentary evolution of forearc basins in the Colombian Caribbean: insights from middle-upper Eocene to Lower Miocene deposits

Sergio A. Celis^{a,b,c*}, Francisco J. Rodríguez-Tovar^a, Carlos A. Giraldo-Villegas^{a,b,c}, Andrés Pardo-Trujillo^{b,c}, Angelo Plata-Torres^{b,c}

^a Departamento de Estratigrafía y Paleontología, Universidad de Granada, 18002 Granada, Spain.

^b Grupo de Investigación en Estratigrafía y Vulcanología (GIEV) Cumanday, Universidad de Caldas, Manizales, Colombia.

^c Instituto de Investigaciones en Estratigrafía-IIES, Universidad de Caldas, 170004, Manizales, Colombia.

*Corresponding author sergiocelis11@gmail.com; sergiocelis@correo.ugr.es (Sergio A. Celis).

Paper submitted to Journal of Sedimentary Research



Abstract

The middle-upper Eocene to Lower Miocene successions in the Colombian Caribbean are reservoir rocks that represent coarse- and fine-grained systems deposited in accretion-dominated subduction complexes with fluvial-dominated and pervasively tide-influenced dynamics. Using outcrops and well-cores, an integrative sedimentological and ichnological analysis was conducted, allowing for the characterization of 12 facies associations, definition of facies stacking patterns, and establishment of the lateral continuity of deltaic bodies. During the middle to late Eocene, coarse-grained systems are characterized by hyperconcentrated to hyperpycnal flows from continental areas reaching the coastline. Ichnological and sedimentological features—e.g. the presence of *Ophiomorpha*, fluid muds, and mud drapes—indicate occasional marine manifestations associated with tidal modulation or wave reworking during upstream avulsion or a sediment input decrease. The limited accommodation space favored the accumulation of amalgamated successions in this compressional accretionary forearc basin, with no evidence of delta plains recorded.

In the earliest Oligocene, transgressive fine-grained deposits overlie the Eocene successions despite a global eustatic sea-level drop, likely overridden by tectonic activity and high sediment input. These successions exhibit meandering fluvial deposits, increased fungal remains, morichal palm pollen, mudrocks, and rhizoliths, indicating water-logged interdistributary bays and gallery flood forests, and pointing to the onset of a lower delta plain supply system. Vertical changes in depositional style occurred under a dramatic global change (Eocene to Oligocene Transition Zone), but the tectonically active basin makes it very difficult to correlate variations in the effectiveness of fluvial and tide influence with fluctuations in eustatic sea-level. Therefore, the accommodation space/sediment supply ratio is controlled principally by active tectonics and fault-controlled subsidence increases. In the Oligocene to Early Miocene, sedimentation is characterized by repetitive coarsening-upward successions typical of fluvio-dominated deltaic settings. These patterns reflect a progradational trend with increasing fluvial-marine interaction and rising accommodation space as compared to the Eocene. The changes in depositional style coincide with lower plate convergence velocities and plate obliquities, indicating margin stabilization in a subduction accretion scenario with a flat slab. This tectonic setting promotes reduced sedimentation rates in forearc basins due to the absence of the magmatic arc, allowing significant sediment accumulation. Deltaic deposits are characterized by hyperpycnite coalescence, where ichnological (tubular tidalites, burrow size) and sedimentological features (fluid muds, and mud drapes) suggest mouth bar migration upstream, laterally, or downstream, depending on basin morphology and tectonic dynamics, with highlighted tidal influence or wave modulation during short episodes, with a possible increase into Early Miocene. Tropical systems in northern South America may correlate more closely with high and mid-latitude fluvio-dominated rivers due to the relationship with mountain ranges than with tropical south-eastern Asian environments, which are more influenced by monsoons or tides in other tectonic scenarios. Present research improves our understanding of the influence of tectonics versus climatic factors on sedimentation in tropical regions.

VII.1. Introduction

Sediment progradation may occur during a slow and steady sea-level rise or at periods of large sea-level fall, or else when sedimentation rates are greater than the creation of accommodation space (Swift and Thorne,

1991; Boyd et al., 1992). Yet deciphering the particular depositional processes involved in the geological record is challenging, because allogenic (climate, tectonism, subsidence and eustatic sea-level) and autogenic (channel avulsion or delta-lobe switching) factors also control the filling of sedimentary basins (Einsele, 2000; Allen and Allen, 2005; Miall, 2014; Catuneanu, 2019). Moreover, while facies models of progradational systems may be similar on a vertical scale, there is considerable lateral variation, especially when deltaic systems are involved, making it difficult to establish the effect of depositional processes (Zavala et al., 2020; Winsemann et al., 2021; Syvitski et al., 2022). These lateral changes, linked to lithological variations, have significant implications for reservoir distribution in hydrocarbon-producing basins (e.g., Olariu et al., 2010; Cole et al., 2021). A valuable approach is the use of multi-proxy techniques to reliably interpret sedimentary processes in detail, and thus obtain regional (basin scale) models of higher resolution. Ichnology coupled with sedimentology and stratigraphy proves key in revealing depositional parameters; and when studied in the framework of regional tools such as seismicity and tectonics, it helps refine knowledge about depositional systems (e.g., Algheryafi et al., 2022; Ahmad et al., 2024).

Marine basins that form along active margins are closely linked to orogenic zones, where tectonic loading from thrust and nappe emplacement generate accommodation space (Fuller et al., 2006; Noda, 2016). This loading induces flexure in the subducting oceanic and continental lithosphere, resulting in the creation of significant depositional spaces. These spaces lead to the formation of accretionary wedges and forearc or back-arc foreland or foredeep basins, which are influenced by various forcing factors (e.g., Beaumont, 1981; Allen et al., 1986; DeCelles and Giles, 1996; Noda, 2016). Ongoing convergence at the leading edge subsequently scrapes off the previously deposited sediments in the flexural accommodation. These sediments become part of the orogenic system as highly deformed accretionary prisms, external fold-and-thrust belts, or deformed foredeeps, where the depositional records may undergo significant erosion (Matenco and Haq, 2020). This is a major problem when studying accretionary systems, hence their record is considered exceptional. Analysis of these sedimentary deposits can reveal whether relative sea-level variations are primarily influenced by allogenic or autogenic factors (Catuneanu and Zecchin, 2013; Noda, 2016; Manteco and Haq, 2020), or help determine the importance of modulation by climatic factors in the case of tropical environments.

The middle-upper Eocene to lowermost Miocene deposits in the Colombian Caribbean are characterized by progradational systems of significant thickness (~1000 m), where multiple tectonic scenarios occurred during their accumulation (e.g., Mora-Bohórquez et al., 2020). The most widely accepted models suggest a shift in subduction from oblique to orthogonal during the early to middle Eocene, with multiple scenarios of compressional accretionary-type forearc basins (Mantilla-Pimiento et al., 2009; Bernal-Olaya et al., 2015; Mora et al., 2018), which most likely had an impact on sedimentary systems. Although two different research scales would prevent a direct correlation, this study focuses on discerning the allochthonous and autochthonous factors that control sedimentation in the northern basins to understand their cause-and-effect relationship within the tectonic context. Since the distribution pattern of sedimentary deposits is a direct response to tectonics and/or eustasy, it sheds light on the movements of thrust loading during subduction, or eustatic variations in a period of strong global change (i.e., Eocene Oligocene transition). In settings deposited with

active tectonic this purpose is commonly hindered by the often-concurrent effects of eustasy and subsidence, which influence spatial and temporal variations in sediment supply and accumulation (Matenco and Haq, 2020). Despite the intricate accumulation scenario, a careful assessment of unconformity-bounded sediment wedges and lateral features of bounding surfaces can prove instrumental in elucidating stratigraphic relationships. This approach helps distinguish whether fluctuations in relative sea-level are driven by eustatic changes or tectonic controls (e.g., Howell and Flint, 1996; Carr et al., 2003; Zecchin et al., 2006; Celma and Cantalamessa, 2007) and constitutes a step forward in comprehending the sedimentation in forearc basins. At the same time, although the types of fills of sedimentary successions are largely influenced by such collisional tectonic scenarios, sedimentation in tropical basins—and the high erosion rates produced by the fast climatic changes of tropical latitudes—can drastically modify the type of resulting successions (e.g., Nummedal et al., 2003). Thus, in addition to changes in subduction processes, the high input of continental sediments into fluvio-deltaic systems during this period must be deciphered in view of the dominant processes.

The primary aim of this study is to analyze the sedimentary record within the forearc basin of the Colombian Caribbean, contextualizing it within the broader framework of Caribbean Plate dynamics and basin evolution. This research is driven by three main objectives: (1) to enhance the existing understanding by updating the stratigraphic framework of the studied region; (2) to develop a comprehensive depositional model that elucidates the processes governing the accumulation of infilling sediments, particularly in relation to the tectonic context; and (3) to infer the paleogeographic evolution of the area through an examination of sedimentation patterns ranging from coarse- to fine-grained scenarios, as well as decipher the dominant sedimentation processes in coastal environments. By achieving these objectives, this study seeks to contribute to our knowledge of tropical sedimentation dynamics within accretion-dominated subduction complexes.

VII.2. Geological background

The development and evolution of sedimentary basins in the Caribbean and western Colombian margin was conditioned by the oblique collision of allochthonous terrains on the continental margin, coupled with intermittent subduction episodes since the Late Cretaceous (Montes et al., 2019; Mora-Paez et al., 2019). This evolution is closely related to the SW to NE migration of the Caribbean Plate, and its interaction with NW margin of South America (Pindell et al., 1998, 2005; Moreno-Sanchez and Pardo-Trujillo, 2003; Pindell and Kennan, 2009; Spikings et al., 2015; Cardona et al., 2018; Hincapié-Gómez et al., 2018; Montes et al., 2019; Mora-Paez et al., 2019).

Currently, the margin displays the morphological and tectonic characteristics of a typical accretion-dominated subduction complex (Mantilla-Pimiento et al., 2009). Seismic data suggest that from the Late Cretaceous to the late Eocene, the convergence between northwest South America and the Caribbean plate was oblique, while nearly orthogonal convergence has taken place from the Oligocene to the present (Pindell et al., 2005; Villagómez et al., 2011; Bayona et al., 2012; Bernal-Olaya et al., 2015; Montes et al., 2019; Mora-Bohórquez et al., 2020).

The primary tectonic features of the margin, from west to east, include the trench, active accretionary prism, outer high and forearc basins (Mantilla-Pimiento et al., 2009). The trench axis aligns with the base of the active accretionary prism, which forms the outer section of the Sinú-Colombia accretionary wedge (Fig. VII.1). The

outer high domain encompasses a significant structural complex comprising the easternmost part of the Sinú-Colombia accretionary wedge and the San Jacinto fold belt (SJFB; Fig. VII.1). This SW-NE trending structure is part of the subduction complex and exposes Cretaceous to Miocene rocks at the surface. The fossil portion of the accretionary prism now serves as a dynamic backstop to the active accretionary prism (Mantilla-Pimiento et al., 2009). The outer high consists of several small sedimentary basins containing post-kinematic Plio-Pleistocene deposits that fossilize the complex structure of the outer high (San Jorge and Plato forearc basins). The landward boundary of the outer high is delineated by the well-developed positive flower structure of the Romeral North or San Jacinto Fault System, representing a structural divide between the smaller basins deformed by mud diapirism to the west and the main, deeper forearc Lower Magdalena Valley Basin to the east. This basin, bounded by the Romeral Fault System to the west, and the Central Cordillera, San Lucas, and the Cáchira Structural High to the east (Mora et al., 2018), is the most prominent feature at the transition between the highly deformed forearc domain to the west (SSJB) and the less deformed one to the east (Mantilla-Pimiento et al., 2009; Fig. VII.1).

The SJFB presents an oceanic igneous basement of Cretaceous age (Silva-Arias et al., 2016; Mora et al., 2017), and the sedimentary record spans from the Late Cretaceous to recent times (Dueñas and Gómez, 2013; Mora et al., 2017, 2018; Montes et al., 2019; Pardo-Trujillo et al., 2020; Angulo-Pardo et al., 2023; Rincón-Martínez et al., 2023; Vallejo-Hincapié et al., 2023; Plata-Torres et al., 2024).

The tectonic evolution of the margin and its interaction with sedimentary environments remains a topic of ongoing debate. However, it is widely agreed that the Ciénaga de Oro Formation, which is the focal point of the stratigraphic analysis conducted in this study, was deposited in shallow marine and deltaic systems from the Eocene (?) to early-middle Miocene (Dueñas and Duque-Caro, 1981; Dueñas, 1986; Guzmán et al., 2004; Bermúdez et al., 2009; Bermúdez, 2016; Mendoza et al., 2018; Manco-Garcés et al., 2020; Celis et al., 2021, 2023; Pardo-Trujillo et al., 2023; Vallejo-Hincapié et al., 2023). Deposits of the same age described mainly northwest and northeast of the basin, e.g. El Floral and El Carmen formations, respectively (Duque-Caro et al., 1996; Raigosa, 2018; Arias-Villegas et al., 2023; Domínguez-Giraldo et al., 2023), would be associated with the distal facies of the Ciénaga de Oro Formation, those mainly associated with the shelf. Private studies by oil companies also report sequences of this age in slope and basin plain environments in the offshore basins, possibly corresponding to the El Carmen Formation.

Deposits preceding the Ciénaga de Oro and El Carmen formations are associated with coarse-grained sedimentation during middle to late Eocene (Duque-Caro et al., 1996; Clavijo and Barrera, 2001; Guzmán, 2007; Mora et al., 2017; Salazar-Ortiz et al., 2020a; Celis et al., 2023, 2024). In the study area, however, this relationship is not well discerned in outcrops, and the deposits associated with the Ciénaga de Oro Formation overlie Paleocene - Eocene conglomerates, sandstones, and mudrocks of the San Cayetano Formation (Duque-Caro et al., 1996; Cardona et al., 2012; Mora et al., 2017) (Fig. VII.2) and middle to upper Eocene deposits of the Toluviejo Formation characterized by bioclastic limestones (Raigosa, 2018; Mendoza et al., 2019; Salazar-Ortiz et al., 2020b). Overlying the Ciénaga de Oro Formation is the Porquera Formation, characterized by a

predominance of fine-grained deposits accumulated from shelf and deep marine systems (Duque-Caro et al., 1996; Mora et al., 2018; Duque-Castaño et al., 2023).

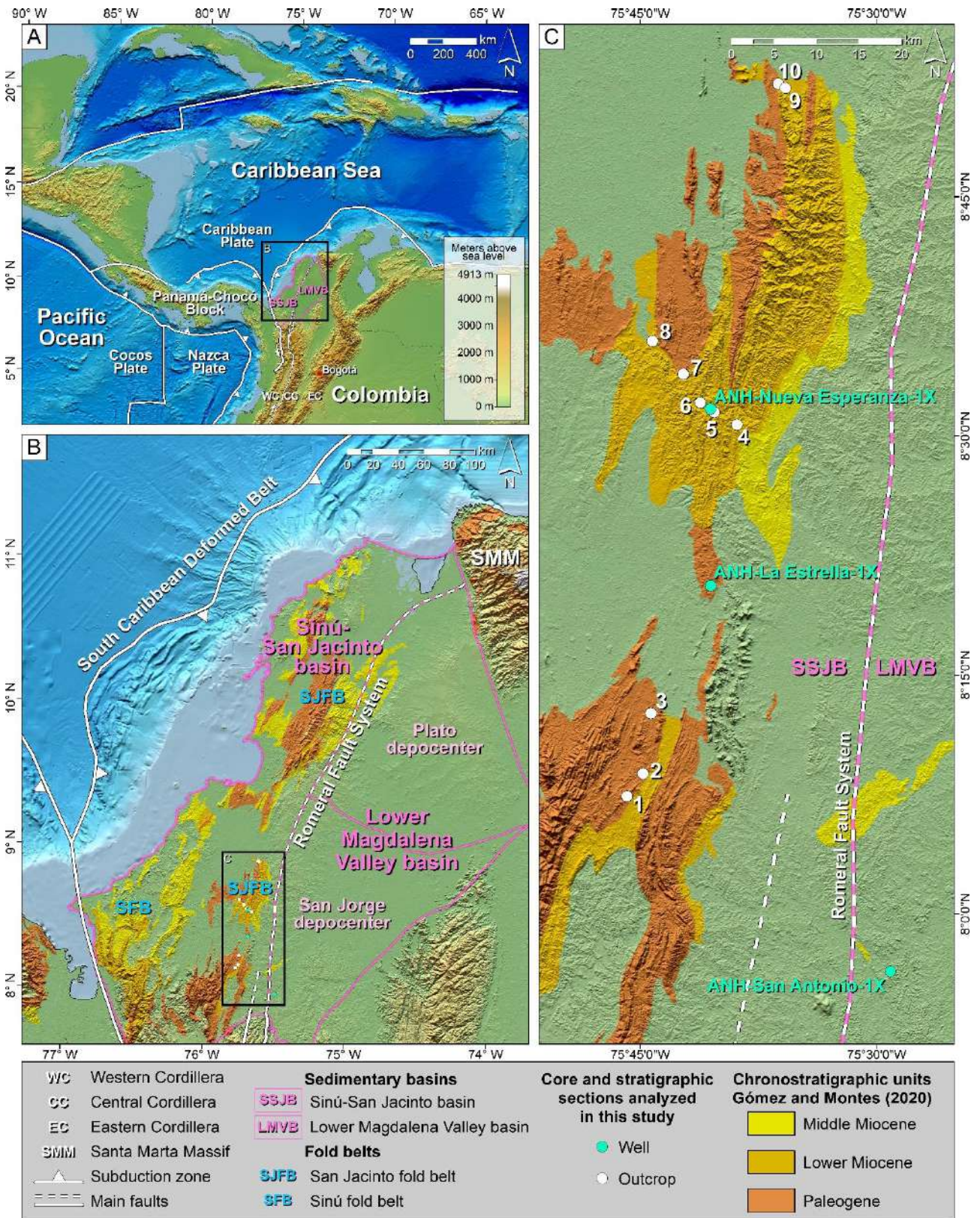


Fig. VII.1. A. Location of the Colombian Caribbean basins. B. Study area in the San Jacinto fold belt and Lower Magdalena Valley basin. C. Outcrop and well-core locations. Paleogene, Lower and Middle Miocene deposits are indicated in the Sinú-San Jacinto Basin (Source: WGS-1984 coordinate system; CIOH, SRTM, NOAA elevation, and ocean models; geology from Gómez and Montes, 2020).

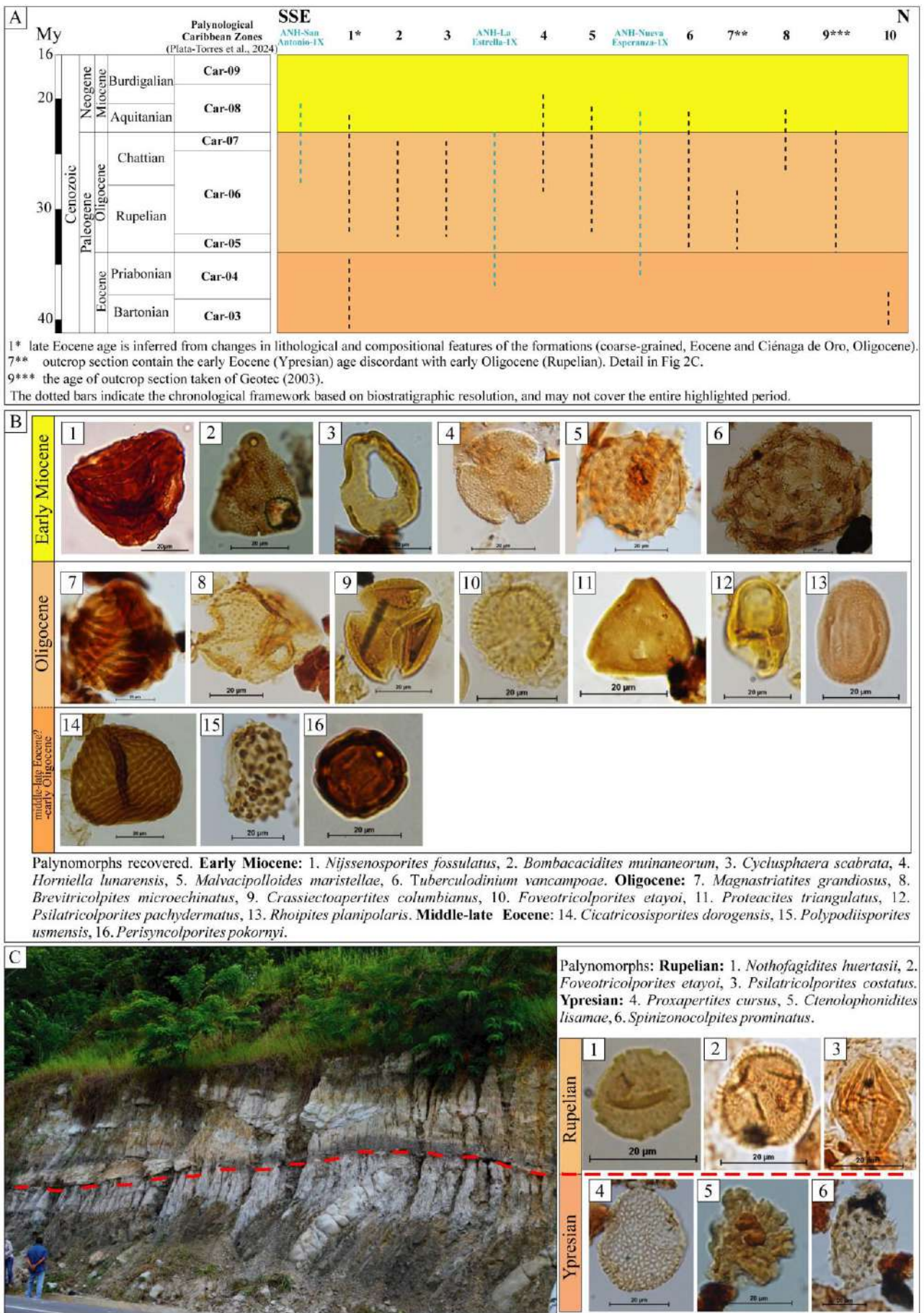


Fig. VII.2. Biostratigraphy of studied outcrops and well-cores. **A.** Stratigraphic distribution of the sections. **B.** Main palynomorphs. **C.** Unconformity between Ypresian and Rupelian from outcrop 7 (see SM1 for coordinates).

VII.3. Dataset and methodology

This study encompasses ten outcrop sections and three well-cores from the San Jacinto and Ciénaga de Oro formations, located in the southern region of the San Jacinto Fold Belt (Fig. VII.1; Supplementary Material VII.1). The outcrop sites are distributed as follows: three outcrops in the San Francisco del Rayo area, five between Montería and Planeta Rica road, and two outcrops near the town of Ciénaga de Oro (Figs. VII.1 and VII.2; Supplementary Material VII.1). The well-cores include ANH-SSJ-San Antonio-1X (~290 m thick), ANH-SSJ-La Estrella-1X (~420 m thick), and ANH-SSJ-NuevaEsperanza-1X (~691 m thick), all located in the Montería-Planeta Rica area, near the town of Montelíbano (Fig. VII.1C). ANH-SSJ-La Estrella-1X drilled rocks older than the study interval, but only their depth from 0 to 420 m (0 ft to 1378 ft) was considered. Rocks from ANH-SSJ-La Estrella-1X are tectonically deformed so its thickness was recalculated (see SM1).

The focus of this study lies in the sedimentological, ichnological and photo-panel analysis of outcrops and well cores. Systematic stratigraphic records were made bed by bed using a Jacob's staff. Observations included analysis of geometry, lithology (texture, grain size, sorting, roundness, sphericity), thickness, sedimentary structures, body fossils, and ichnological features. Bed thickness was classified as very thin (<1 cm), thin (1-10 cm), medium (11-30 cm), thick (31-100 cm), or very thick (>100 cm) according to Nichols' scheme (2009); however, we always try to report the thickness of beds greater than 1 m with accurate numbers. Mudrocks were defined as rocks with grain size <1/16 mm (Wentworth, 1922). The gravel-clast fabric terminology used follows Walker's (1975) classification. For mixed rocks, textural and compositional information followed Mount's (1985) proposal, with the allochemic term modified to bioclastic, because the mixed rocks often consist of fragments of broken shells and extraclasts.

Ichnological attributes, including ichnodiversity, distribution, and abundance, were assessed; the latter using the Bioturbation Index (BI) *sensu* Taylor and Goldring (1993). Ichnotaxonomic assignments of trace fossils were based on core images (Frey and Pemberton, 1985; Gerard and Bromley, 2008; Knaust, 2017). Given the limitations of the core samples, ichnotaxonomic identification was performed at the ichnogenus level, emphasizing general morphology and the presence of specific diagnostic criteria or ichnotaxobases (Bromley, 1996; Bertling et al., 2006, 2022). Despite the cores not being slabbed, confidently identifiable trace fossils were included in the analysis, while uncertain identifications were marked with a question mark and carefully considered in the interpretations. Ichnological analysis was applied to characterize ecological and depositional conditions, and then to improve paleoenvironmental interpretations (Tables VII.2 and VII.3). Throughout fieldwork and the analysis of photo panels, as well as correlation with well-cores, the three-dimensional arrangement of architectural features and bounding surfaces was documented to capture the larger-scale stacking pattern of facies associations, following some ideas proposed by Howell et al. (2008; 2014). Paleoflow directions were determined from features such as planar and trough cross-bedding, asymmetric ripple lamination, and clast imbrications. The interpretation of facies associations and stacking patterns heavily relied on understanding paleoflow conditions, including their spatial variations and temporal evolution.

Sampling was focused on mudrocks to obtain detailed biostratigraphic frameworks and possible paleoenvironmental indicators. Micropaleontological analyses, involving palynomorphs, foraminifera, and calcareous nannoplankton, were performed to support biostratigraphic and paleoenvironmental interpretations.

However, due to poor recovery of calcareous nannoplankton and foraminifera, primary biostratigraphic considerations relied on palynology. A total of 148 palynological samples (3 well-cores: 118 samples; 3 outcrop areas: 30 samples) were processed using the standard technique outlined by Traverse (2007). Slides were examined with a high-resolution Nikon Eclipse 80i microscope at 40x and 100x magnification (Table VII.1). The palynological age model was based on the Cenozoic zonation by Jaramillo et al. (2011) and Plata-Torres et al. (2024). Thermal maturation estimates were determined using Pearson's (1984) color chart, which was correlated with Thermal Alteration Index (TAI) values as described by Traverse (2007).

Table VII.1. Palynological samples used in this study.

| Type | Name | Samples |
|----------------------|------------------------|------------|
| Well-cores | ANH-San Antonio-1X | 10 |
| | ANH-La Estrella-1X | 36 |
| | ANH-Nueva Esperanza-1X | 72 |
| Outcrops | 1-3 (South) | 3 |
| | 4-8 (Central) | 25 |
| | 9-10 (North) | 2 |
| Total samples | | 148 |

VII.4. Biostratigraphy

The biostratigraphy for the well-cores was published recently by Plata-Torres et al. (2024). In the interval 1447.6 - 23ft of the ANH-La Estrella-1X well-core, a Middle-Late Eocene to Oligocene age range (corresponding from Car-03 to Car-07 palynological Caribbean zones) was assigned based on occurrences of *Cicatricosisporites dorogensis*, *Perisyncolporites pokorny*, *Retistephanoporites crassiannulatus*, *Polypodiisporites usmensis*, *Psilatricolporites pachydermatus* and *Magnastriatites grandiosus* (Fig. VII.2A-B). For the ANH-Nueva Esperanza-1X, along the well-core a Middle Eocene to Early Miocene range age, related to Car-03 until Car-08 zones, was assigned and characterized by the occurrences of *P. pokorny*, *P. usmensis*, *M. grandiosus*, *Crassiectoapertites columbianus*, *Retitriletes sommeri*, *Rhoipites planipolaris*, *Psilatricolporites pachydermatus*, *Cicatricosisporites dorogensis*, *Spinizonocolpites prominatus*, *Bombacacidites echinatus*, *Bombacacidites muinaneorum*, *Nijssenosporites fossulatus*, *Echitriporites cricotriporatiformis*, *Cyclusphaera scabrata*, and *H. lunarensis* (Fig. VII.2A-B). For the ANH-San Antonio-1X well-core, a Late Oligocene to Early Miocene age, spanning from Car-07 to Car-09 zones, was assigned. Registered within the palynomorph assemblage were *Proteacidites triangulatus*, *Verrutricolporites rotundiporus*, *Psilatricolporites pachydermatus*, *R. planipolaris*, *C. columbianus*, *Brevitricolpites microechinatus*, *Malvacipolloides maristellae*, *N. fossulatus*, *Clavainaperturites microclavatus*, *Bombacacidites araracuarensis*, and *C. scabrata* (Fig. VII.2A-B). Outcrop palynological samples suggest mainly two age groups. The first group, restricted to outcrop 7 (Fig. VII.2A-C), reveals an age not younger than Early Eocene (Ypresian), corresponding to Car-02 zone, and based on the occurrences of *Proxapertites cursus*, *Ctenolophonidites lisamae*, and *Spinizonocolpites prominatus* discordant with an Earliest Oligocene age, corresponding to Car-05 and based on the co-occurrences of *Nothofagidites huertasii* and *Foveotricolporites etayoi* (Fig. VII.2C). For the second group, similar to that found for the well-cores, a Late

Eocene (?)–Oligocene to Early Miocene age range was assigned, corresponding from Car-04(?)–Car-05 to Car-08 palynological Caribbean zones, based on the occurrences of common taxa such as *C. dorogensis*, *P. pokorny*, *P. usmensis*, *M. grandiosus*, *P. triangulatus*, *B. muinaneorum*, *G. minor* and *C. scabrata* (Fig. VII.2A–B).

VII.5. Sedimentary facies and facies association

A total of 26 facies from middle-late Eocene to Early Miocene were identified (Supplementary Material VII.2, SM VII.2), grouped into twelve facies associations —FA from the more proximal FA1 to the more distal FA9 and FA12 (SM2). The legend for lithology, sedimentary structures, ichnology (Tables VII.2 and VII.3) and FA's features is seen in Figure VII.3. The described well-cores and outcrops are shown in Figures VII.4, VII.5, VII.6 and VII.7.

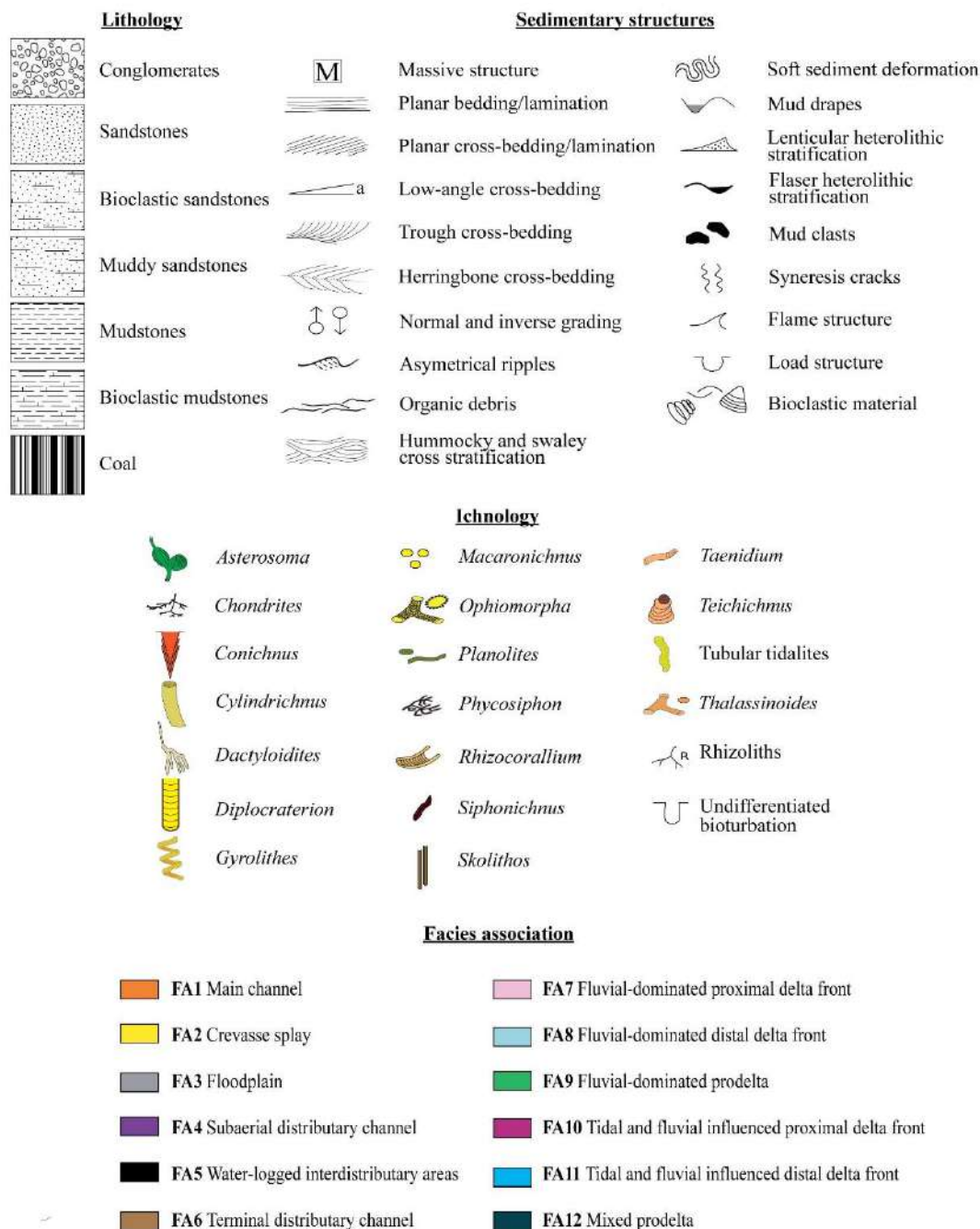


Fig. VII.3. Key for lithologies, sedimentary structures, post depositional features, and facies.

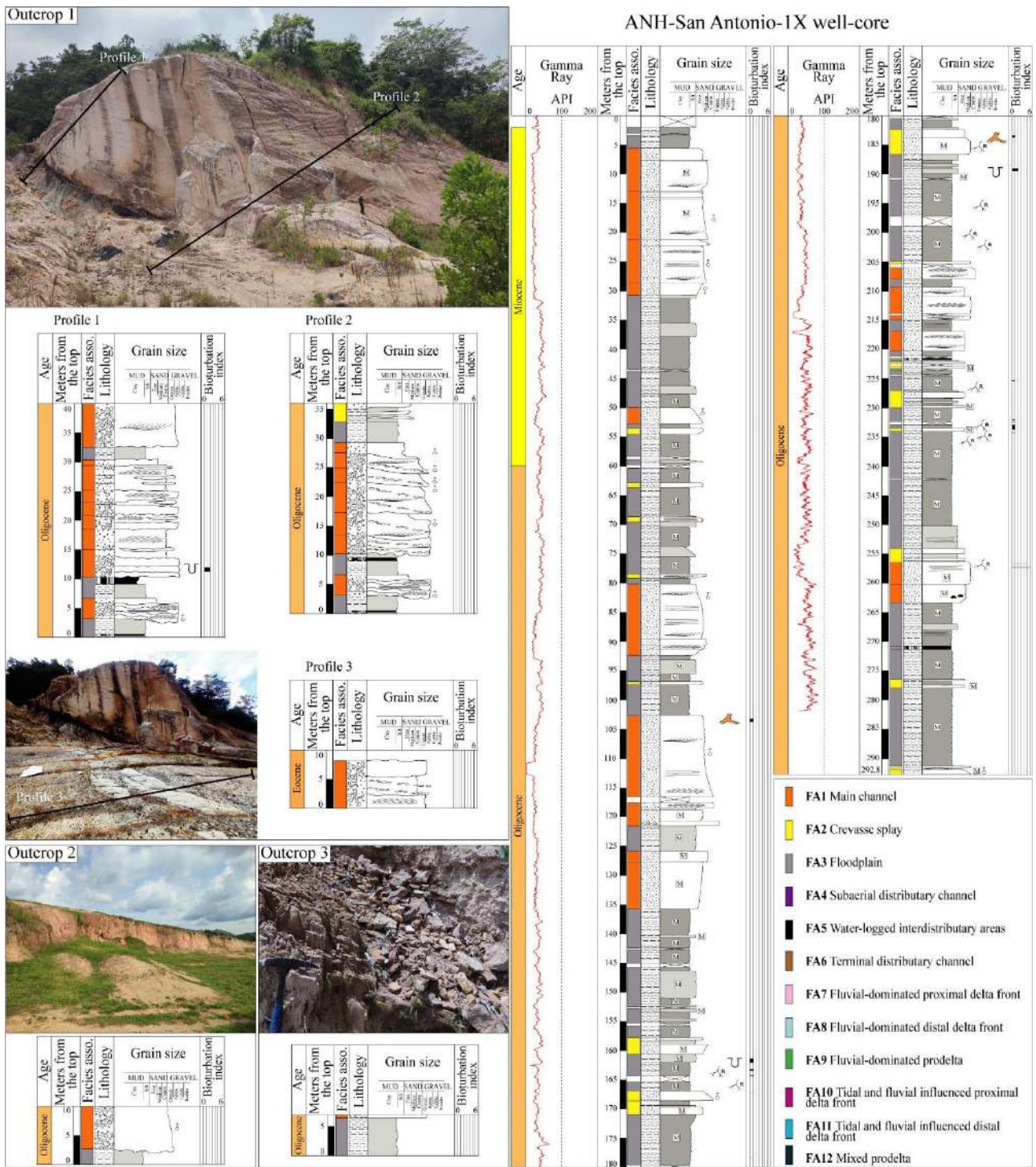


Fig.VII. 4. Continental successions from outcrops 1, 2, 3, and ANH-San Antonio-1X well-core. For legend see Figure VII.3.

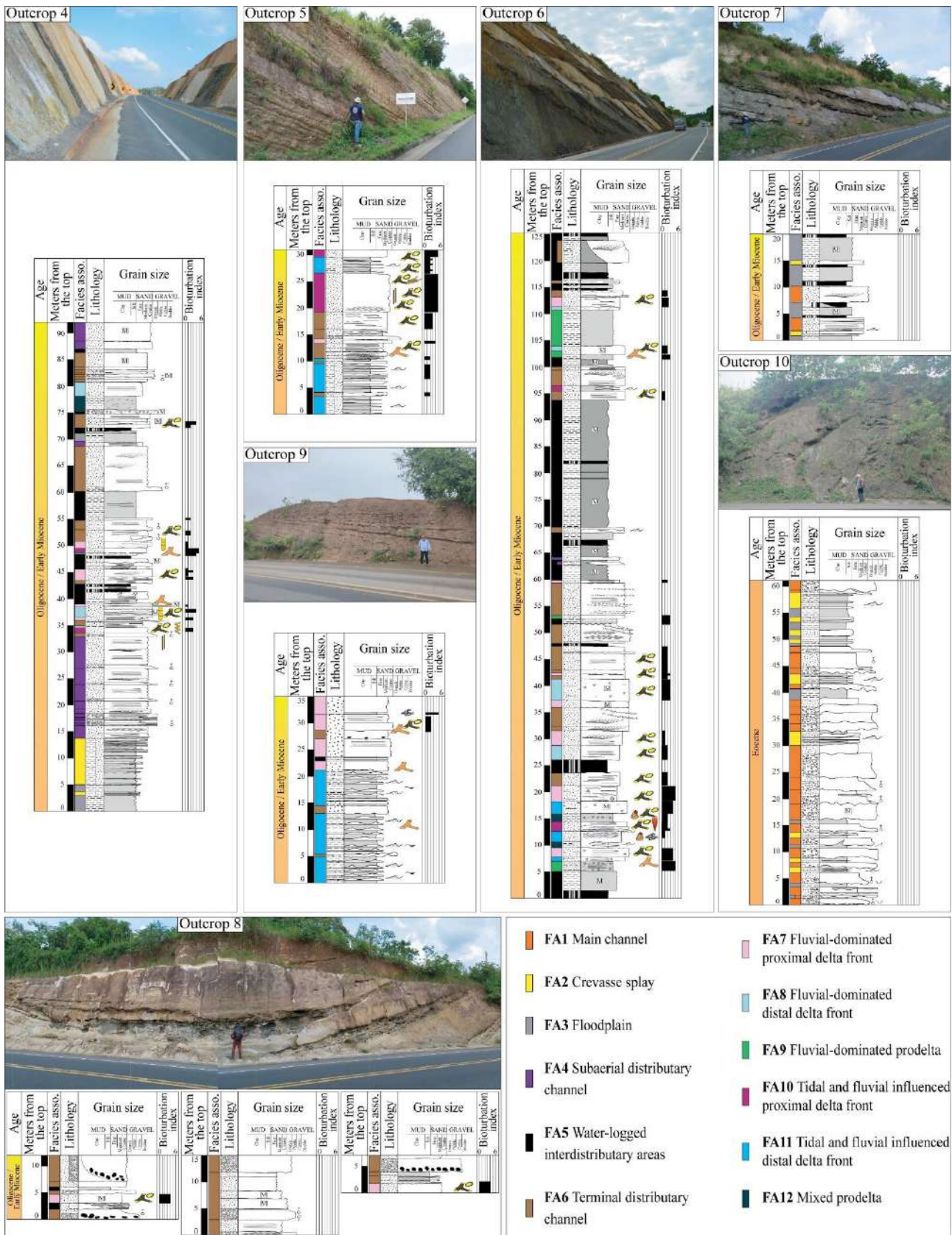


Fig. VII.5. Outcrop sections showing the transition from continental middle-upper Eocene deposits to deltaic Oligocene deposits. For legend see Figure VII.3.

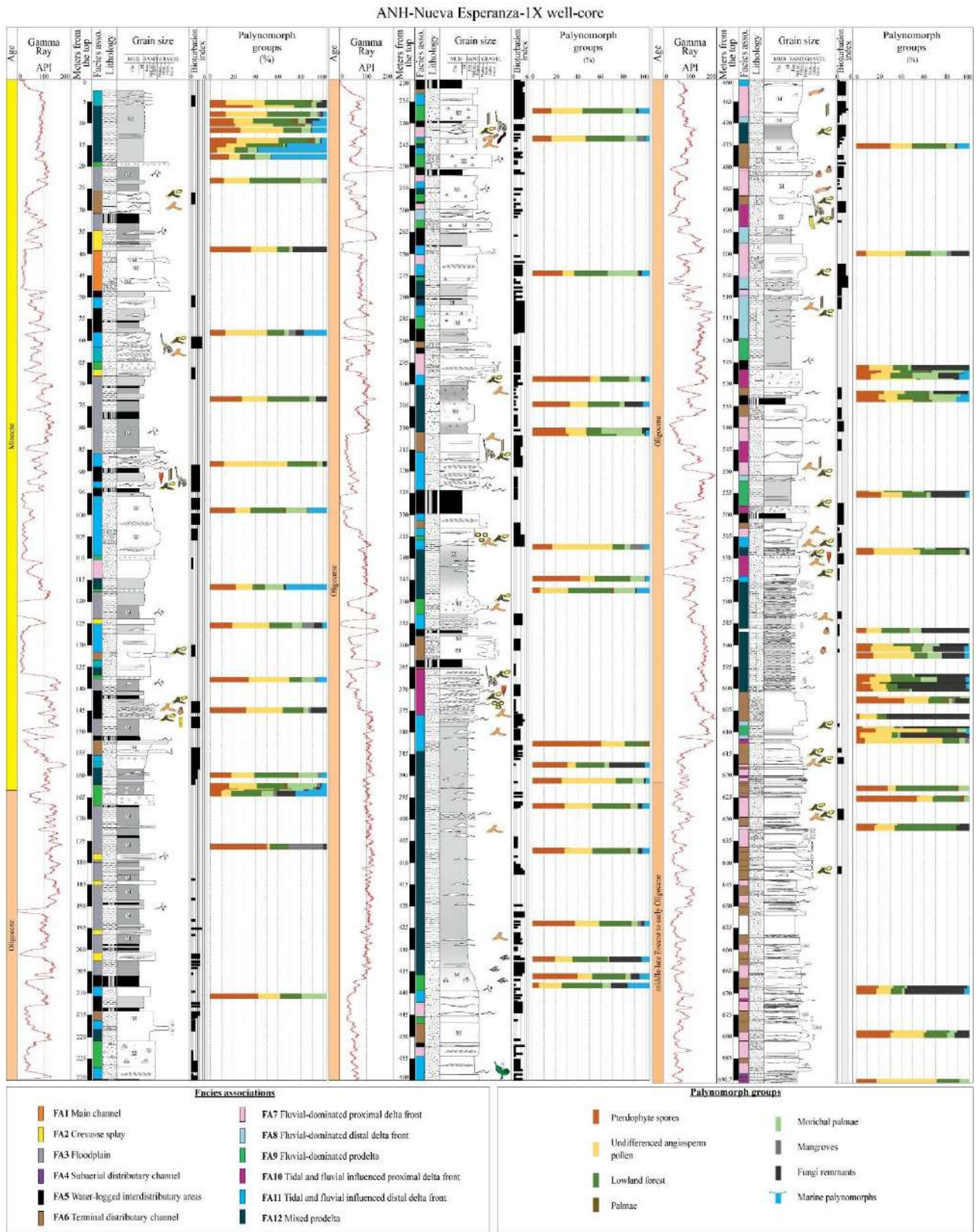


Fig. VII.6. The ANH-Nueva Esperanza-1X well-core showing the transition from continental to transitional middle-upper Eocene deposits to deltaic Early Miocene deposits. For legend see Figure VII.3.

ANH-La Estrella-1X well core

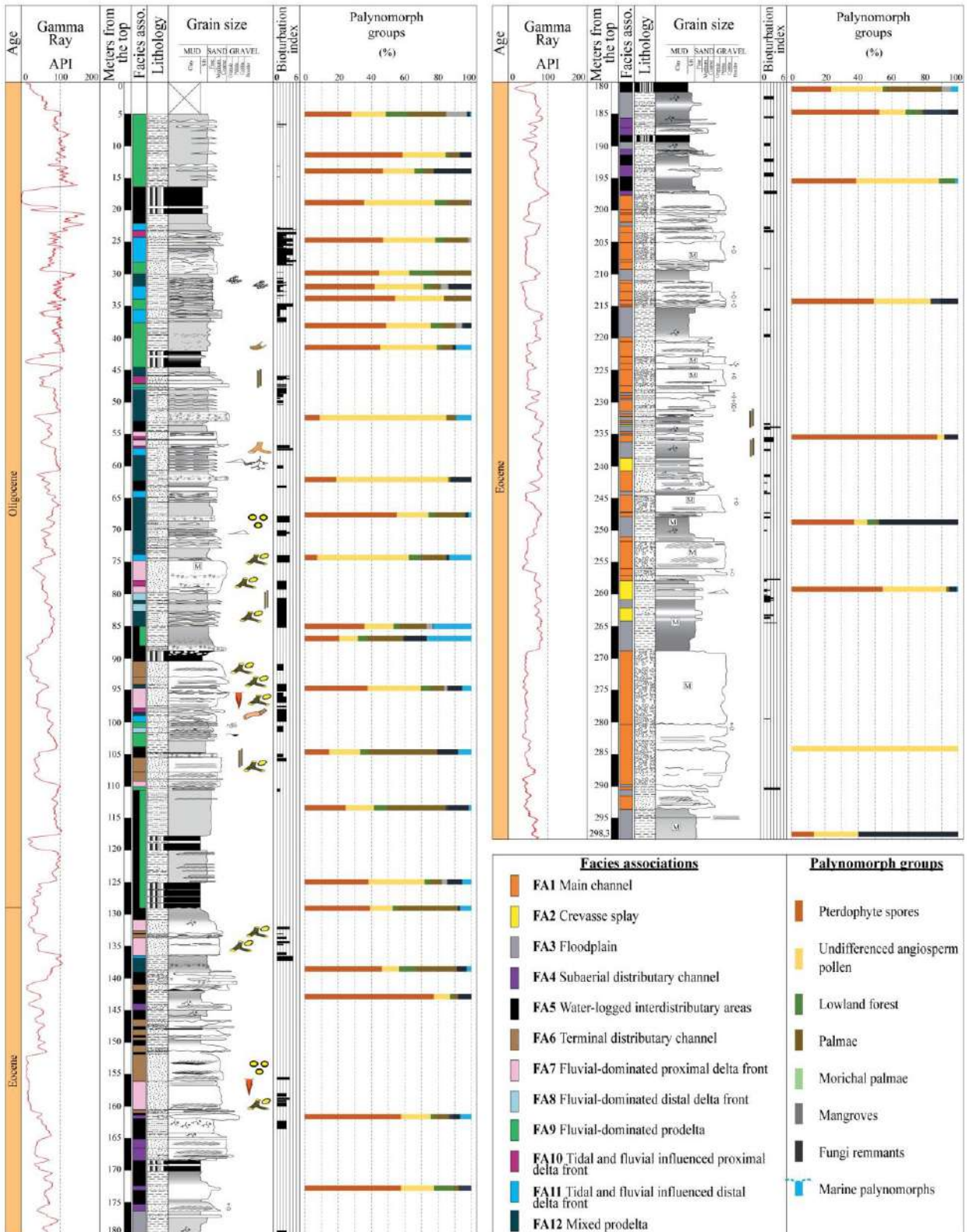


Fig.VII.7. The ANH-La Estrella-1X well-core shows the transition from continental to transitional middle-upper Eocene deposits to deltaic Oligocene deposits. For legend see Figure VII.3.

Table VII.2. Ichnological features of the registered ichnogenus (i.e., lining, abundance and ethology of the tracemakers).

| <u>Ichnogenus</u> | <u>Burrow Lining</u> | <u>Ethology</u> | | | | |
|-----------------------|----------------------|-----------------|-------------------------------|-----------------------|------------------------|-----------------------|
| | | <u>Domicile</u> | <u>Sediment Stabilization</u> | <u>Filter Feeding</u> | <u>Deposit Feeding</u> | <u>Equilibrichnia</u> |
| <i>Asterosoma</i> | | | | | | |
| <i>Chondrites</i> | | | | | | |
| <i>Conichnus</i> | | | | | | |
| <i>Cylindrichnus</i> | | | | | | |
| <i>Dactyloidites</i> | | | | | | |
| <i>Diplocraterion</i> | | | | | | |
| <i>Gyrolithes</i> | | | | | | |
| <i>Macaronichnus</i> | | | | | | |
| <i>Ophiomorpha</i> | | | | | | |
| <i>Phycosiphon</i> | | | | | | |
| <i>Planolites</i> | | | | | | |
| <i>Rhizocorallium</i> | | | | | | |
| <i>Siphonichnus</i> | | | | | | |
| <i>Skolithos</i> | | | | | | |
| <i>Taenidium</i> | | | | | | |
| <i>Teichichnus</i> | | | | | | |
| <i>Thalassinoides</i> | | | | | | |
| Root structures | | | | | | |

| <u>Burrow Lining</u> | <u>Ethological association</u> | | | |
|---|---|---|--|---|
|  |  |  |  |  |
| Lined | Strong | Common | Rare | None |
|  | | | | |
| Unlined | | | | |

VII.5.1. FA1 – Main channel

Description. FA1 overlies the deposits of FA2 with erosive surfaces, incising as well into deposits of FA3. Moreover, FA1 intervals occasionally occur with a fining-upward trend to FA2 and FA3 and amalgamate beds with soft fining-upward trends or in sharp contact directly to FA3. FA1 corresponds to lenticular-shaped bodies with concave up base and single-storey stacking, occasionally with internal erosion surfaces, and thickness between 1 and 3 m. Moreover, there are lenticular bodies with multi-storey offset stacked, bounded by erosion surfaces, that exhibit thickness of up to 5 m and lateral accretion lengths of up to 20 m. In outcrops, internally, FA1 (Fig. VII.8A-F), are matrix-supported by coarse-grained sandstones, and clasts of medium- to very coarse-size pebbles with planar cross-bedding (~50 cm to 1 m; Fig. VII.8A-F) and horizontal stratification, as well as massive structure. In addition, well-cores show massive structure, asymmetrical ripple lamination, soft-sediment deformation structures, and horizontal lamination (Fig. VII.8A-F). Where FA1 grades into or presents sharp contacts with FA3, it exhibits clast-supported medium- to coarse-size pebbles, sandy conglomerates with coarse grained sandstone matrix, and organic debris (Fig. VII.8A-F). This facies association is best represented in outcrops 1, 2, 3, 4, 7 and ANH-SSJ-San Antonio-1X and ANH-SSJ-La Estrella-1X well-cores.

Ichology. FA1 is typically unburrowed (BI 0).

Interpretation. The erosional bases overlain by medium- to coarse-size pebbles, sandy conglomerates, and coarse-grained dominated successions, occasionally with fining-upward trends, are interpreted as channel deposits; and when these successions are amalgamated and show lateral accretion, they are interpreted as multi-storey channels eroded each other (Miall, 1978, 1996, 2014; Donselaar and Overeem, 2008; Swan et al., 2018). Vertical variations in sedimentary structures, ranging from dune-scale to ripple-scale bedforms and stratified bedsets were originated in unidirectional currents associated with channel fills (e.g., Bhattacharya, 2006; Olariu and Bhattacharya, 2006). Two fluvial styles were identified: (i) internal lateral accretion surfaces suggest point bars of high-sinuosity channels, and the fining-upward pattern may be associated with lateral migration and sudden channel abandonment due to avulsion (e.g., Ghazi and Mountney, 2009; Smith et al., 2011; Ghinassi et al., 2018); and (ii) clast-supported successions of amalgamated beds of medium- to fine-grained pebbles with incipient transitions to FA3 may be related to hyperconcentrated gravity flows linked to sudden episodic rainstorms (e.g., Miall, 1977, 1978, 2014; Einsele, 2000; Zavala et al., 2020), where downstream sandy deposits would represent medial to distal sectors of the system (e.g., Coronel et al., 2020). However, outcrop limitations impede conclusive determination of the fluvial style in ii. The environmental conditions, characterized by physico-chemical stress, were inhabitable for tracemaker colonization due to the absence of prolonged stability that would allow for the development of pedogenetic processes (e.g., Retallack, 2001). No evidence of marine influence would allow the interpretation of river-dominated channels that developed in continental areas or on the upper delta plain.

VII.5.2. FA2 – Crevasse splay

Description. FA2 overlies FA1 (i), and it is composed of ~50 cm thick lenticular bodies (Fig. VII.8G-L) with lateral accretion of fining-upward successions of medium-grained to fine-grained sandstones having trough cross-bedding, and interbedded with ~1 to 2 m thick mudrocks (Fig. VII.8G-L), and some thin coal beds. In well-cores, there are several reactivation surfaces in this FA. Occasionally seen are soft-sediment deformation, plant debris and root structures. Frequently, this FA2 forms fining-upward successions from FA1. The best representation of FA2 is found in outcrops 1, 2, 3, 7 and the ANH-SSJ-San Antonio-1X well-core.

Ichology. FA2 presents root structures in life position (BI 1-2), with a subvertical trend up to 7 cm.

Interpretation. Sandstones, and mudrocks containing rhizoliths indicate deposition under fluctuating high- and low-energy conditions typical of crevasse splay deposits, such as overflows or dikes (e.g., Yeste et al., 2020, 2021). These environments are located at a considerable distance from the main channel and tend to accumulate sediment during and after flood events. Cross-lamination is linked to instances where the river breaches its natural levees (Selley, 1985; Einsele, 2000; Yeste et al., 2020; Esperante et al., 2021). The soft-sediment deformation bounded by carbonaceous sandstone or planar cross-laminated sandstone suggests overbank collapse sediments (e.g., Lecce, 1997; Yeste et al., 2020). Some coal beds suggest deposition of large amounts of organic matter under anaerobic periods during low-energy conditions associated with swamps or bogs (Myers and Bristow, 1989).

VII.5.3. FA3 – Floodplain

Description. FA3 overlies FA2, although on a minor scale FA2 and FA3 are interbedded (Fig. VII.8M-R). Although FA3 completes the fining-upward successions from FA1(i), sometimes medium- to thick beds of FA3 appear in transitional contacts with FA1 (ii). FA3 reaches thicknesses up to 4-5 m of mudrocks, and moreover contains fine- to medium-grained sandstones with root structures (Fig. VII.8M-R), rooted to variegated mudrocks (Fig. VII.8M-R). Common calcrete nodules and mudrocks with reddish to green reduction bands and spots are observed. Sedimentary structures are absent. The best representation of this facies association is in outcrops 3, 7, 10, and ANH-SSJ-San Antonio-1X and ANH-SSJ-Nueva Esperanza-1X well-cores.

Ichology. FA3 shows root structures in life position (BI 2-3), ranging in diameter from ~1 mm to ~2 cm. These root structures are irregularly spaced, unbranched, and filled with carbonaceous material, sandy sediment, or sand lined with a thin carbonaceous layer.

Interpretation. Variegated mudrocks, and some fine- to medium-grained sandstone beds containing rhizoliths (BI 2) indicate the transition from active fluvial discharge to the establishment of permanent vegetation. These deposits are associated with extensive floodplains and soil development, reflecting low energy conditions and subaerial exposure (Makaske, 2001; Retallack, 2001; Bridge, 2003, 2006; Miall, 2014).

VII.5.4. FA4 - Subaerial distributary channels

Description. FA4 consists of beds with erosional lower contact overlying FA5 (Fig. VII.8S-X), and interbedded with thin beds from FA2. The basal scours are covered with medium pebbles size and granule to coarse-grained sandstones. There are occasional sharp contacts with massive mudrocks <20 cm thick (Fig. VII.8S-X). FA4 shows lenticular-shaped, fine-grained pebbly sandstones, very coarse- to medium-grained sandstones with planar and trough cross-bedding, and planar lamination marked by organic debris. Beds are stacked, forming 5 m thick, fining-upward intervals. These deposits tend to be finer-grained, having thinner beds than FA1 (main fluvial channels), yet coarser than FA6. Internal erosional surfaces are common. This facies association is best represented in the outcrops 4, 6, and well-cores from ANH-SSJ-La Estrella-1X and ANH-SSJ-Nueva Esperanza-1X.

Ichology. Trace fossils are absent.

Interpretation. Erosional lower contact and fining-upward trends observed are characteristic of deposits related to channel fills with migration of two-dimensional and three-dimensional dunes (Lowe, 1979; Miall, 2014; Viseras et al., 2018). The finer grain sizes and association with crevasse splay deposits and water-logged interdistributary areas suggest deposition in moderate sinuosity channels, indicative of lowland areas within the delta plain downstream of FA1. Multiple internal erosional surfaces are associated with multi-storey channels from overbank discharges (Bhattacharya, 2006; Olariu and Bhattacharya, 2006; Fielding, 2010; Moyano Paz et al., 2020). However, sharp contacts with mudrocks could be associated with mud fluids in tidal-influence scenarios (e.g., McIlroy, 2004). The presence of high inputs of continental palynomorphs, no record of marine microfossils, and absence of marine trace fossils suggest deposition in high-energy distributary channels linked to subaerial delta plain.

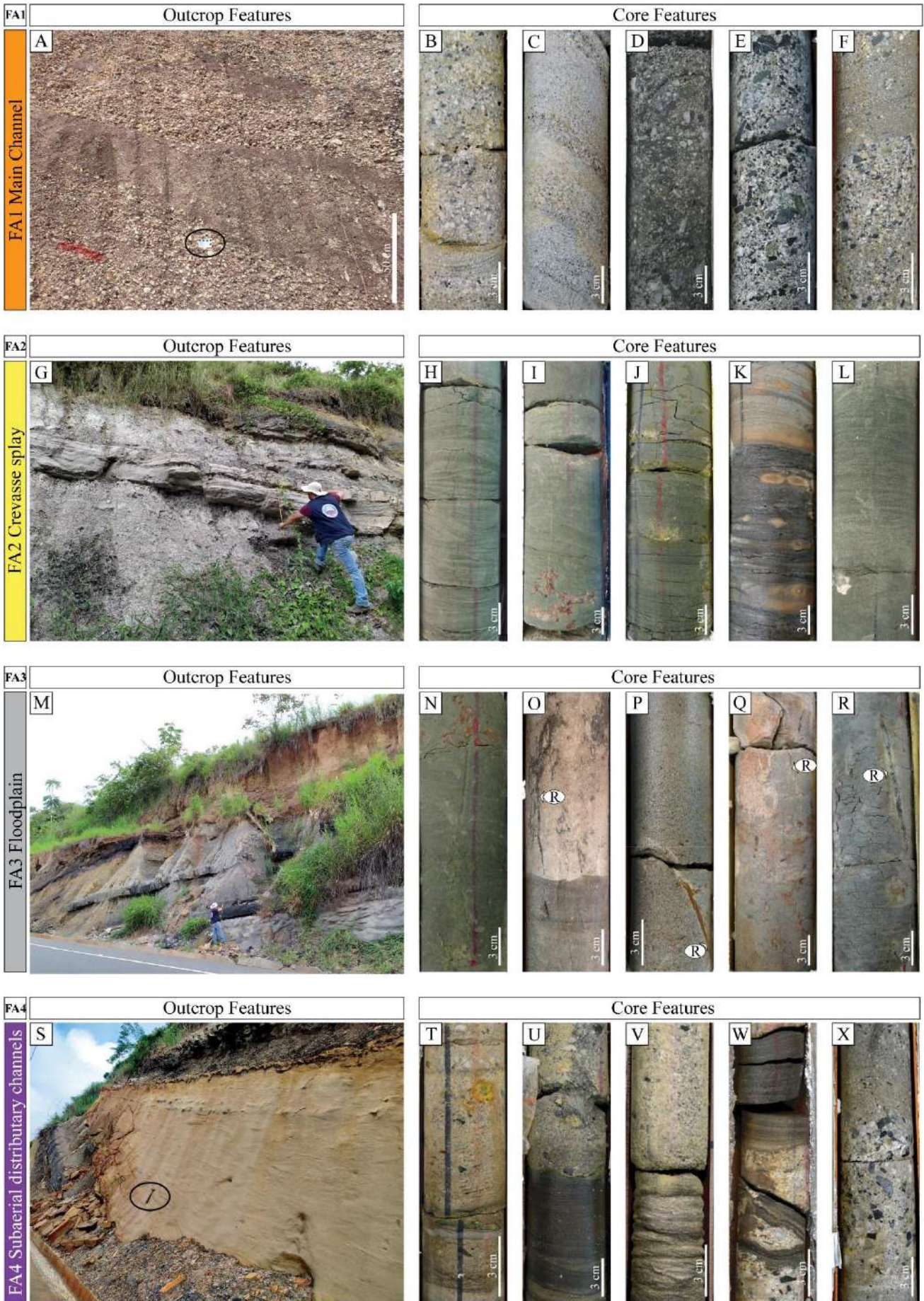


Fig. VII.8. FA1 Main channel. **A.** Interbedding between pebble size conglomerates and coarse- to medium-grained sandstones with planar cross-bedding. Some laminae of pebbles with trough cross-bedding in sandstone beds. **B.** Massive granule size conglomerate. **C.** Planar cross-lamination in coarse-grained sandstone. **D.** Massive granule size conglomerate with high organic matter. **E.** Pebble size clast-supported conglomerate with planar cross-lamination. **F.** Interbedding between granule size conglomerates and medium-grained sandstones with planar cross-bedding. **FA2 Crevasse splay.** **G.** Lenticular-shaped bed of medium- to fine-grained sandstone embedded in massive mudrocks of FA3. **H.** Fine-grained sandstones with trough- and planar-cross lamination. **I.** Fine-grained sandstone with planar cross-lamination overlying mudrocks with ferruginous nodules (associated with paleosols) of FA3. **J.** Fine-grained sandstones with horizontal lamination overlain by massive mudrocks. **K.** Mudrock rich in organic matter overlain by fine-grained sandstone with planar cross-lamination. **L.** Fine-grained sandstones with planar and trough cross-lamination with root structures. **FA3 Floodplain.** **M.** Tabular-shaped beds of mudrocks interbedded with lenticular-shaped bodies of FA2. **N.** Massive mudrock with root structures and ferruginous nodules. **O.** Massive mudrock overlain by fine-grained sandstones with root structures. **P.** Structureless fine-grained sandstone with small ferruginous nodules and root structures filled with iron nodules. **Q.** Massive mudrock with root structures and mottling possibly associated with paleosols. **R.** Massive mudrock with carbonized root structure. **FA4 Subaerial distributary channel.** **S.** Lenticular-shaped bed of fine to medium-grained sandstone with erosive base, planar and trough cross-bedding. **T.** Granule conglomeratic sandstone with organic debris and planar cross-lamination. **U.** Massive mudrock overlain by massive medium-grained sandstone with erosive base. **V.** Fine-grained sandstone with planar cross-lamination overlain by massive medium to coarse-grained sandstone. **W.** Mudrock and granule-size conglomerate interbedding. **X.** Structureless granule to medium-size pebble conglomerate overlies by fine- to medium-grained sandstone with planar cross-lamination.

VII.5.5. FA5 – Water-logged interdistributary areas

Description. FA5 comprises tabular- and lenticular-shaped bodies of 2-3m thick beds, occasionally interrupted by erosional surfaces from FA4, FA6, and FA7 (Fig. VII.9A-F). It consists of organic-rich, structureless black mudrocks (Fig. VII.9A-F), together with horizontal laminated mudrocks interbedded with lenticular-shaped beds of fine-grained sandstones that sometimes show asymmetrical ripple cross-lamination. Syneresis cracks and siderite nodules are commonly observed (Fig. VII.9A-F). Variegated mudstones exhibit slickensides. Medium to thick beds of horizontal laminated coal seams and structureless coal —sometimes containing rhizoliths— are also common in FA5 (Fig. VII.9A-F). In addition, alternations of laminae of fine-grained sandstones and mudrocks are recorded. Notably, structureless bioclastic tabular beds up to 10 m thick occur above FA5. Allochemical components, represented by fossils (including bivalves, gastropods) are often randomly distributed in the beds, accompanied in lesser proportions by muddy intraclasts. The boundary with the underlying bed (either coal or mudrocks) is irregular. Towards the top, transitional variations to FA9 or FA12 (more distal environments) are evident. The most noteworthy occurrences of FA5 are documented in outcrops 4, 6, and in the ANH-SSJ-La Estrella-1X and ANH-SSJ-Nueva Esperanza-1X well-cores.

Ichnology and paleontology. This FA exhibits generalized low bioturbation indexes (BI 0-2) associated with *Taenidium* and rhizoliths. *Taenidium* show diameters ranging from ~1 to 3 cm and widths of ~5-6 cm; they lack lining or present very thin linings, are unbranched, and feature widely spaced meniscate fills. Rhizoliths are irregularly distributed, unbranched, and ~1 mm wide. Occasionally a high bioturbation index (BI 4-5) is observed in some upper beds (bioclastic deposits) at the top of FA5, mainly by *Thalassinoides* (Fig. VII.9D-F), showing a dominant horizontal framework with vertical axes, circular to elliptical in cross-sections, with an average diameter of ~3-4 cm, and passive filling. Local occurrences of bivalve and gastropod fragments

(*Aclis* spp. and *Turritella* spp.), fragments of scaphopod, indeterminate shells, as well as abundant pollen, spores, fungal remains, and mangrove pollen.

Interpretation. The abundance of black mudrocks, siderite nodules, syneresis cracks, low bioturbation indexes, and abundant fungal remains would indicate deposition in low-energy environments under brackish-water conditions (e.g., Rossi and Steel, 2016). In addition, the presence of coal seams containing rhizoliths (BI 0-2) points to the formation of peat bogs in swampy areas (Retallack, 2001). Consequently, persistent water-logged conditions would have facilitated both the accumulation and preservation of organic matter, which underwent reducing conditions, as evidenced by blackish and dark-gray colors (Everett, 1983; Retallack, 2001). Lenticular bedding, asymmetric ripple sandstones containing marine bivalve and gastropod fragments, and *Taenidium*, suggest bidirectional flow in interdistributary bays (e.g., Rossi and Steel, 2016). FA5's close vertical alignment with the subaerial distributary channel deposits of FA4 reveals a connection between them in the lower delta plain. Furthermore, the bioclastic deposits with erosive bases overlying FA5 suggest rapid transgressive pulses or storms that transitioned to deeper-water deposits during the abandonment of the delta-lobe, drowning the river-dominated delta plain (Savrda et al., 1993; Cattaneo and Steel, 2003; Schultz et al., 2020). Thus, *Thalassinoides* could be attributed to bioturbation in firmgrounds (*Glossifungites* ichnofacies) associated with ravinement surfaces (Pemberton et al., 1992, 2004; MacEachern et al., 2007a, 2007b).

VII.5.6. FA6 – Terminal distributary channels

Description. FA6 consists of amalgamated thick beds with lenticular-shaped and erosive bases, and it is characterized by matrix-supported medium-size pebble conglomerates, fine-size pebbly sandstones, and coarse- to medium-grained sandstone beds (Fig. VII.9G-L) up to 3-4 m thick, structureless or with asymmetric ripple lamination and dune cross-bedding (Fig. VII.9G-L). The conglomerates contain clasts that are angular to very angular in shape, with low sphericity, embedded in a matrix of medium- to coarse-grained sand. These lenticular bodies often display normal and inverse grading, and occasionally horizontal lamination accentuated by organic debris (Fig. VII.9G-L), forming fining-upward trends or bigradational trends. Some sandstones exhibit load casts and flame structures with erosional bases, sporadically containing abundant organic debris. Generally, FA6 is observed below FA7 (fluvial-dominated mouth bar) or FA10 (tidally influenced mouth bar). The most notable occurrences of FA6 are documented in outcrops 9, 11, and in the ANH-SSJ-La Estrella-1X and ANH-SSJ-Nueva Esperanza-1X well-cores.

Ichnology and paleontology. Bioturbation in FA6 shows considerable variability, typically absent at the base and gradually increasing towards the top (BI 1-3; Fig. VII.9G). The exclusive presence of *Macaronichnus*, *Ophiomorpha*, *Skolithos*, *Thalassinoides* or *Taenidium* is noted. *Ophiomorpha* is characterized by tunnels and shafts up to 2 cm in diameter, lined with black pellets along the burrow walls. *Skolithos* are predominantly located in the upper parts of sandy bodies, comprising subvertical, cylindrical, unbranched burrows up to 8 cm in length and 3-4 mm in diameter. *Taenidium* correspond to predominantly sub-vertical to oblique meniscate cylindrical burrows, ~1 cm in diameter. *Thalassinoides* present circular and elliptical sections ~3-4 cm in diameter.

Interpretation. The coarse-grained deposits, characterized by erosive bases, large-scale current structures, bigradational or fining-upward trends, and high organic content, indicate channel deposition (Miall, 1996;

Shiers et al., 2018). Horizontal laminations in high-organic gravelly beds are associated with high-velocity unidirectional currents, likely resulting from bedload under hyperpycnal flow conditions during periods of torrential rainfall (Hein and Walker, 1977; Miall, 1996; Zavala, 2020). In turn, the bigradational trend, and poorly sorted and angular clasts sometimes covered by soft deformation, may be linked to short-lived gravity flows (Talling et al., 2012; Zavala, 2020). The exclusive presence of *Ophiomorpha* indicates marine influence on the system, and the presence of *Skolithos* is evidence of suspension feeding behavior due to multiple subaqueous distributary channels reaching the shoreline (Bhattacharya, 2006; Olariu and Bhattacharya, 2006; MacEachern and Bann, 2022). However, the angular to very angular clasts are characteristic of poorly transported high-gradient settings with a nearby source area (Olariu and Bhattacharya, 2006; Zavala, 2020). These channels likely provided hypopycnal conditions during normal river flow or hyperpycnal conditions during extraordinary discharges (Bhattacharya and MacEachern, 2009; Buatois et al., 2011; Zavala et al., 2024). An increase in the BI and diversity vertically may indicate a shift from fluvial-dominated to marine-influenced settings linked to the channel abandonment. Physic-chemically stressed conditions inhibiting colonization by tracemakers suggest brackish water and high energy conditions (MacEachern et al., 2005; Tonkin, 2012; MacEachern and Bann, 2022).

The complete succession of facies associations from the mouth bars (FA7 or FA10) provides interpretations of terminal distributary channels. Record of *Macaronichnus* assemblage may suggest specifically beach-like conditions in point bars (MacEachern et al., 2007; Nara and Seike, 2019).

VII.5.7. FA7 – Fluvial-dominated proximal delta-front (mouth bars)

Description. FA7 is represented by amalgamated thick beds of lenticular-shape, forming successions between 4-5 m thick and a few meters wide (Fig. VII.9M-R). These beds consist of medium- to coarse-grained structureless sandstones (Fig. VII.9 M-R) and fine-grained pebbly sandstones with horizontal lamination. They show coarsening- to fining-upward trends, from thick beds of coarse-grained sandstones to fine-size pebble conglomerates, and then coarse-grained sandstones. Meter-scale 3D cross-bedding is observed. Plant remains including carbonaceous detritus, often highlight the lamination (Fig. VII.9 M-R). In some cases, the conglomerates transition towards the top into medium- and fine-grained sandstones featuring soft-sediment deformation structures. FA7 overlies FA8 and is overlain either by the coarser-grained channelized deposits of FA6 or by mudrocks of FA5. The most prominent examples of this facies association are recorded in outcrops 4, 6, 8, and 9, along with the ANH-SSJ-La Estrella-1X and ANH-SSJ-Nueva Esperanza-1X well-cores.

Ichnology and paleontology. Trace fossils are represented by low abundant (BI 1-2) *Ophiomorpha* (Fig. VII.9K-L), characterized by tunnels and shafts measuring up to 5 cm in diameter, accentuated by black pellets lining the burrow walls and occasionally with a carbonaceous halo. Moreover, *Skolithos* and *Thalassinoides* are recognized. Abundant pollen and spores were found in FA7.

Interpretation. These deposits represent traction and suspension phases during flow deceleration in a lower-flow regime (Mulder et al., 2003; Slater et al., 2017; Zavala et al., 2024). Horizontal lamination and soft-sediment deformation structures indicate rapid deposition and dewatering through loading, typical of mouth bars in a delta-front (van Yperen et al., 2020; Cole et al., 2021). Therefore, FA7 records deposition and flow

widening as mouth bar deposits formed in a fluvial-dominated proximal delta-front (Enge et al., 2010; Olariu et al., 2010; Kurcinka et al., 2018; Moyano-Paz et al., 2020). The transition to FA6 could occur with increased water flow and the distribution of river discharge among several smaller channels, forming a multi-channel delta where scarce and sparsely distributed *Ophiomorpha*, *Skolithos* and *Thalassinoides* indicate environmental conditions favoring deposit-feeders linked to unfavorable high-energy conditions (e.g., Ponce et al., 2023). In such cases, the sedimentary succession may shift from typical mouth bar deposits, such as gravels and coarse sands, to finer and laminated deposits associated with terminal distributary channels.

VII.5.8. FA8 – Fluvial-dominated distal delta-front

Description. FA8 is characterized by medium to thick beds of lenticular-shaped bodies (Fig. VII.9S-X) composed of muddy sandstones and fine-grained sandstones, with planar cross-bedding and asymmetric ripple cross-lamination highlighted by plant remains and carbonaceous detritus (Fig. VII.9S-X). Amalgamated successions can reach thicknesses of ~4 m. Coarsening-upward trends from muddy sandstones to very fine to fine-grained sandstones, along with evidence of soft sediment deformation, are observed (Fig. VII.9S-X). However, some normal grading structures can be also identified. Some beds display incipient planar cross-bedding, and reactivation surfaces (Fig. VII.9S-X). FA8 shows a gradual transition to FA7. The notable occurrences of FA8 are documented in outcrops 4 and 6, and within the ANH-SSJ-La Estrella-1X and ANH-SSJ-Nueva Esperanza-1X well-cores.

Ichnology and paleontology. This FA exhibits low to moderate bioturbation indexes (BI 0–3), attributed to *Ophiomorpha*, *Skolithos*, *Taenidium*, and *Thalassinoides*. *Ophiomorpha* is characterized by 3D systems with vertical shafts and horizontal tunnels measuring up to 2 cm in diameter. *Skolithos* occurs as vertical to subvertical straight-lined burrows, oriented perpendicular to the horizontal lamination, with an average thickness of ~0.2 cm and lengths ranging from ~4 cm to ~10 cm. *Taenidium* occurs as oblique cylindrical burrows with diameters of ~1 cm and lengths ranging from 2 to 3 cm. *Thalassinoides* comprises burrows having horizontal frameworks with vertical axes, with circular and elliptical sections ~2-3 cm in diameter. Sporadic occurrences of calcareous microfossils and morichal palm pollen exist as well as plant remains.

Interpretation. Coarsening upward trends in the sandstones indicate a progradational and transitional evolution of the system, with velocity fluctuations within persistent turbulent flows (e.g., Gamero et al., 2011; Zavala et al., 2024). Combined with the low diversity and scarcity of trace fossil suites and the paucity of marine calcareous microfossils, the observed sedimentary features suggest proximal environments within the deltaic system with high-water turbidity or brackish conditions (Moslow and Pemberton, 1988; Gingras et al., 1998; MacEachern and Bann, 2022). Episodic sedimentation of turbidity currents is inferred in a fluvial-dominated distal delta-front environment associated with occasional normal grading. This could be triggered by collapses of the FA7 mouth bar deposits or by high density hyperpycnal flows, where reactivation surfaces and planar cross-bedding could be associated with rapid energy decay and tidal influence (Mulder and Syvitski, 1995; Rossi and Steel, 2016; Kurcinka et al., 2018; Ponce et al., 2023).

VII.5.9. FA9 – Fluvial-dominated prodelta

Description. FA9 is made up of tabular bodies of thick beds, resulting in successions of mudrocks and sandy mudrocks up to 20 m thick, except in well-core ANH-Nueva Esperanza-1X (up to 45 m). These deposits exhibit horizontal lamination marked by organic debris (Fig. VII.10A-F), or structureless and asymmetric ripple cross-lamination forming lenticular bedding (Fig. VII.10A-F). Occasionally, very fine-grained sandy rocks with normal grading to mudrocks are observed (Fig. VII.10A-F). These deposits transition to interbedding of thick beds of mudrocks and very fine-to fine-grained sandstones featuring horizontal lamination, structureless, or with asymmetrical ripple cross-lamination; often accompanied by syneresis cracks, ferruginous and siderite nodules, and organic debris (Fig. VII.10A-F). Bioclastic deposits atop FA5 represent transitions to FA9, and FA9 gradually transitions to FA8 (fluvial-dominated distal delta-front). Notable occurrences of FA9 are documented in outcrops 4 and 6, and within the ANH-SSJ-La Estrella-1X and ANH-SSJ-Nueva Esperanza-1X well-cores.

Ichnology and paleontology. FA9 is characterized by a variable bioturbation index (BI 0-5) and the presence of *Planolites* and locally exclusive and abundant *Phycosiphon* (BI 4-5; Fig. VII.10D). *Planolites* display circular sections of ~2 cm in diameter. *Phycosiphon* is found in patches with varying lobe orientations, resulting in a random arrangement characterized by narrow U-shaped burrows, ranging in length from ~0.1 cm to ~0.5 cm, rarely reaching 1 cm. Upward, there is a gradual increase in diversity, associated with *Teichichnus* and *Thalassinoides*. *Teichichnus* (BI 0-2) shows typical subvertical spreite structures, ~1 cm wide and ~3 cm long. *Thalassinoides* is circular to elliptical in cross-section, unlined, with an average diameter of ~1 cm. Calcareous nannofossils, foraminifers, and abundant terrestrial palynomorphs were recovered.

Interpretation. Dominant fine-grained lithologies may be associated with deposition by low-energy suspension fallout in environments with low oxygen or limited benthic food availability, as indicated by the trace fossil record (e.g., MacEachern and Bann, 2022). This sedimentation could occur during fair-weather conditions in offshore environments. However, the occurrence of sandstones with asymmetrical ripples and high input in continental palynomorphs could be attributed to seasonal muddy hyperpycnal flows that originate at the mouth of the river during floods or torrential rains, transporting clastic sediments further into the prodelta or offshore areas (e.g., Lamb and Mohrig, 2009; Zavala et al., 2016; Zavala, 2020; Chalabe et al., 2022; Irastorza et al., 2024). Monospecific occurrence of *Phycosiphon* (BI 4–5) may indicate increases in benthic food and oxygen by hyperpycnal flows in full-marine environments (e.g., Rodríguez-Tovar et al., 2014; Celis et al., 2018). Intervals showing a low diversity of trace fossils, high content of terrestrial palynomorphs, syneresis cracks, and siderite nodules suggest salinity fluctuations associated with freshwater fluvial influence (MacEachern et al., 2005; Tonkin, 2012; Wilson and Schieber, 2014). Bioclastic deposits on top of FA5 transitioning to FA9 could reveal transgressive phases allowing for the establishment of prodelta systems over water-logged interdistributary areas.

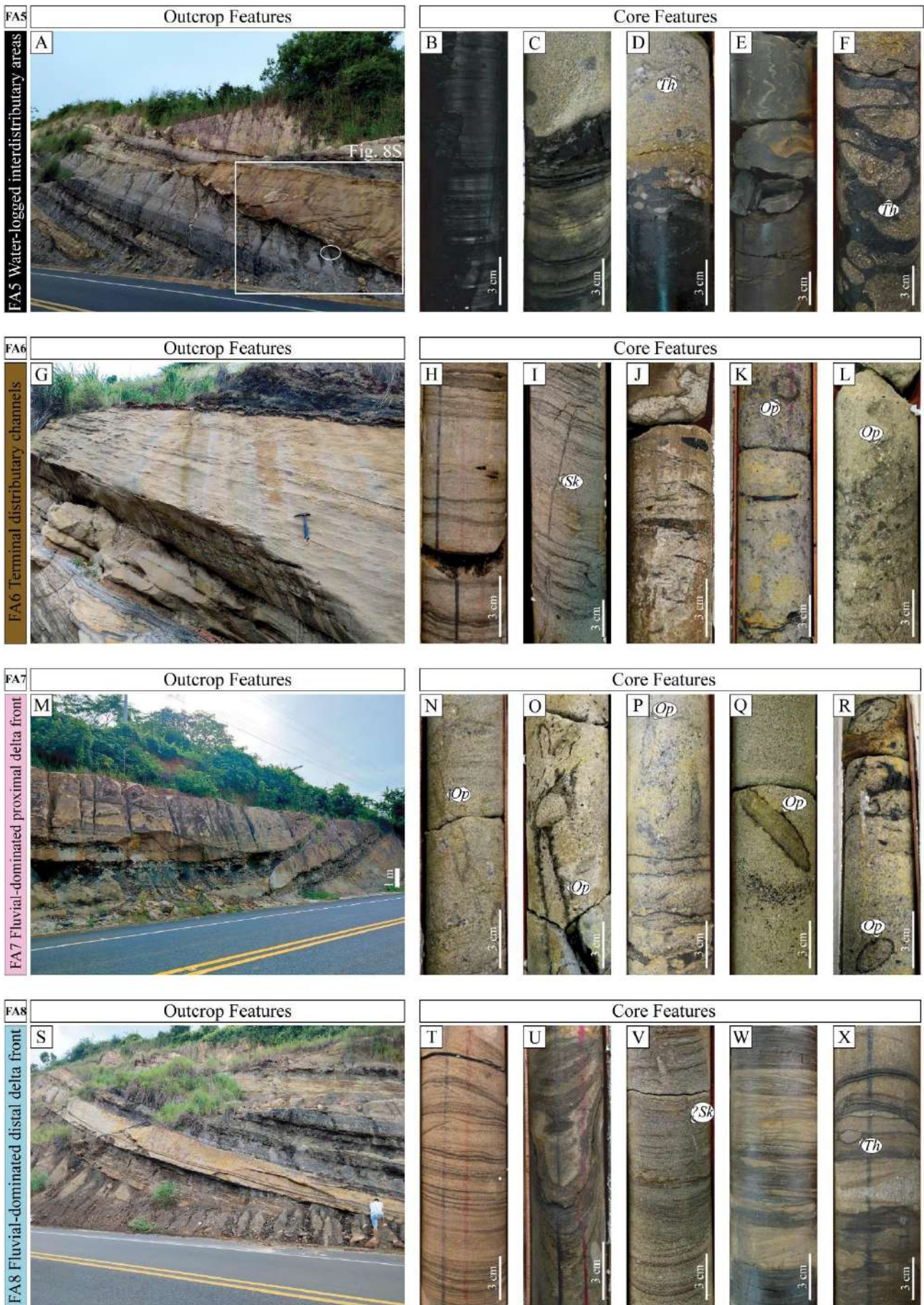


Fig. VII.9. FA5 Water-logged interdistributary areas. **A.** Tabular-shaped beds of mudrocks and carbonized mudrocks overlain by lenticular-shaped bed of fine to medium-grained sandstone with erosive base related to FA4. **B.** Structureless coal. **C.** Carbonized mudrock overlain by fine- to medium-grained sandstone. **D.** Coal bed overlain by medium-grained sandstone with granule-size clasts in *Thalassinoides* (*Th*). **E.** Muddy sandstone with syneresis cracks. **F.** Coal bed and *Thalassinoides* (*Th*) structures refilled with bioclastic deposits associated with *Glossifungites* ichnofacies. **FA6 Terminal distributary channels.** **G.** Lenticular-shaped bed of medium- to fine-grained sandstone having an irregular base and planar to trough cross-bedding. **H-I.** Fine-grained sandstones with horizontal lamination highlighted by organic debris and bioturbated by *Skolithos* (*Sk*). **J.** Medium- to coarse-grained sandstone with organic debris and some granule-size clasts. **K.** Granule-size conglomerate to conglomeratic sandstone with organic debris and *Ophiomorpha* (*Op*). **L.** Structureless granule-size conglomerate with *Ophiomorpha* (*Op*) refilled with granule-size and organic debris clasts. **FA7 Fluvial-dominated proximal delta front.** **M.** Channel with erosive base and boulder-size rip-up clasts, overlying *Ophiomorpha* dominated beds. Lenticular-like morphology corresponds to tectonic deformation and not to the morphology of the original channel. **N.** Medium- to coarse-grained sandstone with *Ophiomorpha* (*Op*). **O.** Fine-grained sandstone with *Ophiomorpha* (*Op*). **P.** Coarse-grained sandstone with *Ophiomorpha* (*Op*). **Q.** Medium-grained sandstone with concentration of black magnetic grains, and *Ophiomorpha* (*Op*). **R.** Medium- to coarse-grained sandstone with organic debris and *Ophiomorpha* (*Op*) with carbonaceous halo. **FA8 Fluvial-dominated distal delta-front.** **S.** Wide lenticular-shaped beds of fine- to medium-grained sandstone with planar and trough cross-bedding highlighted by organic debris. Toward the top, massive mudrocks, carbonaceous mudrocks and coal beds associated with FA5. **T.** Fine- to medium-grained sandstone with organic debris highlighting planar lamination. Possible reactivation surfaces toward the top. **U.** Soft-sediment deformation structure in fine-grained to muddy sandstone. **V.** Fine- to medium-grained sandstone with planar lamination highlighted by organic debris and possible *Skolithos* (*Sk*). **W.** Interbedding of mudrocks, carbonaceous mudrocks and fine-grained sandstone with organic debris highlighting lamination. Some intervals present planar-cross lamination. **X.** Fine-grained sandstone with organic debris and carbonaceous mudrocks with *Thalassinoides* (*Th*).

VII.5.10. FA10 – Tidal and fluvial influenced proximal delta-front

Description. FA10 is characterized by lenticular-shaped bodies up to 10 m thick and tens of meters in lateral continuity. They consist of fine- to coarse-grained structureless sandstones with a coarsening-upward trend (Fig. VII.12G-L) or with horizontal lamination, interbedded with planar and trough cross-bedded sandstones, in occasions with low angle bedding (Fig. VII.10G-L). Organic debris is scarce, although medium to thick beds of sandstones with ripple cross-lamination highlighted by organic remains are present at the top. Asymmetrical ripple cross-lamination and dune cross-bedding with mud drapes are also common. Occasionally increased plant remains (i.e., leaves) are found. In addition, subordinate, medium beds of fine- to medium-grained sandstones with wavy bedding are recorded. FA10 overlies FA11 and is truncated either by channelized incisions of FA6 or by FA7 deposits across flood surfaces. The most notable occurrences of FA10 are documented in outcrops 4, 5, 6, 9, and in the ANH-SSJ-La Estrella-1X and ANH-SSJ-Nueva Esperanza-1X well-cores.

Ichnology and paleontology. The sandbodies of FA10 are typically bioturbated (Fig. VII.10G-L), showing bioturbation indexes from low to moderate (BI 1-4) and containing an ichnoassemblage consisting of *Asterosoma*, *Conichnus*, *Cylindrichnus*, *Dactyloidites*, *Gyrolithes*, *Macaronichnus*, *Ophiomorpha*, *Skolithos*, and *Thalassinoides*. *Asterosoma* was observed in the well-cores, although its diagnostic features are uncertain. *Conichnus* is characterized by large conical sections measuring ~8 cm long and ~2 cm wide. *Cylindrichnus* exhibit arched-shaped with a passive fill and a concentric laminated lining, ranging from ~4 - ~6 cm in length, and ~1 cm in width. *Dactyloidites* can be identified by radial elements in cross-section with diameters of ~0.5

cm, appearing isolated or grouped. *Gyrolithes* are recognizable by parallel circles in cross-section. *Macaronichnus* show sand infill lighter than the embedded sediment, with a rim made up of black minerals, ranging from 0.1 cm to 0.4 cm in diameter and at least 2 cm long, observed occasionally as monospecific ichnoassemblage. *Ophiomorpha* show typical pellet lining and burrow diameters ranging from ~0.5 cm to ~3 cm, with longitudinal sections from ~3 cm to ~12 cm, in some cases exhibiting infill with rhythmic lamination (tubular tidalites) (Fig. VII.10H). *Skolithos* occurs as subvertical cylindrical tubes with lengths ranging from ~4 cm to 12 cm. *Thalassinoides* appear as elliptical cross-sections measuring ~3 cm in diameter. Occasional calcareous microfossils were found.

Interpretation. Alternation of beds with horizontal- and planar cross-bedding is interpreted to reflect fluctuations in river discharge, where the migration of three-dimensional dunes suggest non-oscillatory flow conditions (Charms, 1969; Southard and Boguchwal, 1990; Dumas et al., 2005). Heterolithic deposits with mud drapes and tubular tidalites, as well as moderate to high bioturbation indexes, suggest subordinate tidal influence (e.g., Rossi and Steel, 2016; Rossi et al., 2017a). Coarsening-upward trends suggest progradation, possibly from mouth bars, under high energy conditions; thus, FA10 is interpreted as mouth bar deposits, developed in a tidal-influenced proximal delta-front (e.g., Rossi and Steel, 2016; Rossi et al., 2017b; Kurcinka et al., 2018). Evidence for this interpretation includes the moderate bioturbation index (BI) and biogenic structures related to variable energetic and sedimentation rates conditions and tidal influence (e.g., tubular tidalites of *Ophiomorpha*) (Wetzel et al., 2014; Gingras, and Zonneveld, 2015). The scarcity of biogenic structures correlated with suspension feeding behaviors (i.e., *Skolithos*) further supports the interpretation of depositional settings having high turbidity (Moslow and Pemberton, 1988; Li et al., 2011; MacEachern and Bann, 2022). Furthermore, the monospecific record of *Macaronichnus* assemblage may suggest specifically beach-like conditions in tidal bars (MacEachern et al., 2007; Nara and Seike, 2019).

VII.5.11. FA11 – Tidal and fluvial influenced distal delta-front

Description. FA11 encompasses thick beds of muddy sandstones with coarsening-upward trends from mudrocks and sandy mudrocks, transitioning to fine-to medium-grained structureless sandstones or showing asymmetric ripple cross-lamination, reaching thicknesses of up to ~4.5 m (Fig. VII.10M-R). FA11 exhibits lateral continuity over tens of meters. Additionally, it is characterized by interbedded medium to thick beds of medium-grained sandstones with horizontal lamination, alongside fine- to medium-grained sandstones displaying planar cross-bedding, asymmetric ripple cross-lamination, or through cross-bedding. These features are found within couplets of muds on foresets, often amalgamated to thicknesses of up to 4-5 m, exhibiting internal erosion and reactivation surfaces (Fig. VII.10M-R). In one case, symmetric ripples and convolute lamination are recorded. FA11 shows transitional variation to FA10 (fluvial, and tidally influenced mouth bar) and may overlie FA12 and FA9 over flood surfaces. It is overlain by deposits of FA10 or incised by channelized deposits of FA6 and FA7. This facies association is most prominent in outcrops 4, 5, 6, and 9, and in the well-cores of ANH-SSJ-La Estrella-1X and ANH-SSJ-Nueva Esperanza-1X.

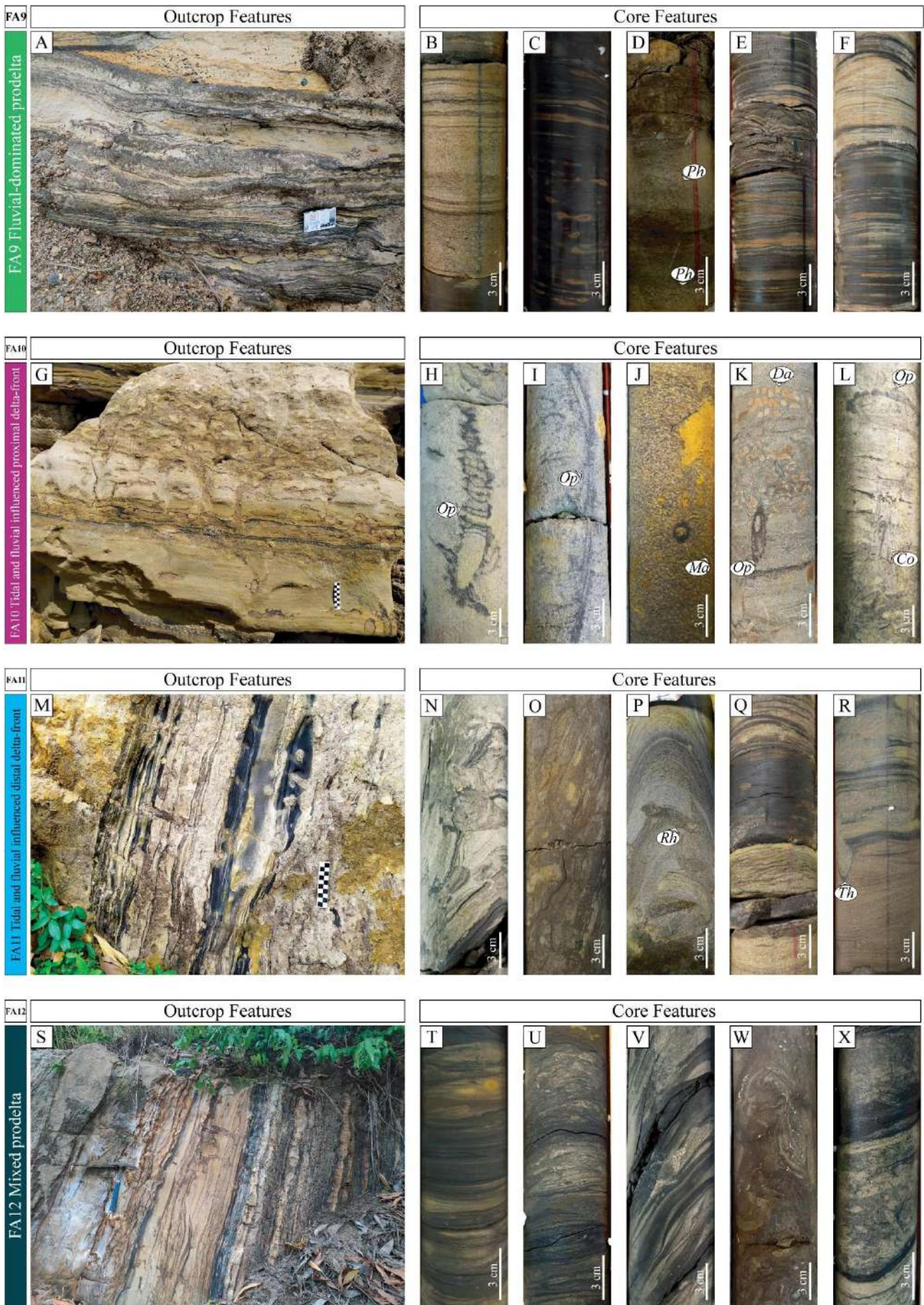


Fig. VII.10. FA9 Fluvial-dominated prodelta. **A.** Fine-grained sandstone and muddy sandstone with high content in organic debris highlighting planar lamination. **B.** Fine-grained sandstone with planar lamination highlighted by high content in organic debris. **C.** Horizontal laminated carbonaceous mudrock with ferruginous nodules and asymmetric ripple cross-lamination. **D.** Structureless mudrock and sandy mudrock beds dominated by *Phycosiphon* (*Ph*). **E.** Alternation of millimetric laminae of mudrocks and fine-grained sandstones with a deformed interval. **F.** Carbonaceous mudrock and mudrock showing planar lamination interbedded with fine-grained sandstone having planar-cross lamination and possible reactivation surfaces. **FA10 Tidal and fluvial influenced proximal delta-front.** **G.** Fine- to medium-grained sandstone with planar lamination at the base highlighted by organic debris and increased bioturbation toward the top. **H.** Fine-grained sandstone with tubular tidalite in *Ophiomorpha* (*Op*). **I.** Fine-grained sandstone highly bioturbated by *Ophiomorpha* (*Op*). **J.** Massive sandstone bed dominated by *Macaronichnus* (*Ma*). **K.** Fine- to medium-grained sandstone with organic debris highlighting planar lamination at the base and bioturbated by *Dactyloidites* (*Da*) and *Ophiomorpha* (*Op*). **L.** Fine-to medium-grained sandstone with planar lamination highlighted by organic debris and bioturbated by *Conichnus* (*Co*) and *Ophiomorpha* (*Op*). **FA11 Tidal and fluvial influenced distal delta-front.** **M.** Fine- to medium-grained sandstones with planar lamination, planar cross-lamination and beds of carbonaceous mudrocks bioturbated by *Ophiomorpha* and *Thalassinoides*. Increased bioturbation index toward the top. **N-O.** Fine-grained sandstone with high content in organic debris and high values in bioturbation index. **P.** Fine-grained sandstones with organic debris and bioturbated by *Rhizocorallium* (*Rh*). **Q.** Fine-grained sandstone with organic debris and carbonaceous mudrocks. **R.** Fine-grained sandstone with planar cross-lamination and possible reactivation surfaces, bioturbated by *Thalassinoides* (*Th*), overlain by medium-grained sandstone with high content in organic debris highlighting planar lamination. **FA12 Mixed prodelta.** **S.** Coarsening-upward succession from carbonaceous mudrocks and mudrocks with planar lamination (FA12) to fine- to medium-grained sandstones with planar lamination, planar and trough cross-lamination, and some mud drapes, bioturbated by *Ophiomorpha* and *Thalassinoides* (FA11 and FA10). Increasing bioturbation index from base to the top. **T.** Muddy sandstone and fine-grained sandstone with high content in organic debris highlighting planar lamination; interrupted by fine-grained bioturbated sandstone intervals with planar cross-bedding. **U.** Alternation of millimetric laminae of mudrocks and fine-grained sandstones with high bioturbation indexes. **V.** Fine-grained sandstone with planar and irregular lamination highlighted by carbonaceous mudrocks and organic debris. **W.** Bioturbated muddy sandstones with shell fragments. **X.** Fine-grained sandstone with high content in organic debris and high bioturbation indexes.

Technology and paleontology. FA11 has low to moderate bioturbation indexes (BI 0-4; Fig. VII.10M-R), and includes *Diplocraterion*, *Ophiomorpha*, *Planolites*, *Rhizocorallium*, *Teichichnus*, and *Thalassinoides*. In coarser deposits, a decrease in the bioturbation index is observed (BI 0-2; *Ophiomorpha*). *Diplocraterion* occurs as vertical U-shaped structures with spreiten ~3 cm in diameter and ~20 cm in length. *Ophiomorpha* appears as vertical and horizontal tunnels with branches, often lined with ovoid pellets, or sometimes showing infilling rhythmic laminations, and cross-sections ~2 cm in diameter and ~5 to ~10 cm in length. *Planolites* are characterized by straight cylindrical tunnels in horizontal bedding, from ~1 to ~2 cm in diameter. *Rhizocorallium* is recognized in vertical cross-section with tubes connected by spreiten, subparallel to the bedding, with the tubes separated by ~4 cm. *Teichichnus* occurs as a subvertical stack of subhorizontal spreiten with a diameter of ~1 cm and a length of ~4 cm. *Thalassinoides* is recognized only in cross-sections as subcircular structures with diameters of ~2 or ~3 cm. Some calcareous microfossils and dinoflagellates were recovered. Plant remains, including leaves and wood fragments, are common.

Interpretation. Interbedding between massive and asymmetric ripple laminations, along with heterolithic deposits featuring mud drapes, suggests periods of high current velocities interspersed with significant energy reductions, during which muddy sediments accumulated either through suspension due to clay flocculation or by bedload transport (e.g., Rossi et al., 2017a; MacEachern and Bann, 2022). Trough and planar cross-stratification highlighted by mud drapes foresets, along with reactivation surfaces, reflect rhythmic fluctuations

in flow strength and direction, often attributed to tidal influences at various scales (Longhitano et al., 2012; Rossi and Steel, 2016; MacEachern and Bann, 2022).

Current structures and a decrease in the diversity and abundance of trace fossils (BI 0-2; *Ophiomorpha*) in some intervals would represent continuous fluvial flooding events (e.g., Li, et al., 2011; Ponce et al., 2023), where biogenic structures reflect adaptations to colonize substrates under both high energy and high sedimentation rates. Heterolithic facies and mud drapes laminae, lamina-sets and intercalated beds, as well as increases in abundances and diversity (BI 1-4; *Diplocraterion*, *Ophiomorpha*, *Planolites*, *Rhizocorallium*, *Teichichnus*, *Thalassinoides*), together with the presence of dinoflagellates, foraminifera, and calcareous nanofossils, may indicate tidal influence in a mixed system with fluvial domain characteristic of the distal delta-front (MacEachern et al., 2005; Bhattacharya, 2006). Highly bioturbated beds indicate extensive reworking by burrowers during fair-weather conditions (e.g., Li et al., 2011). Symmetric ripples and convolute lamination could be indicative of the influence of occasional waves and storms (e.g., Bann et al., 2008).

VII.5.12. FA12 – Mixed prodelta

Description. FA12 is formed by thick beds, forming tabular bodies up to 5 m thick (Fig. VII.10S-X), with lateral continuity exceeding 20 m, resulting in aggradational successions reaching up to 15 m thick. These beds consist of structureless mudrocks interbedded with layers of mudrocks and fine-grained sandstones, occasionally showing asymmetric ripple cross-lamination (Fig. VII.10S-X). Additionally, horizontally laminated mudrocks alternate with medium to thick beds of structureless sandy mudrocks and fine-grained sandstones exhibiting horizontal lamination (Fig. VII.10S-X). FA12 shows a transitional gradation to FA11 (mixed distal delta-front). The bioclastic deposits on top of FA5 show a transition to FA12. This facies association is prominent in outcrops 4 and 6 and is also well represented in the ANH-SSJ-La Estrella-1X and ANH-SSJ-Nueva Esperanza-1X well-cores.

Ichnology and paleontology. The bioturbation index ranges from low to moderate (BI 1-4; Fig. VII.10S-X), and is characterized by the presence of *Chondrites*, *Planolites*, *Siphonichnus*, *Teichichnus*, and *Thalassinoides*. *Chondrites* appears as small root-like tunnels and shafts arranged in a dendritic pattern, typically with diameters less than ~1 cm. *Planolites* is observed as horizontal, simple structures with diameters of ~1 cm. *Siphonichnus* appears as vertical structures with concave backfilled meniscate shapes, measuring ~1 cm in diameter and ~10 cm in length. *Teichichnus* can be identified by its subvertical trend and spreiten, measuring ~2 cm in length. *Thalassinoides* occurs as cylindrical burrows ~1 cm in diameter and ~3 cm in length. These facies have a high abundance of dinoflagellates and foraminifers, and a moderate abundance of calcareous nanofossils. Fragments of bivalves, gastropods, and shell hash are also present. There are abundant plant remains, e.g. leaves, wood fragments and carbonaceous detritus.

Interpretation. FA12 represents alternating phases of low-energy deposition characterized by the suspension settling of fine-grained sediments during fair-weather conditions, interspersed with coarser-grained beds deposited during episodic events that mark large river floods (e.g., Bhattacharya, 2006, 2010; Ganni et al., 2007; Bhattacharya and MacEachern, 2009). Interbedded mudrocks and sandstones may indicate the presence of turbidity current deposits associated with unconfined lobes within the distal areas of the system with absence of suspension feeding behavior by increased water turbidity (hyperpycnites; Moslow and Pemberton, 1988;

Gingras et al., 1998; Zavala et al., 2011). The continuous progradation to shallower facies makes it difficult to interpret a uniquely tide- or wave-dominated environment (shoreface to offshore), suggesting a dynamic mixed prodeltaic system (e.g., Rossi and Steel, 2016; Rossi et al., 2017b; MacEachern and Bann, 2022). Flooding events are characterized by low bioturbation indexes, while a limited trace fossil diversity—often associated with detrital feeding behaviors (e.g., *Planolites*) in organic-rich mudrock beds—may indicate bottom oxygen fluctuations (MacEachern et al., 2005). Following flood events, sandy and heterolithic substrates with moderate bioturbation indexes were colonized by tracemakers reflecting stable and favorable sedimentary conditions. However, the presence of *Siphonichnus* may indicate vertical shifts in the sediment-water interface due to erosion and/or high sedimentation rates (Knaust, 2015).

Table VII.3. Dimensions and relative occurrence of the registered ichnogenus in the facies associations.

| Ichnogenus | FA1 | FA2 | FA3 | FA4 | FA5 | FA6 | FA7 | FA8 | FA9 | FA10 | FA11 | FA12 |
|-----------------------|---------------------|-----------------------|-------------------|--------------------------------------|---|--------------------------------------|---|---|-----------------------------------|--|--|--|
| | <u>Main channel</u> | <u>Crevasse splay</u> | <u>Floodplain</u> | <u>Suacrial distributary channel</u> | <u>Water-logged interdistributary areas</u> | <u>Terminal distributary channel</u> | <u>Fluvial-dominated proximal delta front</u> | <u>Fluvial-dominated distal delta front</u> | <u>Fluvial-dominated prodelta</u> | <u>Fluvial- and tide-influenced proximal delta front</u> | <u>Fluvial- and tide-influenced distal delta front</u> | <u>Fluvial- and tide-influenced prodelta</u> |
| <i>Asterosoma</i> | | | | | | | | | | /5cm | | |
| <i>Chondrites</i> | | | | | | | | | | | | 1cm/ |
| <i>Conichnus</i> | | | | | | | | | | 2cm/8cm | | |
| <i>Cylindrichnus</i> | | | | | | | | | | 1cm/4-6cm | | |
| <i>Dactyloidites</i> | | | | | | | | | | 0.5cm/ | | |
| <i>Diplocraterion</i> | | | | | | | | | | | 3cm/20cm | |
| <i>Gyrolithes</i> | | | | | | | | | | 2cm/ | | |
| <i>Macaronichnus</i> | | | | | | 0.1-0.4cm/2cm | | | | 0.1-0.4cm/2cm | | |
| <i>Ophiomorpha</i> | | | | | | 2cm/4cm | 3cm/5cm | 2cm/5cm | | 0.5-3cm/3-12cm | 2cm/5-10cm | |
| <i>Phycosiphon</i> | | | | | | | | | 0.1-0.5cm/ | | | |
| <i>Planolites</i> | | | | | | | | | 2cm/ | | 1-2cm/ | 1cm/ |
| <i>Rhizocorallium</i> | | | | | | | | | | | 4cm/ | |
| <i>Siphonichnus</i> | | | | | | | | | | | | 1cm/10cm |
| <i>Skolithos</i> | | | | | | 3mm/8cm | | 0.2cm/4-10cm | | 1cm/4-12cm | | |
| <i>Taenidium</i> | | | | | 5-6cm/1-3cm | 1cm/3cm | | 1cm/2-3cm | | | | |
| <i>Teichichnus</i> | | | | | | | | | 1cm/3cm | | 1cm/4cm | 2cm/2cm |
| <i>Thalassinoides</i> | | | | | 3-4cm/5cm | 2-3cm/ | | 2-3cm/ | 1cm/3cm | 3cm/ | 2-3cm | 1cm/3cm |
| Root structures | | | | | 1mm/5cm | | | | | | | |

Dimensions and occurrence

| | | | |
|--------------|--------------|--------------|--------|
| width/length | width/length | width/length | |
| Abundant | Medium | Rare | Absent |

VII.6. Evolution of depositional systems

VII.6.1. Upper Eocene – Lower Oligocene system

Continental. Spanning from the late Eocene to early Oligocene, the depositional system is represented by continental and transitional or marginal deposits. Coarse-grained facies to the base (ANH-La Estrella-1X and ANH-Nueva Esperanza-1X well-cores, and outcrops 1 and 10; Fig. VII.11A) from the main channel (FA1; Fig. VII.11A), subaerial distributary channel (FA4) and terminal distributary channel (FA6), indicate an aggradational sedimentary trend. Within this context, continental systems are associated with hyperpycnal and hyperconcentrated flows (Fig. VII.11B), occasionally interrupted by fine-grained episodic sedimentation linked to floodplains (FA3) (Fig. VII.11C) (e.g., Fielding et al., 2018). Despite the variable facies record, the paucity of outcrops impedes discrimination of the fluvial system type. The absence of typical fluvial successions associated with braided or meandering rivers, interbedded with hyperconcentrated and hyperpycnal flows, prevents their characterization. Moreover, the presence of a small floodplain successions is distinctive, depending on the context. Braiding and meandering are furthermore linked to processes that can occur simultaneously in the same river, meaning some rivers can be described using both terms (Bridge, 2006; Miall, 2014). Therefore, coarse-grained flows could potentially be triggered by different fluvial styles. While these high-energy conditions may be conducive to short, high-gradient river systems, the apparent seasonality of floodplain-breached successions points to the likely influence of torrential tropical rainfall alternating with dry periods (e.g., Fielding et al., 2009). The intricate internal lithological variations into the channel bodies can create highly heterogeneous reservoirs. Without careful consideration, many of these bodies might be misidentified as floodplain deposits based solely on subsurface well core information, potentially leading to an underestimation of their reservoir potential (e.g., Fielding et al., 2012; Yeste et al., 2020).

Transitional. Along the coastline, as the flows enter the sea, the successions are characterized by diluted hyperconcentrated deposits and mouth-bar facies dominated by hyperpycnal flows, resulting in the transitional or marginal settings (Fig. VII.11D- to G). Initially, in a context of unfavorable environmental conditions for macrobenthic tracemakers communities, hence an absence of trace fossils, associated with excessive background energy, certain environmental variations occurred along with an increase in the influence of waves or tides, determining posteriorly the reworking of the mouth bars over a considerable period of time, leading to more favorable conditions, and then the record of macrobenthic activity (*Ophiomorpha*) by the end of the earliest Oligocene (e.g., Gani et al., 2007; Gingras and MacEachern, 2012; Eide et al., 2016; van Yperen et al., 2020).

The aggradational trend mirrors that of the continental systems, indicating amalgamated mouth bars with high-energy deposition, most likely within a coarse-grained delta (e.g., Olariu and Bhattacharya, 2006; Enge et al., 2010; van Yperen et al., 2020; Cole et al., 2021; Longhitano et al., 2021) (Fig. VII.11H). Low proportions of lowland forest pollen could be associated with the absence of a lower delta plain. This suggests that the high gradients inhibit the development of meandering systems and therefore without rapid avulsions or lateral channel displacements, favoring instead braided river systems that become coarse-grained deltas as they reach the coastline; they are represented elsewhere in the basin by the lateral continuation of hyperconcentrated flows at least up to the slope break (Celis et al., 2024). As the energy of gravity flows decreases, however, a

significant degree of tidal reworking can be interpreted. In such a scenario, the main channel continues its fluvial-dominated activity, but adjacent channels during avulsion episodes may be controlled by tidal systems refilling abandoned distributary channels (e.g., Johnson and Dashtgard, 2014; Dalrymple et al., 2015).

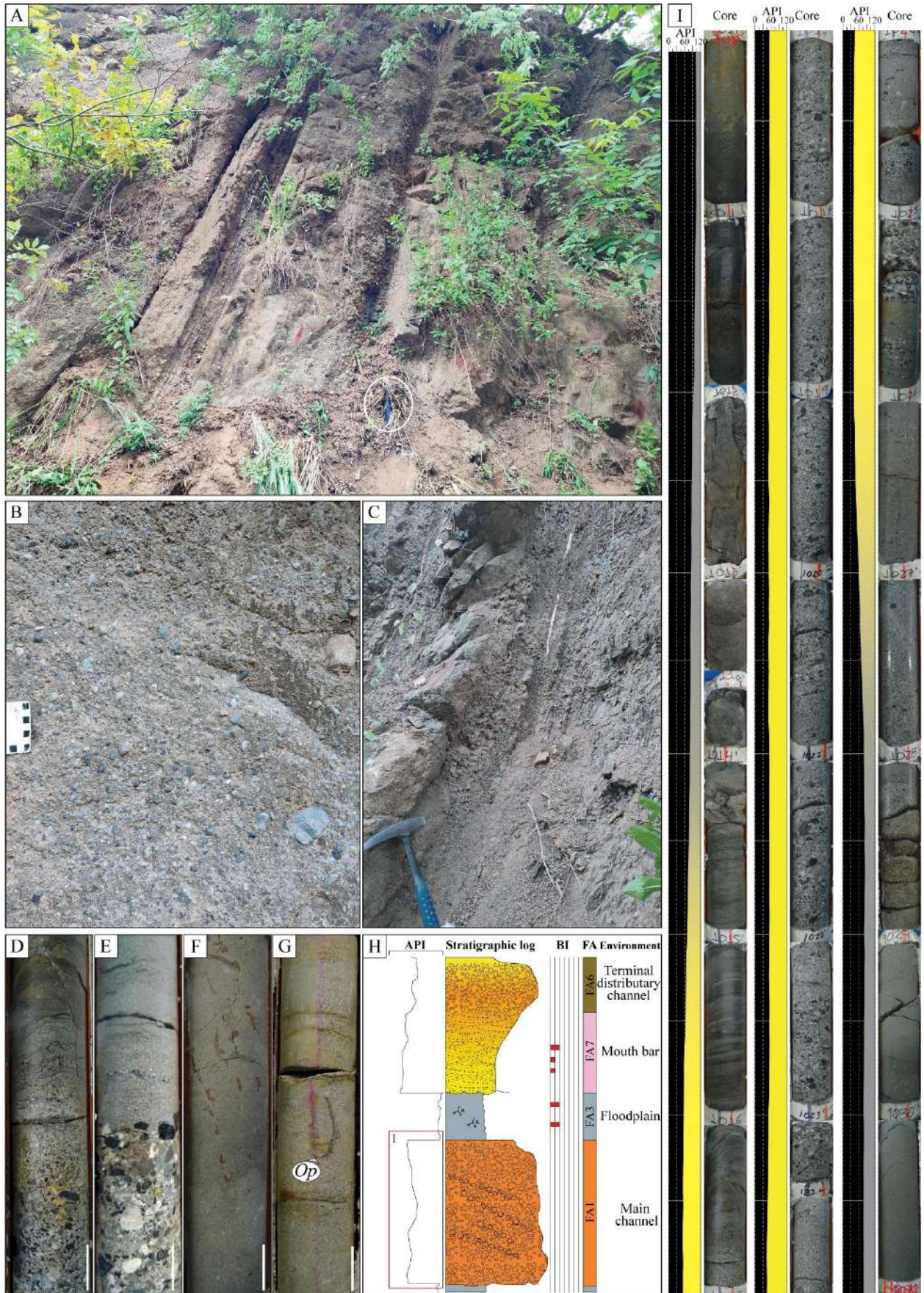


Fig. VII.11. middle to late eocene continental and transitional deposits. **a.** irregular surface to the base (to the right of the photo) and lenticular shaped bodies of channel conglomerates overlain by floodplain mudrocks. **b.** details of massive conglomerates with pebbles and cobbles clasts. **c.** detail of mudrocks associated with floodplains. **d.** granule-size conglomerate and transition from coarse to medium-grained sandstones with organic debris associated with hyperpycnal flows. **e.** pebble-sized conglomerates from hyperconcentrated flows overlain by medium-grained sandstones with organic debris. **f.** root structures in floodplain mudrocks. **g.** medium-grained sandstone with planar horizontal lamination and *ophiomorpha* (*op*). **h.** typical idealized succession from middle to late eocene deposits with hyperconcentrated to hyperpycnal mouth bars, and transitions or sharp contacts to floodplains and/or occasional reworking by tides. **i.** example of interbedding between floodplain and fluvial hyperconcentrated succession from anh-la estrella-1x well-core and gamma ray. note: a.p.i – american petroleum institute; bi – bioturbation index; fa – facies association. scale: each subdivision corresponds to 1 ft.

VII.6.2. Lower Oligocene to Lower Miocene system

During the earliest Oligocene, there was a significant decrease in hyperconcentrated flows from continental areas and a reduction in amalgamated successions of coarse-grained mouth bars along the coast. This change was driven by a sudden marine transgression, which covered the previous facies, and extended even into continental areas (e.g., ANH-La Estrella-1X); transgressive lags appeared to inundate the entire fluvio-dominated system. Yet their duration must have been relatively short, and fluvial-continental systems subsequently resumed progradation over them.

Continental. The evidence for FA1, FA2, FA3, arranged vertically, from the ANH-San Antonio-1X well-core and outcrops 1, 2, and 3, suggests the establishment of a meandering fluvial system in continental areas (Fig. VII.12A). This system is characterized by successions of channels (Fig. VII.12B through D), crevasse splays, and floodplains (Fig. VII.12E-F) showing distinct transitional increases in the gamma-ray record (well-core and gamma ray record in Fig. VII.12I). The main channel can be registered in outcrops 1 and 2, with all the dominant characteristics of point bars along with some areas of crevasse splays and floodplains, even containing coal beds. The development of fining- and thinning-upward successions is characteristic of meander channel/bar deposits, where recorded successions of 7-8 m in thickness correspond to the depth of the channel at maximum discharge (e.g., Ghinassi et al., 2018; Swan et al., 2018). In addition, successions of abandoned channels can be observed in outcrops 1 and 2. This occurs when part of the flow begins to pass through one of the depressions located between the meanders and gradually migrates to a new position, causing an eventual decrease in flow in the old main channel, which is progressively abandoned until it becomes inactive (Burns et al., 2017; Yeste et al., 2020). Such dynamics hinder the preservation of crevasse splay deposits proximal to the main channel, as these areas are prone to erosion from channel migration —cannibalization— (Burns et al., 2017). The ANH-San-Antonio-1X well-core represents areas far from the main channel, or sudden avulsions from the main channel, rather than gradual abandonment processes, allowing for excellent preservation of these crevasse splay and floodplain deposits. Abundant floodplain and crevasse splay deposits relatively far from the channel accumulate because of sediment settling during floods when the river breaks its natural levees (Burns et al., 2017). Thus, completely meandering fluvial successions are identified (Fig. VII.12G-H).

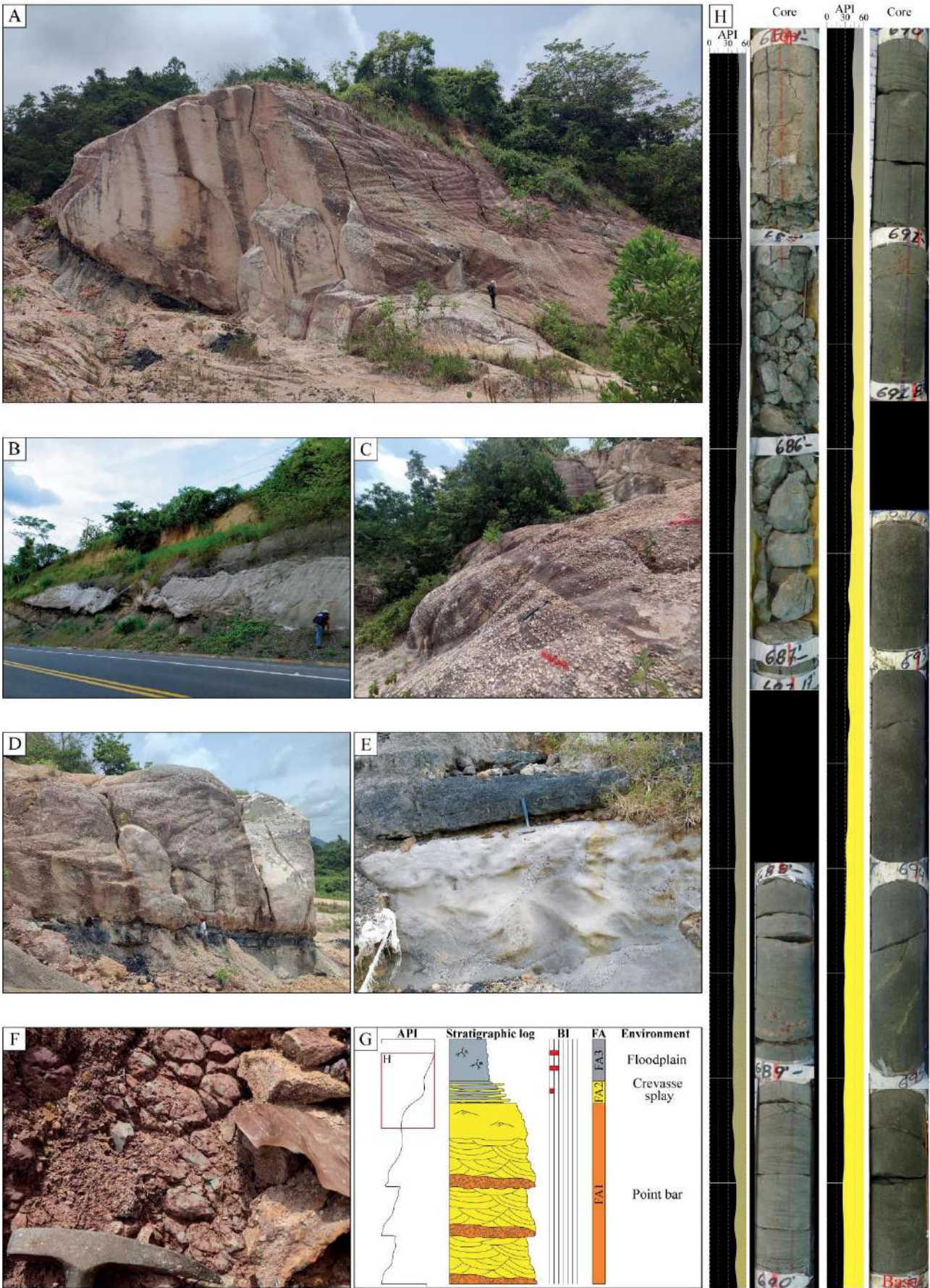


Fig. VII.12. Oligocene fluvial deposits. **A.** General outcrop view channel-floodplain system. **B.** Irregular-based beds of conglomerates associated with channels overlying floodplain mudrocks. **C.** Planar cross-bedding in pebble-sized channel conglomerates. **D.** Lenticular-shaped bodies of channel conglomerates overlaying floodplain mudrocks and coals **E.** Detail of medium- to coarse-grained sandstone with soft sediment deformation and coal bed. **F.** Variegated floodplain mudrocks. **G.** Typical idealized succession of continental deposits from Oligocene with meandering succession from point bars, crevasse splay and floodplain. **H.** Example of meandering succession from ANH-San Antonio-1X well-core and gamma ray. Note: A.P.I – American Petroleum Institute; BI – bioturbation index; FA – facies association. Scale: each subdivision corresponds to 1 ft.

Transitional. The sedimentological features observed, such as the frequent progradational trends (coarsening upward), lenticular-shaped bodies of medium- to coarse-grained sandstones and granule- to pebble-size conglomerates with erosive bases, and the prevalence of unidirectional structures (e.g. asymmetrical ripples and dunes, planar and trough cross-bedding), along with sandstone beds with normal grading, can be associated with channel development (FA6, FA7) (e.g., Coates and MacEachern, 2007; Swan et al., 2018). These preceding facies associations, combined with the presence of coal beds, high organic debris content, conglomerates, mud clasts, massive sandstones and massive mudrocks with rhizoliths, and in view of ichnological information, evoke classical deltaic sequences that prograde during the Oligocene. Recognizable coarsening-upward trends —from hyperpycnal prodelta to proximal delta-front with fluvial-dominated mouth bars— are identified within these sequences (e.g., MacEachern et al., 2005; Bhattacharya, 2006). Furthermore, the persistent dominance of these characteristics throughout the Oligocene allows one to interpret a fluvial-dominated deltaic environment, characterized by shoreline fluctuations with continuous shallowing-up sequences (e.g., Johnson and Dashtgard, 2014; Dashtgard and La Croix, 2015; Ainsworth et al., 2017; Maselli et al., 2020) (Fig. VII.13G).

In this fluvio-deltaic transition, particularly in the upper and lower delta plain environments (outcrops 7, 8, and ANH-Nueva Esperanza-1X well-core) established during progradation, a high abundance of *Mauritia* pollen suggests the presence of gallery flood forests near the transitional system (e.g., Ainsworth et al., 2017; Shchepetkina et al., 2019; Maselli et al., 2020). A sudden increase in fungal remains associated with organic-rich mudrocks, suggests the presence of water-logged interdistributary bays within the system, indicating greater stability of distributary channels and mouth bars compared to the latest Eocene period. Subaerial and subsequent terminal distributary channels (Fig. VII.13A), sometimes associated with hyperpycnal deposits reaching the coast (outcrop 8; Fig. VII.13B), indicate riverine flooding of the beach zone and interaction with the shallow marine environments. Deposits above water-logged interdistributary areas separated by erosive surfaces (Fig. VII.13C-D) are characterized by syneresis cracks, siderite nodules, mollusk shell fragments and low bioturbation indexes. Consequently, the delta widened during the Oligocene, reducing the gradient and allowing for the development of a larger lower delta plain (Fig. VII.13E) (e.g., Rossi et al., 2019).

As progradation continues, reaching up to coal beds (well-core and gamma-ray example in Fig. VII.13G-H), bioclastic successions associated with rapid and short-term transgressive pulses reinitiate the successions (e.g., Savrda et al., 1993; Cattaneo and Steel, 2003; Schultz et al., 2020), often with *Glossifungites* ichnofacies at the base of the following transgressive lags (Fig. VII.13F). The lags overlie typical firm substrates exposed by

erosion during the transgressive phase, resulting in ravinement surfaces (e.g., MacEachern et al., 1992, 1998; Gingras et al., 2002; Pemberton et al., 2004). Following the short-term transgressive phase, the sedimentary environment quickly reverted to previous fluvial-dominated conditions. Thus, persistent conditions resembling deeper/distal marine environments did not persist over time, but are locally recorded as hyperpycnal prodelta conditions, characterized by few calcareous microfossils and low bioturbation, as well as asymmetrical ripple cross-lamination and rare combined flow and symmetrical ripple cross-lamination. This phenomenon may be linked to a flooding event within a confined interdistributary bay-like context and/or stagnant waters (e.g., Bhattacharya, 2006). Accordingly, torrential rainfall favored by active tectonics determined sudden changes in sedimentation. Systems dominated by hyperpycnal prodeltas or mouth bars are established suddenly.

FA4 and FA6 exhibit characteristics indicative of high organic debris content, low bioturbation index, deposits with erosive bases, predominantly normal and bigradational gradations. These features are associated with the influence of multiple distributary channels, which deliver hypopycnal flows during typical river discharge and hyperpycnal flows during exceptional discharge events (Mulder et al., 2003; Bhattacharya and MacEachern, 2009; Zavala and Pan, 2018; Zavala et al., 2024). These conditions are expected to increase freshwater input into the marine environment, leading to significant salinity reductions and subsequent fluctuations in a brackish setting (e.g., Buatois et al., 2005; MacEachern and Bann, 2022). The elevated turbidity and sedimentation rates likely had detrimental effects on macrobenthic community development, predominantly influenced by fluvial processes (e.g., Buatois et al., 2005; Moyano-Paz et al., 2020; Ponce et al., 2023). The occasional occurrence of massive clast-supported conglomerates with rip-up clasts indicates the reworking of fine-grained deposits in these high-energy environments (e.g., Mulder and Alexander, 2001; Shiers et al., 2018).

Marine. Alongside the fluvial-dominated deltaic system, and extending into its variations (Fig. VII.14A), there are some beds characterized by flaser and wavy bedding, as well as mud drapes and reactivation surfaces (FA10 and FA11; Fig. VII.14B through D). These features are indicative of increased tidal influence (e.g., Dalrymple et al., 2015; Gugliotta et al., 2016; Rossi and Steel, 2016). In addition, there are minor occurrences of symmetric ripples and convolute laminations, suggesting increased wave and possible storm influences as one moves away from the main channel (e.g., Bhattacharya and Giosan, 2003; Dashtgard and La Croix, 2015; Rossi et al., 2017). Decimeter-scale interbedded consist of coarse-grained beds, indicative of fluvial-dominated environments with riverine flood deposits, and finer-grained beds with through and planar cross-bedding, reactivation surfaces, composite mud drapes, and tubular tidalites (Fig. VII.14B to D).

These features, coupled with a moderate bioturbation index and diversity (Fig. VII.14B to E), suggest a tidal affinity, and likely represent interflood deposits (e.g., Gugliotta et al., 2016). The alternation observed between these bed types (Fig. VII.14F), along with fluvial-dominated beds, gives rise to non-cyclic rhythmites interpreted as reflections of variations in river discharge magnitude (e.g., Gugliotta et al., 2016). This is due to the variable magnitude of river floods in tropical systems, in contrast to the cyclic and predictable nature of tides. The interpreted fluvial signature is evident in a range of deposits, spanning from distal environments (such as distal delta-front and mouth-bar deposits, FA11 and FA10 in outcrops 4 and 5) to more proximal

facies such as terminal distributary channels (FA6 in outcrop 9) (well-core and gamma-ray example from Fig. VII.14G-H).

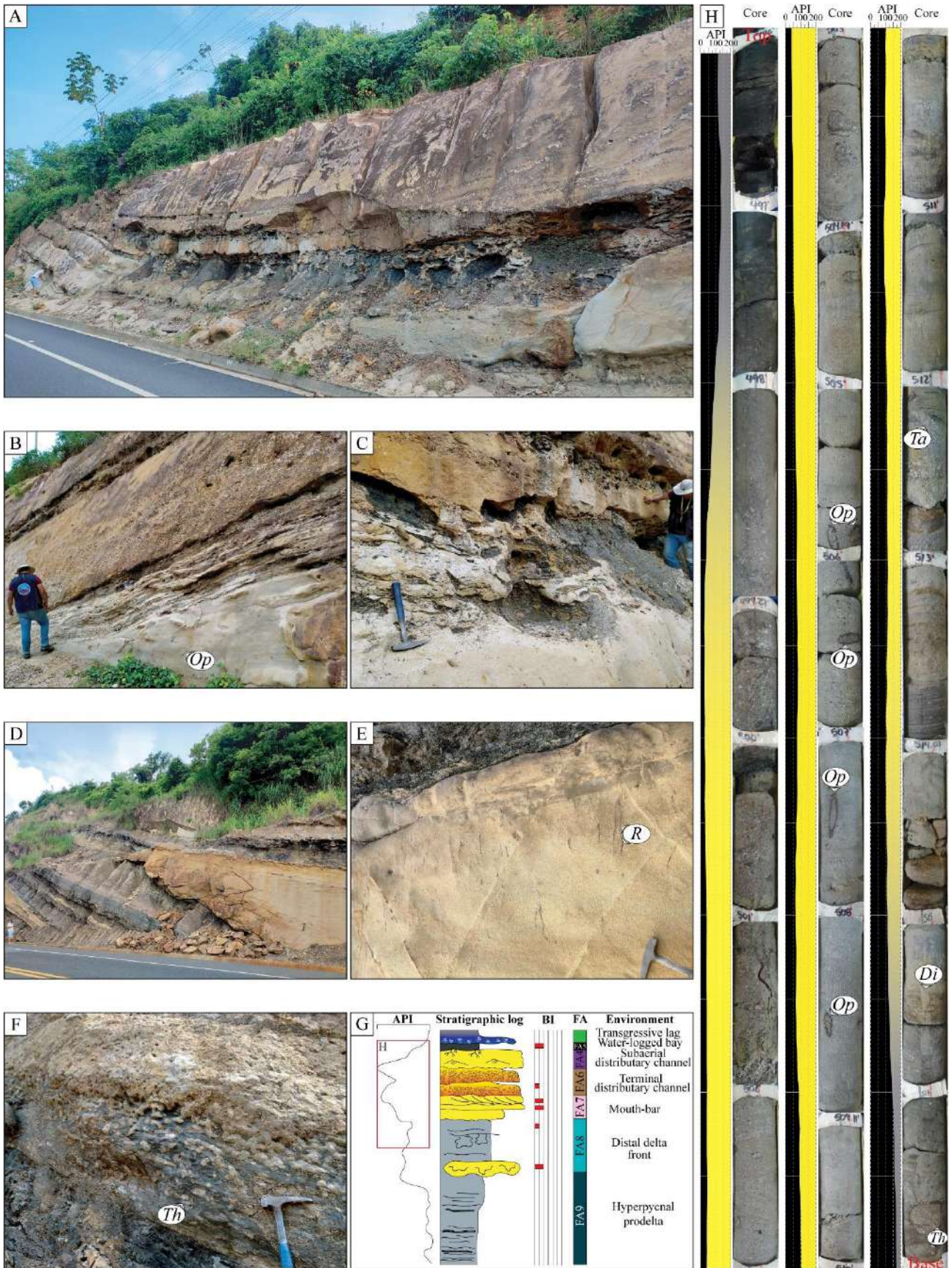


Fig. VII.13. Oligocene fluvial-dominated deltaic deposits. **A.** General outcrop view. Irregular-based channel with boulder to cobble size rip-up clasts overlying delta-front deposits. Lenticular-like morphology corresponds to tectonic deformation and not to the morphology of the original channel. **B.** Proximal delta-front deposits with *Ophiomorpha* (*Op*) overlain by irregular-based pebble-size conglomerates associated with terminal distributary channel. **C.** Detail of cobble-size mud clasts towards the base of the channel. **D.** Terminal distributary channel overlying mudrocks from water-logged interdistributary bay. **E.** Medium-grained sandstones with root structures (R) from water-logged interdistributary bay. **F.** Coal and organic mudrocks bioturbated by *Thalassinoides* (*Th*) representing a ravinement surface. **G.** Typical idealized succession of fluvial-dominated deltaic deposits from Oligocene with progradation from hyperpycnal prodelta to water-logged interdistributary bay. **H.** Example of fluvial-dominated deltaic succession from ANH-Nueva Esperanza-1X well-core and gamma ray: distal delta-front bioturbated by *Diplocraterion* (*Di*) and *Taenidium* (*Ta*), proximal delta-front (mouth bar) bioturbated by *Ophiomorpha* (*Op*), transition to terminal distributary channel and water-logged interdistributary bay. Note: A.P.I – American Petroleum Institute; BI – bioturbation index; FA – facies association. Scale: each subdivision corresponds to 1 ft.

The presence of well-preserved bar deposits with medium beds of fine- to medium-grained sandstones displaying horizontal lamination and low angle cross-bedding, along with bioturbation associated with *Macaronichnus*, and/or *Ophiomorpha* (BI 3-4) —which typically occur twice at the top of the progradation cycle— likely reflect high-energy conditions in beach-like environments, i.e., stable marine-influenced point bars or tidal bars (e.g., Pemberton et al., 2001; Seike et al., 2011). In fact, it suggests episodic stages of torrential rains and other times with greater stability and marine influence on the system. Distinctive features typical of flashy discharge channels, such as pedogenically modified mud partings, abundant planar bedding, and in situ rhizoliths (e.g., Fielding, 2006; Fielding et al. 2009; Gulliford et al. 2014; Wilson et al. 2014) indicate the dominance of fluvial processes despite tidal influences on the system. Additionally, this fluvial-deltaic system probably served as one of the main tributaries of the Colombian Caribbean at that time (e.g., Pardo-Trujillo et al., 2023), draining large catchments capable of absorbing local precipitation and primarily recording seasonal discharge variations. During the latest Oligocene to Earliest Miocene, a significant increase in mangrove pollen, especially *Zonocostites* and *Lanagiopollis crassa*, supports the establishment of a stable transitional environment with continuous flooding/interflooding phases; extensive floodplains and soil development in the upper and lower delta plain environment suggest prolonged subaerial exposure, with increases in marine influence by tidal signal (e.g., Bhattacharya, 2006; Hansen and MacEachern, 2007; Ainsworth et al., 2017; Collins et al., 2020). As one moves away from the distributary system, successions dominated by the tidal environment can be recognized, indicating increased reworking and a possible reduction of sediment input from the fluvio-deltaic system.

VII.7. Discussion

VII.7.1. Tectonics and sedimentation: from coarse- to fine-grained sedimentary systems in forearc basins

The mayor controls on sediment deposition and preservation in deltaic environments have long been attributed to factors external to the depositional system (allogenic), such as glacio-eustasy, tectonics, subsidence, and climate change (e.g., Einsele, 2000; Miall et al., 2014). These large-scale, extrinsic controls are interrelated and force changes in other internal (autogenic) parameters of the depositional system, such as channel avulsion frequency, autoretreat processes and delta-lobe switching (Catuneanu and Zecchin, 2013). Furthermore, in

active margins, tectonics and relative sea-level control the generation of accommodation space and sediment supply, which is partly influenced by climate (e.g., Ainsworth et al., 2008; Armitage et al., 2011).

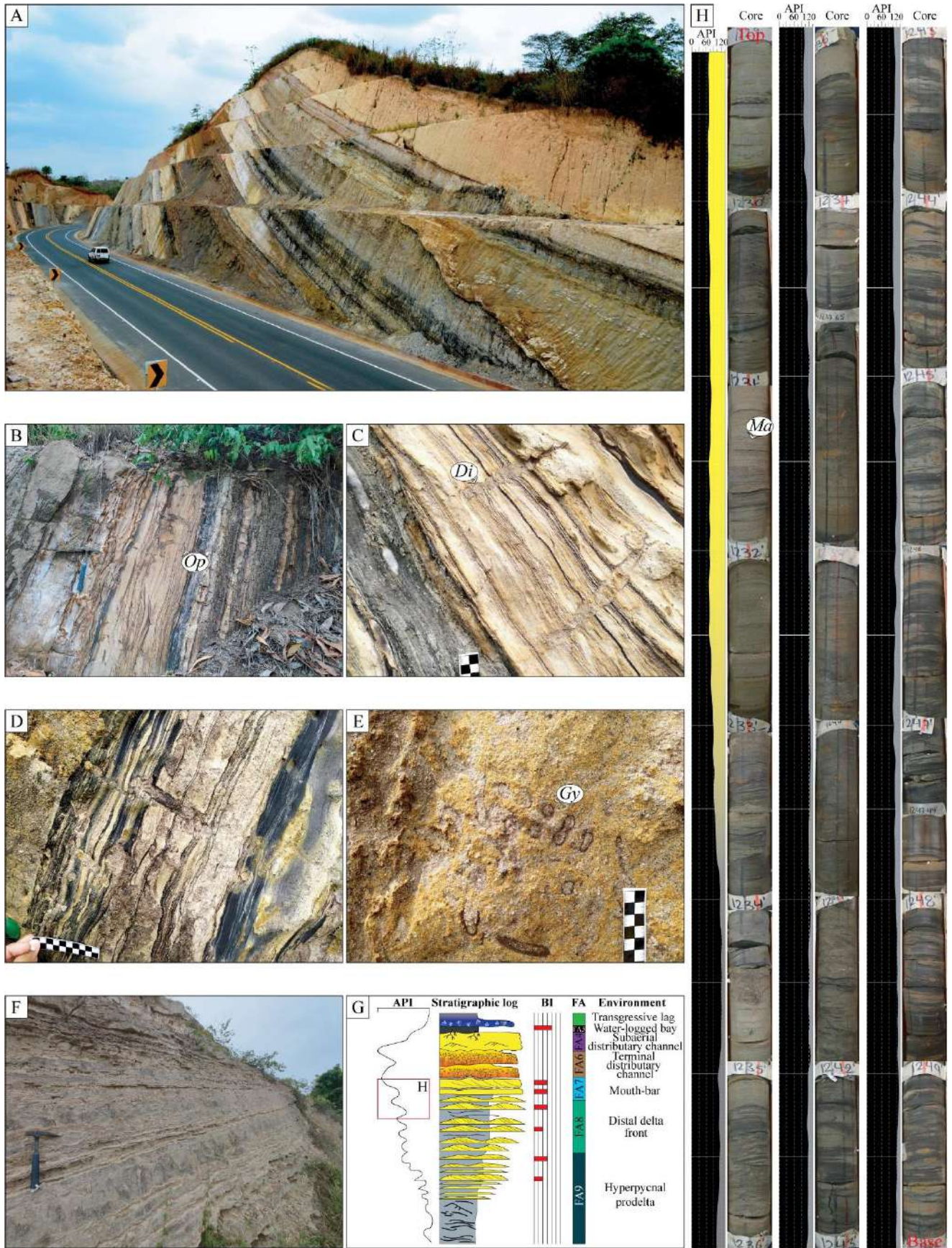


Figure 14. Oligocene tidal and fluvial influenced deltaic deposits. **A.** General outcrop view with water-logged interdistributary bay deposits overlain by irregular-based terminal distributary channel. **B.** Hyperpycnal prodelta and transition to distal delta-front and proximal delta-front with trough cross-bedding and some mud drapes indicating tidal influence. **C-D.** Sub horizontal bedding with organic laminae highlighting lamination and bioturbated by *Diplocraterion* (*Di*) associated with the delta front. **E.** Medium to coarse-grained sandstones bioturbated by *Gyrolithes* (*Gy*) related to delta-front deposits. **F.** Wavy and flaser heterolithic stratification with asymmetrical ripples and planar cross-bedding from medium- to coarse-grained sandstones and mudrocks representing the non-cyclic rhythmites. **G.** Typical idealized succession of fluvial-dominated deltaic deposits with tidal influence from Oligocene, with prograding from hyperpycnal prodelta to water-logged interdistributary bay with tidal influence. **H.** Example of fluvial-dominated deltaic succession with tidal influence from ANH-Nueva Esperanza-1X well-core and gamma ray: distal delta-front and transition to proximal delta-front (mouth bar) bioturbated by *Macaronichnus* (*Ma*). Note: A.P.I – American Petroleum Institute; BI – bioturbation index; FA – facies association. Scale: each subdivision corresponds to 1 ft.

Thus, the deltaic depositional system may be controlled by a mixture of external and internal factors whose relative contributions are difficult to discern, which requires detailed analysis.

The interpreted coarse-grained mouth-bar environments with hyperconcentrated fluvial deposits input during the middle-late Eocene and earliest Oligocene are associated with coarse-grained deltas (Figs. 15 and 16). Climatic conditions induce highly variable runoff in tropical regions that, coupled with the distribution of nearby mountain ranges and sea-level fluctuations, facilitated the generation of gravity flows that arrive to the shoreline. These flows likely originated from nearby basement highs —such as the present-day Magangué-Cicuco high and the northern South American Andes (Central Cordillera)— contributing to basin sedimentation from a mixed source. The source includes the recycled orogen and a magmatic arc south-southeast of the study area (Mora et al., 2017). Furthermore, sedimentary facies trends associated with this tectonic uplift suggest patterns indicative of the later stages of a forced regression, likely triggered by a relative drop in base level localized at the active margin of the basin. In this tectonic scenario, although the deposits may be linked to post-sedimentation of the forced regression, they are more likely related to the re-activation of the basin following collisional changes. During the early to middle Eocene (50–45 Ma), there was a significant cessation of magmatism in northern Colombia, coinciding with a plate-tectonic readjustment characterized by a decrease in convergence velocity and obliquity (Bayona et al., 2012; Matthews et al., 2016; Leal-Mejía et al., 2019). This period also marked the emergence of a new basin from middle Eocene to Recent called the Lower Magdalena Basin (Mora et al., 2017). However, the unconformity registered in the lower to middle Eocene rocks of the San Jacinto Basin, and the subsequent changes in the middle to upper Eocene deposits may be linked to these shifts in the collisional scenario (e.g., Kroehler et al., 2011; Mora-Bohórquez et al., 2020; González et al., 2023), making their exact timing difficult to establish. In this context, the deposits of the latest-middle to late Eocene could be the result of tectonic readjustment and represent renewed forearc extension. Still, the limited accommodation space in this tectonic setting, combined with abundant gravity flows input from near paleo-highs and the tropical climatic conditions, favored the accumulation of amalgamated coarse-grained deposits (e.g., ANH-SSJ-La Estrella-1X and ANH-SSJ-Nueva Esperanza-1X well-cores, outcrops 1 and 10).

Middle to upper Eocene continental and shallow-marine deposits, with increasing marine influence toward the top, are finally overlain by transgressive fine-grained deposits having abundant marine calcareous microfossils

and thicknesses up to ~30 m. Evidence for a discontinuity remains inconclusive, due to the limited biostratigraphic resolution, making precise determination difficult. Additionally, the coarse-grained and transitional nature of these deposits hinders effective microfossil recovery, complicating efforts to distinguish whether the transgressive surface occurred during the latest Eocene or earliest Oligocene.

In deposits toward the northeastern part of the basin, representing more distal palaeoenvironments but showing the same rapid transition from coarse- to fine-grained sedimentation (e.g., Alférez Creek (jet and curve sections), Piedra Azul Creek, San Jacinto Creek, and Salvador Creek; Celis et al., 2024), some authors report a time gap of ~0.8 Myr (Arias-Villegas et al., 2023 in well-core ANH-San Jacinto-1). In these settings, better recovery of marine microfossils enables more accurate calibration. This evidence supports an unconformity at the end of the Eocene, between ~35.2 and ~34.4 Myr, slightly above a sharper boundary between very coarse-grained sandstones and mudstones. However, this data should be used with caution, as the more distal deposits likely represent facies variations from the shallower areas to the east of the study zone, where fluvio-dominated deltaic systems are less prominent. This could potentially influence interpretations. Even so, the occurrence of this change at the Eocene-Oligocene transition, or at least in the earliest Oligocene, is evident.

The sea-level dropped significantly during this period according to the global eustatic curve, marking the Eocene-Oligocene boundary. This event is linked to the establishment of the permanent ice sheet in Antarctica (Fig. VII.15; Katz et al., 2008; Miller et al., 2020; Simmons et al., 2020; Hutchinson et al., 2021), which caused a decrease in accommodation space (e.g., Goodbred Jr et al., 2003). The studied deposits, being associated with a significant system transgression, represent the opposite situation, so that the global eustatic signal is dismissed. However, in the more distal palaeoenvironmental section toward the northeastern part of the basin (ANH-San Jacinto-1 well-core), some biotic variations in marine and terrestrial microfossils (calcareous nannofossils, palynomorphs, and benthic foraminifera) may be associated with ecosystem responses to global climatic changes during the Eocene-Oligocene transition (EOT) (Trejos Tamayo et al., 2024). Therefore, even though there may not be a clear response in the depositional systems, there could be an influence on the biotic response to decreasing global temperatures and a new climatic regime.

After the transgression, the successions underwent a complete change compared to the previously observed amalgamated deposits (Figs. VII.15 and VII.16). A sudden increase in fungal remains, and the high abundance of morichal palm pollen (*Mauritia*) associated with muddy deposits, suggest the star of interdistributary bays and gallery flood forests near the transitional system, may even signal the beginning of the lower delta plain supply system, which was a sub environment absent in the coarse-grained underlying deposits (Fig. VII.16).

The prograding successions reveal the onset of fluvial-marine interaction during this period, with increasing accommodation space for the sediments (fine-grained delta) that began with the tectonic realignment in the early-middle Eocene, a decrease in plate obliquity (Matthews et al., 2016) and evidently increased subsidence (Fig. VII.15) probably associated with fault-controlled due to cooling of magmatic arc (Mora-Bohórquez et al., 2020). The onset of subsidence reported by Mora et al. (2018) indicates decreases in plate obliquity since ~30 My and marks an increase from 200 up to 500 m of accommodation space (Fig. VII.15). These changes coincide with lower plate convergence velocities and plate obliquities, hence margin stabilization in a subduction accretion scenario with flat slab (Mora-Bohórquez et al., 2020). In this context, the onset of flat

subduction would promote reduced sedimentation rates in forearc basins due to the absence of the magmatic arc, allowing sediment accumulation without significant erosion and amalgamation (up to ~1000 m for a deltaic system), meaning basin dynamics and morphology controlled the sedimentation (e.g., Ainsworth et al., 2008; Fielding et al., 2014; van Yperen et al., 2019). In the deposits from the northeastern part of the study area, a new 2 Myr unconformity is reported in the early Oligocene (~32.4 Myr to ~30 Myr; Arias-Villegas et al., 2023). However, the fluvio-deltaic deposits do not show significant changes in sedimentation. This gap cannot be entirely ruled out, as erosional surfaces between the fluvio-deltaic channels could account for this time lapse, but it remains difficult to determine at this point.

The accommodation space in the basin continued to increase during the middle-latest Oligocene (Figs. VII.15 and VII.16). A relative rise in global sea-level is recorded in the late Oligocene, however. The autoretreat could be an autogenic process acting on the system, although it is a challenge to decipher its signal in this scenario. This process highlights the inability of constant sediment supply to keep up with accommodation space to sustain progradation (Catuneanu and Zecchin, 2013). Sedimentation would be controlled by regional tectonic rather than eustatic factors, while the global signal could also play a role. Accordingly, changes in fluvial styles from continuous gravity flows to a stable meandering system were mainly controlled by tectonic and climatic factors.

After the autoretreat phase, transgressive-regressive cycles have been documented regardless of fluctuations in sediment supply and accommodation space. Thus, it is unlikely that the accommodation space and sediment supply have remained constant over an extended period, suggesting that the autoretreat process likely occurred alongside allocyclic changes in accommodation space and sediment supply ratios.

The deltaic system described here for the late Oligocene to Early Miocene shows a stronger aggradational trend of continental systems, in conjunction with a greater significance of marine influence phases (Fig. VII.16). It correlates with the tectonic stability phase of the middle to late Oligocene (Mora et al., 2018). Nonetheless, short environmental changes from distal to shallow in the latest Oligocene could be related to drastic tectonic changes in the margin associated with the interaction between the Andes and the arrival of the Panama Choco Block (e.g., Farris et al., 2011; Vallejo-Hincapié et al., 2024).

The stability of the system during the Early Miocene is probably reflected in a greater predominance of tidal influence and wave action (Fig. VII.16). Thus, the deposits preceding the Middle Miocene regional inundation (Porquera Formation) may be associated with the initial inputs of the transgressive event.

Towards the eastern sector of the Colombian Caribbean, specifically in the Lower Magdalena Valley Basin during the Oligocene to Early Miocene, a second-order transgressive sequence is inferred to have filled the lowest paleo-topographic areas formed by the basin's basement, extending from northwest to southeast (Duque-Caro, 1979; Mora et al., 2018). These sequences likely correspond to transgressive pulses identified in the uppermost part of the studied successions.

The transition to a continental environment (upper delta plain) by the Early Miocene, despite the retrogradational basin pattern, documents the aggradation and stability of a fluvial-deltaic system. However, tectonic dynamics contributed to the uplift of structural highs in the forearc, including mountain range as the Western Cordillera and therefore, high sedimentation rates facilitated the development of other fluvial systems

along the margin during the Miocene (e.g., Farris et al., 2011; Mora et al., 2017; Lara et al., 2018; León et al., 2018; Zapata et al., 2020). Analogous deltaic systems might have been the source of certain Oligocene to Early Miocene successions documented near the Plato depocenter, but with a predominance of wave and tidal processes.

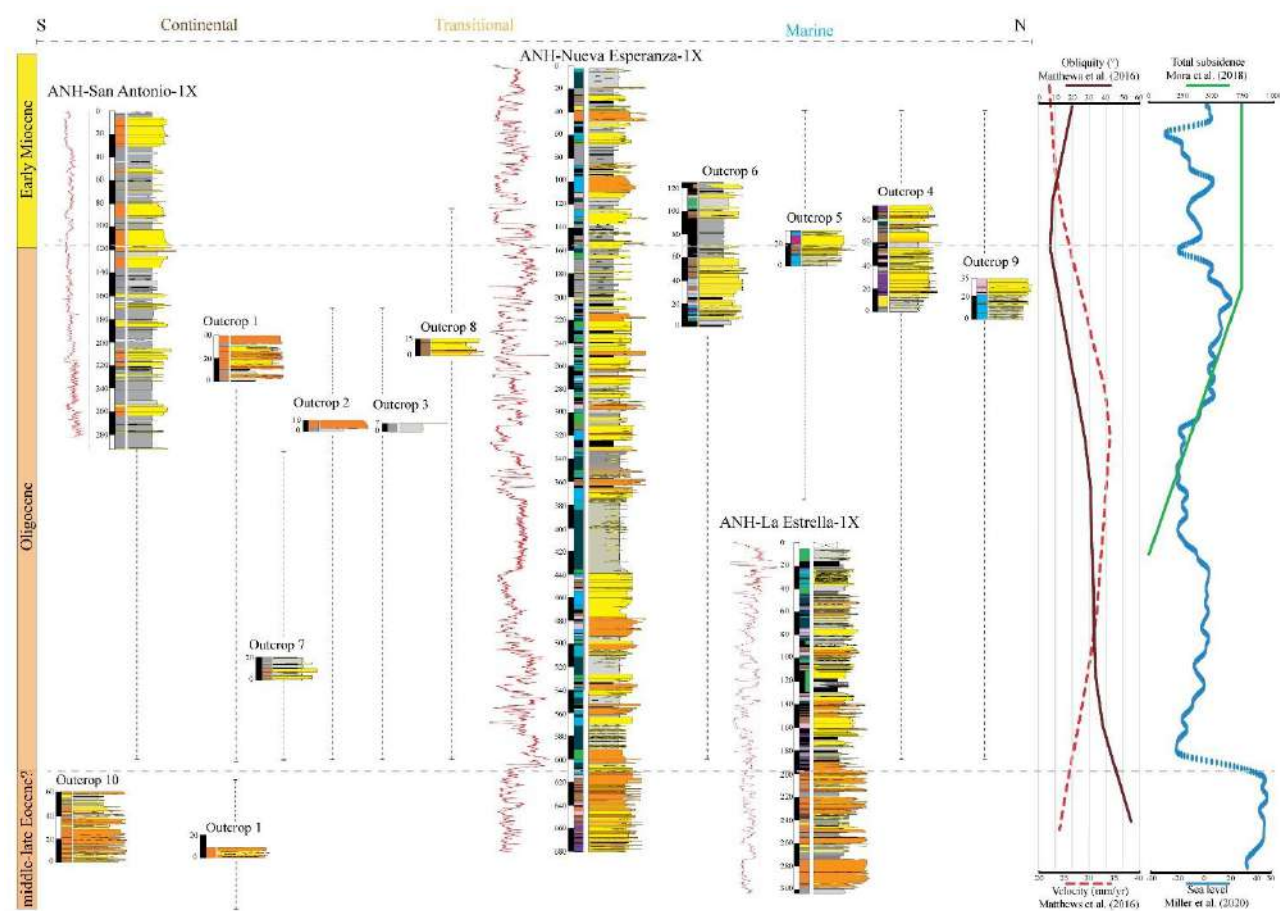


Fig. VII.15. Outcrop and well-core sections and tectonic scenario: obliquity and velocity reconstructions of the plate (Matthews et al., 2016), sea-level (Miller et al., 2020) and total subsidence of the basin (Mora et al., 2018). See Figure VII.3 for facies associations legend.

VII.7.2. Flood – interflood depositional deltaic systems: uniqueness of tropical conditions?

The vertical and lateral architecture of transitional facies has been widely described based on its relative progradation and aggradation, from different settings worldwide. Most of the conventional general models currently applied are based on high- and mid-latitude fluvio-deltaic systems such as those of the Mississippi, Po, Rhône, Ebro and other rivers. Yet in some cases these models needed to be reconsidered, highlighting the complexity of these land-ocean systems (e.g., the Brent Delta Front, Rannoch Formation, northern North Sea; Wei et al., 2016; or Lower Wilcox Delta; Gulf of Mexico; Zhang et al., 2019).

Some tropical examples illustrate processes with tidal dominance, such as in the Mahakam (Indonesia; Storms et al., 2005), Gulf of Carpentaria (Australia; Jones et al., 2003), Mekong (southern Vietnam; Ta et al., 2002; Tamura et al., 2012), or Fly (Papua New Guinea; Dalrymple et al., 2003) deltas, which also present variations in subsidence and in fluvial input. Other examples—including the Niger River delta (Nigeria; Doust and

Omatsola, 1989; George et al., 2019) or Ayeyarwady River delta (Myanmar; Anthony et al., 2019)— show multiple processes associated with rivers, waves, and tides in the same period. Furthermore, some of these deltas are significantly influenced by monsoons that temporarily increase the effect of the waves and turn them into mixed systems (e.g., Mekong, Ayeyarwady, Fly delta). Although the influence of the monsoons is very well documented, few works show the effect of torrential rains in active margins of tropical regions, registering the relationship between the Andes and the adjacent sedimentary basins (e.g., Amazonas River, Hoorn et al., 2010; Orinoco River, Buatois et al., 2012; Peng et al., 2020; Magdalena and Cauca rivers, López-Ramos et al., 2021). Research on mixed-energy coastal systems under tropical conditions is increasing (mainly in Southeast Asia), but the deltaic system in forearc basins is poorly documented.

The fluvial discharges within the fluvio-deltaic system of northern South America are dominated by hyperpycnal flows, which can even generate the largest submarine fans in the world (e.g., Idárraga-García et al., 2019; Naranjo-Vesga et al., 2022). This has been evident since the Eocene-Oligocene transition, as demonstrated in this research, with a river that was likely the main one during the late Paleogene in northern South America. The flows transport a substantial load of suspended sediment, including abundant fragments of organic matter and terrestrial palynomorphs, resulting in underflow that is manifest in distal delta-front and prodelta systems. In addition, the flows can incise shallow channels and incorporate intrabasinal clasts, predominantly rip-up clasts, into the system. This sediment load, coupled with the high textural maturity of the deposits, may be temporarily stored in shallower depositional environments; subsequently these sediments would be periodically mobilized and transported into the basin by rivers during major flood events (e.g., Fielding et al., 2005; Celis et al., 2024). Such changes can be temporally variable, especially under tropical conditions with torrential rains (e.g., Warne et al., 2002).

Syneresis cracks and siderite nodules are frequently observed, indicating fluctuating salinity levels, which could result from either river discharge or mud flocculation within buoyant plumes that transport brackish water to the sediment-water interface (e.g., MacEachern and Bann, 2022). Hence, these processes significantly disrupt the marine signal, affecting macrobenthic tracemaker communities, particularly suspension-feeders (e.g., Perkins, 1974; MacEachern et al., 2005; Bhattacharya and MacEachern, 2009; MacEachern and Bann, 2022), resulting in depauperate, monospecific, or stress-dominated trace fossil assemblages and isolated occurrences of *Ophiomorpha*- or *Phycosiphon*-bearing beds during long-periods. The ichnological assemblage is low in abundance but moderately diverse, comprising *Ophiomorpha*, *Skolithos*, and *Thalassinoides* in fluvio-dominated mouth bars; *Ophiomorpha*, *Skolithos*, *Taenidium*, and *Thalassinoides* in the fluvio-dominated distal delta front; and *Phycosiphon*, *Planolites*, *Teichichnus*, and *Thalassinoides* in fluvio-dominated prodelta successions.

While the studied fluvio-deltaic system is an important tributary catchment and has a long-life span, extending over 250 km since the Oligocene (Celis et al., 2023), the frequency of tropical torrential rains continuously modifies its dynamics and involved processes, interfering with the development of typical tidal modulation or wave re-working (i.e., Olariu et al., 2012; Maselli et al., 2020). In the Colombian Caribbean deposits, the loss of channel confinement at the channel-lobe transition triggers a significant reduction in shear forces, leading to reduced bedload transport as the flow loses competence. It is noteworthy that the record of prodeltaic

hyperspycnal systems occurs in sedimentary catchments proximal to the paleo-shore, as indicated by the described sections and distances from continental sections. As the primary flow decreases, suspended-load sediments progressively settle to the lower flow boundary, a consequence of reduced flow capacity.

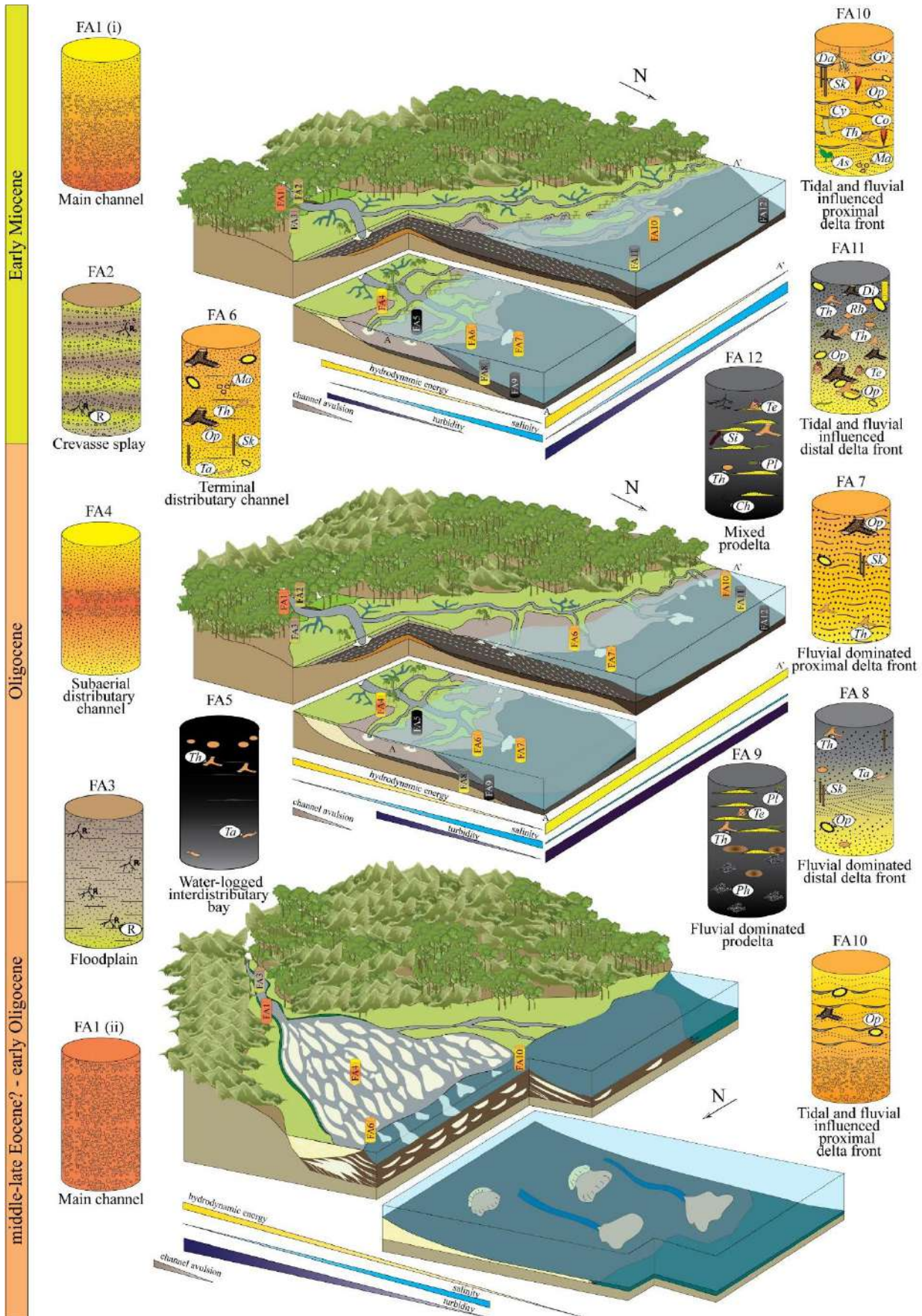


Fig. VII.16. Sedimentation model from middle-late Eocene to Early Miocene. Not to scale. Middle to upper Eocene – early Oligocene: Distributary channels to mouth-bars units of river-dominated, with some tidal- and wave-influenced mouth-bar delta. Oligocene: Fluvio-deltaic system with fluvial-domain. Latest Oligocene to Early Miocene: Fluvio-deltaic system with increase in tidal-influenced.

As a result, mouth bars exhibit dominant fluvial processes, and the exclusive occurrences of *Ophiomorpha* tracemakers, which capitalize on reduced energetic discharges and therefore indicate significant variations in river discharge. In some of the study profiles, higher abundances of trace fossils, including *Ophiomorpha* as tubular tidalites, are locally observed, often accompanied by abundant migrating asymmetric bedforms such as trough and planar cross-bedding, highlighted by mud drapes and mud laminae. Reactivation surfaces are occasionally visible, leading to the interpretation of tidal affinity beds as interflood deposits. Higher bioturbation indexes (BI 3-4) associated with interflood-dominant intervals, along with the increased size of burrows, suggest prolonged time for bioturbation (e.g., Gingras et al. 2002; Gingras and MacEachern 2012; Gugliotta et al., 2016). Therefore, mouth bars also exhibit mud drapes and flaser bedding, with increased bioturbation index and diversity, including *Asterosoma*, *Conichnus*, *Cylindrichnus*, *Dactyloidites*, *Gyrolithes*, *Macaronichnus*, *Ophiomorpha*, *Skolithos*, and *Thalassinoides*.

However, in more distal deposits such as prodelta environments, it becomes difficult to differentiate the tidal signal. These settings are predominated by mudrock dominated heterolithic successions, characterized by composite bedsets with lenticular and occasional wavy bedding, often interspersed with current ripple cross-lamination. Such intervals reflect rapid mud deposition interrupted by episodes of sand transport induced by currents, which hinder bioturbation (e.g., MacEachern and Bann, 2022). It is characterized by *Chondrites*, *Planolites*, *Siphonichnus*, *Teichichnus*, and *Thalassinoides*.

In distal delta-front successions where wavy-dominated, and occasional lenticular heterolithic facies occur due to current activity, the abundance of trace fossils tends to increase, suggesting periods of reduced flood deposition rates or temporary pauses or sections where the hyperpycnal flows continue their offshore/platform trajectory. Distal delta front successions show wavy bedding with scarce mud drapes and a trace fossil assemblage of *Diplocraterion*, *Ophiomorpha*, *Planolites*, *Rhizocorallium*, *Teichichnus*, and *Thalassinoides*.

In comparison with the southeastern Asian deltas, where monsoons and tidal effects play a significant role, the tropical deltas of northern South America present a unique scenario dominated by torrential rains and consequent hyperpycnal flows due to the active tectonic. These rains, associated with the topographic/geomorphological characteristics of mountain ranges create more variable and intense sediment transport events, significantly altering the deltaic architecture and sedimentary processes by reducing wave modulation and tidal influence. Such complexity underlines the importance of detailed studies to identify periods where fluvial-dominated conditions may diminish, allowing marine processes, particularly tidal influence, to act on the system. Indicators such as tubular tidalites, burrow size, mud drapes, and fluid muds in mouth bars, delta-front or prodelta environments can help distinguish these periods. In such scenarios, the models might resemble mid- and high-latitude fluvial-dominated systems rather than the Asian tropical models where despite the occurrence of monsoons, the tectonics of the systems favor that the deltaic systems do not suffer drastic changes in their trends of influence, modulation or dominance. The successions under study show

a close relationship between terminal distributary channels and mouth bars, both in the coarse-grained system (Eocene Oligocene transition) and the fine-grained system (Lower Oligocene Miocene). Channels frequently undergo passive infilling during abandonment phases, influenced by the aggradation and lateral or upstream migration of mouth bars (e.g., Wax Lake Delta, Atchafalaya Delta, Lena Delta, and Volga Delta, Olariu and Bhattacharya, 2006; Siena Basin, Martini and Sandrelli, 2014). Their amalgamation and packing vary depending on accommodation space and sediment input. Consequently, mouth bar migration can occur upstream, laterally, or downstream, depending on the sink's morphology or, on a larger scale, tectonic dynamics (e.g., Olariu and Bhattacharya, 2006). Still, the coalescence of hyperpycnites is characteristic, and some episodes of channel abandonment or low river discharge phases have been reported (e.g., Olariu et al., 2010).

VII.8. Conclusions

Integrative sedimentological, ichnological, gamma-ray, and micropaleontological analysis conducted on outcrops and well-cores from Colombian Caribbean enabled the identification of distinct facies associations and trace fossil assemblages, revealing significant vertical variations in depositional style spanning from the middle-late Eocene to the Early Miocene. This comprehensive study delineates twelve facies associations, ranging from continental to deltaic environments, with variations attributed to accommodation space dynamics and sediment input fluxes.

During the Eocene, coarse-grained sedimentation prevailed, characterized by hyperconcentrated to hyperpycnal flows reaching the coastline, and the development of amalgamated mouth bars, indicative of limited accommodation space. The transition to the earliest Oligocene witnessed a notable shift towards transgressive deposits, marking a pivotal change in sedimentation patterns. From the Oligocene to the Early Miocene, the dominance of meandering fluvial and deltaic fine-grained deposits underscores a shift in depositional control. Integration of these interpretations with extensive tectonic data reveals a correlation between increased accommodation space and tectonic realignment during the Oligocene and Miocene, leading to heightened subsidence. This shift is intricately linked to changes in tectonic regimes and sediment supply dynamics. Our study highlights that tectonic activity emerges as the primary driver of sedimentation within the compressional accretionary type forearc of the Colombian Caribbean basin, superseding the influence of dramatic eustatic sea-level changes during Eocene-Oligocene transition. The tectonically active nature of the basin exerts a profound influence on sediment accommodation and deposition patterns, emphasizing the need for a nuanced understanding of tectonic processes in deciphering basin evolution and stratigraphic architecture in active margins. Moreover, the low diversity of trace fossils, small burrow sizes, high detrital input, and a direct relation between terminal distributary channels and mouth bars, altogether suggest hyperpycnite coalescence during the Oligocene-Miocene established system. Ichnological features such as the presence of tubular tidalites and burrow size, along with sedimentological attributes such as muddy fluids and mud drapes, point to mouth bar migration upstream, laterally, or downstream, depending on basin morphology and tectonic dynamics, with highlighted tidal influence or wave modulation during short episodes. Our findings suggest that tropical systems in northern South America share more similarities with fluvio-dominated rivers of high and mid-latitudes due to its relationship with mountain ranges rather than deltaic tropical southeastern Asian

environments. This has broader implications for understanding the influence of tectonics versus climatic factors (e.g., monsoons) on sedimentation in tropical regions.

Acknowledgements

This research was funded by Grants TED2021-131697B-C21 funded by MCIN/AEI/10.13039/501100011033. The National Program for Doctoral Formation provided financial support to Celis and Giraldo-Villegas (Minciencias grants 885-2020, 906-2021, respectively). We wish to thank the National Hydrocarbons Agency-ANH, and Ministerio de Ciencia, Tecnología e Innovación - Minciencias for allowing the study of well-cores (Convenio 730/327 - 2016). The Vicerrectoría de Investigaciones y Posgrados and the Instituto de Investigaciones en Estratigrafía-IIES of Universidad de Caldas gave economic and logistic support; special thanks to Juan P. Betancourt for Figure VII.1, location and geological map. The research was conducted within the “Ichnology and Palaeoenvironment RG” (UGR). Financial support for Rodríguez-Tovar was provided by scientific Projects PID2019-104625RB-100 (funded by MCIN/AEI/10.13039/501100011033), P18-RT- 4074 (funded by FEDER/Junta de Andalucía-Consejería de Economía y Conocimiento), B-RNM-072-UGR18 and A-RNM-368-UGR20 (funded by FEDER Andalucía).

Supplementary Material VII.1. Coordinates, thicknesses, figures location.

Chapter VIII

RECORDS OF THE ESTABLISHMENT OF DELTAIC SYSTEMS IN THE
OLIGOCENE-EARLY MIOCENE

Deciphering influencing processes in a tropical delta system (middle-late Eocene? to Early Miocene, Colombian Caribbean): Signals from a well-core integrative sedimentological, ichnological, and micropaleontological analysis

Sergio A. Celis^{a,b,c,*}, Francisco J. Rodríguez-Tovar^{a,}, Andrés Pardo-Trujillo^{b,c,d}, Fernando García-García^a, Carlos A. Giraldo-Villegas^{a,b,c}, Fabián Gallego^{b,c}, Ángelo Plata^{b,c,e}, Raúl Trejos-Tamayo^{b,c,e}, Felipe Vallejo-Hincapié^{b,c,e}, Francisco Javier Cardona^f**

a Departamento de Estratigrafía y Paleontología, Universidad de Granada, 18002, Granada, Spain

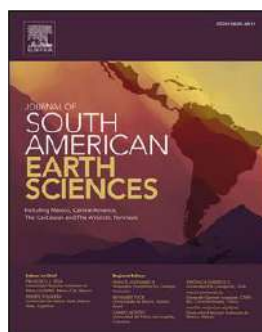
b Instituto de Investigaciones en Estratigrafía-IIES, Universidad de Caldas, 170004, Manizales, Colombia

c Grupo de Investigación en Estratigrafía y Vulcanología (GIEV) Cumanday, Universidad de Caldas, Manizales, Colombia

d Departamento de Ciencias Geológicas, Universidad de Caldas, 170004, Manizales, Colombia

e Departamento de Geología, Universidad de Salamanca, 37008, Salamanca, Spain f Consultant Geologist, Colombia

Journal of South American Earth Sciences, 127 (2023), 104368



<https://doi.org/10.1016/j.jsames.2023.104368>

Highlights

- Integrated sedimentological/ichnological/micropaleontological analysis.
- Subsidence, relief uplifting, and possible relative sea level changes in tropical mixed-energy coastal systems.
- Amalgamated mouth bars settings during middle-late Eocene? to early Oligocene.
- Retrograding to prograding, hyperpycnal-dominated heterolithic delta deposits during the Oligocene.
- Gently (poorly drained), well-developed delta plain during Oligocene to Early Miocene.

Abstract

Deltaic depositional systems are characterized by a complex interaction of physical, chemical, and biological factors. Although fluvial-, wave- and tidal-dominated deltaic environments have been extensively studied, evaluation of the processes in tropical mixed sedimentary systems has not been fully documented. Tropical regions with active margins are tectonic environments where these multiple factors act on the development of coastal systems. An onshore well-core from this tropical setting (Sinú-San Jacinto Basin, Colombian Caribbean) revealed that a middle-upper Eocene?-lower Oligocene coarse-grained deltaic setting is replaced by a thick coal-bearing mixed-energy fine-grained deltaic succession from the Oligocene to Early Miocene. The integrated analysis of facies associations, ichnological data, and terrestrial/marine micropaleontological assemblages (palynomorphs, foraminifera, and calcareous nannofossils) of this well-core allowed us to identify changes in dominance and influence of coastal processes (fluvial-, wave- and tide) and shoreline evolution. Using this information, as well as the sediment supply and accommodation space ratio, we were able to distinguish three intervals from the bottom to the top of the siliciclastic succession: (i) middle-late Eocene?-early Oligocene, prograding, fluvial-dominated, wave- and tide-influenced coarse-grained deltas with amalgamation of hyperpycnal-dominated mouth bars with hyperconcentrated flow input, (ii) Oligocene, retrograding to prograding, hyperpycnal-dominated heterolithic delta deposits punctuated by transgressive pulses, and (iii) late Oligocene to Early Miocene, aggradational, coal-bearing fine-grained delta plain with a higher proportion of transgressive phases over the continental environment. The complete succession represents long-term (~14 Myr) mixed-energy nearshore siliciclastic systems, showing different lithological arrangements and sedimentation styles. A long-term evolution is observed from a middle-late Eocene? steep, short and coarse-grained sedimentary system with tropical humid lowland forest and punctual development of macrobenthic tracemaker communities (Interval I) to an Early Miocene gently (poorly drained), well-developed delta plain with mangroves and wave- and storm-influence record through trace fossils assemblages (Interval III). A combination of factors, including subsidence, relief uplifting, and possible relative sea level changes, are interpreted as the main controls on the stratigraphic evolution of sedimentary styles throughout the entire succession. Minor-order sedimentary successions into each interval (e.g., prograding distributary mouth-bar channel) revealed short-term cycles presumably controlled by an internal delta dynamic. Multidisciplinary analysis is essential for recognizing the influence of fluvial, wave, and tidal processes on tropical deltas, where high spatial and temporal variability makes it difficult to determine dominant processes for long periods of time.

Keywords. Fluvial/wave/tidal influence, Coarse-grained deltas, Hyperpycnal prodelta, Coal-bearing delta plain, Palynological analysis.

VIII.1. Introduction

The characterization of fluvial-, wave-, and tidal-dominated sedimentary successions in tropical regions has had broad attention in scientific and exploratory studies owing to the high sediment loads and their potential as reservoirs (e.g., Howell et al., 2008; Dalrymple et al., 2003; Shchepetkina et al., 2019, and references therein). The interplay of the fluvial, wave, and tidal processes over short spatial and temporal scales generates

a high variability of marine mixed shoreline systems observed from modern environments and outcrops (Yang et al., 2005; Rossi and Steel, 2016). To highlight the great variability and complexity of ancient mixed-process shoreline systems, classifications that use qualitative descriptors (dominated-, influenced-, affected-) of fluvial, wave, and tidal processes have often been used to characterize sedimentary deposits (Ainsworth et al., 2011). Alternative ways of characterizing the internal facies complexity include methods that quantify the likelihood that a deposit was formed by wave, tide, or fluvial processes on the basis of dominant sedimentary structures, texture, and bioturbation. This is especially useful in core data where 3D features of the sedimentary bodies (e.g., bed geometry) are difficult to observe (MacEachern et al., 2005; Bhattacharya, 2006; Wei et al., 2016; Rossi et al., 2017).

Nonetheless, although specific sedimentary environments within coastal successions have characteristic facies associations, their recognition should not be based only on physical structures; under certain depositional conditions, they can appear similar depending on the interactions of various parameters (MacEachern et al., 2005; Bhattacharya, 2006; Dalrymple and Choi, 2007; Ainsworth et al., 2011). For this reason, ichnological and micropaleontological analyses integrated into the detailed sedimentological description have become fundamental tools for interpreting such settings (Nagy, 1992; MacEachern et al., 2005; Gani et al., 2007; MacEachern and Bann, 2008, 2020; Slater et al., 2017; Chalabe et al., 2022), although studies integrating all three tools are scarce (e.g., MacEachern et al., 1999).

Ichnology is useful for paleoenvironmental interpretation because of the extreme sensitivity of tracemakers—their behavior, hence the generated structures—to specific environmental conditions (MacEachern et al., 2005; MacEachern and Bann, 2008). Although depositional systems are widely studied, a sound understanding of organism responses to the interplay of processes and environmental conditions operating in coastal depositional settings is still being developed (MacEachern and Bann, 2020 and references therein).

In addition to ichnology, the characterization of organic matter is key to deciphering the fluvial signal in mixed-energy coastal systems (Zavala et al., 2012). Macroscopic and microscopic vegetal remains (e. g., coal, wood fragments, leaves, pollen, and spores) are abundant components of fluvial-dominated deposits accumulated at the river mouth during flooding events (Slater et al., 2017). Analysis of palynomorphs, which are well preserved in hyperpycnal-dominated subaqueous delta subenvironments (e.g., prodelta), is important for reconstructing subaerial deltaic subenvironments (e.g., feeder system, upper delta plain, interdistributary bays). This information is highly useful in tropical or subtropical settings where coastal systems represent reservoirs of organic matter (Hoorn, 1994; Birgenheier et al., 2017).

Here we apply a multidisciplinary approach to a study of a ~700 m-thick middle-late Eocene to Early Miocene well-core in a tropical basin (Colombian Caribbean onshore region, Fig. VIII.1), to reconstruct dominant processes of sedimentation and depositional environments evolution in mixed-energy coastal systems. The Oligocene-Miocene coastal systems of the Colombian Caribbean have been extensively studied because some of their deposits are proven hydrocarbon reservoirs (Flinch, 2003). Nonetheless, published data from sedimentological, ichnological and micropaleontological studies for detailed paleoenvironmental purposes of this time interval are still in their early stages. Accordingly, the objectives of this paper are: (a) to document tracemaker-substrate interactions to establish the paleoenvironmental (depositional and ecological) variations

in the coastal systems occurred from the middle-late Eocene? to Early Miocene in the Colombian Caribbean; and (b) to discuss paleogeographical implications supported by previous regional models.

VIII.2. Geological setting

The ongoing interaction of the Caribbean Plate against the NW margin of South America has influenced the sedimentation of the Colombian Caribbean basins since the Cretaceous (Montes et al., 2019; Mora-Páez et al., 2019; Romito and Mann, 2020). GPS and seismic data have shown that coeval oblique convergence of NW South America and the Caribbean from the Upper Cretaceous to the lower Eocene, nearly orthogonally convergence from the Oligocene until today (Mora-Bohórquez et al., 2020 and references contained herein). The Sinú-San Jacinto Basin (SSJB) of northern Colombia (Fig. VIII.1A) is considered a forearc basin with an oceanic igneous basement of Cretaceous age (Geotec, 2003; Guzmán, 2007; Bermúdez et al., 2009; Silva-Arias et al., 2016; Mora et al., 2017). Its sedimentary fill includes rocks from the Upper Cretaceous to Pleistocene with several unconformities and variations in accommodation space linked to the multi-stage tectonic interaction of the Caribbean and South American plates (Mantilla-Pimiento et al., 2009; Noda, 2016; Mora et al., 2017, 2018; Montes et al., 2019; Pardo-Trujillo et al., 2020). Tectonic evolution of the Colombian Caribbean has generated a folded belt with a current SW-NE direction, which exposes the Upper Cretaceous to the Pliocene-Pleistocene rocks of the basin at the surface in what is now referred to as the San Jacinto Fold Belt (SJFB; Fig. VIII.1A).

The ANH-SSJ-Nueva Esperanza-1X stratigraphic well-core drilled deposits in the San Jacinto Fold Belt associated with the Ciénaga de Oro Formation (COF) (Gómez et al., 2015) and possibly with the San Jacinto Formation, owing to interest as hydrocarbon reservoirs (Fig. VIII.1B) (Flinch, 2003). Even though the tectonic evolution of the continental margin and its relationship with sedimentary environments is still a matter of debate, there is a consensus that the COF was deposited in shallow marine and deltaic systems with dominant fluvial processes favoring the development of mangrove areas and accumulations of coal beds in the SW Colombian Caribbean (Dueñas and Duque-Caro, 1981; Dueñas, 1983, 1986; Guzmán et al., 2004; Bermúdez et al., 2009; Bermúdez, 2016; Manco-Garcés et al., 2020; Celis et al., 2021). Dueñas (1980, 1983, 1986) and Guzmán et al. (2004) assigned a late Eocene to Early Miocene age to the COF based on palynological and foraminiferal biostratigraphic studies. Dueñas (1983) concluded that the coastal mangrove areas during the Oligocene were affected by sea-level variations. Their carbonaceous content could correlate with the Amagá Formation outcropping in the Amagá sub-basin in the Cauca depression in central Colombia.

The stratigraphic relationship of the COF to the overlying and underlying units in the south-southwest of the SJFB is not yet clearly established. In this part of the basin, rocks of this unit crop out in unconformable contact on rocks possibly associated with the Paleocene- Eocene San Cayetano Formation (Dueñas and Duque-Caro, 1981; Dueñas, 1983, 1986; Mora et al., 2017). However, based on the compilation of unpublished information from the hydrocarbon industry, some outcrop studies from the central and central-northeastern regions of the SJFB (Guzmán et al., 2004; Raigosa, 2018; SGC, 2019; Salazar-Ortiz et al., 2020), and the results obtained in this work, we suggest that in the southern part of the basin there are two formations underlying the COF in addition to the San Cayetano Formation (Fig. VIII.1B): the San Jacinto Formation consisting of conglomerates,

sandstones, and sandy siltstones of late Eocene to early Oligocene age (Duque-Caro, 1972; Duque-Caro et al., 1996; SGC, 2019), and the Toluviejo Formation with bioclastic limestones from the upper Eocene (Guzmán et al., 2004; Raigosa, 2018). Mora et al. (2018), using seismic data, suggested that an Early to Middle Miocene unconformity (LMU) divides the COF. However, in some sectors of the basin, this unconformity has not been identified. The COF is overlain by marine siltstones and, in a lesser proportion, sandstones corresponding to the Porquera Formation accumulated during the Early-Middle to Late Miocene (Guzmán, 2007; Mora et al., 2017).

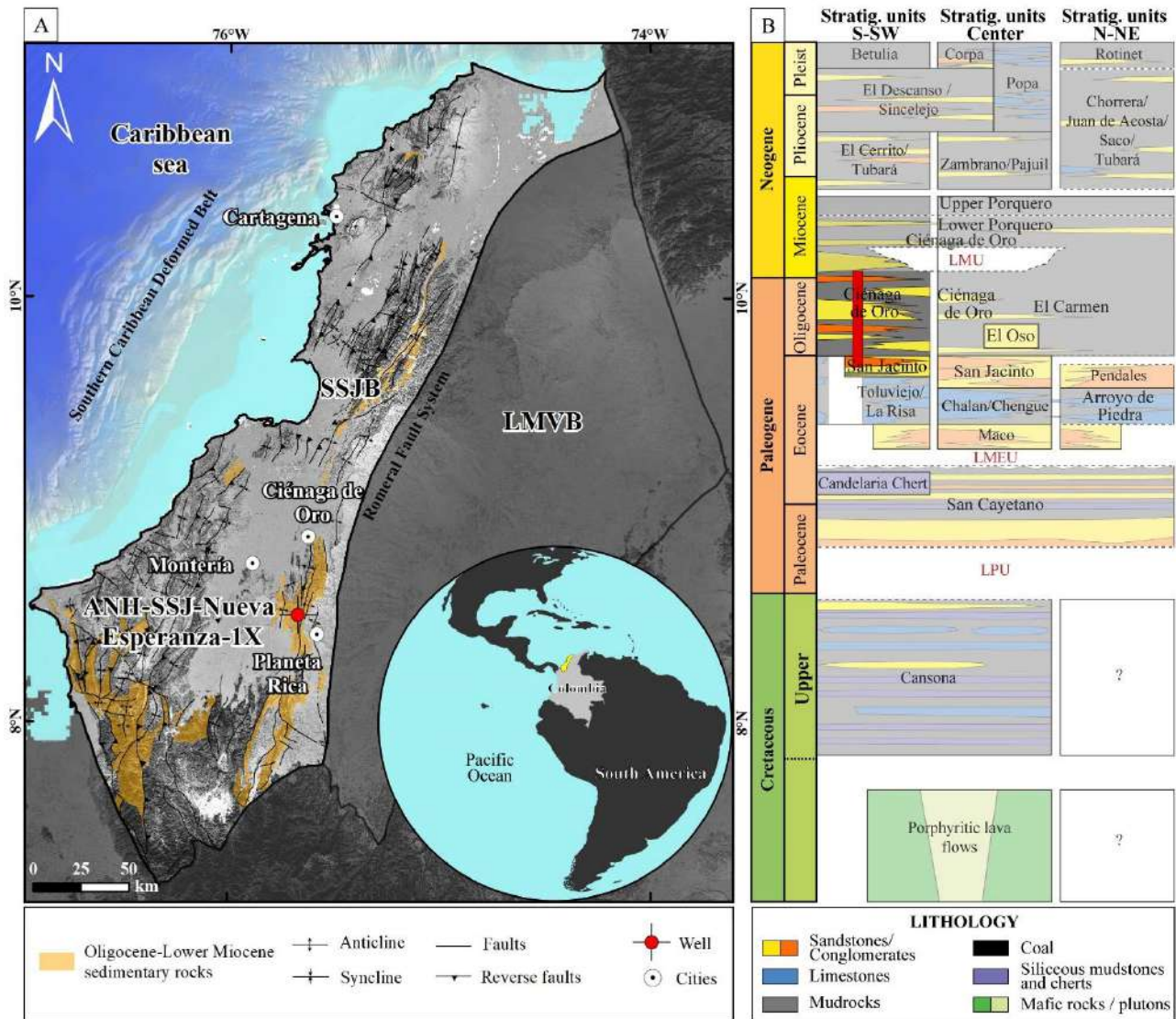


Fig. VIII.1. A. Location of Colombia in South America (yellow polygon for the SSJB) and location of the SSJB in the Colombian Caribbean. Only Oligocene-Lower Miocene deposits are indicated in the SSJB (Source: WGS-1984 coordinate system; CIOH, SRTM, NOAA elevation, and ocean models; geology from Gómez et al., 2015). **B.** Schematic chronostratigraphic chart of the SJFB (modified from Mora et al., 2017, 2018; Osorio-Granada et al., 2020). LPU: lower Paleocene unconformity; LMEU: lower-middle Eocene unconformity; LMU: lower Miocene unconformity. Red bar: cored section.

VIII.3. Materials and methods

The studied cored section corresponds to the ANH-SSJ-Nueva Esperanza-1X stratigraphic well (~691 m in thickness) drilled in the south-western zone of the SJFB (Fig. VIII.1). The new specific data and the well-

established chronostratigraphic framework presented in this study have made it possible to specify the depositional models based on an earlier study that was published in this journal (Celis et al., 2021). Detailed logging (scale 1:5) considered the lithology (texture: grain size, sorting, roundness, sphericity), bed thickness and contact types, fossil content, and sedimentary structures (physical, biogenic, and chemical). Mudrocks refer to rocks with grain size $<1/16$ mm, and claystones to those where the $<1/256$ mm fraction was recognized (Wentworth, 1922). For textural and compositional information about mixed rocks, we followed the proposal of Mount (1985), modifying the allochemic term to bioclastic, because the mixed rocks often consist of fragments of broken shells and extraclasts. Additionally, the conglomerate grain-size was included in this nomenclature. In that sense, the terms conglomerate, sandstone, or mudrock refer to the grain-size of the terrigenous portion, and the term bioclastic refers to the bioclastic material independent of the grain-size of the bioclasts. Facies codes were assigned following Reading (1996) and Collinson and Mountney (2019), based on lithology and sedimentary structures.

Bed thickness was classified as very thin (<1 cm), thin (1–10 cm), medium (11–30 cm), thick (31–100 cm), and very thick (>100 cm) (Nichols, 2009 and references therein). Detailed ichnological analyses were conducted, including major ichnological attributes such as ichnodiversity, distribution, abundance (Bioturbation Index BI *sensu* Taylor and Goldring, 1993) of the structures and their relationship with the facies and stratigraphic surfaces. We used an ichnological atlas on core images (Frey and Pemberton, 1985; Gerard and Bromley, 2008; Knaust, 2017) to make ichnotaxonomic assignments of trace fossils based on the overall shape and the presence of specific diagnostic criteria or ichnotaxobases (Bromley, 1996; Bertling et al., 2006). Due to core limitations, ichnotaxonomic classification was made to the ichnogenus level (Bromley, 1996). Although the well-core was not slabbed, only ichnotaxa that could be confidently identified by ichnotaxonomic features were considered in the analysis. Those that posed any doubts were marked with a question mark and used with caution in the interpretations.

To undertake a detailed analysis of a complex environment, such as coastal settings, in which different processes are interrelated (e.g., fluvial, tidal, and waves), we follow the nomenclature used by MacEachern et al. (2005) and Bhattacharya (2006) for paleoenvironmental zonation. Sampling was carried out in mudrocks lithologies. Micropaleontological analyses (of palynomorphs, foraminifera, calcareous nannoplankton) were conducted for biostratigraphic and paleoenvironmental purposes. A total of 72 palynological samples were treated using the standard technique described by Traverse (2007). Slides were scanned using a high-resolution Nikon Eclipse 80i microscope at 40x and 100x magnification. Abundance of each sample was estimated by counting palynomorphs up to 300 specimens as far as possible and then assigned to the following categories: 1) barren: no palynomorphs recorded; 2) moderate to scarce: 1–200 palynomorphs; and 3) abundant: >200 palynomorphs. The palynological age model relied on the Cenozoic zonation of Jaramillo et al. (2011). The palynomorphs were grouped by botanical affinities and ecological significance, with the sum of the groups totaling 100%. The ecological assignments were based on Hoorn (1994), Jaramillo et al. (2010), Pardo-Trujillo and Jaramillo (2014), and D’Apolito et al. (2021). Thermal maturation estimations were made using Pearson’s (1984) color chart correlated with corresponding Thermal Alteration Index (TAI) values, as illustrated in Traverse (2007).

The preparation of 71 foraminiferal samples follows the methodology of Thomas and Murney (1985). Samples were wet washed using a 63 µm and 125 µm mesh sieve. This fraction was analyzed under a high-resolution Nikon PET SMZ1500 optical stereomicroscope. The photographs were taken using the ESEM-Quanta 250 and the mini-sputtering technique. Abundances, based on the total of foraminifera per gram of sediment (f/g), were categorized as very abundant (VA): >150 f/g, abundant (A): 70–150 f/g, common (C): 30–70 f/g, rare (R): 1–30 f/g, and barren (B): no recovery. Preservation was defined in terms of poor, moderate, and good. Taxonomic criteria follow Wade et al. (2018), and planktonic foraminiferal zonation follows Wade et al. (2011). Seventy-one calcareous nannofossil slides were prepared after applying the smear slide technique, then analyzed under a petrographic microscope Nikon Eclipse LV100 optical microscope at 1000x coupled with a high-resolution Nikon DS-F11 camera. Calcareous nannofossils were quantified by counting up to 500 specimens per sample or, in cases of very rare nannofossils, up to a total of 500 fields of view. Preservation was qualitatively evaluated as follows: poor (1): recrystallized and/or dissolved specimens, preventing taxonomic classification; moderate (2): slight dissolution and/or recrystallization that does not preclude species identification, although some diagnostic characteristics have been affected; and good (3): little evidence of dissolution and/or regrowth, the morphology of the specimen is clear. Classification of calcareous nannofossils was based on usual taxonomic concepts and catalogues (Perch-Nielsen, 1985; Bown, 1998; Young et al., 2003, 2017; Aubry, 2014a, 2014b, 2015b, 2015a, 2021). Biostratigraphic information of this group followed the biozonation of Martini (1971). Chronostratigraphic assignments relied on the International Chronostratigraphic Chart (Cohen et al., 2013) and nomenclature formally established by the Subcommissions of the International Commission on Stratigraphy (<http://stratigraphy.org/subcommissions>).

VIII.4. Results

VIII.4.1. Biostratigraphy

Biostratigraphy in the ANH-SSJ-Nueva Esperanza-1X core section is based on palynomorphs, planktonic foraminifera, and calcareous nannofossils (Figs. VIII.2 and VIII.3). The preservation of palynomorphs is moderate to good, and the abundance ranges from low to very abundant. The thermal alteration index based on the color of spores suggests immature rocks (TAI: 2 to 2+). Planktonic foraminifera and calcareous nannofossils are scarce and poorly to moderately preserved. Benthic foraminifera are nearly absent and poorly preserved, and, therefore, they could not be recognized even at the genus level and were not used as paleoenvironmental indicators.

According to the stratigraphic distribution, microfossil abundance patterns, and the presence of some key taxa, the cored section can be divided into three intervals, from base to top (Figs. VIII.2 and VIII.3).

Interval 1 at the base of the core (~690 m–~625 m) is characterized by the exclusive recovery of palynomorphs that include *Perisyncolporites pokorny* and *Polypodiisporites usmensis*. The assemblage indicates an age younger than or equal to the middle Eocene, and constraints the top of interval 1 to younger than or equal to the late Eocene (Figs. VIII.2 and VIII.3), T06 to T07 zones of Jaramillo et al. (2011). No marine microfossils were found.

Interval 2 (~623–~164 m) is characterized by a palynological assemblage consisting of *Bombacacidites echinatus*, *Cicatricosisporites dorogensis*, *Crassiectoapertites columbianus*, *Magnaperiporites spinosus*,

Magnastriatites grandiosus, *Psilatricolporites pachydermatus*, *Rhoipites planipolaris* and *Spinizonocolpites echinatus*, indicating a biozonal range from T08 to T11, restricted to the Oligocene (Jaramillo et al., 2011). Planktonic foraminifera identified at ~533 m consist of *Catapsydrax unicavus*, *Ciperoella anguliofficialis*, *C. angulisuturalis*, *C. ciperoensis*, *Globorotaloides hexagonus*, *G. variabilis*, *Globoturborotalita bassriverensis*, *G. gnaucki*, *G. ouachitaensis*, *G. pseudopraebulloides*, *G. woodi*, *Tenuitella angustiumbilitata*, *Turborotalita praequinqueloba*, *Paragloborotalia nana*, and *Subbotina eocaena*. These taxa coexisted in biozone O4 of Wade et al. (2011) from the younger part of the early Oligocene. Calcareous nannofossils consist of abundant *Cyclicargolithus abisectus*, *Cyclicargolithus floridanus*, *Coccolithus pelagicus*, *Discoaster deflandrei*, *Reticulofenestra* spp., and *Sphenolithus* spp., and sporadic *Reticulofenestra bisecta*. Among them, *C. abisectus*, observed from ~526 to ~433 m, indicates a biozonal interval from NP23 to NN1 (Martini, 1971) whose age range is from Oligocene to the earliest Miocene (Perch-Nielsen, 1985; Backman et al., 2012; Agnini et al., 2014). Although *R. bisecta* was observed only at ~526 m, this species became extinct in the late Oligocene (Perch-Nielsen, 1985; Backman et al., 2012; Agnini et al., 2014), supporting a Paleogene age for this interval. These considerations of interval 2 indicate that interval 1 is neither older than middle-late Eocene? Nor younger than early Oligocene age.

Interval 3 from ~164 m to ~5 m, yielded the palynomorphs *Bombacacidites gonzalezii*, *Bombacacidites muinaneorum*, *Cyclusphaera scabrata*, *Nijssenosporites fossulatus*, and *Proteacidites triangulatus* indicating the Early Miocene (T12 palynologic zone). The occurrence of *Bombacacidites echinatus*, *Cicatricosisporites dorogensis*, and *Spinizonocolpites echinatus*, is interpreted as a consequence of reworking from Paleogene beds. Toward the top of the well-core (~15 m–~18 m), planktonic foraminifera *Paragloborotalia continuosa*, *Tenuitella angustiumbilitata*, *Globoturborotalita woodi*, *G. pseudopraebulloides*, *G. ouachitaensis*, *G. gnaucki*, *Globorotalia bella*, and *Globigerina bulloides* indicate M1b-M5 biozones, spanning the Early to Middle Miocene (Figs. VIII.2 and VIII.3). The occurrence of *G. gnaucki* reveals reworking from the lower Oligocene beds. New taxa of calcareous nannofossils such as *Helicosphaera euphratis*, *H. vedderi*, *H. truempyi*, *Umbilicosphaera jafari*, and *Sphenolithus conicus* are registered. The occurrence of *H. vedderi* and *H. truempyi*, between 164 m and ~8 m, indicates biozone NN2 (Young, 1998; Boesiger et al., 2017), supporting an Early Miocene age. Moreover, calcareous nannofossil taxa similar to those of the previous interval are recorded, providing evidence of reworking of Oligocene marine deposits in the third interval.

VIII.4.2. Palynomorph groups with ecological significance

The groups of palynomorphs observed were classified according to their taxonomic affinities: pteridophyte spores, undifferentiated angiosperm pollen, lowland forest, palmae, morichal palmae, mangroves, fungal remnants, and marine palynomorphs (Fig. VIII.4; SM VII.1). In general, the palynological record indicates humid tropical lowland forests. High concentrations of fungal remnants suggest high humidity, and the common record of moriche palms points to typical flooded zones along riverbanks. Mangrove pollen indicate areas near the coast.

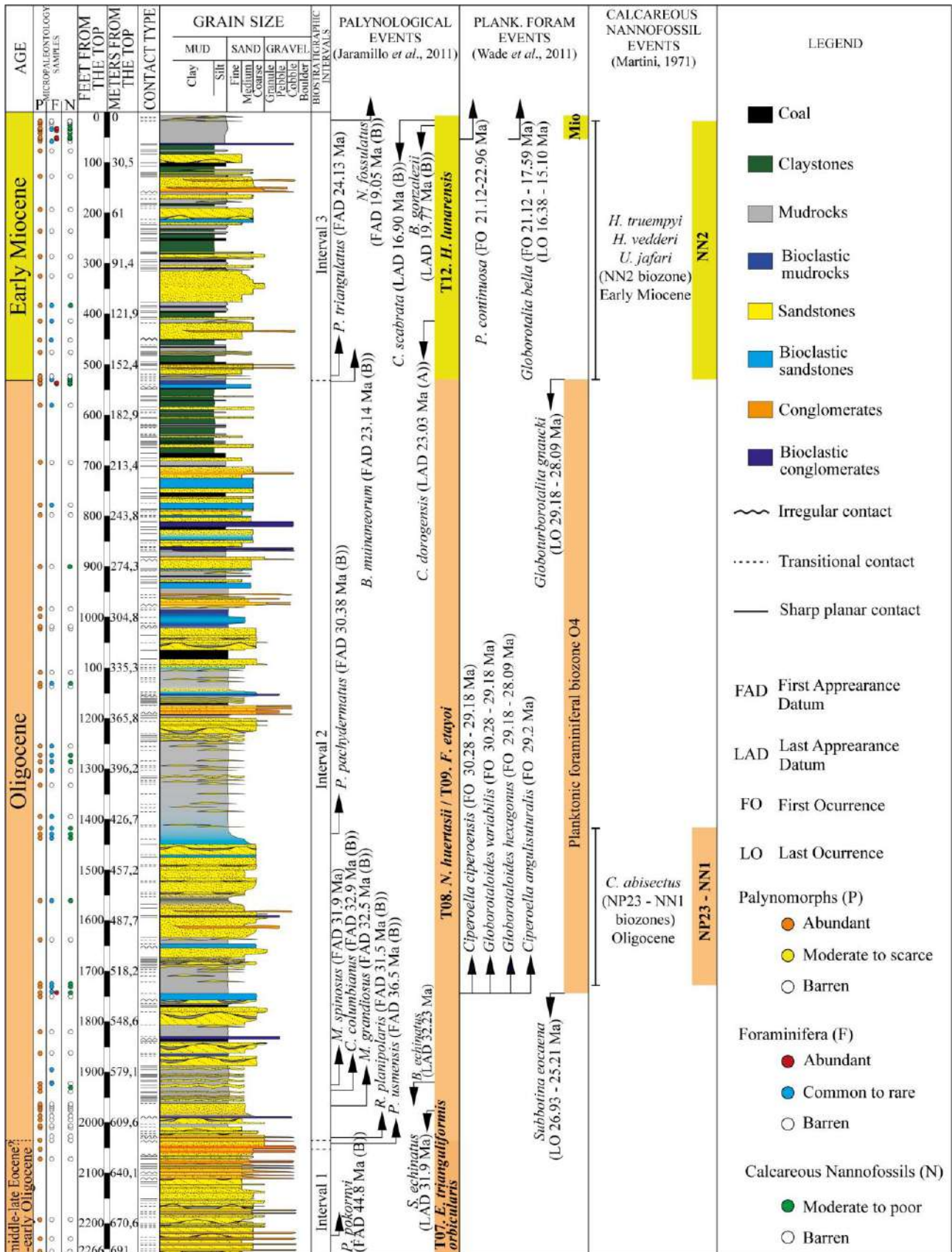


Fig. VIII.2. Age, biostratigraphic samples distribution, stratigraphic log, and bioevents found in the ANH-SSJ-Nueva Esperanza-1X stratigraphic well.

Marine palynomorphs can be useful for identifying relative variations in the sea level. Interval I, the lower portion of the section (between ~690 m and ~625 m) is characterized by abundant pollen and spores (~25%–~30% on average), some of them of lowland forests (~10%–~50%) (Fig. VIII.4; SM VIII.1). In addition, fungal remains (~10%) are identified (Fig. VIII.4; SM VIII.1). Local variation in abundance is significant, however; the lowland forest component varies from 10% to ~50% and abundance of fungal remnants varies from ~10% to ~53%. In Interval 2 (from ~614 m), we found a decrease in pollen and spores (~20%–~25% on average) and abundances of lowland forest similar to those in the previous interval (~25%). Local increases in fungal remnants of up to 50% are seen mainly in this interval (~50%) (Fig. VIII.4). Palynomorphs of palmae show very low recovery in the section (~1% on average). Instead, morichal palm forest becomes evident—an ecological group that varies only slightly throughout the studied section (~10% on average), although it shows a slight increase in the middle-upper part (~15% on average) (from ~350 to ~91 m) (Fig. VIII.4; SM VIII.1). Interval three sees a gradual increase in marine palynomorphs such as dinoflagellate cysts and foraminiferal organic linings (~2% on average, and an increase to ~11% at the top; from ~164 m) (Fig. VIII.4; SM VIII.1). Similarly, an increase in *Zonocostites* and *Lanagiopollis crassa*, which are associated with mangrove ecosystems, is observed at ~176 m (~30%). However, mangrove palynomorphs are particularly rare along the entire record (~1% on average). The average abundance of spores, pollen, and lowland forest is maintained.

VIII.4.3. Facies associations analysis

Twenty-eight sedimentary facies were defined throughout the ANH-SSJ-Nueva Esperanza-1X stratigraphic cored section (Table VIII.1) (see Celis et al., 2021 for a previous detailed study of some of them). The recognized lithofacies have been grouped into 12 facies associations (FA; Table VIII.2) described below (Table VIII.3).

Table VIII.1. Sedimentary facies identified in the ANH-SSJ-Nueva Esperanza-1X well-core.

| Facies Code | Lithology and sedimentary structures | Components and texture (Note: also include microfossil content) | Ichnology | Bed/set thickness (cm) |
|-------------|---|--|---------------------------------|------------------------|
| Gmm | Massive matrix-supported massive conglomerates | - Matrix: fine- to medium-grained sandstone. - Clasts: granule-size and a lesser extent, pebble-size. Quartz; feldspars in less proportion; metamorphic lithic occasionally. Sub-rounded to rounded and low sphericity. - Moderately to poorly sorted; occasionally well sorted. | BI=0-3; <i>Ophiomorpha</i> . | 5 - 150 |
| Gcm | Massive clast-supported massive conglomerates | - Clasts: granule-size and a lesser extent, pebble-size. Quartz; feldspars in less proportion. Sub-rounded to rounded and low sphericity. - Moderately to poorly sorted. - Matrix: fine-grained sandstone. | | 5 – 20 |
| Gng | Normally graded, matrix-supported conglomerates to sandstones | - Matrix: fine-grained sandstone. - Conglomerates: granule-sized and a lesser extent, pebble-sized clasts. Quartz; feldspars in less proportion. Sub-rounded to rounded and high sphericity. Moderately sorted. to - Sandstones: coarse- to medium-grained, mainly quartz. | BI=0-3; <i>Ophiomorpha</i> . | 5 - 80 |

| Facies Code | Lithology and sedimentary structures | Components and texture (Note: also include microfossil content) | Ichnology | Bed/set thickness (cm) |
|-------------|--|---|--|------------------------|
| Sig | Inversely graded sandstones, conglomeratic sandstone to matrix-supported conglomerates | - Sandstones: coarse- to medium-grained, mainly quartz. to - Matrix: fine-grained sandstone. - Conglomerates: granule-sized and a lesser extent, pebble-sized clasts. Quartz and feldspars. Sub-rounded to rounded and high sphericity. Moderately to poorly sorted. | | 5 - 60 |
| Sng | Normally graded sandstones | Medium- to coarse-grained to fine and very fine-grained. Quartz; feldspars in less proportion. Moderately to poor sorted. | BI=0-3; <i>Ophiomorpha</i> . | 5 - 60 |
| Sm | Massive sandstones | Fine- to coarse-grained. Quartz; feldspars and metamorphic lithics in less proportion. Moderately to well sorted. | BI=0-6; <i>Dactyloidites</i> , <i>Macaronichnus</i> , <i>Ophiomorpha</i> , <i>Siphonichnus</i> . | 5 - 200 |
| Sh | Horizontal laminated sandstones | Fine- to medium-grained. Quartz; feldspars in less proportion. Well sorted. | BI=0-4; <i>Conichnus</i> , <i>Cylindrichnus</i> , <i>Dactyloidites</i> , <i>Macaronichnus</i> , <i>Ophiomorpha</i> , <i>Skolithos</i> , <i>Thalassinoides</i> , rhizoliths. | 5 - 60 |
| Sa | Low-angle cross-bedded sandstones | Fine- to medium-grained. Quartz; feldspars in less proportion. Well sorted. | BI=0-3; <i>Dactyloidites</i> , <i>Ophiomorpha</i> . | 5 - 30 |
| Sp | Planar cross-bedded sandstones | Fine- to medium-coarse-grained Quartz; feldspars in less proportion. Moderately to well sorted. | BI=0-3; <i>Ophiomorpha</i> , <i>Skolithos</i> . | 5 - 60 |
| St | Trough cross-bedded sandstones | Fine- to medium-grained Quartz; feldspars in less proportion. Moderately to well sorted. | BI=0-2; <i>Ophiomorpha</i> . | 5 - 30 |
| Sr | Sandstones with asymmetric ripple cross-lamination | Fine- to medium-grained. Quartz; feldspars in less proportion. Moderately to well sorted. | BI=0-1; <i>Teichichnus</i> . | <5 |
| Sw | Sandstones with symmetric ripple cross-lamination | Fine- to medium-grained. Quartz; feldspars in less proportion. Well sorted. | BI=0-2; <i>Teichichnus</i> . | <5 |
| Sc | Sandstones with soft-sediment deformation structure | Fine- to medium-grained. Quartz; feldspars in less proportion. Moderately to poor sorted. | | 5 - 30 |
| Shcs | Sandstones with hummocky cross-stratification | Fine- to medium-grained. Quartz; feldspars in less proportion. Well sorted. | | 2 - 10 |
| Ss | Sandstones with swaley cross-stratification | Fine- to medium-grained. Quartz; feldspars in less proportion. Well sorted | | 2 - 10 |
| Htf | Heterolithic mudstone-sandstone alternation with flaser bedding | - Sandstones: Fine-grained, and occasionally medium- to coarse-grained. Quartz and feldspars. Moderately to well sorted. | BI=0-4; <i>Conichnus</i> , <i>Cylindrichnus</i> , <i>Dactyloidites</i> , <i>Macaronichnus</i> , <i>Ophiomorpha</i> , <i>Skolithos</i> , <i>Thalassinoides</i> , rhizoliths. | 5 - 60 |
| Htw | Heterolithic mudstone-sandstone alternation with wavy bedding | - Sandstones: Fine-grained. Quartz and feldspars. Moderately to well sorted. | BI=0-2; <i>Skolithos</i> and <i>Ophiomorpha</i> . | 5 - 30 |
| Htl | Heterolithic mudstone-sandstone alternation with lenticular bedding | - Sandstones: Fine-grained. Quartz and feldspars. Moderately sorted. | BI=0-2; <i>Taenidium</i> , <i>Teichichnus</i> . | 5 - 3000 |
| Slc, Sf | Load casts and flame structures in sandstones, conglomerates, and mudrocks | Occur at the bases of Gmm, Gcm, Gng, Sm, Sh, Mm. | | <5 |

| Facies Code | Lithology and sedimentary structures | Components and texture (Note: also include microfossil content) | Ichnology | Bed/set thickness (cm) |
|-------------|--------------------------------------|--|--|------------------------|
| Mm | Massive mudrocks | | BI=0-6; <i>Phycosiphon</i> , rhizoliths. | 5 - 300 |
| Mh | Horizontal laminated mudrocks | | BI=0-2; <i>Teichichmus</i> . | 5 - 500 |
| Ms | Mudrocks with syneresis cracks | | | <5 |
| Cm | Claystones | | BI=0-1; rhizoliths. | 5 - 150 |
| Col | Laminated coal | | BI=0-3; <i>Thalassinoides</i> . | 10 - 100 |
| Com | Massive coal | | | 10 - 20 |
| Gbm | Massive bioclastic conglomerates | - Terrigenous grains: granule size, quartz. Poor sorted. - Bioclastic grains: granule- and pebble size, bivalves and gastropod, moderately sorted. - Matrix: fine- to medium- grained. Quartz, feldspars, and micrite. | BI=0-2; <i>Ophiomorpha</i> . | 10 - 200 |
| Sbm | Massive bioclastic sandstones | - Terrigenous grains: fine- to medium-grained, quartz, moderately sorted. - Bioclastic grains: granule-sized, bivalves and gastropods, moderately to poorly sorted. | BI=0-3; <i>Ophiomorpha</i> . | 10 - 300 |
| Mbm | Bioclastic mudrocks | - Bioclastic grains: granule-sized, bivalves and gastropods, moderately to poorly sorted. | BI=0-3; <i>Ophiomorpha</i> . | 10 - 300 |

VIII.4.3.1. Facies association 1 (FA1)

Description. FA1 presents thick beds up to 8 m thick (commonly 3–4 m thickness) of structureless bioclastic deposits (bioclastic sandstones, Sbm; bioclastic conglomerates, Gbm; bioclastic mudrocks, Mbm). Allochemical components are represented by fossils (bivalves, gastropods [*Aclis* spp., *Turritella* spp.], scaphopod fragments, indeterminate shells and shell hash), which are frequently randomly distributed, and in lesser proportion by muddy intraclasts (Fig. VIII.5A-B; Table VIII.3). The contact with the underlying bed (coal or mudrocks) is irregular and bioturbated by *Thalassinoides* (BI = 0–3). Occasionally and transitionally to the top, these lithologies present a decrease in shells and are bioturbated by *Ophiomorpha* in the upper part of the bioclastic deposits (e.g., ~223 m). To the top, FA1 exhibits transitional variation to FA2 (fluvial-dominated prodelta) or FA3 (mixed prodelta).

Interpretation. *Transgressive lag.* The bases of these deposits are irregular, over coal and mudrock beds (FA10), reflecting an erosive process. Bioclastic sediments (Sbm, Gbm, Mbm) and shell hash distributed randomly (FA1) suggest rapid transgressive pulses, or storms (Savrda et al., 1993; Schultz et al., 2020). The bases are invariably bioturbated by *Thalassinoides* in coal and mudrock beds, which could be attributed to bioturbation in a firmground associated with *Glossifungites* ichnofacies (Pemberton et al., 1992, 2004; MacEachern et al., 2007a, 2007b). The decrease in the accumulation of random shells and softground bioturbation represented by *Ophiomorpha* suggest colonization of the substrate during a period of decreasing energy towards the top of the bioclastic deposits, allowing the establishment of a macrobenthic community.

This FA represents a transition to deeper-water deposits, during delta-lobe abandonment, drowning of the river-dominated delta plain, or a wave-dominated strandplain (Cattaneo and Steel, 2003; Buatois et al., 2012).

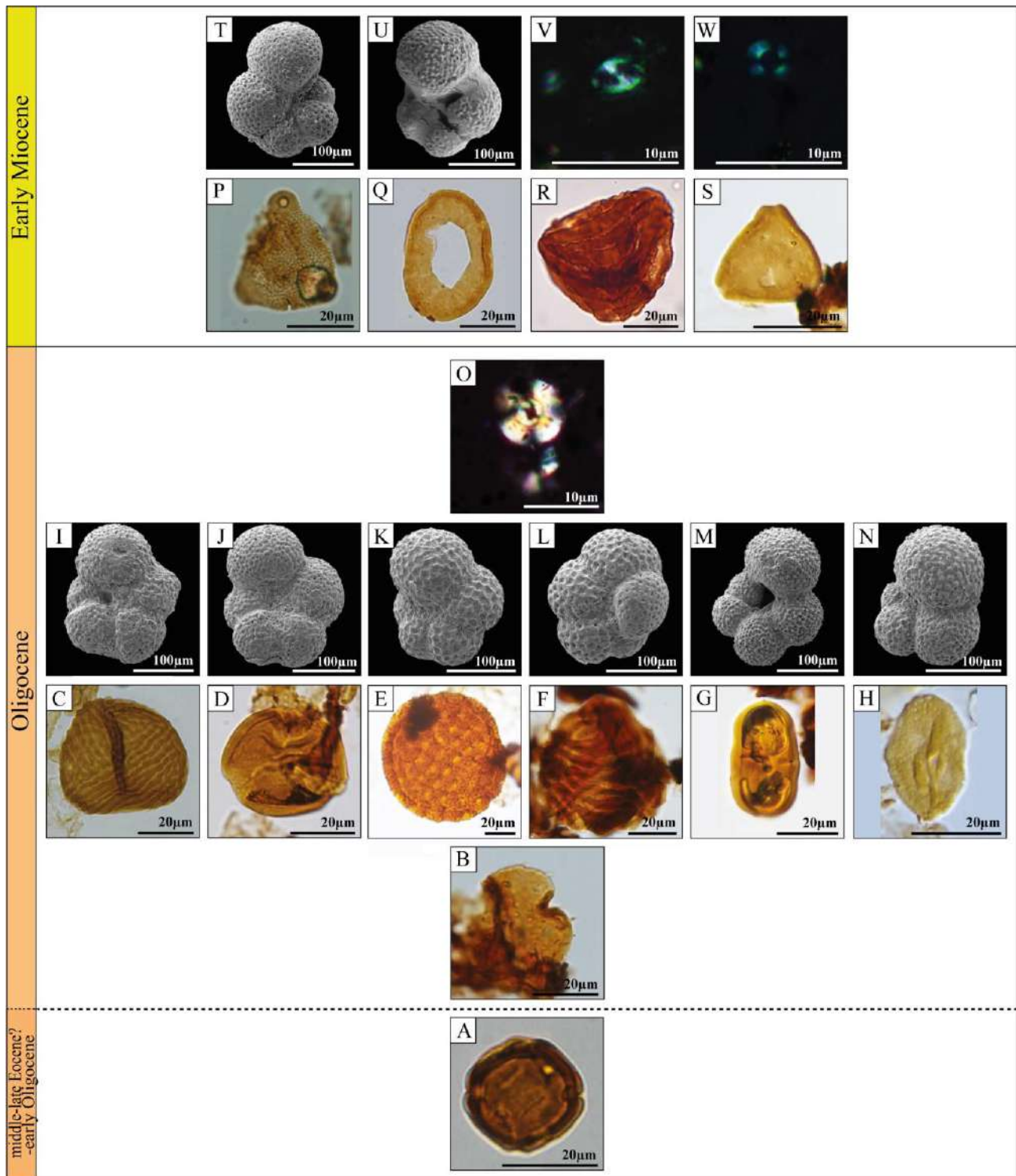


Fig. VIII.3. Some micropaleontological key taxa. **Interval 1. Palynomorphs:** A. *Perisyncolporites pokornyi*. **Interval 2. Palynomorphs:** B. *Bombacacidites echinatus*. C. *Cicatricosisporites dorogensis*. D. *Crassiectoapertites columbianus*. E. *Magnaperiporites spinosus*. F. *Magnastriatites grandiosus*. G. *Psilatricolporites pachydermatus*. H. *Rhoipites planipolaris*. **Foraminifera:** I. *Ciperoella angulisuturalis*. J. *C. ciperoensis*. K. *Globorotaloides hexagonus*. L. *G. variabilis*. M. *Globoturborotalita gnaucki*. N. *Subbotina eocaena*. **Calcareous nannofossil:** O. *Cyclicargolithus abisectus*. **Interval 3. Palynomorphs:** P. *B. muinaneorum*. Q. *Cyclusphaera scabrata*. R. *Nijssenosporites fossulatus*. S. *Proteacidites triangulatus*. **Foraminifera:** T. *Globorotalia bella*. U. *Paragloborotalia continua*. **Calcareous nannofossil:** V. *Helicosphaera vedderi*. W. *Umbilicosphaera jafari*.

VIII.4.3.2. Facies association 2 (FA2)

Description. FA2 presents thick beds (31–100 cm) resulting in successions up to 45 m thick of mudrocks and sandy mudrocks, structureless (Mm) or with horizontal lamination (Mh); it has a low bioturbation index (BI = 0–1) and is associated with *Planolites* and locally exclusive and abundant *Phycosiphon* (BI = 4–5; Fig. VIII.5C-D). Further, we recovered some calcareous nannofossils and foraminifera (Table VIII.3). Occasionally, there are very fine-grained sandy mudrocks with normal grading to mudrocks (Sng), as well as palynomorphs (Fig. VIII.5C; Table VIII.3). These deposits vary transitionally to intercalations of thick beds of mudrocks and very fine-to fine-grained sandstones with horizontal lamination (Mh, Sh), or with massive structure (Mm, Sm), or with asymmetrical ripple lamination (Sr); they are characterized by low bioturbation indexes (BI = 0–2) related to *Teichichnus* and *Thalassinoides*, by syneresis cracks (Ms), siderite nodules, and organic debris, and by an absence of marine calcareous microfossils (Fig. VIII.5D; Table VIII.3). FA2 (fluvial-dominated prodelta) presents a gradual transition to FA4 (fluvial-dominated distal delta front).

Interpretation. *Fluvial-dominated prodelta.* The record of Mm and marine calcareous microfossils and the low bioturbation (BI = 0–1; *Planolites*) are interpreted as sediments deposited by low-energy suspension fallout of fine-grained sediments during fair-weather conditions in offshore environments with low oxygenation or benthic food availability. However, the occasional occurrence of Sng and the recovery of palynomorphs could be related to seasonal muddy hyperpycnal flows originating at the river mouth during floods/torrential rains and moving a volume of clastic sediments farther prodelta/offshore (Lamb and Mohrig, 2009; Zavala et al., 2016; Zavala, 2020; Chalabe et al., 2022). The presence of *Phycosiphon* (BI = 4–5) thus reveals an eventual increase in benthic food and oxygen linked to the variable area influenced by hyperpycnal flows. The transition toward the top to Mm, Sm, Mh, Sh, and Sr, with *Teichichnus* and *Thalassinoides*, is interpreted as deposited from dilute river-derived turbidity currents (hyperpycnal flows) with organic debris transported in suspension. The low diversity of trace fossils, high content in palynomorphs, syneresis cracks, and siderite nodules reveal salinity fluctuations associated with freshwater fluvial domination (MacEachern et al., 2005).

VIII.4.3.3. Facies association 3 (FA3)

Description. FA3 is recognized by thick beds (31–100 cm) of structureless mudrocks (Mm), as well as intercalations of mudrocks and fine-grained sandstones occasionally with symmetric ripple lamination (Sw). Horizontally laminated mudrocks (Mh) interbedded with medium to thick beds of structureless sandy mudrocks (Sm), and fine-grained sandstones with horizontal lamination (Sh) also are observed. Moreover, there are scarce fine-grained sandstones with micro-hummocky cross-stratification (Shcs), micro-swaley cross-stratification (Ss), and soft-sediment deformation structure (Sc). These successions reach up to ~15 m thick. The bioturbation index ranges goes from low to moderate (BI = 0–4) with *Ophiomorpha*, *Planolites*, *Siphonichnus*, *Teichichnus*, and *Thalassinoides*. Also recognized in this facies is a high abundance of dinoflagellates and foraminifera, and moderate abundance of calcareous nannofossils. Fragments of bivalves, gastropods, and shell hash also occur (Fig. VIII.5E-F; Table VIII.3). FA3 (mixed prodelta) shows a transitional gradation to FA5 (mixed distal delta front).

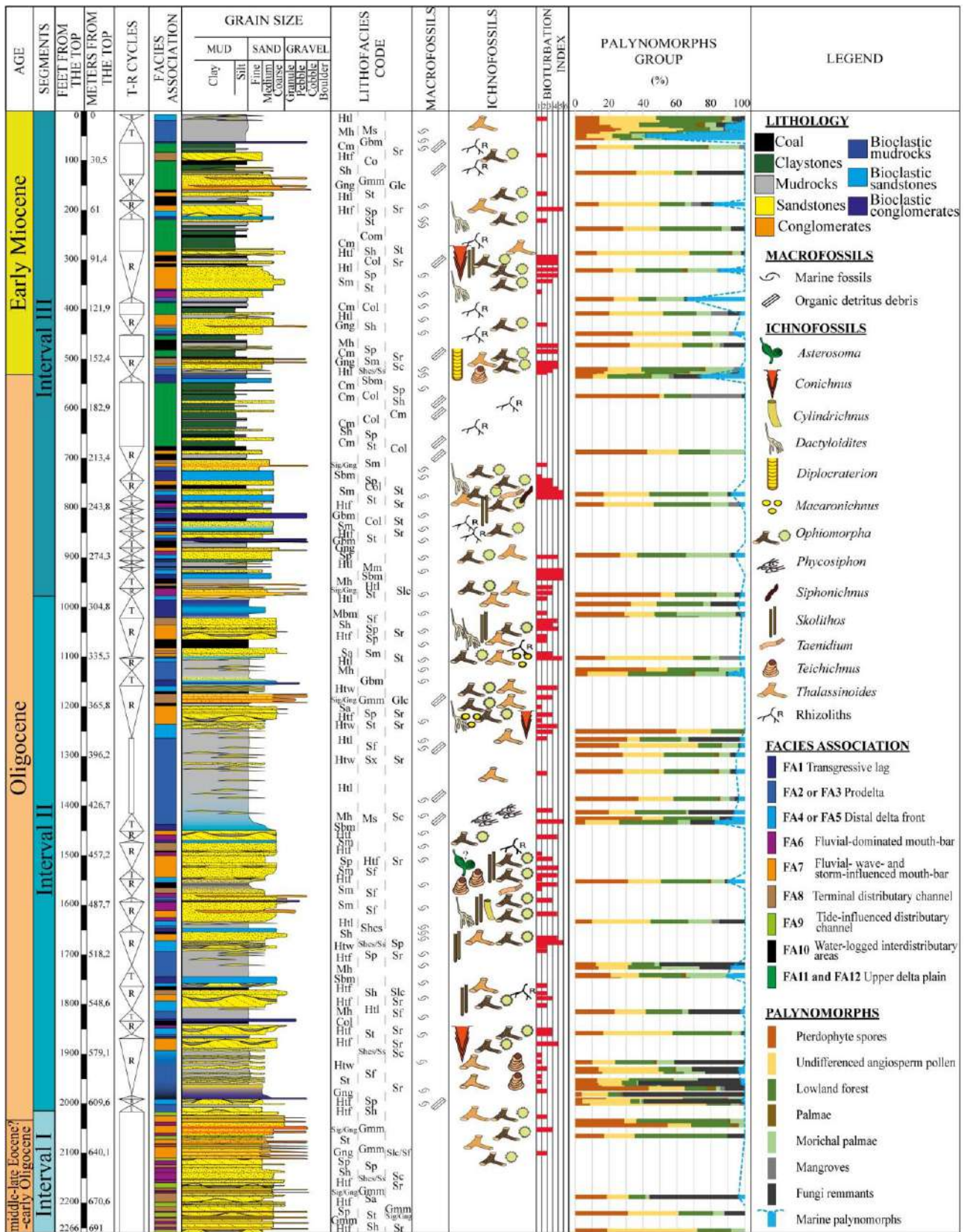


Fig. VIII.4. Stratigraphic log of the cored section (scale 1:2000), including Transgressive-Regressive cycles (T-R cycles), sedimentological (lithology, sedimentary structures, and facies associations), and paleontological features (macrofossils, ichnofossils, Bioturbation Index, and palynomorph groups). Table VIII.1 provides detailed information about the facies code.

Interpretation. *Mixed prodelta.* The dominance of Mm, and the subordination of Sw, with variable bioturbation indexes (BI = 0–4; *Ophiomorpha*, *Planolites*, *Siphonichnus*, *Teichichnus*, and *Thalassisnoides*),

along with the high abundance of marine microfossils, the fragments of bivalves and gastropods, and the presence of shell hash all suggest marine conditions at the lower limit of fair-weather wave base level in a prodelta–distal delta front/offshore environment domination (MacEachern et al., 2005). Mh, interbedded with Sm, and Sh may represent unconfined lobes in the distal domain of turbidity current deposits (hyperpycnites; Zavala et al., 2011). Occasionally, the record of Shcs/Ss, and of Sc not associated with bioturbation, could signal storm episodes below a fair-weather wave base affecting previous conditions (Arnott and Southard, 1990). The continuous progradation to shallower facies impedes the interpretation as a wave-dominated environment (shoreface to offshore), pointing instead to a mixed fluvial-wave prodelta system (Dalrymple et al., 1990, 1992; Shchepetkina et al., 2019).

VIII.4.3.4. Facies association 4 (FA4)

Description. FA4 is composed of medium to thick beds (11–100 cm) of mudrocks (Mm), muddy sandstones, and coarsening-upward trend to sandstones with massive structure (Sm), planar cross-bedding (Sp), asymmetric ripple lamination (Sr), horizontal lamination (Sh), and low to moderate bioturbation indexes (BI = 0–3) linked to *Ophiomorpha*, *Taenidium*, and *Thalassinoides*, with a sparse record of calcareous microfossils, occasionally morichal palms, and organic debris (Fig. VIII.5G and VIII.H; Table VIII.3). These successions reach thicknesses of up to ~6 m. FA4 (fluvial-dominated distal delta front) displays a gradual shift to FA6 (fluvial-dominated mouth bar).

Interpretation. *Fluvial-dominated distal delta front.* Coarsening-upward trends above represent a progradation and a transitional evolution of different tractive sedimentary structures within the sandstones, indicating fluctuating velocity in sustained turbulent flows (Gamero Diaz et al., 2011). All these features, together with the low to moderate bioturbation indexes (BI = 0–3; *Ophiomorpha*, *Taenidium*, and *Thalassinoides*) and the scarcity of marine calcareous microfossils (FA4), suggest more proximal environments within the deltaic system than the two previous FAs (MacEachern et al., 2005; Gingras et al., 2011). Absence of dwelling structures of suspension-feeding organisms, low ichnodiversity, variable concentrations of organic debris, and a prograding trend from sustained turbulent flows may reflect fluvial currents in a fluvial-dominated distal delta-front, associated with the collapse of mouth-bar deposits (MacEachern et al., 2005; Bhattacharya and MacEachern, 2009).

VIII.4.3.5. Facies association 5 (FA5)

Description. FA5 consists of thick beds (31–100 cm) of muddy sandstones and a coarsening-upward trend to fine-to medium-grained sandstones with massive structure (Mm, Sm) and symmetric ripple lamination (Sw), that reach thicknesses of up to ~4.5 m. These facies show low to high bioturbation indexes (BI = 0–5), with *Diplocraterion*, *Ophiomorpha*, *Planolites*, *Teichichnus*, and *Thalassinoides*, and some calcareous microfossils (Fig. VIII.5I–J; Table VIII.3). In addition, there are medium to thick beds of fine-to medium-grained sandstones with planar cross-bedding (Sp), asymmetric ripple lamination (Sr) or horizontal lamination (Sh), and a decrease in bioturbation indexes (BI = 0–2; *Ophiomorpha*). To a lesser extent, micro-hummocky cross-stratification (Shcs) and micro-swaley cross-stratification (Ss) can also be observed. FA5 (mixed distal delta front) exhibits transitional variation to FA7 (fluvial-, wave- and storm-influenced mouth bar).

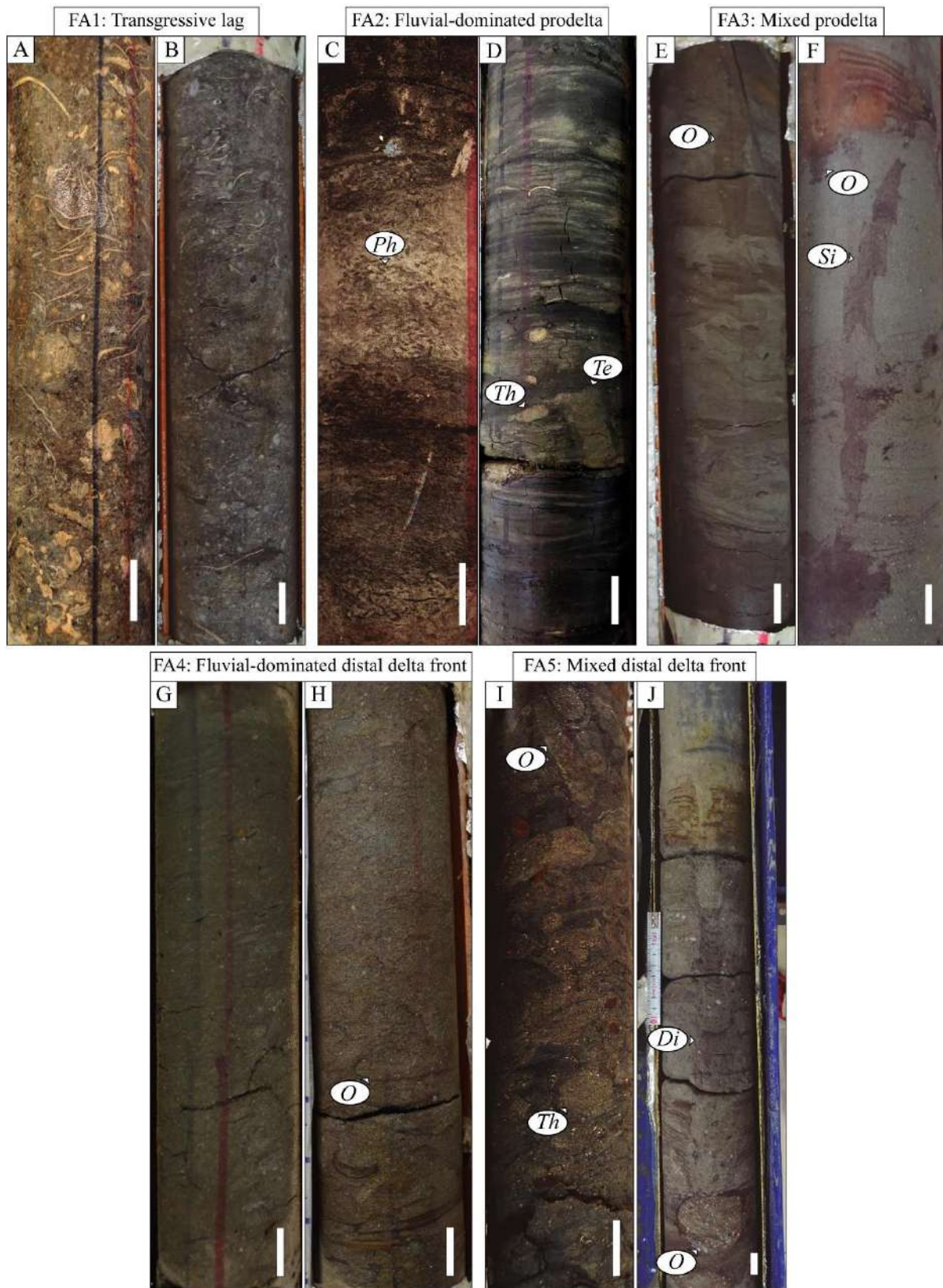


Fig. VIII.5. Facies associations FA1 to FA5. FA1: **A.** Structureless bioclastic sandstone. **B.** Structureless bioclastic conglomerate. FA2: **C.** Structureless mudrock and sandy mudrock with *Phycosiphon* (*Ph*). **D.** Laminated sandy mudrock interbedded with fine-grained sandstone with *Teichichnus* (*Te*) and *Thalassinoides* (*Th*), and bivalves. FA3: **E.** Laminated mudrock bioturbated by *Ophiomorpha* (*O*). **F.** Laminated sandy mudrock and fine-grained sandstone with *Ophiomorpha* (*O*) and *Siphonichnus* (*Si*). FA4: **G-H.** Bioturbated muddy sandstone with *Ophiomorpha* (*O*). FA5: **I.** Massive muddy sandstone highly bioturbated by *Ophiomorpha* (*O*) and *Thalassinoides* (*Th*). **J.** Laminated fine-grained sandstone with *Diplocraterion* (*Di*) and *Ophiomorpha* (*O*). Scale bar 2 cm.

Interpretation. *Mixed distal delta front.* The coarsening-upward trend from Mm to Sm in addition to Sw, the low to high bioturbation indexes (BI = 0–5; *Diplocraterion*, *Ophiomorpha*, *Planolites*, *Teichichnus*, *Thalassinoides*), and the presence of dinoflagellates, foraminifera, and calcareous nannofossils (FA5) may reflect an environment controlled by fair-weather waves, characteristic of the distal delta front (MacEachern et al., 2005; Bhattacharya, 2006; Moyano-Paz et al., 2020). These lithofacies are interbedded with Sp and Sh that locally show Sr, and they display a decrease in the diversity and abundance of trace fossils (BI = 0–2; *Ophiomorpha*). These features reveal a continuous fluvial influence and therefore evidence a mixed system (e.g., Bhattacharya, and Giosan, 2003; Bayet-Goll and Neto de Carvalho, 2020). Beds with Shcs, Ss, and non-bioturbation suggest storm episodes (Arnott and Southard, 1990; Pemberton et al., 1992).

VIII.4.3.6. Facies association 6 (FA6)

Description. FA6 consists of thick beds (31–100 cm) resulting in successions up to ~3 m of medium-to coarse-grained sandstones with massive structure (Sm), and conglomeratic sandstones with horizontal lamination (Sh). Also seen are inverse grading and bigradational trends from thick beds of coarse-grained sandstones to conglomeratic coarse-grained sandstones and granule- and pebble-size conglomerates that are matrix-supported (Gmm-Gng; Gcm-Sig; Fig. VIII.6A). The clasts are angular to very angular with low sphericity, and the matrix is medium-to coarse-grained sand without organic debris. Thick beds of fine-to medium-grained sandstones with planar cross-bedding (Sp), trough cross-bedding (St), and asymmetrical ripple lamination (Sr) are also observed (Table VIII.3). The occurrence of organic debris highlighting the lamination is also common (Fig. VIII.6B). Abundant pollen and spores were found in this facies association. On some occasions, the conglomerates present, towards the top, variations to medium- and fine-grained sandstones with soft-sediment deformation structure (Sc; Fig. VIII.6C). Trace fossils are absent (BI = 0) (Table VIII.3). FA6 (fluvial-dominated mouth bar) present transition contact to FA8 (terminal distributary channel).

Interpretation. *Fluvio-dominated mouth bar.* The coarse-grained sandstones with massive structure (Sm), conglomeratic sandstones with Sh, and organic debris highlighting the lamination and abundant pollen and spores (FA6) are interpreted as a record of high-velocity currents, probably associated with bedload under hyperpycnal flow conditions during times of torrential rains. Sr, St, and Sp, could be associated with traction and suspended load during flow slowdowns in a low-flow regime (Mulder et al., 2003; Zavala et al., 2011; Slater et al., 2017). Towards the top of the hyperpycnal deposits, thick beds of Sm, Gmm, Gng show a bigradational trend, with poorly sorted and angular clasts, sometimes overlain by Sc (FA6) that would be related to gravity flows (Shanmugam, 2009; Talling et al., 2012; Zavala, 2020). Deposits whose internal cohesion is the main grain support mechanism can transport a wide range of textural elements (up to giant blocks) floating in a matrix; they are generally associated with cohesive debris flows (Zavala, 2020). The high concentration of coarse and very coarse sand in the matrix of the studied deposits points to an intermediate stage between cohesive debris flow and hyperconcentrated flows (Zavala, 2020). The soft-sediment deformation structures observed could be related to water penetrating the plastic flow layer and becoming trapped in cavities beneath the bed, then escaping by bursting open the top of the cavity (Zavala, 2020; Shanmugam, 2021). They furthermore indicate rapid deposition and dewatering by loading, typical for mouth-

bars in a delta front deposition (Bann et al., 2008; van Yperen et al., 2019; Cole et al., 2021). The angular to very angular clasts, lacking organic debris, are related to high-gradient settings with a source area very close to the coastline (Olariu and Bhattacharya, 2006; Zavala, 2020). Transition to FA8 can occur when the flow of water decreases and the river discharge is distributed in several smaller channels, forming a multi-channel delta. In this context, the sedimentary succession can change from typical mouth-bar deposits, such as gravels and coarse sands, to finer and more laminated deposits associated with terminal distributary channels. Although the observed features are consistent with this interpretation, it is important to note that further analyses, such as additional core data or outcrop data, would be necessary to confirm and refine these interpretations.

VIII.4.3.7. *Facies association 7 (FA7)*

Description. FA7 encompasses thick beds (31–100 cm) resulting in successions up to ~4.5 m of coarse-to fine-grained sandstones with massive structure (Sm), planar cross-bedding (Sp), trough cross-bedding (St), or horizontal lamination structures (Sh); with scarce organic debris; and/or with medium to thick beds to the top of sandstones with ripple lamination (Sr). Some sheets of mudrocks demarcate lamination. These structures, but mainly massive sandstones, show low to high bioturbation indexes (BI = 0–5) and an ichnoassemblage consisting of ? *Asterosoma*, *Conichnus*, *Cylindrichnus*, *Dactyloidites*, *Macaronichnus*, *Ophiomorpha*, *Skolithos*, *Thalassinoides*, and some calcareous microfossils (Fig. VIII.6D; Table VIII.3). These successions of ~4.5 m are interbedded with medium to thick beds of ~1–2 m thickness (planar contact) of coarse-to fine-grained sandstones that are structureless (Sm) or with planar cross-bedding (Sp) or trough cross-bedding (St); they contain organic debris and are bioturbated either by a trace fossil assemblage or by the exclusive presence of *Dactyloidites*, *Macaronichnus*, *Ophiomorpha*, *Skolithos* and/or *Thalassinoides* (BI = 0–3) (Fig. VIII.6E). In the latter case, pollen and spores are common (Table VIII.3). Though less recurrent, also evident are medium beds of fine-to medium-grained sandstones with possible micro-swaley structure (Ss) and less abundant micro-hummocky cross-stratification (Shcs) where trace fossils are absent (BI = 0) (Fig. VIII.6F; Table VIII.3).

Interpretation. *Fluvial-, wave- and storm-influenced mouth bar.* Sm, Sp, and Sh could indicate high-energy environments with sheet flows and migration of two-dimensional dunes (MacEachern et al., 2005; Coates and MacEachern, 2007). Presence of a diverse ichnoassemblage (?*Asterosoma*, *Conichnus*, *Cylindrichnus*, *Dactyloidites*, *Macaronichnus*, *Ophiomorpha*, *Skolithos*, and *Thalassinoides*; BI = 0–5) is evidence of high-energy marine conditions and most likely well-oxygenated waters. Thus, sheet flows and two-dimensional dunes, along with St, and Sr at the top, could indicate sandwaves (e.g., Davidson-Arnott and Van Heyningen, 2003) with possible wave reworking of temporary mouth-bar constructions probably during dry times (Bhattacharya, 2006; Olariu and Bhattacharya, 2006; Slater et al., 2017). However, these structures need to be detailed in the outcrop. The interbedding of organic debris with beds of sandstones with Sm, Sp, St could be associated with traction load during flow slowdowns in a low-flow regime during wet times (Mulder et al., 2003; Zavala et al., 2011; Slater et al., 2017). Exclusive presence of *Dactyloidites*, *Macaronichnus*, *Ophiomorpha*, *Skolithos* and/or *Thalassinoides* (BI = 0–3) is evidence of decreased in abundance and diversity associated with increased sedimentation rates and possibly with changes in salinity. Less abundant micro-Shcs,

Ss, Sm, yet without bioturbation, are also related to unidirectional and oscillatory currents linked to storm and wave events (Arnott and Southard, 1990). The sedimentary environment energy, however, appears to have been much higher than that of the aforementioned conditions, and the development of bioturbation was inhibited. These aspects indicate high-energy deposition in a proximal mouth-bar setting with fluvial, wave, and storm influence (van Yperen et al., 2019).

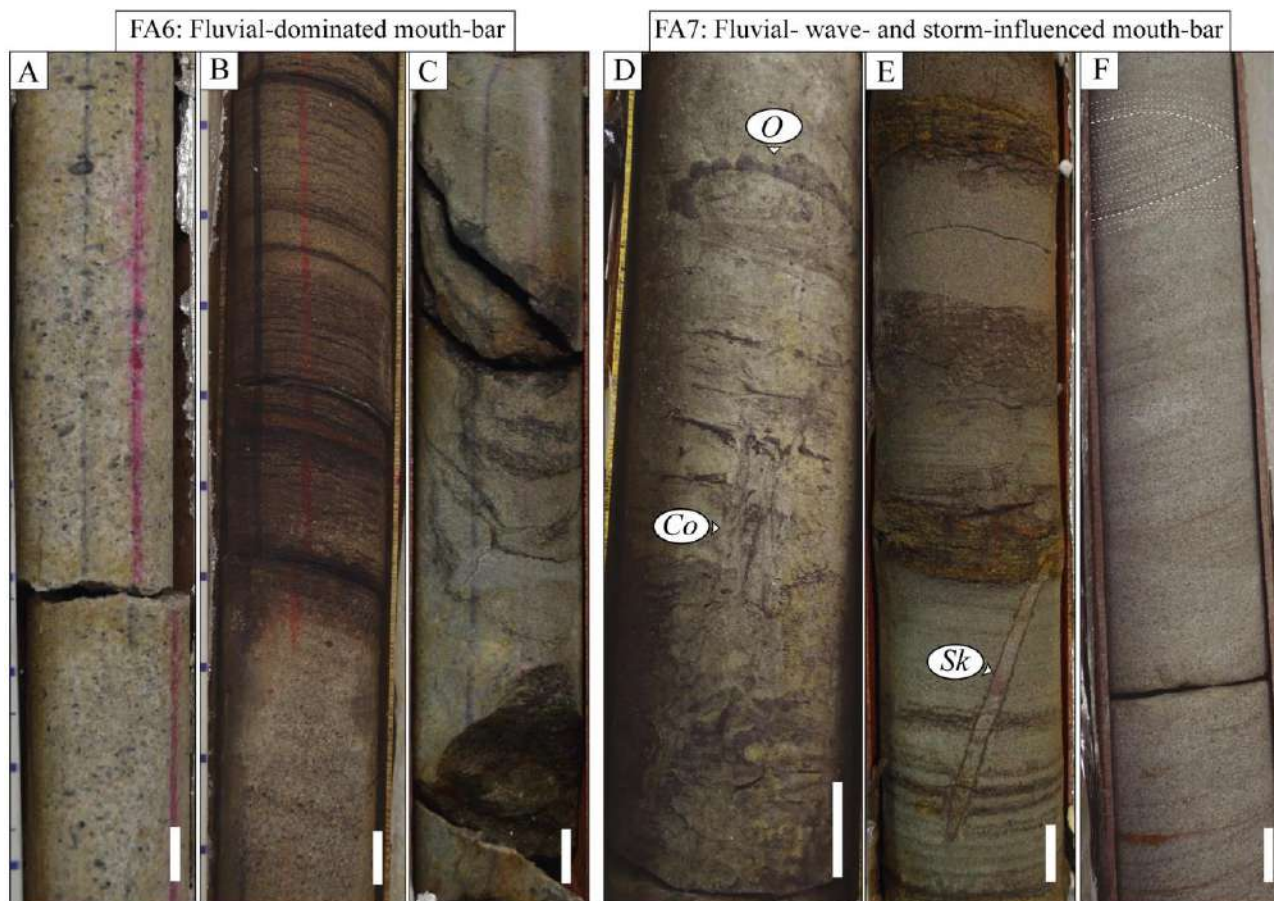


Fig. VIII.6. Facies associations FA6 and FA7. **FA6:** **A.** Conglomeratic sandstone to conglomerate with coarsening-upward structure. **B.** Fine-to medium-grained sandstone with horizontal lamination highlighted by organic debris. **C.** Soft-sediment deformation structure in sandstone. **FA7:** **D.** Laminated fine-to medium-grained sandstone with some very thin beds of mudrocks bioturbated by *Conichnus* (*Co*) and *Ophiomorpha* (*O*). **E.** Interbedding of medium-grained sandstones and bioturbated mudrocks with *Skolithos* (*Sk*). **F.** Micro-hummocky and micro-swaley cross-stratification (dashed white lines) in sandstone. Scale bar 2 cm.

VIII.4.3.8. Facies association 8 (FA8)

Description. FA8 is formed by thick beds (31–100 cm) of conglomeratic sandstones, and of sandstones with massive structure (Sm), normal grading (Sng), and inverse grading (Sig), with erosive bases resulting in sand- and conglomeratic sand bodies up to ~2.4 m. Moreover, there are thick beds of sandstones with horizontal lamination (Sh), ripple lamination (Sr), and trough cross-bedding (St). Some sandstones have load casts and flame structures (Slc/Sf), occasionally having a high content of organic debris; horizontal laminated mudrocks (Mh), and the exclusive presence of *Ophiomorpha* or *Taenidium* (BI = 0–2) are observed (Fig. VIII.7A-B) Table VIII.3. Generally, FA8 (terminal distributary channel) occurs after the recording of FA6 (fluvial-dominated mouth bar) or FA7 (fluvial-, wave- and storm-influenced mouth bar).

Interpretation. *Terminal distributary channel.* A high content of organic debris, coarse-grained deposits with erosive bases (Sng, Sig), and bigradational trend, along with the exclusive presence of *Ophiomorpha* or *Taenidium* (BI = 0–2) (FA8), could attest to the influence of multiple subaqueous distributary channels providing hypopycnic conditions during normal fluvial discharge or hyperpycnic during extraordinary river discharges (Bhattacharya and MacEachern, 2009; Buatois et al., 2011; Zavala et al., 2011; Zavala and Pan, 2018). This denotes more significant continental influence in the proximal delta front or lower delta plain. Such a situation would increase the input of freshwater into the environment in relation to the former FAs, and therefore substantially reduce salinity. Along with the increase in turbidity and sedimentation rate, this would prevent the development of macrobenthic communities, as described for the facies types of fluvial-dominated systems (Gingras et al., 1998; MacEachern et al., 2005). The interpretations associated with terminal distributary channels are based on the complete succession from the facies associations from mouth bars (FA6 and FA7). Because our interpretations about terminal distributary channel are limited to a single well-core, they should be confirmed with other well-cores or outcrops.

VIII.4.3.9. Facies association 9 (FA9)

Description. FA9 comprises thick beds (31–100 cm) of heterolithic beddings composed of medium-to fine-grained sandstones and mudrocks with a prevalence of flaser (Htf) out of wavy bedding (Htw), and some beds where the mud-drapes are very well registered. Reactivation surfaces are common. Structureless mudrock beds (Mm) are scarce, although their occurrence stands out in thin beds atop some FA6, which occasionally are part of lenticular beddings (Htl). Continental palynomorphs such as pollen and spores dominate, and lowland forests and fungi remnants are identified. Trace fossils are absent (BI = 0) (Fig. VIII.7C-D; Table VIII.3). On some occasions, FA6 (fluvial-dominated mouth bar) is intercalated with FA9. FA9 is restricted to interval I of the study section (Fig. VIII.4).

Interpretation. *Tide-influenced distributary channel.* The presence of Htf, Htw, and mud-drapes, together with the reactivation surfaces in sandstones, suggests cyclic sedimentation, probably associated with a bidirectional flow (Dalrymple et al., 1990, 1992; Dashtgard et al., 2009). The intercalation with FA6 indicates that tidal currents filled abandoned distributary channels (Martinius and Gowland, 2011). The scarcity of mudrocks in some intervals allows us to infer a generalized absence of slack water as well as the development of high-energy conditions (Dalrymple et al., 1990; Desjardins et al., 2012). Nonetheless, mudrock beds atop some FA6 with Htl support variations in fluvial discharge, even possible dropouts from the main channel (Gugliotta et al., 2016).

VIII.4.3.10. Facies association 10 (FA10)

Description. FA10 is made up of thick beds (31–100 cm) resulting in successions up to ~2.4 m of structureless mudrocks (Mm), laminated mudrocks (Mh), and lenticular beddings (Htl) with asymmetric ripple lamination (Sr). Moreover, syneresis cracks (Ms) and siderite nodules are common (Fig. VIII.7E), showing low bioturbation indexes (BI = 0–2) associated with *Teichichnus* and rhizoliths. Locally, bivalves and gastropod fragments, along with abundant pollen and spores, fungal remnants, and mangrove pollen, are recorded (Table VIII.3). Also common in FA10 are medium to thick beds (11–100 cm) of laminate coals seams (Col) and

structureless coal (Cm), on some occasions with rhizoliths (BI = 0–2) (Fig. VIII.7F; Table VIII.3). Alternations of millimetric laminae of mudrocks and fine-grained sandstones are also recorded (Fig. VIII.7G).

Interpretation. *Water-logged interdistributary areas.* Altogether, the record of Mm, Mh, Ms, siderite nodules, low bioturbation indexes, and abundant fungal remnants clearly suggest low-energy accumulation zones in brackish-water conditions. The record of Htl and Sr and the alternation of millimetric mudrocks and sandstone with marine bivalve and gastropod fragments as well as *Teichichnus* suggest cyclic sedimentation, probably associated with a bidirectional flow in interdistributary bays (Rossi and Steel, 2016). The presence of coal seams and Mm with rhizoliths (BI = 0–2) attest to the development of peat bogs in swampy areas. Constantly waterlogged conditions would have enabled both the accumulation and preservation of organic matter subjected to reducing conditions (Retallack, 2001).

VIII.4.3.11. Facies association 11 (FA11)

Description. FA11 comprises thick beds (31–100 cm) generating successions up to ~3 m thick composed of fining-upward trend from conglomerates, conglomeratic medium-grained sandstones, coarse-grained sandstones with massive structure (Sm; Gmm), to medium-grained sandstones with horizontal bedding (Sh), planar cross-bedding (Sp), asymmetric ripples (Sr), and low-angle cross-bedding (Sa), without bioturbation (Fig. VIII.7H-I-J; Table VIII.3). FA11 is restricted to interval III of the study section.

Interpretation. *Distributary channel.* Thickly bedded Sp, Sh, Sa, and Sr, all without evidence of bioturbation are originate in high-energy currents that force the migration of bottom forms (dunes) associated with fill of channel successions, where Gmm, Sm, represent the base of channel (Einsele, 2000; Miall, 2014). The dunes may partially represent bars associated with fluvial channels that transported sediment as bottom load, and the fining-upward pattern may be related to lateral migration and sudden abandonment of the canals by avulsion (Einsele, 2000). There is no evidence of marine influence in the system.

VIII.4.3.12. Facies association 12 (FA12)

Description. FA12 is represented by medium to thick beds (31–100 cm), which cumulatively may reach thicknesses of up to ~45 m, of fine-to coarse-grained sandstones with planar cross-bedding (Sp), as well as thin, horizontally laminated mudrock beds (Mh) and massive fine-grained sandstones (Sm) (Fig. VIII.7K) that occasionally contain rhizoliths (BI = 0–3) (Fig. VIII.7L); also found in FA are medium to thick beds of massive claystones (Cm) and laminated coals (Col) with rhizoliths (BI = 0–1) (Fig. VIII.7M). Pollen and spores are recorded, and mangrove palynomorphs are scarce (Table VIII.3). FA12 is restricted to interval III of the study section.

Interpretation. *Crevasse splay and floodplains.* Sandstones, coals, and claystones with rhizoliths suggest deposition during alternating high- and low-energy conditions associated with crevasse splay deposits (e.g., dikes or overflows), and floodplains. Such environments are relatively distant from the channel and tend to accumulate sediments during and after floods when the river breaks its natural levees (Selley, 1985; Einsele, 2000; Esperante et al., 2021). Sandstone beds with rhizoliths mark the cessation of current discharge and establishment of permanent vegetation (Retallack, 2001; Bridge, 2006). From the presence of Cm with

rhizoliths (BI = 0–1) and mottled textures (FA12) we can infer relatively low-energy conditions associated with vast floodplains and soil development, recording prolonged subaerial exposure (Makaske, 2001; Retallack, 2001; Miall, 2014).

Table VIII.2. Relationship between lithofacies and facies associations (FA).

| Facies Code | FA1 | FA2 | FA3 | FA4 | FA5 | FA6 | FA7 | FA8 | FA9 | FA10 | FA11 | FA12 |
|-------------|------|------|------|------|------|-----|-------|-------|------|------|------|------|
| Gmm | | | | | | 10% | | | | | ~25% | |
| Gcm | | | | | | 5% | | | | | | |
| Gng | | | | | | 15% | | | | | | |
| Sig | | | | | | 10% | | ~5% | | | | |
| Sng | | ~5% | | | | | | ~20% | | | | |
| Sm | | ~5% | ~10% | ~30% | ~25% | 25% | ~45% | ~35% | | | ~40% | 25% |
| Sh | | ~10% | ~5% | ~10% | ~5% | 10% | ~10% | ~10% | | | ~10% | |
| Sa | | | | | | | | | | | ~5% | |
| Sp | | | | ~20% | ~10% | 10% | ~20% | | | | ~10% | 15% |
| St | | | | | | 5% | ~5% | ~7,5% | | | | |
| Sr | | ~5% | | ~10% | ~5% | 5% | ~10% | ~15% | | ~5% | ~10% | |
| Sw | | | ~15% | | ~10% | | | | | | | |
| Sc | | | ~5% | | | 5% | | | | ~5% | | |
| Shcs | | | ~5% | | ~5% | | ~2,5% | | | | | |
| Ss | | | ~5% | | ~5% | | ~2,5% | | | | | |
| Htf | | | | | | | | | ~40% | | | |
| Htw | | | | | | | | | ~30% | | | |
| Htl | | | | | | | | | ~20% | ~10% | | |
| Slc, Sf | | | | | | | | ~2,5% | | | | |
| Mm | | ~35% | ~45% | ~30% | ~35% | | ~5% | | ~10% | ~40% | | |
| Mh | | ~35% | ~10% | | | | | ~5% | | ~10% | | 15% |
| Ms | | ~5% | | | | | | | | ~5% | | |
| Cm | | | | | | | | | | | | 40% |
| Col | | | | | | | | | | ~20% | | 5% |
| Com | | | | | | | | | | ~5% | | |
| Gbm | ~25% | | | | | | | | | | | |
| Sbm | ~65% | | | | | | | | | | | |
| Mbm | ~10% | | | | | | | | | | | |

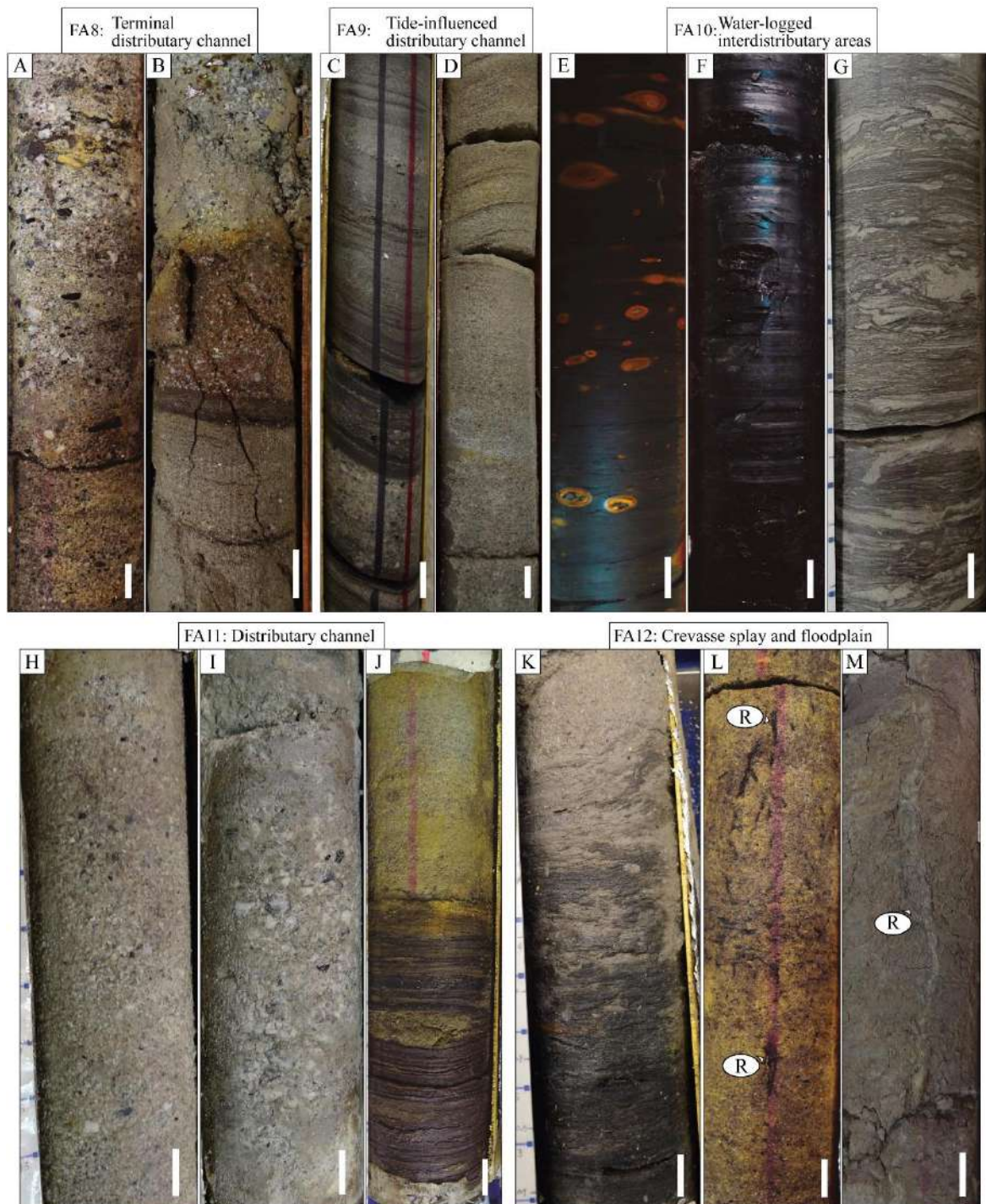


Fig. VIII.7. Facies associations FA8 to FA12. **FA8:** **A.** Massive granule-size polymictic conglomerate (Gmm). **B.** Medium-grained sandstone with horizontal lamination (Sh) and sharp contact with coarse-grained sandstone to conglomeratic sandstone. **FA9:** **C.** Alternations of millimetric laminae of mudrocks and millimeter to centimeter intervals of sandstones and conglomeratic sandstones poorly selected with net base, sometimes erosive, and planar cross-bedding. **D.** Medium-grained sandstone with a massive structure (Sm) that varies transitionally to medium-grained sandstone with planar cross-bedding (Sp) highlighted by millimetric laminae of mudrocks. **FA10:** **E.** Horizontal laminated carbonaceous mudrock with ferruginous nodules (Mh). **F.** Laminated coal (Col). **G.** Alternation of millimetric laminae of mudrocks and fine-grained sandstones. **FA11:** **H.** Coarse-grained sandstone to conglomeratic sandstone with planar cross-bedding (Sp). **I.** Massive granule-size conglomerate (Gmm). **J.** Mudrock with lenticular bedding (Htf) overlain by medium-grained massive sandstone (Sm). **FA12:** **K.** Carbonaceous mudrock that varies transitionally to massive muddy to medium-grained sandstone (Sm). **L.** Massive sandstone with rhizoliths (R). **M.** Massive claystone with rhizoliths (R). Scale bar 2 cm.

Table VIII.3. Summary of the main features of the facies associations recognized.

| <u>Facies Association</u> | <u>Lithology</u> | <u>Simple facies codes</u> | <u>Ichnology</u> | <u>Micropaleontology</u> | <u>Interpretation</u> |
|---------------------------|--|--|---|--|---|
| FA1 | Bioclastic sediments (bioclastic conglomerates, bioclastic sandstones, bioclastic mudrocks). | Sbm, Gbm, Mbm. | <i>Ophiomorpha</i> (BI = 0-3). | Bivalves, gastropods (<i>Aclis</i> spp., <i>Turritella</i> spp.), scaphopod fragments, and indeterminate shells. | Transgressive lag |
| FA2 | Mudrocks, and intercalation of mudrocks, sandy mudrocks and fine-grained sandstones. | Mm, Mh, Sh, Sr, Sm, Sng, Ms, and siderite nodules. | BI = 0-1; <i>Planolites</i> and exclusive presence of <i>Phycosiphon</i> where the bioturbation index increases (BI = 4-5). BI = 0-2; <i>Teichichnus</i> , and <i>Thalassinoides</i> . | Some foraminifera and calcareous nannofossils, as well as, palynomorphs. | Fluvial-dominated prodelta |
| FA3 | Mudrocks, sandy mudrocks, intercalation of mudrocks, and fine-grained sandstones. | Mm, Sw. Mh, Sm, Sh. Shcs, Ss, Sc. | BI = 0-4; <i>Ophiomorpha</i> , <i>Planolites</i> , <i>Siponichnus</i> , <i>Teichichnus</i> , <i>Thalassinoides</i> . | Abundant dinoflagellates (<i>Lingulodinium</i> spp.), foraminifera, and moderate amounts of calcareous nannofossils, besides bivalves and gastropod fragments as well as undifferentiated shell hash. | Mixed prodelta (fluvial, wave, and storm influence) |
| FA4 | Muddy sandstones and fine- to medium-grained sandstones. | Mm, Sm, Sp, Sr, Sh. | BI = 0-3; <i>Ophiomorpha</i> , <i>Taenidium</i> , and <i>Thalassinoides</i> . | Calcareous microfossils (foraminifera and calcareous nannofossils) in low proportions. Occasionally morichal palms. | Fluvial-dominated distal delta front |
| FA5 | Coarsening upward trends from muddy sandstones to fine-medium-grained sandstones. | Mm, Sm, Sw. Sp, Sr, Sh. Shcs, Ss. | BI = 0-5; <i>Diplocraterion</i> , <i>Ophiomorpha</i> , <i>Planolites</i> , <i>Teichichnus</i> , <i>Thalassinoides</i> . BI = 0-2; <i>Ophiomorpha</i> . | Some calcareous microfossils (foraminifera and calcareous nannofossils). | Mixed distal delta-front (fluvial, wave, and storm influence) |
| FA6 | Fine- to coarse-grained sandstones and the occurrence of organic debris highlighting lamination. Coarse-grained sandstones, conglomeratic coarse-grained sandstones and granule- and pebble-size conglomerates without the presence of organic debris, with floating clasts and granules. On some occasions, the conglomerates present, towards the top, variations to medium- fine-grained sandstones. | Sm, Gmm-Gng, Gcm-Sig, Sp, Sh, St, Sr, Sc. | Trace fossils are usually absent (BI = 0). | Abundant pollen and spores. | Proximal delta front (fluvial-dominated mouth-bar) |

| <u>Facies Association</u> | <u>Lithology</u> | <u>Simple facies codes</u> | <u>Ichnology</u> | <u>Micropaleontology</u> | <u>Interpretation</u> |
|---------------------------|---|--|--|--|---|
| FA7 | Fine- medium- to coarse-grained sandstones with occasional organic debris. | Sm, Sp, St, Sh, Sr. Sm, Shcs, Ss. | BI = 0-3; ichnological association or the exclusive presence of <i>Dactyloidites</i> , <i>Macaronichnus</i> , <i>Ophiomorpha</i> , <i>Skolithos</i> and / or <i>Thalassinoides</i> . Or BI = 0-5; ,?Asterosoma, <i>Conichnus</i> , <i>Cylindrichnus</i> , <i>Dactyloidites</i> , <i>Macaronichnus</i> , <i>Ophiomorpha</i> , <i>Skolithos</i> , <i>Thalassinoides</i> . | Pollen and spores are common, and some calcareous microfossils. | Proximal delta front (fluvial- wave- and storm- influenced mouth bar) |
| FA8 | Granule-size conglomerates, conglomeratic medium-grained sandstones, and medium- to coarse-grained sandstones with high content of organic debris. | Sm, Sng, Sig, Sh, Sr, St, Slc, Sf, Mh and erosive bases. | BI = 0-2; exclusive presence of <i>Ophiomorpha</i> or <i>Taenidium</i> . | Abundant pollen and spores. | Lower delta plain (terminal distributary channel) |
| FA9 | Fine- medium- to coarse-grained sandstones. Some mudrocks and fine-grained sandstones interbedding. | Htf, Htw, Htl, Mm, mud-drapes. | There is no a trace fossil (BI = 0) record. | Continental palynomorphs such as pollen, spores, lowland forest, and fungi remnants. | Lower delta plain (Tidal-influenced distributary channel) |
| FA10 | Mudrocks, muddy sandstones and intercalation of mudrocks and fine-grained sandstones, and coal seams. Rhythm of millimetric sheets of mudrocks and fine-grained sandstones with some micro soft-sediment deformation structure. | Mm, Col, Mh, Htl, Sr, Ms, siderite nodules, Com, and Sc. | BI = 0-2; <i>Teichichnus</i> , rhizoliths. | Abundant pollen and spores, fungi remnants and mangrove pollen (<i>Lanagiopollis crassa</i>), and occasional bivalves and gastropod fragments. | Lower delta plain (Water-logged interdistributary areas) |
| FA11 | Granule-size conglomerates, conglomeratic medium-grained sandstones, and medium- to coarse-grained sandstones. | Sm, Gmm, Sp, Sh, Sr, Sa. | BI = 0. | -- | Upper delta plain (Distributary channel) |
| FA12 | Fine- to coarse-grained sandstones, some thin beds of mudrocks, coal seams and claystones. | Cm, Sm, Sp, Mh, Col. | BI = 0-3; rhizoliths. | Pollen and spores. Mangrove palynomorphs are scarce. | Upper delta plain (Crevasse splay and Floodplain) |

VIII.5. Depositional systems and evolution

The established chrono-stratigraphic framework and detailed sedimentological, ichnological, and micropaleontological results allow us to interpret the temporal evolution of the sedimentary settings. Three different intervals are recognized in the cored section (Fig. VIII.4). The lowest, interval I, comprises FA6, FA7, FA8, and FA9 (Fig. VIII.8A). Facies associations from FA1 to FA10 are components of intervals II and

III. Assemblages of FA11 and FA12 are identified in the upper part of the section, helping to distinguish interval II from interval III (Fig. VIII.8B-C). We therefore propose the following succession: (i) a setting likely controlled by fluvial-dominated and tide- or wave-influenced mouth-bars in the middle-late Eocene? to early Oligocene (interval I); (ii) subsequent development of a fine-grained deltaic system initially mixed and influenced by river, waves, and storms during most of the Oligocene (interval II); and finally (iii) a general mixed fine-grained deltaic system, with aggradation of continental and marine systems, that stabilizes toward the end of the Oligocene/Early Miocene (interval III) (Fig. VIII.8).

VIII.5.1. Interval I – middle-late Eocene? to early Oligocene: fluvial-dominated coarse-grained delta with wave- and tidal-influenced

Interval I corresponds roughly to ~691–614 m at the base of the studied section (Fig. VIII.4). A succession of facies with an aggradational trend is marked by an alternation of facies from FA6 to FA9 (Fig. VIII.8A). This succession features hyperpycnal-dominated mouth bars (FA6), followed by hyperconcentrated flows (FA6, FA8; Fig. VIII.8A). FA7 reveals environmental variations, notably an increase in the influence of waves and sometimes conditions allowing macrobenthic activity (*Ophiomorpha*) (Fig. VIII.8A). The record of tide-influenced distributary channels (FA9) at the top of some alternations suggests a filling of abandoned distributary channels through the action of tides (Fig. VIII.8A) (e.g., Johnson and Dashtgard, 2014; Dalrymple et al., 2015).

A coarsening-upward succession of facies types FA6 to FA9 repeats along this interval, without the periodic occurrence of FA7 (zoom interval I, Fig. VIII.8A). The thickness of this zoom succession is ~3–5 m associated with amalgamated mouth bars settings.

During the middle-late Eocene? to early Oligocene, then, we see aggradational trend successions that indicate high-energy deposition indicative of distributary channels and mouth-bars settings, most likely within a coarse-grained delta (Olariu and Bhattacharya, 2006; Enge et al., 2010; van Yperen et al., 2019; Cole et al., 2021). Contributions from wet tropical lowland forests are inferred from continental palynomorphs such as pollen and spores. Rapid avulsions and lateral displacements of channels (probably high gradient) would have prevented the development of interdistributary bays and swamps (lower delta plain). This interaction of fan deposits and forests has been characterized in other stratigraphical sequences (e.g., Wilford et al., 2005).

Under the high-energy conditions generated by hyperpycnal and hyperconcentrated flows from short river systems, biogenic structures were either not produced or not preserved due to excessive background instability ($BI = 0$) (Gani et al., 2007; Gingras and MacEachern, 2012). Even a short period of wave or tidal influence may prevent the develop of trace fossils in a sedimentary environment, a re-working of mouth-bars by waves, absent the influence of gravity flows for a considerable time, could, however, generate conditions more favorable for the record of bioturbation at the end of the interval I (from ~645 m). In sum, trace fossils in this period likely were affected by both hydrodynamic conditions and changes in salinity. Increased sedimentation rates further impede the construction and maintenance of permanent domiciles by benthic organisms. The result is a reduced concentration of food resources per unit volume of sedimentary debris at the sea floor and rapid burial of sedimentary material beyond the reach of even deep-probing deposit feeders (MacEachern et al., 2005).

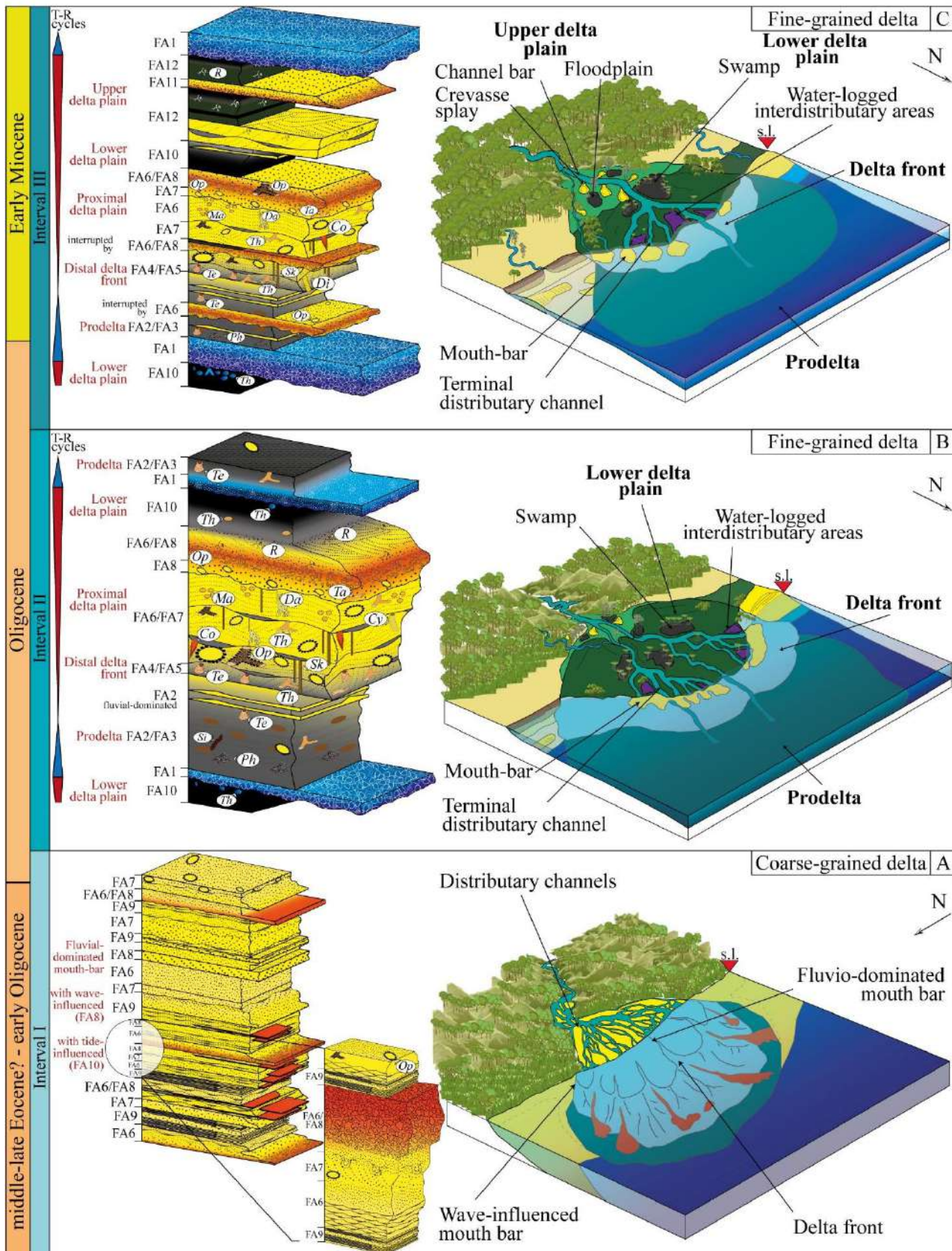


Fig. VIII.8. Succession of facies types for intervals I to III, evolution of sedimentary settings, and a sketch of the interpreted evolution of the coastline from the middle-late Eocene? to the Early Miocene in the area represented by the studied core. s.l.: sea-level. **A.** Interval I: Succession of the mouth-bar to distributary channel units of river-dominated, tidal- and wave-influenced mouth-bar type delta. **B.** Interval II: Sequence of facies types of deltaic system for the succession of the interval II. **C.** Interval III: Sequence of facies types of deltaic system frequently interrupted by the progradation of continental systems.

VIII.5.2. Interval II - Oligocene: mixed fine-grained deltaic environment (fluvial, wave, and storm influenced)

The transition zone to interval II (~614 m) is marked by a drastic reduction of hyperconcentrated flows and amalgamated successions of mouth-bars. The change is driven by a sudden marine transgression that overlies the previous facies. The first record of FA2 shows the onset of hyperpycnal prodelta development and the prograding fluvial system that restarted after transgressions (FA1 – transgressive cycles; Fig. VIII.4). This zone is also characterized by a sudden increase in fungal remnants, suggesting that swamps and interdistributary bays occupied the proximal part of the sedimentary system. For this reason, the distributary channels and mouth-bars had greater stability (Fig. VIII.8B). Interval II, corresponding to ~614 m to ~297 m (Fig. VIII.4), displays alternating progradational trends to form a succession facies type (Fig. VIII.8B). This succession may show coarsening-upward fluvial dominance (FA2-FA4-FA6) up to 46 m thick or coarsening-upward of a mixed system (FA3-FA5-FA7) up to ~24–30 m thick. It always ends in terminal distributary channels (FA8) and water-logged interdistributary areas (FA10); we thus see the alternation of transgressive cycles (F1) and regressive cycles (T-R cycles Fig. VIII.4; VIII.8 B–C). Deposits with erosive bases, high organic debris, and coal beds (FA6 to FA8) can be linked to classical deltaic sequences (Ainsworth et al., 2017; Shchepetkina et al., 2019; Maselli et al., 2020). The FA8 and FA10 always restarted in the wake of transgressive lags with *Glossifungites* ichnofacies at the base (FA1), typical of firm substrates exhumed by erosion during a transgression phase that determines ravinement surfaces (T-R cycles; Figs. VIII.4 and VIII.8B-C). Such features led us to interpret a generalized mixed deltaic environment for interval II, varying between fluvial-dominated phases and others more significantly influenced by waves and storms (in both scenarios from prodelta to lower delta plain–succession facies type) (e. g., Dashtgard and La Croix, 2015; Rossi and Steel, 2016; Rossi et al., 2017). The high abundance of morichal palm pollen suggests gallery flood forests close to the transitional system. Therefore, the beginning of these regular alternations with erosive bases associated with FA1 to FA10 marks interval II and its boundary with interval I; here the delta widens, reducing the gradient and developing a greater lower delta plain with more stable sub-environments than in interval I. The evolution of fresh/brackish/marine salinity settings generated by this intensive interaction between the fluvial-deltaic system had a direct impact on the macrobenthic tracemaker communities (Gingras et al., 1999; MacEachern et al., 2005; Bhattacharya and MacEachern, 2009). The fluvial discharge likely ranged from hyperpycnal to homopycnal; such changes may be temporally variable, especially in tropical conditions (Warne et al., 2002; Buatois et al., 2012). Higher fluvial discharges are generally characterized by elevated sedimentation rates in proximal positions, resulting in lower bioturbation intensities as evidenced in the interpreted lower delta plain. Still, salinity exerts first-order control upon benthic fauna (Díez-Canseco et al., 2015). Other stress factors, e.g., hypopycnal conditions, commonly result in the development of buoyant mud plumes that extend from the delta front to the prodelta region. This clear influence of the deltaic plumes in the sequence of facies types is evident. It drives the decrease of abundance and diversity of the macrobenthic tracemaker communities when water turbidity increases and there is freshwater input in the system (e.g., Warne et al., 2002). In sum, this sequence of facies types develops from the prodelta to the proximal delta front with fluvial-dominated input and higher specific recovery of palynomorphs. Meanwhile, the infaunal diversity,

abundance, feeding strategy, and overall behaviors increase drastically when there is a mixed influence (waves and rivers).

VIII.5.3. Interval III – late Oligocene to Early Miocene: mixed deltaic environment (fluvial, wave, and storm influenced) with aggradation of continental and marine systems

Interval III, corresponding to ~297–0 m (Fig. VIII.4), bears similarities with interval II, e.g., the repetitive record from prodelta to lower delta plain settings of the facies successions (Fig. VIII.8B-C). In the transition zone and during the first stages of interval III, rapid changes between regressive and transgressive cycles stand out, revealing some instability in the fluvial-deltaic system (Figs. VIII.4 and VIII.8B-C). However, a subsequent and more significant aggradational trend in the continental environment is apparent (FA11 and FA12). Interval III is further differentiated by its diverse frequency of facies associations and by sedimentological and ichnological differences from interval II. Thus, distributary channels (FA11) to crevasse splay and floodplains (FA12) occur above terminal distributary channels (FA8) to water-logged interdistributary areas (FA10), thus indicating the end of the succession facies types in this interval. Then, the more frequent FA6 and FA8, and the less frequent FA2-FA4 and FA3-FA5, lead us to infer a progradation of continental deposits (Fig. VIII.8C). A distinctive feature of interval III is the continuous repetition of FA11 to FA12 associated with an aggradational continental sedimentation (upper delta plain) into the fluvio-deltaic system with vast floodplains and soil development, indicating prolonged subaerial exposure. An increase in mangrove pollen (*Zonocostites* and *Lanagiopollis crassa*) supports the establishment of a transitional environment in this interval. The record of continental facies is interpreted as evidence that the upper delta plain continues to increase, at least from ~221 m (e.g., Bhattacharya, 2006; Hansen and MacEachern, 2007; Ainsworth et al., 2017; Collins et al., 2020). Nevertheless, increased marine palynomorphs (dinoflagellates and foraminifera organic lining) and the development of a tracemaker community under mixed conditions (e.g., *Conichnus*, *Diplocraterion*, and *Ophiomorpha*) signal a higher significance of transgressive phases into interval III on the continental environment. We therefore interpret this as a general mixed deltaic system similar to interval II, yet with a higher influence of fluvial-dominated processes and recurrence of wave processes. Aggradation of continental and marine systems stabilizes.

When a mixed system is established, trace fossil diversity is maximum in apparent normal salinity conditions associated with spikes of abundant dinoflagellates. It gradually decreases by diluting salinity in brackish water environments (upper and lower delta plain). Bioturbation varies, however, from sporadic distribution in the subaqueous distributary channels (mouth bar) to a remarkable paucity associated with fully upper delta plain. In freshwater environments, an inland location could favor a secondary peak of diversity (Pemberton and Wightman, 1992; Buatois et al., 2005), although this is not evidenced in the studied record. The fluvial influence signal prevails in the studied system, and establishing control of other processes for long periods is not possible. The influence of waves is noticeable in some intervals, but suddenly the ichnological and palynological signal reveals the entry of fluvial systems, modifying the previous conditions. Systems dominated by hyperpycnal prodeltas or mouth bars are created suddenly, probably in association with torrential rains.

VIII.6. Paleogeographic implications

Reconstructed hyperpycnal-dominated mouth-bar environments with hyperconcentrated flow input (coarse-grained deltas) in the context of the middle-late Eocene? and earliest Oligocene are correlated with the deposition of the San Jacinto Formation, interpreted as fan delta deposits by some authors (e.g., Guzmán, 2007 and references here contain; Mora-Bohórquez et al., 2020). Coarse-grained delta systems could be generated from nearby basement highs, as those were exhumed by that time. The sources of detritus would have been the orogen and magmatic arc at the south-southeastern of the well-core location (e.g., Cretaceous magmatic arc in the Central Cordillera) and the Magangué-Cicuco High (e.g., recycled sedimentary rocks exposed in the basement highs) to the east of the well-core location (Mora et al., 2017; Osorio-Granada et al., 2020). Moreover, the global eustatic curve for this period depicts a significant drop in sea level associated with the Eocene-Oligocene Transition (EOT) caused by the onset of the permanent ice sheet in Antarctica (Katz et al., 2008; Simmons et al., 2020; Hutchinson et al., 2021). This would point to a decrease in accommodation space, thereby suggesting some degree of correlation with amalgamated deposits (Interval I).

The sedimentary environments interpreted in this work reflect transitional variations in the final stages of gravity flow sedimentation during the middle-late Eocene?-early Oligocene, delimited by a transgression in the early Oligocene. In turn, palynology indicates the start of the lower delta plain supply system since that time. The prograding successions reveal the onset of fluvial/marine interaction, with more sediment accommodation space (fine-grained delta), which might be linked to the onset of subsidence processes reported by Mora-Bohórquez et al. (2020) in the Lower Magdalena Valley Basin. The identification of unconformities near the geological contact between the San Jacinto Formation and COF, as reported by Mora et al. (2017, 2018), is challenging due to limitations in biostratigraphic resolution. Additionally, the advance of continental systems with high sedimentation rates generates instability in marine systems (e.g., submarine slides, Mutti et al., 2003), and therefore unconformities would be registering only in more distal environments (e.g., Villegas et al. this volume). Moreover, these unconformities are difficult to document and estimate due to the lack of clear marine biostratigraphic markers in transitional environments.

We attribute the transition zone from coarse-grained delta upward to fine-grained delta in the early Oligocene to the continued increase in accommodation space in the basin during the Oligocene. This scenario, tied to the COF in the SW of the SJFB, might correspond to early phases of the proto-Cauca River delta development (at least from Amagá Formation), whose formation was driven by sedimentation from the Amagá fluvial system (the most important deltaic systems of the northern Andes during the Oligocene–Early Miocene). Detrital U/Pb geochronology data of Oligocene age from sandstones of Amagá (Lower Member) and Ciénaga de Oro Formations show similar signals in age populations (Lara et al., 2018; Manco-Garcés et al., 2020; Osorio-Granada et al., 2020, Fig. VIII.9). In turn, contributions to the Lower Amagá member from Late Cretaceous igneous rocks from the Central and Western cordilleras, and Permo-Triassic metamorphic basement of the Central Cordillera have been recorded (e.g., Zapata et al., 2020). The interpretation of both cordilleras (Central and Western cordilleras) as source of sediments for the Amagá Formation in the Oligocene has also been based on interpretation of a north-trending paleocurrent direction for the river systems (Silva-Tamayo et al., 2008, 2020; Lara et al., 2018). The COF, during the Oligocene, has a source area from Lower Magdalena Valley

Basin basement and/or Central Cordillera rocks and, to a lesser extent, from igneous rocks of the Western Cordillera (Mora et al., 2018; Manco-Garcés et al., 2020; Osorio-Granada et al., 2020). This interpretation is further supported by paleocurrents of rivers from south to north, and shorter systems from the east or southeast (Manco-Garcés et al., 2020) (Fig. VIII.9).

The deltaic system interpreted in detail here for the late Oligocene to Early Miocene presents a greater aggradational trend. Therefore, the delta front could harbor a greater influence of waves, even showing delta aggradational tendencies (e.g., Moyano-Paz et al., 2022). Thus, because the accommodation space and sediment supply are unlikely to remain constant for any significant period, we would predict instead aggradation and stability of a possible fluvial-deltaic system such as the proto-Cauca River (at least from Amagá Formation), with a possible greater reworking of the waves in the delta front (Fig. VIII.9). Previous authors invoke a regional unconformity at the top of the lower COF during the Early Middle Miocene (Mora et al., 2018). Our biostratigraphic data are inconclusive, and there is no physical evidence of this unconformity.

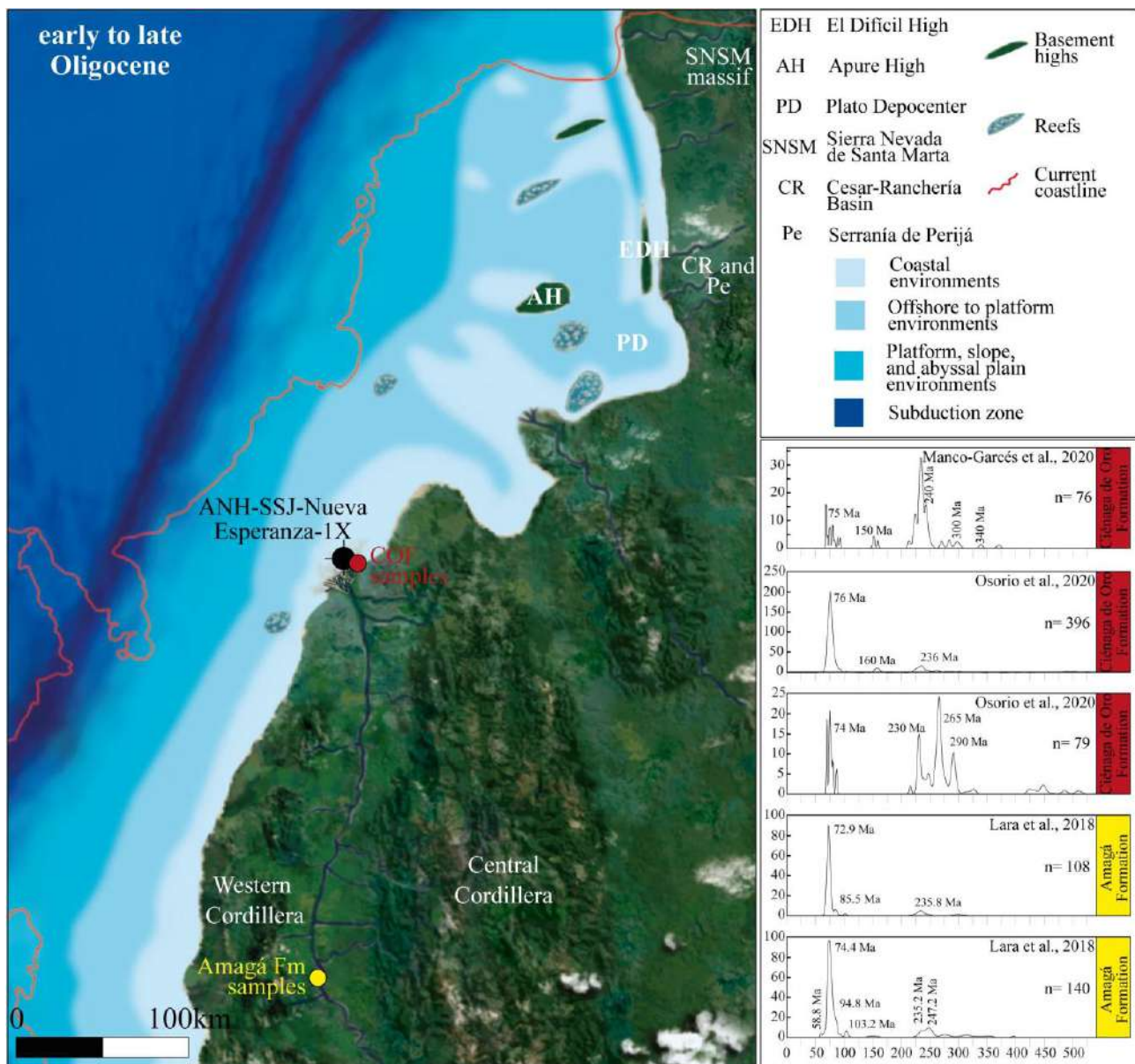


Fig. VIII.9. Paleogeographic reconstruction of the proto-Cauca River delta in the SW SSJB during the early-late Oligocene. Detrital geochronology from Amagá Formation (Lara et al., 2018) and Ciénaga de Oro Formation (Manco-Garcés et al., 2020; Osorio-Granada et al., 2020). Modified from Mora et al. (2018).

VIII.7. Conclusions

We used a multidisciplinary approach to study the influences on a mixed-energy deltaic setting on the SW Caribbean coast of Colombia during the middle-Eocene to Early Miocene. Our approach, using facies associations, trace fossils, and analysis of palynomorphs versus calcareous foraminifera/nannofossils from the well-core ANH-SSJ-Nueva Esperanza-1X, revealed a high variability of fluvial, wave, storm, and tidal processes, with long-term influence on this tropical deltaic environment. Twelve facies associations representing different deltaic subenvironments (from upper delta plain to prodelta), grouped in three stratigraphic intervals, show changes from the middle-late Eocene? to the Early Miocene. Interval I (middle-late Eocene? to early Oligocene) is represented by the amalgamation of hyperpycnal-dominated mouth bars with hyperconcentrated flow input capped by fine-grained, wave-influenced, and heterolythic deposits infilling distributary channels with land-derived palynomorphs. It is interpreted as the stacking of prograding units of fluvial-dominated, wave- and tide-influenced coarse-grained deltas, with humid tropical forest in the land and sources of sedimentation from nearby paleohighs. Our findings reveal a noteworthy impact of these high-energy conditions on the macrobenthic tracemaker community. Interval II (Oligocene) is represented by retrograding to prograding units of dominantly heterolythic deposits with a high content in morichal palm pollen alternating with thin transgressive lags. It is interpreted as flood-forested delta plain and hyperpycnal-dominated delta front to prodelta settings punctuated by transgressive wave pulses. Interval III (late Oligocene to Early Miocene) is represented by coal-bearing, thick, fine-grained packages containing mangrove pollen, and paleosols alternating with deposits showing the same facies associations as the underlying interval. It is interpreted as an aggradational, well-developed, flood-forested delta plain, commonly drowned during transgressions, thus allowing a tracemaker community to develop under mixed conditions. During the middle-late Eocene? to Early Miocene, the Colombian Caribbean presents the evolution from a steep, short, and presumably narrow margin (with coarse-grained deltas in coastal settings, interval I) to a more gentle and wide margin with a fine-grained delta (e.g., well-developed delta plain with swamps sporadically drowned, intervals II and III) reflecting both a long-term decrease in sediment supply, increase in accommodation ratio, and an increase of tropical flooded forests in the coastline associated with the evolution of perhaps the most important deltaic systems of the northern Andes during the Oligocene - Early Miocene (proto-Cauca river delta; at least from Amaga Formation). Sedimentological, ichnological, and micropaleontological analyses attempt to evaluate in detail the variations that may exist in the stratigraphic record within a tropical deltaic system, where it is complicated to determine dominant processes over long periods of time owing to the changing factors.

Acknowledgements. The National Program for Doctoral Formation provided financial support to Celis and Giraldo-Villegas (Minciencias grants 885-2020, 906-2021, respectively). We want to thank the National Hydrocarbons Agency-ANH, and *Ministerio de Ciencia, Tecnología e Innovación - Minciencias* for allowing the study of well-core (Convenio 730/327-2016). The Vicerrectoría de Investigaciones y Posgrados and the Instituto de Investigaciones en Estratigrafía-IIES of Universidad de Caldas gave economic and logistic support.

The research was conducted within the “Technology and Palaeoenvironment RG” (UGR). Financial support for Rodríguez-Tovar was provided by scientific Projects PID 2019- 104625RB-100 (funded by MCIN/AEI/10.13039/501100011033), P18- RT- 4074 (funded by FEDER/Junta de Andalucía-Consejería de Economía y Conocimiento), B-RNM-072-UGR18 and A-RNM-368-UGR20 (funded by FEDER Andalucía). We want to thank to Dra. Beatriz Bádenas for constructive comments and suggestions on the earliest version of manuscript. Moreover, thanks to the editor Andrés Folguera and three anonymous reviewers for the comments and suggestions, which improved the manuscript. Funding for open access charge: Universidad de Granada / CBUA.

SM VIII.1. Supplementary material VIII.I

Supplementary data to this article can be found online at:

<https://ars.els-cdn.com/content/image/1-s2.0-S0895981123001797-mmc1.xlsx>

Supplementary paper of Chapter VIII

Sediment provenance signal of the Northern Andes during the Oligocene-Pliocene: Insights from the detrital record of the forearc and intra-arc basins, northwestern Colombian margin

Sebastián Echeverri^{1, 2, 3, 4*}, Sergio A. Celis^{1, 2, 5}, Andrés Pardo-Trujillo^{1, 2, 6}

¹ *Grupo de Investigación en Estratigrafía y Vulcanología (GIEV) “Cumanday” Universidad de Caldas, Manizales, Colombia.*

² *Instituto de Investigaciones en Estratigrafía – IIES, Universidad de Caldas, Manizales, Colombia.*

³ *Departamento de Geociencias, Facultad de Ciencias, Universidad Nacional de Colombia – sede Bogotá, Colombia.*

⁴ *Grupo de Investigación en Geología y Geofísica (EGEO), Universidad Nacional de Colombia – sede Medellín.*

⁵ *Departamento de Estratigrafía y Paleontología, Universidad de Granada, 18002, Granada, Spain.*

⁶ *Departamento de Ciencias Geológicas, Universidad de Caldas, Manizales, Colombia.*

Journal of South American Earth Sciences, 152 (2025), 105316



Highlights

- Oligocene to Pliocene exhumation signals in the northwestern Colombian Andes are described.
- Insights of the topographic configuration of the Western and Central cordilleras from the Oligocene to the Miocene-Pliocene are shown.
- Paleogeographic contributions from the detrital signals of the Oligocene-Pliocene strata in forearc and intra-arc basins.

Abstract

The Cenozoic uplift and relief history of the Colombian Andes controlled the evolution of drainage systems and the filling history of sedimentary basins. The understanding of the associated polyphasic orogenic history has been reconstructed from the history of hinterland and foreland basins in eastern Colombia. In contrast, the tectonostratigraphic record of the forearc and intra-arc basins is less known, despite their potential to record both the exhumation and magmatic history of the orogen and the lesser-known history of the Central and Western cordilleras. A review of the regional stratigraphy together with provenance constraints from sandstone petrography, and U-Pb zircon geochronology ($n = 2738$ new and 2456 published data) of the Oligocene-Pliocene successions in the Caribbean and Pacific forearc basins and the Amagá and Cauca intra-arc basins (NW Colombia) is used to infer the topographic evolution of the Central and Western cordilleras, as well as the distribution of depositional environments and ancient drainage systems. The results indicate that the Oligocene-Lower Miocene sandstones of the intra-arc and Caribbean forearc basins document the uplift of both the Central and Western cordilleras, as seen by the quartz-rich character with fragments associated to the Pre-Cenozoic sources, while sandstones of the Pacific forearc segment show a lithic character with volcanic fragments derived from the Cretaceous and Eocene-Oligocene sources of the proto-Western Cordillera. After the Lower-Middle Miocene, sandstones are more immature including sources derived from the cordilleran basement and volcanic fragments from the upper Oligocene-Middle Miocene magmatic arc located exclusively in the Western Cordillera. The Upper Miocene-Pliocene sandstones in general exhibit a lithic character with fragments derived from upper Oligocene-Middle Miocene and Middle Miocene-Pliocene magmatic rocks located in the Western Cordillera and intra-arc region. When the provenance record between basins is compared, changes in topographic continuity are seen through time, with some marine passages connecting the Pacific forearc with the Cauca intra-arc basin during the Oligocene-Miocene, followed by the formation of a continuous cordilleran system after the Middle Miocene that interrupts marine passages. The integrated detrital zircon signature from the different basins show that within a regional perspective, Miocene-Pliocene magmatism was continuous along the northwestern South American margin.

Keywords: Sedimentary provenance; Intra-arc and forearc basins; Panamá-Chocó arc; Western Cordillera; Paleodrainages.

**PART V FINAL REMARKS, CONCLUSIONS AND
FORTHCOMING RESEARCH**

Chapter IX

CONCLUSIONS

The integrative analysis of sedimentological, ichnological, gamma-ray, and micropaleontological data from outcrops and well-cores in the southwestern Colombian Caribbean (with a particular emphasis on the Sinú-San Jacinto Fold Belt) has enabled the identification of distinct facies and facies associations, as well as trace fossil assemblages, revealing significant vertical variations in depositional style from the middle-late Eocene to the Early Miocene. This study delineates facies associations ranging from continental to slope break and slope settings, with deltaic sedimentation being dominant. These variations are attributed to accommodation space dynamics and sediment input fluxes, subsidence, avulsion processes, and minor evidence of relative sea level changes. Our main conclusions resolve the specific objectives initially proposed:

- (i) During the middle-late Eocene, coarse-grained sedimentation prevailed, driven by hyperconcentrated to hyperpycnal flows reaching the coastline and forming amalgamated mouth bars, indicative of limited accommodation space. Some of these flows advanced to the shelf and slope, where the coarse-grained deposits record the development of a submarine channel system, characterized by cohesionless debris flows and high-density turbidity currents under highly variable flow conditions. Gravelly cyclic step sets, formed under supercritical flow conditions, mark the onset of the confined channel segment. More distal settings reflect the channel-levee and terrace systems, as well as lobes and off-axis lobes. These deposits represent the transition from supercritical to subcritical flows in a shelf-break context, with coarse-grained material being routed from the channel mouth to the Channel-Lobe Transition Zone, thus suggesting that the head of the slope channel/canyon intersected a shallow marine system fed by a high-gradient fluvial system. A significant shift occurred during the latest Eocene to earliest Oligocene, with transgressive deposits marking a change in sedimentation patterns. Oligocene to lower Miocene successions exhibit meandering fluvial deposits, abundant fungal remains, morichal palm pollen, and terminal distributary channels reaching waterlogged interdistributary areas and shallow marine zones, reflecting increased accommodation space and tectonic realignment. This process generated fluvio-dominated mouth bars, along with distal delta front and prodelta systems, reactivated by transgressive lag deposits. The system is dominated by the coalescence of hyperpycnites. The evolution of this complex sedimentary system throughout the Oligocene is reflected in the repetitive coarsening-upward succession, which also show variations in sedimentological features (e.g., fluid muds, mud drapes) and ichnological content (e.g., tubular tidalites, burrow size). Such changes episodically increase the impact of tidal modulation or wave reworking on the deltaic system, which may have intensified during the Early Miocene. The Eocene to Oligocene shift, coupled with heightened subsidence, underscores the influence of tectonics over sea level changes during the Eocene-Oligocene transition. Tectonic activity emerged as the dominant driver of sedimentation in the Colombian Caribbean forearc, exerting a profound influence on accommodation space and depositional patterns.
- (ii) The animal-substrate relationship and, accordingly, the ichnological record help identify marine influences in coarse-grained systems, as sedimentological evidence is often difficult to distinguish in transitional, complex, environments. This makes ichnological analysis a crucial tool for

reconstructing paleoenvironments. Sedimentological and ichnological features —presence of *Conichnus*, *Ophiomorpha*, *Thalassinoides*, fluid muds, and mud drapes— indicate that the arrival of hyperconcentrated to hyperpycnal flows at the coastline triggers an interaction between gravitational flow and marine processes, highlighting the interplay between the feeder system and the receiving basin.

When these flows reach deep marine zones, the *Nereites* ichnofacies is characterized, the occurrence of *Ophiomorpha* and *Thalassinoides* being associated with the record of *Ophiomorpha rudis* ichnosubfacies interbedded with *Nereites*, and *Phycosiphon* related to the *Nereites* ichnosubfacies. These ichnological assemblages help identify flow transitions into less confined areas and deposition from turbidity currents in channel-levee and terrace systems. Lobes and off-axis lobe areas show bioturbation of *Ophiomorpha*, *Scolicia*, *Taenidium* and *Thalassinoides*, all part of the *Ophiomorpha rudis* ichnosubfacies.

During the Oligocene, the ichnological assemblage is low in abundance but moderately diverse, comprising *Ophiomorpha*, *Skolithos*, and *Thalassinoides* in fluvio-dominated mouth bars; *Ophiomorpha*, *Skolithos*, *Taenidium*, and *Thalassinoides* in the fluvio-dominated distal delta front; and *Phycosiphon*, *Planolites*, *Teichichnus*, and *Thalassinoides* in fluvio-dominated prodelta successions. Mouth bar migration upstream, laterally, or downstream, depending on basin morphology and tectonic dynamics highlighted tidal influence or wave modulation during short episodes. Therefore, occasionally mouth bars also exhibit mud drapes and flaser bedding, with increased bioturbation index and diversity, including *Asterosoma*, *Conichnus*, *Cylindrichnus*, *Dactyloidites*, *Gyrolithes*, *Macaronichnus*, *Ophiomorpha*, *Skolithos*, and *Thalassinoides*, reflecting tidal and fluvial influences. Distal delta front successions show wavy bedding with scarce mud drapes and a trace fossil assemblage of *Diplocraterion*, *Ophiomorpha*, *Planolites*, *Rhizocorallium*, *Teichichnus*, and *Thalassinoides*. The prodelta is characterized by lenticular and episodic mud drapes and mudrock domains, with *Chondrites*, *Planolites*, *Siphonichnus*, *Teichichnus*, and *Thalassinoides*, indicating tidal and fluvial influences.

Fluvio-deltaic processes significantly disrupt the marine signature, impacting macrobenthic tracemaker communities, and leading to depauperate, monospecific, or stress-dominated trace fossil assemblages.

- (iii) In recent years, the surge in studies related to the impact of physicochemical stresses on benthic communities has largely focused on deltaic depositional systems, even leading to new Seilacherian ichnofacies proposals such as the *Rosselia* and *Phycosiphon* ichnofacies. However, the influence of these stresses, and consequently the occurrence, composition, and distribution of stressed ichnological assemblages, impeded the assignment of preconceived ichnofacies models that could be easily applied in environments where macrobenthic communities are less affected. In the case of tidally modulated coasts, this remains a topic warranting further exploration within coastal sedimentary basin analysis. In fluviually dominated deltaic systems and tropical environments

featuring torrential rains, the characterization and interpretation of each ecological niche will allow for a more detailed understanding of coastal-marine systems having high fluvial influence.

- (iv) The paleogeographic model for the middle-late Eocene reveals a tectonically active, steep, and abrupt basin margin during the late Eocene, with nearby basement highs acting as sources of coarse sediments. However, the transition to the Oligocene, primarily associated with the development of a gentler, wider, fine-grained delta, reflects changes in subsidence, sediment supply, accommodation space, and the expansion of tropical forests along the coastline. This period marks the establishment of a much more extensive and stable fluvio-deltaic margin, corresponding to the early stages of development for the most significant deltaic systems of the northern Andes. Nonetheless, the frequency of tropical torrential rains continuously altered the system dynamics, the variations suggesting mouth bar migrations upstream, laterally, or downstream, depending on basin morphology and tectonic influences.

The paleoenvironmental analysis of two onshore basins in the southwestern Colombian Caribbean, with emphasis on the Sinú-San Jacinto Fold Belt, from the middle-late Eocene to the Early Miocene, reveals complex coastal to marine systems with river mouth influence, within the broader framework of tectonic basin evolution. This research identified key autogenic and allogenic controls on sedimentation, emphasizing the most significant changes in sedimentary patterns. Sedimentary dynamics in such complex settings depend on multiple interacting parameters, a fact that highlights the importance of detailed data analysis to confirm, reassess, and refine the initial hypotheses. Tectonic activity, particularly marked by increased subsidence, appears to obscure evidence of the sea level fall during the Eocene-Oligocene Transition. Nevertheless, at a palaeoceanographic scale, a potential effect of this sea level drop could be discerned. Furthermore, a relative sea level rise during this period is evidenced by depositional changes, giving rise to a shift in sedimentation styles.

CONCLUSIONES

El análisis integrado de datos sedimentológicos, icnológicos, de rayos-gamma y micropaleontológicos de afloramientos y testigos de sondeos en el Caribe colombiano (Cinturón Plegado de San Jacinto y la región occidental de la Cuenca del Valle Inferior del Magdalena, subcuenca de San Jorge) ha permitido la identificación de distintas facies y asociaciones de facies, así como de asociaciones de trazas fósiles, revelando variaciones verticales significativas en el patrón de depósito desde el Eoceno medio-tardío hasta el Mioceno Temprano. Este estudio diferencia asociaciones de facies que varían desde ambientes continentales hasta las zonas de ruptura de talud, siendo la sedimentación deltaica la dominante. Estas variaciones se atribuyen a variaciones del espacio de acomodación, los flujos de aporte de sedimentos, los procesos de avulsión y la evidencia menor de cambios eustáticos. Las principales conclusiones responden a los objetivos específicos inicialmente propuestos:

- (i) Durante el Eoceno medio-tardío, predominó la sedimentación de grano grueso, generada por flujos hiperconcentrados a hiperpícnicos que alcanzaban la costa, formando barras de desembocadura amalgamadas, lo que indica un espacio de acomodación limitado. Algunos de estos flujos avanzaron hasta la plataforma y el talud, donde los depósitos de grano grueso registran el desarrollo de un sistema de canales submarinos, caracterizado por flujos de detritos no cohesivos y corrientes de turbidez de alta densidad bajo condiciones de flujo altamente variables. Registros cíclicos de conglomerados, formados bajo condiciones de flujo supercrítico, marcan el inicio del segmento confinado del canal. Los ambientes más distales reflejan los sistemas de canal-dique y terrazas, así como lóbulos y lóbulos alejados del eje principal del canal. Estos depósitos representan la transición de flujos supercríticos a subcríticos en un contexto de ruptura de talud, con material de grano grueso siendo canalizado desde la desembocadura del canal hacia la Zona de Transición Canal-Lóbulo, lo que sugiere que la cabecera del canal/cañón de talud intersectaba un sistema marino somero alimentado por un sistema fluvial de alto gradiente. Un cambio significativo ocurrió durante el Eoceno tardío al Oligoceno Temprano, con depósitos transgresivos que marcan un cambio en los patrones de sedimentación. Las sucesiones del Oligoceno al Mioceno inferior muestran depósitos fluviales meandriformes, restos abundantes de hongos, polen de palma de *Mauritia*, y canales distributarios terminales que alcanzan áreas interdistributarias anegadas y zonas marinas, lo que refleja un aumento en el espacio de acomodación y un realineamiento tectónico. Este proceso generó barras de desembocadura dominadas por sistemas fluviales, junto con sistemas distales de frente deltaico y prodeltas, reactivados por depósitos de *lag* transgresivos. El sistema está dominado por la coalescencia de hiperpícnitas. La evolución de este complejo sistema sedimentario a lo largo del Oligoceno se refleja en que estas sucesiones granocrecientes repetitivas también muestran variaciones en las características sedimentológicas (por ejemplo, fluidos de lodos, láminas de lodo) y contenido icnológico (por ejemplo, tidalitas tubulares, tamaño de madrigueras). Estos cambios indican el aumento episódico del impacto de la modulación de mareas o el retrabajamiento por olas en el sistema deltaico, los cuales pudieron haberse intensificado durante el Mioceno Temprano. El cambio del Eoceno al Oligoceno está asociado con

un aumento en la subsidencia, lo que resalta el predominio de la tectónica sobre los cambios del nivel del mar durante la transición Eoceno-Oligoceno. La actividad tectónica se revela como el principal factor que controla la sedimentación en las cuencas de antearco del Caribe colombiano, ejerciendo una profunda influencia sobre el espacio de acomodación y los patrones de depósito.

- (ii) La relación entre los organismos y el sustrato, y por tanto las estructuras biogénicas que se generan, ayuda a identificar influencias marinas en sistemas de grano grueso, ya que la evidencia sedimentológica a menudo es difícil de distinguir en los complejos ambientes de transición. Esto lo convierte en una herramienta crucial para reconstruir los paleoambientes. Las características sedimentológicas e icnológicas, como la presencia de *Conichnus*, *Ophiomorpha*, *Thalassinoides*, fluidos de fangos y láminas de fango, indican que la llegada de flujos hiperconcentrados o hiperpícnicos a la costa desencadena una interacción entre los procesos de flujo gravitacional y los procesos marinos, destacando la interacción entre las áreas de aporte y la cuenca receptora. Cuando estos flujos alcanzan zonas marinas profundas las asociaciones de trazas permiten la asignación a las icnofacies de *Nereites*, con estructuras de *Ophiomorpha* y *Thalassinoides* asociadas con la icnosubfacies *Ophiomorpha rudis*, intercaladas con trazas de *Nereites* y *Phycosiphon* propias de la icnosubfacies de *Nereites*. Estas asociaciones icnológicas ayudan a identificar transiciones de flujo en áreas menos confinadas y el depósito de corrientes de turbidez en los sistemas de canal-dique y terrazas. Las áreas de lóbulos y lóbulos alejados del eje muestran bioturbación por *Ophiomorpha*, *Scolicia*, *Taenidium* y *Thalassinoides*, pertenecientes a la icnosubfacies *Ophiomorpha rudis*.

Durante el Oligoceno, las asociaciones icnológicas son poco abundantes, pero moderadamente diversas, con *Ophiomorpha*, *Skolithos* y *Thalassinoides* en las barras de desembocadura dominadas por sistemas fluviales; *Ophiomorpha*, *Skolithos*, *Taenidium* y *Thalassinoides* en el frente deltaico distal dominado por los ríos; y *Phycosiphon*, *Planolites*, *Teichichnus* y *Thalassinoides* en las sucesiones del prodelta dominado por los ríos. Ocasionalmente, las barras de desembocadura también exhiben láminas de fango y estratificación flaser, con el aumento del índice de bioturbación y la diversidad, incluyendo *Asterosoma*, *Conichnus*, *Cylindrichnus*, *Dactyloidites*, *Gyrolithes*, *Macaronichnus*, *Ophiomorpha*, *Skolithos* y *Thalassinoides*, lo que refleja influencias mareales y fluviales. Las sucesiones del frente deltaico distal muestran estratificación ondulada con escasas láminas de fango e icnoasociaciones de *Diplocraterion*, *Ophiomorpha*, *Planolites*, *Rhizocorallium*, *Teichichnus* y *Thalassinoides*. El prodelta está controlado por episódicas láminas de fango, estratificación lenticular y lutitas, con *Chondrites*, *Planolites*, *Siphonichnus*, *Teichichnus* y *Thalassinoides*, indicando influencias mareales y fluviales.

Los procesos fluvio-deltaicos interrumpen significativamente la señal marina, impactando a las comunidades macrobentónicas generadoras de trazas, lo que determina icnoasociaciones empobrecidas, monoespecíficas o dominadas por icnotaxones que reflejan ese estrés.

- (iii) En los últimos años, el aumento de estudios relacionados con el impacto de los factores de estrés físico-químico en las comunidades bentónicas generadoras de trazas se ha centrado en los sistemas deposicionales deltaicos, incluso con propuestas de nuevas icnofacies Seilacherianas, como las icnofacies de *Rosselia* y *Phycosiphon*. Sin embargo, la influencia de estos factores de estrés físico-químico modifica la ocurrencia, composición y distribución de las asociaciones icnológicas, dificultando la asignación directa a los modelos de icnofacies tradicionales. Podrían intentar usarse, con algunas variaciones, en ambientes con mayor retrabajamiento por olas, donde las comunidades macrobentónicas están menos afectadas. Incluso en costas moduladas por mareas sigue siendo un aspecto que merece más atención en el análisis de cuencas sedimentarias costeras. En sistemas deltaicos dominados por ríos y ambientes tropicales con lluvias torrenciales, la caracterización e interpretación de cada nicho ecológico permite un análisis más detallado de los sistemas costero-marinos con alta influencia fluvial.
- (iv) El modelo paleogeográfico para el Eoceno medio-tardío revela un margen de cuenca tectónicamente activo, inclinado y abrupto durante el Eoceno tardío, con relieves de basamento cercanos que actuaban como áreas fuente de los sedimentos gruesos. Sin embargo, la transición al Oligoceno, asociada principalmente con el desarrollo de un delta más amplio y de grano fino, refleja cambios en la subsidencia, el aporte de sedimentos, el espacio de acomodación y la expansión de los bosques tropicales a lo largo de la costa. Este período marca el establecimiento de un margen con dominio fluvio-deltaico mucho más extenso y estable, reflejando las etapas tempranas de desarrollo de los sistemas deltaicos más significativos de los Andes del norte. No obstante, la frecuencia de lluvias torrenciales tropicales alteró continuamente la dinámica del sistema, con variaciones que sugieren migraciones de las barras de desembocadura aguas arriba, lateralmente o aguas abajo, dependiendo de la morfología de la cuenca y las influencias tectónicas.

El análisis paleoambiental de dos cuencas continentales en el Caribe colombiano, con énfasis en el Cinturón Plegado de San Jacinto, desde el Eoceno medio-tardío hasta el Mioceno Temprano, revela complejos sistemas costeros a marinos con influencia de desembocaduras de ríos, dentro del marco más amplio de la evolución tectónica de la cuenca. La investigación ha permitido identificar controles autogénicos y alogénicos sobre la sedimentación, enfatizando los cambios más significativos en los patrones sedimentarios. Las dinámicas sedimentarias en estos ambientes complejos dependen de múltiples parámetros que interactúan entre sí, destacando la importancia de un análisis detallado de los datos para confirmar, reevaluar y refinar las hipótesis iniciales. La actividad tectónica, particularmente marcada por el aumento de la subsidencia, parece enmascarar la evidencia de la caída del nivel del mar durante la transición Eoceno-Oligoceno. A escala paleoceanográfica, se podría interpretar un efecto potencial de esta caída del nivel del mar. Sin embargo, una subida relativa del nivel del mar durante este período se refleja en los cambios deposicionales, determinando variaciones en los patrones de sedimentación.

Chapter X

FUTURE PERSPECTIVES AND OTHER COASTAL SYSTEMS

This section outlines potential future research directions based on the findings of this thesis, which primarily focused on deltaic environments. While this work has enhanced our understanding of delta systems, several open questions and challenges remain, requiring further exploration. Emerging methodologies and advanced approaches, such as quantitative process estimation, numerical modeling in coastal systems, and the distinction between tropical and high-latitude coastal and shelf environments, offer exciting opportunities to expand research into other coastal systems.

In this context, the following paper presents an integrated ichnological and sedimentological study of a shallow marine system, specifically the Puerto Madryn Formation (Late Miocene, Argentine Patagonia). This study opens new research avenues and methodological insights beyond deltas, highlighting the complexity of coastal settings and the environmental stresses within shoreface/offshore and estuarine systems. The findings provide a more nuanced interpretation of depositional processes, bioturbation patterns, and ichnological assemblages, with a focus on wave- and tide-dominated systems. Incorporating these new approaches enables the investigation of similar coastal environments and fosters a deeper understanding of sedimentary processes in coastal and marine settings, where much remains to be discovered.

Ichnological indicators of physico-chemical stresses in wave- to tide-dominated Miocene shallow marine environments (Argentine Patagonia)

Sergio A. Celis^{1,2*}, Damián Moyano-Paz³, Sebastián Richiano⁴, José I. Cuitiño⁴, Francisco J. Rodríguez-Tovar¹

¹ Departamento de Estratigrafía y Paleontología, Universidad de Granada, 18002, Granada, Spain.

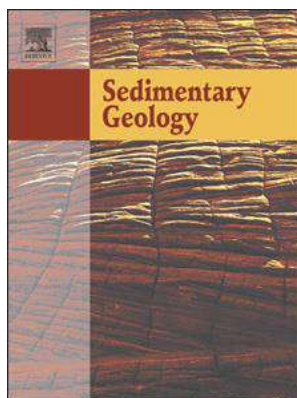
² Grupo de Investigación en Estratigrafía y Vulcanología (GIEV) Cumanday, Universidad de Caldas, Manizales, Colombia.

³ Centro de Investigaciones Geológicas (CONICET-UNLP), Diagonal 113 #275, B1904DPK, La Plata, Buenos Aires, Argentina.

⁴ Instituto Patagónico de Geología y Paleontología (IPGP, CCT CONICET-CENPAT), Boulevard Brown 2915, Puerto Madryn (9120), Chubut, Argentina.

*Corresponding author: sergiocelis11@gmail.com; sergiocelis@correo.ugr.es (Sergio A. Celis).

Sedimentary Geology, 472 (2024), 106755



<https://doi.org/10.1016/j.sedgeo.2024.106755>

Highlights

- Ichnological analysis as indicators of physico-chemical stresses.
- Ecosystems evolution from wave-dominated to tide-dominated environments.
- Non-tidal shorefaces in transgressive phase.
- Tide-dominated estuarine system in regressive phase.
- Physico-chemical stressors challenge traditional ichnofacies analysis.

Abstract

An integrated analysis of ichnological and sedimentological features in ancient successions provides a robust dataset of high-resolution interpretations of environmental parameters, encompassing both depositional and ecological aspects. By characterising discrete and recurring bioturbation patterns in the Puerto Madryn Formation (Late Miocene, Argentine Patagonia), we arrive at key knowledge about predominant environmental stresses within transgressive phase shallow marine and estuarine systems, shedding light on their palaeoenvironmental implications. Given the inherent complexities of coastal settings, including the challenges posed by omission/erosion surfaces, it becomes imperative to consider the intricate interplay of multiple depositional processes and environmental factors.

Through a detailed integration of sedimentological and ichnological approaches, we discern the establishment of a wave-dominated system overlain by a tide-dominated estuarine system.

The wave-dominated marine system involves tabular bodies extending laterally over tens of kilometres, with upward fining and coarsening successions from the mid- to lower-shoreface to offshore-shelf environments. The influence of waves and tides on these systems is discussed in the absence of physical sedimentary structures and the need to find elements that bring us closer to elucidating whether waves or tidal processes influence shoreface to offshore systems. The ichnological assemblages allow for the characterisation of *Cruziana* ichnofacies with proximal (*Taenidium* and *Thalassinoides*), archetypal (*Asterosoma*, *Chondrites*, *Cylindrichnus*, *Ophiomorpha*, *?Rhizocorallium*, *Rosselia*, *Scolicia*, *Sinusichnus*, *Siphonichnus*, *Teichichnus*, and *Thalassinoides*), and distal expressions (*Chondrites*, *Helicodromites*, *Phycodes*, *Thalassinoides*, and *?Zoophycos*) in the lower shoreface to lower offshore and transitional settings with the shelf. However, the transition from these deposits to *Chondrites*-dominated beds associated with lower offshore to shelf environments—determined by changes in oxygenation, nutrients, and energy conditions—impedes assignment of all the successions to a particular ichnofacies.

The tide-dominated estuarine system features wide, channel-shaped bodies filled with sandy to heterolithic facies, interpreted as intertidal and subtidal deposits. To differentiate between estuary mouths and other settings, the analysis involved characterisation of transgressive and regressive surfaces, ichnological assemblages, and facies distribution, determining net sediment movement—whether landwards or seawards—and its influence on system classification. The ichnological assemblages could be assigned to the *Skolithos* (*Arenicolites*, *Gyrolithes*, *Maiakarichnus*, *Ophiomorpha*, *Schaubcylindrichnus*, *Skolithos*, and *Thalassinoides*) and *Cruziana* ichnofacies (*Ophiomorpha*, *Rosselia*, *Scolicia*, and *Siphonichnus*). Variations in diversity and abundance often help to determine certain stressful conditions, although the transition to more open areas is discussed, addressing how it could modify the typical models linked with a direct relationship between abundance/diversity and physico-chemical stress.

Keywords: Puerto Madryn Formation, shoreface-offshore-shelf system, estuarine system, *Cruziana* ichnofacies, *Skolithos* ichnofacies, ecological and depositional conditions, palaeoenvironmental analysis.

X.1. Introduction

Coastal environments encompass those accumulation sedimentary systems situated at the interface between continental and marine realms (Boyd et al., 1992). They are dynamic and complex depositional systems that coexist laterally along the same shoreline and can evolve into one another over time. The relative dominance of wave (fair-weather and storm), tidal and river depositional processes operating in a coastal system would respond to wave and tide energies, sediment supply (intrabasinal and extrabasinal), shoreline morphology and relative sea level changes (Dalrymple, 1992; Ainsworth et al., 2008, 2011). A complex interaction among these depositional processes shapes the morphology of coastal systems, their relative dominance being commonly used to define and classify coastal systems (Boyd et al., 1992; Yang et al., 2005; Ainsworth et al., 2011).

Ichnological datasets are invaluable for deciphering the relative dominance of wave, tide, and river processes along coastal settings (e.g., MacEachern et al., 2005; Gingras et al., 2011; Buatois et al., 2012; Moyano-Paz et al., 2020, 2022; Celis et al., 2023). The interaction of these processes generates a variety of physico-chemical stresses, including hydrodynamic energy, substrate consistency, sedimentation and erosion rates, water turbidity, bottom water de-oxygenation, salinity fluctuations, and channel avulsions, all of which impact benthic communities (e.g., MacEachern et al., 2005, 2007; Gingras et al., 2011; Buatois et al., 2012; Schwarz and Buatois, 2012; Bayet-Goll et al., 2015; Moyano-Paz et al., 2022; Ponce et al., 2023). Such stresses cause trace fossil assemblages to depart from the archetypal expression of the Seilacherian Ichnofacies, leading to ichnological assemblages dominated by facies-crossing elements, an overall reduction in the diversity of structures and a prevalence of simple structures (MacEachern et al., 2005, 2007; MacEachern and Bann, 2020, 2022).

In the last few years, the upsurge in studies related to the impact of physico-chemical stresses on benthic communities has been largely focused on deltaic depositional systems—even leading to new Seilacherian Ichnofacies proposals such as the *Rosselia* and the *Phycosiphon* ichnofacies (MacEachern and Bann, 2020, 2022). However, the influence of physico-chemical stresses, and consequently the occurrence, composition, and distribution of stressed ichnological assemblages in non-deltaic coasts, remains a topic that warrants further exploration in coastal sedimentary basin analysis.

The Puerto Madryn Formation is a non-deltaic coastal unit accumulated during the regional Late Miocene (Entrerriense) transgression in Patagonia, Argentina (Scasso and del Río, 1987; Cuitiño et al., 2017). The stratigraphic record of the Puerto Madryn Formation is divided into three depositional phases: transgressive, maximum flooding and regressive phases (Cuitiño et al., 2017). The transgressive phase includes wave-dominated nearshore to shelf deposits that grade vertically into thoroughly bioturbated shelf deposits of the maximum flooding phase (Cuitiño et al., 2017). The overlying regressive phase represents a transition from the shallow marine deposits towards an estuarine tidal-fluvial transition (Cuitiño et al., 2017). Such stratigraphic and palaeoenvironmental complexity makes the Puerto Madryn Formation an excellent case study for evaluating the relationship between depositional processes, ichnological assemblages, and physico-chemical stressful conditions. Accordingly, on the basis of field sedimentologic and ichnologic analyses, the aims of this paper are: i) to evaluate the role of wave, tide and river processes on the distribution of physico-

chemical stresses in non-deltaic coastal systems, and ii) to determine dissimilarities from the archetypal expression of Seilacherian Ichnofacies in order to improve preexisting ichnological models.

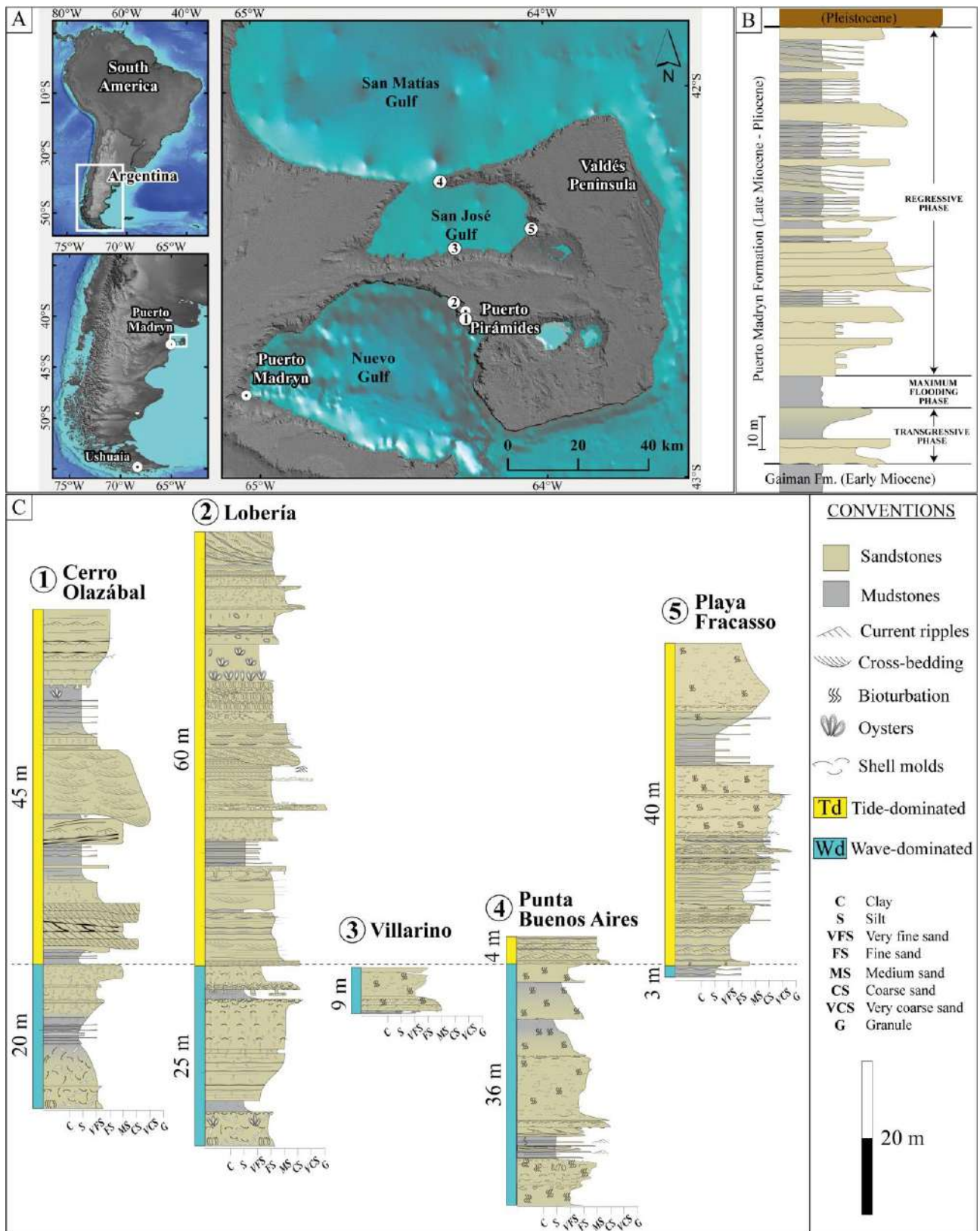


Fig. X.1. Geographic and stratigraphic context of the studied successions. **A.** Location map of the studied localities in Puerto Madryn and Peninsula Valdés region. **B.** Composite stratigraphic column of the Puerto Madryn Formation in the Valdés Peninsula (modified from Scasso and Cuitiño, 2017). **C.** Synthetic stratigraphic logs for the five studied localities.

X.2. Geological background

The study area lies in the western part of the Valdés Basin in northeast Chubut province, Argentina (eastern coast of Patagonia) (Fig. X.1A-B). The Neogene succession of the Puerto Madryn-Valdés Peninsula region (Fig. X.1C) comprises strata overlying a Jurassic volcanic basement to the west, south, and north of the study area, and overlying older sedimentary strata of the Aquitanian-Burdigalian rocks to the south (Cortés, 1987; Scasso et al. 2010; Cuitiño et al., 2023). In a Neogene stratigraphic column, the lowermost units are represented by the Early Miocene Gaiman Formation and the Trelew Member of the Sarmiento Formation (Haller, 1979; Scasso and del Río, 1987; Cuitiño et al., 2023). Above, an unconformable boundary has an extensive ravinement surface, separating them from the overlying Late Miocene sedimentary layers referred to as the Puerto Madryn Formation (Fig. X.1B). The Gaiman and Puerto Madryn formations have been associated with two significant Miocene marine flooding events observed in the Patagonian region: the Early Miocene Patagoniense Transgression (Parras and Cuitiño, 2021), and the Late Miocene Entrerriense Transgression (Scasso and del Río, 1987; Cuitiño et al., 2017). Other studies have documented Miocene deltaic systems advancing into the Patagonian shelf and could be correlated in age with those deposits (e.g., Lower Miocene Chenque Formation, Carmona et al., 2008, 2009; Lower Miocene Monte León Formation, Parras and Cuitiño, 2018).

The Puerto Madryn Formation is dated from the Late Miocene to Pliocene (Serravalian, 12 Ma to Piacenzian, 2.7 Ma; del Río et al., 2018; Cuitiño et al., 2023), an age assignment also supported by information on malacofauna (del Río, 2000; del Río et al., 2001), palynology (Palazzesi et al., 2006, 2014), foraminifera (Marengo, 2015) and mammals (Dozo et al., 2010). This formation crops out extensively in Valdés Peninsula and is well exposed at the coastal cliffs. It consists of about 150 m of shallow-marine deposits: mudstones, sandy mudstones, bioclastic mudstones, bioturbated muddy sandstones, bioclastic sandstones, bioturbated sandstones, heterolithic beds, and minor tuffs (Scasso and del Río, 1987; Scasso and Cuitiño, 2017; Cuitiño et al., 2023; Farroni et al., 2024). The high marine fossil diversity observed in the Upper Miocene deposits of Península Valdés may be attributed to upwelling processes, which enhance primary productivity and support the development of complex food webs (Cuitiño et al., 2017). The Puerto Madryn Formation was divided into three stratigraphic stages from base to top: the Transgressive Stage, the Maximum Flooding Stage and the Regressive Stage (Fig. X.1B) (del Río et al., 2001; Cuitiño et al., 2017, 2023). The transgressive stage is characterised by bioclastic mudstones and sandstones separated from the overlying phase by a maximum flooding surface, and mudstone deposits that accumulated when the sea level was at its maximum (del Río et al., 2001). The sediments of the upper part (regressive phase) accumulated in a fluvial-tidal transition zone within an estuary, and feature cross-bedded sandstones, heterolithic and herringbone bedding, inclined heterolithic stratification, and intraformational channel lag conglomerates. Hence, they reveal multiple tidal-channel infills, the interplay of tidal currents, fluvial processes, seasonal variations, and erosional surfaces associated with fluvial ravinement surfaces that characterise the bases of retrograding successions, highlighting the intermix between progradational fluvial and retrogradational deposits linked to estuarine conditions (Scasso et al., 2012; Scasso and Cuitiño, 2017). Some erosional surfaces are overlain, and even truncated, by

tidal ravinement surfaces; high-energy bioclastic conglomerates, mainly formed in the tidally/fluvially dominated estuary, further influence estuarine dynamics (Scasso and Cuitiño, 2017). Point bars were deposited from the freshwater fluvial source to the saltwater tidally dominated estuary, where the channel infill contains volcanoclastic sandy to muddy heterolithic seasonal rhythmites (Scasso and Cuitiño, 2017). Volcanic ashes from large explosive volcanic eruptions on land contributed to high sedimentation rates and favoured rapid burial, allowing the preservation of fossil vertebrates and invertebrates that inhabited the inner shelf (Maguire et al., 2016; Farroni et al., 2024) or off-channel, freshwater, low-energy environments such as marshes and ponds (Scasso et al., 2012; Scasso and Cuitiño, 2017). Assessments of marine-derived amorphous organic matter, phytoclasts, palynomorphs, and calcareous nannofossils, together with sedimentological and stratigraphic observations, also indicate a sporadic increase in fluvial, mud-laden freshwater input into the marine depositional system because of deltaic channel switching processes (Fuentes et al., 2019).

X.3. Methodology

This study is based on extensive observations from the exceptionally well exposed coastal cliffs of the Puerto Madryn Formation in the Valdés Peninsula (Argentine Patagonia; Fig. X.1). Detailed ichnological and lithological characteristics were noted and described for five localities, including Cerro Olazábal, Lobería, Playa Villarino, Punta Buenos Aires, and Playa Fracasso (Fig. X.1C). Sedimentary facies were defined based on bed thickness, grain size, sorting, sedimentary structures, stratal architectures, bioturbation index (BI *sensu* Taylor and Goldring, 1993), and the trace-fossil assemblage, which enabled interpretation of dominant depositional processes along each section (Table X.1). Correlation of the studied sections entailed identifying common lithological and ichnological features and detailing the similarity of vertical variations. Key stratigraphic surfaces were identified and traced laterally to ensure a reliable correlation. The lateral and vertical distribution of facies allowed us to construct a composite stratigraphic column (Figs. X.2 and X.3) for the studied sections of the Puerto Madryn Formation, following the maximum flooding surface cropping out across all sections, as well as the regressive surface between Interval 1 and Interval 2 (Fig. X.2). Additionally, surfaces of lower hierarchical order, such as other maximum flooding surfaces and, in some cases, maximum regression surfaces, were used as correlation datums. We then attempted to identify these surfaces laterally based on ichnological, sedimentological, and fossil records, and selected the section that best showcased the characteristics of each interval for representation in the generalised column (Figs. X.2 and X.3). In this way, we established a general distribution of facies associations and defined their surrounding depositional systems.

X.4. Sedimentological and ichnological features

The composite stratigraphic succession has a thickness of ~90 m (Fig. X.3). These deposits have been divided into eight facies associations (FAs), including moderately bioturbated structureless mudstones (FA1), highly bioturbated sandstones and mudstones (FA2), tabular and lenticular bioturbated shell beds (FA3), moderately bioturbated flaser bedding (FA4), moderately to highly bioturbated wavy and lenticular bedding (FA5), unbioturbated wavy and lenticular bedding (FA6), cross-bedded crushed shell beds (FA7), and occasional low-bioturbated structureless mudstones (FA8). A detailed sedimentological and ichnological description of each facies association is presented below (Table X.1).

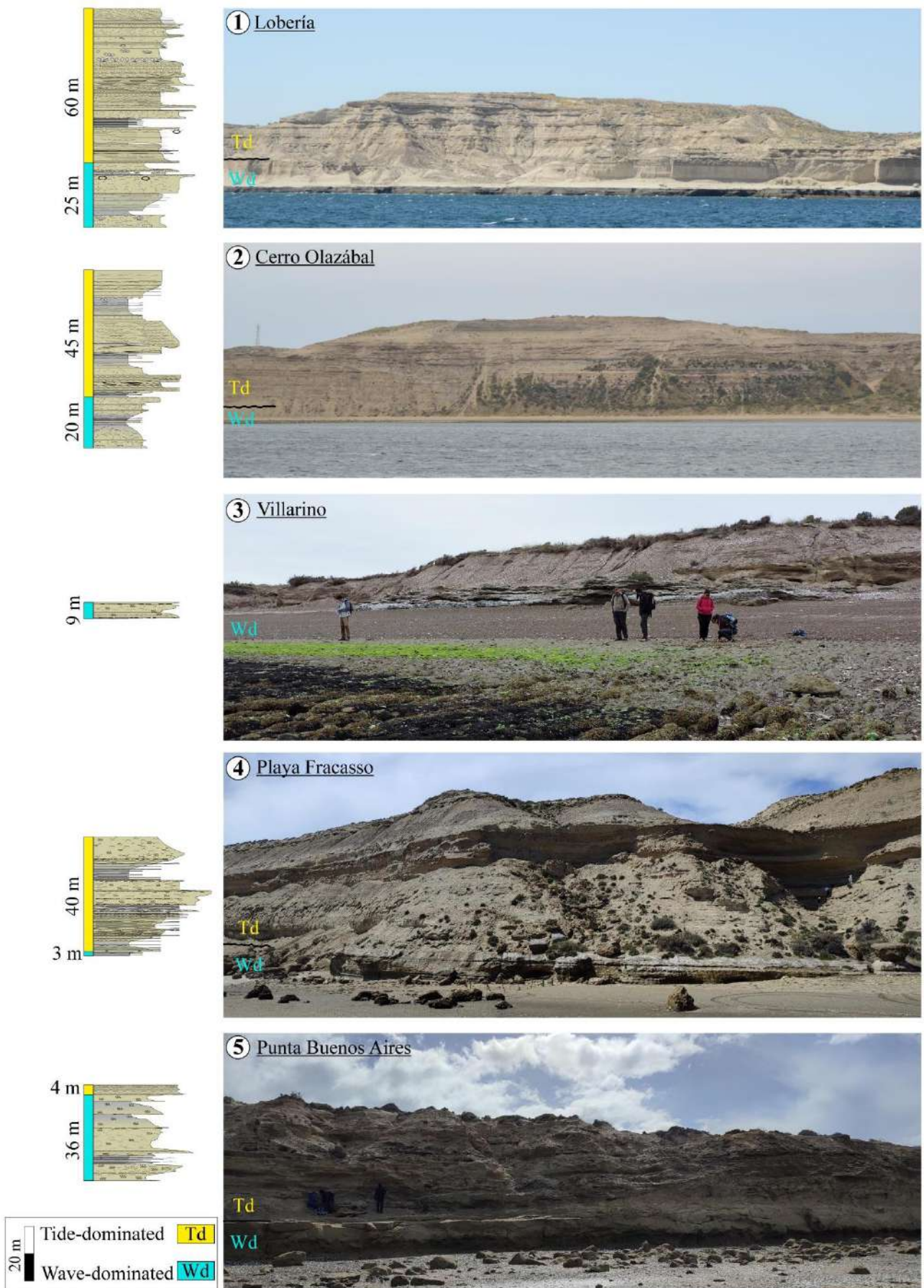


Fig. X.2. Outcrop profiles with wave- and tide-dominated intervals.

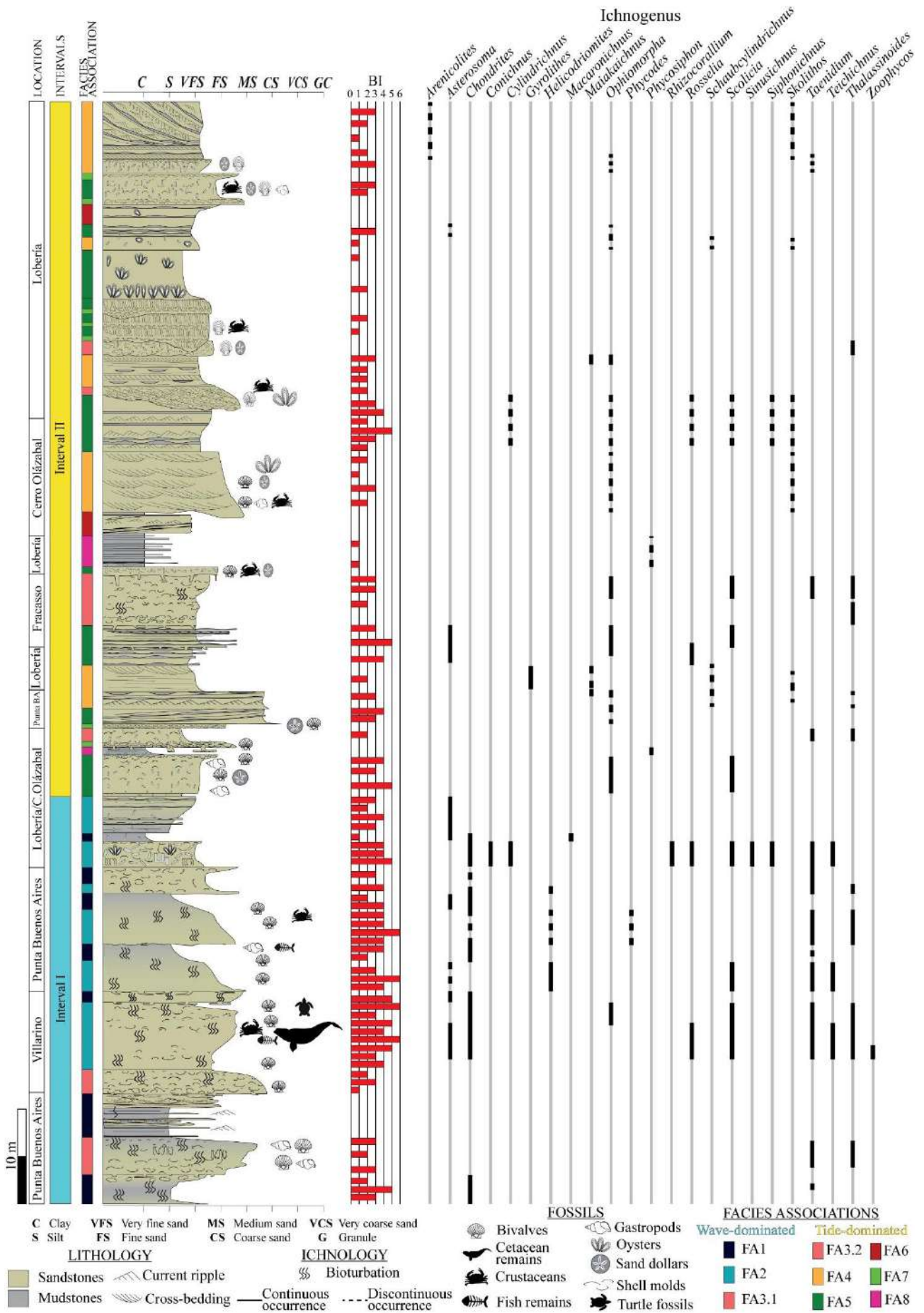


Fig. X.3. Composite stratigraphic log of the Puerto Madryn Formation where the dominant processes, facies associations, bioturbation index, and ichnogenus distribution are indicated.

Table X.1. Description and interpretation of Facies Associations.

| Facies Association | Lithology | Sedimentary Structures | Ichnology | | Geometry | Interpretation |
|--------------------|---|---|----------------|--|---|---|
| | | | BI most common | Ichnological assemblage | | |
| FA1 | Moderately bioturbated structureless mudstones | Structureless, bioturbated, ripple lamination, lenticular bedding. | 4 | (i) <i>Asterosoma</i> , <i>Chondrites</i> , <i>Macaronichnus</i> , and <i>Taenidium</i> . | Tabular; 1-3 m thick. | Offshore to shelf (Bromley and Ekdale, 1984; Baniak et al., 2014). |
| FA2 | Highly bioturbated mudstones, sandy mudstones, bioclastic sandy mudstones, and fine-grained sandstones. | Structureless, bioturbated. | 5 | (i) <i>Taenidium</i> and <i>Thalassinoides</i> with some <i>Chondrites</i> and <i>Phycodes</i> superimposed; (ii) <i>Asterosoma</i> , <i>Chondrites</i> , <i>Cylindrichnus</i> , <i>Ophiomorpha</i> , <i>?Rhizocorallium</i> , <i>Rosselia</i> , <i>Scolicia</i> , <i>Sinusichnus</i> , <i>Siphonichnus</i> , <i>Teichichnus</i> , and <i>Thalassinoides</i> ; (iii) <i>Helicodromites</i> , <i>Phycodes</i> , <i>Thalassinoides</i> , and <i>?Zoophycos</i> . | Tabular; 2-5 m thick. | Lower shoreface to offshore transition (Buatois and Mángano, 2011). |
| FA3 | Bioturbated bioclastic sandstones and mudstones. | Structureless, diffuse stratification. | 2 | FA3.1: <i>Ophiomorpha</i> , <i>?Scolicia</i> , <i>Taenidium</i> , and <i>Thalassinoides</i> . FA3.2: <i>Thalassinoides</i> , <i>?Ophiomorpha</i> , and <i>Taenidium</i> . | Tabular; from 2 to 5 m thick. Lenticular, sharp-based bodies up to 8 m thick. | Tabular: condensed shoreface; Lenticular: tidal channel (Cattaneo and Steel, 2003). |
| FA4 | Moderately bioturbated medium- to fine-grained sandstones, mudstones, and mud drapes. | Flaser bedding, cross-bedding, horizontal bedding, and combined-flow structures. | 2 | (i) <i>Arenicolites</i> , <i>Schaubcylindrichnus</i> , and <i>Skolithos</i> ; (ii) <i>Gyrolithes</i> , <i>Maiakarichnus</i> , and <i>Ophiomorpha</i> . | Lenticular bodies; 3-7 m thick. | Outer estuary (Dalrymple et al., 1992; Dalrymple and Choi, 2007). |
| FA5 | Moderately to highly bioturbated medium- to fine grained sandstones, mudstones, and oyster buildups. | Wavy- and lenticular bedding, cross-bedding, and structureless. | 3 | (i) <i>Ophiomorpha</i> , and crowded <i>Ophiomorpha</i> ; (ii) <i>Ophiomorpha</i> , <i>Scolicia</i> , and <i>Siphonichnus</i> ; (iii) <i>Rosselia</i> , <i>Scolicia</i> , and <i>Siphonichnus</i> . | Cuneiform up to 10 m thick. | Middle to outer estuary (Dalrymple and Choi, 2007). |
| FA6 | Unbioturbated medium- to fine grained sandstones, and mudstones. | Wavy- and lenticular bedding, climbing ripples, and inclined heterolithic stratification. | 0 | | Cuneiform up to 5 m thick. | Middle to inner estuary (Dalrymple and Choi, 2007). |
| FA7 | Crushed bioclastic sandstones. | Planar cross-bedding. | 0 | | Lenticular up to 1 m. | Tidal channel (Brett and Baird, 1986). |
| FA8 | Occasionally bioturbated mudstones. | Structureless | 1 | <i>Phycosiphon</i> . | Cuneiform up to 3 m thick. | Fluid-muds in channels subjected to marine flooding events (McIlroy, 2004; Ichaso and Dalrymple, 2009). |

X.4.1 Facies Association 1: moderately bioturbated structureless mudstones

Sedimentology: Facies Association 1 (FA1) shows tabular bodies between 1 and 5 m thick. FA1 consists of structureless mudstones and sandy mudstones that are occasionally bioturbated. Moreover, one interval 4–5 m in thickness has interbedded unbioturbated mudstones and sandy mudstones with asymmetrical ripple lamination forming lenticular bedding; it is associated with a soft-sediment deformation bed ~2 m thick.

FA1 grades vertically upwards to bioturbated sandy mudstones, bioclastic sandy mudstones, and fine-grained sandstones of the FA2, forming coarsening-upward successions. Moreover, FA1 overlies FA2 deposits, forming fining-upward successions (Fig. X.4A–B).

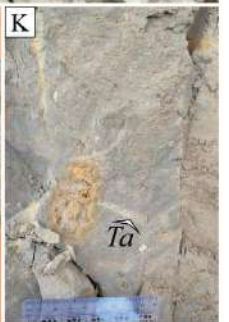
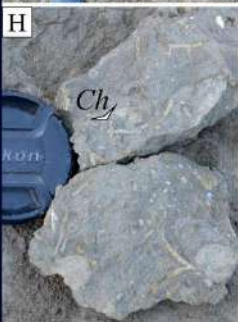
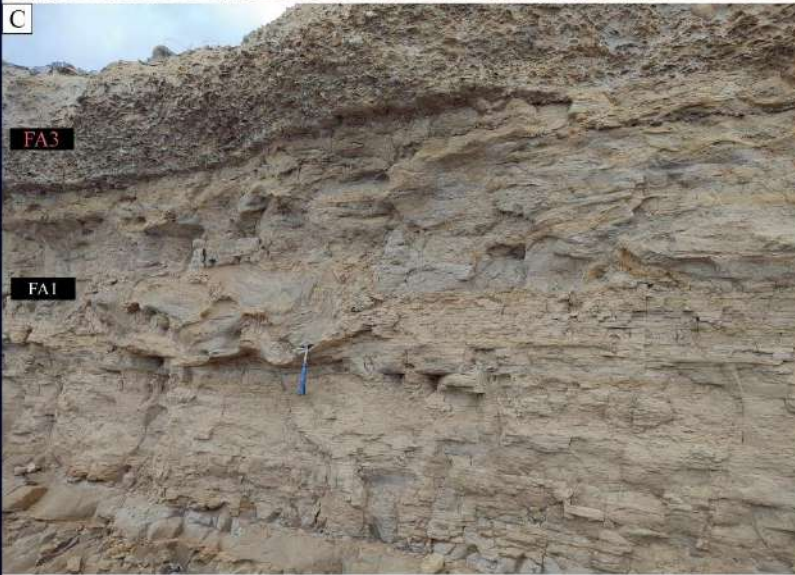
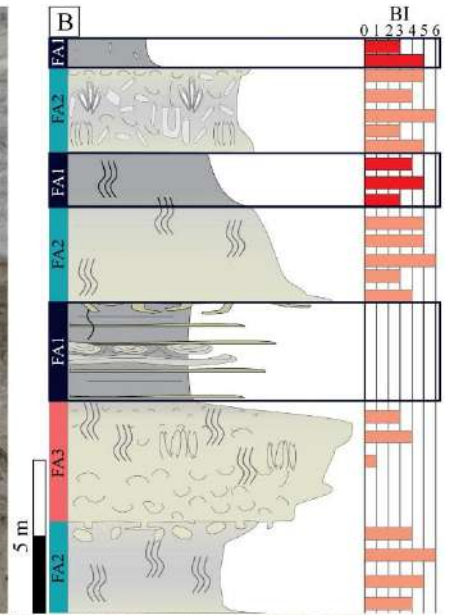
Ichthyology: Bioturbation intensities in the mudstone and sandy mudstone beds are unevenly distributed, mostly observed as dense patches (BI ~4). Beds completely devoid of bioturbation (BI = 0) are uncommon. The ichnoassemblage is dominated almost exclusively by *Chondrites*, with rare *Asterosoma*, *Macaronichnus*, and *Taenidium* (Fig. X.4E–K). *Chondrites* are present in two sizes: an association dominated by *Chondrites* smaller than 0.3 cm in width, and a whitish *Chondrites* association over 1 cm wide. Crosscutting relationships — *Chondrites* overlapping *Taenidium* — are common in this ichnoassemblage (Fig. X.4C–D).

Interpretation: FA1 is interpreted as the accumulation of fine-grained sediments from suspended loads in low-energy, fully marine shelf environments below the storm-wave base level. However, transitions to lower offshore zones can be interpreted through the presence of sandy mudstones, which indicate some influence and remnants of storm events (Baniak et al., 2014). The absence of marine macrofauna, unevenly distributed bioturbation intensities, and the ichnoassemblage with dominant deep-tier sessile deposit feeding structures (*Chondrites*) point to reduced bottom water and water column oxygenation conditions (Bromley and Ekdale, 1984). The accumulation of sandy mudstones suggests across-shelf currents (Pearson et al., 2007), causing mixing of the water column and the re-establishment of well-oxygenated conditions that favoured a recolonisation of the substrate evidenced by sessile (*Asterosoma*) and mobile (*Macaronichnus* and *Taenidium*) deposit feeding structures (Martin, 2004). In this case, *Macaronichnus* would likely correspond to *M. segregatis degiberti*, an ichnosubspecies found in distal marine environments (Rodríguez-Tovar and Aguirre, 2014; Nara and Seike, 2019; Rodríguez-Tovar and García-García, 2023).

The 4–5 m interval, which lacks clear lateral continuity, exhibits a high concentration of palynomorphs exclusively within that interval (Fuentes et al., 2019), whilst the presence of asymmetrical ripple lamination and soft-sediment deformation suggest an episodic and sudden influx of a fluvio-deltaic system. This event most likely led to high sedimentation rates in relatively steep systems, associated with hyperpycnal prodelta flows reaching the shelf (Arnott and Southard, 1990; Zavala, 2020).

Fig. X.4. Field examples of FA1: moderately bioturbated structureless mudstones. **A.** Outcrop view of moderately bioturbated structureless mudstones. **B.** Stratification trends of FA1 and their relationship to the other facies associations. **C.** Outcrop view of mudstones and sandy mudstones overlain by mudstones with soft-sediment structure (FA1), and further overlain by bioclastic shell bed of FA3. **D.** Outcrop view of interbedding of unbioturbated mudstones and sandy mudstones (FA1). **E to K.** Field examples of bioturbation structures of FA1: *Asterosoma* (*As*); *Chondrites* (*Ch*); *Macaronichnus* (*Ma*); *Taenidium* (*Ta*).

FA1: moderately bioturbated structureless mudstones



X.4.2 Facies Association 2: highly bioturbated sandstones and mudstones

Sedimentology: Facies Association 2 (FA2) forms tabular bodies 2-5 m thick (Fig. X.5A-C). FA2 consists of moderately to pervasively bioturbated mudstones, sandy mudstones, bioclastic sandy mudstones (Fig. X.5D), and fine-grained sandstones where the mechanic sedimentary structures are obliterated by intense bioturbation. Furthermore, these deposits contain centimetre-thick accumulations of gastropods, bivalves, bryozoans, echinoids (sand dollars), and vertebrate fossils, sometimes with scour surfaces at the bottom. FA2 can be found grading vertically upwards to the fine-grained deposits of FA1, forming fining-upward successions (Fig. X.5), or else to shell beds of FA3 forming coarsening-upward successions.

Ichnology: The deposits associated with FA2 are moderately to intensely burrowed (BI = 3-6). Sixteen ichnotaxa are recorded, comprising *Asterosoma*, *Chondrites*, *Conichnus*, *Cylindrichnus*, *Helicodromites*, *Ophiomorpha*, *Phycodes*, *Rhizocorallium*, *Rosselia*, *Scolicia*, *Sinusichnus*, *Siphonichnus*, *Taenidium*, *Teichichnus*, *Thalassinoides*, and *Zoophycos*. This facies association presents three ichnological assemblages:

(i) *Taenidium* and *Thalassinoides* with some *Chondrites*, *Helicodromites* and *Phycodes* superimposed (Fig. X.5E-I); this assemblage is present in sandy mudstones, fine-grained sandstones and some mudstones, with bioturbation index values between 3 and 4. *Taenidium* is the most abundant ichnogenus, even bioturbating previous *Thalassinoides* burrows. Some cross-cutting relationships are observed, including *Taenidium* overlapping *Thalassinoides*, and *Chondrites-Phycodes* overlapping *Taenidium* and *Thalassinoides*.

(ii) *Asterosoma*, *Chondrites*, *Cylindrichnus*, *Ophiomorpha*, ?*Rhizocorallium*, *Rosselia*, *Scolicia*, *Sinusichnus*, *Siphonichnus*, *Taenidium*, *Teichichnus*, and *Thalassinoides* (Fig. X.6A-L). This trace fossil assemblage occurs in sandy mudstones, and fine-grained sandstones with bioturbation index values ranging between 3 and 6. *Thalassinoides* cross-cut by *Chondrites* and by *Taenidium* were identified.

(iii) *Chondrites*, *Helicodromites*, *Phycodes*, *Thalassinoides*, and ?*Zoophycos* (Fig. X.6M-R). This ichnoassemblage appears in mudstones and sandy mudstones, with bioturbation index values of 3 to 4. *Helicodromites* is the most abundant trace. Several cross-cutting relationships were observed, including *Helicodromites* over *Thalassinoides*, *Phycodes* over *Helicodromites* and *Thalassinoides*, and *Zoophycos* over *Thalassinoides*.

Interpretation: The abundant bioturbation and the high ichnodiversity recorded in the deposits of FA2, in addition to the abundant vertebrate and invertebrate fossils, suggest accumulation in a shelf to shoreface environment with normal salinity (Clifton, 2006). The dominance of *Taenidium* and *Thalassinoides* in the ichnoassemblage i points to moderate to high-energy levels, as well as moderate sedimentation rates (e.g., Malpas et al., 2005). A very diverse ichnoassemblage ii is often registered in shallow marine, moderate-energy environments with sandy substrates (Pemberton et al., 2012) that allow bioturbation by a variety of tracemakers of different behaviour. The occurrence of *Thalassinoides*, which is a trace fossil often produced by burrowing crustaceans, along with *Asterosoma* would suggest the presence of a well-oxygenated bottom water environment (Monaco et al., 2007; MacEachern and Bann, 2008; Pemberton et al., 2012). In turn, *Rosselia* has been interpreted as the dwelling structure of detritus-feeding tolerant polychaetes found in different shallow

marine conditions with variations in the colonisation style (e.g., Carmona et al., 2009; Aguirre et al., 2010; Netto et al., 2014; Bayet-Goll et al., 2022). In this case, given the diversity and abundance of the ichnoassemblage, *Rosselia* represents a typical component of the fair-weather community without major system disturbances in quiet fully marine conditions (e.g., Bayet-Goll et al., 2022), not associated with unstable and physically controlled substrates (e.g., crowded *Rosselia*, Netto et al., 2014). *Siphonichnus* indicates the presence of suspension- and deposit-feeders adjusting their position in response to erosion and deposition in high-energy environments; but likewise suggests the activity of vagile endobenthic organisms for locomotion and partial deposit-feeding, possibly indicating a community without apparent stressor conditions (e.g., Knaust, 2015). The presence of *Rhizocorallium* and *Taenidium* suggests that the substrate was colonised by deposit-suspension feeders, and locomotion-detritus-feeding, respectively (e.g., Rodríguez-Tovar and Pérez-Valera, 2008; Knaust, 2013).

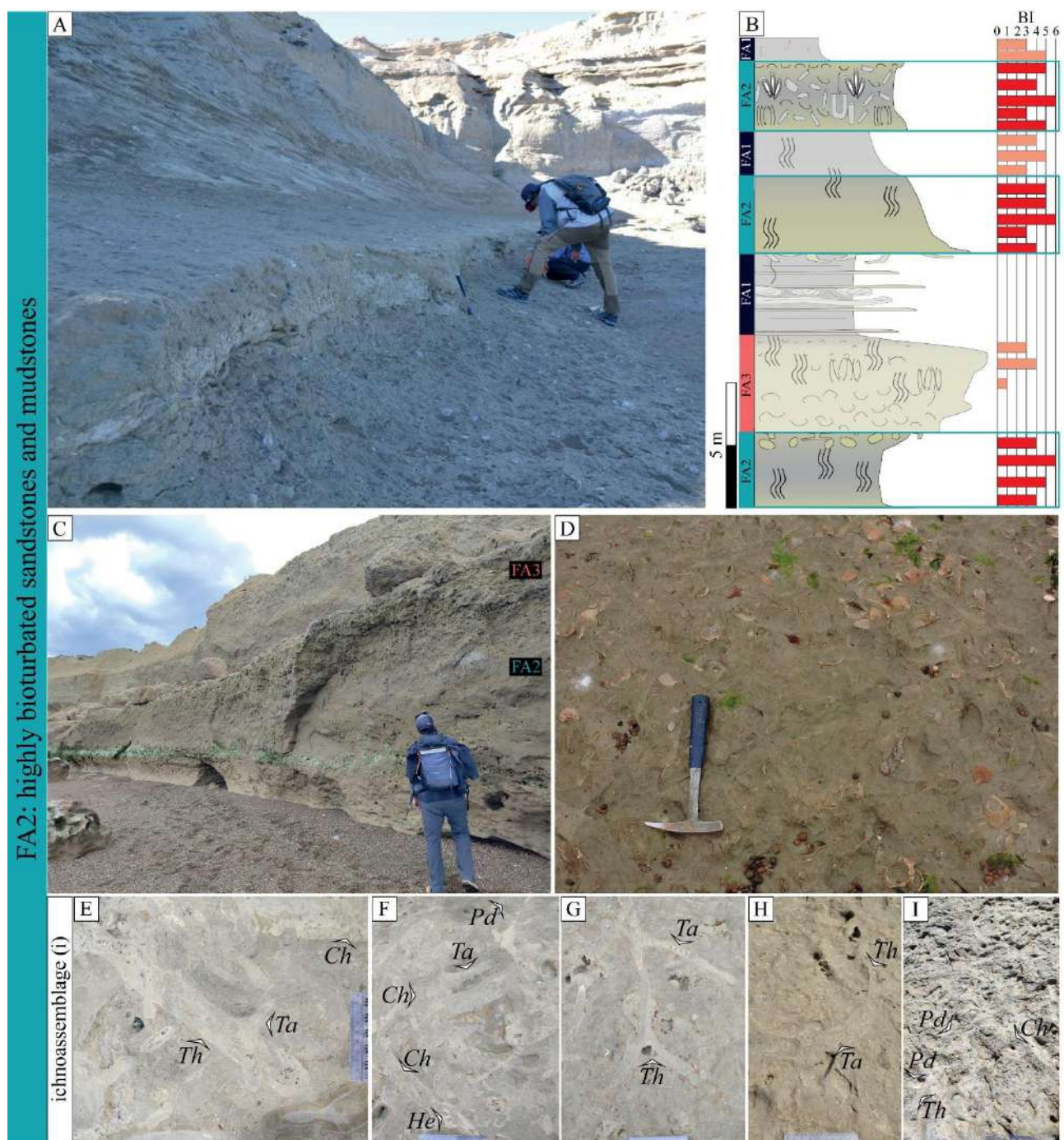


Fig. X.5. Field examples of FA2: highly bioturbated sandstones and mudstones. **A.** Outcrop view of FA2. **B.** Stratification trends of FA2 and their relationship to the other facies associations. **C.** Outcrop view of bioturbated bioclastic sandy mudstones of FA2 and coarsening upward trend to FA3. **D.** Bioturbated bioclastic sandy mudstones with randomly distributed bivalve shells. **E to I. Field examples of bioturbation structures of FA2.** Ichnoassemblage i: *Chondrites* (*Ch*), *Helicodromites* (*He*), *Phycodes* (*Pd*), *Taenidium* (*Ta*) and *Thalassinoides* (*Th*).

Moreover, *Sinusichnus* represents deposit-feeding crustaceans, probably associated with some storm remnants, as it has been linked to shallow marine, offshore to nearshore transition environments (de Gibert, 1996; Buatois et al., 2009; Belaústegui et al., 2013). Ichnoassemblage iii signals a depositional environment of low to moderate water energy and oxygen levels, but with a relatively high input of organic matter (e.g., Baucon et al., 2020). This is typical of offshore to shelf environments, where the sedimentation rate is relatively low, and the bottom water oxygen levels are often lower due to a combination of factors, e.g. water stratification, limited mixing, and the decomposition of organic matter. The presence of bioturbating organisms—such as deposit-feeding polychaetes and echinoderms— suggests that the sediment was nutrient-rich and able to support a diverse benthic community (e.g., Vesal et al., 2023). Thus, the three ichnoassemblages are characteristic of lower shoreface to offshore transitional environments (MacEachern et al., 2012; Pemberton et al., 2012).

X.4.3 Facies Association 3: tabular and lenticular bioturbated shell beds

Sedimentology: Facies Association 3 (FA3) is constituted by m-thick accumulations of bioclastic-dominated deposits (=shell beds). Two types are discerned within this facies association: FA3.1 related to FA1 and FA2; and FA3.2 associated with FA4, FA5, FA6, FA7, and FA8.

FA3.1 is composed of tabular amalgamated bodies that range between 1 and 5 m thick, with internal discontinuities, showing fine to coarse sandy matrix, diffuse stratification, moderate to intense bioturbation, and a highly diverse fossil invertebrate association dominated by bivalves, gastropods, bryozoans, sand dollars, and barnacles, as well as phosphatic concretions, marine mammal remains, and shark teeth, with a low degree of fragmentation (Fig. X.7A-E). They are included in the invertebrate assemblage association A of del R o et al. (2001). The matrix comprises fine- to medium-grained sandstone with volcanic lithics, plagioclase and quartz, and some shell fragments. The relationship between the shell and matrix in the beds varies. Although they are predominantly shell-supported, variations to matrix-supported structures do occur. Beds of FA 3.1 may transitionally or sharply cover beds of FA2 or FA1.

FA3.2 is formed by lenticular sharp-based bodies up to 8 m in thickness, consisting of light grey and grey sandy matrix, massive structure and in some occasions diffuse cross-stratification, as well as moderate bioturbation. The bioclastic fraction is constituted mainly by boulder-sized oysters, with some pectinids, echinoids, bryozoans and gastropods, the shell hash having a high degree of fragmentation being included in the invertebrate assemblage association C of del R o et al. (2001). The matrix is composed of medium- to coarse-grained sandstone with abundant shell fragments, and some lithics and quartz. The bases of these deposits are invariably irregular, lying atop deposits of FA4, 5, or 6, and transitionally covered by cross-bedded sandstones of FA4 (Fig. X.7F-J).

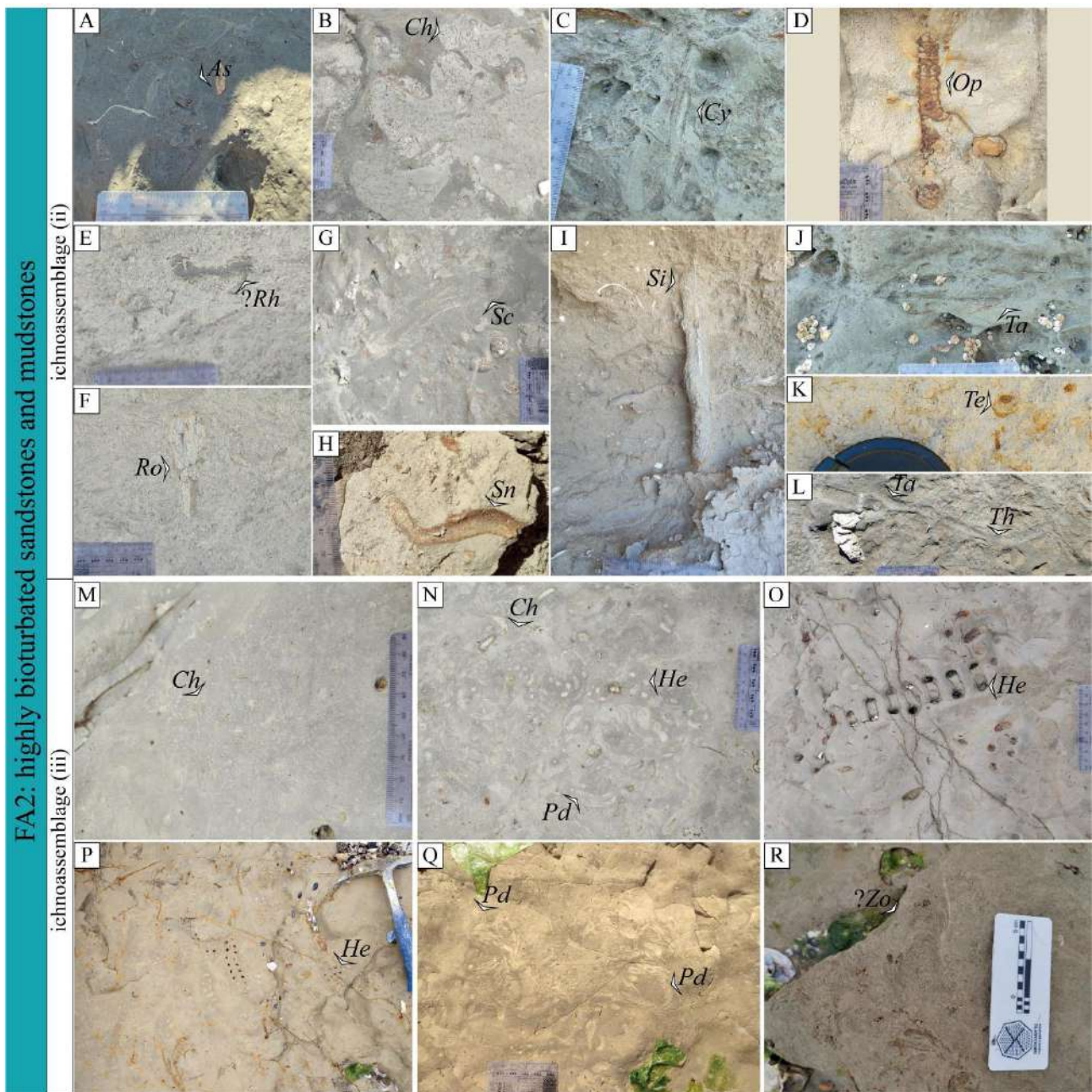
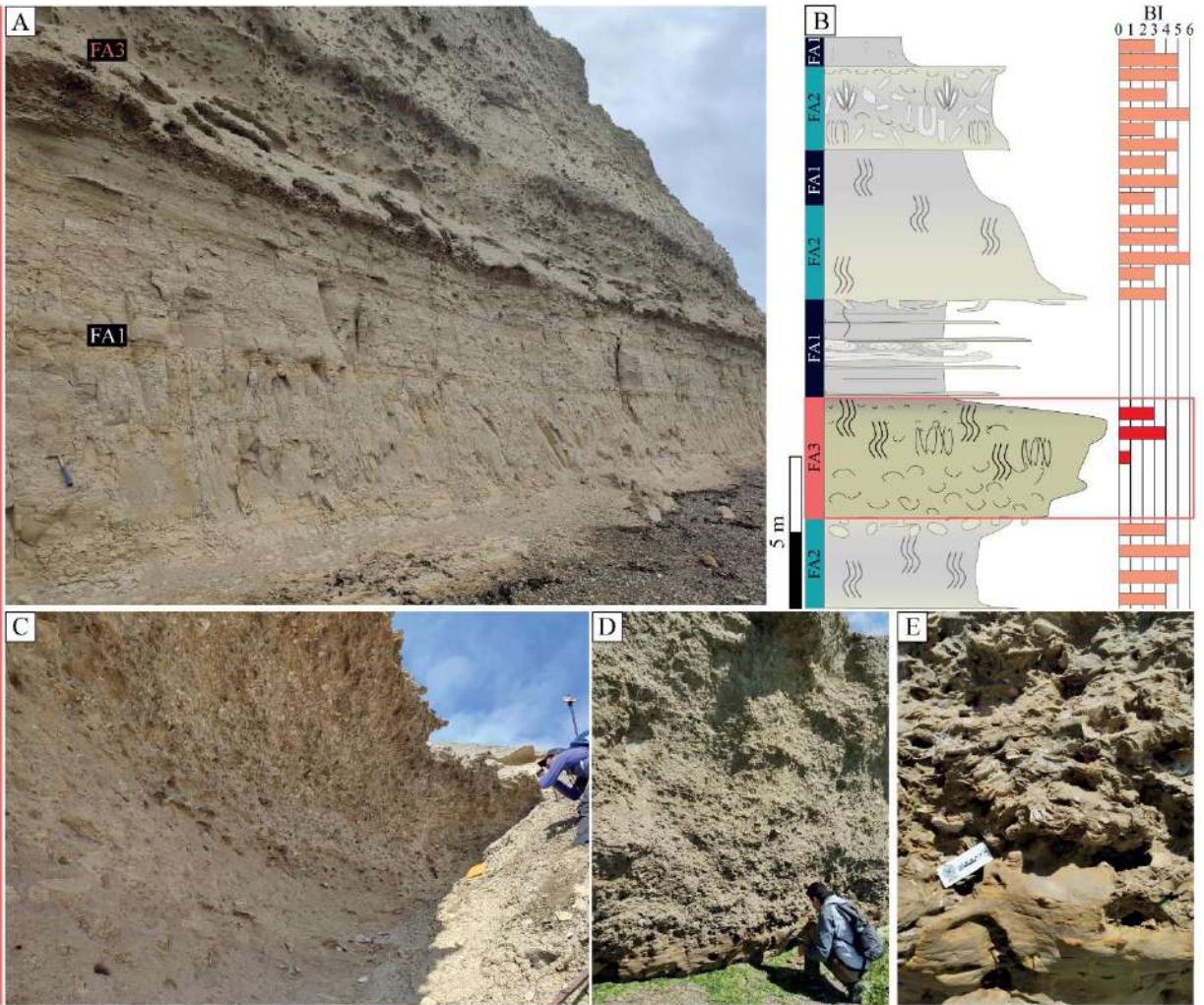


Fig. X.6. Field examples of bioturbation structures of FA2. A to L: ichnoassemblage ii and **M to R:** ichnoassemblage iii: *Asterosoma* (*As*); *Chondrites* (*Ch*); *Helicodromites* (*He*); *Ophiomorpha* (*Op*); *Phycodes* (*Pd*); *?Rhizocorallium* (*?Rh*); *Rosselia* (*Ro*); *Scolicia* (*Sc*); *Sinusichnus* (*Sn*); *Siphonichnus* (*Si*); *Taenidium* (*Ta*); *Teichichnus* (*Te*); *Thalassinoides* (*Th*); *Zoophycos* (*Zo*).

Ichnology: Bioclastic beds of both tabular morphology and lenticular morphology are unbioturbated to moderately bioturbated (BI = 0-3), with a slight decrease in bioturbation in the lenticular beds (FA3.2). Soft-ground trace fossils such as *Ophiomorpha*, *?Scolicia*, *Taenidium*, and *Thalassinoides* are present in FA3.1. In FA3.2 the ichnoassemblage is dominated by trace fossils like *Thalassinoides* produced in soft but cohesive substrates (Rodríguez-Tovar et al., 2008), and superimposed soft-ground trace fossils such as *Taenidium* and *?Ophiomorpha* (Fig. X.8). Some *Thalassinoides* may be bioturbated by *Taenidium* in both types of facies.

FA3.1: tabular bioturbated shell beds



FA3.2: lenticular bioturbated shell beds

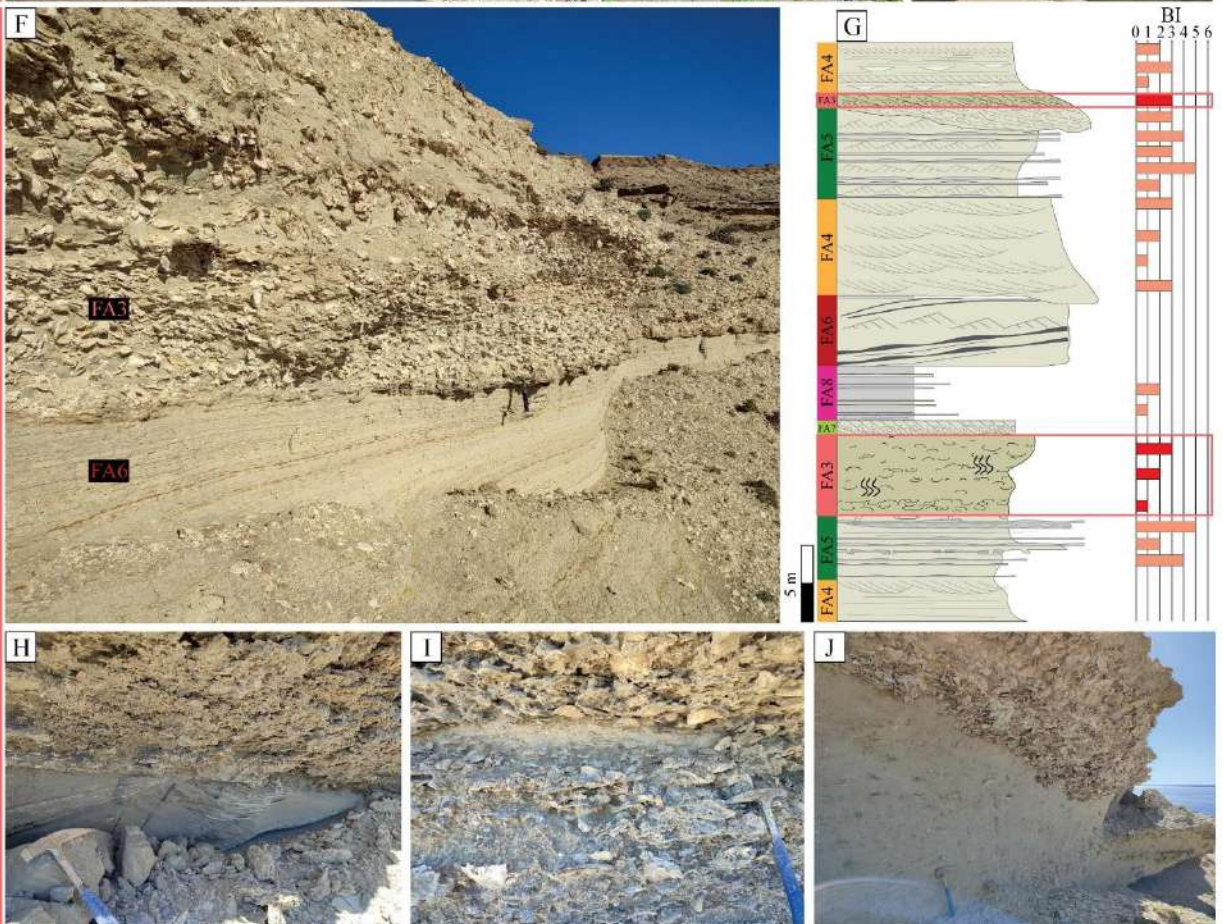


Fig. X.7. Field examples of FA3: bioturbated shell beds. A to E: tabular bioturbated shell beds. **A.** Outcrop view of tabular shell beds overlying FA1. **B.** Stratification trends of FA3.1 and their relationship to the other facies associations. **C.** Massive tabular shell bed. **D.** Irregular surface of massive tabular shell bed over FA1. **E.** Detail of oyster concentrations in tabular shell bed. **F to J: lenticular bioturbated shell beds.** **F.** Outcrop view of lenticular shell beds overlying FA4. **G.** Stratification trends of FA3.2 and their relationship to the other facies associations. **H.** Detailed outcrop of lenticular shell beds overlying FA4. **I.** Close-up view of bivalve concentrations. **J.** Irregular surface of massive lenticular shell bed over FA4.

Interpretation: The presence of bioclastic conglomerates and sandstones rich in fossil invertebrates points to a shallow marine environment under high-energy conditions. The intense bioturbation by softground trace fossils suggests the activity of infaunal organisms that actively burrow and feed within the sediment. This behaviour likely reflects a response to the rapid accumulation of buried nutrients during fair-weather conditions (e.g., Pemberton et al., 1992; Kim and Heo, 1997). Yet the bioturbation of previous *Thalassinoides* by softground trace fossils may indicate two separate colonisation phases in the soft-ground substrates. It is also possible that the *Thalassinoides* formed during a depositional hiatus, representing firmground colonisation, followed by bioturbation by softground trace fossils. Still, without clear evidence of pauses in sedimentation, deciphering the phases of bioturbation during these events remains challenging.

Shell-supported tabular beds (FA3.1) containing shelf molluscs with low fragmentation and a bioturbated bioclastic sandy matrix may indicate prolonged exposure on the seafloor, with minimal transport of shells away from their original habitat (Kidwell et al., 1986; del Río et al., 2001). Invertebrate shell-rich deposits with sandy matrix and bioturbation are commonly formed in shoreface environments (shallow marine and inner shelf zones under wave or tidal current reworking; see discussion in 6.1), during periods when the rate of carbonate production surpasses the rate of clastic deposition (Cattaneo and Steel, 2003; Tomasovych et al., 2006). Additionally, these processes agree with the in situ macrobenthic tracemakers activity observed in soft substrates. In contrast, lenticular shell beds (FA3.2) with irregular sharp bases are interpreted as allochthonous, multi event, shell-supported deposits associated with channel environments (del Río et al., 2001). The dominance of oyster shells, as well as the presence of cross-bedding interbedded with mud drapes (FA4), would mean that FA3.2 represents tidal channel or tidal inlet deposits (e.g., Gingras et al., 2012a). Traces of softground substrate may correspond to periods of bioturbation during the waning phases of high-energy events (e.g., Kim and Heo, 1997).

X.4.4 Facies association 4: moderately bioturbated flaser bedding

Sedimentology: Facies Association 4 (FA4) comprises lenticular-shaped bodies up to 1 km wide, with invariably irregular bases, commonly 3 to 7 m in thickness. These deposits contain metric grey fine- to medium-grained sandstones, and centimetric-millimetric light yellow mudstones that occasionally form heterolithic bedding with mud drapes. The dominant sedimentary structures are flaser bedding and planar cross-bedding. Climbing-ripple cross-bedding, horizontal bedding on some occasions, and in one interval (Cerro Olázabal) oscillatory and combined-flow structures are observed (Fig. X.9A). FA4 transitionally or sharply covers beds of FA5 (Fig. X.9B).

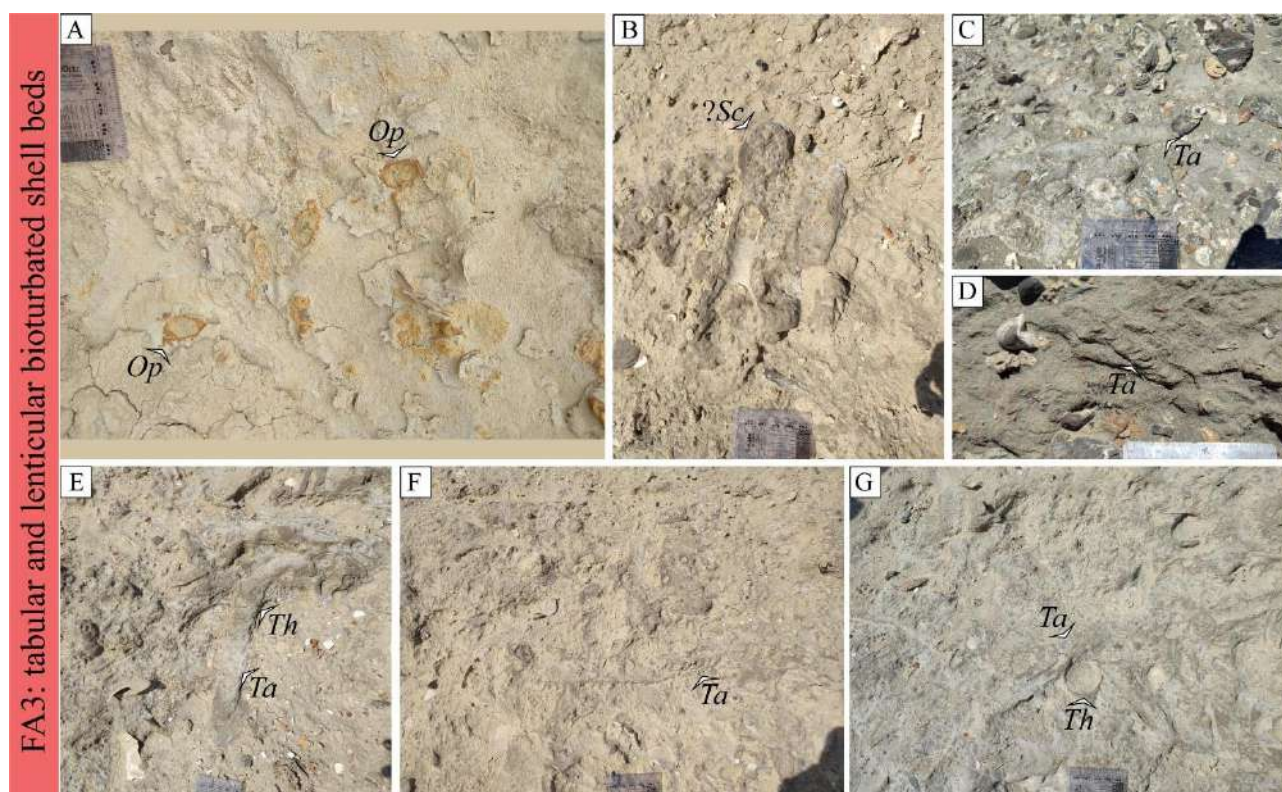


Fig. X.8. Field examples of bioturbation structures of FA3. Ichnoassemblage of FA3: *Ophiomorpha* (*Op*); *?Scolicia* (*Sc*); *Taenidium* (*Ta*); *Thalassinoides* (*Th*).

Ichnology: Sandstone beds are occasionally bioturbated (BI = 0-3) by suspension feeding structures such as (i) *Arenicolites*, *Skolithos* and *Schaubcylindrichnus* (Fig. X.9C-E), or by a less recurrent ichnoassemblage characterised by (ii) *Gyrolithes*, *Maiakarichnus*, *Ophiomorpha* and *Thalassinoides* with fill that is generally finer-grained (mud) than the host sediment (Fig. X.9F-H). Cross-cutting relationships were not observed.

Interpretation: The presence of channelised bodies showing irregular bases, flaser and planar cross-bedding with asymmetrical ripples, and occasionally with mud drapes, suggests deposition by traction under a lower flow regime dominated by tidal currents within tidal channels (Dalrymple et al., 1992; Dalrymple and Choi, 2007). Mud drapes are typically associated with periods of reduced flow velocity and increased settling of fine particles during the slack water tidal phase (Mackay and Dalrymple, 2011). The dominance of suspension feeding traces such as *Arenicolites*, *Skolithos*, and *Schaubcylindrichnus*, along with unbioturbated intervals in the sandstone beds, indicates high-energy settings (Pemberton, 2001; MacEachern et al., 2007). Together with the fine- to medium grain size of the sediments, high hydrodynamic energy conditions, and their vertical relationship with FA5 and FA6 (see below), such settings invoke the bottomset of subtidal sand bodies and the core of subtidal sandbars (Dalrymple et al., 1992; Bromley, 1996). The presence of some mixed oscillatory and combined flow structures in this environment suggests a complex interplay between tidal currents and wave energy (e.g., Yang et al., 2008).

The ichnoassemblage ii (*Gyrolithes*, *Maiakarichnus*, *Ophiomorpha* and *Thalassinoides*), consisting of suspension-feeder burrows with fine-grained fill, indicates that these traces were created during brief windows of slightly reduced energy (e.g., Gingras et al., 2008, 2011) when mud was deposited in subtidal sandflats. The

architecture of large, channelled bodies may be consistent with deposition in an outer estuarine setting (Beynon et al., 1988; Bromley, 1996; Dalrymple and Choi, 2007).

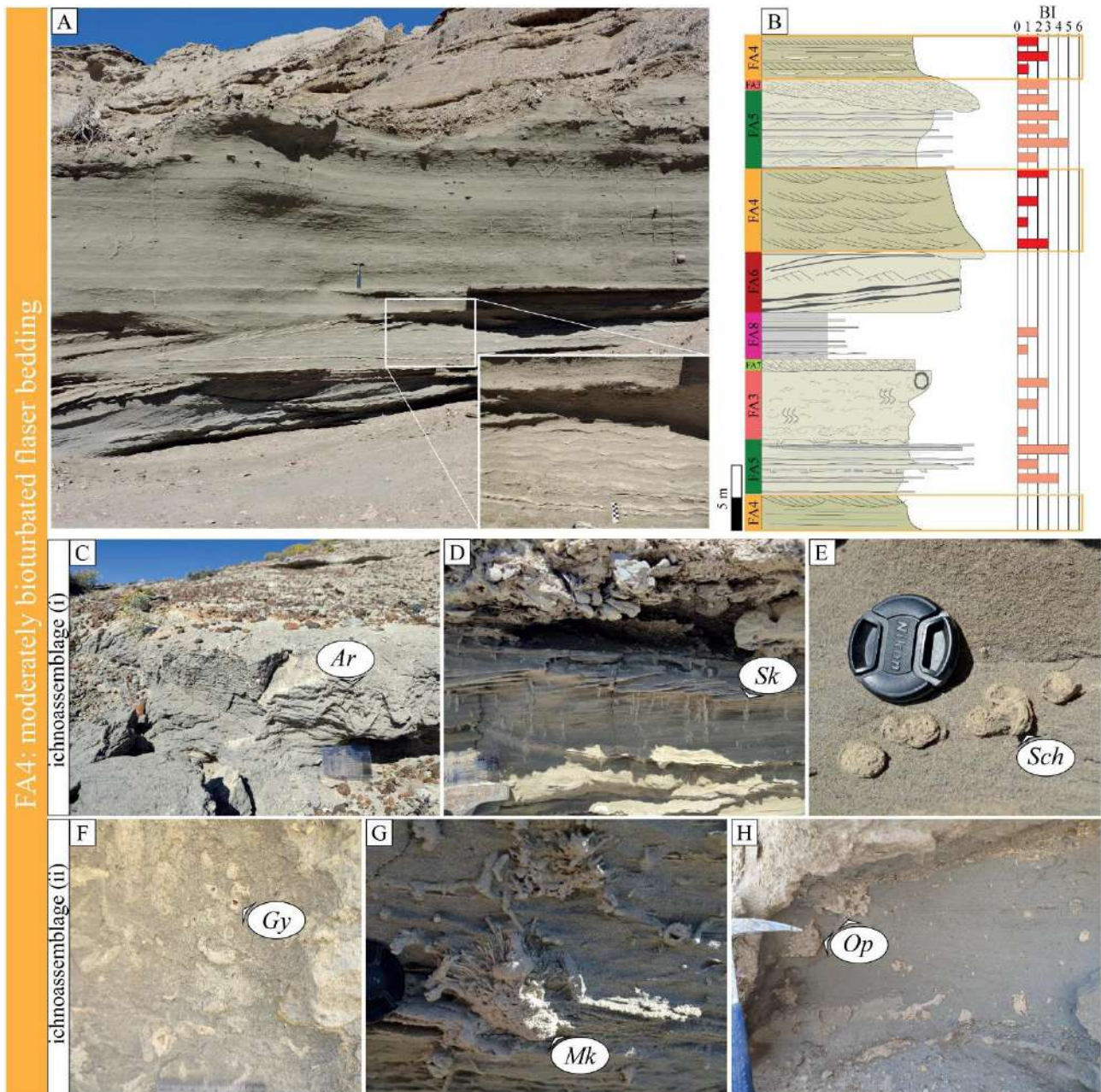


Fig. X.9. Field examples of FA4: moderately bioturbated flaser bedding. A. Outcrop view of flaser bedding with cross-bedding and horizontal bedding and zoom detail of mud drapes. B. Stratification trends and their relationship to the other facies associations. C-H: Field examples of bioturbation structures of FA4. C-E: ichnoassemblage i: *Arenicolites* (Ar); *Skolithos* (Sk); *Schaubcylindrichnus* (Sch). F-H: ichnoassemblage ii: *Gyrolithes* (Gy); *Maiakarichnus* (Mk); *Ophiomorpha* (Op).

X.4.5 Facies association 5: moderately to highly bioturbated wavy and lenticular bedding

Sedimentology: Facies Association 5 (FA5) consists of wedge-shaped beds up to 10 m thick of grey medium- to fine-grained sandstones and light-yellow mudstones with heterolithic wavy and lenticular bedding structures (Fig. X.10A-E). Locally, planar and trough cross-bedding structures are observed. FA5 transitionally or

sharply covers beds of FA4. Oyster buildups (biostromes) in life position are commonly intercalated within FA5 (Fig. X.10E).

Ichtnology: Heterolithic facies show an increase in the bioturbation index with respect to those observed in FA4 (BI = 0-5). Variations in abundance from suspension feeding behaviours to deposit- and detritus feeding behaviours and vice versa are observed. The ichnoassemblages are characterised by: (i) in wavy bedding, suspension-feeders such as *Ophiomorpha* just on top of FA4 deposits, and crowded *Ophiomorpha* with passively filled rhythmic laminations reflecting tubular tidalites (Fig. X.11A-F); (ii) suspension-feeders such as *Ophiomorpha*, abundant deposit-feeders such as *Scolicia*, and suspension- and deposit-feeders such as *Siphonichnus* (Fig. X.11G-I); and in lenticular bedding, (iii) detritus-feeding such as *Rosselia*, deposit-feeding such as *Scolicia*, and abundant suspension- and deposit-feeders such as *Siphonichnus* are seen (Fig. X.11J-M). Cross-cutting relationships were not observed.

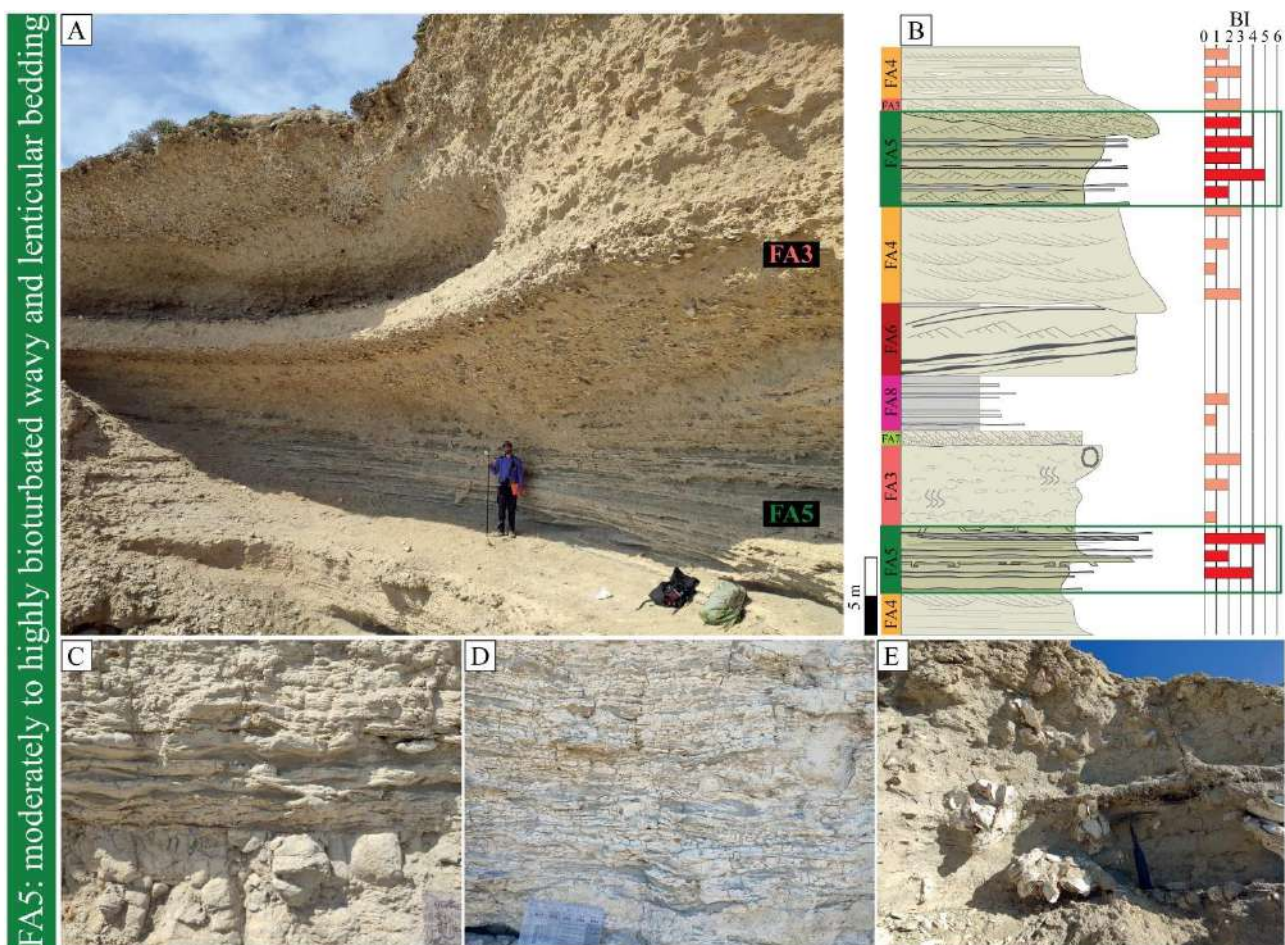


Fig. X.10. Field examples of FA5: moderately to highly bioturbated wavy and lenticular bedding. **A.** Outcrop view of wavy and lenticular bedding overlain by lenticular shell bed (FA3.2). **B.** Stratification trends and their relationship to the other facies associations. **C.** Detail of lenticular bedding (beige: mudstones; grey: sandstones). **D.** Detail of wavy bedding (beige: mudstones; grey: sandstones). **E.** Oyster buildups (biostromes) in life position. **F.** Structureless mudstones overlain by FA4. **G.** Detailed structureless mudstones with *Thalassinoides* (*Th*) from the top bed.



Fig. X.11. Field examples of bioturbation structures of FA5. **A-F:** ichnoassemblage i: *Ophiomorpha* (*Op*). **G-I:** ichnoassemblage ii: *Scolicia* (*Sc*); *Siphonichnus* (*Si*). **J-M:** ichnoassemblage iii: *Rosselia* (*Ro*), *Scolicia* (*Sc*); *Siphonichnus* (*Si*).

Interpretation: The frequent occurrence of heterolithic facies with a higher proportion of mud and clay suggests a more sheltered, lower-energy environment compared to FA4, characteristic of middle to lower intertidal sandflats (e.g., Dalrymple and Rhodes, 1995; Dalrymple and Choi, 2007; Ahmad et al., 2024). Wavy and lenticular bedding, along with tubular tidalites, would attest to fluctuations in hydraulic energy within the depositional system, likely influenced by tidal currents (e.g., Wetzel et al., 2014; Gingras and Zonneveld,

2015). Cross-bedding results from the migration of subaqueous dunes or bars, and in some cases, ripple migration. These features reflect episodic high-energy events against a background low-energy context, or rhythmic alternation between high and low-energy conditions, driven by the changing direction and strength of the tidal currents (Dalrymple et al., 1990). *Ophiomorpha* and tubular tidalites (i) are consistent with sedimentation in tidal flats or shallow tidal channels affected by tides, where wavy bedding signals sand deposited during active tidal currents and mudstones deposited during calm times (e.g., Wetzel et al., 2014; Gingras and Zonneveld, 2015; Rodríguez-Tovar et al., 2019). Ichnoassemblage ii, with *Ophiomorpha*, *Scolicia*, and *Siphonichnus*, in conjunction with heterolithic facies and oyster biostromes, reflects a dynamic intertidal to shallow subtidal environment with fluctuating tidal currents and abundant organic matter (e.g., Desjardins et al., 2012; Gingras and MacEachern, 2012; Díez-Canseco et al., 2015).

Oyster buildups tend to occur in shallow, well-lit marine environments with low turbidity and a steady supply of food (Johnson et al., 2007), although estuarine monospecific oyster bioherms are also well known (Pufahl and James, 2006). Oysters are able to thrive and rapidly colonise new substrates, resulting in the formation of extensive biostromes (Kidwell and Bosence, 1991). The dominance of articulated oysters with low fragmentation suggests autochthonous preservation of bioherms in tidal flat areas (Pufahl and James, 2006). On the other hand, the occasional dominance of suspension- and deposit-feeders such as *Siphonichnus* over detritus feeders (ichnoassemblage iii), along with the presence of small channels and tidal flat heterolithic successions, suggests middle to outer estuary zones in restricted shallow marine areas. Despite having wide channel architectures, these areas exhibit relatively lower-energy conditions than FA4 in interbar areas, probably due to tides or river inflow (Dalrymple, 1992, 2006).

X.4.6 Facies association 6: unbioturbated wavy and lenticular bedding

Sedimentology: Facies Association 6 (FA6) consists of cuneiform beds, up to 5 m thick, of grey medium- to fine-grained sandstones and light-yellow mudstones with heterolithic bedding, showing a prevalence of wavy and lenticular bedding structures, as well as mud drapes (Fig. X.12A-D). Occasionally, climbing-ripples and locally inclined heterolithic stratification are recognised. FA6 transitionally or sharply covers beds of FA5.

Ichnology: This facies association is completely devoid of bioturbation (BI = 0).

Interpretation: Climbing ripples are commonly linked to the tidal channel levees located within the inner channel region of a fluvio-estuarine transition (Lanier and Tessier, 1998). Mud drapes suggest tidal influence during periods of low fluvial discharge (Dalrymple and Choi, 2007; Mángano et al., 2023). Inclined heterolithic stratification reflects point-bar lateral accretion in tidally influenced rivers and creeks draining intertidal mudflats (Thomas et al., 1987; Dalrymple et al., 2003; Olariu et al., 2015; Ahmad et al., 2024); hence this facies association represents intertidal creek point-bar deposits in an estuarine channel. The lack of trace fossils signals unfavourable conditions for the trace-maker community under high turbidity and high sedimentation rates, or extremely brackish waters in proximal areas of the estuary (Gingras et al., 2012b).

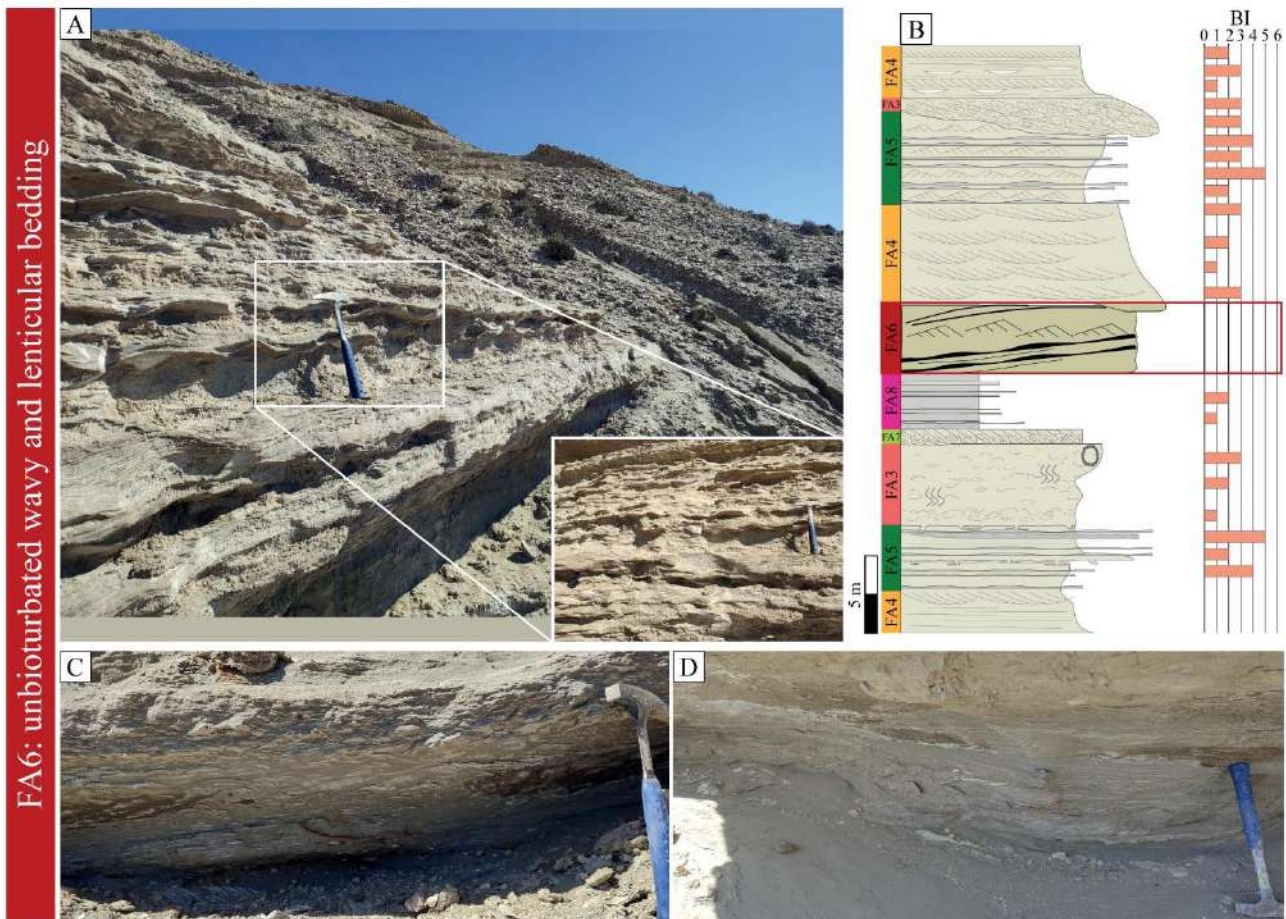


Fig. X.12. Field examples of FA6: unbioturbated wavy and lenticular bedding. **A.** Outcrop view of wavy bedding and 4x zoom detail of mud drapes. **B.** Stratification trends of FA6 and their relationship to the other facies associations; **C-D.** Close-up views of wavy stratification with some climbing ripples.

X.4.7 Facies association 7: planar cross-bedded and crushed shell beds

Sedimentology: This facies association is characterised by lenticular bodies <1 m thick (thinner than FA3) comprising highly fragmented bioclasts with tractive structures such as planar cross-bedding (Fig. X.13A-E). Erosive bases are present above FA4 and occasionally above FA5.

Ichnology: This facies association does not show bioturbation (BI = 0).

Interpretation: The heavily crushed and small-sized shells suggest prolonged, intense abrasion and sorting due to long-lived, high-energy currents, and therefore represent condensed sections at the bases of tidal channels (e.g., Brett and Baird, 1986; Kidwell et al., 1986). The planar cross-bedding structures reveal that the sediments were deposited by migrating bedforms, most likely dunes, driven by the tidal currents (Kidwell et al., 1986). The sorting process is more effective in high-energy environments, where the currents are strong enough to transport and sort the sediment. They are included in the invertebrate assemblage B of del Río et al. (2001).

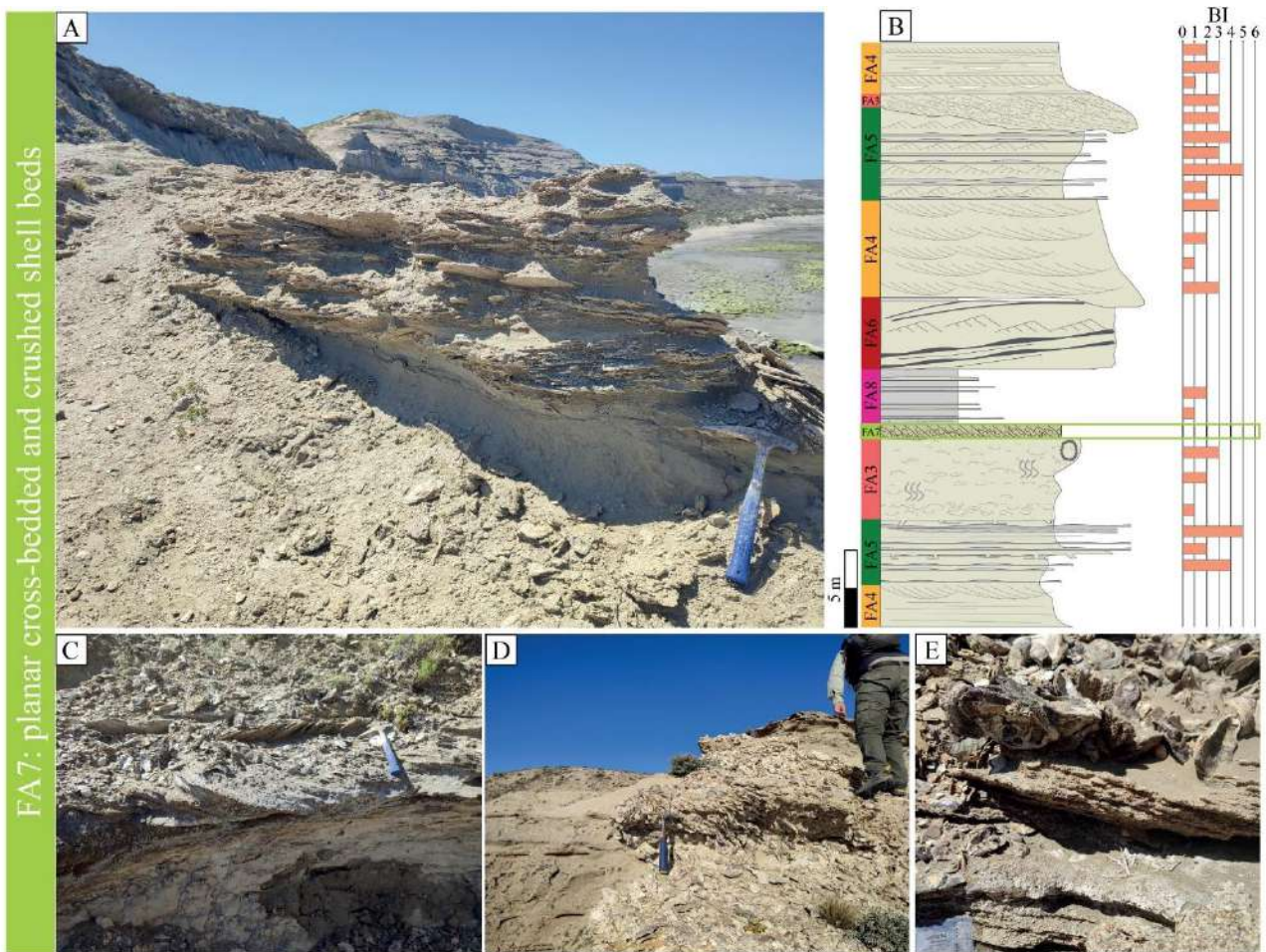


Fig. X.13. Field examples of FA7: planar cross-bedded and crushed shell beds. **A.** Outcrop view of cross-bedding structures of crushed shell beds. **B.** Stratification trends of FA7 and their relationship to the other facies associations. **C.** Detail of traction structures and crushed shell beds. **D-E.** General view and detail of cross-bedding crushed shell beds overlain by oyster buildups (biostromes).

X.4.8 Facies association 8: occasional low-bioturbated structureless mudstones

Sedimentology: This facies association presents 2-3 m thick lenticular beds of structureless mudstones in sharp contact with FA4, FA5 or FA6 (Fig. X.14A-B).

Ichnology: Structureless mudstones present sporadic patches of *Phycosiphon* (BI=0-1) smaller than 1 mm (Fig. X.14C-D).

Interpretation: The presence of mudstones with a massive structure and *Phycosiphon*, interbedded with tidal channel sandstones, suggests deposition from fluid-muds in maximum turbidity zones (McIlroy, 2004; Ichaso and Dalrymple, 2009; Mackay and Dalrymple, 2011), where the facies and opportunistic colonisation may reflect transgressive conditions with respect to previous facies. This marks channels subjected to marine flooding events, probably during periods of low discharge (McIlroy, 2004; Mackay and Dalrymple, 2011).

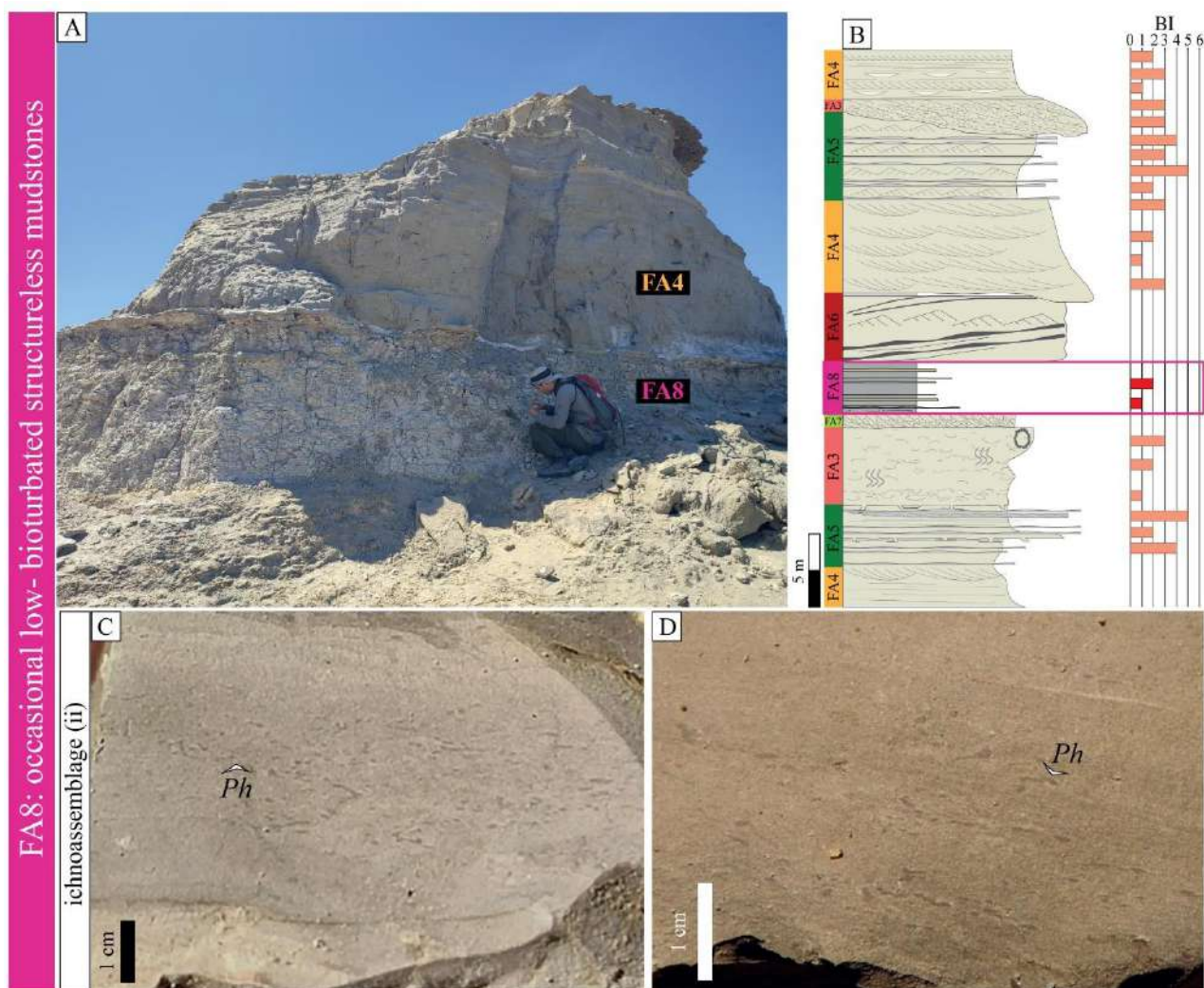


Fig. X.14. Field examples of FA8: structureless mudstone occasionally bioturbated. **A.** Outcrop view of FA8 overlain by FA4. **B.** Stratification trends of FA8 and their relationship to the other facies associations. **C-D.** Detail of bioturbation by *Phycosiphon* (*Ph*).

X.5. Vertical facies distribution

The key factors controlling transgressions and regressions—or the directional migration of shorelines over time—include eustatic fluctuations, accommodation space changes, sediment supply or erosion rates, and vertical displacement or tilting of the depositional surface (Collier et al., 1990; Muto and Steel, 1997; Allen and Allen, 2013). The Entrerriense Transgression is a continental-scale Late Miocene marine transgression that is well registered in the Puerto Madryn Formation in northern Patagonia. This event encompasses a complete marine sedimentation cycle, including both transgressive and regressive phases that took at least 4 Myr to accumulate (Scasso and del Río, 1987; del Río et al., 2001, 2018; Cuitiño et al., 2017, 2023). In this context, the high-order T–R stratigraphic cycle begins with a Transgressive Phase (del Río et al., 2001), marked by continuous upward deepening of the marine environment above a basal erosive ravinement surface (Fig. X.1) (del Río et al., 2001; Cuitiño et al., 2017). The Transgressive Phase culminates in a Maximum Flooding Phase (del Río et al., 2001), characterised by a 10–15 m thick, mud-dominated bed of laminated or thoroughly bioturbated shelf deposits, marking the maximum marine depths during the deposition of the Puerto Madryn

Formation. Afterward, the Regressive Phase reflects a gradual upward shallowing of the marine depositional system, involving tidal-fluvial domain deposits (del Río et al., 2001; Cuitiño et al., 2017). Besides this overall stratigraphic trend, the Puerto Madryn Formation shows several (yet undetermined) lower order cycles, punctuated by erosion or condensation surfaces. The cycles are interpreted as lower rank relative sea-level fluctuations having a duration of <1 Myr.

It was suggested that global sea-level fluctuations were not the primary drivers of the sedimentation patterns observed in the Puerto Madryn Formation (Cuitiño et al., 2023). Instead, a combined influence of thermal subsidence and differential compaction of the underlying sedimentary column are thought to have played a crucial role in accommodation space creation throughout the Cenozoic (Lovecchio, 2018; Cuitiño et al., 2023). High sedimentation rates are additionally detected for the volcanoclastic-rich regressive phase in the Puerto Madryn Formation, tied to explosive volcanic activity in the context of the Andean orogeny, allowing for preservation of the morphology of tidal channels (Scasso et al., 2012; Scasso and Cuitiño, 2017; Cuitiño et al., 2023). Only the high-frequency cycles could be assigned as mainly controlled by eustatic sea-level changes.

In this setting, the eight facies associations defined here for the Puerto Madryn Formation are vertically distributed and grouped into lower and upper informal stratigraphic intervals (Figs. X.2 and X.3) that roughly coincide with the previously defined Transgressive and Regressive phases, respectively, separated by a maximum flooding surface. We noted that each stratigraphic interval is dominated by either wave or tidal processes, showing specific ichnological assemblages whose significance is discussed below.

X.5.1 Wave-dominated system in the transgressive phase

The lower interval has recorded several low hierarchy cycles, stacked in tabular beds over several kilometres, with an overall retrogradational pattern —i.e. coincide with the high rank Transgressive Phase previously defined for the Puerto Madryn Formation (del Río et al., 2001). These cycles show fining- and coarsening-upward trends from lower shoreface (FA2) to offshore and shelf environments (FA1), and vice versa, interrupted by shoreface shell beds (FA3.1) with non-depositional surfaces at the base (Figs. X.3 and X.15). The large-scale tabular geometry, the grain-size trends (lower-rank progradational and retrogradational stacking patterns), and the predominance of abundant and highly diverse trace and invertebrate fossil assemblages clearly point to fully marine conditions. This could be linked to sedimentation in a wave-dominated (i.e., shoreface to offshore) system with negligible fluvial influence (Figs. X.3 and X.15). The latter can be associated with relative small-scale sea level rises and falls during an overall sea level rise (e.g., Proust et al., 2001; Olsen et al., 2002; Hampson and Storms, 2003; Willis et al., 2022).

Due to the obliteration of physical sedimentary structures by bioturbation, determining the relative influence of tides on the wave-dominated system is challenging. Shoreface deposits are typically considered as indicative of environments highly influenced by wave processes (Dalrymple et al., 1992); they are found in a variety of coastal settings influenced by changes in relative sea level, including transgressive, normal regressive, and forced regressive settings (e.g., Posamentier et al., 1992; Plint and Nummendal, 2000; Posamentier and Morris,

2000; Dashtgard et al., 2012). The preserved characteristics of these deposits are further shaped by autogenic factors, particularly the relative influence of fair-weather waves, storm waves, and tides (Anthony and Orford, 2002; Dashtgard et al., 2012). Diagnostic sedimentological and ichnological features such as trough-cross stratification have been highlighted sometimes overlain by planar-cross bedding, current or wave-ripples, hummocky and swaley cross-stratification, and/or highly bioturbated sediments (e.g., Yang et al., 2005; Dashtgard et al., 2012, 2021).

The offshore and lower shoreface sections of tidally influenced shorefaces are identified by sedimentary structures reflecting fair-weather conditions. They may feature beds of granulometry similar to that of the upper shoreface, and typically exhibit high bioturbation indices (Dashtgard et al., 2012). Fair-weather sandy beds tend to be extensively bioturbated. The presence of strong tidal currents in the lower shoreface and offshore zones encourages the settlement of infauna, leading to burrow patterns characteristic of the *Skolithos* ichnofacies (Dashtgard et al., 2012, 2021). In contrast, tidally modulated shorefaces are marked in the proximal lower shoreface by a low abundance and diversity of benthic activity. The ichnoassemblage includes elements common to both the *Skolithos* and *Cruziana* ichnofacies, but lacks grazing behaviours, elaborated deposit-feeding behaviours, and deep-probing structures (Dashtgard et al., 2012, 2021). In the Puerto Madryn Formation, the lower shoreface and offshore areas exhibit high BI values and a high diversity of structures, with archetypal and distal expressions of the *Cruziana* ichnofacies. Because this suggests a low tidal influence on the system, these environments most likely developed in settings having a small tidal prism and limited tidal-current energy—essentially non-tidal shorefaces (e.g., Dashtgard et al., 2012, 2021).

Conversely, wave-dominated shorefaces, with no significant tidal influence, feature intensely bioturbated silty and sandy mud beds in the lower and upper offshore, offshore transition, and lower shoreface zones, representing fair-weather deposition (Pemberton, 2001; Pemberton et al., 2012). These are interbedded with sand and silt beds deposited during storms. However, depending on the storm energy levels (increasing from storm-affected, storm-influenced, to storm-dominated; Clifton 2006; Dashtgard et al. 2012), the ichnological trends might be affected. In the Puerto Madryn Formation, the ichnoassemblages are typical of fair-weather conditions (archetypal *Cruziana* in offshore transition to upper offshore and distal *Cruziana* in lower offshore to shelf), but some storm influence cannot be ruled out because the sediments could be reworked by bioturbation. Other research efforts involving the Entrerriense Transgression in Uruguay have underlined the local occurrence of waves and tides affecting coastal dynamics (Aumond et al., 2021). Meanwhile, in storm-affected shorefaces, the lower shoreface is characterised by an erosional surface and graded bedding showing hummocky cross stratification, and heavily bioturbated muddy sand with high mud content to the top, transitioning into heavily bioturbated silty sand with lower mud content at the top of the middle shoreface successions (Dashtgard et al., 2012). Storm beds are generally thin and commonly bioturbated, so they could have been present in this system and have an unclear record.

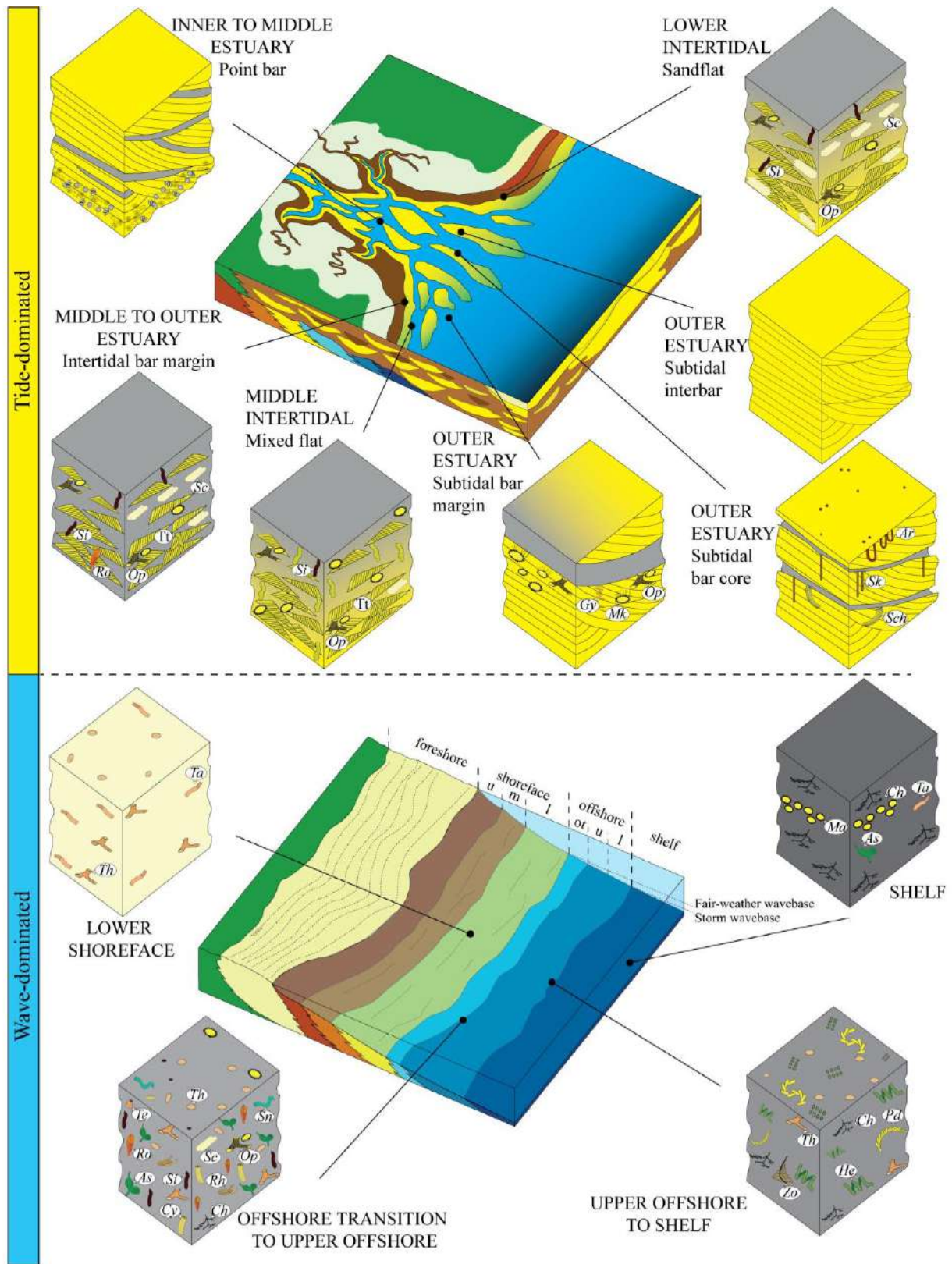


Fig. X.15. Depositional model and sub-environments in wave-dominated from lower shoreface to shelf, and tide-dominated systems from inner-middle estuary to outer estuary and variations to lower and middle intertidal zones with a possible embayment. *Ar*: Arenicolites, *As*: Asterosoma, *Ch*: Chondrites, *Cy*: Cylindrichnus, *Gy*: Gyrolithes, *He*: Helicodromites, *Ma*: Macaronichnus, *Mk*: Maiakarichnus, *Op*: Ophiomorpha, *Pd*: Phycodes, *Rh*: Rhizocorallium, *Ro*: Rosselia, *Sc*: Scolicia, *Sch*: Schaubcylindrichnus, *Sk*: Skolithos, *Sn*: Sinusichnus, *Si*: Siphonichnus, *Ta*: Taenidium, *Th*: Thalassinoides, *Tt*: tubular tidalites, *Zo*: Zoophycos.
 u: upper; l: lower; ot: offshore transition.

X.5.2 Tide-dominated estuarine system in the regressive phase

The identification of estuaries in the geological record is highly complex (Dalrymple et al., 1992), although their sedimentation and ichnological patterns should be consistent with at least four discernible conditions (Gingras et al., 2012b): brackish-water sedimentation, transgressive backstepping of sedimentary environments, tidally influenced sedimentation—even if not limited to estuaries, it provides evidence of sedimentation in marginal-marine settings—and the presence of a transgressed valley floor. Still, it is important to acknowledge that not all characteristics need to be present within a dataset, and ichnological content can vary from estuary to estuary (Gingras et al., 2012b). For example, as the transgressed base of the estuary is not always demarcated by omission suites, discerning the outer part of the estuary can be challenging, especially since the stratigraphically higher units may not display brackish-water trace-fossil assemblages (Gingras et al., 2012b). Adding to this complexity, estuaries receive sediments from both fluvial and tidal sources, and in more intricate basins, episodes of increased continental sedimentation can complicate the interpretation even further. This is seen in the McMurray Formation (Canada), where aspects of both deltaic sedimentation and estuarine sedimentation are present (Gingras et al., 2012b).

The upper interval of the Puerto Madryn Formation comprises FA4 to FA6 and FA8, sometimes interrupted by erosive (transgressive) surfaces associated with condensed intervals of transported and crushed shells (FA7) and tidal channel shell beds (FA3.2), indicating the persistent transgressive nature of the system fill. These bodies are predominantly channel-shaped, and their lateral margins correspond to the contact with adjacent channelised bodies. Heterolithic-dominated flaser, wavy, and lenticular bedding—showing current ripples and occasional planar cross-bedding—would indicate flood and ebb tidal flows, and therefore an alternation of traction and suspension fallout processes (e.g., Dalrymple and Choi, 2007; Scasso and Cuitiño, 2017). Mud lamina draping ripple and dune foresets mark variations in the speed of water currents and the settling of mud particles during periods of reduced water flow, typically occurring during slack water (e.g., Willis, 2005; Shchepetkina et al., 2019). This upper interval thus records sediment distribution controlled by tidal processes (e.g., Dalrymple and Choi, 2007; Shchepetkina et al., 2019). The erosive bases and general aggradational and fining-upward trends of the successions point to sedimentation within amalgamated tidal channels (Scasso et al., 2012). Volcaniclastic materials, delivered to the tidal channels by river systems (Scasso and del Río, 1987), significantly influenced the overall regressive trend by shifting the depocentres (Scasso et al., 2012). Notwithstanding, the presence of crushed shell beds (FA7) with tractive structures, which limit each sedimentary cycle, suggests they are environmentally condensed deposits. These beds indicate periods of prolonged non-deposition and signal flooding surfaces within elongate sand bars and sand flats (Scasso et al., 2012). The final net landward movement of sediment, derived from outside the estuary mouth, distinguishes the estuary from a deltaic system, where the net sediment transport is seawards (e.g., Dalrymple et al., 1992). Additionally, it should be stressed that as a result of a very large tidal prism, tide-dominated estuaries tend to be large, and their physiographic boundaries greatly attenuated (Dalrymple et al., 1992). In such estuaries, facies changes are gradational over a scale of several kilometres to tens of kilometres, owing to the significant influence of fluvial discharges (Gingras et al., 2012b; Choi et al., 2021).

The ichnological distinction between tide-dominated estuaries and tide-dominated deltas remains uncertain and is therefore still a topic of ongoing research (e.g., Gingras et al., 2012b; Shchepetkina et al., 2019). The fluvio-tidal zone from tide-influenced and tide-dominated estuaries and deltas is often treated as a single entity, as no major sedimentological or ichnological differences have been clearly identified (e.g., Shchepetkina et al., 2019). However, some morphological differences between deltas and estuaries could prove crucial in deciphering the behaviour of macrobenthic fauna. Variations in distributary channel geometries can, for instance, significantly impact tidal dynamics and the extent of salinity intrusion. In large deltaic systems, the fluvio-tidal zone may extend hundreds of kilometres offshore during periods of high fluvial discharge, whereas in estuaries, fluvial influence typically does not extend beyond the estuary mouth. The results presented here suggest that brackish systems might not play a major role in this area, and that creek point-bars from FA6 are confined to the inner estuary, with a rapid transition to fully marine conditions. Moreover, abundances and diversities could be higher than what is typically observed in tide-dominated deltas (e.g., MacEachern and Bann, 2022). Further research is needed to fully understand these processes.

In turn, the fact that tidal processes are the dominant force within this system (tide-dominated estuary) further suggests that no barrier existed to close off the estuary mouth. Hence, no shoreface/barrier island system limited interaction with a central muddy basin (which would be typical of a wave-dominated estuary; Dalrymple et al., 1992). We should also consider the possibility that the estuarine system is alike an embayment due to the wide tidal channels and the presence of ichnoassemblages that are not highly stressed, or indicative of environments heavily influenced by brackish water. The embayment model would admit a greater influx of fully marine waters into the bay. However, this model requires further investigation; as detailed in the following facies associations some areas appear to be more restricted.

FA4 is associated with the bottom set of the core of subtidal sandbars, which are unbioturbated due to areas of maximum energy and high-current velocities (e.g., Desjardins et al., 2012). In the subtidal interbar bodies, pauses in sedimentation or reductions in energetic conditions were sufficient to allow the development of ichnoassemblage i (*Arenicolites*, *Skolithos* and *Schaubcylindrichnus*), characterised by suspension-feeders. Yet ichnoassemblage ii (*Gyrolithes*, *Maiakarichnus*, *Ophiomorpha* and *Thalassinoides*) and a wide lenticular architecture could be associated with lower intertidal sandflats or the subtidal bar margin in a more restricted environment, consistent with deposition in an outer estuary (e.g., Dalrymple et al., 1992; Gingras et al., 2012b; Mángano et al., 2023). Therefore, variations in ichnoassemblages represent colonisation at the margins of the estuarine complex and within the outer estuary, evidencing prolonged changes in sedimentation rates (e.g., Dalrymple et al., 1992; Gingras et al., 2012b).

FA5 records a dynamic intertidal to shallow subtidal environment, where variations in trace fossil assemblages and the predominance of specific behaviours also indicate sedimentation at the margins of the open estuarine system associated with the intertidal zone such as ichnoassemblages i and ii (mixed flat, e.g., Ahmad et al., 2024), or restricted to the outer-middle estuary itself with ichnoassemblage iii (e.g., Gingras et al., 2019; Buatois et al., 2023; Mángano et al., 2023). FA6 registers inclined heterolithic stratification related to lateral accretion in point bars, whose absence of bioturbation could signal turbidity or high sedimentation rates, or

brackish conditions and unstable channel margins feeding the estuarine system, or even incising from supratidal zones to intertidal flat zones (e.g., Ahmad et al., 2024). The bases of some tidal channels contain crushed shell beds indicating condensed sections (FA7), whereas some tops of the estuarine system are restricted to fluid mud deposits (FA8) associated with flooding events (e.g., McIlroy, 2004).

Therefore, as previously suggested by Scasso et al. (2012) and Scasso and Cuitiño (2017), the upper part of the Puerto Madryn Formation—in view of bed geometry, ichnological analysis, and sedimentary structures—can be related to the intertidal to subtidal sandflat zones in an inner/middle and outer estuary or embayment in a tide-dominated system (Figs. X.3 and X.15).

X.6. Ichnological signature and physico-chemical stresses

X.6.1. The wave-dominated system

The ichnoassemblages identified in the lower interval of the Puerto Madryn Formation indicate full-marine conditions, i.e., without revealing brackish-water trace fossils. The ichnoassemblage i related with FA2 is characterised by detritus-feeding, locomotion, and dwelling behaviours as that of *Taenidium*, and deposit-feeding behaviours including *Thalassinoides* with some *Chondrites* and *Phycodes* superimposed (MacEachern et al., 2007, 2012; Vallon et al., 2016). This scenario, including with the presence of certain invertebrate macrofossils, indicates a shallow marine setting influenced by frequent wave agitation. Such conditions can be related to the *Cruziana* ichnofacies, spanning from lower shoreface to upper offshore environments (e.g., Seilacher, 1964; MacEachern et al., 2007; 2012; Buatois and Mángano, 2011). Specific sedimentary structures remain unidentified, impeding a more precise characterisation of the depositional environment; however, the observed increase in grain-size, in comparison to sedimentary rocks from ichnoassemblages ii (*Asterosoma*, *Chondrites*, *Cylindrichnus*, *Ophiomorpha*, *?Rhizocorallium*, *Rosselia*, *Scolicia*, *Sinusichnus*, *Siphonichnus*, *Taenidium*, *Teichichnus*, and *Thalassinoides*) and iii (*Chondrites*, *Helicodromites*, *Phycodes*, *Thalassinoides*, and *?Zoophycos*), points to a rise in energy conditions, hinting at a shallower water depositional setting. It is probable that some *Thalassinoides* represent previous colonisation on softground or compacted (cohesive) substrates (e.g., Pemberton et al., 1992). Subsequently, *Taenidium* and the new *Thalassinoides* ichnoassemblage appear to be associated with early endobenthic detritus- and deposit-feeders, taking advantage of the pre-existing galleries left by *Thalassinoides*. The increasing distality of the system is documented by the presence of deeper overlying tiering faunas (*Chondrites* and *Phycodes*), which may be linked to a successive change to ichnoassemblage ii or iii.

The ichnoassemblage ii, also related to FA2, is one of the most common ones pertaining to the wave-dominated stratigraphic interval. Whilst mobile and sessile deposits and detritus feeding structures prevail, suspension feeding also occurs. Deposit- and suspension-feeding structures such as *Asterosoma*, *Ophiomorpha*, *Rhizocorallium*, and *Siphonichnus*, deposit-feeding as *Scolicia*, *Sinusichnus*, and *Teichichnus*, suspension-feeding such as *Cylindrichnus*, and detritus-feeding as *Rosselia* and *Thalassinoides*, characterise this ichnoassemblage. The predominance of horizontal structures produced by mobile organisms indicates an accumulation of organic detritus within the sediment during periods of moderate- to low-energy (e.g., MacEachern and Pemberton, 1992; Pemberton et al., 2012). The variable ethologies, along with the high

diversity and abundance of trace fossils, commonly reflect favourable conditions for the development of a macrobenthic trace-maker community, associated with times of lower physico-chemical stress due to low to moderate sedimentation and erosion rates. This is typically associated with an assemblage of archetypal *Cruziana* ichnofacies (e.g., Seilacher, 1964; MacEachern et al., 2007; 2012; Buatois and Mángano, 2011) occurring between the fair-weather and storm-wave bases, i.e., from the upper offshore to offshore transition in wave-dominated systems (MacEachern and Pemberton, 1992; MacEachern et al., 1999).

In scenarios dominated by the ichnoassemblage iii of FA2, we find subsurface deposit-feeding behaviours such as those related to *Chondrites*, *Phycodes*, ?*Zoophycos*, and dwelling structures such as *Helicodromites*. These specialised feeding traces may be linked to distal expressions of the *Cruziana* ichnofacies, occurring from the upper offshore to the offshore transition zones within shelf environments (Seilacher, 1964; MacEachern et al., 2007; 2012; Buatois and Mángano, 2011). However, the dominance of deep-tier deposit-feeding structures could also be related to variations within the *Zoophycos* ichnofacies (MacEachern et al., 2007; Buatois and Mángano, 2011). In any case, the ichnoassociation (iii) indicates that although *Chondrites* and ?*Zoophycos* penetrate deeply into oxygen-depleted sediments, this does not necessarily reflect poor oxygenation of bottom waters. Intense bioturbation by *Helicodromites* and *Phycodes*, for instance, argues against oxygen depletion (Baucon et al., 2020), making distal expressions of the *Cruziana* ichnofacies the most probable scenario.

In all scenarios, FA2 grades vertically from or towards FA1. The ichnoassemblage recorded for FA1 is dominated by deposit-feeding traces attributable to *Chondrites*, with sparse meniscate traces of *Taenidium*, occasionally *Asterosoma*, and in one interval a dominance of *Macaronichnus*. The change in the trace fossil assemblage, together with the dramatic reduction in diversity and abundance with respect to that of FA2, reveals an abrupt change in the palaeoenvironmental conditions affecting the trace-maker community, with no record of a gradual transition. For some clarification, an intra-ichnofacies analysis with careful consideration of bed- and bed set-scale juxtapositions of genetically related assemblages, spatial variations in bioturbation index, and the range of ethological responses expressed by the various ichnogenera and ichnospecies is required (e.g., MacEachern et al., 2005; MacEachern and Bann, 2020, 2022; Moyano-Paz et al., 2020, 2022). Notwithstanding, the dominance of deposit-feeding, deep-tier structures (*Chondrites*), together with the fining-upward trend from FA2 to FA1, attests to deepening/flooding events in the wave-dominated system. Coarsening-upward trends are rarer but could also be linked to stressful changes in the environment.

Dissolved oxygen content, nutrient concentration, or variations in sedimentation rates may be the main controlling factors in normal salinity marine environments. Still, the occurrence of some fluvial pulses with freshwater loading reported for specific beds in these depositional systems of the Puerto Madryn Formation (e.g., Fuentes et al., 2019) suggests the impact of salinity fluctuations —interval of 4-5 m in thickness from FA1. The eventual freshwater input may be associated with the non-bioturbated layers of interbedded mudstones and sandy mudstones showing ripple lamination, probably related to short-duration currents sourced in continental areas —i.e. hyperpycnal prodelta flows reaching the shelf—.

X.6.1.1 Dissolved-oxygen content and nutrient concentration

Ichnoassemblages ii and iii recorded in FA2, assigned to the *Cruziana* ichnofacies, present a data on diversity, abundance, and size of biogenic structures indicative of favourable oxic conditions, without any evidence of significant oxygen depletion.

The change from FA2 to the more distal settings of FA1 reflects a significant reduction in diversity and abundance, producing a *Chondrites*-dominated assemblage that highlights a significant environmental variation. *Chondrites* has traditionally been considered a reliable marker of low-oxygen conditions (Bromley and Ekdale, 1984) when present as dense concentrations in organic-rich layers beneath storm event beds (Vossler and Pemberton, 1988). Nevertheless, it is important to note that the presence of *Chondrites* in a substrate does not necessarily imply low oxygen (or dysoxic) pore-water; it has also been observed in highly oxygenated and nutrient-poor (oligotrophic) environments (Leszczyński and Uchman, 1993; Hertweck et al., 2007; Baucon et al., 2020).

The studied successions present beds with an exclusive presence of *Chondrites* having sizes under 0.3 cm wide, probably associated with low oxygen (i.e., dysoxic) conditions. High concentrations of *Chondrites*-dominated beds up to 1 cm wide with whitish colorations could reveal oxygenated oligotrophic environments; thus, their occasional occurrence with other traces and decrease in size would respond to upwelling scenarios that eutrophise the waters (e.g., Leszczyński and Uchman, 1993). It has been proposed that primary productivity and the development of complex food webs were influenced by upwelling processes in this basin during the Miocene (Cuitiño et al., 2017).

X.6.1.2 Sedimentation rates and hydrodynamic energy

The dominance of horizontal traces observed for ichnoassemblages FA2-ii-iii comes to support the low to moderate sedimentation rates, assumed to be significantly higher for ichnoassemblage FA2-i as evidenced by detritus-feeding behaviours. Overlying the ripple-laminated layers of FA1, there are unbioturbated, structureless mud layers. Accordingly, if these pulses are associated with currents from the mainland, they did not recover the oxygenation patterns; so that the high sedimentation rates in these episodes also play a fundamental role in suppressing benthic bioturbation activity.

FA3.1, in terms of shell concentrations, reveals relative increases in the input rates of hard parts, thereby suggesting important increases in sedimentation rates, hence physical stressors. Most bioclastic beds exhibit massive successions that indicate a high-energy shallow marine system subjected to storm currents (e.g., Bayet-Goll et al., 2015). Altogether, the wide variety of grain-sizes and fossils, grading patterns, and bioturbation indexes indicate that storms were intercalated with fair-weather periods that allowed colonisation by the tracemakers producing the soft ground ichnological assemblages (*Ophiomorpha*, *?Scolicia*, *Taenidium*, and *Thalassinoides*) (MacEachern et al., 2007).

X.6.1.3 Water turbidity

Unbioturbated, ripple-laminated layers, and structureless mud layers of FA1 —plus associated syn-sedimentary structures— deposited during high sedimentation rates further reveal important changes in water

turbidity. The absence of dwelling structures corresponding to suspension feeding organisms is consistent with elevated water turbidity, which inhibits this type of feeding behaviour due to the rapid fall of suspended sediments (Moslow and Pemberton, 1988; Gingras et al., 1998; MacEachern et al., 2005).

X.6.2. The tide-dominated system

The ichnoassemblage identified for FA4, in the upper interval of the Puerto Madryn Formation, exhibits low ichnodiversity, a dominance of vertical traces over horizontal traces, some U-shaped dwelling structures of suspension-feeders such as *Arenicolites*, and a dominance of simple, vertical suspension-feeder traces including *Skolithos* and deposit-feeder traces as *Ophiomorpha*. In addition, there are dwelling/feeding structures of a solitary funnel-feeder such as *Schaubcylindrichnus* (Nara, 2006). Dominance of vertical burrows of suspension feeders agrees with *Skolithos* ichnofacies (e.g., Seilacher, 1964; MacEachern et al., 2007; Buatois and Mángano, 2011), suggesting a high abundance of organic particles kept in suspension by currents in a well-oxygenated water column (Gingras et al., 2012a). FA5 shows simple-vertical suspension-feeding structures including *Siphonichnus*, detritus-feeders like *Rosselia* and *Thalassinoides*, and deposit-feeders like *Scolicia*. This association could be linked to a lower-energy environment relative to FA4 and the *Cruziana* ichnofacies, representing intertidal environments in middle to outer estuary or marginal zones of the estuary (Desjardins et al., 2012). The ichnological differences between FA4 and FA5, reveal a variable impact of physico-chemical stress factors in the estuarine environment. Nonetheless, identifying an exact boundary that separates subtidal areas from intertidal zones is challenging. Although tidal flats are generally situated landward and lateral to subtidal sandbars, ichnology is crucial for their differentiation. Lower hydrodynamic energy and sedimentation rates in tidal flats allow for more uniformly distributed bioturbation compared to the subtidal sandbar complex, even within estuarine systems (Gingras et al., 2012a; 2012b). Moreover, comparing FA4 and FA5, bioturbation intensities tend to increase upwards: from subtidal to intertidal estuary. FA6 deposits lack trace fossils, thus reflecting unfavourable habitats for macrobenthic tracemakers under unstable environmental conditions typical of tidal creek point bars (Fig. X.15) (e.g., Dalrymple and Choi, 2007; Shchepetkina et al., 2019). Accordingly, the hydrodynamic (tidal) energy, elevated water turbidity, sea-bottom consistency and grain size, and salinity fluctuations, can be invoked as the main stress factors to be identified in tide-dominated estuarine environments.

X.6.2.1 Sedimentation rate and hydrodynamic energy

The vertical arrangement of most burrows (*Arenicolites* and *Skolithos*) in FA4 suggests relatively high-energy and short periods of erosion, revealing short-term colonisation windows during slack water processes in sand bars of the outer estuary (Díez-Canseco et al., 2015). Furthermore, though dominated by suspension-feeding structures, FA5 includes some structures produced by detritus and deposit feeders (e.g., *Rosselia*) and suspension-feeders (e.g., *Ophiomorpha*), which would reveal decreases in energy in middle areas of the estuary (Gingras et al., 2012a, 2012b). In this case the *Cruziana* ichnofacies could be associated with more proximal environments than the *Skolithos* ichnofacies, generating the singular upward increase of bioturbation intensities.

The occurrence of *Gyrolithes*, *Maiakarichnus*, *Ophiomorpha*, and *Thalassinoides* in FA4 in conjunction with periods of lower system energy reflects their colonisation during stress conditions in sub- to inter-tidal flats. These areas are marked by turbulent waters carrying a high load of suspended particles, creating favourable conditions for the settlement of infaunal organisms specialising in both deposit feeding and suspension feeding—which in this case take advantage of the periods of decreasing energy to colonise the substrate (e.g., *Maiakarichnus*; Verde and Martínez, 2004). However, identifying a shift that separates subtidal areas from intertidal zones proves challenging, as ichnological evidence may be limited, and even *Cruziana* and *Skolithos* ichnofacies can overlap.

X.6.2.2 Water turbidity

The presence of thick mudstone layers interpreted as fluid mud deposits—cm-thick mud drapes intercalated within sandstone deposits—and the presence of some marine trace fossils (*Phycosiphon*) could reveal high suspended sediment concentrations and the development of a turbidity maximum due to fluvial fine-grained sediment supply to tidal channels (Allen et al., 1980; Wolanski and Gibbs, 1995; Wolanski et al., 1995; MacEachern et al., 2005). The resulting soupgrounds are colonised by mobile, deposit-feeding *Phycosiphon*-type traces, excluding large endobenthic deposit-feeders and suspension-feeders.

X.6.2.3 Salinity

Brackish-water environments are characterised by faunas showing less diversity and abundance than their marine equivalents, tending to be opportunistic (Mángano et al., 2023). FA4 and FA5 exhibit a decrease in abundance and diversity with respect to the lower interval, but trace sizes are not drastically reduced, meaning there is no direct impact of fresh-water or brackish-water conditions on the ichnological assemblages. Usually, a size decrease reflects a strategy to cope with harsh conditions in terms of salinity changes or oxygen availability (Gingras et al., 2011; Łaska et al., 2017; Rodríguez-Tovar et al., 2017). The absence of a transitional ichnoassemblage, in the strict sense (e.g., *Psilonichnus ichnofacies*; Frey and Pemberton, 1987), could furthermore indicate unregistered more proximal environments. The greater ichnodiversity seen in FA5 compared to FA4 probably indicates normal marine salinities and moderate hydrodynamic energy found in a more distal position from the mouth of tidal channels. The absence of biogenic structures in the heterolithic tidal flat deposits of FA6 may be attributed to unfavourable factors such as brackish conditions, subaerial exposure, and/or high sedimentation rates. Yet none of these factors taken alone would necessarily restrict bioturbation. Alternatively, it is possible that the trace fossils initially generated were not preserved due to the high energetic and erosive conditions prevalent in this part of the estuary.

X.7. Conclusions

Ichnological and sedimentological approaches, applied to the Late Miocene Puerto Madryn Formation (Argentine Patagonia) in Valdés Peninsula, lead us to interpret a sedimentary succession deposited in two main shallow/coastal marine depositional systems: a wave-dominated system, overlain by a tide-dominated estuarine system where the conditions in transgressive and regressive phases, respectively, configure an interesting challenge for discussion.

Lower shoreface to offshore transition environments characterised the wave-dominated system during a transgressive phase. It includes typical elements of the *Cruziana* ichnofacies (proximal, archetypal, and distal expressions). The transition to more distal shelf settings is characterised by an abrupt reduction in diversity, revealing the impact of environmental stressors such as dissolved oxygen content or food availability. Unidirectional currents and storm events determine alterations in sedimentation rates within the system, also inducing changes in the trace-maker community. Although sedimentary structures are discrete, the abundance and diversity of trace fossils as well as ichnoassemblages allowed us to determine low tidal influence on the system, indicating that these environments most likely developed in settings featuring a small tidal prism and limited tidal-current energy, i.e. essentially in non-tidal shorefaces.

Following a significant drop in eustatic sea level, the tide-dominated depositional system is established, representing an environment where multiple stressors may act. The erosive bases and overall aggradational and fining-upward trends observed in the sedimentary successions indicate deposition within amalgamated tidal channels. The presence of volcanoclastic materials, delivered by river systems to these tidal channels, played a significant role in shifting depocentres and influencing a general regressive trend. Despite this influence, the discovery of crushed shell beds with tractive structures, which cap each sedimentary cycle, suggests the beds represent environmentally condensed deposits. They indicate extended periods of non-deposition and mark flooding surfaces punctuated by short-term, high-order, relative sea level rises in an estuarine system, thereby highlighting a complex sedimentary environment. Typical *Skolithos* ichnofacies develop in the subtidal bar deposits in an outer estuary from the bottomset of subtidal sandbars to intertidal sandflats, whereas the *Cruziana* ichnofacies develop in the middle to outer estuary, from lower intertidal sandflats to intertidal mixed flats. The occasional lack of trace fossils in some horizons reflects unfavourable conditions for trace-maker communities under highly variable environmental conditions in proximal areas of the estuary (inner to middle estuary), including high sedimentation rates and hydrodynamic energy, water turbidity and sea-bottom consistency, and salinity fluctuations.

The conducted research supports that multiple physico-chemical stress factors, such as hydrodynamic energy, dissolved oxygen, water turbidity, sea-bottom consistency, and salinity, greatly impact the abundance and distribution of trace fossil assemblages in wave- and tide-dominated environments. This research confirms certain conclusions drawn by other researchers, whilst highlighting the complex and never unidirectional distribution of ichnoassemblages in highly dynamic environments that undergo pronounced variations in most of the parameters of the study. The consequently complex assemblages, sometimes discrete, that record a range of faunal responses to such persistently changing physico-chemical conditions, make it very difficult to determine the typical Seilacherian ichnofacies arrangements in some episodes. In the case expounded here, the keys underlying reconstruction include bioturbation intensity, distribution and ethological diversity, variations in sizes, backfill and lining of trace fossils (e.g., tubular tidalites), and ichnoassemblages and their relationship with the sedimentary physical environment.

Acknowledgements

This research was funded by Grants PID2019-104625RB-100 and TED2021-131697B-C21 funded by MCIN/AEI/ 10.13039/501100011033. The National Program for Doctoral Formation provided financial support to Celis (Miniciencias grants Colombia 885-2020). We thank the Asociación Universitaria Iberoamericana de Posgrado (AUIP) and the Santander Open Academy (Becas Santander Movilidad Internacional Doctorado 23/24) for their financial support, which enabled S. Celis to complete doctoral stays at the Instituto Patagónico de Geología y Paleontología (IPGP CONICET-CENPAT; Puerto Madryn, Argentina) and the Centro de Investigaciones Geológicas (CIG CONICET-UNLP; La Plata, Argentina), respectively. Thanks to the staff of IPGP and CIG for all their logistical support. Further thanks to Aylén Allende, Nicolás Farroni, Damián Pérez, and rangers from Punta Buenos Aires Reserve for their support in the field. This work was done with the permission of Ministerio de Turismo y Áreas Protegidas de Chubut and Administración de Parques Nacionales (Argentina), which the authors gratefully acknowledge. Financial support for fieldwork was provided by the Agencia Nacional de Investigaciones Científicas y Técnicas (Argentina) through grant PICT 2019-0390 to JIC and SMR. Thanks to Diana E. Fernández for comments made at an early stage of the manuscript. We would like to express our gratitude to Massimo Moretti (Editor-in-Chief), as well as Daniel Sedorko and one anonymous reviewer for their constructive comments and suggestions. Funding for open access charge: Universidad de Granada / CBUA.

Agradecimientos / Acknowledgements

Susy, gracias por creer, querer, y hacer una pareja pingüina durante estos cinco años. Gracias a tu apoyo, este proceso se hizo más fácil. Gracias por tu paciencia y amor. Por aguantar los bajones, y caminar juntos en los subidones. En Patagonia vimos lo difícil que puede llegar a ser para un pingüino esperar y esperar... Gracias, porque cada vez que nos tiramos al océano, siempre volvimos ¡Lo logramos!

A papá y mamá, siempre con un 'sí' para cualquier decisión. Gracias por siempre tener tiempo para un saludo cada noche.

A More, mi compañero y ángel vivo de cuatro patas, porque terminó de llenar mi corazón de amor. Su presencia irradia felicidad y amor en cualquier instante de la vida.

El común denominador para hacer ciencia a nivel mundial es hacerlo con lo mínimo y aguantar al máximo. Los países invierten cada día menos en ciencia, y se sostiene gracias al amor y la pasión de muchos. Sin embargo, por más amor que haya, se requiere al menos, de las condiciones mínimas. Después de cinco años, no vale la pena hacerlo sino es al menos con lo mínimo. Estoy convencido. No merece tener más tiempo de tu mente pensando en cómo sobrevivir que en cómo resolver tus preguntas de investigación. Un doctorado requiere al menos 4 años; con dinero para 3 o incluso menos, se hace muy complejo. Aun así, gracias a ese gobierno que comprendía que aún debe enviarse a un colombiano afuera para luego retornar a tratar de cambiar el sistema. Desde adentro, es imposible cambiarlo, incluso, querer cambiarlo, incluso, darse cuenta de que hay que cambiarlo. Gracias a las personas que creen que la ciencia y la educación son la clave para el progreso de una sociedad.

A Carlos Giraldo porque siempre estuvo dispuesto para ir al campo, discutir y compartir muchas experiencias personales y académicas paralelas.

A mis directores Francisc y Andrés, por involucrarse con mi proyecto. Para el futuro, tomaré lo bueno, y aprenderé de lo malo. El tiempo, cuan valioso es el tiempo.

A Fernando García-García por su colaboración y asesoría en algunos capítulos de la tesis.

A Francisca Martínez-Ruiz por sus gestiones como tutora.

To those who agreed to be part of my thesis committee and evaluate it from different perspectives: Domenico Chiarella... A los que aceptaron hacer parte del comité-tribunal de mi tesis y evaluarla desde diferentes ópticas: Alice Giannetti, y Ángel Puga Bernabeu. Además, a los evaluadores externos Josué Alejandro Mora y Augusto Nicolás Varela. Gracias a quienes estuvieron siempre dispuestos a colaborar con sus evaluaciones y comentarios para la tesis: Noelia Carmona, Ana Guerreiro dos Santos, Miquel Poyatos-More, Javier Dorador. I am also grateful to those who were always willing to collaborate with their evaluations and feedback on the thesis, or on some of its chapters: Jutta Winsemann, Adam McArthur, Daniel Sedorko and Anna van Yperen.

A Sebastian Richianno, Damián Moyano Paz y José Cuitiño por recibirme y abrirme las puertas de su vida académica y personal. Experiencias y días inolvidables para mí.

Al CENPAT y al CIG, sus directores Pablo Bouza y Gonzalo Veiga, así como los chic@s que me recibieron en sus nichos como uno más. Me sentí en Argentina, como en casa.

Gracias por mi espacio de trabajo, a los que, durante mi estadía estos cinco años, fueron directores del Departamento de Estratigrafía y Paleontología de la Universidad de Granada: Francisco J. Rodríguez-Tovar y Ángel Puga-Bernabéu.

A la organización de la IAS Summer School 2023 – Beatriz Bádenas, Marcos Aurell, Miquel Poyatos More, una experiencia inolvidable. Gracias a todos los amig@s. “Amig@s que aún no se conocían”.

Al Instituto de Investigaciones en Estratigrafía IIES por su apoyo económico el último año del doctorado. A Juan Pablo Betancourt por su disposición para la creación del mapa asociado a la Fig. I.7.

Para quienes, en dos momentos, formaron en Granada los sitios más similares a casa para llegar en las noches – *roommates*: a Hernán Maltz, charlas increíbles de la vida y la ciencia... por muchos mates, muchos cafés y muchas parrilladas más; a Carlos, mi maestro en la nieve, gracias por tantas horas con los esquí, sembraste un hobby que me saca del mundo; a Raúl, por muchas risas a las 6 am en la puerta de casa: el llegando de la fiesta, yo saliendo a correr; los dos en paralelo, en nuestras mentes, pensando: ¿qué piensa este hombre de la vida?. Muchas noches de *Champions League* con ellos tres. A Belén, por muchas pelis y series con cerveza. A Patri, por las risas ante los dramas de su vida.

A Henry Osorio, siempre listo para lo que fuese. Gracias a Marta Marchegiano por unos lindos últimos años: *Ti voglio bene amica*. A Albert y Mariola, dos maravillas que llegaron desde el minuto 1. A Álvaro Bremer, un gran amigo.

A Felipe Vallejo, Raúl Trejos y Angelo Plata por colaborar en los análisis bioestratigráficos. A ellos y a Mónica Duque, gracias por muchas charlas de la vida. Gracias a Daniel Piedrahita por la incondicionalidad. Gracias a Hugo Murcia por sus consejos e infinitas noches de discusiones los primeros años del doctorado... mucha más salsa y ron: *“la salsa es la expresión festiva del provinciano en la gran ciudad”*. Gracias a Sebastián Echeverri por mostrarme su forma de ver la geología... una pasión desbordada por los arcos y su denudación.

A quienes estuvieron, permanecieron y trataron de entender lo que hago. No es fácil ser amigo de alguien que vive tratando de entender cómo cayeron y se acomodaron los granitos de arena, menos si le sumamos, los rastros de bichos en esos granitos. No los menciono por temor de olvidar alguno. Pero cada uno de ellos sin importar el momento, sabe su importancia en este proceso. Perdón por el poco tiempo para ellos.

En varias campañas de campo, nos cruzamos con niñ@s que formaban parte de grupos armados y organizaciones ilegales. Era obligatoria su compañía para acceder a ciertas zonas y describir las rocas. Gracias a ellos. Esta tesis también está dedicada a ellos, con la esperanza de que algún día pueda volver y ayudar a cambiar el curso de muchas vidas.

Al fútbol, irracional y abstracto para muchos, pero media vida para otros. *“Cómo vas a saber querido amigo, cómo vas a saber lo que es la vida, si nunca jamás, jugaste al fútbol”*. Las horas de agobio lejos de casa se hicieron más amenas viendo fútbol y jugando al fútbol. Gracias a mi OC por existir... valió la pena cada amanecer. Gracias a los chicos de las peñas que siempre me recibieron en Puerto Madryn, Granada, y La Plata. Mención especial para una noche en Patagonia, con tormenta, cayendo granizo, mucha neblina y nadie se fue ¡Que viva la pelota!

A los que reflejan integridad, profesionalismo, anti-corrupción, rectitud y orden. Me inspiran. Gracias a quienes creen en las futuras generaciones y son capaz de apartarse cuando ya están en fuera de juego.

Todo el sufrimiento que hemos enfrentado y toda la alegría que hemos irradiado, han surgido del mismo lugar: nuestra propia mente; dependiendo de cómo interpretamos y asumimos cada situación. Por eso, me doy las gracias. La pasión, la constancia y la dedicación pueden superar cualquier escenario, incluso aquellos que parecen reservados para la brillantez.

References

- Aagard, T., 2011. Sediment transfer from beach to shoreface: The sediment budget of an accreting beach on the Danish North Sea Coast. *Geomorphology*, 135, 143-157.
- Abad, M., Ruiz, F., Pendón, J.G., Tosquella, J., González-Regalado, M.L., 2006. Escape and equilibrium trace fossils in association with *Conichnus conicus* as indicators of variable sedimentation rates in Tortonian littoral environments of SW Spain. *Geobios*, 39, 1–11.
- Agirrezabala, L.M., de Gibert, J.M., 2004. Paleodepth and paleoenvironment of *Dactyloidites otto* (Geinitz, 1849) from Lower Cretaceous deltaic deposits (Basque–Cantabrian Basin, west Pyrenees). *Palaios*, 19, 276–291.
- Agnini, C., Fornaciari, E., Raffi, I., Catanzariti, R., Pälke, H., Backman, J., Rio, D., 2014. Biozonation and biochronology of Paleogene calcareous nannofossils from low and middle latitudes. *Newsletters on Stratigraphy*, 47, 131-181.
- Aguirre, J., de Gibert, J.M., Puga-Bernabéu, A., 2010. Proximal–distal ichnofabric changes in a siliciclastic shelf, Early Pliocene, Guadalquivir Basin, southwest Spain. *Palaeogeography, Palaeoclimatology, Palaeoecology*, 291(3–4), 328-337.
- Ahmad, W., Gingras, M.K., Ranger, M.J., MacEachern, J.A., Zonneveld, P., 2024. Depositional setting and trace fossil suites of the early Cambrian (series 2, stage 4) Khussak Formation, east-central salt range, north-west sub-Himalayas, Pakistan. *Marine and Petroleum Geology*, 165, 106858.
- Ainsworth, R.B., Flint, S.S., Howell, J.A., 2008. Predicting coastal depositional style: Influence of basin morphology and accommodation to sediment supply ratio within a sequence stratigraphic framework. In: Hampson, G.J., Steel, R.J., Burgess, P.M., Dalrymple, R.W. (Eds.), *Recent advances in models of shallow-marine stratigraphy*, Tulsa, Oklahoma, SEPM Special Publication, 90, 237–263.
- Ainsworth, R.B., Vakarelov, B.K., Nanson, R.A., 2011. Dynamic spatial and temporal prediction of changes in depositional processes on clastic shorelines: toward improved subsurface uncertainty reduction and management. *APPG Bulletin*, 95, 267–297.
- Ainsworth, R.B., Vakarelov, B.K., MacEachern, J.A., Nanson, R.A., Lane, T.I., Rarity, F., Dashtgard, S.E., 2016. Process-driven architectural variability in mouth-bar deposits: a case study from a mixed-process mouth-bar complex, Drumheller, Alberta, Canada. *Journal of Sedimentary Research*, 86(5), 512-541.
- Ainsworth, R.B., Vakarelov, B.K., MacEachern, J.A., Rarity, F., Lane, T.I., Nanson, R.A., 2017. Anatomy of a shoreline regression: implications for the high–resolution stratigraphic architecture of deltas. *Journal of Sedimentary Research*, 87, 425–459.
- Alasad, R., Olariu, C., Steel, R.J., 2023. Alluvial fan and fan delta facies architecture recording initial marine flooding in the Mio-Pliocene syn-rift sequence of the Fish Creek-Vallecito Basin, southern California. *Basin Research*, 35(4), 1619-1649.
- Alexander, J., Bridge, J.S., Cheel, R.J., Leclair, S.F., 2001. Bedforms and associated sedimentary structures formed under supercritical water flows over aggrading sand beds. *Sedimentology* 48, 133–152.

- Alfaro, E., Holz, M., 2014. Review of the chronostratigraphic charts in the Sinú–San Jacinto basin based on new seismic stratigraphic interpretations. *Journal of South American Earth Sciences*, 56, 139–169.
- Algheryafi, H., Viseras, C., Polo, C., Al-Ramadan, K., 2022. Facies architecture and paleogeography evolution of regressive wave-dominated shorelines transitioning into tide-dominated estuaries: Early Devonian Subbat Member, Jauf Formation, Saudi Arabia. *Journal of Sedimentary Research*, 92, 955-987.
- Allen, J.R.L., 1977. The possible mechanics of convolute lamination in graded sand beds. *Journal of the Geological Society* 134, 19–31.
- Allen, J.R.L., 1983. Studies in fluvial sedimentation: bars, bar-complexes and sandstone sheets (low-sinuosity braided streams) in the brownstones (L. Devonian), Welsh Borders. *Sedimentary Geology*, 33, 237-293.
- Allen, J.R.L., 1985. *Principles of Physical Sedimentology*. George Allen and Unwin, London, 272 pp.
- Allen, P.A., Allen, J.R., 2005. *Basin Analysis. Principles and Applications*. Second Edition. 562 p.
- Allen, P.A., Allen, J.R., 2013. *Basin Analysis: Principles and Application to Petroleum Play Assessment*, 3rd Edition 640 p.
- Allen, G.P., Salomon, J.C., Bassoullet, P., Du Penhoat, Y., De Grandpre, C. 1980. Effects of tides on mixing and suspended sediment transport in macrotidal estuaries. *Sedimentary Geology*, 26, 69-90.
- Allen, P.A., Homewood, P., Williams, G.D., 1986. Foreland basins: an introduction. In: Allen, P.A., Homewood, P. (Eds.), *Foreland Basins*. Spec. Publs. Int. Ass. Sediment 8. Blackwell Scientific Publications, Oxford, p. 3-14.
- Alpert, S.P., 1974. Systematic review of the genus *Skolithos*. *Journal of Paleontology*, 48, 661–669.
- Angulo-Pardo, E., Vallejo-Hincapié, F., Do Monte Guerra, R., Pardo-Trujillo, A., Giraldo-Villegas, C.A., García Gonzáles, J., Hernández Duran, S., Herrera Quijano, S., Plata Torres, A., Trejos-Tamayo, R., 2023. Late Cretaceous calcareous nannofossil assemblages from Colombia: Biostratigraphic contributions to northwestern South American Basins. *Journal of South American Earth Sciences*, 127, 104315.
- Anthony, E.J., Orford, J.D., 2002. Between wave- and tide-dominated coasts: the middle ground revisited. *Journal of Coastal Research*, Special Issue, 36, 8-15.
- Anthony, E.J., Besset, M., Dussouillez, P., Goichot, M., Loisel, H., 2019. Overview of the Monsoon-influenced Ayeyarwady River delta, and delta shoreline mobility in response to changing fluvial sediment supply: *Marine Geology*, v. 417, 106038.
- Arias-Villegas, V., Bedoya Agudelo, E.L., Vallejo-Hincapié, F., Aubry, M-P., Pardo-Trujillo, A., 2023. Late Eocene to Early Miocene calcareous nannofossil biostratigraphy from the ANH-San Jacinto- 1 well: Stratigraphic implications for the Sinú-San Jacinto basin in the Caribbean region of Colombia. *Journal of South American Earth Sciences*, 128, 104470.
- Armitage, J.J., Duller, R.A., Whittaker, A.C., Allen, P.A., 2011. Transformation of tectonic and climatic signals from source to sedimentary archive: *Nature geoscience*, 4, 231-235.
- Armitage, D.A., McHargue, T., Fildani, A., Graham, S.A., 2012. Postavulsion channel evolution: Niger Delta continental slope. *AAPG Bulletin*, 96, 823-843.
- Arnott, R.W., Southard, J.B., 1990. Exploratory flow–duct experiments on combined–flow bed configurations, and some implications for interpreting storm event stratification. *Journal of Sedimentary Petrology*, 60, 211–219.

- Arregui, M.G., Buatois, L.A., Rodríguez, E., 2019. Shrimps and leaves: phytodetrital pulses and bioturbation in deposits of a river-dominated delta (Middle Jurassic Lajas formation, Neuquén basin, Argentina). *Palaeogeography, Palaeoclimatology, Palaeoecology*, 516, 179-189.
- Aslan, A., 2013. Fluvial environments. In: Elias, S.A., Mock, C.J. (Eds.), *Encyclopedia of Quaternary Science* (Second Edition), 663-675.
- Astin, T.R., Rogers, D.A., 1991. 'Subaqueous shrinkage cracks' in the Devonian of Scotland reinterpreted. *Journal of Sedimentary Petrology*, 61, 850-859.
- Aubry, M.-P. 2014a. *Cenozoic coccolithophores: Discoasterales (CC-B)*.: New York, Micropaleontology Press. Atlas of Micropaleontology series, 431 p.
- Aubry, M.-P. 2014b. *Cenozoic Coccolithophores: Discoasterales (CC-C)*.: New York, Micropaleontology Press. Atlas of Micropaleontology series, 328 p.
- Aubry, M.-P. 2015a. *Cenozoic coccolithophores: Discoasterales (CC-D)*.: New York, Micropaleontology Press. Atlas of Micropaleontology series, 433 p.
- Aubry, M.-P. 2015b. *Cenozoic coccolithophores: Discoasterales (CC-E)*. (M. Aubry, Ed.): New York, Micropaleontology Press. Atlas of Micropaleontology series, 532 p.
- Aubry, M.-P. 2021. *Coccolithophores: Cenozoic Discoasterales—Biology, Taxonomy, Stratigraphy*: SEPM Society for Sedimentary Geology, v. 14.
- Aumond, G.N., Kochhann, K.G.D., Netto, R.G., de Souza, L.V., Sedorko, D., Horodyski, R.S., Almeida Junior, F.N., Verde, M., 2021. Paleoenvironmental conditions of the late Miocene "Entrerriense" epicontinental sea: A case study of the Camacho Formation, SW Uruguay, *Journal of South American Earth Sciences* 110, 103421.
- Azpiroz-Zavala, M., Cartigny, M.J.B., Summer, E.J., Clare, M.A., Talling, P.J., Parsons, D.R., Cooper, C., 2017. A General Model for the Helical Structure of Geophysical Flows in Channel Bends. *Geophysical Research Letters* 44 (23), 932-941.
- Baas, J.H., Best, J.L., Peakall, J., 2016. Predicting bedforms and primary current stratification in cohesive mixtures of mud and sand. *Journal of the Geological Society*, 173, 12-45.
- Babonneau, N., Savoye, B., Cremer, M., Bez, M., 2004. Multiple terraces within the deep incised Zaire Valley (ZaiAngo Project): are they confined levees? In: *Geological Society, London, Special Publications* 222, 91-114.
- Backman, J., Raffi, I., Rio, D., Fornaciari, E., Pälke, H., 2012. Biozonation and biochronology of Miocene through Pleistocene calcareous nannofossils from low and middle latitudes. *Newsletters on Stratigraphy*, 45, 221-244.
- Baniak, G.M., Gingras, M.K., Burns, B.A., Pemberton, S.G., 2014. An example of a highly bioturbated, storm-influenced shoreface deposit: Upper Jurassic Ula Formation, Norwegian North Sea. *Sedimentology* 61, 1261-1285.
- Bann, K.L., Tye, S.C., MacEachern, J.A., Fielding, C.R., Jones, B.G., 2008. Ichnological and sedimentologic signatures of mixed wave- and storm-dominated deltaic deposits: examples from the Early Permian Sidney Basin, Australia. In: Hampson, G.J., Steel, R.J., Burgess, P.B., Dalrymple, R.W. (Eds.), *Recent Advances in Models of Siliciclastic Shallow-Marine Stratigraphy*. Society for Sedimentary Geology, Special Publication, 90, 292-332.

- Barbosa-Espitia, Á.A., Kamenov, G.D., Foster, D.A., Restrepo-Moreno, S.A., Pardo-Trujillo, A., 2019. Contemporaneous Paleogene arc-magmatism within continental and accreted oceanic arc complexes in the northwestern Andes and Panama. *Lithos*, 348–349.
- Barnes, H.A., Hutton, J.F., Walters, K., 1989. *An Introduction to Rheology*. Elsevier, Amsterdam, 199 p.
- Barrell, J., 1912. Criteria for the recognition of ancient delta deposits. *Bulletin of the Geological Society of America*, 23; 377-446.
- Barrera, R., Reyes, G.A., Guzmán, G., Franco, J.V., 2001. Geología de la plancha 31 Campo de la Cruz, Escala 1:100000. Memoria explicativa, INGEOMINAS, Bogotá. (in Spanish)
- Barrett, P.J., 2007. Cenozoic climate and sea level history from glacial marine strata off the Victoria Land coast, Cape Roberts Project, Antarctica. In: Hambrey, M.J., Christoffersen, P., Glasser, N.F., Hubbard, B. (Eds.), *Glacial Processes and Products*. International Association of Sedimentologists, Oxford, Special Publication, 39, 259-287.
- Bates, C.C., 1953. Rational theory of delta formation. *American Association of Petroleum Geologists Bulletin*, 37, 2119-2162.
- Baucon, A., Ronchi, A., Felletti, F., Neto de Carvalho., 2014. Evolution of crustaceans at the edge of the end-Permian crisis: ichnonetwork analysis of the fluvial succession of Nurra (Permian–Triassic, Sardinia, Italy). *Palaeogeography, Palaeoclimatology, Palaeoecology*, 410, 74–103.
- Baucon, A., Bednarz, M., Dufour S., Felletti, F., Malgesini, G., Neto de Carvalho, C., Niklas, K.J., Wehrmann, A., Batstone, R., Bernardini, F., Briguglio, A., Cabella, R., Cavalazzi, B., Ferretti, A., Zanzerl, H., McIlroy, D., 2020. Ethology of the trace fossil *Chondrites*: Form, function and environment. *Earth-Science Reviews* 202, 102989.
- Baucon, A., Breda, A., Neto de Carvalho, C., Piazza, M., Briguglio, A., 2023. Life in a Gilbert-type delta system: Ichnoassociations of the Ventimiglia palaeovalley and their sequence stratigraphic significance (Pliocene, NW Italy). *Palaeogeography, Palaeoclimatology, Palaeoecology* 627, 111718.
- Bayet-Goll, A., Neto de Carvalho, C., 2020. Architectural evolution of a mixed-influenced deltaic succession: Lower-to-Middle Ordovician Armorican Quartzite in the southwest Central Iberian Zone, Penha Garcia Formation (Portugal). *International Journal of Earth Sciences*, 109, 2495–2526.
- Bayona, G., Cardona, A., Jaramillo, C., Mora, A., Montes, C., Valencia, V., Ayala, C., Montenegro, O., Ibañez, M., 2012. Early Paleogene magmatism in the northern Andes: insights on the effects of Oceanic Plateau–continent convergence. *Earth and Planetary Science Letters*, 331–332, 97–111.
- Bayet-Goll, A., Neto De Carvalho, C., Mahmudy-Gharaei, M.H., Nadaf, R., 2015. Ichnology and sedimentology of a shallow marine Upper Cretaceous depositional system (Neyzar Formation, Kopet-Dagh, Iran): Palaeoceanographic influence on ichnodiversity. *Cretaceous Research* 56, 628-646.
- Bayet-Goll, A., Knaust, D., Daraei, M., Bahrami, N., Bagheri, F., 2022. *Rosselia* ichnofabrics from the Lower Ordovician of the Alborz Mountains (northern Iran): palaeoecology, palaeobiology and sedimentology. *Palaeobiodiversity and Palaeoenvironments* 102, 103-128.
- Bayet-Goll, A., Sharafi, M., Daraei, M., Nasiri, Y., 2023. The influence of hybrid sediment gravity flows on distribution and composition of trace-fossil assemblages: Ordovician succession of the north-eastern Alborz Range of Iran. *Sedimentology* 70 (3), 783–827.
- Beaumont, C., 1981, Foreland basins: *Geophysical Journal International*, v. 65, 291-329.

- Beddow, H.M., Liebrand, D., Sluijs, A., Wade, B.S., Lourens, L.J., 2016. Global change across the Oligocene-Miocene transition: High-resolution stable isotope records from IODP Site U1334 (equatorial Pacific Ocean). *Paleoceanography and Paleoclimatology*, 31, 81-97.
- Belaústegui, Z., de Gibert, J.M., 2013. Bow-shaped, concentrically laminated polychaete burrows: a *Cylindrichnus concentricus* ichnofabric from the Miocene of Tarragona, NE Spain. *Palaeogeography, Palaeoclimatology, Palaeoecology*, 381–382, 119–127.
- Belaústegui, Z., de Gibert, J.M., López-Blanco, M., Bajo, I., 2013. Recurrent constructional pattern of the crustacean burrow *Sinusichnus sinuosus* from the Paleogene and Neogene of Spain. *Acta Palaeontologica Polonica* 59(2), 461-474.
- Benvenuti, M., Martini, I.O., 2002. Analysis of terrestrial hyperconcentrated flows and their deposits. In: Martini, I.P., Baker, V.R., Garzón, G. (Eds.), *Flood and Megaflood Processes and Deposits: Recent and Ancient Examples. Alluvial-fan floods. Special Publication Number 32 of the International Association of Sedimentologists*, 32, 167-93.
- Bermúdez, H.D., 2016. Esquema estratigráfico de secuencias del registro sedimentario del Cinturón Plegado de San Jacinto, Caribe colombiano. Extended abstract presented at the XII Simposio Bolivariano Exploración Petrolera en Cuencas Subandinas, September 26–28, Bogotá, (in Spanish).
- Bermúdez, H.D., Alvarán, M., Grajales, J.A., Restrepo, L., Rosero, J.S., Guzmán, C., Ruiz, E., Navarrete, R., Jaramillo, C., Osorno, F., 2009. Estratigrafía y evolución geológica de la secuencia sedimentaria del Cinturón Plegado de San Jacinto. XII Congreso Colombiano de Geología. Paipa, Colombia, p. 1-28, (in Spanish).
- Bernal-Olaya, R., Mann, P., Escalona, A., 2015. Cenozoic Tectonostratigraphic Evolution of the Lower Magdalena Basin, Colombia: An Example of an Under- to Overfilled Forearc Basin. In: Batolini, C., Mann, P. (Eds.), *Petroleum Geology and Potential of the Colombian Caribbean Margin*, 108, 345–398.
- Bertling, M., Braddy, S., Bromley, R.G., Demathieu, G.D., Genise, J.F., Mikuláš, R., Nielsen, J-K., Nielsen, K.S.S., Rindsberg, A.K., Schlirf, M., Uchman, A., 2006. Names for trace fossils: a uniform approach. *Lethaia*, 39, 265-286.
- Beverage, J.P., Culbertson, J.K., 1964. Hyperconcentrations of suspended sediment. *J. Hydraulics Div., Am. Soc. Civ. Eng.*, 90, 117-128.
- Beynon, B.M., Pemberton, S.G., Bell, D.D., Logan, C.A., 1988. Environmental implications of ichnofossils from the Lower Cretaceous Grand Rapids Formation; Cold Lake Oil Sand Deposits. In: James, D.P., Leckie, D.A. (Eds.), *Sequences, Stratigraphy, Sedimentology: Surface and Subsurface. Canadian Society of Petroleum Geologists, Memoir 15*, 275-290.
- Bhattacharya, J.P., 2006. Deltas. In: Posamentier, H.W., Walker, R.G. (Eds.), *Facies Models revisited. Society of Economic Paleontologists and Mineralogists Special Publication*, 84, 237–292.
- Bhattacharya, J.P., 2010. Deltas. In: *Facies Models 4*, James, N.P., Dalrymple, R.W. (Eds.), *The Geological Association of Canada*, 6, 233-264.
- Bhattacharya, J.P., Walker, R.G., 1991. Facies and facies successions in river- and wave-dominated depositional systems of the Upper Cretaceous Dunvegan Formation, northwestern Alberta. *Bulletin of Canadian Petroleum Geology*, 39, 165–191.
- Bhattacharya, J.P., Walker, R.G., 1992. Deltas. In: Walker, R.G., James, N.O. (Eds.), *Facies Models: Response to Sea-Level Change. Geological Association of Canada, St Johns*, 157–177.

- Bhattacharya, J.P., Giosan, L., 2003. Wave-influenced deltas: geomorphological implications for facies reconstruction. *Sedimentology*, 50, 187–210.
- Bhattacharya, J.P., MacEachern, J.A., 2009. Hyperpycnal rivers and prodeltaic shelves in the Cretaceous seaway of North America. *Journal of Sedimentary Research*, 79, 184–209.
- Birgenheier, L. P., Horton, B., McCauley, A.D., Johnson, C. L., Kennedy, A., 2017. A depositional model for offshore deposits of the lower Blue Gate Member, Mancos Shale, Uinta Basin, Utah, USA. *Sedimentology*, 64, 1402-1438.
- Bloom, A.L., 1978. *Geomorphology. A systematic analysis of late Cenozoic land forms*. Englewood Cliffs, New Jersey: Prentice-Hall. xvii + 510 pp.
- Boesiger, T.M., de Kaenel, E., Bergen, J.A., Browning, E., Blair, S.A., 2017. Oligocene to Pleistocene taxonomy and stratigraphy of the genus *Helicosphaera* and other placolith taxa in the circum North Atlantic Basin. *Journal of Nannoplankton Research*, 37(2-3), 145-175.
- Botero-Garcia, M., Vinasco, C.J., Restrepo-Moreno, S.A., Foster, D.A., Kamenov, G.D., 2023. Caribbean–South America interactions since the Late Cretaceous: Insights from zircon U–Pb and Lu–Hf isotopic data in sedimentary sequences of the northwestern Andes. *Journal of South American Earth Sciences*, 123, 104231.
- Bown, P. 1998. *Calcareous nannofossil biostratigraphy*: Chapman and Hall; Kluwer Academic.
- Boyd, C., McIlroy, D., 2016. Three–dimensional morphology and palaeobiology of the trace fossil *Dactyloidites jordii* nov. isp. from the Carboniferous of England. *Geobios*, 49, 257–264.
- Boyd, R., Dalrymple, R., Zaitlin, B.A., 1992. Classification of clastic coastal depositional environments. *Sedimentary Geology*, 80, 139–150.
- Brandes, C., Winsemann, J., 2018. From incipient island arc to doubly-vergent orogen: A review of geodynamic models and sedimentary basin-fills of southern Central America. *Island Arc*, 27 (5), e12255.
- Brenna, A., Marchi, L., Borga, M., Ghinassi, M., Zaramella, M., Surian, N., 2021. Sediment–water flows in mountain catchments: insights into transport mechanisms as responses to high-magnitude hydrological events. *Journal of Hydrology*, 602, 126716.
- Brett, C.E., Baird, G.C., 1986. Comparative taphonomy: a key to paleoenvironmental interpretation based on fossil preservation. *Palaios* 207-227.
- Bridge, J.S., 2003. *Rivers and Floodplains*. Blackwell Sciences, Oxford, 491 pp.
- Bridge, J.S., 2006. Fluvial facies models: recent developments. In: Posamentier, H.W., Walker, R.G. (Eds), *Facies Models Revisited*. SEPM (Society for Sedimentary Geology), Special Publications, 84, 85-170.
- Bridge, J.S., Tye, R.S., 2000. Interpreting the dimensions of ancient fluvial channel bars, channels, and channel belts from wireline-logs and cores. *AAPG Bulletin*, 84, 1205-1228.
- Bromley, R.G., 1990. *Trace fossils; Biology and Taphonomy*. London, Unwin Hyman, Special Topics in Paleontology, 3, 280 p.
- Bromley, R.G., 1996. *Trace fossils. Biology, Taphonomy and Applications*. Chapman and Hall, London.
- Bromley, R.G., Ekdale, A.A., 1984. *Chondrites*: a trace fossil indicator of anoxia in sediments. *Science* 224, 872-874.
- Bromley, R.G., Ekdale, A.A., 1986. Composite ichnofabrics and tiering of burrows. *Geological Magazine*, 123, 59-65.

- Bromley, R.G., Milàn, J., Uchman, A., Hansen, K.S., 2009. Rheotactic *Macaronichnus*, and human and cattle trackways in Holocene beachrock, Greece: reconstruction of paleoshoreline orientation. *Ichnos*, 16, 103–117.
- Brooks, H.L., Hodgson, D.M., Brunt, R.L., Peakall, J., Hofstra, M., Flint, S.S., 2018. Deepwater channel-lobe transition zone dynamics: processes and depositional architecture, an example from the Karoo Basin, South Africa. *GSA Bulletin* 130, 1723–1746.
- Brooks, H.K., Ito, M., Zuchuat, V., Peakall, J., Hodgson, D.M., 2022. Channel-lobe transition zone development in tectonically active settings: Implications for hybrid bed development. *The Depositional Record* 8, 829–868.
- Buatois, L.A., Mángano, M.G., 2011. *Ichnology: Organism–Substrate Interactions in Space and Time*. Cambridge University Press, 358 p.
- Buatois, L.A., Macsotay, O., Quiroz, L.I., 2009. *Sinusichnus*, a trace fossil from Antarctica and Venezuela: expanding the dataset of crustacean burrows. *Lethaia* 42(4), 511–518.
- Buatois, L.A., Saccavino, L.L., Zavala, C., 2011. Ichnologic signatures of hyperpycnal flow deposits in Cretaceous river-dominated deltas, Austral Basin, southern Argentina. In: Slatt, R.M., Zavala, C. (Eds.), *Sediment transfer from shelf to deep water—revisiting the delivery system*. AAPG Studies in Geology, 61, 153–170.
- Buatois, L.A., Mángano, M.G., Pattison, S.A.J., 2019. Ichnology of prodeltaic hyperpycnite-turbidite channel complexes and lobes from the Upper cretaceous Praire Canyon Member of the Mancos Shale, Book Cliffs, Utah, USA. *Sedimentology*, 66 (5), 1825–1860.
- Buatois, L.A., Mángano, M.G., Maples, C.G., Lanier, W.P., 1997. The paradox of nonmarine ichnofaunas in tidal rhythmites: Integrating sedimentologic and ichnologic data from the Late Carboniferous of Eastern Kansas. *Palaios*, 12, 467–481.
- Buatois, L.A., Gingras, M.K., MacEachern, J.A., Mángano, M.G., Zonneveld, J.P., Pemberton, S.G., Netto, R.G., Martin, A.J., 2005. Colonization of Brackish–water systems through time, Evidence from the trace–fossil record. *Palaios*, 20, 321–347.
- Buatois, L.A., Santiago, N., Herrera, M., Plink–Björklund, P., Steel, R.J., Espin, M., Parra, K., 2012. Sedimentological and ichnological signatures of changes in wave, river and tidal influence along a Neogene tropical deltaic shoreline. *Sedimentology*, 59, 1568–1612.
- Buatois, L.A., Mángano, M.G., Rossi, V.M., Longhitano, S.G., Leva Lopez, J., Chiarella, D., Gugliotta, M., 2023. Trace fossils from Miocene to Pleistocene tidal straits in southern Italy: implications for the ichnofacies model. 36th International Meeting of Sedimentology, Dubrovnik, Croatia, 354 p.
- Burgess, P.M., Allen, P.A., Steel, R.J., 2016. Introduction to the future of sequence stratigraphy: evolution or revolution?. *Journal of the Geological Society*, 173, 801–802.
- Burns, C.E., Mountney, N.P., Hodgson, D.M., Colombera, L., 2017. Anatomy and dimensions of fluvial crevasse-splay deposits: examples from the Cretaceous Castlegate sandstone and Neslen formation, Utah, USA. *Sedimentary Geology*, 351, 21–35.
- Callow, R.H.T., Kneller, B., Dykstra, M., McIlroy, D., 2014. Physical, biological, geochemical and sedimentological controls on the ichnology of submarine canyon and slope channel systems. *Marine and Petroleum Geology* 54, 144–166.

- Canale, N., Ponce, J.J., Carmona, N.B., Parada, M.N., Drittanti, D.I., 2020. Sedimentología e icnología de un delta fluvio-dominado, Formación Lajas (Jurásico Medio), cuenca Neuquina, Argentina. *Andean Geology*, 47, 179–206.
- Cardona, A., Valencia, V., Bustamante, C., García-Casco, A., Ojeda, G., Ruiz, J., Saldarriaga, M., Weber, M., 2010. Tectonomagmatic setting and provenance of the Santa Marta Schists, northern Colombia: Insights on the growth and approach of Cretaceous Caribbean oceanic terranes to the South American continent. *Journal of South American Earth Sciences*, 29(4), 784-804.
- Cardona, A., Montes, C., Ayala, C., Bustamante, C., Hoyos, N., Montenegro, O., Ojeda, C., 2012. Tectonophysics From arc–continent collision to continuous convergence, clues from Paleogene conglomerates along the southern Caribbean–South America plate boundary. *Tectonophysics*, 580, 58–87.
- Cardona, A., Weber, M., Valencia, V., Bustamante, C., Montes, C., Cordani, U., Muñoz, C.M., 2012. Geochronology and geochemistry of the Parashi granitoid, NE Colombia: Tectonic implication of short-lived Early Eocene plutonism along the SE Caribbean margin. *Journal of South American Earth Sciences*, 50, 75-92.
- Cardona, A., León, S., Jaramillo, J., Montes, C., Valencia, V., Vanegas, J., Bustamante, C., Echeverri, S., 2018. The Paleogene arcs of the northern Andes of Colombia and Panama: insights on plate kinematic implications from new and existing geochemical, geochronological and isotopic data. *Tectonophysics*, 749, 88-103.
- Carmona, N.B., Buatois, L.A., Mángano, M.G., Bromley, R.G., 2008. Ichnology of the Lower Miocene Chenque Formation, Patagonia, Argentina: animal - substrate interactions and the Modern Evolutionary Fauna. *Ameghiniana* 45(1), 93-122.
- Carmona, N.B., Buatois, L.A., Ponce, J.J., Mángano, M.G., 2009. Ichnology and sedimentology of a tide-influenced delta, Lower Miocene Chenque Formation, Patagonia, Argentina: Trace-fossil distribution and response to environmental stresses. *Palaeogeography, Palaeoclimatology, Palaeoecology* 273, 75-86.
- Carr, I.D., Gawthorpe, R.L., Jackson, C.A.L., Sharp, I.R., Sadek, A., 2003. Sedimentology and sequence stratigraphy of early syn-rift tidal sediments: the Nukhul Formation, Suez Rift, Egypt. *Journal of Sedimentary Research*, 73, 407-420.
- Cartigny, M.J.B., Ventra, D., Postma, G., Van Den Berg, J.H., 2014. Morphodynamics and sedimentary structures of bedforms under supercritical-flow conditions: new insights from flume experiments. *Sedimentology* 61, 712–748.
- Carvajal, C., Steel, R., 2009. Shelf-edge architecture and bypass of sand to deep water: influence of shelf-edge processes, sea level, and sediment supply. *Journal of Sedimentary Research*, 79, 652-672.
- Cattaneo, A., Steel, R.J., 2003. Transgressive deposits: a review of their variability. *Earth Science Reviews*, 62 (3–4), 187–228.
- Catuneanu, O., 2006. Principles of sequence stratigraphy. Elsevier, Amsterdam, 375pp.
- Catuneanu, O., 2019. Scale in sequence stratigraphy. *Marine and Petroleum Geology*, 106, 128-159.
- Catuneanu, O., Zecchin, M., 2013. High-resolution sequence stratigraphy of clastic shelves II: controls on sequence development. *Marine and Petroleum Geology*, 39, 26-38.
- Cawood, P.A., Kröner, A., Collins, W.J., Kusky, T.M., Mooney, W.D., Windley, B.F., 2009. Accretionary orogens through Earth history. In: Cawood, P.A., Kröner, A. (Eds.), *Earth Accretionary Systems in Space and Time*, Geological Society of London, Special Publication, 318(1), 1-36.

- Cediel, F., Shaw, R., Cáceres, C., 2003. Tectonic assembly of the northern Andean block. In: Bartolini C, Buffer RT, Blickwede J. (Eds.), *The circum—Gulf of Mexico and the Caribbean: hydrocarbon habitats, basin formation and plate tectonics*. American Association of Petroleum Geologists, Tulsa, AAPG Memoir, 79, 815-848.
- Celis, S.A., Rodríguez–Tovar, F.J., Pardo–Trujillo, A., 2018, *The *Phycosiphon* record in the ladrillos–Juanchaco section (Miocene, Colombian Pacific): palaeoecological implications*. Spanish Journal of Palaeontology, 33(2), 277-288.
- Celis, S.A., Rodríguez–Tovar, F.J., Giraldo-Villegas, C.A., Pardo–Trujillo, A., 2021. Evolution of a fluvial-dominated delta during the Oligocene of the Colombian Caribbean: Sedimentological and ichnological signatures in well-cores. *Journal of South American Earth Sciences*, 111, 103440.
- Celis, S.A., Rodríguez-Tovar, F.J., Pardo-Trujillo, A., García-García, F., Giraldo-Villegas, C.A., Gallego, F., Plata, A., Trejos-Tamayo, R., Vallejo-Hincapié, F., Cardona, J., 2023. Deciphering influencing processes in a tropical delta system (middle-late Eocene? to Early Miocene, Colombian Caribbean): Signals from a well-core integrative sedimentological, ichnological, and micropaleontological analysis. *Journal of South American Earth Sciences*, 127, 104368.
- Celis, S.A., García-García, F., Rodríguez-Tovar, F.J., Giraldo-Villegas, C.A., Pardo-Trujillo, A., 2024. Coarse-grained submarine channels: from confined to unconfined flows in the Colombian Caribbean (late Eocene). *Sedimentary Geology*, 459, 106550.
- Celma, C.D., Cantalamessa, G., 2007, *Sedimentology and high-frequency sequence stratigraphy of a forearc extensional basin: The Miocene Caleta Herradura Formation, Mejillones Peninsula, northern Chile*. *Sedimentary Geology*, 198, 29-52.
- Cerón, J.F., Kellogg, J.N., Ojeda, G.Y., 2007. Basement configuration of the Northwestern South America - Caribbean margin from recent Geophysical data. *CT&F- Ciencia, Tecnología y Futuro* 3, 25-49.
- Chakraborty, C., Bose, P.K., 1992. Ripple/dune to upper stage plane bed transition: some observations from the ancient record. *Geological Journal* 27, 349–359.
- Chalabe, A.C., Matrínez., M.A., Olivera, D.E., Canale, N., Ponce, J.J., 2022. Palynological analysis of sandy hyperpycnal deposits of the Middle Jurassic, Lajas Formation, Neuquén Basin, Argentina. *Journal of South American Earth Sciences*, 116, 103867.
- Charms, J.C., 1969, *Hydraulic Significance of Some Sand Ripples*, *GSA Bulletin*, v. 80(3), p. 363-396.
- Charvin, K., Hampson, G.J., Gallagher, K.L., Labourdette, R., 2010. Intra-parasequence architecture of an interpreted asymmetrical wave-dominated delta. *Sedimentology*, 57, 760-785.
- Choi, K., Jo, J., Kim, D., 2021. Tidal and seasonal controls on the stratigraphic architecture of blind tidal channel deposits in the fluvial-tidal transition of the macrotidal Sittaung River estuary, Myanmar. *Sedimentary Geology*, 426, 106029.
- Clark, J.D., Pickering, K.T., 1996. *Submarine Channels: Processes and Architecture*. Vallis Press, London.
- Clavijo, J., Barrera, R., 2001. *Geología de las planchas 44 Sincelejo y 52 Sahagún. Escala 1:100.000. Memoria Explicativa. INGEOMINAS. Bogotá, (in Spanish)*.
- Clifton, H.E., 2006. A Re-examination of Facies Models for Clastic Shorelines. In: Posamentier, H.W., Walker, R.G. (Eds.), *Facies Models Revisited*. Society for Sedimentary Geology Special Publication 84, 293-337.
- Clifton, H.E., Thompson, J.K., 1978. *Macaronichnus segregatis*: a feeding structure of shallow marine polychaetes. *Journal of Sedimentary Petrology*, 48, 1293–1302.

- Cloos, M., Shreve, R.L. 1988. Subduction-channel model of prism accretion, melange formation, sediment subduction, and subduction erosion at convergent plate margins: 1. Background and description. *Pure and Applied Geophysics*, 128(3), 455-500.
- Coates, L., MacEachern, J.A., 2007. The ichnological signatures of river- and wave-dominated delta complexes: differentiating deltaic and non-deltaic shallow marine successions, Lower Cretaceous Viking Formation and Upper Cretaceous Dunvegan Formation, West-Central Alberta. In: MacEachern, J.A., Bann, K.L., Gingras, M.K., Pemberton, S.G. (Eds.), *Applied Ichnology*. Society for Sedimentary Geology, Short Course Notes, 52, 227–255.
- Cochrane, R., Spikings, R., Gerdes, A., Ulianov, A., Mora, A., Villagómez, D., Putlitz, B., Chiaradia, M., 2014. Permo-Triassic anatexis, continental rifting and the disassembly of western Pangaea. *Lithos*, 190–191, 383–402.
- Cohen, K.M., Finney, S.C., Gibbard, P.L., Fan, J.-X. 2013. The ICS International Chronostratigraphic Chart: Episodes, 36, 199–204.
- Cole, G., Jerrett, R., Watkinson, M.P., 2021. A stratigraphic example of the architecture and evolution of shallow water mouth bars. *Sedimentology*, 68, 1227-1254.
- Coleman, J.M., Wright, L.D., 1971. Analysis of major river systems and their deltas: procedures and rationale: with two examples, 95. Baton Rouge, LA: Louisiana State University Press, p. 125.
- Collier, R.E.L., Leeder, M.R., Maynard, J.R., 1990. Transgression and regression: A model for the influence of tectonic subsidence, deposition and eustasy, with application to Quaternary and Carboniferous examples. *Geological Magazine* 127, 117-128.
- Collins, S.D., Johnson, H.D., Baldwin, C.T., 2020. Architecture and preservation in the fluvial to marine transition zone of a mixed-process humid-tropical delta: Middle Miocene Lambir Formation, Baram Delta Province, north-west Borneo. *Sedimentology*, 67, 1–46.
- Collinson, J., Mountney, N., 2019. *Sedimentary structures – Fourth Edition*. Dunedin Academic Press Ltd. 340p.
- Collinson, J., Mountney, N., Thompson, D., 2006. *Sedimentary Structures - Third Edition*. Terra publishing. 302p.
- Condie, K.C., 2007. Accretionary orogens in space and time. In: Hatcher, Jr. R.D., Carlson, M.P., McBride, J.H., Martínez Catalán, J.R. (Eds.), *4-D Framework of Continental Crust*. Geological Society of America, 200, 145-158.
- Cooper, M., Addison, F., Alvarez, R., Coral, M., Graham, R., Hayward, A., Howe, S., Martinez, J., Naar, J., Penas, R., Pulham, A., Taborda, A., 1995. Basin development and tectonic history of the Llanos Basin, Eastern Cordillera, and Middle Magdalena Valley, Colombia. *AAPG Bulletin*, 79, 1421-1443.
- Cooper, A.K., Brancolini, G., Escutia, C., Kristoffersen, Y., Larter, R., Leitchenkov, G., O'Brien, P., Jokat, W., 2009. Cenozoic Climate History from Seismic Reflection and Drilling Studies on the Antarctic Continental Margin. In: Florindo, F., Siegert, M. (Eds.), *Antarctic Climate Evolution, Developments in Earth & Environmental Sciences*, 8. Chapter 5, 120 p.
- Cornard, P.H., Pickering, K.T., 2019. Supercritical-flow Deposits and Their Distribution in a Submarine Channel System, Middle Eocene, Ainsa Basin, Spanish Pyrenees. *Journal of Sedimentary Research* 89 (6), 576–597.
- Coronel, M.D., Isla, M.F., Veiga, G.D., Mountney, N.P., Colombera, L., 2020. Anatomy and facies distribution of terminal lobes in ephemeral fluvial successions: Jurassic Tordillo Formation, Neuquén Basin, Argentina: *Sedimentology*, v. 67(5), p. 2596-2624.

- Cortes, J.E., Aguilera, R., Wilches, O., Osorno, J.F., Cortes, S.I., 2018. Organic geochemical insights from oil seeps, tars, rocks, and mud volcanoes on the petroleum systems of the Sinú-San Jacinto basin, Northwestern, Colombia. *Journal of South American Earth Sciences*, 86, 318-341.
- Cortés, J.M., 1987. Descripción geológica de la Hoja 42h Puerto Lobos, Provincia del Chubut, 202. Dirección Nacional de Geología y Minería, boletín, p. 93. [In Spanish].
- Coussot, Ph., Meunier, M., 1996. Recognition, classification and mechanical description of debris flows. *Earth Science Review*, 40, 209-227.
- Covault, J.A., Kostic, S., Paull, C.K., Ryan, H.F., Fildani, A., 2014. Submarine channel initiation, filling and maintenance from sea-floor geomorphology and morphodynamic modelling of cyclic steps. *Sedimentology* 61, 1031–1054.
- Cowell, P.J., Stive, M.J., Niedoroda, A.W., de Vriend, H.J., Swift, D.J., Kaminsky, G.M., Capobianco, M., 2003. The coastal-tract (part 1): a conceptual approach to aggregated modeling of low-order coastal change. *Journal of Coastal Research*, 812-827.
- Coxall, H.K., Wilson, P.A., 2011. Early Oligocene glaciation and productivity in the eastern equatorial Pacific: insights into global carbon cycling. *Paleoceanography and Paleoclimatology*, 26(2).
- Coxall, H.K., Wilson, P.A., Pälike, H., Lear, C.H., Backman, J., 2005. Rapid stepwise onset of Antarctic glaciations and deeper calcite compensation in the Pacific Ocean. *Nature*, 433, 53-57.
- Cronin, S.J., Lecointre, J.A., Palmer, A.S., Neall, V.E., 2000. Transformation, internal stratification, and depositional processes within a channelised, multi-peaked lahar flow. *New Zealand Journal of Geology & Geophysics*, 43, 117-128.
- Cuitiño, J.I., Dozo, M.T., del Río, C.J., Buono, M.R., Palazzesi, L., Fuentes, S., Scasso, R. A., 2017. Miocene marine transgressions: paleoenvironments and paleobiodiversity. In: Bouza, P., Bilmes, A. (Eds.), *Late Cenozoic of Península de Valdés, Patagonia Argentina: an interdisciplinary approach*. Springer Earth System Sciences 3, 47-84.
- Cuitiño, J.I., Bilmes, A., Buono, M.R., Bordese, S., Herazo, L., Scasso, R.A., 2023. Stratigraphy, provenance, and timing of Neogene sedimentation in the western Valdés Basin, Patagonia. Accurate paleogeographic reconstructions as a key piece for Andean-passive margin integration. *Journal of South American Earth Sciences*, 124, 104278.
- Curray, J.R., 1964. Transgressions and regressions. In: Miller, R. (Ed.), *Papers in Marine Geology*, Shepard Commemorative Volume, Macmillan, New York, 175-203.
- D'Apolito, C., Jaramillo, C., Harrington, G., 2021. Miocene Palynology of the Solimões Formation (Well 1-AS-105-AM), Western Brazilian Amazonia. *Smithsonian Contributions to Paleobiology*, No. 105. Smithsonian Institution Scholarly Press, Washington, D.C.
- D'Alessandro, A., Bromley, R.G., 1987. Meniscate trace fossils and the *Muensteria-Taenidium* problem. *Palaeontology*, 30, 743–763.
- Dalrymple, R.W., 1979. Wave-induced liquefaction: a modern example from the Bay of Fundy. *Sedimentology*, 26, 835-844.
- Dalrymple, R.W., 1992. Tidal depositional systems. In: Walker, R.G., James, N.P. (Eds.), *Facies Models: Response to Sea Level Change*, Geological Association of Canada, St. John's, 195-218.

- Dalrymple, R.W., 2006. Incised-valleys in time and space: An introduction to the volume and an examination of the controls on valley formation and infilling. In: Dalrymple, R.W., Leckie, D.A., Tillman, R.W. (Eds.), *Incised Valleys in Time and Space*. Society for Sedimentary Geology Special Publications 85, 5-12.
- Dalrymple, R.W., Rhodes, R.N., 1995. Estuarine dunes and bars. In: Perillo, G.M.E. (Ed.), *Geomorphology and Sedimentology of Estuaries*. Developments in Sedimentology 53, 359-422.
- Dalrymple, R.W., Choi, K., 2007. Morphologic and facies trends through the fluvial– marine transition in tide–dominated depositional systems: a schematic framework for environmental and sequence–stratigraphic interpretation. *Earth Science Review*, 81, 135–174.
- Dalrymple, R.W., Zaitlin, B.A., Boyd, R., 1992. Estuarine facies models: conceptual basis and stratigraphic implications. *Journal of Sedimentary Petrology*, 62, 147–173.
- Dalrymple, R.W., Knight, R.J., Zaitlin, B.A., Middleton, G.V., 1990. Dynamics and facies model of a macrotidal sand–bar complex, Cobequid Bay—Salmon River Estuary (Bay of Fundy). *Sedimentology*, 37, 577–612.
- Dalrymple, R.W., Baker, E.K., Harris, P.T., Hughes, M.G., 2003. Sedimentology and stratigraphy of a tide-dominated, foreland-basin delta (Fly river, Papua New Guinea). In: Sidi, F.H., Nummedal, D., Imbert, P., Darman, H., Posamentier, H.W. (Eds.), *Tropical Deltas of Southeast Asia—Sedimentology, Stratigraphy, and Petroleum Geology*. SEPM (Society for Sedimentary Geology), 76, 147–173.
- Dalrymple, R.W., Kurcinka, C., Jablonski, B., Ichaso, A., Mackay, D., 2015. Deciphering the relative importance of fluvial and tidal processes in the fluvial–marine transition. In: Ashworth, P.J., Best, J.L., Parsons, D.R. (Eds.), *Fluvial–Tidal Sedimentology*. Developments in Sedimentology, Elsevier, 68, 3–45.
- Dashtgard, S.E., La Croix, A.D., 2015. Sedimentological trends across the tidal–fluvial transition, Fraser River, Canada: a review and some broader implications. In: Ashworth, P.J., Best, J.L., Parsons, D.R. (Eds.), *Fluvial–Tidal Sedimentology*. Developments in Sedimentology, 111–126.
- Dashtgard, S.E., Gingras, M.K., MacEachern, J.A., 2009. Tidally modulated shorefaces. *Journal of Sedimentary Research*, 79, 793–807.
- Dashtgard, S.E., MacEachern, J.A., Frey, S.E., Gingras, M.K., 2012. Tidal effects on the shoreface: Towards a conceptual framework. *Sedimentary Geology* 279, 42-61.
- Dashtgard, S.E., Vaucher, R., Yang, B., Dalrymple, R., 2021. Hutchison Medallist 1. Wave-Dominated to Tide-Dominated Coastal Systems: A Unifying Model for Tidal Shorefaces and Refinement of the Coastal Environments Classification Scheme. *Geoscience Canada*, 48(1), 5-22.
- Davidson-Arnott, R.G.D., Van Heyningen, A.G., 2003. Migration and sedimentology of longshore sandwaves, Long Point, Lake Erie, Canada. *Sedimentology*, 50, 1123-1137.
- Davies, J.L., 1964. A morphogenic approach to world shorelines. *Zeit fur Geomorph*, 8, 27-42.
- Davis, R.A., Dalrymple, R.W., 2012. *Principles of Tidal Sedimentology*. Springer, New York, p. 621.
- de Gibert, J.M., 1996. A new decapod burrow system from the NW Mediterranean Pliocene. *Revista Española de Paleontología* 11, 251-254.
- de Gibert, J.M., Martinell, J., Domènech, R., 1995. The rosetted feeding trace fossil *Dactyloidites ottoi* (Geinitz) from the Miocene of Catalonia. *Geobios*, 28 (6), 769–776.
- DeCelles, P.G., Giles, K.A., 1996. Foreland basin systems. *Basin Research*, 8, 105-123.

- del Río, C.J., 2000. Malacofauna de las Formaciones Paraná y Puerto Madryn (Mioceno marino, Argentina): su origen, composición y significado bioestratigráfico. En: Aceñolaza F.G., Herbst, R. (Eds.), *El Neógeno de Argentina*. INSUGEO, Serie Correlación Geológica, 14, 77-101. [In Spanish].
- del Río, C.J., Martínez, S.A., Scasso, R.A., 2001. Nature and origin of spectacular marine Miocene Shell beds of northeastern Patagonia (Argentina): paleoecological and bathymetric significance. *Palaios* 16, 3-25.
- del Río, C.J., Martínez, S.A., McArthur, J.M., Thirlwall, M.F., Pérez, L.M., 2018. Dating late Miocene marine incursions across Argentina and Uruguay with Sr-isotope stratigraphy. *Journal of South American Earth Sciences*, 85, 312-324.
- Denniellou, B., Droz, L., Jacq, C., Babonneau, N., Bonnel, C., Picot, M., Le Saout, M., Saout, J., Bez, M., Savoye, B., Olu, K., Rabouille, C., 2017. Morphology, structure, composition and build-up processes of the active Congo channel-mouth lobe complex with inputs from remotely operated underwater vehicle (ROV) multibeam and video surveys. *Deep Sea Research Part II: Topical Studies in Oceanography* 142, 25–49.
- Desjardins, P.R., Buatois, L.A., Mángano, M.G., 2012. Tidal flats and subtidal sand bodies. In: Knaust, D., Bromley, R.G. (Eds.), *Trace fossils as indicators of sedimentary environments*. *Developments in Sedimentology*, 64, 529–561.
- Díez-Canseco, D., Buatois, L.A., Mángano, M.G., Rodríguez, W., Solorzano, E., 2015. The ichnology of the fluvial–tidal transition: Interplay of ecologic and evolutionary controls. In: Ashworth, P.J., Best, J.L., Parsons, D.R. (Eds.), *Fluvial–Tidal Sedimentology*. *Developments in Sedimentology*, Elsevier, 283–321.
- Domínguez-Giraldo, V., Arias-Díaz, A., Vallejo-Hincapié, F., Plata-Torres, A., Gallego, N.F., Pardo-Trujillo, A., 2023. Middle-late Eocene to Early Miocene micropaleontology of the ANH–TIERRALTA–2–X–P well: Biostratigraphic implications for southwestern deposits of the Sinú-San Jacinto belt (Colombian Caribbean). *Journal of South American Earth Sciences*, 128, 104420.
- Donselaar, M.E., Overeem, I., 2008. Connectivity of fluvial point-bar deposit: An example from the Miocene Huesca fluvial fan, Ebro Basin, Spain. *AAPG Bulletin*, 92, 1109-1129.
- Dorador, J., Rodríguez-Tovar, F.J., Miguez-Salas, O., 2021. The complex case of *Macaronichnus* trace fossil affecting rock porosity. *Scientific Reports*, 11, 1975.
- Dosut, H., Omatsola, E., 1989. Niger Delta. In: Edwards, J.D., Santogrossi, P.A. (Eds.), *Divergent/Passive Margins*. *AAPG Memoir*, 48, 201-238.
- Dozo, M.T., Bouza, P., Monti, A., Palazzesi, L., Barreda, V., Massaferró, G., Scasso, R.A., Tambussi, C., 2010. Late Miocene continental biota in northeastern Patagonia (Península Valdés, Chubut, Argentina). *Palaeogeography, Palaeoclimatology, Palaeoecology* 297, 100-109.
- Duarte, L.M., 1997. L’Eocène et le Miocène du Bassin de la Vallée Inférieure de la Magdalena, Colombie: Sédimentologie, Litho- et Argilostratigraphie, Paléogéographie et Paleoclimatologie. University of Liège, Belgium, PhD thesis, 128 pp. (In French)
- Dueñas, H., 1980. Palynology of Oligocene-Miocene strata of borehole Q-E-22, Planeta Rica, Northern Colombia. *Review of paleobotany and palynology*, 30, 313–328.
- Dueñas, H., 1983. Fluctuaciones del nivel del mar durante el depósito de los sedimentos basales de la Formación Ciénaga de Oro. Instituto nacional de investigaciones geológico mineras, INGEOMINAS. Bogotá, D.E. *Revista de la academia colombiana de ciencias exactas, físicas y naturales*, XV, 58.
- Dueñas, H., 1986. Geología y palinología de la Formación Ciénaga de Oro, Región Caribe Colombiana: *Publicaciones Geológicas Especiales del Ingeominas*, 18, 1-56, (in Spanish).

- Dueñas, H., Duque-Caro, H., 1981. Geología del Cuadrángulo F-8 (Planeta Rica): Boletín Geológico Ingeominas, 24(1), 1-35. (in Spanish).
- Dueñas, H., Gómez, C., 2011. Bioestratigrafía y paleogeografía de la Formación Cansona (Quebrada Peñitas, región Caribe colombiana). In: Memorias XIV Congreso Latinoamericano de Geología y XIII Congreso Colombiano de Geología, Medellín, pp. 361. (in Spanish).
- Dueñas, H., Gómez, C., 2013. Bioestratigrafía de la Formación Cansona en la Quebrada Penitas, Cinturón de San Jacinto. Implicaciones paleogeográficas: Revista de la Academia Colombiana de Ciencias Exactas, Físicas y Naturales, v. 145, p. 527-539, (in Spanish).
- Dumas, S., Arnott, R.W.C., Southard, J.B., 2005. Experiments on Oscillatory-Flow and Combined-Flow Bed Forms: Implications for Interpreting Parts of the Shallow-Marine Sedimentary Record. *Journal of Sedimentary Research*, 75(3), 501-513.
- Dunne, L.A., Hempton, M.R., 1984. Deltaic sedimentation in the Lake Hazar pull-apart basin, south-eastern Turkey. *Sedimentology*, 31, 401-412.
- Duque, H., 1973. The geology of the Montería area. Society of Petroleum Geology and Geophysics. Annual field conference, Bogotá.
- Duque-Castaño, M., Trejos-Tamayo, R., Osorio-Tabares, L.C., Angulo-Pardo, E., Vallejo, F., Plata, A., Pardo-Trujillo, A., 2023. Lower to Middle Miocene multiproxy biostratigraphy of the P-18 core-stratigraphic well in Sinú-San Jacinto Basin, Caribbean region of Colombia. *Journal of South American Earth Sciences* 123, 104228.
- Duque-Caro, H., 1968. Observaciones generales a la bioestratigrafía y geología regional en los departamentos de Bolívar y Córdoba. *Boletín Geológico*, 24, 71–87.
- Duque-Caro, H., 1972. Ciclos tectónicos y sedimentarios en el Norte de Colombia y sus relaciones con la paleoecología. *Boletín Geológico de Ingeominas*, 19, 1–23. (in Spanish)
- Duque-Caro, H., 1979. Major structural elements and evolution of northwestern Colombia. In: Watkins, J.S., Montadert, L., Dickerson, P.W. (Eds.), *Geological and geophysical investigations of continental margins*. AAPG Memoir 29, 329–351.
- Duque-Caro, H., 1984. Structural Style, diapirism and accretionary episodes of the Sinú-San Jacinto terrane, southwestern Caribbean borderland. *GSA Memoir* 162, 303–316.
- Duque-Caro, H. 1990a. Neogene stratigraphy, paleoceanography and paleobiogeography in northwest South America and the evolution of the Panama Seaway. *Palaeogeography, Palaeoclimatology, Palaeoecology*, 77, 203-234.
- Duque-Caro, H. 1990b. The Choco Block in the northwestern corner of South America: Structural, tectonostratigraphic, and paleogeographic implications. *Journal of South American Earth Science*, 3(1), 71-84.
- Duque-Caro, H. 1990c. El Bloque Chocó en el noroccidente Suramericano: Implicaciones estructurales, tectonoestratigráficas y paleogeográficas. *Boletín Geológico, Ingeominas*, 31(1), 48-71.
- Duque-Caro, H., 1991. Contributions to the Geology of the Pacific and the Caribbean Coastal Areas of Northwestern Colombia and South America. Ph.D. Thesis. Princeton University. Nueva Jersey. Estados Unidos. 132 p.
- Duque-Caro, H., Guzmán Ospitia, G., Hernández, R., 1996. Geología de la plancha 38 Carmen de Bolívar, Escala 1:100.000. Instituto Colombiano de Geología y Minería INGEOMINAS, Bogotá, 96 p, (in Spanish).

- Echeverri, J.S., 2019. Cenozoic tectonic evolution of the Sierra Nevada of Santa Marta, northern Colombia: a record of transcurrent tectonics along the southern Caribbean Plate. PhD Thesis, University of Sao Paulo. 170 p.
- Eide, C.H., Howell, J.A., Buckley, S.J., Martinius, A.W., Oftedal, B.T., Henstra, G.A., 2016. Facies model for a coarse-grained, tide-influenced delta: gule horn formation (early Jurassic), Jameson Land, Greenland. *Sedimentology*, 63(6), 1474-1506.
- Einsele, G., 2000, *Sedimentary Basins. Evolution, Facies, and Sediment Budget. Second, Completely Revised and Enlarged Edition.* Springer. 795 p.
- Ekdale, A.A., Lewis, D.W., 1991. Trace fossils and paleoenvironmental control of ichnofacies in a late Quaternary gravel and loess fan delta complex, New Zealand. *Palaeogeography, Palaeoclimatology, Palaeoecology*, 81, 253-279.
- Ekdale, A.A., Harding, S.C., 2015. *Cylindrichnus concentricus* Toots in Howard, 1966 (trace fossil) in its type locality, Upper Cretaceous, Wyoming. *Annales Societatis Geologorum Poloniae*, 85, 427–432.
- Ekdale, A.A., Bromley, R.G., Pemberton, S.G., 1984. Ichnology: Trace fossils in sedimentology and stratigraphy. *SEPM, Short Course*, 15, 317 p.
- Ekdale, A.A., Bromley, R.G., Knaust, D., 2012. The ichnofabric concept. In: Knaust, D., Bromley, R.G. (Eds.), *Trace Fossils as Indicators of Sedimentary Environments, Developments in Sedimentology*, 64, 139e155.
- Elliott, T., 1996. Deltas. In: Reading, H.G. (Ed.), *Sedimentary Environments and Facies.* Oxford, UK: Blackwell Scientific Publications, 113-154.
- Enge, H.D., Howell, J.A., Buckley, S.J., 2010. The geometry and internal architecture of stream mouth bars in the Panther Tongue and the Ferron Sandstone Members, Utah, U.S.A. *Journal of Sedimentary Research*, 80, 1018-1031.
- Escalona, A., Mann, P., 2011. Tectonics, basin subsidence mechanisms, and paleogeography of the Caribbean-South American plate boundary zone. *Marine and Petroleum Geology*, 28, 8–39.
- Escutia, C., Brinkhuis, H., Klaus, A., The Expedition 318 Scientists., 2011. Wilkes Land Glacial History: Cenozoic East Antarctic Ice Sheet evolution from Wilkes Land margin sediments. *Proceedings of the Integrated Ocean Drilling Program, 318.* Integrated Ocean Drilling Program Management International Inc., Tokyo.
- Escutia, C., Brinkhuis, H., the Expedition 318 Scientists., 2014. From Greenhouse to Icehouse at the Wilkes Land Antarctic margin: IODP Expedition 318 Synthesis of Results. In: Stein, R., Blackman, D.K., Inagaki, F., Larsen, H-C. (Eds.), *Earth and Life Processes Discovered from Subseafloor Environments. A Decade of Science Achieved by the Integrated Ocean Drilling Program (IODP).* *Developments in Marine Geology*, Chapter 3.3, 7, 295-328.
- Esperante, R., Rodríguez-Tovar, F.J., Nalin, R., 2021. Rhizoliths in Lower Pliocene alluvial fan deposits of the Sorbas Basin (Almería, SE Spain). *Palaeogeography, Palaeoclimatology, Palaeoecology*, 567, 110281.
- Everet, K.R., 1983. Histosols. In: Wilding, L.P., Smeck, N.E., Hall, G.F. (Eds), *Pedogenesis and Soil Taxonomy: the Soil Orders.* Elsevier Science Publishers, 1-53.
- Falk, P.D., Dorsey, R.J., 1998. Rapid development of gravelly high-density turbidity currents in marine Gilberttype fan deltas, Loreto Basin, Baja California Sur, Mexico. *Sedimentology*, 45, 331-349.

- Farris, D.W., Jaramillo, C., Bayona, G., Restrepo-Moreno, S.A., Montes, C., Cardona, A., Mora, A., Speakman, R.J., Glascock, M.D., Valencia, V., 2011. Fracturing of the Panamanian Isthmus during initial collision with South America. *Geology*, 39, 1007-1010.
- Farroni, N.D., Cuitiño, J.I., Lazo, D.G., Buono, M.R., 2024. Taphonomic analysis of an articulated baleen whale (Cetacea; Mysticeti) from upper Miocene inner shelf deposits of Península Valdés, Patagonia, Argentina. *Palaios* 39(3),97-112.
- Fedele, J.J., Hoyal, D.C., Barnaal, Z., Tulenko, J., Awalt, S., 2016. Bedforms created by gravity flows. In: Budd, D., Hajek, E., Purkis, S. (Eds.), *Autogenic Dynamics and Self-organization in Sedimentary Systems*. 106. SEPM, Special Publications, 95–121.
- Fidolini, F., Ghinassi, M., 2016. Friction- and Inertia-Dominated Effluents In A Lacustrine, River-Dominated Deltaic Succession (Pliocene Upper Valdarno Basin, Italy). *Journal of Sedimentary Research*, 86(9), 1083-1101.
- Fielding, C.R., 2006. Upper flow regime sheets, lenses and scour fills: Extending the range of architectural elements for fluvial sediment bodies. *Sedimentary Geology*, 190, 227–240.
- Fielding, C.R., 2010. Planform and facies variability in asymmetric deltas: facies and depositional architecture of the Turonian Ferron Sandstone in the Western Henry Mountains, south-central Utah, U.S.A: *Journal of Sedimentary Research*, 80, 455-479.
- Fielding, C.R., Trueman, J.D., Alexander, J., 2005. Sharp-based, flood-dominated mouth bar sands from the Burdekin River Delta of northeastern Australia: extending the spectrum of mouth-bar facies, geometry, and stacking patterns: *Journal of Sedimentary Research*, 75, 55-66.
- Fielding, C.R., Hutsky, A.J., Hurd, T.J, 2014. Deltaic deposits formed under spatially and temporally variable accommodation regimes: a plausible alternative explanation for isolated shallow-marine sandstone bodies. *AAPG Bulletin*, 98, 893-909.
- Fielding, C.R., Alexander, J., Allen, J.P., 2018. The role of discharge variability in the formation and preservation of alluvial sediment bodies: *Sedimentary Geology*, 365, 1-20.
- Fielding, C.R., Allen, J.P., Alexander, J., Gibling, M.R., 2009. Facies model for fluvial systems in the seasonal tropics and subtropics. *Geology*, 37(7), 623-626.
- Fielding, C.R., Ashworth, P.J., Best, J.L., Prokocki, E.W., Sambrook Smith, G.H., 2012. Tributary, distributary and other fluvial patterns: what really represents the norm in the continental rock record? *Sedimentary Geology*, 261-262, 15-32.
- Fildani, A., Normark, W.R., Kostic, S., Parker, G., 2006. Channel formation by flow stripping: large-scale scour features along the Monterey East Channel and their relation to sediment waves. *Sedimentology* 53, 1265–1287.
- Fildani, A., Kostic, S., Covault, J.A., Maier, K.L., Caress, D.W., Paull, C.K., 2021. Exploring a New Breadth of Cyclic Steps on Distal Submarine Fans. *Sedimentology* 68, 1378–1399.
- Fischer, R.V., 1983. Flow transformations in sediment gravity flows. *Geology*, 11, 273-274.
- Flinch, J.F., 2003. Structural evolution of the Sinú-Lower Magdalena area (Northern Colombia). In: Bartolini, C., Buffler, R.T., Blickwede, J. (Eds.), *The Circum-Gulf of Mexico and the Caribbean: Hydrocarbon habitats basin formation, and plate tectonics*. AAPG Memoir, 79, 776–796.
- Fredrickson, A.G., 1964. *Principles and Applications of Rheology*. Prentice-Hall, Englewood Cliffs, N.J., 326 p.

- Frey, R.W., 1990. Trace fossils and hummocky cross-stratification, Upper Cretaceous of Utah. *Palaios*, 5, 203–218.
- Frey, R.W., Howard, J.D., 1981. *Conichnus* and *Schaubcylindrichnus*: redefined trace fossils from the Upper Cretaceous of the Western Interior. *Journal of Paleontology*, 55, 800–804.
- Frey, R.W., Pemberton, G.S., 1985. Biogenic structures in outcrops and cores. Approaches to ichnology. *Bulletin of Canadian Petroleum Geology*, 33(1), 72–115.
- Frey, R.W., Pemberton, S.G., 1987. The *Psilonichnus* ichnocoenose, and its relationship to adjacent marine and nonmarine ichnocoenoses along the Georgia coast. *Bulletin of Canadian Petroleum Geology*, 35, 333–357.
- Frey, R.W., Howard, J.D., Pryor, W.A., 1978. *Ophiomorpha*: its morphologic, taxonomic, and environmental significance. *Palaeogeography, Palaeoclimatology, Palaeoecology*, 23, 199–229.
- Fuentes, S.N., Cuitiño, J.I., Martz, P., Panera, J.P.P., Guler, V., Palazzesi, L., Barreda, V.D., Scasso, R.A. 2019. Palaeoenvironmental reconstruction of the Puerto Madryn Formation (middle to late Miocene), northeast of Patagonia: palynology, nannofossils and stratigraphy. *Ameghiniana* 56, 28–52.
- Fuller, C.W., Willett, S.D., Brandon, M.T., 2006. Formation of forearc basins and their influence on subduction zone earthquakes. *Geology*, 34, 65–68.
- Fürsich, F.T., 1974. On *Diplocraterion* Torell 1870 and the significance of morphological features in vertical, spreiten-bearing, U-shaped trace fossils. *Journal of Paleontology*, 48, 952–962.
- Fürsich, F.T., Bromley, R.G., 1985. Behavioural interpretation of a rosetted spreite trace fossil: *Dactyloidites otto* (Geinitz). *Lethaia*, 18, 199–207.
- Gábris, G., Nagy, B., 2005. Climate and tectonically controlled river style changes on the Sajó-Hernád alluvial fan (Hungary). In: Harvey, A.M., Mather, A.E., Stokes, M. (Eds.), *Alluvial Fans: Geomorphology, Sedimentology, Dynamics*. Geological Society, London, Special Publications 61–67.
- Galeotti, S., DeConto, R., Naish, T., Stocchi, P., Florindo, F., Pagani, M., Barrett, P., Bohaty, S.M., Lanci, L., Pollard, D., Sandroni, S., Talarico, F.M., Zachos, J.C., 2016. Antarctic Ice Sheet variability across the Eocene-Oligocene boundary climate transition. *Science*, 76–80.
- Galloway, W.E., 1975. Process framework for describing the morphologic and stratigraphic evolution of deltaic depositional systems. In: Broussard, M.L., (Ed.), *Deltas, Models for Exploration*. Houston Geological Society, *Memories*, 13, 87–98.
- Gamero, H., Contreras, C., Lewis, N., Welsh, R., Zavala, C., 2011. Evidence of a shelfal hyperpycnal deposition of Pliocene sandstones in the Oilbird field, southeast coast, Trinidad: impact on reservoir distribution. In: Slatt, R.M., Zavala, C. (Eds.), *Sediment transfer from shelf to deep water—revisiting the delivery system*. AAPG Studies in Geology, 61, 193–214.
- Gan, Y., Júnior, F.N. de Almeida., Rossi, V.M., Steel, R.J., Olariu, C., 2022. Sediment transfer from shelf to deepwater slope: How does it happen? *Journal of Sedimentary Research*, 92(6), 570–590.
- Gani, M.R., Bhattacharya, J.P., 2005. Lithostratigraphy versus chronostratigraphy in facies correlations of Quaternary deltas: application of bedding correlation. In: Bhattacharya, J.P., Giosan, L. (Eds.), *River deltas: concepts, models, and examples*, SEPM Special Publication, 83, 31–48.
- Gani, M.R., Bhattacharya, J.P., MacEachern, J.A., 2007. Using Ichnology to Determine the Relative Influence of Waves, Storms, Tides, and Rivers in Deltaic Deposits: Examples from Cretaceous Western Interior Seaway, U.S.A. In: MacEachern, J.A., Bann, K.L., Gingras, M.K., Pemberton, S.G. (Eds.), *Applied Ichnology*. Society for Sedimentary Geology, Short Course Notes, 52, 209–225.

- García-García, F., Fernández, J., Viseras, C., Soria, J.M., 2016. High frequency cyclicity in a vertical alternation of Gilbert-type deltas and carbonate bioconstructions in the late Tortonian, Tabernas Basin, Southern Spain. *Sedimentary Geology*, 192, 123-139.
- García-García, F., Rodríguez-Tovar, F.J., Poyatos-Moré, M., Yeste, L.M., Viseras, C., 2021. Sedimentological and ichnological signatures of an offshore-transitional hyperpycnal system (Upper Miocene, Betic Cordillera, southern Spain). *Palaeogeography, Palaeoclimatology, Palaeoecology*, 561, 110039.
- Ge, Z., Nemeč, W., Vellinga, A.J., Gawthorpe, R.L., 2022. How is a turbidite actually deposited? *Science Advances* 8 (3): eabl9124.
- George, C.F., Macdonald, D.I.M., Spagnolo, M., 2019. Deltaic sedimentary environments in the Niger Delta, Nigeria. *Journal of African Earth Sciences*, 160, 103592.
- Geotec., 2003. Geología de los cinturones Sinú–San Jacinto. Planchas 50, 51, 59, 060, 61, 69, 70, 71, 79, 80. Bogotá. Geotec Ltda–Ingeominas., 135 p. (in Spanish)
- Gerard, J.R.F., Bromley, R.G., 2008. *Ichnofabrics in Clastic Sediments: Applications to Sedimentological Core Studies*. Jean R.F. Gerard, Madrid, 97 pp.
- Ghazi, S., Mountney, N.P., 2009. Facies and architectural element analysis of a meandering fluvial succession: The Permian Warchha Sandstone, Salt Range, Pakistan. *Sedimentary Geology*, 221(1-4), 99-126.
- Ghinassi, M., Colombera, L., Mountney, N.P., Reesink, A.J.H., 2018. Sedimentology of meandering river deposits: advances and challenges. In: Ghinassi, M., Colombera, L., Mountney, N.P., Reesink, A.J.H., Bateman, M. (Eds), *Fluvial Meanders and Their Sedimentary Products in the Rock Record*, 1-14.
- Giannetti, A., Baeza–Carratalá, J.F., Soria–Mingorance, J.M., Dulai, A., Tent–Manclús, J.E., Peral–Lozano, J., 2018. New paleobiogeographical and paleoenvironmental insight through the Tortonian brachiopod and ichnofauna assemblages from the Mediterranean–Atlantic seaway (Guadix Basin, SE Spain). *Facies*, 64 (3), 24 p.
- Gingras, M., MacEachern, J.A., 2012. Tidal Ichnology of Shallow–Water Clastic Settings. In: Davis Jr, R.C., Dalrymple, R.W. (Eds.), *Principles of Tidal Sedimentology*, 4, 57–77.
- Gingras, M.K., Zonneveld, J-P., 2015. Tubular tidalites: a biogenic sedimentary structure indicative of tidally influenced sedimentation. *Journal of Sedimentary Research*, 85, 845-854.
- Gingras, M.K., MacEachern, J.A., Pemberton, S.G., 1998. A comparative analysis of the ichnology of wave- and river-dominated allomembers of the Upper Cretaceous Dunvegan Formation. *Bulletin of Canadian Petroleum Geology*, 46, 1-26.
- Gingras, M.K., MacEachern, J.A., Dashtgard, S.E., 2011. Process ichnology and the elucidation of physico–chemical stress. *Sedimentary Geology*, 237, 115–134.
- Gingras, M.K., MacEachern, J.A., Dashtgard, S.E., 2012a. The potential of trace fossils as tidal indicators in bays and estuaries. *Sedimentary Geology* 279, 97-106.
- Gingras, M.K., Pemberton, S.G., Saunders, T., Clifton, H.E., 1999. The ichnology of brackish water Pleistocene deposits at Willapa Bay, Washington: variability in estuarine settings. *Palaios*, 14, 352–374.
- Gingras, M.K., Räsänen, M., Pemberton, S.G., Romero, L., 2002. Ichnology and sedimentology reveal depositional characteristics of bay-margin parasequences in the Miocene Amazonian Foreland Basin. *Journal of Sedimentary Research*, 72(6), 871–883.
- Gingras, M.K., Pemberton, S.G., Dashtgard, S.E., Dafoe, L., 2008. How fast do invertebrates burrow? *Palaeogeography, Palaeoclimatology, Palaeoecology*, 270, 280-286.

- Gingras, M.K., MacEachern, J.A., Dashtgard, S.E., Zonneveld, J-P., Schoengut, J., Ranger, M.J., Pemberton, S.G., 2012b. Estuaries. Chapter 16. In: Knaust, D., Bromley, R.G. (Eds.), Trace Fossils as Indicators of Sedimentary Environments. *Developments in Sedimentology* 64, 463-505.
- Gingras, M.K., Dashtgard, S.E., La Croix, A., Bann, K., MacEachern, J.A., 2019. The Neoichnological Basis for a Brackish-Water Ichnofacies. AAPG Annual Convention and Exhibition, San Antonio, Texas.
- Giraldo-Villegas, C.A., Rodríguez-Tovar, F.J., Celis, S.A., Pardo-Trujillo, A., Duque-Castaño, M.L., 2023. Paleoenvironmental conditions over the Caribbean Large Igneous Province during the Late Cretaceous in NW of South American Margin: A sedimentological and ichnological approach. *Cretaceous Research*, 142, 105407.
- Giraldo-Villegas, C.A., Rodríguez-Tovar, F.J., Celis, S.A., Pardo-Trujillo, A., 2024. Variable Ophiomorpha ichnofabric: Improving the understanding of mouth bar environments in fan-delta complex depositional settings from the Upper Cretaceous of NW South America. *Cretaceous Research*, 154, 105730.
- Gladstone, C., McClelland, H.L., Woodcock, N.H., Pritchard, D., Hunt, J.E., 2018. The formation of convolute lamination in mud-rich turbidites. *Sedimentology* 65, 1800–1825.
- Goldring, R., Pollard, J.E., 1995. A re-evaluation of *Ophiomorpha* burrows in the Wealden Group (Lower Cretaceous) of southern England. *Cretaceous Research*, 16, 665–680.
- Goldring, R., Pollard, J.E., Taylor, A.M., 1991. *Anconichnus horizontalis*: a pervasive ichnofabric-forming trace fossil in post-Paleozoic offshore siliciclastic facies. *Palaios*, 6, 250–263.
- Gómez, J., Montes, N.E., 2020. Mapa Geológico de Colombia en Relieve 2020. Escala 1:1000000. Servicio Geológico Colombiano.
- Gómez, E., Jordan, T.E., Allmendinger, R.W., Hegarty, K., Kelley, S., Heizler, M., 2003. Controls on Architecture of the Late Cretaceous to Cenozoic Southern Middle Magdalena Valley Basin, Colombia. *GSA Bulletin*, 115(2), 131–147.
- Gómez, J., Nivia, A., Montes, N., Jiménez, D., Tejada, M., Sepúlveda, J., Osorio, J., Gaona, T., Diederix, H., Uribe, H., Mora, M., 2007. Mapa geológico de Colombia. Escala 1:2'800.000. Reporte técnico, INGEOMINAS, 2 Edición.
- Gómez, J., Montes, N.E., Nivia, Á., Diederix, H., 2015. Mapa Geológico de Colombia 2015. Escala 1:1 000 000. Bogotá. Ingeominas.
- Gong, C., Chen, L., West, L., 2017. Asymmetrical, inversely graded, upstream-migrating cyclic steps in marine settings: Late Miocene-early Pliocene Fish Creek-Vallecito Basin, southern California. *Sedimentary Geology* 360, 35–46.
- González, R., Oncken, O., Faccenna, C., Le Breton, E., Bezada, M., Mora, A., 2023. Kinematics and convergent tectonics of the Northwestern South American plate during the Cenozoic. *Geochemistry, Geophysics, Geosystems*, 24(7), e2022GC010827.
- Goodbred Jr, S.L., Kuehl, S.A., Steckler, M.S., Sarker, M.H., 2003. Controls on facies distribution and stratigraphic preservation in the Ganges–Brahmaputra delta sequence. *Sedimentary Geology*, 155(3-4), 301-316.
- Gouw, M.J.P., Berendsen, H.J.A., 2007. Variability of channel belt dimensions and the consequences for alluvial architecture: observations from the Holocene Rhine-Meuse delta (The Netherlands) and Lower Mississippi Valley (USA). *Journal of Sedimentary Research*, 77, 124-138.

- Govers, R., Wortel, M.J.R., 2005. Lithosphere tearing at STEP faults: Response to edges of subduction zones. *Earth and Planetary Science Letters*, 236(1–2), 505–523.
- Gradstein, F., Ogg, J.G., Schmitz, M.D., Ogg, G.M., 2020. *Geologic Time Scale 2020*, 2, Elsevier, Amsterdam.
- Grundvåg, S-A., Helland-Hansen, W., Johannssen, E.P., Eggenhuisen, J., Pohl, F., Spychala, Y., 2023. Deep-water sand transfer by hyperpycnal flows, the Eocene of Spitsbergen, Arctic Norway. *Sedimentology*, 70(7), 2057-2107.
- Gugliotta, M., Saito, Y., 2019. Matching trends in channel width, sinuosity, and depth along the fluvial to marine transition zone of tide-dominated river deltas: The need for a revision of depositional and hydraulic models. *Earth-Science Reviews*, 191, 93-113.
- Gugliotta, M., Kurcinka, C.E., Dalrymple, R.W., Flint, S.S., Hodgson, D.M., 2016. Decoupling seasonal fluctuations in fluvial discharge from the tidal signature in ancient deltaic deposits: an example from the Neuquén Basin, Argentina. *Journal of the Geological Society*, 173, 94-107.
- Gulliford, A.R., Flint, S.S., Hodgson, D.M., 2014, Testing Applicability of Models Of Distributive Fluvial Systems Or Trunk Rivers In Ephemeral Systems: Reconstructing 3-D Fluvial Architecture In the Beaufort Group, South Africa: *Journal of Sedimentary Research*, v. 84(12), p. 1147-1169.
- Guzmán, G., 2007. Stratigraphy and Sedimentary Environment and Implications in the Plato Basin and the San Jacinto Belt Northwestern Colombia. University of Liège, Belgium, PhD thesis, 185 pp.
- Guzmán, G., Gómez, E., Serrano, B.E., 2004. Geología de los cinturones del Sinú, San Jacinto y borde occidental del Valle Inferior del Magdalena. *Caribe Colombiano*. Escala 1:300.000, 24, 134 p, (in Spanish).
- Hage, S., Cartigny, M.J.B., Clare, M.A., Sumner, E.J., Vendettuoli, D., Hughes Clarke, J.E., Hubbard, S.M., Talling, P.J., Lintern, D.G., Stacey, C.D., Englert, R.G., Vardy, M.E., Hunt, J.E., Yokokawa, M., Parsons, D.R., Hizzett, J.L., Azpiroz-Zabala, M., Vellinga, A.J., 2018. How to recognize crescentic bedforms formed by supercritical turbidity currents in the geologic record: Insights from active submarine channels. *Geology* 46 (6), 563–566.
- Haller, M.J., 1979. Estratigrafía de la región al poniente de Puerto Madryn, provincia del Chubut, República Argentina. *Actas 7º Congreso Geológico Argentino* 1, 285-297 (Buenos Aires). [In Spanish].
- Hampson, G.J., Storms, J.E.A., 2003. Geomorphological and sequence stratigraphic variability in wave-dominated, shoreface-shelf parasequences. *Sedimentology* 50(4), 667-701.
- Hampson, G.J., Steel, R., Burgess, P., Dalrymple, R., 2008. Recent advances in models of siliciclastic shallow – marine stratigraphy: Introduction and perspectives. In: Hampson, G.J., Steel, R.J., Burgess, P.M., Dalrymple, R.W. (Eds.), *Recent Advances in Models of Siliciclastic Shallow-Marine Stratigraphy*, SEPM Special Publication, 90, 03-14.
- Hampson, G.J., 2016. Towards a sequence stratigraphic solution set for autogenic processes and allogenic controls: Upper Cretaceous strata, Book Cliffs, Utah, USA. *Journal of the Geological Society (London)*, 173, 817-836.
- Hand, B.M., 1974. Supercritical flow in density currents. *Journal of Sedimentary Petrology* 44, 637–648.
- Hand, B.M., 1997. Inverse grading resulting from coarse-sediment transport lag. *Journal of Sedimentary Research*, 67, 124–129.
- Hansen, C.D., MacEachern, J.A., 2007. Application of the asymmetric delta model to along-strike facies variations in a mixed wave- and river-influenced delta lobe, Upper Cretaceous Basal Belly River

- Formation, central Alberta. In: MacEachern, J.A., Pemberton, S.G., Gingras, M.K., Bann, K.L. (Eds.), *Applied Ichnology*. Society for Sedimentary Geology, Tulsa, USA, 256–272.
- Hansen, L.A.S., Callow, R.H.T., Kane, I., Gamberi, F., Rovere, M., Cronin, B.T., Kneller, C., 2015. Genesis and character of thin-bedded turbidites associated with submarine channels. *Marine and Petroleum Geology* 67, 852–879.
- Hansen, L.A.S., Healy, R.S., Gomis-Cartesio, L., Lee, D.R., Hodgson, D.M., Pontén, A., Wild, R.J., 2021. The Origin and 3D Architecture of a Km-Scale Deep-Water Scour-Fill: Example from the Skoorsteenberg Fm, Karoo Basin, South Africa. *Frontiers Earth Sciences* 9, 737932.
- Harbitz, C.B., Glimsdal, S., Bazin, S., Zamora, N., Lovholt, F., Bungum, H., Smebye, H., Gauer, P., Kjekstad, O., 2012. Tsunami hazard in the Caribbean: Regional exposure derived from credible worst case scenarios. *Continental Shelf Research*, 38, 1-23.
- Hardenbol, J., Thierry, J., Farley, M.B., Jacquin, T., De Graciansky, P.-C., Vail, P.R., 1998. Jurassic sequence chronostratigraphy SEPM Spec. Publ. 60, chart.
- Hasiotis, S.T., 2010. Continental trace fossils. *SEPM Short Course Notes* 51, 1–132.
- Heard, T.G., Pickering, K.T., 2008. Trace fossils as diagnostic indicators of deep-marine environments, middle Eocene Ainsa-Jaca basin, Spanish Pyrenees. *Sedimentology* 55, 809–844.
- Hein, F.J., Walker, R.G., 1977. Bar evolution and development of stratification in the gravelly, braided, Kicking Horse River, British Columbia. *Canadian Journal of Earth Sciences*, 14(4), 562-570.
- Heldreich, G., Redfern, J., Legler, B., Gerdes, K., Williams, B.P.J., 2017. Challenges in characterizing subsurface paralic reservoir geometries: a detailed case study of the Mungaroo Formation, North West Shelf, Australia. In: Hampson, G.J., Reynolds, A.D., Kostic, B., Wells, M.R. (Eds.), *Sedimentology of Paralic Reservoirs: Recent Advances*, Geological Society, London, Special Publications, 444.
- Heller, P.L., Burns, B.A., Marzo, M., 1993. Stratigraphic solution sets for determining the roles of sediment supply, subsidence, and sea level on transgressions and regressions. *Geology*, 21(8), 747-750.
- Hertweck, G., Wehrmann, A., Liebezeit, G., 2007. Bioturbation structures of polychaetes in modern shallow marine environments and their analogues to *Chondrites* group traces. *Palaeogeography, Palaeoclimatology, Palaeoecology* 245, 382-389.
- Hessler, A.M., Sharman, G.R., 2018. Subduction zones and their hydrocarbon systems. *Geosphere*, 14(5), 2044-2067.
- Hincapié-Gómez, S., Cardona, A., Jiménez, G., Monsalve, G., Ramírez, L., Bayona, G., 2018. Paleomagnetic and gravimetrical reconnaissance of Cretaceous volcanic rocks from the Western Colombian Andes: paleogeographic connections with the Caribbean Plate. *Studia Geophysica & Geodaetica*, 62, 485-511.
- Hodgson, D.M., Peakall J., Maier, K.L., 2022. Submarine channel mouth settings: Processes, geomorphology, and deposits. *Frontiers in Earth Science* 10:790320.
- Hofstra, M., Hodgson, D.M., Peakall, J., Flint, S.S., 2015. Giant scour-fills in ancient channel-lobe transition zones: Formative processes and depositional architecture. *Sedimentary Geology* 329, 98–114.
- Hofstra, M., Peakall, J., Hodgson, D., Stevenson, C.J., 2018. Architecture and morphodynamics of subcritical sediment waves in an ancient channel-lobe transition zone. *Sedimentology* 65, 2339–2367.
- Hoorn, M.C. 1994. An environmental reconstruction of the palaeo-Amazon River system (Middle to Late Miocene, NW Amazonia). *Palaeogeography, Palaeoclimatology, Palaeoecology*, 112, 187-238.

- Hoorn, C., Wesselingh, P., ter Steege, H., Bermudez, M.A., Mora, A., Sevink, J., Sanmartín, I., Sanchez-Meseguer, A., Anderson, C.L., Figueiredo, J.P., Jaramillo, C., Riff, D., Negri, F.R., Hooghiemstra, H., Lundberg, J., Stadler, T., Sarkinen, T., Antonelli, A., 2010. Amazonia Through Time: Andean Uplift, Climate Change, Landscape Evolution, and Biodiversity. *Science*, 330, 927-931.
- Hornung, J.J., Aspiron, U., Winsemann, J., 2007. Jet-efflux deposits of a subaqueous ice-contact fan, glacial Lake Rinteln, northwestern Germany. *Sedimentary Geology*, 193, 167-192.
- Howell, J.A., Flint, S.S., 1996. A model for high resolution sequence stratigraphy within extensional basins, in: Howell, J.A., Aitkin, J.F. (Eds.), *High Resolution Sequence Stratigraphy: Innovations and Applications*, Special Publications Geological Society of London, 104, 129-137.
- Howell, J.A., Martinius, A.W., Good, T.R., 2014. The application of outcrop analogues in geological modelling: a review, present status and future outlook. In: Martinius, A.W., Howell, J.A., Godd, T.R. (Eds.), *Sediment-Body Geometry and Heterogeneity: Analogue Studies for Modelling the Subsurface*, Geological Society, London, Special Publications, 387, 1-25.
- Howell, J.A., Skorstad, A., MacDonald, A., Fordham, A., Flint, S., Fjellvoll, B., Manzocchi, T., 2008. Sedimentological parameterization of shallow-marine reservoirs. *Petroleum Geoscience*, 14, 17–34.
- Hubbard, S.M., Romans, B.W., Graham, S.A., 2008. Deep-water foreland basin deposits of the Cerro Toro Formation, Magallanes basin, Chile: architectural elements of a sinuous basin axial channel belt. *Sedimentology*, 55 (5), 1333-1359.
- Hubbard, S.M., de Ruig, M.J., Graham, S.A., 2009. Confined channel-levee complex development in an elongate depo-center: deep-water Tertiary strata of the Austrian Molasse basin. *Marine and Petroleum Geology*, 26(1), 85-112.
- Hubbard, S.M., MacEachern, J.A., Bann, K.L., 2012. Slopes (Chapter 20). In: Knaust, D., Bromley, R.G. (Eds.), *Trace Fossils as Indicators of Sedimentary Environments*, *Developments in Sedimentology*, vol. 64. Elsevier, Amsterdam, 607–642.
- Hughes Clarke, J.E., 2016. First wide-angle view of channelized turbidity currents links migrating cyclic steps to flow characteristics. *Nature Communications*, 1–13.
- Hughes Clarke, J.E., Shor, A.N., Piper, D.J.W., Mayer, L.A., 1990. Large-scale current-induced erosion and deposition in the path of the 1929 Grand Banks turbidity current. *Sedimentology*, 37, 613–629.
- Husinec, A., Read, J.F., 2011. Microbial laminite versus rooted and burrowed caps on peritidal cycles: Salinity control on parasequence development, Early Cretaceous isolated carbonate platform, Croatia. *GSA Bulletin*, 123, 1896–1907.
- Hutchinson, D.K., Coxall, H.K., Lunt, D.J., Steinthorsdottir, M., de Boer, A.M., Baatsen, M., von der Heydt, A., Huber, M., Kennedy-Asser, A.T., Kunzmann, L., Ladant, J.-B., Lear, C.H., Moraweck, K., Pearson, P.N., Piga, E., Pound, M.J., Salzmann, U., Scher, H.D., Sijp, W.P., Śliwińska, K.K., Wilson, P.A., Zhang, Z., 2021. The Eocene–Oligocene transition: a review of marine and terrestrial proxy data, models and model–data comparisons. *Climate of the Past*, 17, 269–315.
- Ibañez-Mejía, M., Cordani, U.G., 2020. Zircon U–Pb geochronology and Hf–Nd–O isotope geochemistry of the Paleo- to Mesoproterozoic basement in the westernmost Guiana Shield. In: Gómez, J., Mateus–Zabala, D. (Eds.), *The Geology of Colombia, Volume 1 Proterozoic–Paleozoic*. Servicio Geológico Colombiano, Publicaciones Geológicas Especiales 35, 65–90. Bogotá.
- Ichaso, A.A., Dalrymple, R.W. 2009. Tide-and wave generated fluid mud deposits in the Tilje Formation (Jurassic), offshore Norway. *Geology*, 37, 539-542.

- Ichaso, A., Buatois, L.A., Mangano, M.G., Thomas, P., Marion, D., 2022. Assessing the expansion of the Cambrian Agronomic Revolution into fan-delta environments. *Scientific Reports*, 12, 14431.
- Idárraga-García, J., Masson, D.G., García, J., León, H., Vargas, C.A., 2019. Architecture and development of the Magdalena Submarine Fan (southwestern Caribbean). *Marine Geology*, 414, 18-33.
- Ilgar, A., Nemeč, W., Tuncay, E., Alçiçek, M.C., Hakyemez, A., Bozkurt, A., Çiner, A., Ergen, A., 2024. The coeval development of conglomeratic, shoal–water and Gilbert-type deltas in the post-orogenic extensional Çardak Basin, SW Türkiye: implications for accommodation and sediment supply. *Mediterranean Geoscience Reviews*, 20 p.
- Inman, D.L., Nordstrom, C., 1971. On the tectonic and morphologic classification of coasts. *Journal of Geology*, 79, 1-21.
- Irastorza, A., Zavala, C., Campetella, D.M., Turienzo, M., Sánchez, N., Durán, T., Peñalva, G., 2024. Origin and evolution of shallowing-upward clastic successions: A case example from the Lower Cretaceous Agrio Formation, Neuquén Basin, Argentina. *Journal of South American Earth Sciences*, 137, 104855.
- Isla, M.F., Schwarz, E., Veiga, G.D., 2020. Record of a nonbarred clastic shoreline. *Geology*, 48(4), 338-342.
- Isla, M.F., Moyano-Paz, D., FitzGerald, D.M., Simontacchi, L., Veiga, G.D., 2023. Contrasting beach-ridge systems in different types of coastal settings. *Earth Surf. Process. Landforms*, 1-25.
- Ito, M., Ishikawa, K., Nishida, N., 2014. Distinctive erosional and depositional structures formed at a canyon mouth: A lower Pleistocene deep-water succession in the Kazusa forearc basin on the Boso Peninsula, Japan. *Sedimentology* 61, 2042–2062.
- Jaramillo, C.A., Rueda, M., Torres, V., 2011. A palynological zonation for the Cenozoic of the Llanos and Llanos Foothills of Colombia. *Palynology*, 35, 46–84.
- Jaramillo, C., Ochoa, D., Contreras, L., Pagani, M., Carvajal-Ortiz, H., Pratt, L.M., Krishnan, S., Cardona, A., Romero, M., Quiroz, L., Rodriguez, G., Rueda, M., De la Parra, F., Moron, S., Green, W., Bayona, G., Montes, C., Quintero, O., Ramirez, R., Mora, A., Schouten, S., Bermudez, H., Navarrete, R.E., Parra, F., Alvaran, M., Osorno, J., Crowley, J.L., Valencia, V., Vervoort, J., 2010. Effects of Rapid Global Warming at the Paleocene-Eocene Boundary on Neotropical Vegetation. *Science*, 330, 957-961.
- Jenson, M.A., Pedersen, G.K., 2010. Architecture of vertically stacked fluvial deposits, Atane formation, Cretaceous, Nuussuaq, central West Greenland. *Sedimentology*, 57, 1280-1314.
- Johnson, D.W., 1919. *Shore processes and shoreline development*. Wiley, New York, 584 pp.
- Johnson, A.L.A., Liquorish, M.N., Sha, J., 2007. Variation in growth-rate and form of a Bathonian (middle Jurassic) oyster in England, and its environmental implications. *Palaeontology*, 50(5), 1155-1173.
- Johnson, S.M., Dashtgard, S.E., 2014. Inclined heterolithic stratification in a mixed tidal–fluvial channel: Differentiating tidal versus fluvial controls on sedimentation. *Sedimentary Geology*, 301, 41–53.
- Jones, B.G., Woodroffe, C.D., Martin, G.R., 2003. Deltas in the Gulf of Carpentaria, Australia: Forms, Processes, and Products. In: Sidi, F.H., Nummedal, D., Imbert, P., Darman, H., Posamentier, H.W. (Eds.), *Tropical Deltas of Southeast Asia—Sedimentology, Stratigraphy, and Petroleum Geology*, SEPM (Society for Sedimentary Geology), 76, 21-44.
- Kane, I.A., Hodgson, D.M., 2011. Sedimentological criteria to differentiate submarine channel levee sub environments: Exhumed examples from the Rosario Fm. (Upper Cretaceous) of Baja California, Mexico, and the Fort Brown Fm. (Permian), Karoo Basin, S. Africa. *Marine and Petroleum Geology*, 28, 807–823.

- Kane, I.A., Dykstra, M.L., Kneller, B.C., Tremblay, S., McCaffrey, W.D., 2009. Architecture of a coarse-grained channel-levee system: the Rosario Formation, Baja California, Mexico. *Sedimentology*, 56, 2207–2234.
- Katz, M., Miller, E.K.G., Wright, J.D., Wade, B.S., Browning, J.V., Cramer, B.S., Rosenthal, Y., 2008. Stepwise transition from the Eocene greenhouse to the Oligocene icehouse. *Nature Geoscience*, 1, 329–334.
- Kenyon, N.H., Amir, A., Cramp, A., 1995. Geometry of the younger sediment bodies of the Indus Fan. In: Pickering, K.T., Hiscott, R.N., Kenyon, N.H., Lucchi, R.R., Smith, R.D.A. (Eds.), *Atlas of Deep-Water Environments: Architectural Style in Turbidite Systems*. Chapman and Hall, London, 89–93.
- Kerr, A., Tarney, J., Marriner, G.F., Nivia, A., Klaver, G.T., Saunders, A.D., 1996. The geochemistry and tectonic setting of late Cretaceous Caribbean and Colombian volcanism. *Journal of South American Earth Sciences*, 9(1-2), 111–120.
- Kidwell, S.M., Bosence, D.W.J., 1991. Taphonomy and time-averaging of marine shelly faunas. In: Allison, P.A., Briggs, D.E.G. (Eds.), *Taphonomy, releasing the data locked in the fossil record*. Plenum Press, New York 560, 115–209.
- Kidwell, S.M., Fursich, F.T., Aigner, T., 1986. Conceptual framework of the analysis and classification of fossil concentrations. *Palaios* 228–238.
- Kim, J-Y K., Heo, W-H., 1997. Shell beds and trace fossils of the Seogwipo Formation (Early Pleistocene), Jeju Island, Korea. *Ichnos* 5, 89–99.
- Kim, W., Paola, C., Swenson, J.B., Voller, V.R., 2006. Shoreline response to autogenic processes of sediment storage and release in the fluvial system. *Journal of Geophysical Research*, 111, F4.
- Kleinspehn, K.L., Steel, R.J., Johannessen, E., Netland, A., 1984. Conglomeratic fan-delta sequences, late Carboniferous – early Permian, western Spitsbergen. In: Koster, E.H., Steel, R.J. (Eds.), *Sedimentology of Gravels and Conglomerates*, Canadian Society of Petroleum Geologists, 10, 279–294.
- Knaust, D., 2009. Ichnology as a tool in carbonate reservoir characterization: a case study from the Permian—Triassic Khuff Formation in the Middle East. *GeoArabia*, 14, 17–38.
- Knaust, D., 2013. The ichnogenus *Rhizocorallium*: classification, trace makers, palaeoenvironments and evolution. *Earth-Science Review* 126, 1–47.
- Knaust, D., 2015. *Siphonichnidae* (new ichnofamily) attributed to the burrowing activity of bivalves: ichnotaxonomy, behaviour and palaeoenvironmental implications. *Earth Science Review*, 150, 497–519.
- Knaust, D., 2017, *Atlas of Trace Fossils in Well Core: Appearance, Taxonomy and Interpretation*. Springer, Cham, Switzerland, 206 p.
- Knaust, D., 2018. The ichnogenus *Teichichnus* Seilacher, 1955. *Earth Science Reviews*, 177, 386–403.
- Knaust, D., Bromley, R., 2012. Trace Fossils as Indicators of Sedimentary Environments. *Developments in Sedimentology*, 64. 924pp.
- Kneller, B.C., Branney, M.J., 1995. Sustained high density turbidity currents and the deposition of thick massive sands. *Sedimentology* 42, 607– 616.
- Kneller, B., Buckee, C., 2000. The structure and fluid mechanics of turbidity currents: a review of some recent studies and their geological implications. *Sedimentology*, 47(1), 62–94.
- Kneller, B.C., McCaffrey, W.D., 2003. The interpretation of vertical sequences in turbidite beds: the influence of longitudinal flow structure. *Journal of Sedimentary Research* 73, 706–713.

- Komar, P.D., 1985. The hydraulic interpretation of turbidites from their grain sizes and sedimentary structures. *Sedimentology* 32 (3), 395–407.
- Kostaschuk, R.A., 1985. River mouth processes in a fjord-head delta, British Columbia, Canada. *Marine Geology*, 69, 1-23.
- Kostaschuk, R.A., McCann, S.B., 1983. Observations on delta-forming processes in a fjord-head delta, British Columbia, Canada. *Sedimentary Geology*, 36, 269-288.
- Kroehler, M.E., Mann, P., Escalona, A., Christeson, G.L., 2011. Late Cretaceous-Miocene diachronous onset of back thrusting along the South Caribbean deformed belt and its importance for understanding processes of arc collision and crustal growth. *Tectonics*, 30(6), 1-31.
- Kurcinka, C., Dalrymple, R.W., Gugliotta, M., 2018. Facies and architecture of river dominated to tide-influenced mouth bars in the lower Lajas Formation (Jurassic), Argentina. *AAPG Bulletin*, 102, 885-912.
- Lamb, M.P., Mohrig, D., 2009. Do hyperpycnal-flow deposits record river-flood dynamics? *Geology, GSA*, 37(12), 1067-1070.
- Lang, J., Winsemann, J., 2013. Lateral and vertical facies relationships of bedforms deposited by aggrading supercritical flows: From cyclic steps to humpback dunes. *Sedimentary Geology* 296, 36–54.
- Lang, J., Brandes, C., Winsemann, J., 2017. Erosion and deposition by supercritical density flows during channel avulsion and backfilling: Field examples from coarse-grained deepwater channel-levée complexes (Sandino Forearc Basin, southern Central America). *Sedimentary Geology* 349, 79–102.
- Lang, J., Fedele, J.J., Hoyal, D.C., 2021. Three-dimensional submerged wall jets and their transition to density flows: morphodynamics and implications for the depositional record. *Sedimentology* 68 (4), 1297–1327.
- Lanier, W.P., Tessier, B., 1998. Climbing-ripple bedding in the fluvio-estuarine transition: a common feature associated with tidal dynamics (modern and ancient analogues). *SEPM Special Publications* 61, 109-117.
- Lara, M., Salazar-Franco, A.M., Silva-Tamayo, J.C. 2018. Provenance of the Cenozoic siliciclastic intramontane Amagá Formation: Implications for the early Miocene collision between Central and South America. *Sedimentary Geology*, 373, 147– 162.
- Larsen, E., Nemec, W., Ellingsen, T-R., 2024b. The frontal facies and sedimentation processes of a shoal-water fan delta in the Köprü Basin of southern Türkiye. *Mediterranean Geoscience Reviews*, 35 p.
- Larsen, E., Nemec, W., Alçiçek, M.C., Helland, O.M., 2024a. The Göktaş fan delta complex in Manavgat Basin, South Türkiye: a model for stratigraphic development of coarse-clastic littoral wedges and spatial-facies prediction. *Mediterranean Geoscience Reviews*, 33 p.
- Larsen, E., Puigdefábregas, C., Nemec, W., Dreyer, T., Ellingsen, T-R., 2024c. The Altinkaya fan-delta complex in Köprü Basin (south Türkiye): relative sea-level changes and basin margin dynamics. *Mediterranean Geoscience Reviews*, 24 p.
- Łaska, W., Rodríguez-Tovar, F.J., Uchman, A., 2017. Evaluating macrobenthic response to the Cretaceous-Palaeogene event: A high-resolution ichnological approach at the Agost section (SE Spain). *Cretaceous Research* 70, 96-110.
- Lavigne, F., Suwa, H., 2004. Contrasts between debris flows, hyperconcentrated flows and stream flows at a channel of Mount Semeru, East Java, Indonesia. *Geomorphology*, 61, 41-58.
- Lazo, D.G., Palma, R.M., Piethé, R.D., 2008. La traza *Dactyloidites ottoi* Geinitz en la Formación La Manga, Oxfordiano de Mendoza. *Ameghiniana* (Nota Paleontológica) 45 (2), 000–000.

- Leal-Mejía, H., Shaw, R.P., Melgarejo i Draper, J.C., 2019. Spatial-Temporal Migration of Granitoid Magmatism and the Phanerozoic Tectono-Magmatic Evolution of the Colombian Andes. In: Cediél, F., Shaw, R.P. (Eds.), *Geology and Tectonics of Northwestern South America: Frontiers in Earth Sciences*. Springer, Cham.
- Lecce, S.A., 1997. Spatial patterns of historical overbank sedimentation and floodplain evolution, Blue River Wisconsin: *Geomorphology*, v. 18, p. 265-277.
- León, S., Cardona, A., Parra, M., Robel, E.R., Jaramillo, J.S., Glodny, J., Valencia, V.A., Chew, D., Montes, C., Posada, G., Monsalve, G., Pardo-Trujillo, A., 2018. Transition From Collisional to Subduction-Related Regimes: An Example from Neogene Panama-Nazca-South America Interactions. *Tectonics*, 37(1), 119–139.
- Leszczyński, S., Uchman, A., 1993. Biogenic structures of organic-poor siliciclastic sediments: examples from Paleogene variegated shales, Polish Carpathians. *Ichnos* 2, 267-275.
- Li, W., Bhattacharya, J.P., Zhu, Y., Garza, D., Blankenship, E., 2011. Evaluating delta asymmetry using three-dimensional facies architecture and ichnological analysis, Ferron ‘Notom Delta’, Capital Reef, Utah, USA. *Sedimentology*, 58(2), 478-507.
- Liebrand, D., Lourens, L.J., Hodell, D.A., de Boer, B., van de Wal, R.S.W., Pälike, H., 2011. Antarctic ice sheet and oceanographic response to eccentricity forcing during the early Miocene. *Climates of the Past*, 7, 869-880.
- Longhitano, S., Mellere, D., Steel, R.J., Ainsworth, R.B., 2012. Tidal depositional systems in the rock record: a review and new insights. *Sedimentary Geology*, 279, 2-22.
- Longhitano, S., Chiarella, D., Gugliotta, M., Ventra, D., 2021. Coarse-grained deltas approaching shallow-water canyon heads: A case study from the Lower Pleistocene Messina Strait, Southern Italy. *Sedimentology*, 68(6), 2523-2562.
- López-Quirós, A., 2020. Cenozoic paleoenvironmental and paleoceanographic reconstructions in the Drake-Scotia gateway. PhD Thesis. University of Granada, 220 p.
- López-Quirós, A., Escutia, C., Etourneau, J., Rodríguez-Tovar, F.J., Roignant, S., Lobo, F.J., Thompson, N., Bijl, P.K., Bohoyo, F., Salzmann, U., Evangelinos, D., Salabarnada, A., Hoem, F.S., Sicre, M-A., 2021. Eocene-Oligocene paleoenvironmental changes in the South Orkney Microcontinent (Antarctica) linked to the opening of Powell Basin. *Global and Planetary Change*, 204, 103581.
- López-Ramos, E., Rincón-Martínez, D., Moreno, N., Gómez, P-D., 2021. Mass balance of Neogene sediments in the Colombia Basin relationship with the evolution of the Magdalena and Cauca River Basins: CT&F – Ciencias, Tecnología y Futuro, 11, 65-95.
- Lovecchio, J.P., 2018. Seismic Stratigraphy of the Offshore Basins of Argentina: Characterization and Modeling of the South Atlantic Passive Margin Dynamics. PhD Thesis, University of Buenos Aires, p. 322.
- Lowe, D.R., 1976. Grain flow and grain flow deposits. *Journal of Sedimentary Petrology* 46, 188– 199.
- Lowe, D.R., 1979. Sediment gravity flows: their classification and some problems of application to natural flows and deposits. In: Doyle, L.J., Pilkey, O.H. (Eds), *Geology of Continental Slopes*, 27. Claremore, OK: SEPM Special Publications, 75–82.
- Lowe, D.R., 1982. Sediment gravity flows: II. Depositional models with special reference to the deposits of high-density turbidity currents. *Journal of Sedimentary Petrology*, 52, 279-297.

- Lowe, D.R., 1988. Suspended-load fallout rate as an independent variable in the analysis of current structures. *Sedimentology*, 35, 765-776.
- MacEachern, J.A., Pemberton, S.G., 1992. Ichnological aspects of Cretaceous shoreface successions and shoreface variability in the Western Interior Seaway of North America. In: Pemberton, S.G. (Ed.), *Applications of Ichnology to Petroleum Exploration: A Core Workshop*. Society for Sedimentary Geology Core Workshop 17, 57-84.
- MacEachern, J.A., Gingras, M.K., 2007. Recognition of brackish-water trace-fossil suites in the Cretaceous Western Interior Seaway of Alberta, Canada. In: Bromley, R.G., Buatois, L.A., Mángano, M.G. (Eds.), *Sediment-organism interactions: a multifaceted ichnology*, SEPM Special Publication, 88, 149-193.
- MacEachern, J.A., Bann, K.L., 2008. The role of ichnology in refining shallow marine facies models. In: Hampson, G.J., Steel, R.J., Burgess, P.M., Dalrymple, R.W. (Eds.), *Recent Advances in Models of Siliciclastic Shallow-Marine Stratigraphy*. SEPM Special Publication No 90, 73-116.
- MacEachern, J.A., Bann, K.L., 2020. The *Phycosiphon* Ichnofacies and the *Rosselia* Ichnofacies: Two new Seilacherian Ichnofacies for marine deltaic environments. *Journal of Sedimentary Research*, 90, 855-886.
- MacEachern, J.A., Bann, K.L., 2022. Departures from the archetypal deltaic ichnofacies. Geological Society, London, Special Publications, 522 p.
- MacEachern, J.A., Bechtel, D.J., Pemberton, S.G., 1992. Ichnology and sedimentology of transgressive deposits, transgressively related deposits and transgressive systems tracts in the Viking Formation of Alberta. In: Pemberton, S.G. (Ed.), *Applications of Ichnology to Petroleum Exploration: A Core Workshop*. Society of Economic Paleontologists and Mineralogists, Core Workshop, 17, 251-290.
- MacEachern, J.A., Zaitlin, B.A., Pemberton, S.G., 1998. High-resolution sequence stratigraphy of early transgressive deposits, Viking Formation, Joffre Field, Alberta, Canada. *American Association of Petroleum Geologists Bulletin*, 82, 729-756.
- MacEachern, J.A., Stelck, C.R., Pemberton, S.G., 1999. Marine and marginal marine mudstone deposition: Paleoenvironmental interpretations based on the integration of ichnology, palynology and foraminiferal paleoecology. In: Bergman, K.M., Snedden, J.W. (Eds.), *Isolated Shallow Marine Sand Bodies: Sequence Stratigraphic and Sedimentologic Interpretation*. SEPM, Special Publication 64, 205-225.
- MacEachern, J.A., Zaitlin, B.A., Pemberton, S.G., 1999. A sharp based sandstone of the Viking Formation, Joffre Field, Alberta, Canada: criteria for recognition of transgressively incised shoreface complexes. *Journal of Sedimentary Research* 69, 876-892.
- MacEachern, J.A., Bann, K., Bhattacharya, J.P., Howell, C.D., 2005. Ichnology of deltas: organism responses to the dynamic interplay of rivers, waves, storms and tides. In: Bhattacharya, B.P., Giosan, L. (Eds.), *River Deltas: Concepts, Models and Examples*, SEPM Special Publication, 83, 45-85.
- MacEachern, J.A., Bann, K.L., Pemberton, S.G., Gingras, M.K., 2007a. The ichnofacies paradigm: high-resolution paleoenvironmental interpretation of the rock record. In: MacEachern, J.A., Bann, K.L., Gingras, M.K., Pemberton, S.G. (Eds.), *Applied Ichnology*. Society for Sedimentary Geology, Short Course Notes, 52, 27-64.
- MacEachern, J.A., Pemberton, S.G., Gingras, M.K., Bann, K.L., Dafoe, L.T., 2007b. Use of trace fossils in genetic stratigraphy. In: Miller, W.III. (Ed.), *Trace Fossils: Concepts, Problems, Prospects*. Elsevier, 110-134.
- MacEachern, J.A., Pemberton, S.G., Gingras, M.K., Bann, K.L., 2010. Ichnology and facies models. In: Dalrymple, R.G., James, N.P. (Eds.), *Facies Models 4*, vol. 3, Geological Association of Canada. *Geotext*, 19-58.

- MacEachern, J.A., Bann, K.L., Gingras, M.K., Zonneveld, J-P., Dashtgard, S.E., Pemberton, S.G., 2012. The Ichnofacies Paradigm. Chapter 4. In: Knaust, D., Bromley, R.G. (Eds.), Trace Fossils as Indicators of Sedimentary Environments. *Developments in Sedimentology*, 64, 103-138.
- Mackay, D.A., Dalrymple, R.W., 2011. Dynamic Mud Deposition In A Tidal Environment: The Record of Fluid-Mud Deposition In the Cretaceous Bluesky Formation, Alberta, Canada. *Journal of Sedimentary Research*, 81(11-12), 901-920.
- Maestrelli, D., Maselli, V., Kneller, B., Chiarella, D., Scarselli, N., Vannuchi, P., Jovane, L., Iacopini, D., 2020. Characterisation of submarine depression trails driven by upslope migrating cyclic steps: Insights from the Ceará Basin (Brazil). *Marine and Petroleum Geology* 115, 104291.
- Maguire, E.P., Feldmann, R.M., Casadio, S., Schweitzer, C.E., 2016. Distal volcanic ash deposition as a cause for mass kills of marine invertebrates during the Miocene in Northern Patagonia, Argentina. *Palaios* 31(12), 577-591.
- Maier, K. L., Johnson, S. Y., Hart, P., 2018. Controls on submarine canyon head evolution, migration, and fill in Monterey Bay, offshore central California. *Marine Geology*, 404, 24–40.
- Maier, K.L., Fildani, A., Paull, C.K., Grahan, S.A., McHargue, T.R., Caress, D.W., McGann, M., 2011. The elusive character of discontinuous deep-water channels: New insights from Lucia Chica channel system, offshore California. *Geology*, 39(4), 327–330.
- Maier, K.L., Paull, C.K., Caress, D.W., Anderson, K., Nieminski, N.M., Lundsten, E., Erwin, B.E., Gwiazda, R., Fildani, A., 2020. Submarine-fan development revealed by integrated high-resolution datasets from La Jolla Fan, offshore California, USA. *Journal of Sedimentary Research*, 90, 468–479.
- Makaske, B., 2001. Anastomosing rivers: a review of their classification, origin and sedimentary products. *Earth-Science Reviews*, 53 (3-4), 149-196.
- Malpas, J.A., Gawthorpe, R.L., Pollard, J.E., Sharp, I.R., 2005. Ichnofabric analysis of the shallow marine Nukhul Formation (Miocene), Suez Rift, Egypt: implications for depositional processes and sequence stratigraphic evolution. *Palaeogeography, Palaeoclimatology, Palaeoecology* 215, 239-264.
- Manco–Garcés, A., Marín–Cerón, M.I., Sánchez–Plazas, C.J., Escobar–Arenas, L.C., Beltrán–Triviño, A., von Quadt, A., 2020. Provenance of the Ciénaga de Oro Formation: unveiling the tectonic evolution of the Colombian Caribbean margin during the Oligocene - Early Miocene. *Boletín de Geología*, 42(3), 205-226. (in Spanish).
- Mángano, M.G., Waisfeld, B.G., Buatois, L.A., Vaccari, N.E., Muñoz, D.F., 2023. Evolutionary and ecologic controls on benthos distribution from an upper Cambrian incised estuarine valley: Implications for the early colonization of marginal-marine settings. *Palaeogeography, Palaeoclimatology, Palaeoecology* 626, 111692.
- Mann, P., 2021. Gulf of Mexico, Central America, and the Caribbean. In: Aldaberto, D., Elias, S.A. (Eds.), *Encyclopedia of Geology (Second Edition)*, 47–67.
- Mantilla-Pimiento, A., Jentzsch, G., Kley, J., Alfonso-Pava, C., 2009. Configuration of the Colombian Caribbean Margin: Constraints from 2D Seismic Reflection data and Potential Fields Interpretation. In: Lallemand, S., Funicello, F. (Eds.), *Subduction Zone Geodynamics: Frontier in Earth Sciences*, 247-272.
- Marengo, H., 2015. Neogene Micropaleontology and Stratigraphy of Argentina. The Chaco-Paranense Basin and the Península de Valdés. *Springer Briefs in Earth System Sciences* p. 218.
- Marín, J.P., Bermúdez, H.D., Aguilera, R., Jaramillo, J.M., Rodríguez, J.V., Ruiz, E.C., Cerón, M.R., 2010. Evaluación geológica y prospectividad sector Sinú – Urabá. *Boletín de Geología*, 32(1), 145–153.

- Marín-Cerón, M.I., Leal-Mejía, H., Bernet, M., Mesa-García, J., 2019. Late Cenozoic to Modern-Day Volcanism in the Northern Andes: A Geochronological, Petrographical, and Geochemical Review. In: Cediel, F., Shaw, R.P. (Eds.), *Geology and Tectonics of Northwestern South America. The Pacific-Caribbean-Andean Junction*. *Frontiers in Earth Sciences*, 603–648.
- Martin, K.D., 2004. A re-evaluation of the relationship between trace fossils and dysoxia. In: McIlroy, D. (Ed.), *The Application of Ichnology to Palaeoenvironmental and Stratigraphic Analysis*, Geological Society, London, Special Publications 228, 141-156.
- Martínez, C., Jaramillo, C., Martínez-Murcia, J., Crepet, W., Cárdenas, A., Escobar, J., Moreno, F., Pardo-Trujillo, A., Caballero-Rodríguez, D., 2021. Paleoclimatic and paleoecological reconstruction of a middle to late Eocene South American tropical dry forest. *Global and Planetary Change* 205, 103617.
- Martini, E., 1971. Standard Tertiary and Quaternary calcareous nannoplankton zonation. In: Farinacci, A. (Ed.), *Proceedings 2nd International Conference Planktonic Microfossils Roma: Rome* (Ed. Tecnosci.), 2, 739–785.
- Martini, I., Sandrelli, F., 2014. Facies analysis of a Pliocene river-dominated deltaic succession (Siena Basin, Italy): Implications for the formation and infilling of terminal distributary channels. *Sedimentology*, 62(1), 234-265.
- Martinius, A.W., Gowland, S., 2011. Tide-influenced fluvial bedforms and tidal bore deposits (Late Jurassic Lourinhã Formation, Lusitanian Basin, Western Portugal). *Sedimentology*, 58, 285–324.
- Maselli, V., Normandeau, A., Nones, M., Tesi, T., Langone, L., Trincardi, F., Bohacs, K.M., 2020. Tidal modulation of river–flood deposits: How low can you go?. *Geology*, 48, 663–667.
- Matenco, L.C., Haq, B.U. 2020. Multi-scale depositional successions in tectonic settings. *Earth-Science Reviews*, 200, 102991.
- Matthews, K., Maloney, K., Zahirovic, S., William, S., Seton, M., Muller, D., 2016, Global plate boundary evolution and kinematics since the late Paleozoic: *Global and Planetary Change*, v. 146, p. 226-250.
- Mayall, M., Jones, Ed., Casey, M., 2006. Turbidite channel reservoirs—Key elements in facies prediction and effective development. *Marine and Petroleum Geology*, 23(8), 821-841.
- McArthur, A., Kane, I., Bozetti, G., Hansen, L., Kneller, B.C., 2020. Supercritical flows overspilling from bypass-dominated submarine channels and the development of overbank bedforms. *The Depositional Record*, 6, 21-40.
- McIlroy, D. 2004. Ichnofabrics and sedimentary facies of a tide-dominated delta: Jurassic Ile Formation of Kristin Field, Haltenbanken, Offshore Mid-Norway. In: McIlroy, D. (Ed.), Geological Society, London, Special Publications 1 (228), 237-272.
- McIlroy, D. 2008. Ichnological analysis: the common ground between ichnofacies workers and ichnofabric analysts. *Palaeogeography, Palaeoclimatology, Palaeoecology*, 270, 332-338.
- Mejía-Molina, A., Flores, J.A., Torres Torres, V., Sierro, F.J., 2010. Distribution of calcareous nannofossils in Upper Eocene-Upper Miocene deposits from Northern Colombia and the Caribbean Sea. *Revista Española de Micropaleontología*, 42(3), 279–300.
- Melchor, R.N., Genise, J.F., Buatois, L.A., Umazano, A.M., 2012. Fluvial environments. In: Knaust, D., Bromley, R.G. (Eds), *Trace fossils as indicators of sedimentary environments*. *Developments in Sedimentology*, 64, 329-378.

- Melstrom, E.M., Birgenheier, L.P., 2021. Stratigraphic architecture of climate influenced hyperpycnal mouth bars. *Sedimentology*, 68, 1580-1605.
- Mendoza-Rodríguez, G.A., Buatois, L.A., Rincón-Martínez, D.A., Mángano, M.G., Gómez, P.D., 2018. Ichnology and sedimentology of a tropical delta and associated shallow-marine environments, Oligocene Ciénaga de Oro Formation, San Jacinto Fold Belt Basin, Colombia: Trace-fossil distribution and depositional dynamics, Simposio Latinoamericano de Icnología – SLIC.
- Mendoza-Rodríguez, G., Buatois, L.A., Rincón-Martínez, D.A., Mángano, M.G., Baumgartner-Mora, C., 2019. The armored burrow *Nummipera eocenica* from the upper Eocene San Jacinto Formation, Colombia: morphology and paleoenvironmental implications. *Ichnos*, 27(2), 81-91.
- Miall, A.D., 1977, A review of the braided river depositional environment: *Earth Sciences Review*, v. 13, p. 1-62.
- Miall, A.D., 1978, Lithofacies types and vertical profile models in braided river deposits: a summary: *Fluvial Sedimentology*, v. 5, p. 597-600.
- Miall, A.D., 1988. Reservoir heterogeneities in fluvial sandstones: lessons from outcrop studies. *AAPG Bulletin*, 72, 682–697.
- Miall, A.D., 1996. *The Geology of Fluvial Deposits. Sedimentary Facies, Basin Analysis, and Petroleum Geology*, Springer Berlin, Heidelberg, 582 p.
- Miall, A.D., 2014. *Fluvial Depositional Systems*. Springer Geology, 322 p.
- Middleton, G.V., Hampton, M.A., 1973. *Sediment Gravity Flows: Mechanics of Flow and Deposition*. Society of Economic Paleontologists and Mineralogists, Pacific Section, Los Angeles, CA, 1-37.
- Miguez–Salas, O., Rodríguez–Tovar, F.J., 2019. Stable deep–sea macrobenthic trace maker associations in disturbed environments from the Eocene Lefkara Formation, Cyprus. *Geobios*, 52, 37–45.
- Miguez–Salas, O., Rodríguez–Tovar, F.J., De Weger, W., 2020. *Macaronichnus* and contourite depositional settings: Bottom currents and nutrients as coupling factors. *Palaeogeography, Palaeoclimatology, Palaeoecology*, 545, 109639.
- Miller, K.G., Wright, J.D., Katz, M.E., Wade, B.S., Browning, J.V., Cramer, B.S., Rosenthal, Y., 2009. Climate threshold at the Eocene-Oligocene transition: Antarctic ice sheet influence on ocean circulation. In: Koeberl, C., Montanari, A. (Eds.), *The late Eocene Earth-Hothouse, Icehouse, and Impacts*. Geological Society of America Special Paper, 452, 169-178.
- Miller, K.G., Browning, J.V., Schmelz, W.J., Kopp, R.E., Mountain, G.S., Wright, J.D., 2020. Cenozoic sea-level and cryospheric evolution from deep-sea geochemical and continental margin records. *Science Advances*, 6, eaaz1346.
- Molinares, C.E., Martinez, J.I., Fiorini, F., Escobar, J., Jaramillo, C., 2012. Paleoenvironmental reconstruction for the Lower Pliocene Arroyo Piedras section (Tubará – Colombia): Implications for the Magdalena River – paleodelta’s Dynamic. *Journal of South American Earth Sciences*, 39, 170–183.
- Monaco, P., Caracuel, J.E., Giannetti, A., Soria, J.M., Yébenes, A., 2007. *Thalassinoides* and *Ophiomorpha* as cross-facies trace fossils of crustaceans from shallow-to-deep-water environments: Mesozoic and Tertiary examples from Italy and Spain. 3rd Symposium on Mesozoic and Cenozoic Decapod Crustaceans - Museo di Storia Naturale di Milano, May 23-25, 2007. *Memorie della Società Italiana di Scienze Naturali e del Museo Civico di Storia Naturale di Milano Volume XXXV - Fascicolo II*.

- Monaco, P., Caracuel, J.E., Giannetti, A., Soria, J.M., Yébenes, A., 2009. *Thalassinoides* and *Ophiomorpha* as cross-facies trace fossils of crustaceans from shallow-to-deep-water environments: Mesozoic and Tertiary examples from Italy and Spain. In: Garassino, A., Feldmann, R.M., Teruzzi, G., (Eds.), 3rd Symposium on Mesozoic and Cenozoic Decapod Crustaceans—Museo di Storia Naturale di Milano, May 23–25, 2007. *Memorie della Società Italiana di Scienze Naturali e del Museo Civico di Storia Naturale di Milano*, 35, 79–82.
- Montes, C., Guzman, G., Bayona G., Cardona, A., Valencia, V., Jaramillo, C., 2010. Clockwise rotation of the Santa Marta massif and simultaneous Paleogene to Neogene deformation of the Plato-San Jorge and Cesar-Rancheria basins. *Journal of South American Earth Sciences*, 29(4), 832–848.
- Montes, C., Cardona, A., Mcfadden, R., Morón, S.E., Silva, C.A., Restrepo-Moreno, S., Ramírez, D.A., Hoyo, N., Wilson, J., Farris, D., Bayona, G.A., Jaramillo, C.A., Valencia, V., Bryan, J., Flores, J.A., 2012. Evidence for middle Eocene and younger land emergence in central Panama: Implications for Isthmus closure. *Geological Society of America Bulletin*, 124(5-6), 780-799.
- Montes, C., Rodríguez-Corcho, A.F., Bayona, G., Hoyos, N., Zapata, S., Cardona, A., 2019. Continental margin response to multiple arc-continent collisions: The northern Andes-Caribbean margin. *Earth Science Reviews*, 198, 102903.
- Mora, J.A., Oncken, O., Le Breton, E., Ibáñez-Mejía, M., Faccena, C., Veloza, G., Vélez, V., de Freitas, M., Mesa, A., 2017. Linking Late Cretaceous to Eocene tectonostratigraphy of the San Jacinto fold belt of NW Colombia with Caribbean plateau collision and flat subduction. *Tectonics*, 36, 2599-2629.
- Mora, J.A., Oncken, O., Le Breton, E., Mora, A., Veloza, G., Vélez, V., de Freitas, M., 2018. Controls on forearc basin formation and evolution: Insights from Oligocene to Recent tectonostratigraphy of the Lower Magdalena Valley basin of northwest Colombia: *Marine and Petroleum Geology*, 97, 288-310.
- Mora-Bohórquez, J.A., Oncken, O., Le Breton, E., Ibáñez-Mejía, M., Veloza, G., Mora, A., Vélez, V., de Freitas, M., 2020. Formation and Evolution of the Lower Magdalena Valley Basin and San Jacinto Fold Belt of Northwestern Colombia: Insights from Upper Cretaceous to Recent Tectono-Stratigraphy. In: Gómez, J., Mateus-Zabala, D. (Eds.), *The Geology of Colombia, Volume 3 Paleogene – Neogene*. Servicio Geológico Colombiano, *Publicaciones Geológicas Especiales*, 37, 21-66.
- Mora-Páez, H., Kellogg, J.N., Freymueller, J., Mencin, D., Fernandes, R.M.S., Diederix, H., LaFemina, P., Cardona-Piedrahita, L., Lizarazo, S., Peláez-Gaviria, J-R., Díaz-Mila, F., Bohórquez-Orozco, O., Giraldo-Londoño, L., Corchuelo-Cuervo, Y., 2019. Crustal deformation in the northern Andes – A new GPS velocity field. *Journal of South American Earth Sciences*, 89, 76–91.
- Morales, J.A., 2022. *Coastal Geology*, Springer Textbooks in Earth Sciences, Geography and Environment. Switzerland. 463 p.
- Morang, A., 2004. *Coastal geology*. University Press of the Pacific, US Army Corps of Engineers, 297 p.
- Moreno-Sánchez, M., Pardo-Trujillo, A., 2002. Western Colombia geological history. *Geo-Eco-Trop* 26, 91-113.
- Moreno-Sánchez, M., Pardo-Trujillo, A., 2003. Stratigraphical and sedimentological constraints on Western Colombia: implications on the evolution of the Caribbean Plate. In: Bartolini, C., Buffler, R., Blickwede, J. (Eds.), *The Circum-Gulf of Mexico and the Caribbean: Hydrocarbon Habitats, Basin Formation and Plate Tectonics*. AAPG Memoir, 79, 891-924.
- Moslow, T.F., Pemberton, S.G., 1988. An integrated approach to the sedimentological analysis of some Lower Cretaceous shoreface and delta front sandstone sequences. In: James, D.P., Leckie, D.A. (Eds.),

Sequences, Stratigraphy, and Sedimentology: Surface and Subsurface, Canadian Society of Petroleum Geologists, Memoir 15, 373-386.

- Mount, J., 1985, Mixed siliciclastic and carbonate sediments: a proposed first-order textural and compositional classification: *Sedimentology*, v. 32, p. 435-442.
- Moyano-Paz, D., Richiano, S., Varela, A.N., Gómez Decál, A.R., Poiré, D.G., 2020. Ichnological signatures from wave- and fluvial-dominated deltas: The La Anita Formation, Upper Cretaceous, Austral-Magallanes Basin, Patagonia. *Marine and Petroleum Geology*, 114, 104168.
- Moyano-Paz, D., Isla, M.F., MacEachern, J.A., Richiano, S., Gómez-Dacal, A.R., Varela, A.N., Poiré, D.G., 2022. Evolution of an aggradational wave-dominated delta: Sediment balance and animal-substrate dynamics (Upper cretaceous La Anita Formation, Southern Patagonia). *Sedimentary Geology*, 106193.
- Mudelsee, M., Bickert, T., Lear, C.H., Lohmann, G., 2014. Cenozoic climate changes: a review based on time series analysis of marine benthic $\delta^{18}\text{O}$ records. *Reviews of Geophysics*, 52(3), 333-374.
- Mukti, M.M., Ito, M., 2010. Discovery of outcrop-scale fine-grained sediment waves in the lower Halang Formation, an upper Miocene submarine-fan succession in West Java. *Sedimentary Geology* 231, 55–62.
- Mulder, T., Alexander, J., 2001. The physical character of subaqueous sedimentary density flows and their deposits. *Sedimentology*, 49, 269-299.
- Mulder, T., Syvitski, J.P.M., 1995. Turbidity currents generated at river mouths during exceptional discharges to the world oceans. *The Journal of Geology*, 103, 285–298.
- Mulder, T., Syvitski, J.P.M., Migeon, S., Faugeres, J.C., Savoye, B., 2003. Marine hyperpycnal flows: initiation, behavior and related deposits: A review. *Marine and Petroleum Geology*, 20, 861–82.
- Muto, T., Steel, R.J., 1997. Principles of regression and transgression; the nature of the interplay between accommodation and sediment supply. *Journal of Sedimentary Research*, 67(6), 994-1000.
- Muto, T., Steel, R.J., Swenson, J.B., 2007. Autostratigraphy: a framework norm for genetic stratigraphy. *Journal of Sedimentary Research*, 77, 2-12.
- Mutti, E., 1992. Turbidite sandstones. San Donato, Milanese, Università di Parma, Agip, 275 p.
- Mutti, E., Normark, W.R., 1987. Comparing examples of modern and ancient turbidite systems: problems and concepts, in Leggett, J.K., Zuffa, G.G., eds., *Marine Clastic Sedimentology*: Springer, The Netherlands, 1–38.
- Mutti, E., Davoli, G., Tinterri, R., Zavala, C., 1996. The importance of ancient fluvio-deltaic systems dominated by catastrophic flooding in tectonically active basins. *Memorie di Scienze Geologiche*, 48, 233-291.
- Mutti, E., Tinterri, R., Benevelli, G., di Biase, D., Cavanna, G., 2003. Deltaic, mixed and turbidite sedimentation of ancient foreland basins. *Marine and Petroleum Geology*, 20(6-8), 733-755.
- Myers, K.J., Bristow, C.S., 1989. Detailed sedimentology and gamma-ray log characteristics of a Namurian deltaic succession II: gamma-ray logging. In: Whateley, M.K.G., Pickering, K.T. (Eds), *Deltas Sites and Traps for Fossil Fuels Geological Society Special Publication*, 41, 81-88.
- Nagy, J., 1992. Environmental significance of foraminiferal morphogroups in Jurassic North sea deltas. *Palaeogeography, Palaeoclimatology, Palaeoecology*, 95, 111-134.
- Nara, M., 2006. Reappraisal of *Schaubcylindrichnus*: A probable dwelling/feeding structure of a solitary funnel feeder. *Palaeogeography, Palaeoclimatology, Palaeoecology* 240(3-4), 439-452.

- Nara, M., Seike, K., 2004. *Macaronichnus segregatis*-like traces found in the modern foreshore sediments of the Kujukurihama Coast, Japan. *Journal of the Geological Society of Japan*, 110, 545–551.
- Nara, M., Seike, K., 2019. Palaeoecology of *Macaronichnus segregatis degiberti*: Reconstructing the infaunal lives of the travisiid polychaetes. *Palaeogeography, Palaeoclimatology, Palaeoecology*, 516(15), 284-294.
- Naranjo-Vesga, J., Paniagua-Arroyave, J.F., Ortiz-Karpf, A., Jobe, Z., Wood, L., Galindo, P., Shumaker, L., Mateus-Tarazona, D., 2022. Controls on submarine canyon morphology along a convergent tectonic margin. *The Southern Caribbean of Colombia: Marine and Petroleum Geology*, 137, 105493.
- Naruse, H., Nifuku, K., 2008. Three-dimensional morphology of the ichnofossil *Phycosiphon incertum* and its implication for paleoslope inclination. *Palaios*, 23, 270–279.
- Navarro, L., Arnott, R.W.B., 2020. Stratigraphic record in the transition from basin floor to continental slope sedimentation in the ancient passive-margin Windermere turbidite system. *Sedimentology*, 67, 1710-1749.
- Nemec, W., 1990. Aspects of sediment movement on steep delta slopes. In: Colella, A., Prior, D.B. (Eds.), *Coarse-grained deltas*. *Spec. Publ. Int. Assoc. Sed.* 10, 29-73.
- Nemec, W., 1993. The concept and definition of a fan delta: review and discussion. In: *Extended abstract, 3rd International Workshop of fan deltas, Pohang (South Korea)*, 1-11.
- Nemec, W., 2009. What is a hyperconcentrated flow? Lecture abstract. IAS meeting, Alguero (Sardinia).
- Nemec, W., Muszyński, A., 1982. Volcaniclastic alluvial aprons in the Tertiary of Sofia district (Bulgaria). *Ann. Geol. Soc. Pol.* 52, 239-303.
- Nemec, W., Steel, R.J., 1984. Alluvial and coastal conglomerates: their significant features and some comments on gravelly mass-flow deposits. In: Koster, R.H., Steel, R.J. (Eds.), *Sedimentology of Gravels and Conglomerates (Canadian Society of Petroleum Geologists, Mem, 10)*, 1-31.
- Nemec, W., Steel, R.J., 1988. *Fan Deltas – Sedimentology and Tectonic Settings*. Blackie, London, 464 p.
- Nemec, W., Postma, G., 1993. Quaternary alluvial fans in southwestern Crete: sedimentation processes and geomorphic evolution. In: Marzo, M., Puigdefabregas, C. (Eds.), *Alluvial Sedimentation*. *International Association of Sedimentologists. Special Publications*, 17, 235–276.
- Nemec, W., Özaksoy, V., 2024. Sedimentation in the Late Miocene–Early Pliocene Alanya Bay, southwestern Türkiye. *Mediterranean Geoscience Reviews*, 29 p.
- Netto, R.G., Rossetti, D. de F., 2003. Ichnology and salinity fluctuations: a case study from the early Miocene (Lower Barreiras Formation) of São Luís Basin, Maranhão, Brazil. *Revista Brasileira de Paleontologia*, 6, 5–18.
- Netto, R.G., Tognoli, F.M.W., Assine, M.L., Nara, M., 2014. Crowded *Rosselia* ichnofabric in the Early Devonian of Brazil: An example of strategic behaviour. *Palaeogeography, Palaeoclimatology, Palaeoecology*, 395(1), 107-113.
- Nichols, G., 2009. *Sedimentology and Stratigraphy*. Blackwell Publishing, A John Wiley and Sons, Ltd., Publication, 432 p.
- Nio, S.D., Yang, C.S., 1991. Diagnostic attributes of clastic tidal deposits: a review. In: Smith, D., Reinson, G.G.E., Zaitlin, B.A. Rahmani, R.A. (Eds.), *Clastic Tidal Sedimentology*. *Canadian Society of Petroleum Geologists, Memoir* 16, 3-27.
- Nivia, A. 2001. Mapa Geológico Departamento del Valle del Cauca Escala 1:250.000 (Memoria Explicativa). *Ingeominas*, 1-148. (in Spanish)

- Noda, A., 2016. Forearc basins: Types, geometries, and relationships to subduction zone dynamics. *Geological Society of America Bulletin*, 128 (5-6), 879–895.
- Normark, W.R., Paull, C.K., Caress, D.W., Ussler III, W., Sliter, R., 2009. Fine-scale relief related to Late Holocene channel shifting within the floor of the upper Redondo Fan, offshore Southern California. *Sedimentology* 56, 1690–1704.
- Nummedal, D., Sidi, F.H., Possamentier, H.W., 2003. A framework for deltas in southeast Asia. In: Sidi, F.H., Nummedal, D., Imbert, P., Darman, H., Posamentier, H.W. (Eds.), *Tropical Deltas of Southeast Asia—Sedimentology, Stratigraphy, and Petroleum Geology*. SEPM (Society for Sedimentary Geology), 76, 5–17.
- Nyberg, B., Helland-Hansen, W., Gawthorpe, R.L., Sandbakken, P., Haug Eide, C., Sømme, T., Hadler-Jacobsen, F., Leiknes, S., 2018. Revisiting morphological relationships of modern source-to-sink segments as a first-order approach to scale ancient sedimentary systems. *Sedimentary Geology*, 373, 111-113.
- O'Brien, P.E., Cooper, A.K., Richter, C., et al., 2001. *Proceedings of the Ocean Drilling Program, Initial Reports*, 188.
- Olariu, C., Bhattacharya, J.P., 2006. Terminal distributary channels and delta front architecture of river-dominated delta systems. *Journal of Sedimentary Research*, 76 (2), 212-233.
- Olariu, C., Steel, R.J., Petter, A.L., 2010. Delta-front hyperpycnal bed geometry and implications for reservoir modeling: Cretaceous Panther Tongue delta, Book Cliffs, Utah. *AAPG Bulletin*, 94(6), 819-845.
- Olariu, C., Steel, R.J., Olariu, M.I., Choi, K.S., 2015. Facies and architecture of unusual fluvial-tidal channels with inclined heterolithic strata. In: Ashworth, P.J., Best, J.L., Parsons, D.R. (Eds.), *Fluvial-Tidal Sedimentology. Developments in Sedimentology*, 353-394.
- Olariu, M.I., Olariu, C., Steel, R.J., Dalrymple, R.W., Martinius, A.W., 2012. Anatomy of a laterally migrating tidal bar in front of a delta system: Esdolomada Member, Roda Formation, Tremp-Graus Basin, Spain: *Sedimentology*, 59, 356-378.
- Olsen, T.R., Mellere, D., Olsen, T., 2002. Facies architecture and geometry of landward-stepping shoreface tongues: the Upper Cretaceous Cliff House Sandstone (Mancos Canyon, south-west Colorado). *Sedimentology* 46(4), 603-625.
- Ono, K., Plink-Bjorklund, P., 2018. Froude supercritical flow bedforms in deepwater slope channels? Field examples in conglomerates, sandstones and fine-grained deposits. *Sedimentology* 65, 639–669.
- Ono, K., Plink-Bjorklund, P., Eggenhuisen, J.T., Cartigny, M.J.B., 2021. Froude supercritical flow processes and sedimentary structures: New insights from experiments with a wide range of grain sizes. *Sedimentology*, 68 (4), 1328–1357.
- Orton, G.J., 1988. A spectrum of Middle Ordovician fan deltas and braidplain deltas, North Wales: a consequence of varying fluvial clastic input. In: Nemec, W., Steel, R.J. (Eds.), *Fan Deltas*, Blackie & Son Ltd, London., 23-49.
- Orton, G.J., Reading, H.G., 1993. Variability of deltaic processes in terms of sediment supply, with particular emphasis on grain size. *Sedimentology*, 40, 475–512.
- Osorio-Granada, E., Pardo-Trujillo, A., Restrepo-Moreno, S.A., Gallego, F., Muñoz, J., Plata, A., Trejos-Tamayo, R., Vallejo, F., Barbosa-Espitia, A., Cardona-Sánchez, F.J., Foster, D.A., Kamenov, G., 2020. Provenance of Eocene-Oligocene sediments in the San Jacinto Fold Belt: Paleogeographic and geodynamic implications for the northern Andes and the southern Caribbean. *Geosphere*, 16(1), 210-228.

- Osorio-Tabares, L.C., Ochoa, D., Trejos-Tamayo, R., Pardo-Trujillo, A., 2023. Astrobiochronological calibration of an early Oligocene succession from the Colombian Caribe: Tectonostratigraphic implications. *Journal of South American Earth Sciences*, 126, 104328.
- Osorno, J., Rangel, A., 2015. Geochemical Assessment and Petroleum Systems in the Sinú-San Jacinto Basin, Northwestern Colombia. *Marine and Petroleum Geology*, 65, 217–231.
- Ospina-Muñoz, A., Marquez, I., Vallejo-Hincapié, F., Salazar-Ríos, A., Trejos-Tamayo, R., Celis, S.A., Plata, A., Pardo-Trujillo, A., 2023. Calcareous microfossil biostratigraphy of Upper Miocene to Pliocene deposits of the Sinú-San Jacinto Belt, Caribbean region of Colombia. *Journal of South American Earth Sciences* 129, 104468.
- Palanques, A., Kenyon, N.H., Alonso, B., Limonov, A., 1995. Erosional and depositional patterns in the Valencia Channel mouth: an example of a modern channel-lobe transition zone. *Marine Geophysical Researches* 17, 503–517.
- Palazzesi, L., Barreda, V.D., Cuitiño, J.I., Guler, M.V., Tellería, M.C., Ventura Santos, R., 2014. Fossil pollen records indicate that Patagonian desertification was not solely a consequence of Andean uplift. *Nature Communications*, 5, 3558.
- Palazzesi, L., Barreda, V.D., Scasso, R.A., 2006. Early Miocene Spore and Pollen Record of the Gaiman Formation (Northeastern Patagonia, Argentina): Correlations and Paleoenvironmental Implications. IV Congreso Latinoamericano de Sedimentología. XI Reunión Argentina de Sedimentología, San Carlos de Bariloche, Argentina, p. 161.
- Pardo-Trujillo, A., Jaramillo, C., 2014. Palinología y paleoambientes de los depósitos paleógenos del sector central de la Cordillera Oriental Colombiana: 35 millones de años de historia de la vegetación neotropical. In: Rangel, J.O., (Ed), *Colombia Diversidad Biótica XIV: La región de la Orinoquía de Colombia*. Edition 1. Palinología y paleoambientes. Universidad Nacional.
- Pardo-Trujillo, A., Cardona, A., Giraldo, S.A., León, S., Vallejo, D.F., Trejos-Tamayo, R., Plata, A., Ceballos, J., Echeverri, S., Barbosa-Espitia, A., Slattery, J., Salazar-Ríos, A., Botello, G.E., Celis, S.A., Osorio-Granada, E., Giraldo-Villegas, C.A., 2020. Sedimentary record of the Cretaceous–Paleocene arc–continent collision in the northwestern Colombian Andes: insights from stratigraphic and provenance constraints. *Sedimentary Geology*, 401, 105627.
- Pardo-Trujillo, A., Plata-Torres, A., Ramírez, E., Vallejo-Hincapié, F., Trejos-Tamayo, R., 2023. Eocene to Miocene Palynology of the Amagá Basin (Cauca Valley, Colombia) compared to the Caribbean Region: *Revista de la Academia Colombiana de Ciencias Exactas, Físicas y Naturales*, 47(185), 925-942.
- Parker, G., García, M., Fukushima, Y., Yu, W., 1987. Experiments on turbidity currents over an erodible bed. *Journal of Hydraulic Research* 25 (1), 123–147.
- Parras, A.M., Cuitiño, J.I. 2018. The stratigraphic and paleoenvironmental significance of the regressive Monte Observación Member, early Miocene of the Austral-Magallanes Basin, Patagonia. *Latin American Journal of Sedimentology and Basin Analysis* 25, 93-115.
- Parras, A.M., Cuitiño, J.I., 2021. Revised chrono and lithostratigraphy for the Oligocene-Miocene Patagoniense marine deposits in Patagonia: Implications for stratigraphic cycles, paleogeography, and major drivers. *Journal of South American Earth Sciences* 110, 103327.
- Patrino, S., Hampson, G.J., Jackson, C.A.L., Whipp, P.S., 2015. Quantitative progradation dynamics and stratigraphic architecture of ancient shallow-marine clinoform sets: a new method and its application to the Upper Jurassic Sognefjord Formation, Troll Field, offshore Norway. *Basin Research*, 27, 412-452.

- Paull, C., Caress, D., Lundsten, E., Gwiazda, R., Anderson, K., McGann, M., Conrad, J., Edwards, B., Sumner, E., 2013. Anatomy of the La Jolla submarine Canyon system; offshore southern California. *Marine Geology* 335, 16–34.
- Peakall, J., Best, J., Baas, J.H., Hodgson, D.M., Clares, M.A., Talling, P.J., Dorrell, R.M., Lee, D.R., 2020. An integrated process-based model of flutes and tool marks in deep-water environments: Implications for palaeohydraulics, the Bouma sequence and hybrid event beds. *Sedimentology* 67, 1601–1666.
- Pearson, D.L., 1984. Pollen/spore colour 'standard', Version #2. Phillips Petroleum Company Exploration Projects Section, privately distributed. Bartlesville, Oklahoma [privately distributed].
- Pearson, N.J., Gingras, M.K., Armitage, L.A., Pemberton, S.G., 2007. The significance of Atlantic sturgeon feeding excavations, Mary's Point, Bay of Fundy, New Brunswick, Canada. *Palaios* 22, 457–464.
- Pemberton, S.G., 2001. Ichnology & sedimentology of shallow to marginal marine systems. Geological Association of Canada, Short Course 15, p. 343.
- Pemberton, S.G., Frey, R.W., 1984. Ichnology of storm-influenced shallow marine sequence: Cardium Formation (Upper Cretaceous) at Seebe, Alberta. In: Stott, D.F., Glass, D.J. (Eds.), *The Mesozoic of Middle North America. Canadian Society of Petroleum Geologists, Memoir 9*, 281–304.
- Pemberton, S.G., Wightman, D.M., 1992. Ichnological characteristics of brackish water deposits. In: Pemberton, S.G. (Ed), *Applications of Ichnology to Petroleum Exploration. A Core Workshop: SEPM*, 17, 141–167.
- Pemberton, S.G., MacEachern, J.A., Frey, R.W., 1992. Trace fossil facies models: environmental and allostratigraphic significance. In: Walker, R.G., James, N.P. (Eds.), *Facies Models: Response to Sea Level Change, Geological Association Canadian* 47–72.
- Pemberton, S.G., MacEachern, J.A., Ranger, M.J., 1992. Ichnology and event stratigraphy: the use of trace fossils in recognizing tempestites. In: Pemberton, S.G. (Ed.), *Applications of ichnology to petroleum exploration. A core workshop. SEPM Core Workshop*, 17, 85–117.
- Pemberton, S.G., MacEachern, J.A., Saunders, T., 2004. Stratigraphic applications of substrate specific ichnofacies: delineating discontinuities in the rock record. In: McIlroy, D. (Ed.), *The Application of Ichnology to Palaeoenvironmental and Stratigraphic Analysis. Geological Society, Special Publications*, 228, 2962.
- Pemberton, S.G., Spila, M., Pulham, A.J., Saunders, T., MacEachern, J.A., Robbins, J., Sinclair, I.K., 2001. Ichnology and sedimentology of shallow marginal marine systems. Geological Association of Canada. Short Course Notes, 15, 343 p.
- Pemberton, S.G., MacEachern, J.A., Dashtgard, S.E., Bann, K.L., Gingras, M.K., Zonneveld, J-P., 2012. Shorefaces. Chapter 19. In: Knaust, D., Bromley, R.G. (Eds.), *Trace Fossils as Indicators of Sedimentary Environments. Developments in Sedimentology*, 64, 563–603.
- Pemberton, E.A.L., Hubbard, S.M., Fildani, A., Romans, B., Straight, L., 2016. The stratigraphic expression of decreasing confinement along a deep-water sediment routing system: outcrop example from southern Chile. *Geosphere*, 12(1), 114–134.
- Peng, Y., Steel, R.J., Olariu, C., Li, S., 2020. Rapid subsidence and preservation of fluvial signals in an otherwise wave-reworked delta front succession: Early-mid Pliocene Orinoco continental-margin growth, SE Trinidad. *Sedimentary Geology*, 395, 105555.
- Perch-Nielsen, K., 1985. Cenozoic calcareous nannofossils. In: Bolli, H. M., Saunders, J. B., Perch-Nielsen, K., (Eds.), *Plankton Stratigraphy, Cambridge University Press, Cambridge*, 427–554.

- Perkins, E.J., 1974, *The Biology of Estuaries and Coastal Waters*: London, Academic Press, 678 p.
- Picard, M.D., High, L.R., 1973. *Sedimentary Structures of Ephemeral Streams*. Elsevier, Amsterdam. 223p.
- Pickering, K.T., Hiscott, R.N., 2015. *Deep Marine Systems: Processes, Deposits, Environments, Tectonics and Sedimentation*. American Geophysical Union, Wiley, p. 696.
- Pickering, K. T., Clark, J. D., Smith, R. D. A., Hiscott, R. N., Ricci Lucchi, F., Kenyon, N. H., 1995. Architectural element analysis of turbidite systems, and selected topical problems for sand-prone deep-water systems. In: Pickering, K.T., Hiscott, R.N., Kenyon, N.H., Lucchi, R., Smith, R.D.A. (Eds.), *Atlas of Deep-Water Environments; Architectural Style in Turbidite Systems*. London: Chapman and Hall, 1–10.
- Pierson, Th.C., Scott, K.M., 1985. Downstream dilution of a lahar: Transition from debris flow to hyperconcentrated streamflow. *Water resources research*, 21(10), 1511-1524.
- Pindell, J.L., Kennan, L., 2009. Tectonic evolution of the Gulf of Mexico, Caribbean and northern South America in the mantle reference frame: an update. in: James, K.H., Lorente, M.A., Pindell, J.L. (Eds.), *The Origin and Evolution of the Caribbean Plate*, Geological Society, London, Special Publications, 328, 1-55.
- Pindell, J.L., Higgs, R., Dewey, J.F., 1998. Cenozoic palinspastic reconstruction, paleogeographic evolution, and hydrocarbon setting of the northern margin of South America. In: Pindell, J.L., Drake, C. (Eds.), *Paleogeographic evolution and non-glacial eustasy, North America: Society for Sedimentary Geology (SEPM) Special Publication*, 58, 45-86.
- Pindell, J., Kennan, L., Maresch, W.V., Draper, G., 2005. Plate–kinematics and crustal dynamics of circum–Caribbean arc–continent interactions: Tectonic controls on basin development in Proto–Caribbean margins. *Geological Society of America Special Papers*, 394(1), 7–52.
- Plata-Torres, A., Pardo-Trujillo, A., Flores, J.A., 2024. A contribution to the knowledge of Cretaceous to Neogene Palynology in the Colombian Caribbean. *Review of Palaeobotany and Palynology*, 325, 105098.
- Plata-Torres, A., Pardo-Trujillo, A., Vallejo-Hincapié, F., Trejos-Tamayo, R., Flores, J.A., 2023. Early Eocene (Ypresian) palynology of marine sediments from the colombian Caribbean. *Journal of South American Earth Sciences* 121, 104146.
- Plint, A.G., Nummendal, D., 2000. The falling stage systems tract: recognition and importance in sequence stratigraphic analysis. *Sedimentary Responses to Forced Regressions*. In: Hunt, D., Gawthorpe, R.L. (Eds.), Geological Society of London, Special Publication 172, 1-17.
- Pollard, J.E., Goldring, R., Buck, S.G., 1993. Ichnofabrics containing *Ophiomorpha*: significance in shallow–water facies interpretation. *Journal of the Geological Society*, 150, 149–164.
- Ponce, J.J., Carmona, N., 2011. Coarse-grained sediment waves in hyperpycnal clinoform systems, Miocene of the Austral foreland basin, Argentina. *Geology* 39 (8), 763–766.
- Ponce, J.J., Carmona, N., Jait, D., Cevallos, M., Rojas, C., 2023. Sedimentological and ichnological characterization of delta front mouth bars in a river-dominated delta (Upper Cretaceous) from the La Anita Formation, Austral Basin, Argentina. *Sedimentology*, 71(1), 27-53.
- Porebski, S.J., Steel, R., 2006. Deltas and sea-level change. *Journal of Sedimentary Research*, 76, 0-0.
- Posamentier, H.W., Morris, W.R., 2000. Aspects of the stratal architecture of forced regressive deposits. *Sedimentary Responses to Forced Regressions*. In: Hunt, D., Gawthorpe, R.L. (Eds.), Geological Society of London, Special Publication 172, 19-46.

- Posamentier, H.W., Allen, G.P., James, D.P., Tesson, M., 1992. Forced regressions in a sequence stratigraphic framework: concepts, examples, and exploration significance. *American Association of Petroleum Geologists Bulletin* 76, 1687-1709.
- Postma, G., 1990. Depositional architecture and facies of river and fan deltas: a synthesis. In: Colella, A., Prior, D.B. (Eds.), *Coarse-grained deltas*. IAS Special Pub. 10, 13-28.
- Postma, G., Cartigny, M.J.B., 2014. Supercritical and subcritical turbidity currents and their deposits – a synthesis. *Geology* 42, 987–990.
- Postma, G., Kleverlaan, K., 2018. Supercritical flows and their control on the architecture and facies of small-radius sand-rich fan lobes. *Sedimentary Geology*, 364, 53–70.
- Postma, G., Nemeč, W., Kleinspehn, K.L., 1988. Large floating clasts in turbidites: a mechanism for their emplacement. *Sedimentary Geology*, 58, 47–61.
- Postma, G., Cartigny, M.J.B., Kleverlaan, K., 2009. Structureless, coarse-tail graded Bouma Ta formed by internal hydraulic jump of the turbidity current? *Sedimentary Geology*, 219, 1-6.
- Postma, G., Kleverlaan, K., Cartigny, M.J.B., 2014. Recognition of cyclic steps in sandy and gravelly turbidite sequences, and consequences for the Bouma facies model. *Sedimentology*, 61, 2268–2290.
- Postma, G., Hoyal, D.C., Abreu, V., Cartigny, M.J., Demko, T., Fedele, J.J., Kleverlaan, K., Pederson, K.H., 2016. Morphodynamics of supercritical turbidity currents in the channel-lobe transition zone. In: Lamarche, G., Moundjoy, J. (Eds.), *Submarine Mass Movements and their Consequences*. *Advances in Natural and Technological Hazards Research* 469–478. Springer, Dordrecht.
- Postma, G., Lang, J., Hoyal, D.C., Fedele, J.J., Demko, T., Abreu, V., Pederson, K.H., 2021. Reconstruction of bedform dynamics controlled by supercritical flow in the channel-lobe transition zone of a deep-water delta (Sant Llorenç del Munt, north-east Spain, Eocene). *Sedimentology*, 68(4), 1–24.
- Potter, P.E., Maynard, J.B., Depetris, P.J., 2005. *Mud and Mudstones: Introduction and Overview*. Springer Berlin / Heidelberg. 297p.
- Pratt, B.R., 1998. Syneresis cracks: subaqueous shrinkage in argillaceous sediments caused by earthquake-induced dewatering. *Sedimentary Geology*, 117, 1–10.
- Project Contrato RC 494, 2017. Informe de integración del proyecto “Certificación de estratigrafía física y de edad de los núcleos de perforación recuperados por la Agencia Nacional de Hidrocarburos en las cuencas de Sinú-San Jacinto y cordillera”. Informe confidencial.
- Proust, J-N., Mahieux, G., Tessier, B., 2001. Field and seismic images of sharp-based shoreface deposits: Implications for sequence stratigraphic analysis. *Journal of Sedimentary Research* 71(6), 944-957.
- Pufahl, P.K., James, N.P., 2006. Monospecific Pliocene oyster buildups, Murray Basin, South Australia: Brackish water end member of the reef spectrum. *Palaeogeography, Palaeoclimatology, Palaeoecology* 233 (1-2), 11-33.
- Quiroz, L.I., Buatois, L.A., Mángano, M.G., Jaramillo, C.A., Santiago, N., 2010. Is the trace fossil *Macaronichnus segregatis* an indicator of temperate to cold waters? Exploring the paradox of its occurrence in tropical coasts. *Geology*, 38, 651–654.
- Quiroz, L.I., Buatois, L.A., Seike, K., Mángano, M.G., Jaramillo, C., Sellers, A., 2019. The search for an elusive worm in the tropics, the past as a key to the present, and reverse uniformitarianism. *Scientific Reports*, 9, 18402.

- Raigosa, M., 2018. Caracterización estratigráfica, microfacial y diagenética de las formaciones Toluviejo y El Floral en la región onshore del Cinturón Plegado SinúSan Jacinto, Bogotá: Servicio Geológico Colombiano, 119 p, (in Spanish).
- Reading, H., 1996. *Sedimentary Environments: Processes, Facies and Stratigraphy* – Third Edition. Oxford: Blackwell Scientific Ltd. 689p.
- Restrepo, J.J., Toussaint, J.F., 2020. Tectonostratigraphic terranes in Colombia: An update. First part: Continental terranes. In: Gómez, J., Mateus-Zabala, D. (Eds), *The Geology of Colombia, Volume 1 Proterozoic – Paleozoic*. Servicio Geológico Colombiano, Publicaciones Geológicas Especiales, 35, 37-63.
- Restrepo-Moreno, S.A., Foster, D.A., Stockli, D.F., Parra-Sánchez, L.N., 2009. Long-term erosion and exhumation of the “Altiplano Antioqueño”, Northern Andes (Colombia) from apatite (U-Th)/He thermochronology. *Earth and Planetary Science Letters*, 278, 1-12.
- Retallack, G.J., 2001, *Soils of the Past: An Introduction to Paleopedology*. Blackwell Science, Oxford, 549 p.
- Richards, M., Bowman, M., Reading, H., 1998. Submarine-fan systems i: characterization and stratigraphic prediction. *Marine and Petroleum Geology*, 15(7), 689–717.
- Rincón-Martínez, D., Baumgartner, P.O., Sandoval, M.I., Restrepo-Acevedo, S.M., Baumgartner-Mora C., 2023. Late Cretaceous and Paleocene radiolarians from the San Jacinto Fold Belt, northeast Colombia: Biostratigraphic and paleoenvironmental implications. *Journal of South American Earth Sciences*, 126, 104325.
- Rodríguez-López, J.P., Meléndez, N., De Boer, P.L., Soria, A.R., 2010. The action of wind and water in a mid-Cretaceous subtropical erg-margin system close to the Variscan Iberian Massif, Spain. *Sedimentology*, 57(5), 1315-1356.
- Rodríguez-Tovar, F.J., 2022. Ichnological analysis: A tool to characterize deep-marine processes and sediments. *Earth-Sciences Reviews* 228, 104014.
- Rodríguez-Tovar, F.J., Pérez-Valera, F., 2008. Trace Fossil *Rhizocorallium* from the middle Triassic of the Betic Cordillera, southern Spain: characterization and environmental implications. *Palaios* 23(2), 78-86.
- Rodríguez-Tovar, F.J., Aguirre, J., 2014. Is *Macaronichnus* an exclusively small, horizontal and unbranched structure? *Macaronichnus segregatis degiberti* subsp. nov. *Spanish Journal of Palaeontology*, 29(2), 131-142.
- Rodríguez-Tovar, F.J., García-García, F., 2023. *Macaronichnus* ‘co-occurrence’ in offshore transition settings: Discussing the role of tidal versus fluid muds influence. *Geobios*, 80, 73-82.
- Rodríguez-Tovar, F.J., Puga-Bernabéu, A., Buatois, L.A., 2008. Large burrow systems in marine Miocene deposits of the Betic Cordillera (Southeast Spain). *Palaeogeography, Palaeoclimatology, Palaeoecology*, 268, 19–25.
- Rodríguez-Tovar, F.J., Nagy, J., Reolid, M., 2014. Palaeoenvironment of Eocene prodelta in Spitsbergen recorded by the trace fossil *Phycosiphon incertum*. *Polar Research*, 33, 23786.
- Rodríguez-Tovar, F.J., Alcalá, L., Cobos, A., 2016. *Taenidium* at the lower Barremian El Hoyo dinosaur tracksite (Teruel Spain): assessing palaeoenvironmental conditions for the invertebrate community. *Cretaceous Research*, 65, 48–58.

- Rodríguez-Tovar, F.J., Puga-Bernabéu, A., Buatois, L.A., 2008. Large burrow systems in marine Miocene deposits of the Betic Cordillera (Southeast Spain). *Palaeogeography, Palaeoclimatology, Palaeoecology*, 268, 119-125.
- Rodríguez-Tovar, F.J., Miguez-Salas, O., Duarte, L.V., 2017. Toarcian Oceanic Anoxic Event induced unusual behaviour and palaeobiological changes in *Thalassinoides* tracemakers. *Palaeogeography, Palaeoclimatology, Palaeoecology*, 485, 46-56.
- Rodríguez-Tovar, F.J., Mayoral, E., Santos, A., Dorador, J., Wetzel, A., 2019. Crowded tubular tidalites in Miocene shelf sandstones of southern Iberia. *Palaeogeography, Palaeoclimatology, Palaeoecology*, 521(1), 1-9.
- Romito, S., Mann, P., 2020. Tectonic terranes underlying the present-day Caribbean plate: their tectonic origin, sedimentary thickness, subsidence histories and regional controls on hydrocarbon resources. In: Davison, I., Hull, J.N.F., Pindell, J. (Eds.), *The Basins, Orogens and Evolution of the Southern Gulf of Mexico and Northern Caribbean*. Geological Society, London, Special Publications, 504(1), 343.
- Rosello, E., Cossey, S., 2012. What is the evidence for subduction in the Caribbean Margin of Colombia? In: Extended abstract in *Memoirs of the XII Simposio Bolivariano de Cuencas Subandinas: Cartagena, Colombia*. Asociación Colombiana de Geólogos y Geofísicos del Petróleo, 1–7.
- Rossi, V.M., Steel, R., 2016. The role of tidal, wave and river currents in the evolution of mixed-energy deltas: Example from the Lajas Formation (Argentina). *Sedimentology*, 63, 824-864.
- Rossi, V.M., Longhitano, S.G., Mellere, D., Dalrymple, R.W., Steel, R.J., Chiarella, D., Olariu, C., 2017a. Interplay of tidal and fluvial processes in an early Pleistocene, delta-fed, strait margin (Calabria, Southern Italy). *Marine and Petroleum Geology*, 87, 14-30.
- Rossi, V.M., Perillo, M.M., Steel, R.J., Olariu, C., 2017b. Quantifying mixed-process variability in shallow-marine depositional systems: what are sedimentary structures really telling us? *Journal of Sedimentary Research*, 87, 1060-1074.
- Rossi, V.M., Paterson, N.W., Helland-Hansen, W., Klausen, T.G., Eide, C.H., 2019. Mud-rich delta-scale compound clinoforms in the Triassic shelf of northern Pangea (Havert Formation, south-western Barents Sea). *Sedimentology*, 66, 2234-2267.
- Rust, B.R., Koster, E.H. 1984. Coarse alluvial deposits. In: Walker, R.G. (Ed.), *Facies Models*, 2nd Geosci. Can. Reprint Ser. 1, 53-69.
- Salazar-Ortiz, E., Numpaque, J., Bernal, L., Ocampo, E., Matajira, A., Villabona, J., Gómez, D., García, G., Méndez, S., Martínez, E., Sánchez, D., Sotelo, A.P., Aguirre, L., 2020a. Geología del área Sinú – San Jacinto, Planchas 23, 24, 30, 31 y parte de las planchas 37 y 38 a escala 1:50.000. Bogotá: Servicio Geológico Colombiano, (in Spanish).
- Salazar-Ortiz, E.A., Rincón-Martínez, D., Páez, L-A., Restrepo, S.M., Barragán, S., 2020b. Middle Eocene mixed carbonate-siliciclastic systems in the southern Caribbean (NW Colombian margin). *Journal of South American Earth Sciences*, 99, 102507.
- Sánchez, C., Permanyer, A., 2006. Origin and alteration of oils and oil seeps from the Sinú-San Jacinto Basin, Colombia. *Organic Geochemistry*, 37(12), 1831-1845.
- Sarmiento-Rojas, L.F., 2001. Mesozoic rifting and Cenozoic basin inversion history of the Eastern Cordillera, Colombian Andes. Inferences from tectonic models. Ph.D. Thesis Vrije Universiteit, Amsterdam, The Netherlands, 297p.

- Sarmiento-Rojas, L.F., 2019. Cretaceous stratigraphy and Paleofacies maps of Northwestern South America. In: Cediel, F., Shaw, R.P. (Eds.), *Geology and Tectonics of Northwestern South America. The Pacific-Caribbean-Andean Junction*. *Frontiers in Earth Sciences*, 673–747.
- Sarmiento-Rojas, L.F., van Wess, J.D., Cloetingh, S., 2006. Mesozoic transtensional basin history of the Eastern Cordillera, Colombian Andes: Inferences from tectonic models. *Journal of South American Earth Sciences*, 21(4), 383–411.
- Saunderson, H.C., Lockett, F.P.J., 1983. Flume experiments on bedforms and structures at the dune-plane bed transition. In: Collinson, J.D., Lewin, L. (Eds.), *Modern and ancient fluvial systems*. Spec. International Association of Sedimentologists Special Publication, vol. 6. Blackwell Science, Oxford, pp. 49–58.
- Savrda, C.E., 2002. Equilibrium responses reflected in a large *Conichnus* (Upper Cretaceous Eutaw Formation, Alabama, USA). *Ichnos*, 9, 33–40.
- Savrda, C.E., Ozalas, K., Demko, T.H., Hichison, R.A., Scheiwe, T.D., 1993. Log-grounds and the ichnofossil *Teredolites* in transgressive deposits of the Clayton Formation (Lower Paleocene), Western Alabama. *Palaios*, 8, 311–324.
- Savrda, C.E., Blanton-Hooks, A.D., Collier, J.W., Drake, R.A., Graves, R.L., Hall, A.G., Nelson, A.J., Slone, J.C., Williams, D.D., Wood, H.A., 2000. *Taenidium* and associated ichnofossils in fluvial deposits, Cretaceous Tuscaloosa Formation, eastern Alabama, southeastern USA. *Ichnos*, 7, 777–806.
- Scasso, R.A., del Río, C.J., 1987. Ambientes de sedimentación, estratigrafía y proveniencia de la secuencia marina del Terciario superior de la región de Península Valdés, Chubut. *Revista de la Asociación Geológica Argentina* 42(3-4), 291-321. [In Spanish].
- Scasso, R.A., Cuitiño, J.I., 2017. Sequential development of tidal ravinement surfaces in macro to hypertidal estuaries with high volcanoclastic input: the Miocene Puerto Madryn Formation (Patagonia, Argentina). *Geo-Marine Letters*, 37, 427-440.
- Scasso, R.A., Cuitiño, J.I., Escapa, I., 2010. Mesozoic-Cenozoic basins of Central Patagonia with emphasis in their tidal systems. In: del Papa, C., Astini, R. (Eds.), *Field Excursion Guidebook*. 18th International Sedimentological Congress, Mendoza, Argentina, FE-C9, 1-41.
- Scasso, R.A., Dozo, M.T., Cuitiño, J.I., Bouza, P., 2012. Meandering tidal-fluvial channels and lag concentration of terrestrial vertebrates in the fluvial-tidal transition of an ancient estuary in Patagonia. *Latin American Journal of Sedimentology and Basin Analysis*, 19(1), 27-45.
- Scholl, D.W., von Huene, R., 2010. Subduction zone recycling processes and the rock record of crustal suture zones. *Canadian Journal of Earth Sciences*, 47(5), 633-654.
- Seilacher, A., 1964. Biogenic sedimentary structures. In: Imbrie, J., Newell, N. (Eds.), *Approaches to Paleocology*. Wiley, New York, 296e316.
- Shepard, F.P., 1973. *Submarine geology*. Harper and Row, New York, 3rd edition.
- Schultz, S.K., MacEachern, J.A., Catuneanu, O., Dashtgard, S., 2020. Coeval deposition of transgressive and normal regressive stratal packages in a structurally controlled area of the Viking Formation, central Alberta, Canada. *Sedimentology*, 67(6), 2974-3002.
- Schwarz, E., Buatois, L.A., 2012. Substrate-controlled ichnofacies along a marine sequence boundary: The Intra-Valanginian Discontinuity in central Neuquén Basin (Argentina). *Sedimentary Geology*, 277-278, 72-87.

- Seike, K., 2007. Palaeoenvironmental and palaeogeographical implications of modern *Macaronichnus segregatis*-like traces in foreshore sediments on the Pacific coast of central Japan. *Palaeogeography, Palaeoclimatology, Palaeoecology*, 252, 497–502.
- Seike, K., Yanagishima, S., Nara, M., Sasaki, T., 2011. Large *Macaronichnus* in modern shoreface sediments: Identification of the producer, the mode of formation, and palaeoenvironmental implications. *Palaeogeography, Palaeoclimatology, Palaeoecology*, 311, 224–229.
- Seilacher, A., 1964. Biogenic sedimentary structures. In: Imbrie, J., Newell, N. (Eds.), *Approaches to Paleocology*, New York, John Wiley and Sons 296–316.
- Selley, R.C., 1985. *The Reservoir, Elements of Petroleum Geology*. W.H. Freeman and Company, New York, 219–275.
- Sequeiros, O.E., 2012. Estimating turbidity current conditions from channel morphology: A Froude number approach. *Journal of Geophysical Research*, 117, C04003.
- Sequeiros, O.E., Spinewine, B., Beaubouef, R.T., Sun, T., García, M.H., Parker, G., 2010. Bedload transport and bed resistance associated with density and turbidity currents. *Sedimentology*, 57, 1463–1490.
- SGC., 2019. Memoria explicativa de la plancha 81 – Puerto Libertador a escala 1:100000. Departamento de Córdoba. Servicio Geológico Colombiano, 220 p.
- Shanmugam, G., 1997. The Bouma Sequence and the turbidity mindset. *Earth-Science Reviews*, 42, 201–229.
- Shanmugam, G., 2009. Slides, slumps, debris flows, and turbidity currents. In: Steele, J.H., Thorpe, S.A., Turekian, K.K. (Eds.), *Encyclopedia of Ocean Sciences* (second ed.), Academic Press (Elsevier), Waltham, MA, 447–467.
- Shanmugam, G., 2021. Gravity flows: debris flows, grain flows, liquefied/fluidized flows, turbidity currents, hyperpycnal flows, and contour currents. In: Shanmugam, G. (Ed.), *Mass Transport, Gravity Flows, and Bottom Currents. Downslope and Alongslope Processes and Deposits*. Chapter 3. Academic Press (Elsevier), Waltham, 89–148.
- Shchepetkina, A., Gingras, M.K., Mángano, M.G., Buatois, L.A., 2019. Fluvio–tidal transition zone: Terminology, sedimentological and ichnological characteristics, and significance. *Earth Science Reviews*, 192, 214–235.
- Shields, D.J., Strobl, R., 2010. The Wabiskaw D Member, Clearwater Formation: A World Class Oil Sands Reservoir Hosted in an Incised Valley Complex. In: *GeoCanada 2010 – Working with the Earth*. AAPG, 5 p.
- Shiers, M.N., Mountney, N.P., Hodgson, D.M., Colombera, L., 2018. Controls on the depositional architecture of fluvial point-bar elements in a coastal-plain succession. In: Ghinassi, M., Colombera, L., Mountney, N.P., Reesink, A.J.H., Bateman, M. (Eds), *Fluvial Meanders and Their Sedimentary Products in the Rock Record*, 15–46.
- Silva–Arias, A., Páez–Acuña, L.A., Rincón–Martínez, D., Tamara–Guevara, J.A., Gomez–Gutierrez, P.D., López–Ramos, E., Restrepo–Acevedo, S.M., Mantilla–Figuroa, L–C., Valencia, V., 2016. Basement characteristics in the Lower Magdalena Valley and the Sinú and San Jacinto Fold Belts: evidence of a Late Cretaceous magmatic arc at the South of the Colombian Caribbean. *Ciencia, Tecnología y Futuro*, 6, 5–36.
- Silva, A., Paez, L., Rincon, M., Tamara, J., Gomez, P., Lopez, E., Restrepo, S., Mantilla, L., Valencia, V., 2017. Basement characteristics in the Lower Magdalena Valley and the Sinú and San Jacinto Fold belts:

- Evidence of a Late Cretaceous magmatic arc at the south of the Colombian Caribbean. *Ciencia, Tecnología y Futuro*, 6(4), 5–36.
- Silva-Tamayo, J.C., Sierra, G., Correa, L., 2008. Tectonic and climate driven fluctuations in the stratigraphic base level of a Cenozoic continental coal basin, northwestern Andes. *Journal of South American Earth Sciences*, 26-4, 369-382.
- Silva-Tamayo, J.C., Lara, M.E., Yobo, L.N., Erdal, Y.D., Sanchez, J., Zapata-Ramírez, P.A., 2017. Tectonic and environmental factors controlling on the evolution of Oligo – Miocene shallow marine carbonate factories along a tropical SE Circum-Caribbean. *Journal of South American Earth Sciences*, 78, 213–237.
- Silva-Tamayo, J.C., Rincón-Martínez, D., Barrios, L.M., Torres-Lasso, J.C., Osorio-Arango, C., 2020. Cenozoic marine carbonate systems of Colombia. In: Gómez, J., Mateus-Zabala, D. (Eds.), *The Geology of Colombia, Volume 3 Paleogene – Neogene*. Servicio Geológico Colombiano, Publicaciones Geológicas Especiales 37, 249–282. Bogotá.
- Silva-Tamayo, J.C., Lara, M., Salazar-Franco, A.M., 2020. Oligocene – Miocene coal-bearing successions of the Amagá Formation, Antioquia, Colombia: Sedimentary environments, stratigraphy, and tectonic implications. In: Gómez, J., Mateus-Zabala, D. (Eds.), *The Geology of Colombia, Volume 3 Paleogene – Neogene*. Servicio Geológico Colombiano, Publicaciones Geológicas Especiales 37, 23 p. Bogotá.
- Simmons, M.D., Miller, K.G., Ray, D.C., Davies, A., van Buchem, F.S.P., Gréselle, B., 2020. Phanerozoic Eustasy. In: Gradstein, F., Ogg, J.G., Schmitz, M.D., Ogg, G.M. (Eds.), *Geologic Time Scale 2020*. Chapter 13, 357-400.
- Simpson, J. 1997 *Gravity Currents*. Cambridge University Press. 1-244.
- Slater, S.M., McKie, T., Vieira, M., Wellman, C.H., Vajda, V., 2017. Episodic river flooding events revealed by palynological assemblages in Jurassic deposits of the Brent Group, North Sea. *Palaeogeography, Palaeoclimatology, Palaeoecology*, 485, 389-400.
- Slatt, R.M., 2006. Geologic controls on reservoir quality. In: Slatt, R.M. (Ed.), *Stratigraphic Reservoir Characterization for Petroleum Geologists, Geophysicists, and Engineers*. Elsevier, Amsterdam, 61, 159–202.
- Slatt, R.M., Zavala, C., 2011. Sediment transfer from shelf to deep water—Revisiting the delivery system. *AAPG Stud. Geol.*, 61, 1–214.
- Slotman, A., Cartigny, M.J.B., 2020. Cyclic steps: Review and aggradation-based classification. *Earth-Science Reviews* 201, 102949.
- Slott, J.M., Murray, A.B., Ashton, A.D., 2010. Large-scale responses of complex-shaped coastlines to local shoreline stabilization and climate change. *Journal of Geophysical Research: Earth Surface*, 115, F3.
- Smith, D.G., Hubbard, S.M., Lavigne, J., Leckie, D.A., Fustic, M., 2011. Stratigraphy of counter-point-bar and eddy-accretion deposits in low-energy meander belts of the Peace-Athabasca Delta, Northeast Alberta, Canada. In: Davidson, S.K., Leleu, S., North, C.P. (Eds.), *From River to Rock Record: The Preservation of Fluvial Sediments and Their Subsequent Interpretation*. SEPM Special Publications, 97, 143-152.
- Smith, G.A., 1986. Coarse-grained nonmarine volcanoclastic sediment: Terminology and depositional process. *Geological Society of America Bulletin*, 97, 1-10.
- Sohn, Y.K., Rhee, C.W., Kim, B.C., 1999. Debris flow and hyperconcentrated flood-flow deposits in an alluvial fan, northwestern part of the Cretaceous Yongdong Basin, central Korea. *Journal of Geology*, 107, 111-132.

- Sohn, Y.K., Choe, M.Y., Jo, H.R., 2002. Transformation from debris flow to hyperconcentrated flow in a submarine channel (the Cretaceous Cerro Toto Formation, southern Chile). *Terra Nova* 14, 405-415.
- Solórzano, E.J., Buatois, L.A., Rodríguez, W.J., Mángano, M.G., 2017. From freshwater to fullymarine: Exploring animal-substrate interactions along a salinity gradient (Miocene Oficina Formation of Venezuela). *Palaeogeography, Palaeoclimatology, Palaeoecology*, 482, 30–47.
- Southard, J.B., Boguchwal, L.A., 1990, Bed configuration in steady unidirectional water flows; Part 2, Synthesis of flume data: *Journal of Sedimentary Research*, 60(5), 658-679.
- Spikings, R., Cochrane, R., Villagomez, D., Van der Lelij, R., Vallejo, C., Winkler, W., Beate, B., 2015. The geological history of northwestern South America: from Pangaea to the early collision of the Caribbean Large Igneous Province (290–75Ma). *Gondwana Research*, 27, 95–139.
- Steel, R.J., Milliken, K.L., 2013. Major advances in siliciclastic sedimentary geology, 1960–2012. In: Bickford, M.E. (Ed.), *The Web of Geological Sciences: Advances, Impacts, and Interactions: Geological Society of America Special Paper 500*, 121-167.
- Steel, R., Osman, A., Rossi, V.M., Alabdullatif, J., Olariu, C., Peng, Y., Rey, F., 2024. Subaqueous deltas in the stratigraphic record: Catching up with the marine geologists. *Earth-Science Reviews*, 256, 104879.
- Stevenson, C.J., Jackson, C.A.L., Hodgson, D.M., Hubbard, S.M., Eggenhuisen, J.T., 2015. Deep-water sediment bypass. *Journal of Sedimentary Research*, 85, 1058–1081.
- Stevenson, C.J., Talling, P.J., Masson, D.G., Sumner, E.J., Frenz, M., Wynn, R.B., 2014. The spatial and temporal distribution of grain-size breaks in turbidites. *Sedimentology*, 61, 1120–1156.
- Storms, J.E.A., Hoogendoorn, M., Dam, R.A.C., Hoitink, A.J.F., Kroonenberg, S.B., 2005. Late-Holocene evolution of the Mahakam delta, East Kalimantan, Indonesia. *Sedimentary Geology*, 180(3-4), 149-166.
- Stow, D.A.V., 1985. Fine-grained sediments in deep water: An overview of processes and facies models. *Geo-Marine Letters* 5, 17–23.
- Stow, D.A., Piper, D.J.W., 1984. Deep-water fine-grained sediments; history, methodology and terminology. Geological Society, London, Special Publications 15, 3–14.
- Stow, D.A.V., Tabrez, A., 1998. Hemipelagites: processes, facies and model. In: Stoker, M.S., Evans D., Cramp, A. (Eds.), *Geological Processes on Continental Margin: Sedimentation Mass-Wasting and Stability*, Geological Society, London, Special Publications 129, 317–337.
- Stow, D.A., Smillie, Z., 2020. Distinguishing between deep-water sediment facies: turbidites, contourites and hemipelagites. *Geosciences* 10, 1–43.
- Summer, E.J., Talling, P.J., Amy, L.A., Wynn, R.B., Stevenson, C.J., Frenz, M., 2012. Facies architecture of individual basin-plain turbidites: Comparison with existing models and implications for flow processes. *Sedimentology* 59 (6), 1850–1887.
- Svendsen, J., Stollhofen, H., C.B.E, Krapf., Stanistreet, I.G. 2003. Mass and hyperconcentrated flow deposits record, dune damming and catastrophic breakthrough of ephemeral rivers, Skeleton Coast Erg, Namibia, *Sedimentary Geology*, 160, 7-31.
- Swan, A., Hartley, A.J., Owen, A., Howell, J., 2018. Reconstruction of a sandy point-bar deposit: implications for fluvial facies analysis. In: Ghinassi, M., Colombera, L., Mountney, N.P., Reesink, A.J.H., Bateman, M. (Eds.), *Fluvial Meanders and Their Sedimentary Products in the Rock Record*, 48, 445-474.

- Swift, D.J.P., Thorne, J.A., 1991. Sedimentation on continental margins: a general model for shelf sedimentation. In: Swift, D.J.P., Oertel, G.F., Tillman, R.W., Thorne, J.A. (Eds.), *Shelf Sand and Sandstone Bodies: International Association of Sedimentologists, Special Publication*, 14, 3–31.
- Symons, W.O., Sumner, E.J., Talling, P.J., Cartigny, M.J.B., Clare, M.A., 2016. Large-scale sediment waves and scours on the modern seafloor and their implications for the prevalence of supercritical flow. *Marine Geology* 371, 130–148.
- Syvitski, J.P.M., Peckham, S.D., Hilberman, R., Mulder, T., 2003. Predicting the terrestrial flux of sediment to the global ocean: a planetary perspective. *Sedimentary Geology*, 162(1-2), 5-24.
- Syvitski, J.P.M, Anthony, E., Saito, Y., Zăinescu, F., Day, J., Bhattacharya, J.P., Giosan, L., 2022. Large deltas, small deltas: Toward a more rigorous understanding of coastal marine deltas. *Global and Planetary Change*, 218, 103958.
- Ta, T.K.O., Nguyen, V.L., Tateishi, M., Kobayashi, I., Saito, Y., Nakamura, T., 2002. Sediment facies and Late Holocene progradation of the Mekong River Delta in Bentre Province, southern Vietnam: an example of evolution from a tide-dominated to a tide- and wave-dominated delta. *Sedimentary Geology*, 152(3-4), 313-325.
- Taboada, A., Rivera, L.A., Fuenzalida, A., Cisternas, A., Philip, H., Olaya, J., Rivera, C., 2000. Geodynamics of the northern Andes: Subductions and intracontinental deformation (Colombia). *Tectonics*, 19(5), 787–813.
- Talling, P.J., Masson, D.G., Sumner, E.J., Malgestini, G., 2012. Subaqueous sediment density flows: depositional processes and deposit types. *Sedimentology*, 59, 1937–2003.
- Tamura, T., Saito, Y., Nguyen, V.L., Ta, T.K.O., Bateman, M.D., Matsumoto, D., Yamashita, S., 2012. Origin and evolution of interdistributary delta plains; insights from Mekong River delta. *Geology*, 40(4), 303-306.
- Tamura, T., Saito, Y., Nguyen, V.L., Ta, T.K.O., Bateman, M.D., Matsumoto, D., Yamashita, S., 2012. Origin and evolution of interdistributary delta plains; insights from Mekong River delta. *Geology*, 40(4), 303-306.
- Tanner, P.W.G., 2003. Syneresis. In: Middleton, G.V. (Ed.), *Encyclopedia of Sediments and Sedimentary Rocks*. Kluwer Academic, Dordrecht, 718–720.
- Taylor, A.M., Goldring, R., 1993. Description and analysis of bioturbation and ichnofabric. *Journal of the Geological Society of London*, 150, 141-148.
- Taylor, A., Goldring, R., Gowland, S., 2003. Analysis and application of ichnofabrics. *Earth Science Review*, 60, 227–259.
- Thomas, F.C., Murney, M.G., 1985. Techniques for extraction of foraminifers and ostracodes from sediment samples: Canadian Technical Report of Hydrography and Ocean Sciences, 54, 24 p.
- Thomas, R.G., Smith, D.G., Wood, J.M., Visser, J., Calverley-Range, E.A., Koster, E.H., 1987. Inclined heterolithic stratification—Terminology, description, interpretation and significance. *Sedimentary Geology* 53, 123-179.
- Thouret, J-C., Antoine, S., Magill, C., Ollier, C., 2020. Lahars and debris flows: Characteristics and impacts. *Earth-Science Reviews*, 201, 103003.
- Tinterri, R., 2011. Combined Flow Sedimentary Structures and the Genetic Link between Sigmoidal and Hummocky-Cross Stratification. *GeoActa*, 10, 43-85.

- Tinterri, R., Mazza, T., Magalhaes, P.M., 2022. Contained-Reflected Megaturbidites of the Marnoso-arenacea Formation (Contessa Key Bed) and Helminthoid Flysches (Northern Apennines, Italy) and Hecho Group (South-Western Pyrenees). *Frontiers in Earth Sciences* 10:817012.
- Tinterri, R., Civa, A., Laporta, M., Piazza, A., 2020. Turbidities and turbidity currents. In: Scarselli, N., Chiarella, D., Bally, A.W., Adam, J., Roberts, D.G., (Eds.), *Regional Geology and Tectonics (Second Edition) Volume 1: Principles of Geologic Analysis*. Chapter 17, 39 p.
- Todd, S.P., 1989. Stream-driven, high-density gravelly traction carpets: possible deposits in the Trabeg Conglomerate Formation, SW Ireland and some theoretical considerations of their origin. *Sedimentology*, 36, 513–530.
- Toussaint, J., 1993. Introducción - Precámbrico. In *Evolución geológica de Colombia*. Universidad Nacional de Colombia.
- Toussaint, J.F., Restrepo, J.J., 2020. Tectonostratigraphic terranes in Colombia: An update. Second part: Oceanic terranes. In: Gómez, J., Pinilla-Pachon, A.O. (Eds.), *The Geology of Colombia, Volume 2 Mesozoic*. Servicio Geológico Colombiano, Publicaciones Geológicas Especiales, 36, 237-260. Bogotá.
- Tomasovych, A., Fursich, F.R., Wilmsen, M., 2006. Preservation of Autochthonous Shell Beds by Positive Feedback between Increased Hardpart-Input Rates and Increased Sedimentation Rates. *The Journal of Geology* 114(3), 287-312.
- Tonkin, N.S., 2012. Deltas. Chapter 17. In: Knaust, D., Bromley, R.G. (Eds.), *Trace Fossils as Indicators of Sedimentary Environments: Developments in Sedimentology*, 64, 507-528.
- Traverse, A., 2007. *Paleopalynology (second edition)*: Dordrecht, Springer, Topics in Geobiology, 28, 813 p.
- Trejos Tamayo, R., Garzón, D., Arias, V., Plata, A., Vallejo, F., Pardo, A., Flores, J.A., 2024. Microfossils provide evidence of environmental changes during the Eocene-Oligocene transition in northwestern South America. *EGU General Assembly Conference Abstracts*, 1156.
- Uchman, A., 2009. The *Ophiomorpha rudis* ichnosubfacies of the *Nereites* ichnofacies: Characteristics and constraints. *Palaeogeography, Palaeoclimatology, Palaeoecology* 276, 107–119.
- Uchman, A., Pervesler, P., 2007. Palaeobiological and palaeoenvironmental significance of the Pliocene trace fossil *Dactyloidites peniculus*. *Acta Palaeontologica Polonica*, 52(4), 799–808.
- Uchman, A., Wetzel, A., 2012. Deep-Sea Fans. In: Knaust, D., Bromley, R.G. (Eds.), *Trace Fossils as Indicators of Sedimentary Environments*. *Developments in Sedimentology*, 64, 643–671.
- Uchman, A., Johnson, M.E., Rebelo, A.C., Melo, C., Cordeiro, R., Ramalho, R.C., Ávila, S.P., 2016. Vertically-oriented trace fossil *Macaronichnus segregatis* from Neogene of Santa Maria Island (Azores; NE Atlantic) records vertical fluctuations of the coastal groundwater mixing zone on a small oceanic island. *Geobios*, 49, 229–241.
- Vallejo-Hincapié, F., Flores, J-A., Marie-Pierre, A., Pardo-Trujillo, A., 2023. Contribution to the Cenozoic chronostratigraphic framework of the Caribbean Sinú-San Jacinto Belt of Colombia based on calcareous nanofossils. *Journal of South American Earth Sciences*, 127, 104419.
- Vallejo-Hincapié, F., Pardo-Trujillo, A., Barbosa-Espitia, A., Aguirre, D., Celis, S.A., Giraldo-Villegas, C.A., Plata-Torres, Á., Trejos-Tamayo, R., Salazar-Ríos, A., Flores, J-A., Aubry, M-P., Gallego, F., Delgado, E., Foster, D., 2024. Miocene vanishing of the Central American Seaway between the Panamá Arc and the South American Plate. *GSA Bulletin*, 17 p.

- Vallon, L.H., Rindsberg, A.K., Bromley, R.G., 2016. An updated classification of animal behaviour preserved in substrates, *Geodinamica Acta* 28(1-2), 5-20.
- Van der Merwe, W., Hodgson, D.M., Brunt, R.L., Flint, S.S., 2014. Depositional architecture of sand-attached and sand-detached channel-lobe transition zones on an exhumed stepped slope mapped over a 2500 km² area. *Geosphere* 10 (6), 1–18.
- van Yperen, A.E., Holbrook, J.M., Poyatos-Moré, M., Midtkandal, I., 2019. Coalesced delta front sheet-like sandstone bodies from highly avulsive distributary channels: the low-accommodation Mesa Rica Sandstone (Dakota Group, New Mexico, USA). *Journal of Sedimentary Research*, 89, 654–678.
- Van Yperen, A.E., Poyatos-Moré, M., Holbrook, J.M., Midtkandal, I., 2020. Internal mouth-bar variability and preservation of subordinate coastal processes in low-accommodation proximal deltaic settings (Cretaceous Dakota Group, New Mexico, USA). *The Depositional Record*, 6, 431-458.
- Vargas, C.A. 2020. Subduction geometries in northwestern South America. In: Gómez, J., Pinilla-Pachon, A.O. (Eds.), *The Geology of Colombia, Volume 4 Quaternary*. Servicio Geológico Colombiano, Publicaciones Geológicas Especiales 38, 397–422. Bogotá.
- Vargas-González, V., Pardo-Trujillo, A., Gallego-Bañol, N.F., Restrepo-Moreno, S.A., Muñoz-Valencia, J.A., 2022. Procedencia de la Formación El Cerrito en el Cinturón Plegado de San Jacinto: implicaciones paleogeográficas para el Caribe colombiano. *Boletín de Geología*, 44(3), 39–63. In Spanish.
- Vellinga, A.J., Cartigny, M.J.B., Eggenhuisen, J.T., Hansen, E.W.M., 2018. Morphodynamics and depositional signature of low-aggradation cyclic steps: New insights from a depth-resolved numerical model. *Sedimentology* 65, 540–560.
- Verde, M., Martínez, S., 2004. A new ichnogenus for crustacean trace fossils from the Upper Miocene Camacho Formation of Uruguay. *Palaeontology* 47(1), 39-49.
- Vesal, S.E., Nasi, F., Auriemma, R., Del Negro, P., 2023. Effects of Organic Enrichment on Bioturbation Attributes: How Does the Macrofauna Community Respond in Two Different Sedimentary Impacted Areas? *Diversity*, 15(3), 449.
- Villagómez, D., Spikings, R., 2013. Thermochronology and tectonics of the Central and Western Cordilleras of Colombia: early Cretaceous–Tertiary evolution of the northern Andes. *Lithos*, 160, 228–249.
- Villagómez, D., Spikings, R., Magna, T., Kammer, A., Winkler, W., Beltrán, A., 2011. Geochronology, geochemistry and tectonic evolution of the Western and Central cordilleras of Colombia. *Lithos*, 125, 875-896.
- Viseras, C., Henares, S., Yeste, L.M., García-García, F., 2018. Reconstructing the architecture of ancient meander belts by compiling outcrop and subsurface data. In: Ghinassi, M., Colombera, L., Mountney, N.P., Reesink, A.J.H., Bateman, M. (Eds.), *Fluvial Meanders and Their Sedimentary Products in the Rock Record*, 48, 419-444.
- Vossler, S.M., Pemberton, S.G., 1988. Superabundant *Chondrites*: a response to storm buried organic material? *Lethaia* 21, 94.
- Wade, B.S., Pälike, H., 2004. Oligocene climate dynamics. *Paleoceanography and Paleoclimatology*, 19(4).
- Wade, B.S., Pearson, P.N., Berggren, W.A., Pälike, H., 2011. Review and revision of Cenozoic tropical planktonic foraminiferal biostratigraphy and calibration to the geomagnetic polarity and astronomical time scale. *Earth Science Reviews*, 104, 111–142.

- Wade, B.S., Olsson, R.K., Pearson, P.N., Huber, B.T., Berggren, W.A., 2018. Atlas of Oligocene Planktonic Foraminifera. Cushman Foundation for Foraminiferal Research, Special Publication, 46, 1-524.
- Wagreich, M., Strauss, P.E., 2005. Source area and tectonic control on alluvial-fan development in the Miocene Fohnsdorf intramontane basin, Austria. In: Harvey, A.M., Mather, A.E., Stokes, M. (Eds.), Alluvial Fans: Geomorphology, Sedimentology, Dynamics. Geological Society, London, Special Publications, 207–216.
- Walker, R.G., 1975. Generalized facies models for resedimented conglomerates of turbidite association. Geological Society of America Bulletin 86, 737–748.
- Warne, A.G., Meade, R.H., White, W.A., Guevara, E.H., Gibeaut, J., Smyth, R.C., Aslan, A., Tremblay, T., 2002. Regional controls on geomorphology, hydrology, and ecosystem integrity in the Orinoco Delta, Venezuela. *Geomorphology*, 44, 273–307.
- Wasson, R., 1977. Last-glacial alluvial fan sedimentation in the Lower Derwent Valley, Tasmania. *Sedimentology*, 24, 781-799.
- Wathne, E., Larsen, E., Nemeč, W., Alçiçek, M.C., Ilgar, A., Helland, O.M., 2024. The Katırınemeği and Asar fan delta complexes in the Manavgat Basin (southern Türkiye): facies architecture of small shoal-water deltas recording forced and normal regressions. *Mediterranean Geoscience Reviews*, 24 p.
- Wei, X., Steel, R.J., Ravnas, R., Jiang, Z., Olariu, C., Li, Z., 2016. Variability of tidal signals in the Brent Delta Front: New observations on the Rannoch Formation, northern North Sea. *Sedimentary Geology*, 335, 166-179.
- Wentworth, C.K., 1922. A Scale of Grade and Class Terms for Clastic Sediments. *Journal of Geology*, 30, 377-392.
- West, L.M., Perillo, M.M., Olariu, C., Steel, R.J., 2019. Multi-event organization of deepwater sediments into bedforms: Long-lived, large-scale antidunes preserved in deepwater slopes. *Geology*, 47 (5), 391–394.
- Wetzel, A., 2008. Recent bioturbation in the deep South China Sea: a uniformitarian ichnologic approach. *Palaios*, 23, 601–615.
- Wetzel, A., 2010. Deep-sea ichnology: observations in modern sediments to interpret fossil counterparts. *Acta Geologica Polonica*, 60, 125-138.
- Wetzel, A., Bromley, R.G., 1994. *Phycosiphon incertum* revisited: *Anconichnus horizontalis* is its junior subjective synonym. *Journal of Paleontology*, 68, 1396–1402.
- Wetzel, A., Carmona, N., Ponce, J.J., 2014. Tidal signature recorded in burrow fill. *Sedimentology*, 61, 1198-1240.
- Whateley, M.K.G., Pickering, K.T., 1989. Deltas: sites and traps for fossil fuels. Geological Society London, Special Publication, 41, 360 p.
- Whybrow, P.J., McClure, H.A., 1980. Fossil mangrove roots and palaeoenvironments of the Miocene of the eastern Arabian Peninsula. *Palaeogeography, Palaeoclimatology, Palaeoecology*, 32, 213–225.
- Wilford, D.J., Sakals, M.E., Innes, J.K., Sidle, R.C., 2005. Fans with forests: contemporary hydrogeomorphic processes on fans with forests in west central British Columbia, Canada. In: Harvey, A.M., Mather, A.E., Stokes, M. (Eds.), Alluvial Fans: Geomorphology, Sedimentology, Dynamics. Geological Society, London, Special Publications, 25-40.
- Wilkin, J., Cuthbertson, A., Dawson, S., Stow, D., Stephen, K., Nicholson, U., Penna, N., 2023. The response of high-density turbidity currents and their deposits to an abrupt channel termination at a slope break: Implications for channel-lobe transition zones. *Sedimentology*, 70, 1164–1194.

- Willis, B.J., 2005. Deposits of tide-influenced river deltas. In: Giosan, L., Bhattacharya, J.P. (Eds.), *River deltas—Concepts, Models and Examples*, SEPM Special Publication 83, 87-129.
- Willis, B.J., Sun, T., Ainsworth, R.B., 2022. Sharp-based shoreface successions reconsidered in three-dimensions: A forward stratigraphic modelling perspective. *The Depositional Record*, 8(2), 685-717.
- Wilson, R.D., Schieber, J., 2014. Muddy Prodeltaic Hyperpynites In the Lower Genesee Group of Central New York, USA: Implications For Mud Transport In Epicontinental Seas. *Journal of Sedimentary Research*, 84(10), 866-874.
- Wilson, A., Flint, S.S., Payenberg, T.H.D., Tohver, E., Lanci, L., 2014. Architectural styles and sedimentology of the fluvial lower Beaufort Group, Karoo Basin, South Africa. *Journal of Sedimentary Research*, 84(4), 326-348.
- Winsemann, J., Lang, J., Fedele, J.J., Zavala, C., Hoyal, D.C., 2021. Re-examining models of shallow-water deltas: Insights from tank experiments and field examples. *Sedimentary Geology*, 421, 1–19.
- Wolanski, E., Gibbs, R.J., 1995. Flocculation of suspended sediment in the Fly River estuary, Papua New Guinea. *Journal of Coastal Research*, 11, 794-762.
- Wolanski, E., King, B., Galloway, D., 1995. Dynamics of the turbidity maximum in the Fly River estuary, Papua New Guinea. *Estuarine, Coastal and Shelf Science*, 40(3), 321-337.
- Wood, M.L., Ethridge, F.G., 1984. Sedimentology and architecture of Gilbert- and mouth bar-type fan deltas, Paradox Basin, Colorado. In: Nemeč, W., Steel, R.J. (Eds.), *Fan Deltas—Sedimentology and Tectonic Settings*, Blackie, London, UK, 251-263.
- Wright, L.D., 1977. Sediment transport and deposition at river mouths: a synthesis. *Geological Society of America Bulletin*, 88, 857-868.
- Wynn, R.B., Kenyon, N.H., Masson, D.G., Stow, D.A.V., Weaver, P.P.E., 2002. Characterization and recognition of deepwater channel-lobe transition zones. *AAPG Bulletin* 86, 1441–1462.
- Yang, B.C., Dalrymple, R.W., Chun, S.S., 2005. Sedimentation on a wave dominated, open-coast tidal flat, south-western Korea: a summer tidal flat–winter shoreface. *Sedimentology*, 52, 235–252.
- Yang, T., Yingchang, C., Yanzhong, W., 2017. A new discovery of The Early Cretaceous Supercritical Hyperpynal Flow Deposits on Lingshan Island, East China. *Acta Geologica Sinica*, 91(2), 749–750.
- Yang, B., Gingras, M., Pemberton, S.G., Dalrymple, R.W., 2008. Wave-generated tidal bundles as an indicator of wave-dominated tidal flats. *Geology*, 35(1), 39-42.
- Yeste, L.M., Palomino, R., Varela, A.N., McDougall, N.D., Viseras, C., 2021. Integrating outcrop and subsurface data to improve the predictability of geobodies distribution using a 3D training image: a case study of a Triassic Channel – Crevasse-splay complex. *Marine and Petroleum Geology*, 129, 105081.
- Yeste, L.M., Varela, A.N., Viseras, C., McDougall, N.D., García-García, F., 2020. Reservoir architecture and heterogeneity distribution in floodplain sandstones: Key features in outcrop, core and wireline logs. *Sedimentology*, 67(7), 3355-3388.
- Young, J. R., 1998. Neogene. In: Bown, P.R. (Ed.), *Calcareous Nannofossil Biostratigraphy*. British Micropalaeontological Society Publication Series. 225-265.
- Young, J.R., Bown, P.R., Lees, J.A. 2017. Nannotax3 website. International Nannoplankton Association: International Nannoplankton Association, <http://www.mikrotax.org/Nannotax3>.

- Young, J.R., Geisen, M., Cros, L., Kleijne, A., Sprengel, C., Probert, I., Østergaard, J. 2003. A guide to extant coccolithophore taxonomy. *Journal of Nannoplankton Research*, 1, 1–125.
- Zachos, J., Pagani, M., Sloan, L., Thomas, E., Billups, K., 2001. Trends, rhythms, and aberrations in global climate 65 Ma to present. *Science*, 292(5517), 686-693.
- Zapata, S., Patiño, A., Cardona, A., Parra, M., Valencia, V., Reiners, P., Oboh-Ikuenobe, F., Genezini, F., 2020. Bedrock and detrital zircon thermochronology to unravel exhumation histories of accreted tectonic blocks: An example from the Western Colombian Andes. *Journal of South American Earth Sciences*, 103, 102715.
- Zavala, C., 2020. Hyperpycnal (over density) flows and deposits. *Journal of Paleogeography* 9, 17. 21p.
- Zavala, C., Arcuri, M., 2016. Intrabasinal and extrabasinal turbidites: origin and distinctive characteristics. *Sedimentary Geology*, 337, 36-54.
- Zavala, C., Pan, S.X., 2018, Hyperpycnal flows and hyperpycnites: Origin and distinctive characteristics. *Lithologic Reservoirs*, 3(1), 1-27.
- Zavala, C., Arcuri, M., Blanco Valiente, L., 2012. The importance of plant remains as a diagnostic criteria for the recognition of ancient hyperpycnites. *Revue Paléobiologie* 11, 457–469.
- Zavala, C., Arcuri, M., Di Meglio, M., Gamero Diaz, H., Contreras, C., 2011. A genetic facies tract for the analysis of sustained hyperpycnal flow deposits. In: Slatt, R.M., Zavala, C. (Eds.), *Sediment transfer from shelf to deep water revisiting the delivery system*. AAPG Studies in Geology, 61, 31–51.
- Zavala, C., Arcuri, M., Di Meglio, M., Zorzano, A., Goitia Antezana, V.H., Arnez Espinosa, LR., 2016. Prodelta hyperpycnites: Facies, processes and reservoir significance. Examples from the lower cretaceous of Russia. *International Conference and Exhibition, Barcelona, Spain, SEG Global Meeting*, 73 pp.
- Zavala, C., Arcuri, M., Di Meglio, M., Zorzano, A., Otharán, G., Irastorza, A., Torresi, A., 2021. Deltas: a new classification expanding Bates's concepts. *Journal of Palaeogeography*, 10, 23.
- Zavala, C., Arcuri, M., Zorzano, A., Trobbiani, V., Torresi, A., Irastorza, A., 2024, Deltas: New paradigms, *The Depositional Record*, 00, 1-37.
- Zecchin, M., Mellere, D., Roda, C., 2006. Sequence stratigraphy and architectural variability in growth fault-bounded basin fills: a review of Plio-Pleistocene stratal units of the Croton Basin, southern Italy. *Journal of Geological Society (London)*, 163, 471-486.
- Zhang, J., Rossi, V.M., Peng, Y., Steel, R., Ambrose, W., 2019. Revisiting Late Paleocene Lower Wilcox deltas, Gulf of Mexico: River-dominated or mixed-process deltas? *Sedimentary Geology*, 389, 1-12.
- Zuchuat, V., Gugliotta, M., Poyatos-Moré, M., van der Vegt, H., Collins, D.S., Vaucher, R., 2023. Mixed depositional processes in coastal to shelf environments: Towards acknowledging their complexity. *The Depositional Record*, 9(2), 206-212.
- Zuluaga, M., Robledo, S., Arbelaez-Echeverri, O., Osorio-Zuluaga, G.A., Duque-Méndez, N., 2022. Tree of Science - ToS: A web-based tool for scientific literature recommendation. Search less, research more! *Issues In Science And Technology Librarianship*, 100.

Appendix I.

Other peer reviewed publications –JCR (SCI)– indexed journal papers during the doctoral thesis.

- Vallejo-Hincapié, F., Pardo-Trujillo, A., Barbosa-Espitia, A., Aguirre, D., **Celis, S.A.**, Giraldo-Villegas, C., Plata-Torres, A., Trejos-Tamayo, R., Salazar-Ríos, A., Flores, J-A., Aubry, M-P., Gallego, F., Delgado, E., Foster, D., 2024. Miocene vanishing of the Central American Seaway between the Panamá Arc and the South American Plate. *Geological Society of America Bulletin*, <https://doi.org/10.1130/B37499.1>.
- Giraldo-Villegas, C., Rodríguez-Tovar, F.J., **Celis, S.A.**, Pardo-Trujillo, A., 2023. Variable Ophiomorpha ichnofabric: Improving the understanding of mouth bar environments in fan-delta complex depositional settings from the Upper Cretaceous of NW South America. *Cretaceous Research*, 154, 105730.
- Ospina-Muñoz, A., Márquez, I., Vallejo, D.F., Salazar-Ríos, A., Trejos-Tamayo, R., **Celis, S.A.**, Plata, A., Pardo-Trujillo, A. 2023. Calcareous microfossil biostratigraphy of Upper Miocene to Pliocene deposits of the Sinú-San Jacinto Belt, Caribbean region of Colombia. *Journal of South American Earth Sciences*. Accepted.
- Giraldo-Villegas, C., Rodríguez-Tovar, F.J., **Celis, S.A.**, Pardo-Trujillo, A., Duque-Castaño, M.L. 2023. Paleoenvironmental conditions over the Caribbean Large Igneous Province during the Late Cretaceous in NW of South American Margin: A sedimentological and ichnological approach. *Cretaceous Research*, 142, 105407.
- Pardo-Trujillo, A., Echeverri, S., Borrero, C., Arenas, A., Vallejo, F., Trejos, R., Plata, Á., Flores, J.A., Cardona, A., Restrepo, S., Barbosa, Á., Murcia, H., Giraldo, C., **Celis, S.**, López, S.A. 2020. Cenozoic geologic evolution of the southern Tumaco Forearc Basin (SW Colombian Pacific). In: Gómez, J., Mateus-Zabala, D. (Eds.), *The Geology of Colombia, Volume 3 Paleogene – Neogene*. Servicio Geológico Colombiano, *Publicaciones Geológicas Especiales* 37, 215–247.
- Pardo-Trujillo, A., Cardona, A., Giraldo, A.S., León, S., Vallejo, D.F., Trejos-Tamayo, R., Plata, A., Ceballos, J., Echeverri, S., Barbosa-Espitia, A., Slattery, J., Salazar, A., Botello, G.E., **Celis, S.A.**, Osorio-Granada, E., Giraldo-Villegas, C.A. 2020. Sedimentary record of the Cretaceous-Paleocene arc-continent collision in the northwestern Colombian Andes: insights from stratigraphic and provenance constraints. *Sedimentary Geology*, 401, 105627.

Thesis results were published in the following national and international conferences

- Celis, S.A., Rodríguez-Tovar, F.J., García-García, F., Giraldo-Villegas, C., Pardo-Trujillo, A. 2024. From shallow to deep marine coarse-grained deposits: sedimentary systems during the late Eocene, Colombian Caribbean. *International Association of Sedimentology IAS Conference*. Poster communication. Aberdeen, Scotland.
- Celis, S.A., Moyano-Paz, D., Richiano, S., Cuitiño, J., Rodríguez-Tovar, F.J., 2024. Ichnological analysis as indicators of physico-chemical stresses in wave to tide-dominated Miocene shallow marine environments (Argentine Patagonia). Oral communication. *The 5th International Congress on Ichnology ICHNIA*. Florianópolis, Brazil.
- Celis, S.A., Moyano-Paz, D., Richiano, S., Cuitiño, J., Rodríguez-Tovar, F.J., 2023. Physico-chemical stresses in Miocene wave-dominated and tide-dominated coastal settings (Puerto Madryn Formation, Argentine Patagonia). *XVIII Reunion Argentina de Sedimentología - IX Congreso Latinoamericano de Sedimentología*. Oral communication. La Plata, Argentina.

- Celis, S.A., García-García, F., Rodríguez-Tovar, F.J., Pardo-Trujillo, A., Giraldo-Villegas, C. 2023. Coarse-grained channel lobe transition zone and channel levee complex in late Eocene deposits from Colombian Caribbean. International Association of Sedimentology IAS Conference. Poster communication. Dubrovnik, Croatia.
- Celis, S.A., Rodríguez-Tovar, F.J., Pardo-Trujillo, A., García-García, F., Giraldo-Villegas, C., 2023. Evolution of coastline depositional systems in a tropical forearc basin during the Oligocene-Miocene in the Colombian Caribbean: signals from well-cores integrative sedimentological, ichnological, and micropaleontological analysis. International Association of Sedimentology IAS Conference. Oral communication. Dubrovnik, Croatia.
- Celis, S.A., 2022. Life and death in the ocean: stress factors in coastal environments. Oral communication. Granada, Spain.
- Celis, S.A., Rodríguez-Tovar, F.J., Pardo-Trujillo, A. 2022. The record of rhizoliths in Oligocene – Miocene sediments of the Colombian Caribbean: paleoenvironmental implications. XXXVII Jornadas de la Sociedad Española de Paleontología y V Congreso Ibérico de Paleontología. Poster communication. Cuenca, Spain.
- Celis., S.A., Rodríguez-Tovar, F.J., Giraldo-Villegas, C., Gallego, F., Pardo-Trujillo, A. 2021. Evolución de sistemas deltaicos durante el Oligoceno Mioceno en el Caribe colombiano. XVIII Congreso Colombiano de Geología. Oral communication. Colombia.
- Celis, S.A., Giraldo-Villegas, C., Rodríguez-Tovar, F.J., Pardo-Trujillo, A. 2020. Icnología en Colombia: estado del conocimiento, avances y perspectivas. I Congreso Colombiano de Paleontología. Oral communication. Bogotá, Colombia.

**Depositional processes and controlling factors from
river mouths to slope systems in active tectonic margins:**
insights from middle-upper Eocene to Lower Miocene
records in the Colombian Caribbean

Sergio A. Celis
PhD Thesis

The middle-upper Eocene to Lower Miocene successions in the Colombian Caribbean represent complex depositional environments shaped by tectonics and sediment input. The conducted sedimentological, ichnological, and micropaleontological analyses reveal both allogenic and autogenic processes influencing sedimentation.

In the southwestern Colombian Caribbean, south of the San Jacinto Fold Belt, middle-late Eocene coarse-grained systems are characterized by hyperconcentrated and hyperpycnal flows originating from continental areas. These flows undergo transformations upon reaching coastal and marine settings, exhibiting diverse flow behaviors ranging from high-energy sand-rich flows to fluidal gravel beds. Marine influence, reflected in sedimentological and ichnological features, indicate gravitational flow and tidal modulation. In the central region of the San Jacinto Fold Belt, evidence points to the development of submarine channel systems, with coarse-grained channel-lobe transitions marking supercritical to subcritical conditions with sediment transport from land to the marine basin.

During the latest Eocene to earliest Oligocene, transgressive fine-grained deposits overlie coarse-grained successions in the southwestern Colombian Caribbean. Oligocene to Early Miocene successions show meandering fluvial deposits, mudrocks, and rhizoliths, indicating water-logged interdistributary bays and gallery flood forests, marking the beginning of a lower delta plain system. Moreover, typical fluvio-dominated deltaic successions, influenced by tropical torrential rains, show fluctuations in river discharges, with episodic tidal modulation and wave reworking affecting the deltaic system. This period marks a shift in sedimentation patterns, driven by tectonic activity, eustatic sea level changes, and tropical climatic influences. The progradational trend and evolving depositional styles highlight the complex interplay between tectonic convergence, subsidence, and climate, contributing to the understanding of sedimentary processes in tropical regions.



ugr

Universidad
de Granada



Programa Doctorado
Ciencias de la Tierra

